TR A7389 Unrestricted

Report

EERA DeepWind'2014 Conference
22 – 24 January 2014

Royal Garden Hotel, Trondheim

Author:
John Olav Tande (editor)

SINTEF Energy Research
Electric Power Systems
2014-02-24

SINTEF Energi AS
SINTEF Energy Research
Address:
Postboks 4761 Sluppen
NO-7465 Trondheim
NORWAY
Telephone:+47 73597200
Telefax:+47 73598354
energy.research@sintef.no
www.sintef.no/energi
Enterprise /VAT No:
NO 939 350 675 MVA

KEYWORDS:
Keywords

Report

EERA DeepWind'2014 Conference
22 – 24 January 2014

Royal Garden Hotel, Trondheim

VERSION
1.0

DATE
2014-02-24

AUTHOR(S)
John Olav Tande

CLIENT(S)

CLIENT'S REF.

PROJECT NO.
502000389

NUMBER OF PAGES/APPENDICES:
316

ABSTRACT
This report includes the presentations from the 11th Deep Sea Offshore Wind R&D Conference, EERA DeepWind'2014, 22 – 24 January 2014 in Trondheim, Norway.

Presentations include plenary sessions with broad appeal and parallel sessions on specific technical themes:
a) New turbine and generator technology
b) Grid connection and power system integration
c) Met-ocean conditions
d) Operations & maintenance
e) Installation & sub-structures
f) Wind farm modelling
g) Experimental Testing and Validation

Plenary presentations include frontiers of science and technologies and strategic outlook. The presentations and further conference details are also available at the conference web page https://www.sintef.no/Projectweb/Deepwind_2014/

Full papers of selected presentations will be published online in Energy Procedia (Elsevier).

PREPARED BY
John Olav Tande

SIGNATURE

CHECKED BY
Hans Christian Bolstad

SIGNATURE

APPROVED BY
Knut Samdal

SIGNATURE

REPORT NO.	ISBN	CLASSIFICATION	CLASSIFICATION THIS PAGE
TR A7389	978-82-594-3583-5	Unrestricted	Unrestricted

Document history

VERSION	DATE	VERSION DESCRIPTION
1.0	2014-02-24	

Table of contents

Posters

Closing session

Wednesday 22 January

09.00	Registration & coffee	
	Opening session – Frontiers of Science and Technology Chairs: John Olav Tande, SINTEF/NOWITECH and Trond Kvamsdal, NTNU/NOWITECH	
09.30	Opening and welcome by chair	
09.40	*Progress of offshore wind through R&D in FP7 and H2020,* Matthijs Soede, European Commission	
10.10	*Innovations in offshore wind through R&D,* John Olav Tande, SINTEF/NOWITECH	
10.35	*Highlights from NORCOWE*, Kristin Guldbrandsen Frøysa, CMR/NORCOWE	
11.00	*EERA Design Tool for Offshore wind farm Clusters - DTOC*, Charlotte Bay Hasager, DTU Wind Energy	
11.30	*Innovative wind conversion systems for offshore applications – INNWIND.EU.*, Peter Hjuler Jensen, DTU Wind Energy	
11.55	Closing by chair	
12.00	Lunch	
	Parallel sessions	
	A1) New turbine and generator technology Chairs: Karl Merz, SINTEF Prof Gerard van Bussel, TU Delft	**C1) Met-ocean conditions** Chairs: Prof J Reuder, Uni of Bergen Erik Berge, Kjeller Vindteknikk
13.00	Introduction by Chair	Introduction by Chair
13.05	*New generator technology for offshore wind turbines*, prof Robert Nilssen, NTNU	*Using the NORSEWInD lidar array for observing hub-height winds in the North Sea*, Charlotte Bay Hasager, DTU Wind Energy
13.30	*Necessity is the mother of invention: nacelle mounted lidar for measurement of turbine performance,* Matt Smith, Zephir Lidar Ltd.	*Results and conclusions of a floating Lidar offshore test*, Julia Gottschall, Fraunhofer IWES
13.50	*New rotor concepts for future offshore wind farms,* O. Ceyhan ECN	*Metocean analysis of a low-level coastal jet off the Norwegian coast*, Konstantinos Christakos, Polytec R&D
14.10	*Multi Rotor Systems of 20 MW or more for deep water applications,* Peter Jamieson, Strathclyde University	*Air-Sea Interaction Influenced by Swell Waves*, Mostafa Bakhoday Paskyabi, Geophysical Institute, University of Bergen
14.30	Closing by Chair	Closing by Chair
14.35	Refreshments	
	A2) New turbine and generator technology (cont.)	**C2) Met-ocean conditions (cont.)**
15.05	Introduction by Chair	Introduction by Chair
15.10	*DeepWind-from idea to 5 MW concept*, Uwe Scmidt Paulsen, Technical University of Denmark	*Wave refraction analyses at the western coast of Norway for offshore applications*, Ole Henrik Segtnan, Polytec R&D Institute
15.30	*Dynamic analysis of a floating vertical axis wind turbine during emergency shutdown through mechanical brake and hydrodynamic brake*, Kai Wang, NTNU	*Improving Gap Flow Simulations near Coastal Areas of Continental Portugal,* Paulo Costa, LNEG
15.50	*Concept design verification of a semi-submersible floating wind turbine using coupled simulations*, Fons Huijs, GustoMSC	*Wave driven wind and the effect on offshore wind turbine performance,* Siri Kalvig, StormGeo/University of Stavanger
16.10	Closing by Chair	Closing by Chair
16.15	Refreshments	
17.00	**Laboratory visits** a) Smart Grids Lab b) Ocean Basin Lab c) Wind tunnel	
19.00	Conference reception	

Thursday 23 January

	Parallel sessions	
	B1) Grid connection Chairs: Prof Kjetil Uhlen, NTNU Prof Olimpo Anaya-Lara, Strathclyde University	**E1) Installation and sub-structures** Chairs: Prof Hans Gerd Busmann, Fraunhofer IWES Jørgen Krokstad, Statkraft
09.00	Introduction by Chair	Introduction by Chair
09.05	*Power system integration of offshore wind farms,* Tobias Hennig, Fraunhofer IWES	*Experimental Studies and numerical Modelling of structural Behavior of a Scaled Modular TLP Structure for Offshore Wind turbines*, Frank Adam, GICON
09.30	*The Impact of Active Power Losses on the Wind Energy Exploitation of the North Sea*, Hossein Farahmand, SINTEF Energi AS	*Tension-Leg-Buoy Platforms for Offshore Wind Turbines,* Tor Anders Nygaard, IFE
09.50	*Dynamic Series Compensation for the Reinforcement of Network Connections with High Wind Penetration*, Juan Nambo-Martinez, Strathclyde University	*A preliminary comparison on the dynamics of a floating vertical axis wind turbine on three different floating support structures,* Michael Borg, Cranfield University
10.10	*Transient interaction between wind turbine transformer and the collection grid of offshore wind farms,* Andrzej Holdyk, SINTEF Energy Research	*Modelling challenges in simulating the coupled motion of a semi-submersible floating vertical axis wind turbine,* R. Antonutti, EDF R&D – IDCORE
10.30	Refreshments	
	B2) Grid connection (cont.)	**E2) Installation and sub-structures (cont.)**
11.00	*Experimental verification of a voltage droop control for grid integration of offshore wind farms using multi-terminal HVDC,* Raymundo E. Torres-Olguin, SINTEF Energi AS	*Offshore wind R&D at NREL,* Senu Sirnivas, NREL
11.20	*Ancillary Services Analysis of an Offshore Wind Farm Cluster - Technical Integration Steps of an Simulation Tool;* Tobias Hennig, Fraunhofer IWES	*Ringing and impulsive excitation of offshore wind turbines from steep and breaking waves on intermediate depth. Results from the Wave Loads project,* Henrik Bredmose, DTU Wind Energy
11.40	*Sub-sea cable technology*; Hallvard Faremo, SINTEF Energy Research	*Damping of wind turbine tower vibrations by means of stroke amplifying brace concepts,* Mark Brodersen, DTU
12.00	Closing by Chair	Closing by Chair
12.05	Lunch	
	B3) Power system integration Chairs: Prof Kjetil Uhlen, NTNU Prof Olimpo Anaya-Lara, Strathclyde University	**G1) Experimental Testing and Validation** Chairs: Tor Anders Nygaard, IFE Ole David Økland, MARINTEK
13.05	Introduction by Chair	Introduction by Chair
13.10	*Active damping of DC voltage oscillations in multiterminal HVDC systems*; Salvatore D'Arco, SINTEF Energy Research	*Joint test field research – selected results from the RAVE initiative*, Michael Durstewitz, Fraunhofer IWES
13.35	*Analysis and Design of a LCL DC/DC converter for Offshore Wind Turbines*; Rene A. Barrera, PhD Student NTNU	*Testing of towing and installation of Reinertsen self-installing concept*, Marit Reiso, Reinertsen AS
13.55	*Fault Ride Through Enhancement of Multi Technology Offshore Wind Farms*; Arshad, Ali, University of Strathclyde	*Wind turbine wake blind test;* Prof Per-Åge Krogstad, NTNU
14.15	*Reliability of power electronic converters for offshore wind turbines;* Magnar Hernes, SINTEF Energy Research	*Wind Turbine Wake Experiment - Wieringermeer (WINTWEX-W),* Valerie-Marie Kumer, UiB
14.35	Refreshments	
	B4) Power system integration (cont.)	**G2) Experimental Testing and Validation (cont.)**
15.05	*Design and Optimisation of Offshore Grids in Baltic Sea for Scenario Year 2030*, Vin Cent Tai, NTNU	*Design of a 6-DoF Robotic Platform for Wind Tunnel Tests of Floating Wind Turbines,* Marco Belloli, Politecnico di Milano
15.25	*Operation of power electronic converters in offshore wind farms as virtual synchronous machines*; Jon Are Suul, SINTEF Energy Research	*Experimental study on wake development of floating wind turbine models,* Stanislav Rockel, ForWind, Univ Oldenburg
15.45	*The Future of HVDC*; Yiannis Antoniou, University of Strathclyde	*Floating Wind Turbines*, Prof Paul Sclavounos, MIT
16.05	*North-Sea Offshore Network – NSON;* Magnus Korpås, SINTEF Energy Research	*Numerical CFD comparison of Lillgrund employing RANS*, Nikolaos Simisiroglou, WindSim AS
16.25	Closing by Chair	Closing by Chair
16.30	Refreshments	
17.00	Poster session	
19.00	Conference dinner	

Thursday 23 January

17.00	**Poster Session with refreshments** 1. *Numerical simulation of a wind turbine with hydraulic transmission system, Zhiyu Jiang, NTNU* 2. *A DC-OPF Computation for Transmission Network Incorporating HVDC Transmission Systems, Phen Chiak See, NTNU* 3. *Cross-Border Transfer of Electric Power under Uncertainty: A Game of Incomplete Information, Phen Chiak See, NTNU* 4. *FSI-WT: A comprehensive design methodology for Offshore Wind Turbines, Espen Åkervik, FFI* 5. *First verification test and wake measurement results using a Ship-Lidar System, G Wolken-Möhlmann, Fraunhofer IWES* 6. *Buoy-mounted lidar provides accurate wind measurement for offshore wind farm developments*, Jan-Petter Mathisen, Fugro OCEANOR 7. *Characterization of the SUMO turbulence measurement system for wind turbine wake assessment, Line Båserud, UiB* 8. *Field Measurements of Wave Breaking Statistics Using Video Camera for Offshore Wind Application, Mostafa Bakhoday Paskyabi, UiB* 9. *Stochastic Particle Trajectories in the Wake of Large Wind Farm, Mostafa Bakhoday Paskyabi, UiB* 10. *LiDAR Measurement Campaign Sola (LIMECS), Valerie-Marie Kumer, UiB* 11. *Fatigue Reliability-Based Inspection and Maintenance Planning of Gearbox Components in Wind Turbine Drivetrains, Amir Nejad, NTNU* 12. *Engineering Critical Assessment (ECA) of Electron Beam (EB) welded flange connection of wind turbine towers, P. Noury, Luleå University of Technology* 13. *A Multiscale Wind and Power forecast system for wind farms, Adil Rasheed, SINTEF ICT* 14. *NOWITECH Reference Wind Farm, Henrik Kirkeby, SINTEF Energi AS* 15. *Actuator disk wake model in RaNS, Vitor M. M. G. Costa Gomes, Faculdade de Engenharia da Universidade do Porto* 16. *Model reduction based on CFD for wind farm layout assessment, Chad Jarvis, Christian Michelsen Research AS* 17. *Energy yield prediction of offshore wind farm clusters at the EERA-DTOC European project, E. Cantero, CENER* 18. *Sizing of Offshore Wind Localized Energy Storage, Franz LaZerte, NTNU* 19. *Unsteady aerodynamics of attached flow for a floating wind turbine, Lene Eliassen, UiS* 20. *FloVAWT: development of a coupled dynamics design tool for floating vertical axis wind turbines, Michael Borg, Cranfield University* 21. *Use of an industrial strength aeroelastic software tool educating wind turbine technology engineers, Paul E. Thomassen, Simis as* 22. *Offshore ramp forecasting using offsite data, Pål Preede Revheim, UiA* 23. *Significance of unsteady aerodynamics in floating wind turbine design, Roberts Proskovics, Univ of Strathclyde* 24. *Synergy and disadvantage: Offshore wind farm integration with aquaculture farm, W. He, Statoil* 25. *Multiphysics optimization of ironless permanent magnet generator with super computers*, S.M. Muyeen, The Petroleum Institute 26. *Wind Tunnel Testing of a Floating Wind Turbine Moving in Surge and Pitch,* Jan Bartl, NTNU 27. *Sub-sea Energy Storage for Deep-sea Wind Farms*, Ole Christian Spro, SINTEF Energi AS 28. *How can more advanced failure modelling contribute to improving life-cycle cost analyses of offshore wind farms*?, Kari-Marie Høyvik Holmstrøm, University of East London 29. *Will 10 MW wind turbines bring down the operation and maintenance cost of offshore wind farms?,* Matthias Hofmann/Iver Sperstad Bakken, SINTEF Energi AS 30. *Modelling of Lillgrund wind farm: Effect of wind direction,* Balram Panjwani, SINTEF 31. *Lab-scale implementation of a multi-terminal HVDC grid connecting offshore wind farms, Raymundo Torres-Olguin, SINTEF Energi AS*
19.00	Dinner

Friday 24 January

	Parallel sessions	
	D) Operations & maintenance Chairs: Thomas Welte, SINTEF Energi AS Michael Durstewitz, Fraunhofer IWES	**F) Wind farm optimization** Chairs: Prof Trond Kvamsdal, NTNU Thomas Buhl, DTU Wind Energy
09.00	Introduction by Chair	Introduction by Chair
09.05	*Operational experience with offshore wind farms,* Per Christian Kittilsen, Statkraft	*EERA-DTOC: How aerodynamic and electrical aspects come together in wind farm design*, Gerard Schepers, Energy Research Center of the Netherlands
09.25	*Fatigue Reliability-Based Inspection and Maintenance Planning of Gearbox Components in Wind Turbine Drivetrains,* Amir Nejad, NTNU	*Benchmarking of Lillgrund offshore wind farm scale wake models in the EERA-DTOC project,* K.S. Hansen, DTU
09.45	*Cost-Benefit Evaluation of Remote Inspection of Offshore Wind Farms by Simulating the Operation and Maintenance Phase,* Øyvind Netland, NTNU	*Variable Frequency Operation for Future Offshore Wind Farm Design: A Comparison with Conventional Wind Turbines*, Ronan Meere, University College Dublin
10.05	*The effects of using multi-parameter wave criteria for accessing wind turbines in strategic maintenance and logistics models for offshore wind farms*, Iver Bakken Sperstad, SINTEF Energi AS	*Estimation of Possible Power in Offshore Wind Farms during Downregulation, PossPOW Project*, Tuhfe Göçmen Bozkurt, DTU
10.25	Closing by Chair	Closing by Chair
10.30	Refreshments	
	Closing session – Strategic Outlook Chairs: John Olav Tande, SINTEF/NOWITECH and Trond Kvamsdal, NTNU/NOWITECH	
11.00	Introduction by Chair	
11.05	*Floating wind technology – future development;* Johan Slätte, DNV	
11.35	*Results from the Offshore Wind Accelerator Programme*; Jan Matthiesen, Carbon Trust	
12.05	*Offshore wind developments,* Prof Leonard Bohmann, Michigan Tech	
12.35	Poster award and closing	
13.00	Lunch	

List of participants – EERA DeepWind'2014 Conference

Surname	First name	Institution
Adam	Frank	GICON
Anaya-Lara	Olimpo	Strathclyde University
Andersen	Morten Thøtt	Aalborg University
Andreassen	Vidar	Innovasjon Norge
Antoniou	Yiannis	University of Strathclyde
Antonutti	Raffaello	EDF R&D LNHE
Arshad	Ali	University of Strathclyde
Bakken	Iver Sperstad	SINTEF Energi AS
Barrera-Cardenas	Rene Alexander	NTNU
Bartl	Jan	NTNU
Belloli	Marco	Politecnico di Milano
Berge	Erik	Kjeller Vindteknikk
Bergström	Daniel	DB Teknikanalys
Beyer	Hans Georg	Universitetet i Agder
Bohmann	Leonard	Michigan Tech
Bolstad	Hans Christian	SINTEF Energi AS
Borg	Michael	Cranfield University
Boulharts	Habiba	IFP Energies Nouvelles
Bozkurt	Tuhfe Gocmen	Technical University of Denmark, DTU
Bredmose	Henrik	DTU Wind Energy
Brodersen	Mark	Technical University of Denmark, DTU
Buhl	Thomas	DTU
Busmann	Hans-Gerd	Fraunhofer IWES
Båserud	Line	Universitetet i Bergen
Cândido,	José	Wavec Offshore Renewables
Ceyhan	Ozlem	ECN
Chabaud	Valentin	NTNU
Christakos	Konstantinos	Polytec R&D Institute
Costa	Paulo	LNEG
D'Arco	Salvatore	SINTEF Energi AS
Durstewitz	Michael	Fraunhofer IWES
Eliassen	Lene	Statkraft
Ellingsen	Rakel	TEKNISK HJELP (stud NTNU)
Endegnanew	Atsede	SINTEF Energi AS
Farahmand	Hossein	SINTEF Energi AS
Faremo	Hallvard	SINTEF Energi AS

Frøyd	Lars	4Subsea
Frøysa	Kristin Gulbrandsen	Christian Michelsen Research AS
Gao	Zhen	CeSOS, NTNU
Gomes	Vitor	FEUP
Gottschall	Julia	Fraunhofer IWES
Gravdahl	Arne R.	WindSim AS
Hagen	Arnulf	Fedem Technology
Hansen	Kurt S.	DTU Wind Energy
Hasager	Charlotte	DTU Wind Energy
Haug	Roald	Bosch Rexroth
He	Wei	Statoil
Hennig	Tobias	Fraunhofer IWES
Hernes	Magnar	SINTEF Energi AS
Holdahl	Runar	SINTEF
Holdyk	Andrzej	SINTEF Energi AS
Holmstrøm	Kari-Marie Høyvik	University of East London
Hopstad	Anne Lene	DNV GL
Howe	Graham	AXYS Technologies Inc
Huertas Hernando	Daniel	SINTEF Energi AS
Huijs	Fons	GustoMSC
Jakobsen	Jasna Bogunovic	Universitetet i Stavanger
Jamieson	Peter	Strathclyde University
Jarvis	Chad	CMR
Jensen	Peter Hjuler	DTU
Jiang	Zhiyu	NTNU
Kalvig	Siri	StormGeo
Kirkeby	Henrik	SINTEF Energi AS
Kittilsen	Per Christian	Statkraft
Klein	Marian	Boulder Environmental Sciences and Technology,LLC
Klementsen	Kristine	Student
Korpås	Magnus	SINTEF Energi AS
Krogstad	Per-Åge	NTNU
Krokstad	Jørgen	Statkraft
Kumer	Valerie-Marie	University of Bergen
Kvamsdal	Trond	NTNU
Kvinge	Katrine	TEKNISK HJELP (stud NTNU)
Lazerte	Franz	NTNU
Ljøkelsøy	Kjell	SINTEF Energi AS
Lund	Berit Floor	Kongsberg Maritime AS

Maal	Guro Tjomlid	TEKNISK HJELP (stud NTNU)
Manger	Eirik	Acona Flow Technology
Mathisen	Jan-Petter	Fugro OCEANOR
Matthiesen	Jan	Carbon Trust
Meere	Ronan	Electricity Research Centre, UCD
Merz	Karl	SINTEF Energi
Moan	Torgeir	NTNU
Mork	Bruce	Michigan Tech
Muyeen	S.M.	The Petroleum Institute
Myhr	Anders	Dr.tech. Olav Olsen
Nambo-Martinez	Juan Carlos	University of Strathclyde
Nejad	Amir	NTNU
Netland	Øyvind	NTNU
Nielsen	Finn Gunnar	Statoil
Nilssen	Robert	NTNU
Noury	Pourya	Luleå University of Technology
Nygaard	Tor Anders	IFE
Oggiano	Luca	IFE
Ong	Muk Chen	MARINTEK
Palma	Jose	Universidade do Porto
Panjwani	Balram	SINTEF
Paskyabi	Mostafa Bakhoday	Geophysical Institute
Paulsen	Uwe Schmidt	DTU Wind Energy
Pelissier	Sebastien	EDF R&D LNHE
Proskovics	Roberts	University of Strathclyde
Rasheed	Adil	SINTEF
Reiso	Marit	Reinertsen
Reuder	Joachim	UiB
Revheim	Pål Prede	University of Agder
Rockel	Stanislav	ForWind - University of Oldenburg
Ross	William	University of Strathclyde
Ruddy	Jonathan	Electricity Research Centre, (ERC)
Røkenes	Kjersti	Kongsberg Maritime AS
Sandal	Kasper	TEKNISK HJELP (stud NTNU)
Sauder	Thomas	MARINTEK
Schepers	Gerard	ECN
Sclavounos	Paul	MIT
Schramm	Rainer	Subhydro AS
See	Phen Chiak	NTNU
Segtnan	Ole Henrik	Polytec

Simisiroglou	Nikolaos	WindSim AS
Sirnivas	Senu	NREL
Slätte	Johan	DNV GL
Smith	Matthew	ZEPHIR LTD
Soede	Matthijs	European Commission
Spro	Ole Christian	SINTEF Energi AS
Stenbro	Roy	IFE
Suja-Thauvin	Loup	Statkraft
Suul	Jon Are	SINTEF Energi AS
Svendgård	Ole	VIVA - Testsenter for turbiner
Svendsen	Harald	SINTEF Energi AS
Süld	Jakob	Meteorologisk Institutt
Sætertrø	Kristian	Fedem Technology
Tande	John Olav	SINTEF Energi
Thomassen	Paul	Simis AS
Torres-Olguin	Raymundo E.	SINTEF Energi AS
Uhlen	Kjetil	NTNU
van Bussel	Gerard	TU Delft
Vin Cent	Tai	NTNU
Wang	Kai	CeSOS, NTNU
Welte	Thomas	SINTEF Energi
Wolken Möhlmann	Gerrit	Fraunhofer IWES
Zwick	Daniel	NTNU
Økland	Ole David	MARINTEK
Øverli	Jan M.	Professor emeritus NTNU
Åkervik	Espen	FFI

3 Scientific Committee and Conference Chairs

An international Scientific Committee is established with participants from leading research institutes and universities. These include:

Anaya-Lara, Olimpo, Strathclyde
Avia, Felix, CENER
Berge, Erik, Kjeller Vindteknikk
Busmann, Hans-Gerd, Fraunhofer IWES
Eecen, Peter, ECN
Jørgensen, Hans Ejsing, DTU
Kvamsdal, Trond, NTNU
Langen, Ivar, UiS
Leithead, William, Strathclyde
Lekou, Denja, CRES
Madsen, Peter Hauge, DTU
Moan, Torgeir, NTNU
Nielsen, Finn Gunnar, Statoil/UiB
Nygaard, Tor Anders, IFE
Pascual, Pablo Ayesa, CENER
Reuder, Joachim, UiB
Robertson, Amy, NREL
Rohrig, Kurt, Fraunhofer IWES
Sempreviva, Anna Maria, CNR
Tande, John Olav, SINTEF/NOWITECH
Undeland, Tore, NTNU
Van Bussel, Gerard, TU Delft

The Scientific Committee will review submissions and prepare the programme. Selection criteria are relevance, quality and originality.

The conference chairs were

- John Olav Giæver Tande, Director NOWITECH, senior scientist SINTEF Energy Research
- Trond Kvamsdal, Chair NOWITECH Scientific Committee, Associate Professor NTNU

Opening session – Frontiers of Science and Technology

Progress of offshore wind through R&D in FP7 and H2020,
Matthijs Soede, European Commission

Innovations in offshore wind through R&D, John Olav Tande, SINTEF/NOWITECH

Highlights from NORCOWE, Kristin Guldbrandsen Frøysa, CMR/NORCOWE

EERA Design Tool for Offshore wind farm Clusters - DTOC, Charlotte Bay Hasager,
DTU Wind Energy

Innovative wind conversion systems for offshore applications – INNWIND.EU,
Peter Hjuler Jensen, DTU Wind Energy

Progress of offshore wind through R&D in FP7 and H2020

Matthijs SOEDE
Research Programme Officer
Unit G3 Renewable Energy Sources
DG Research and Innovation

Renewable Energy Policy Framework in Europe

- ***EU 2020 strategy:*** *sustainable, smart and inclusive growth encapsulating the three 20 % targets on renewables, energy efficiency and GHG emissions*
  - → *need to boost the renewables industry, promote technological innovation and employment in Europe and achieve:*
- ***EU 2050 roadmap****: reducing GHG emission levels by 80-95% compared to 1990 and becoming less dependent on imported energy*

Wind Energy for Europe

- *Policy context: Europe 2020 strategy comprising the three 20% targets.*
- *Wind energy: 33-49% of the EU's electricity demand by 2050*
- ***Key clean alternative*** *to fossil fuels, contributor to **securing the energy supply** and **reducing GHG emissions***
- Benefits from ***promising and evolving RE technology*** and from widespread distribution of resources across MSs

EU Wind power progress

Focus on offshore wind technology:
sector's full development by 2030

- ***Investment costs in offshore*** *wind farms >> onshore facilities; **partly offset by a higher total electricity generation** due to stronger offshore wind intensity*
- ***EU Policy implementation and financial incentives*** *paved the way for recognizing the offshore wind sector's brimming potential*

EU policy and financial support: at the heart of wind energy growth

- ***SET-Plan****: instrumental role in advancing the deployment and roll-out of wind energy technology*

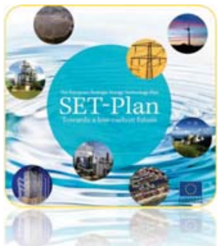

EU contribution *devoted to:*
- ***R&DD:*** *FP7 funding (**€135 million**)*
- ***Demo:*** *European Energy Recovery Programme (**€565 million**), NER300 funding mechanism (**€273.1 million**)*
- ***Commercialisation:*** *IEE, RSFF, loans by EIB and EBRD*
- ***Market diffusion:*** *EIB, EBRD, MS action: feed-in tariffs, portfolios*

External conditions, resource assessment and forecasting for wind energy

NORSEWInD – aug 2008-jul 2012
- **Compiling and analysing LiDAR data resulting in an offshore wind atlas of North, Irish and Baltic Seas – wind mapping for offshore applications**

SAFEWIND – sept 2008- aug 2012
- **Improving wind power predictability - External conditions, resource assessment and forecasting for wind energy**

WINDSCANNER.EU – oct 2012 –sept 2015
- **The European windscanner facility focussed on improving infrastructure and measurement methodologies**

Aerodynamic and structural reliability of wind turbines – wind turbine design

RELIAWIND – march 2008-march 2011

- **Focused on optimising wind energy systems design, operation and maintenance: tools, proof of concepts, guidelines for a new generation**

INNWIND.EU – nov 2012- oct 2017

- **Innovative Wind Conversion Systems (10-20 MW) for Offshore applications – light weight rotor, innovated irect drive generator, and substructure**

AVATAR – nov 2013 –sept 2017

- **AdVanced Aerodynamic Tools for lArge Rotors facilitating the development of large wind turbines (10-20 MW)**

Aerodynamic and structural reliability of wind turbines – wind turbine design

DEEPWIND – okt 2010 –sept 2014

- **Future Deep Sea Wind Turbine technologies – floating wind turbine**

HiPRWind – nov 2010 –oct 2015

- **High Power, high Reliability offshore wind technology – design support structure and mooring system for floating wind turbine**

Development of design tools for offshore wind farm clusters

EERA-DTOC – jan 2012-june 2015

- **Multidisciplinary integrated software tool for an optimised design of individual and clusters of offshore wind farms**

ClusterDesign – dec 2011- may 2016

- **Innovative Wind Conversion Systems (10-20 MW) for Offshore applications – light weight rotor, innovated direct drive generator, and substructure**

Development of offshore multi-purpose RE conversion platforms

ORECCA– march 2010-august 2011

- **Offhshore Renewable Energy Conversion platforms – coordination action – research roadmap for activities in the context of offshore renewable energy**

Marina Platform – jan 2010-june 2014

- **New infrastructures for both offshore wind and ocean energy convertors – design, engineering and economic evaluation of multifunction marine platforms**

TROPOS – feb 2012- jan 2015

- **Modular Multi-use Deep Water Offshore Platform harnessing and servicing mediterranean, subtropical and tropical marine and maritime resources – modular approach including floater concept**

H2Ocean – jan 2012 –dec 2015

- **Wind-wave power open sea platform equipped for hydrogen generation as green energy carrier**

Grid integration

Twenties – april 2010-march 2013

- **Transmission system operation with large penetration of wind and other renewable sources in networks of innovative tools an**

Logistics

LEANWIND – dec 2013–nov 2017

- **Innovative transport and deployment systems for the offshore wind energy sector**

IRPWIND – Start 01/03/2014

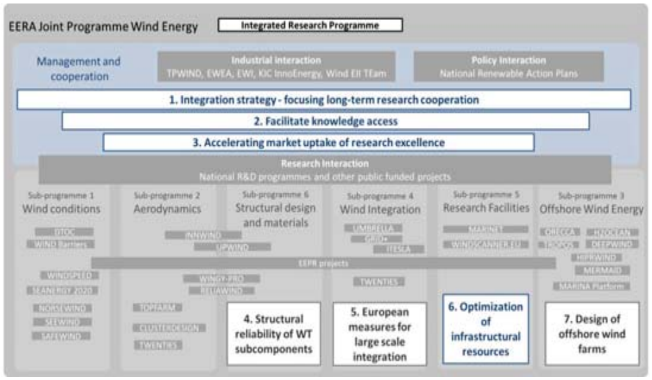

Figure 7- Rationale behind IRPWIND: Identification of gaps within the framework of EERA JP Wind

Implementing actions: Integrated Roadmap

Prioritise the ***development of innovative solutions*** *for the* ***European energy system*** *by 2020, 2030 and beyond*

Challenge-based approach for ***R&I actions*** *to be undertaken in the following* ***6 years****:*

- *holistic perspective on the R&I chain (Actions and Actors)*
- *R&I ⟺ energy policy*
- *expert-based, open and transparent approach*

Integrated Roadmap

Technology & innovation*: key component of EU energy policy and priorities*

I. Energy Efficiency

II. Competitive, efficient, secure, sustainable and flexible energy systems

III. Innovation in real environments, market uptake

IV. Horizontal issues

SETPlan Integrated roadmap – wind challenges

- ✓ *Increase deployment possibilities and repowering process of onshore wind*
- ✓ *Reduce cost, increase reliability and availability of offshore wind*
- ✓ *Mass manufacturing turbines and components*
- ✓ *Infrastructure for offshore wind, dedicated ports*
- ✓ *Enable system integration*
- ✓ *Minimise environmental impact, increase social impact and spatial planning techniques*
- ✓ *Improve wind energy forecasts and understanding conditions*

EWEA report *Deep water – July 2013*

- *Offshore wind is one of the fastest growing sectors*
- *Deep offshore designs are necessary to unlock the promising offshore market potential*
- *The technology is still at very early stage development*
- *Policy, economic and technological recommendations*

Matthijs SOEDE
Research Programme Officer
Unit G3 Renewable Energy Sources
DG Research and Innovation

The Multiannual Financial Framework 2014-2020:

European Council conclusions, 8 February 2013

Key challenge: *stabilise the financial and economic system while taking measures to create economic opportunities*

1. **Smart & inclusive growth (€451 billion)**

Education, Youth, Sport | **Connecting Europe** | **Cohesion** | **Competitive Business SMEs** | **HORIZON 2020**

2. **Sustainable growth, natural resources (€373 billion)**
3. **Security and citizenship (€16 billion)**
4. **Global Europe (€58 billion)**
5. **Administration (€61.6 billion)**

TOTAL €960 billion

What is H2020 and how is it new?

- ***€70.2 billion*** R&I funding programme
- ***A single programme***: brings together 3 separate programmes/initiatives*
- ***Coupling research ⟺ innovation***: from research to retail, all forms of innovation
- ***Focus on societal challenges***: faced by EU society (e.g. health, clean energy)
- ***Simplified access***: for all companies, universities, institutes in the EU & beyond

* The 7th Research Framework Programme (FP7), innovation aspects of Competitiveness and Innovation Framework Programme (CIP), EU contribution to the European Institute of Innovation and Technology (EIT)

Strong focus on SMEs

- **20% of budget**
  - ✓ **from societal challenges and LEITs**
- **New SME instrument**
  - ✓ **> € 500 million in 2014-2015**
- **Support measures under 'Innovation in SMEs'**
- **Access to risk finance**
- **Participation with Member States** (Public-Public) **Eurostars joint programme**

Major Simplification for the benefit of applicants

1. **A single set of rules for all funding under Horizon 2020**
   - ✓ **Fewer, more flexible, funding instruments**
2. **Simpler reimbursement: 1 project = 1 funding rate**
   - ✓ **100% of the total eligible costs** (70% for innovation actions)
   - ✓ **Non-profit legal entities can also receive 100% in innovation actions**
   - ✓ **Single flat rate for indirect costs** (25% of eligible costs)
3. **Faster time to grant**
   - ✓ **Within 8 months of call deadline**

Major Simplification for the benefit of applicants

4. **Fewer, better targeted controls and audits**
5. **Coherent implementation**
   - ✓ **Through dedicated agencies**
   - ✓ **Single IT system**
6. **Simplification in grant agreements**

New approach to Work Programmes and Calls

- **2-year work programmes**
  (2014-2015: > € 15 billion)
- **Less prescriptive calls**
  (64 calls in 2014)
  - ✓ **Challenged-based approach, broader and fewer topics**
  - ✓ **First call deadlines as from March 2014**
- **Cross-cutting actions**
- **Use of *TRLs***

Three priorities

European Commission

Work Programme 2014
Funding for calls

Societal Challenges Pillar: ~ € 2.8 billion

- **Health, demographic change and wellbeing** (2 calls) € 600 million
- **Food Security, Sustainable Agriculture and Forestry, Marine and Maritime and Inland Water Research and the Bioeconomy** (3 calls) € 300 million
- **Secure, clean and efficient energy** (4 calls) € 600 million
- **Smart, green and integrated transport** (3 calls) € 540 million
- **Climate action, environment, resource efficiency and raw materials** (3 calls) € 300 million
- **Europe in a changing world – inclusive, innovative and reflective societies** (5 calls) € 112 million
- **Secure Societies** (4 calls) € 200 million

In addition

- **Spreading Excellence and Widening Participation** (3 calls) € 50 million
- **Science with and for Society** (4 calls) € 45 million

HORIZON 2020

Thematic scope of the Energy Challenge (according to the Horizon 2020 Specific Programme)

- Reducing energy consumption and carbon footprint by smart and sustainable use

New concepts, components and systems for buildings, cities, industry and people

- **Low-cost, low-carbon electricity supply**

Novel RE, efficient and flexible fossil fuel plants & CCS, or CO2 re-use tech

- **Alternative fuels and energy sources for mobility**

Bio-energy, power & heat, all forms of transport, H and fuel cells, new forms

Thematic scope of the Energy Challenge (according to the Horizon 2020 Specific Programme)

- A single, smart European electricity grid

Smart energy grid technologies, storage, systems & market designs for inter-operable networks, standards, emergency

- Market uptake of energy innovation

Applied innovation, standards, non-tech barriers, smart & sustainable use

- **New knowledge and technologies**

Multi-disciplinary research for energy technologies (including visionary actions)

- **Robust decision making & public engagement**

Tools, methods, models and perspectives for a robust and transparent policy support

Four Calls and their indicative budget

1. **Energy efficiency**
2. **Smart cities & communities**
3. **Competitive low-carbon energy**
4. **SME's and Fast Track to Innovation for Energy**

Part B - other actions
-Support to policy development & implementation
-Support to Technology Platforms
-IEA Implementing Agreements
-etc.

Calls	2014 (M€)	2015 (M€)
Energy Efficiency	92	98
Smart Cities and Communities	74	87
Competitive Low-Carbon Energy	359	372
SMEs and Fast Track to Innovation	34	37
Part B – other actions	*77*	*63*

Call LCE: Competitive Low-Carbon Energy

- New knowledge and technologies
- **Renewable electricity and heating/cooling**
- Modernising the single **European electricity grid**
- Flexibility through enhanced **energy storage technologies**
- **Sustainable biofuels and alternative fuels** for the European transport fuel mix
- Enabling the decarbonisation of the use of fossil fuels during the transition to a low-carbon economy
- Supporting the development of a **European Research Area in the field of Energy**
- **Social, environmental and economic aspects of the energy system**
- **Cross-cutting issues**

Call LCE: areas to be addressed

	AREA	TRL	TYPE	Deadline
LCE 1	New knowledge and technologies	2 > 3-4	RIA	01/04/2014 (stage 1) 23/09/2014 (stage 2)
Renewable electricity and heating/cooling				
LCE 2	Developing the next generation technologies of renewable electricity and heating/cooling	3-4 > 4-5	RIA	01/04/2014 (stage 1) 23/09/2014 (stage 2)
LCE 3	Demonstration of renewable electricity and heating/cooling	5-6 > 6-7	IA	10/09/2014
LCE 4	Market uptake of existing and emerging renewable electricity, heating and cooling technologies	7-9	CSA	07/05/2014

Types of Actions

- ***Research and Innovation Actions***

Actions primarily designed to establish new knowledge and/or to explore the feasibility of a new or improved technology, product etc, including testing and validating on a small scale laboratory prototype.

- ***Innovation Actions***

Aimed at producing plans and arrangements or designs for new, altered or improved products, processes or services. May include prototyping, testing, demo, large-scale validation & market replication.

- ***Coordination and Support Activities***

Accompanying measures such as standardisation, dissemination, awareness-raising and communication, networking, policy dialogues, etc.

Technology Readiness Levels

TRL 0: **Idea**. Unproven concept, no testing has been performed.
TRL 1: **Basic research.** Principles postulated and observed but no experimental proof available.
TRL 2: **Technology formulation**. Concept and application have been formulated.
TRL 3: **Applied research**. First laboratory tests completed; proof of concept.
TRL 4: **Small scale prototype** built in a laboratory environment ("ugly" prototype).
TRL 5: **Large scale prototype** tested in intended environment.
TRL 6: **Prototype system** tested in intended environment close to expected performance.
TRL 7: **Demonstration system** operating in operational environment at pre-commercial scale.
TRL 8: **First of a kind commercial system**. Manufacturing issues solved.
TRL 9: **Full commercial application**, technology available for consumers.

Structure of the call topic

- ***Specific Challenge***
- ***Scope***
- ***Expected Impact***
- ***Type of action***

LCE 1 - 2014: New knowledge & technologies

- *Aim: accelerating the development of transformative energy technologies or enabling technologies that have reached **TRL2** ⇨ **TRL 3-4***
- *Activities should also focus on the early identification and clarification of **potential problems to society**, and on the definition of a targeted and quantified **development roadmap***
- ***Novel ideas**: provide impetus to technology pathways and address the energy challenge in Europe & beyond.*

LCE 2: Developing the next generation techn of renewable electricity & heating/cooling

2014 Wind energy:
Develop control strategies and innovative substructure concepts

- *Control strategies and systems for new and/or **large rotors and wind farms** (on- and offshore);*
- ***New innovative substructure concepts**, incl. floating platforms, to reduce production, installation and O&M costs for water depths of more than 50m.*

2015 Wind energy:
Substantially reduce the costs of wind energy

- *There is a need for **innovative integrated dedicated offshore systems** (e.g. with a significant lower mass per unit power installed) to reduce production, installation and O&M costs for water depths of more than 50m.*

LCE 2: Developing the next generation techn of renewable electricity & heating/cooling

Scope

- *From TRL 3-4 to 4-5*
- *Life-cycle perspective*
- *Environment, health and safety issues shall be considered*
- *Increased understanding of risks in each area*
- *Increased performance and reduced costs*
- *Manufacturing Readiness Levels*
- *Indication EU contribution 3-6 million Euro*

LCE 2: Developing the next generation techn of renewable electricity & heating / cooling

Expected impacts of proposals

- *Significantly increased technology performance*
- *Reducing life-cycle impact*
- *Improving EU energy security*
- *More predictable and grid friendly*
- *Strengthening European technology base*
- *Reducing renewable energy technologies installation time and costs*
- *Increasing reliability an lifetime*
- *……see work programme*

LCE 3: Demo of renewable electricity & heating / cooling technologies

2014 Wind energy:

Demonstrating and testing of new nacelle and rotor prototypes

- *Demonstration and testing of* ***new nacelle and rotor prototypes*** *with a significant lower mass and material intensity and applicable to several types of* ***large-scale wind turbines****.*

2015 Wind energy:

Demonstrating innovative substructure and floating concepts

- *Demonstration of* ***innovative bottom-fixed substructure*** *concepts for water depths of 30 to 50m capable of reducing costs;*
- *Demonstration of innovative* ***floating wind turbine*** *concepts.*

LCE 4: Market uptake of existing and emerging renewable electricity, heating & cooling techn

CSA: *focus on best practices and quantified indicators of the market impacts of future policy*

- *Ensuring sustained* ***public acceptance*** *of RE projects;*
- *Speedy and user friendly* ***permitting procedures****;*
- *Implementing* ***RE policies****, codes and legislations at EU, national, regional and local levels in a* ***coordinated way****;*
- ***Capacity building*** *and further development of policy;*
- *Deployment of improved* ***business models*** *and innovative* ***financing schemes***

First H2020 calls
12 focus areas

Some examples:

- ✓ **Personalising health and care**
  (€ 549 million)
- ✓ **Blue growth: unlocking the potential of seas and oceans**
  (€ 100 million)
- ✓ **Overcoming the crisis: new ideas and strategies to overcome the crisis in Europe**
  (€ 35 million)

HORIZON 2020

European Commission

WP in the area of Food security, sustainable agriculture and forestry, marine and maritime and inland water research and the bioeconomy

BG-5-2014: *Call for Blue Growth: Unlocking the potential of Seas and Oceans*

Budget: *€2,000,000*

DDL: ***2014-06-26*** *+17:00:00 (BXL)*

Topic: Preparing for the future innovative offshore economy (CSA)

This should include a review of marine renewable energy farms (both **wind and ocean energy**), offshore aquaculture facilities, multi-use offshore platforms projects and their business models, as well as issues of competing access to marine space between different activities and, more broadly, all social & env. impacts

Other parts of H2020 of direct relevance to Energy

- LEIT – KET materials, nano, electronics, manufacturing, processing
- FET-open and FET-pro-active
- Research Infrastructures
- ERC, EIT
- SME instrument (directly paid from Energy SC budget)
- JRC direct actions (IET, IPTS)

Close links – societal challenges

Thank you for your attention!

More information:
www.ec.europa/research/horizon2020

Innovations in Offshore Wind through R&D

John Olav Giæver Tande
Director NOWITECH
Senior Scientist
SINTEF Energy Research
John.tande@sintef.no

NOWITECH in brief

- A joint pre-competitive research effort
- Focus on deep offshore wind technology (+30 m)
- Budget (2009-2017) EUR 40 millions
- Co-financed by the Research Council of Norway, industry and research partners
- 25 PhD/post doc grants
- Key target: innovations reducing cost of energy from offshore wind
- Vision:
  - large scale deployment
  - internationally leading

A large growing global market for offshore wind

- Battle climate change
- Security of supply
- Industry value creation

Stern Review (2006): ..strong, early action on climate change far outweigh the costs of not acting.

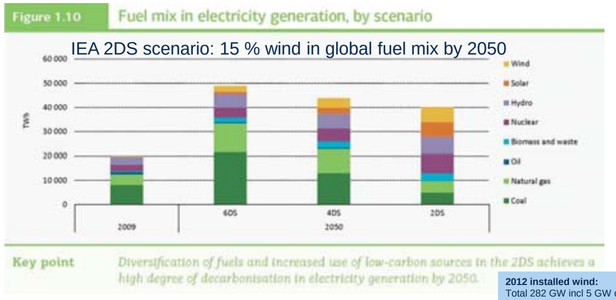

Copy from IEA Energy Technology Perspectives 2012

2012 installed wind:
Total 282 GW incl 5 GW offshore
2050 2DS wind:
6000 TWh/3000 h = 2000 GW
Required annual installations to reach 2DS goal for wind:
2000 GW / 40 y = 50 GW/y
+ end of lifetime replacements

Main challenge: Reduce Cost of Energy

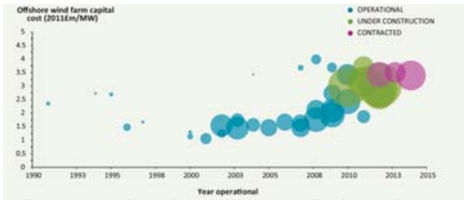

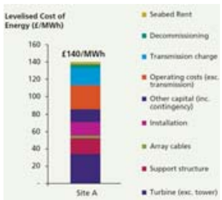

Graphics from: The Crown Estate (2012) Offshore wind cost reduction pathways study

From R&D to innovations to cost reductions

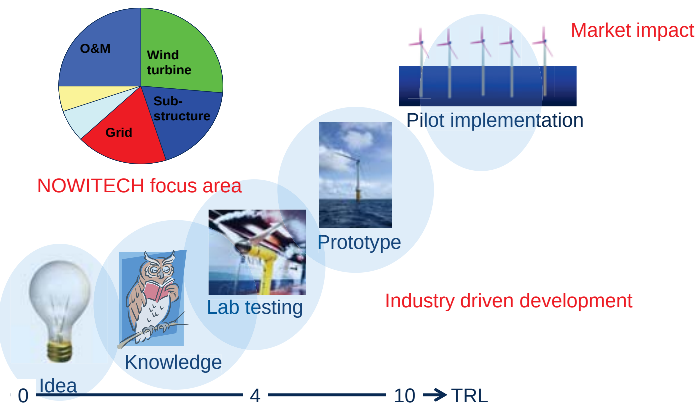

Reducing uncertainties by better models

- Integrated models simulate the behavior of the complete turbine with substructure in the marine environment: SIMO-RIFLEX (MARINTEK) and 3DFloat (IFE)
- Model capability includes bottom fixed and floating concepts
- Code to code comparison in IEA Wind OC3 and OC4
- Model to measurements comparison in progress

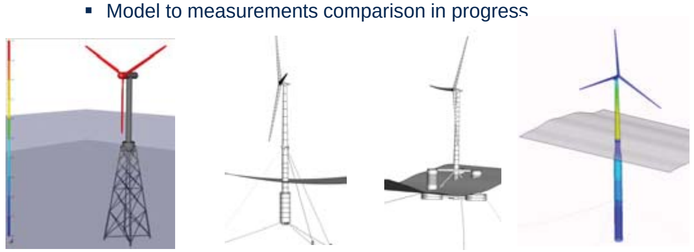

Cost savings by optimising spar buoy design

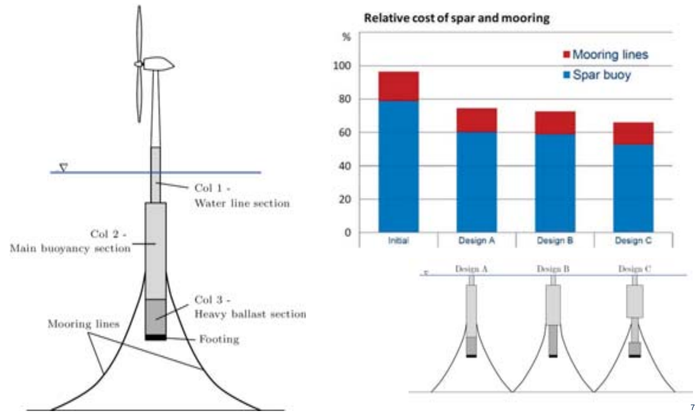

Integrating structural dynamics, control and electric model

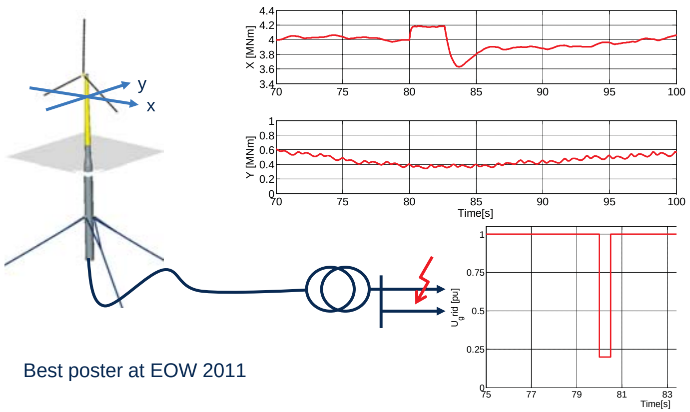

Best poster at EOW 2011

NOWITECH Norwegian Research Centre for Offshore Wind Technology

HVDC generator avoiding need for large sub-station

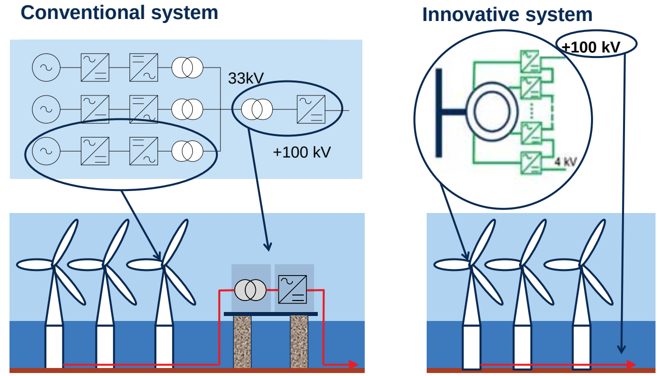

NOWITECH Norwegian Research Centre for Offshore Wind Technology

Lab-scale implementation of multi-terminal HVDC grid connecting offshore wind farm

VSC-HVDC model:
In-house built laboratory VSC converters with FPGA-control

R&D topics:

- Operation and control
- Converter interoperability
- System stability
- Fault handling
- System services

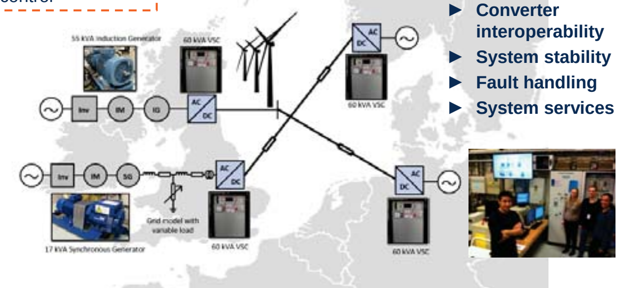

NOWITECH Norwegian Research Centre for Offshore Wind Technology

Optimization of the offshore grid

- Inside and between wind farms
- New market solutions are required
- New technology (HVDC VSC, multi-terminal, hybrid HVDC/HVAC, ..)
- Protection, Fault handling, Operation, Control, Cost, Security of Supply

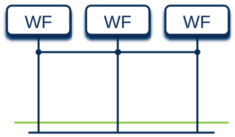

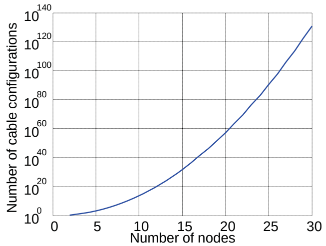

NOWITECH Norwegian Research Centre for Offshore Wind Technology

O&M and logistics cost analysis

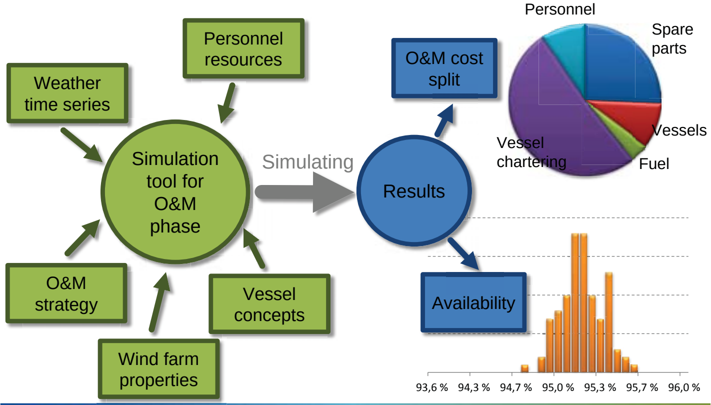

NOWITECH Norwegian Research Centre for Offshore Wind Technology

Coatings for offshore wind turbine blades - Protection against rain droplet

Investigation by
- Erosion testing
- Material characterization
- Numerical modelling

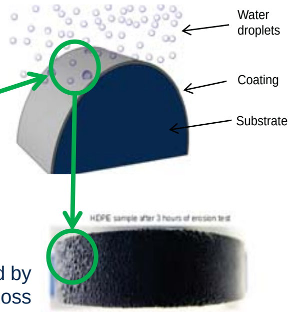

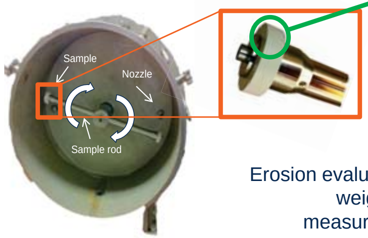

Erosion evaluated by weight loss measurements

Remote presence reduce O&M costs

- It is costly and sometimes impossible to have maintenance staff visiting offshore turbines
- Remote presence:
  - Remote inspection through a small robot on a track in the nacelle equipped with camera / heat sensitive, various probes, microphone etc.
  - Remote maintenance through robotized maintenance actions

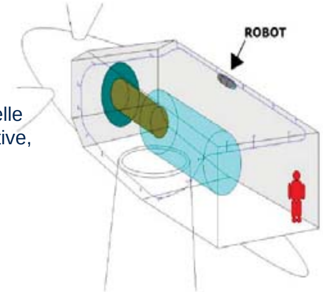

NOWITECH 10 MW reference turbine

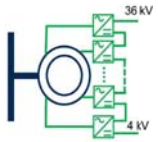

Initial design parameters
- Nominal power output 10.0 MW
- Design wind velocity 13.0 m/s
- Tip speed ratio 7.7
- Hub height 93.5 m
- Turbine diameter 141.0 m
- Design water depth 60.0 m
- Wind & waves ala Doggerbank
- **(work in progress!)**

Best poster at EOW 2013

The NOWITECH 10 MW reference turbine introduces a new generator and support structure concept

SEAWATCH Wind Lidar Buoy

- Cost efficient and flexible compared to offshore met mast
- Measure wind profiles (300 m), wave height and direction, ocean current profiles, met-ocean parameters
- Result of NOWITECH "spin-off" joint industry project by Fugro OCEANOR with Norwegian universities, research institutes and Statoil.

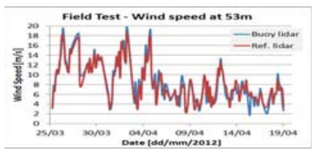

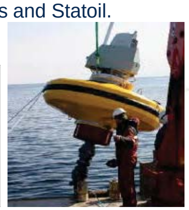

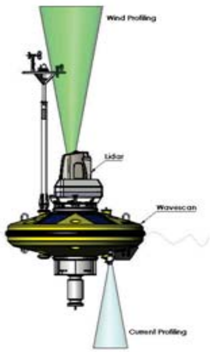

Relevant labs on campus

Wind tunnel 11x3x2 m

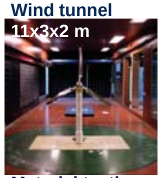

Material testing

SmartGrids lab

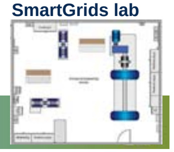

Strong field facilities for R&D in development

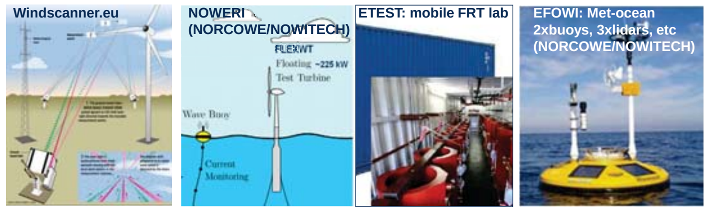

Recruitment and education

- 25 PhD and post doc students are granted by NOWITECH to be finished in 2014-2015
- Some +30 PhD students are funded through other projects and some hundred MSc have specialized within wind energy
- The Erasmus Mundus European Wind Energy Master (EWEM) programme gives further weight to the wind education at NTNU and NOWITECH

NOWITECH achievements

- **NOWITECH is about education, competence building and innovations reducing cost of energy from offshore wind**
- Significant budget and duration: EUR 40 millions (2009-2017)
- Strong consortium with leading research and industry parties
- Excellent master and PhD programme: 25 PhD & post doc grants
- Strong scientific results: good number of peer-reviewed publications
- R&D results give value creation and cost reductions
- Innovation process is enhanced through TRL
- Two new business developments (Remote Presence + SiC coatings)
- Strong infrastructure in development: NOWERI, WindScanner, ++
- A high number of spin-off projects: total volume EUR 125 millions
- **Vision: large scale deployment & internationally leading**

NORCOWE at a glance

We build future industry competence through instrumentation, education and research

- Part of the Research Council of Norway's scheme: Centres of Environment-friendly Energy Research
- Budget of 232 MNOK (29 MEUR; 38 MUSD) for 2009-2017
- Pre-competitive and industry driven research

Partners

R&D partners:

- Christian Michelsen Research
- Uni Research
- University of Agder
- University of Bergen
- University of Stavanger
- Aalborg University (DK)

User partners:

- Statkraft
- Statoil
- Acona Flow Technology
- Meteorologisk institutt (met.no)
- StormGeo
- Leosphere

Memorandum of Understanding

- DTU Wind
- Fraunhofer IWES
- The National Renewable Energy Lab (NREL)
- ECN (the Netherlands)
- Arena NOW

Collaborations in Europa, USA, Australia, South-Africa, China and Japan

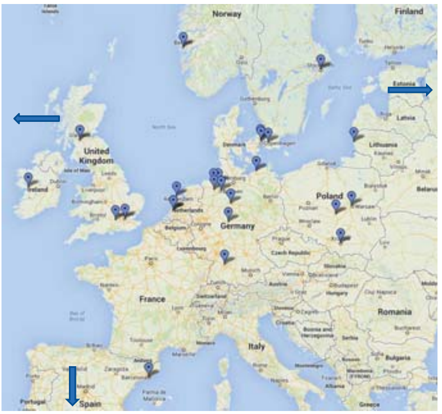

Measurement campaigns

atmosphere – wind turbine / farm interaction

$$P_{out} = \frac{1}{2} C_p A \rho v^3$$

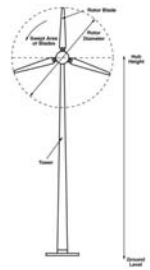

extraction of energy from the mean flow:

- ❑ conversion into mechanical/electrical power (including WT losses)
- ❑ conversion into turbulence kinetic energy (TKE)

the flow behind one (several) turbines is therefore characterized by:

- ❑ reduced average wind speed
- ❑ increased turbulence level

both factors affect the performance of the turbines behind negatively:

- ❑ reduced power output
- ❑ increased load and fatigue

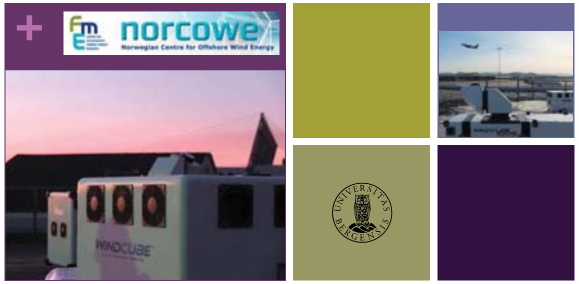

LIMECS -
LiDAR measurement campaign Sola

Valerie Kumer, Jochen Reuder, Birgitte Furevik

Campaign Sola

- 2 Windcubes v1 and a scanning Windcube 100S were located at two sites in Sola from March 2013 to July 2013

Campaign Sola

- Site 1: Airport Stavanger Sola

Campaign Sola

- Site 2 : automatic radiosonde launcher met.no

Intentions and Aims

- Test campaign:
  - Evaluations of the performance of the WindCube 100S, through comparisons among different data sets (Raso,WLSv1,Metsation)
  - Comparison of rawinsonde and LiDAR wind measurements between 40 and 3000 m (cooperation with met.no)
  - Wind vector retrievals
- Development and setup of appropriate and reliable scanning patterns
- Validation of fine scale Numerical Models (cooperation with met.no)
- Investigation of land-sea boundary layer transitions

WINTWEX-W campaign November 2013-April 2014

Meeting NORCOWE – Mitsubishi Electronics
Bergen, 14. November 2013

ECN/NORCOWE LiDAR campaign

- October 2013 - April 2014
- 2 nacelle mounted LiDARs
- 5 LiDARs in the field
  - 1 scanning
- SUMO flights in April

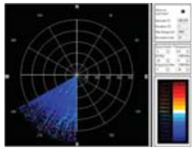



WINTWEX-W campaign November 2013-April 2014

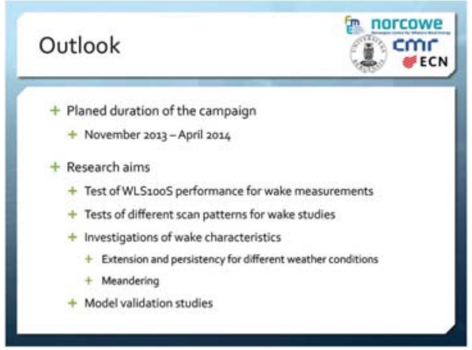
Outlook

- Planed duration of the campaign
  - November 2013 – April 2014
- Research aims
  - Test of WLS100S performance for wake measurements
  - Tests of different scan patterns for wake studies
  - Investigations of wake characteristics
    - Extension and persistency for different weather conditions
    - Meandering
  - Model validation studies

Offshore measurement campaign

- @ North Sea wind farm
- 2014-2015

- Offshore wake propagation
- Boundary layer characterisation
- Power performance
- Structural loading

Lidar needs for offshore campaigns

Nacelle
- Forward looking lidar

Transition piece
- Scanning lidars


Floating (buoy / ship-based)
- Motion compensated lidar


Wind farm layout with model reduction techniques (MRT)

Chad Jarvis and Yngve Heggelund, CMR
chad@cmr.no

Wakes

- Wakes reduce the power production of downstream turbines.
- To find the layout which maximizes power production, it is important to accurately estimate the effect of wakes.

Model reduction based on CFD

- Reduction of the solution space, while keeping the most important degrees of freedom
- The solutions space is constructed from a set of steady state CFD simulations of the RANS equations
- The solution time is reduced from the order of hours to seconds

Results so far

Six turbines

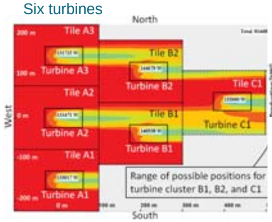

Solution of the x-component of the flow field (m/s) at hub-height for the optimal position of turbine cluster B1, B2, and C1.

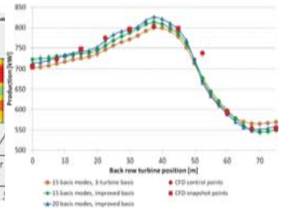

Production estimates for the wind farm for different positions of the three downstream turbines. The value 0 m refers to a center position directly behind turbine A2, and 75 m refers the uppermost position.

Results so far (cont.)

Ten turbines in a row with a distance of 5 rotor diameters

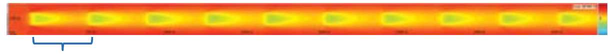

5 rotor diameters

Using the first N turbines of a CFD simulation of ten turbines to construct a basis, which is then used to compute the production in the reduced space.

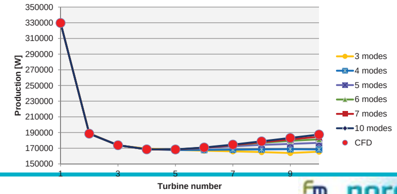

The power production of each turbine. The basis constructed from the first 3 turbines of the CFD simulation is labeled 3 modes etc.

Future plans

- Arbitrary interactive movement of turbines in a wind farm on a grid of empty background tiles

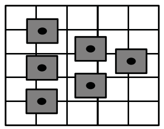

Turbine Tile Empty Tile

- Continued verification with CFD on larger realistic wind farm cases, and for more wind conditions

O&M AND LOGISTICS FOR OFFSHORE WIND TURBINE PARKS

PhD student Ole-Erik Endrerud
Prof. Jayantha P. Liyanage

Centre for Industrial Asset Management
University of Stavanger

norcowe Norwegian Centre for Offshore Wind Energy

Operational infrastructure (OI)

24

The basic physical and organizational structures and facilities

norcowe Norwegian Centre for Offshore Wind Energy

Work management system (WMS)

25

The system of processes used to plan, execute and control industrial assets.

norcowe
Norwegian Centre for Offshore Wind Energy

Purpose

26

Present a maintenance and logistics model of a large-scale wind turbine park in order to investigate how different maintenance strategies and logistics support will affect availability and life-cycle costs.

This model can be a decision tool when designing and optimizing maintenance strategies, operational infrastructure and work management systems.

norcowe
Norwegian Centre for Offshore Wind Energy

UiS O&M Wind Simulation Model

- Created model of Wash-area and vessel market.
- Investigate vessel charter contracts and maintenance management of operating several parks.
- Failure model made more realistic with wind turbine sub-systems instead of failure categories.

UiS O&M Wind Simulation Model

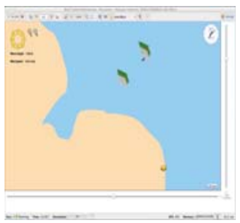

- Investigating possibility for developing wind park development tool for the industry based on this model.

The potential of remotely piloted aircraft systems (RPAS) for wind energy related measurements

Prof. Joachim Reuder
Geophysical Institute, University of Bergen
joachim.reuder@gfi.uib.no

NORCOWE – Arena NOW
Offshore Wind Operations/Science Meets Industry
10. September 2013, Bergen

UNIVERSITETET I BERGEN
Geofysisk institutt

NORCOWE
Norwegian Centre for Offshore Wind Energy

RPAS – some (semi) operational systems

J. Reuder, Geophysical Institute, University of Bergen
Offshore Wind Operations/Science Meets Industry
Bergen, 13. September 2013

NORCOWE

SUMO – turbulence sensor

miniaturized 5-hole probe from Aeroprobe Inc., USA (3 mm diameter)

differential pressure measurements (static-dynamic, left right, up-down)

provides flow velocity and angles of sideslip and attack with 100 Hz resolution

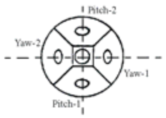

Spin-off Projects

Spin-off project: wave and LiDAR

- LiDAR on Stuart platform
- Controlled wave motion
- Fugro OCEANOR
- Buoy mounted LiDAR

Spin-off project: Gwind

- Floating vertical axis wind turbine
- Gyros used for dampening
- Prototype in Stavanger harbour
- Managed by TTO office Prekubator

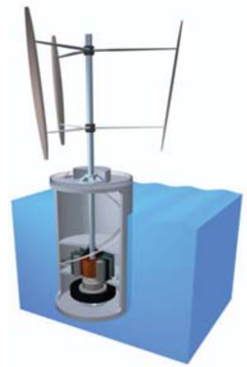

Spin-off project: decision support for installation of offshore wind

- Funding: RCN and Statoil
- Partners: Uni Research, Met.no, Aalborg University, MARINTEK, University of Bergen and Christian Michelsen Research
- Develop methods for decision support based on physical limitations of equipment
- Incorporate uncertainty
- Manage the weather window

Key conferences/activities 2014

- Science Meets Industry, Stavanger: April 2
- Work Package meetings: May 6-7 at UiA (Grimstad)
- PhD Summer School: August 11-15 at Stand Hotel Fevik
- OWO/Science Meets Industry, Bergen: September 9
- NORCOWE day, Bergen: September 10

www.norcowe.no


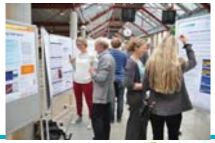


NORCOWE summer school 2014

Innovative methods and concepts in offshore wind energy

- August 11-15 at Strand Hotel Fevik, Aust Agder
- Focus on
  - New methods in analysis and measurements
  - Next generation and new concepts within wind energy
  - Impact of innovation on offshore technology
  - Group work
- Open also for industry employees and non-NORCOWE PhD students

Contact us!

www.norcowe.no
post@norcowe.no


EERA Design Tool for Offshore wind farm Cluster (DTOC)

PETER HAUGE MADSEN. Director
Charlotte Hasager. Senior scientist
DTU Wind Energy

DTOC
THE EUROPEAN ENERGY RESEARCH ALLIANCE
DESIGN TOOLS FOR OFFSHORE WIND FARM CLUSTER

Support by

Project partners

- DTU Wind Energy (former Risø)
- Fraunhofer IWES
- CENER
- ECN
- EWEA
- SINTEF
- ForWind
- CRES
- CIEMAT
- University of Porto
- University of Strathclyde
- Indiana University
- CLS
- Statkraft
- Iberdrola Renovables
- Statoil
- Overspeed
- BARD
- Hexicon
- Carbon Trust
- E.On
- RES

EERA partners

- DTU Wind Energy (former Risø)
- Fraunhofer IWES
- CENER
- ECN
- EWEA
- SINTEF
- ForWind
- CRES
- CIEMAT
- University of Porto
- University of Strathclyde
- Indiana University
- CLS
- Statkraft
- Iberdrola Renovables
- Statoil
- Overspeed
- BARD
- Hexicon
- Carbon Trust
- E.On
- RES

"Design Tool for Offshore wind farm Clusters" is the first EERA project. EERA is based on national science activities.

EERA – European Energy Research Alliance

Background: The EERA JP Wind Energy was officially launched at the SET-Plan conference in Madrid in June 2010. The strategy and main activities of the JP is described in the "Strategic Action Plan" (yearly updated).

The programme vision is:
- to provide strategic leadership for the scientific–technical medium to long term research
- to support the European Wind Initiative and the Technology Roadmap's activities on wind energy, and on basis of this
- to initiate, coordinate and perform the necessary scientific research.

Joint Programme and Sub-programmes
Wind Conditions. Coordinated by Prof. Erik Lundtang Petersen, DTU Wind Energy (DK)
Aerodynamics. Coordinated by Dr. Peter Eecen, ECN (NL)
Offshore Wind Energy. Coordinated by Dr. John O. Tande, SINTEF (NO)
Grid Integration. Coordinated by Dr. Kurt Rohrig, FhG IWES (DE)
Research Facilities. Coordinated by Dr. Pablo Ayesa Pascual, CENER (ES)
Structural design and materials. Coordinated by Dr. Denja Lekou, CRES (GR)

EERA DTOC funding from EC FP7

Topic ENERGY.2011.2.3-2:
Development of design tools for Offshore Wind farm clusters

Open in call: *FP7-ENERGY-2011-1*
Funding scheme: Collaborative project

- EERA DTOC is 3.5 years: January 2012 to June 2015
- Budget is 4 m€ hereof 2,9 m€ from EC
- Parallel project is ClusterDesign coordinated by 3E

FP7: Expected impact

- To contribute to the SET-Plan on the development of offshore wind power.
- To demonstrate the capability of designing virtual wind power plants composed of wind farms and wind farm clusters while minimizing the negative spatial interactions, improving the overall power quality output and providing confidence in energy yield predictions.

ENERGY.2011.2.3-2: Call objective

The objective of this topic is to develop new **design tools** to optimise the exploitation of individual wind farms as well as wind farm clusters, in view of transforming them into virtual power plants.

Such design tools should integrate:

- Spatial modelling: medium (within wind farms) to long distance (between wind farms) **wake effects**
- **Interconnection optimisation**: to satisfy grid connection requirements and provide power plant system service.
- **Precise energy yield** prediction: to ease investment decisions based on accurate simulations

The project should focus on offshore wind power systems and **make optimal use of previously developed models**.

ENERGY.2011.2.3-2: Call objective

EERA DTOC Work Packages (WP)

The objective of this topic is to develop new **design tools** to optimise the exploitation of individual wind farms as well as wind farm clusters, in view of transforming them into virtual power plants.

Such design tools should integrate:

- Spatial modelling: medium (within wind farms) to long distance (between wind farms) **wake effects**
- **Interconnection optimisation**: to satisfy grid connection requirements and provide power plant system service.
- **Precise energy yield** prediction: to ease investment decisions based on accurate simulations

The project should focus on offshore wind power systems and **make optimal use of previously developed models**.

WP1 wake

WP2 grid

WP3 yield

WP4 tool and WP5 demo

WP structure

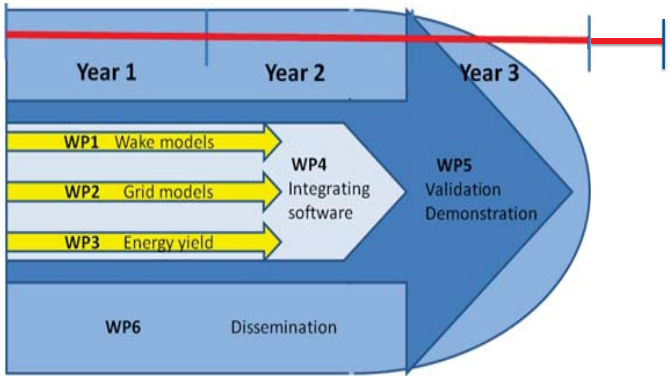

EERA DTOC concept

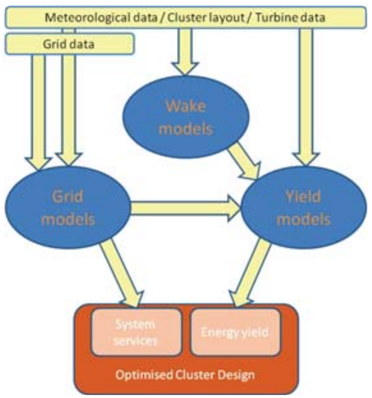

EERA DTOC main components

- Use and bring together existing models from the partners
- Develop open interfaces between them
- Implement a shell to integrate
- Fine-tune the wake models using dedicated measurements
- Validate final tool

EERA DTOC portfolio of models

Name	Partner	Status	Programs	Input/ output	Script/ GUI	Database interface	IPR	Com
CFDWake	CENER		Fluent, C++, OpenFOAM	ASCII	script	Yes		
CorWind	Risoe DTU	Ope	DOS exe Delphi	CSV files	no	no	+	+
CRES-farm	CRES	Ope	Linux/ Fortran77	ASCII	no	no	+	
CRES--flowNS	CRES	Ope	Linux/ Fortran77	ASCII	no	no		
DWM	Risoe DTU	Ope	Fortran, pc, pc-cluster	ASCII	script		+	
ECNS	ECN	Beta	Linux/ Fortran90	ASCII	No	No	+	
EeFarm	ECN	Alpha	Matlab	Matlab scripts	Script/ GUI	yes	+	+
Farm-farm interaction	ECN	Ope	Fortran	ASCII	No	no	+	
FarmFlow	ECN	Ope	Delphi	ASCII/ binary	GUI	Yes	+	+
FlowARSM	CRES	Alpha	Linux/ Fortran77	ASCII	no	no		
FUGA	Risoe DTU	Ope	Fortran, C, Delphi, pc	ASCII	Script/ GUI	No	+	
NET-OP	SINTEF	Proto type	Matlab	ASCII	script	No	+	
Skiron/WAM	CENER	Ope	Unix/ Fortran	GRIB	script	yes		
TOPFARM	Risoe DTU	Beta	Matlab/C/ Fortran	ASCII	script		+	
UAEP	Risoe DTU		Matlab, pc	ASCII/ binary	no	yes		
VENTOS	UPorto	Beta	Unix/ Fortran	ASCII	no	yes	+	+
WAsP	Risoe DTU	Ope	Windows pc	ASCII	Script/ GUI	No	+	+
WCMS	Fraunhofer	Ope	Matlab/JAVA	OracleDB		yes	+	
WRF	Risoe DTU	Ope	Unix, Linux, Fortran90	netCDF	Shell script	yes		
WRF/ROMS	CIEMAT	Ope	Linux/ Fortran	netCDF	script	yes	+	

12

EERA DTOC portfolio of models

Name	Partner	Status	Programs	Input/ output	Script/ GUI	Database interface	IPR	Com
CFDWake	CENER		Fluent, C++, OpenFOAM	ASCII	script	Yes		
CorWind	Risoe DTU	Ope	DOS exe Delphi	CSV files	no	no	+	+
CRES-farm	CRES	Ope	Linux/ Fortran77	ASCII	no	no	+	
CRES--flowNS	CRES	Ope	Linux/ Fortran77	ASCII	no	no		
DWM	Risoe DTU	Ope	Fortran, pc, pc-cluster	ASCII	script		+	
ECNS	ECN	Beta	Linux/ Fortran90	ASCII	No	No	+	
EeFarm	ECN	Alpha	Matlab	Matl[illegible]	Script/ [illegible]	yes	+	+
Farm-farm interaction	ECN	Ope	Fortran	[illegible]	[illegible]	[illegible]	+	
FarmFlow	ECN	Ope	Delp[illegible]	[illegible]	[illegible]	[illegible]	+	+
FlowARSM	CRES	Alpha	Linux/ F[illegible]	[illegible]	[illegible]	[illegible]		
FUGA	Risoe DTU	Ope	Fortran, C, [illegible] pc	[illegible]	[illegible]	[illegible]	+	
NET-OP	SINTEF	Proto type	Matlab	ASCII	script	No	+	
Skiron/WAM	CENER	Ope	Unix/ Fortran	GRIB	script	yes		
TOPFARM	Risoe DTU	Beta	Matlab/C/ Fortran	ASCII	script		+	
UAEP	Risoe DTU		Matlab, pc	ASCII/ binary	no	yes		
VENTOS	UPorto	Beta	Unix/ Fortran	ASCII	no	yes	+	+
WAsP	Risoe DTU	Ope	Windows pc	ASCII	Script/ GUI	No	+	+
WCMS	Fraunhofer	Ope	Matlab/JAVA	OracleDB		yes	+	
WRF	Risoe DTU	Ope	Unix, Linux, Fortran90	netCDF	Shell script	yes		
WRF/ROMS	CIEMAT	Ope	Linux/ Fortran	netCDF	script	yes	+	

Run on Windows, on a single PC

EERA DTOC portfolio of models

Name	Partner	Status	Programs	Input/ output	Script/ GUI	Database interface	IPR	Com
CFDWake	CENER		Fluent, C++, OpenFOAM	ASCII	script	Yes		
CorWind	Risø DTU	Ope	DOS exe Delphi	CSV files	no	no	+	+
CRES-farm	CRES	Ope	Linux/ Fortran77	ASCII	no	no	+	
CRES--flowNS	CRES	Ope	Linux/ Fortran77	ASCII	no	no		
DWM	Risø DTU	Ope	Fortran, pc, pc-cluster	ASCII	script		+	
ECNS	ECN	Beta	Linux/ Fortran90	ASCII	No	No	+	
EeFarm	ECN	Alpha	Matlab	Matlab	Script/ [illegible]	yes	+	+
Farm-farm interaction	ECN	Ope	Fortran	[illegible]	[illegible]	[illegible]	+	
FarmFlow	ECN	Ope	Delphi	[illegible]	[illegible]	[illegible]	+	+
FlowARSM	CRES	Alpha	Linux/ F[illegible]	[illegible]	[illegible]	[illegible]		
FUGA	Risø DTU	Ope	Fortran, C, D[illegible] pc	[illegible]	[illegible]	[illegible]	+	
NET-OP	SINTEF	Proto type	Matlab	ASCII	script	No	+	
Skiron/WAM	CENER	Ope	Unix/ Fortran	GRIB	script	yes		
TOPFARM	Risø DTU	Beta	Matlab/C/ Fortran	ASCII	script		+	
UAEP	Risø DTU		Matlab, pc	ASCII/ binary	no	yes		
VENTOS	UPorto	Beta	Unix/ Fortran	ASCII	no	yes	+	+
WAsP	Risø DTU	Ope	Windows pc	ASCII	Script/ GUI	No	+	+
WCMS	Fraunhofer	Ope	Matlab/JAVA	OracleDB		yes	+	
WRF	Risø DTU	Ope	Unix, Linux, Fortran90	netCDF	Shell script	yes		
WRF/ROMS	CIEMAT	Ope	Linux/ Fortran	netCDF	script	yes	+	

Runs on Cluster under UNIX/Linux

User Requirements

Users

Design and model selection guided by end-users

Two **main user groups** were identified:

- Strategic planners
- Developers of offshore wind farms

Associated users could be:

- Consultants
- Research institutions
- Manufacturers
- System Operators

Selected user stories

- As a developer I can determine the wake effects of neighbouring wind farm clusters on a single wind farm.
- As a developer I can determine the optimum spacing, position, turbine model and hub height of turbines within an offshore wind farm.
- As a strategic planner I can determine the optimum strategic infrastructure to accommodate offshore wind farm clusters.
- *14 relevant user stories in total*

Optimisation process

- As a developer I can **determine the optimum** spacing, position, turbine model and hub height of turbines within an offshore wind farm.

*Software supports the **comparison** of many design scenarios.*

***Comparative** reporting enables selection of optimised configurations.*

Score for comparison: Levelised Cost of Energy

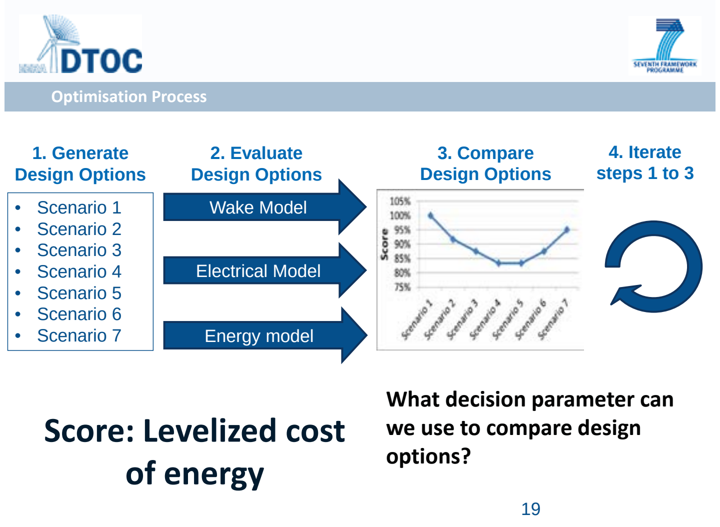
DTOC
Optimisation Process
1. Generate Design Options
2. Evaluate Design Options
3. Compare Design Options
4. Iterate steps 1 to 3
Scenario 1
Scenario 2
Scenario 3
Scenario 4
Scenario 5
Scenario 6
Scenario 7
Wake Model
Electrical Model
Energy model
Score
105%
100%
95%
90%
85%
80%
75%
Scenario 1
Scenario 2
Scenario 3
Scenario 4
Scenario 5
Scenario 6
Scenario 7
Score: Levelized cost of energy
What decision parameter can we use to compare design options?
19

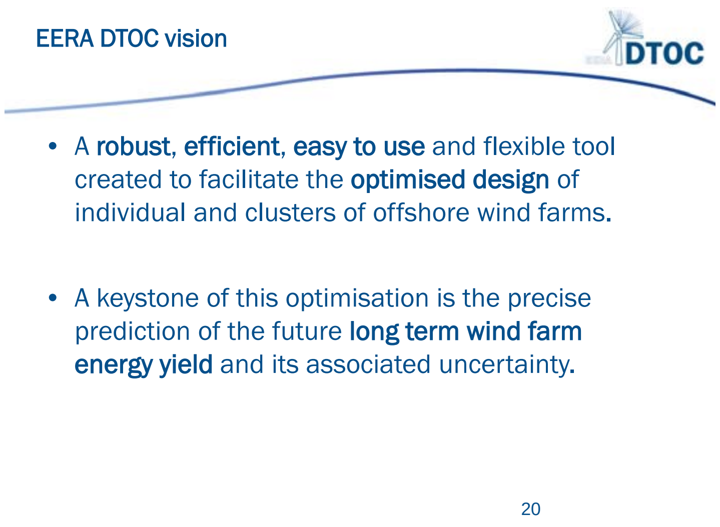
EERA DTOC vision
DTOC
A robust, efficient, easy to use and flexible tool created to facilitate the optimised design of individual and clusters of offshore wind farms.
A keystone of this optimisation is the precise prediction of the future long term wind farm energy yield and its associated uncertainty.
20

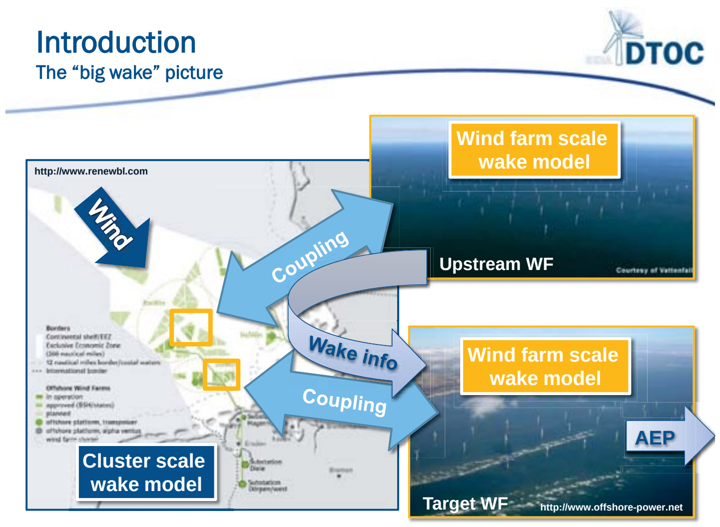
Introduction
The “big wake” picture
DTOC
http://www.renewbl.com
Wind
Coupling
Wind farm scale wake model
Upstream WF
Wake info
Coupling
Wind farm scale wake model
AEP
Cluster scale wake model
Target WF
http://www.offshore-power.net

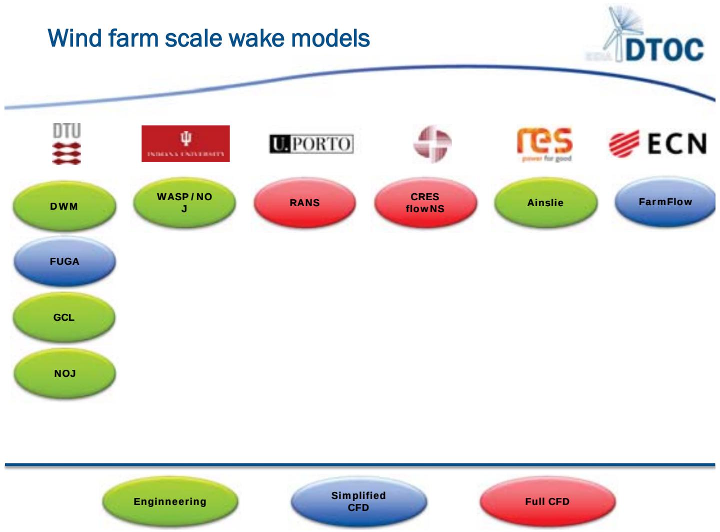
Wind farm scale wake models
DTOC
DTU
UPORTO
res
ECN
DWM
WASP / NOJ
RANS
CRES flowNS
Ainslie
FarmFlow
FUGA
GCL
NOJ
Engineering
Simplified CFD
Full CFD

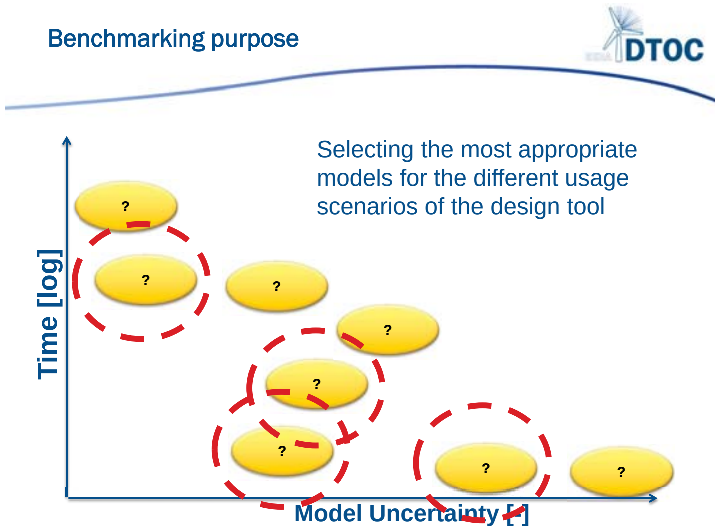
Benchmarking purpose
DTOC
Selecting the most appropriate models for the different usage scenarios of the design tool
Time [log]
Model Uncertainty [-]

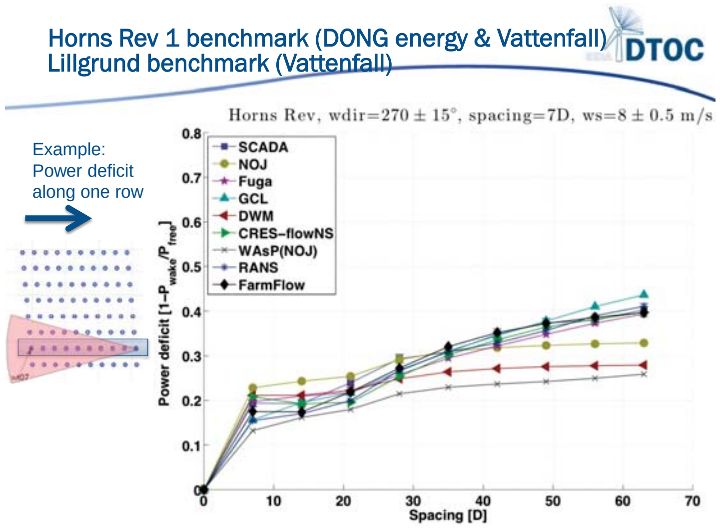
Horns Rev 1 benchmark (DONG energy & Vattenfall)
Lillgrund benchmark (Vattenfall)
DTOC
Example:
Power deficit along one row
Horns Rev, wdir=270 ± 15°, spacing=7D, ws=8 ± 0.5 m/s
SCADA
NOJ
Fuga
GCL
DWM
CRES–flowNS
WAsP(NOJ)
RANS
FarmFlow
Power deficit [1–P_wake/P_free]
Spacing [D]
0
0.1
0.2
0.3
0.4
0.5
0.6
0.7
0.8
10
20
30
40
50
60
70

Gross energy : FINO-1 test case (BMU)

- Wind speed and direction data (10 minutes)
  From 13/01/2005 to 30/06/2012 (total of 7.5 years data)
  (Generic power curve (1.225 kg/m³))

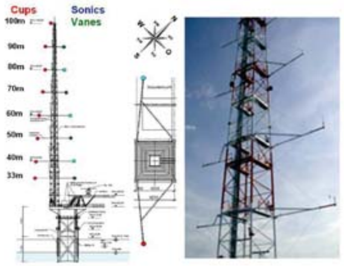

Gross energy – output parameter checks

- Mean wind sped (before filtering)
- Mean wind speed (after filtering)
- Long term mean wind speed, free decision
- Vertical extrapolation between 100m and 120m
- Gross energy P50
- Gross energy P90

Gross energy P90

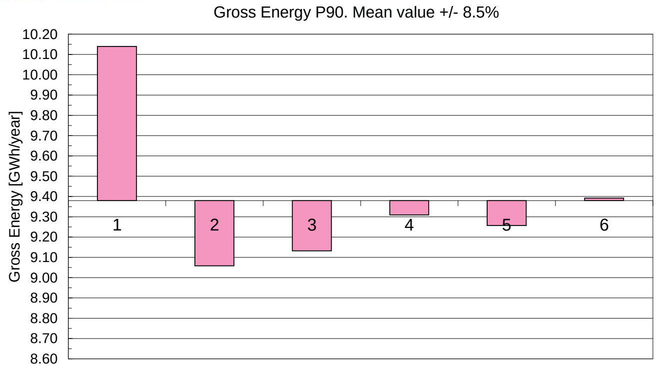

O&M losses

- Offshore Wind Farm
  - o Inputs
    - o Turbine layout and turbine model
    - o Site wave climate
    - o Location of O&M base (from 10 to 150 km)
    - o O&M strategy
  - o SWARM software

Wave Climate Scenario	Description	Mean Wind Speed at 100m [m/s]	% of Time Above Hs Limit	
			1.5 meters	2.0 meters
1	Benign Climate	9.0	16.5%	6.3%
2	Moderate Climate	9.4	21.0%	7.4%
3	Severe Climate	9.5	28.3%	12.6%

Scenario	Number of Workboats	Number of Helicopters	Wave Hs Limit for Boats [m]
1	5	0	1.5
2	5	0	2.0
3	5	2	2.0

Aims of grid layout optimization

- Design tool and procedure assisting the optimization of the electrical design;
- Clustering;
- Grid code compliance;
- Power plant ancillary services;

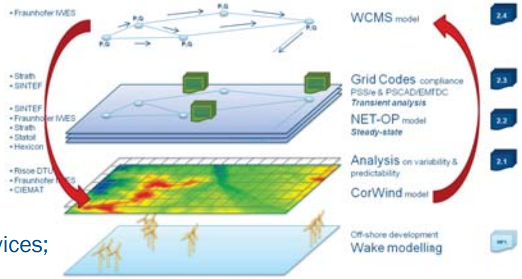

- Evaluate impact of the variability and the predictability.

Methodology

1. Determine the models chain, interactions, I/O;
2. Establish the data flow/ data gaps according to the user cases;
3. Procedure to fill overcome gaps was investigated:
   1. Automatic electrical data generation
   2. User intervention providing accurate data.
   3. Implementation of a new module
4. Dry runs (based on scenarios)
5. Assessment/ convenience evaluation

Kriegers Flak case study

#	Country	Wind farm	Capacity
1	DK	Kriegers Flak A K2	200
2	DK	Kriegers Flak A K3	200
3	DK	Kriegers Flak A K4	200
4	DK	Kriegers Flak B K1	200
5	DE	EnBW Baltic 2	288
6	DE	EnBW Baltic 1	48
7	DE	Baltic Power	500
8	DE	Wikinger	400
9	DE	Arkona Becken Südost	480
10	SE	Kriegers Flak	640

Branch type	max distance	max power
AC	65 km	700 MW
DC-direct		1000 MW
DC-mesh		1000 MW
converter		1000 MW

Kriegers Flak case study results

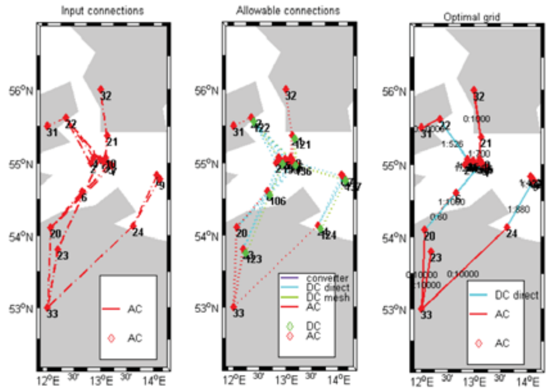

Expected achievements

- Checking planned grid:
  - Fulfillment of full load flows → calculate component utilization factors.
  - Fulfillment of certain average load flows situations.
  - Checking congestions and voltages.
  - Control power:
    - Power reserve
    - Balancing power
  - Voltage control
  - Enabling market/ transport

Model workflow energy yield (WP3)

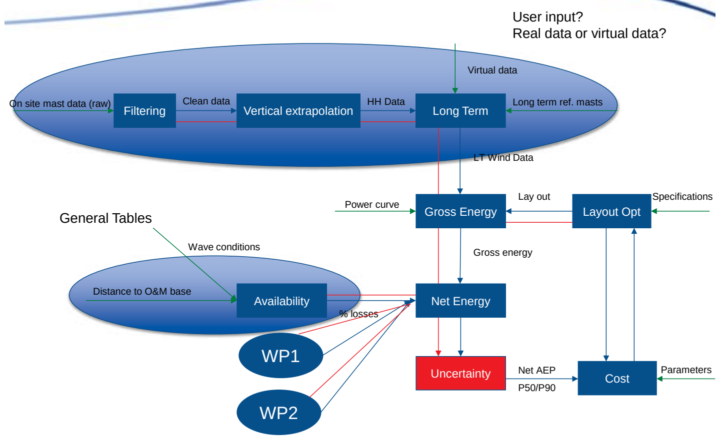

Model workflow wake (WP1)

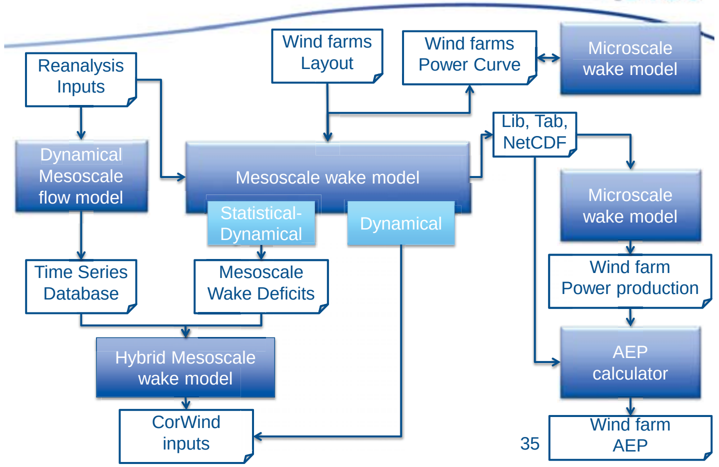

Model workflow "Electrical" (WP2)

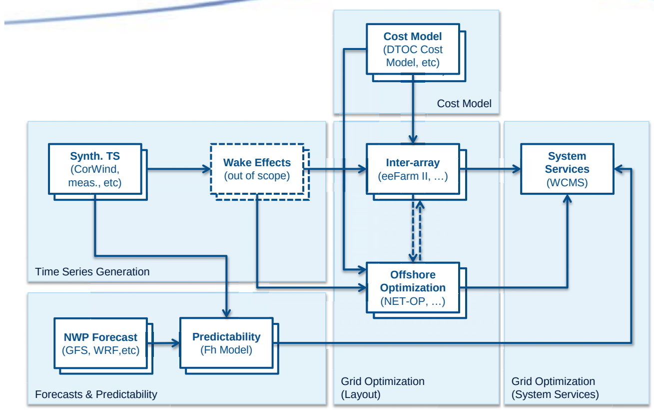

Total tool overview – very complex!

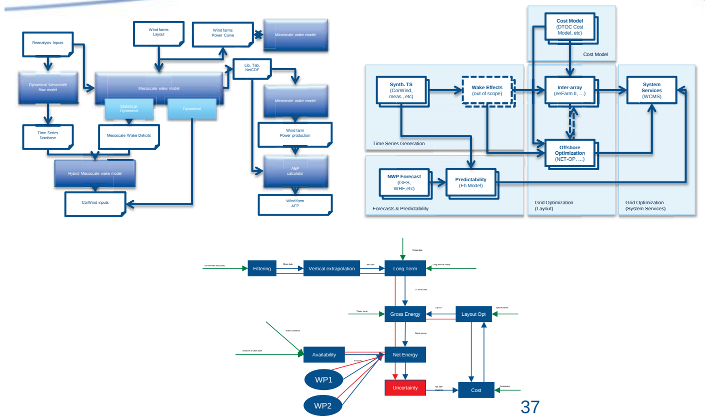

37

Open interfaces

- The sub-models are protected by IPR…
- …but the interfaces in the model chain are going to be open
- File formats for data exchange are based on existing industry standard formats, e.g. the WAsP types based on XML and ESRI shape file standard

38

DTOC software development timeline

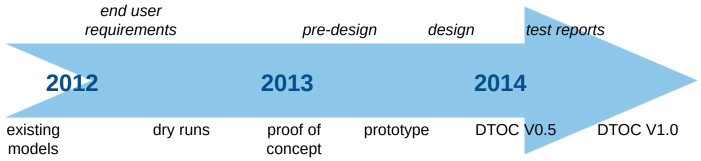

39

Validation and demonstration

29-1-2014
40

Rødsand 2 data (E.On)

10 minute statistical data from meteorological mast and Rødsand 2 turbines
(No data from neighbouring Nysted farm)

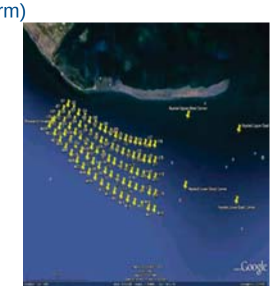

SAR satellite images (CLS, DTU)

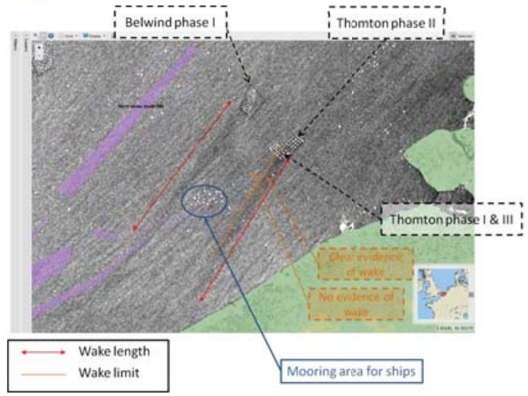

INNWIND.EU

INNWIND.EU
OVER VIEW OF PROJECT and RECENT RESULTS

Peter Hjuler Jensen
Anand Natarajan
DTU Wind Energy

Background for the project

- The UpWind project completed in Feb 2011 produced many results on the technologies required for the next generation 10-20MW wind turbine.
- The UpWind project examined conventional 3 bladed upwind turbines.
- Moving deeper offshore, the need is to design and manufacture large wind turbines that are specifically designed to operate in deeper, farther offshore sites.
- This project INNWIND.EU will use the results from UpWind, but will go beyond the three bladed conventional wind turbine to conceptualize, Prioritize and put forth to the market the best innovations for offshore wind turbines.

Question 2008: Will upscaling continue?

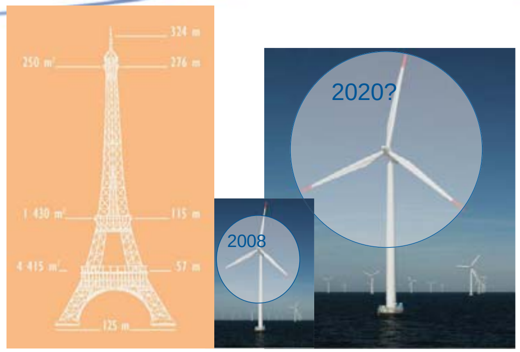

UpWind organisation
Integrated project

with 15 technical and scientific work packages

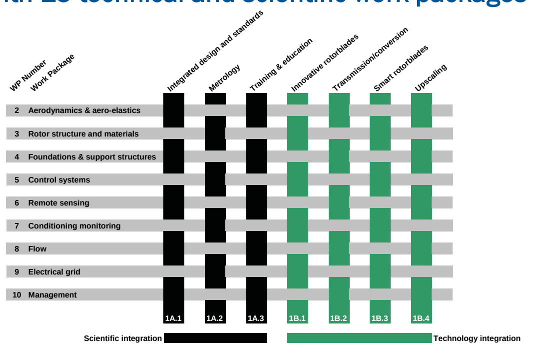

Upwind participants

- **39 participants**

- 11 EU countries
- 10 research institutes
- 11 universities
- 7 turbine & component manufacturers
- 6 consultants & suppliers
- 2 wind farm developers
- 2 standardization bureaus
- 1 branch organisation

UpWind:
Overall result from cost functions

Up scaling – levelised cost

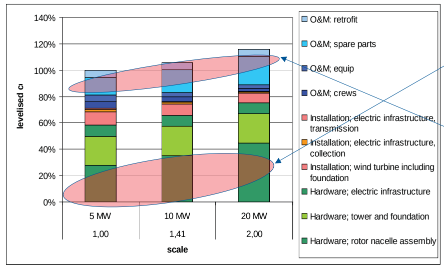

- Levelised cost *increases* with scale
- Reasons:
  - Rotor and nacelle costs scale ~s^3 (?)
  - Spare parts costs follow
- Cost of energy over lifetime increase more than 20 % for increasing the Wind Turbine size from 5 to 20 MW so the power law for the rotor

Economical viability of 20MW W/Ts
Case study: Blades

		PAST						FUTURE		
		GI-P HLU	GI-P RI	GI-Ep RI	GI-Ep Prep	GI-C Hybrid 1	GI-C Hybrid 2	New Tech 1	New Tech 2	New Tech 3
	Single Step r(t)/r(t-1)	1,00	0,59	0,79	0,93	0,86	0,87	0,93	0,93	0,93
	Cummulative r(t)	1,00	0,59	0,47	0,44	0,38	0,33	0,31	0,28	0,26
	Single Step a(t)/a(t-1)	1,00	1,08	1,08	1,10	1,10	1,00	1,03	1,03	1,03
	Cummulative a(t)/a(t0)	1,00	1,08	1,17	1,28	1,41	1,41	1,45	1,50	1,54
WT Power (MW)	Rotor Radius (m)	Mass (tn)	Mass (tn)	Mass (tn)	Mass (tn)	Mass (tn)	Mass (tn)	Mass (tn)	Mass (tn)	Mass (tn)
0,125	10	0,25	0,15	0,12	0,11	0,09	0,08	0,08	0,07	0,07
0,281	15	0,85	0,50	0,40	0,37	0,32	0,28	0,26	0,24	0,22
0,500	20	2,00	1,19	0,94	0,88	0,76	0,66	0,61	0,57	0,53
0,781	25	3,91	2,33	1,84	1,71	1,48	1,28	1,19	1,11	1,03
1,125	30	6,76	4,02	3,17	2,96	2,55	2,22	2,06	1,92	1,78
1,531	35	10,74	6,39	5,04	4,70	4,05	3,52	3,28	3,05	2,83
2,000	**40**	**16,02**	**9,53**	**7,52**	**7,01**	**6,04**	**5,26**	4,89	4,55	4,23
2,531	**45**	**22,82**	**13,57**	**10,71**	**9,99**	**8,60**	**7,49**	6,96	6,48	6,02
3,125	**50**	**31,30**	**18,62**	**14,70**	**13,70**	**11,80**	**10,27**	9,55	8,88	8,26
3,781	**55**	**41,66**	**24,78**	**19,56**	**18,23**	**15,71**	**13,67**	12,71	11,82	11,00
4,500	**60**	**54,08**	**32,17**	**25,40**	**23,67**	**20,39**	**17,75**	16,51	15,35	14,28
5,281	**65**	**68,76**	**40,90**	**32,29**	**30,09**	**25,93**	**22,57**	20,99	19,52	18,15
6,125	70		51,09	40,33	37,58	32,38	28,19	26,21	24,38	22,67
7,031	75		62,84	49,60	46,23	39,83	34,67	32,24	29,98	27,89
8,000	80		76,26	60,20	56,10	48,34	42,07	39,13	36,39	33,84
9,031	85			72,20	67,29	57,98	50,47	46,93	43,65	40,59
10,125	90				79,88	68,82	59,91	55,71	51,81	48,19
11,281	95				93,95	80,94	70,45	65,52	60,94	56,67
12,500	100					94,40	82,18	76,42	71,07	66,10
13,781	105					109,29	95,13	88,47	82,28	76,52
15,125	110					125,65	109,38	101,72	94,60	87,98
16,531	115						124,98	116,23	108,09	100,53
18,000	120						142,00	132,06	122,81	114,22
19,531	125						160,50	149,26	138,81	129,10
21,125	130						180,54	167,90	156,15	145,22

Warsaw, April 21, 2010

Overall UpWind results:
Case study: Blades – technology evolution with size

Innovations drive cost down in the past

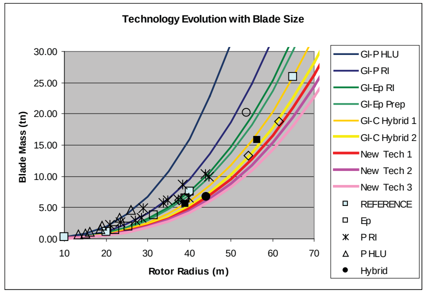

INNWIND.EU

an EERA project

EERA Project - procedure

- Overall project description
- Coordinator and core group
- Call for expression of interest to all EERA members
- Expression of interest send to core group
- Core group makes project proposal
- Project proposal approved by EERA Wind management

Key Objectives

1. Beat the cubic law of weight (and cost) of classical up scaling and render a 10-20 MW offshore design cost-effective.
2. Develop innovative turbine concepts, performance indicators and design targets and assess the performance of components and integrated conceptual designs.
3. Development of new modeling tools capable of analyzing 20MW innovative turbine systems.
4. Integrate the design, manufacturing, installation, operation and decommissioning of support structure and rotor-nacelle assembly in order to optimize the structure and life-cycle as a whole.
5. Establish effective communications channels in the co-ordination of all project activities between the partners and dissemination of the knowledge gained.

Proposal Time line 2013

First core group meeting	Jan 24th
Preliminary budget and partner template	Jan 26th
Confirmation from all partners and feedback with deliverables	Feb 07th
Final decision on partners	Feb 10th
First draft of stage 2 proposal	Feb 16th
First meeting with all partners	Feb 21st
Meet with EU consortium Rep	Feb 24th
Second budget revision	Feb 28th
Second draft of proposal	March 5th
Second core group meeting	March 07th
Partners comments on second draft	March 20th
Final budget and proposal	April 01st

Guidelines for the Proposal development

- A core group decides in co-ordi**nation with all partners the details of the work packages.**
- **The underlying theme** of the proposal is innovation in design.
- There is no requirement for demonstration of an innovation.
- Entities that wish to demonstrate a component or sub component should do so at their own expense.
- Each partner will commit to deliverables that can be tracked on a yearly basis. It is possible for a deliverable to be shared amongst partners.
- The proposal process must be transparent to all partners.

INNWIND.EU Project Overview and Consortium

- Innwind.eu started 1. October 2013 – long negotiation period
- 5 year project, 19.6M€ overall budget
- 27 Participating organizations
- 7 Leading wind energy industries, 19 leading Universities/Research organizations, 1 trade institution
- Main Objectives:
  - a light weight rotor having a combination of adaptive characteristics from passive built-in geometrical and structural couplings and active distributed smart sensing and control
  - an innovative, low-weight, direct drive generator
  - a standard mass-produced integrated tower and substructure that simplifies and unifies turbine structural dynamic characteristics at different water depths

Structure of the Project

Innovative large offshore wind turbine design

1. **Component level innovations** integrated into the wind turbine, virtually tested and further developed.
2. Demonstrations of Innovations include **super conducting generators, pseudo magnetic drives and smart blades**.

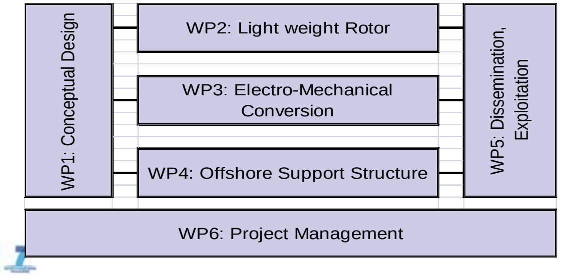

Work Package Overview WG1

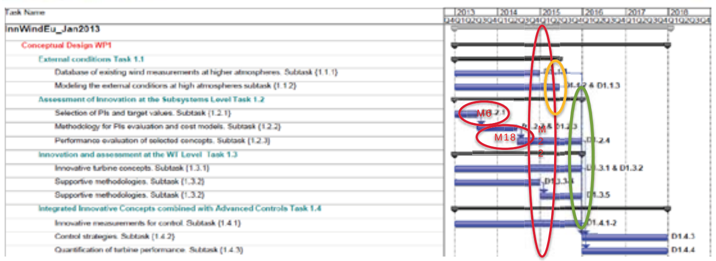

WP1	In Total	Partners														PMs
		AAU	CENER	CRES	DHI	DTU	ECN	FhG	GL-GH	GL-RS	NTUA	OLD	SWE	TUD	UoS	
		18	11,5	29	11	39	15,5	8	15	6	13,5	26	8	42,5	22	265

INNWIND Reference Wind Turbine

- The INNWIND Reference wind turbine is a 10MW turbine designed at DTU mounted on a jacket structure designed by Rambøll at 50m water depth.
- 3 Bladed Up wind, Medium speed drive, variable speed pitch controlled turbine

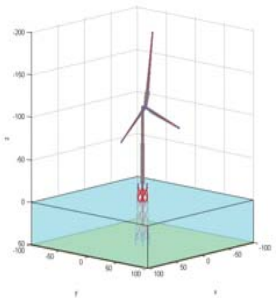

Reference Turbine Parameters

Rated Power [MW]	10
Number of blades [-]	3
Rotor Diameter [m]	178,33
Hub Height from m.s.l. [m]	119
Blade Length [m]	86,36
Rated Wind Speed [m/s]	11,5
Design Extreme Thrust Value [kN]	4600
Minimum Rotor Speed [RPM]	6
Rated Rotor Speed [RPM]	9,6
Optimal TSR [-]	7,5
Gear Ratio [-]	50
Blade Mass [tons]	41.7
Hub Mass [tons]	105.5
Nacelle mass [tons]	446
Tower mass [tons]	628.4
Tower Top Mass, RNA [tons]	676.7
Water depth (mean sea level - m.s.l.) [m]	50
Access Platform a.m.s.l. [m]	25
Jacket Mass [Tons]	720
Transition piece mass [Tons]	400

WP 1.3 - Innovation & Assessment at WT level

Subtask 1.3.1. Innovative turbine concepts e.g.
- ✓ Designs aimed at a low (reduced) tower top mass, e.g.
  - ➢ Lowered bedplate mass
  - ➢ Two bladed down wind machines
  - ➢ Lowered rated wind speeds
- ✓ Turbines with innovative rotors, e.g.
  - ➢ 2- bladed
  - ➢ High rotor speed (to reduce torque in the drive train)
- ✓ More than 3 bladed (braced) rotors
- ✓ Multi rotor concepts on single support structure.

Subtask 1.3.2. Supportive methodologies will be developed like:
- ✓ methodology for support structure design assessment and WT integration (in close cooperation with WP 4, a preliminary design process based on parameterized support structure models will be implemented) and
- ✓ a methodology and tool for integrated system reliability analysis of mechanical, electrical and structural components for innovative wind turbine systems.

New Innovations in the First Year

Kingpin Drive – Superconducting Generator in front of the rotor

Gurney Flap

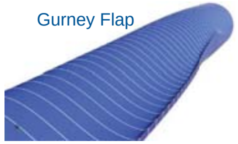

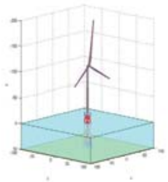

Three Legged Jackets

Work Package Overview

Summary of first year objectives of WG 2:

- To investigate new aerodynamic rotor concepts and
- To benchmark the aerodynamic, aeroelastic and structural design tools that will be used in the project by the different partners for the evaluation of the innovative designs.
- The preliminary investigation of the influence of increased Reynolds number and compressibility effects

Summary of first year achievements

- High tip speed low induction rotors
- Targets for dedicated airfoil families
- Downwind rotor concept, tower wake influence, compressibility- and high Reynolds number effects
- Comparison of the 3 bladed 10MW reference rotor to two-bladed

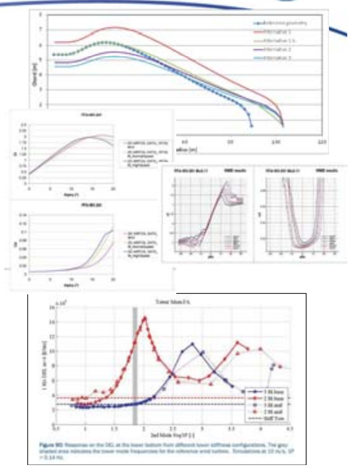

Summary of first year achievements WG 2

- Structural benchmark, stiffness, strength and buckling.
- 2D and 3D Aerodynamic benchmarking.
- Aero-elastic benchmarking

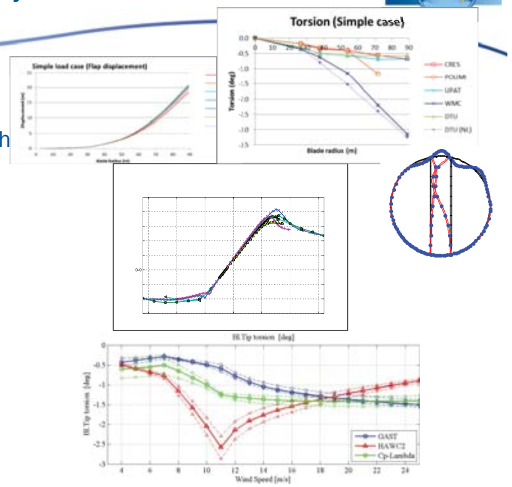

Work Package 3 Objectives

- Investigate innovative wind turbine generator systems (SC and PDD) that have the potential to beat the cubic scaling law
- PI for 10 and 20 MW reference turbine for SC and PDD compared to PMDD
- PI:
  - Size, mass, cost
  - Efficiency
  - Energy yield using Weibul distribution
  - Cost of energy

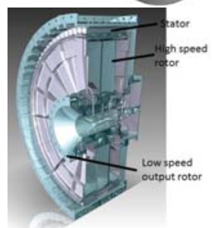

Tasks & Partners

- **3.1. Superconducting Direct Drive (DTU)**
  1. SCDD models (DTU, TUD)
  2. Industrial demonstration of pole pair: 2G YBCO (Siemens, DTU)
  3. MgB_2 coil demonstration (SINTEF, DTU)
- **3.2. Magnetic Pseudo Direct Drive (Magnomatics)**
  1. Analytical model and optimization of PDD (Sheffield)
  2. Industrial demonstration of PDD (Magnomatics)
- **3.3. Power electronics (AAU)**
  1. PE tailored to SCDD & PDD (AAU, Hanover & StrathClyde)
  2. New components and designs (Hanover, Strathclyde & AAU)
- **3.4. Mechanical integration in nacelle (TUD)**
  1. Nacelle design (Garrad Hassan)
  2. Assessment of SCDD & PDD (TUD)
  3. Mechanical support of SC coils (TUD)

First year objectives and achievements (D3.42)

- Superconducting Generators
  - Overview of performance indicators
  - Model of MgB2 and YBCO
  - Definition of demonstrators (MgB2 coil + YBCO pole pair)
- Pseudo Direct Drive
  - Overview of performance indicators
  - Analytical optimization methods
  - Definition of industrial demonstrator
- Power Electronics
  - Overview of converters suitable for SC and PDD
  - Initial performance indicators (efficiency, THD)
- Mechanical integration
  - Nacelle concept defined

Integrated Design of Super Conducting Generator

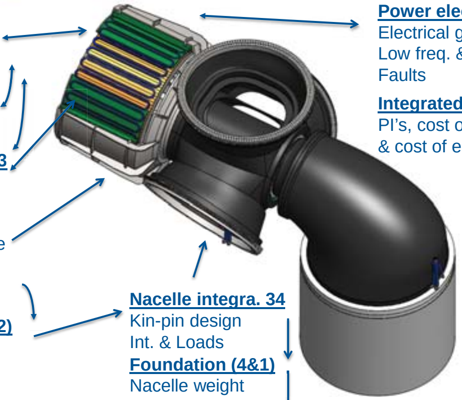

Direct drive trains

10 MW superconducting (DTU)

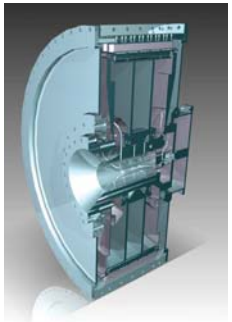

Pseudo direct drive (Magnomatics)

INNWIND LEAFLET www.innwind.eu

WG 4 TECHNOLOGY ROADMAP
BOTTOM-MOUNTED SUPPORT STRUCTURES

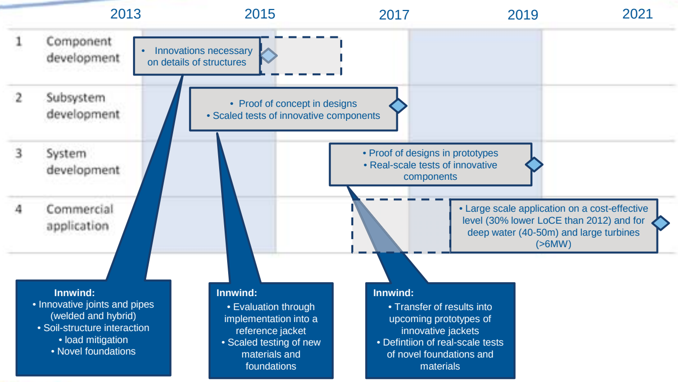

WG 2 TECHNOLOGY ROADMAP
FLOATING SUPPORT STRUCTURES

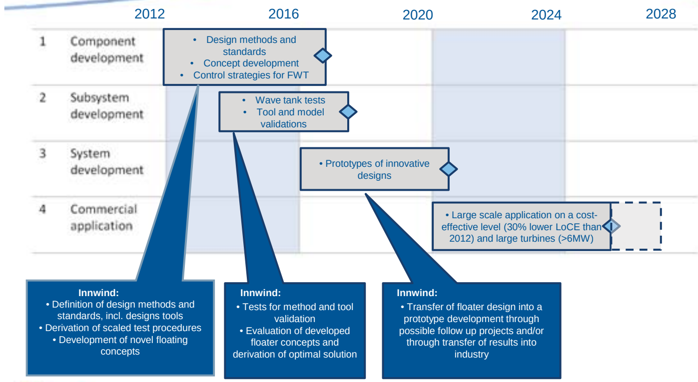

First Project Leaflet

Project Website

- http://www.innwind.eu

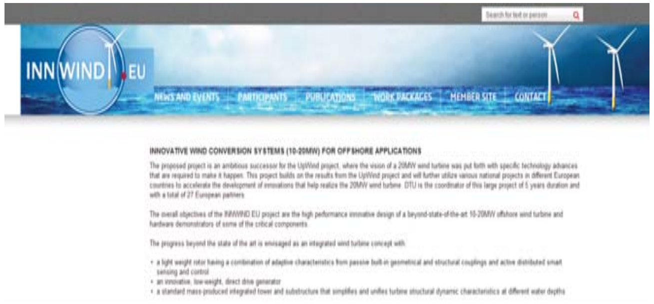

Lidar measurements (ForWind & Fraunhofer IWES)

- Long range wind scanner measurements from fixed positions
- Ship based LIDAR measurements

- EERA DTOC partners requested
- Alpha Ventus SCADA data

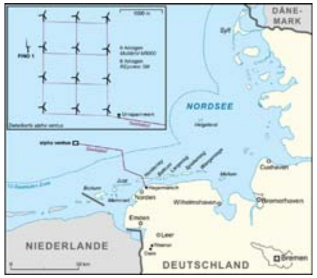

Scenarios

Industry partners are very important!

Iberdrola, Statoil, Carbon Trust, Hexicon, Statkraft, E.On, RES

Purpose of the scenarios

- The tool should fullfill the previously defined user requirements:
  - The tool should be useful, easy to use, complete and robust
- Functionality of all modules in EERA DTOC should be proven → All parts of the tool should be activated during the scenarios
- Inventory of user experiences:
  - How steep is the learning curve?
  - Which tutorials should be added ?
- The results should LOOK realistic from an expert point of view

EERA DTOC web www.eera-dtoc.eu

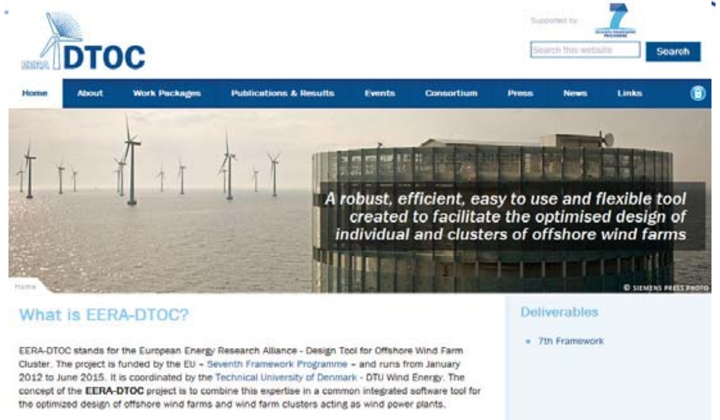

Thank you very much for your attention

Support by

SEVENTH FRAMEWORK PROGRAMME

EERA DTOC project
FP7-ENERGY-2011-1/ n°282797

A1) New turbine and generator technology

New generator technology for offshore wind turbines, prof Robert Nilssen, NTNU

Necessity is the mother of invention: nacelle mounted lidar for measurement of turbine performance, Matt Smith, Zephir Lidar Ltd.

New rotor concepts for future offshore wind farms, O. Ceyhan ECN

Multi Rotor Systems of 20 MW or more for deep water applications, Peter Jamieson, Strathclyde University

1

New Generator Technology for offshore wind turbins

Presented by : Professor Rober Nilssen (NTNU)

Deepwind 2014

2

Totally five types of generators are used in offshore wind farms

- Doubly-Fed induction Generator (DFG),
- Squirrel-Cage induction Generator (SCG),
- Wound-Rotor induction Generator (WRG),
- Permanent Magnet synchronous Generator (PMG)
- Electrically-Excited synchronous Generator (EEG)

3

Gear /generator/converter concepts

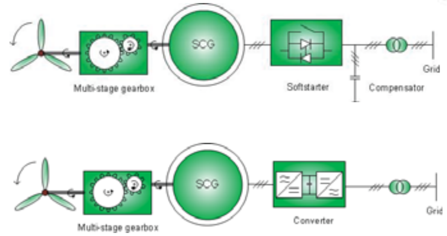

4

Gear /generator/converter concepts

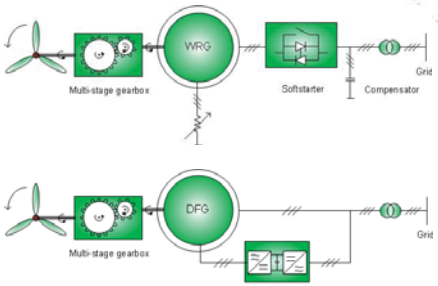

5

Gear /generator/converter concepts

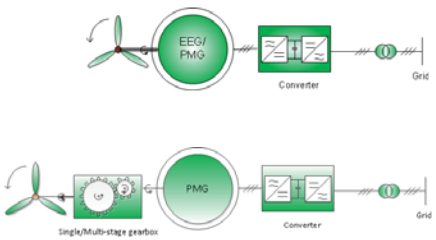

6

Gear /generator/converter concepts

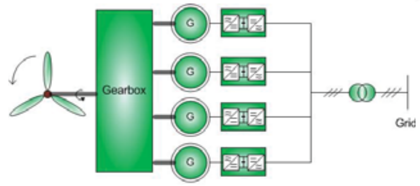

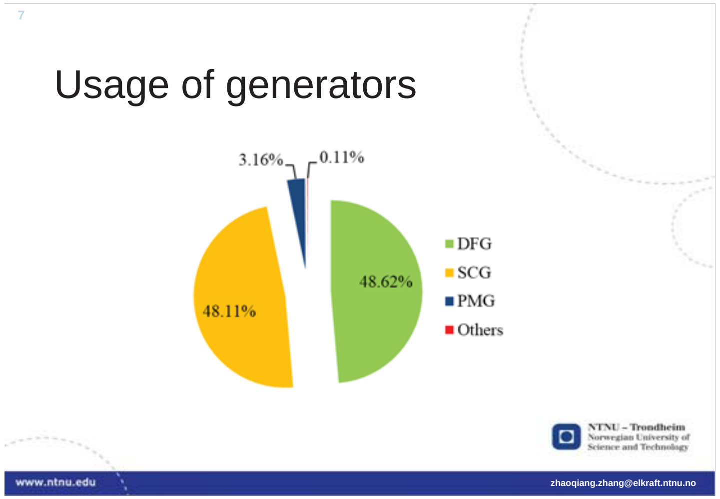
7
Usage of generators
3.16%
0.11%
48.62%
48.11%
DFG
SCG
PMG
Others
NTNU – Trondheim
Norwegian University of Science and Technology
www.ntnu.edu
zhaoqiang.zhang@elkraft.ntnu.no


8
Still focus on Direct Drives
NTNU – Trondheim
Norwegian University of Science and Technology
www.ntnu.edu
zhaoqiang.zhang@elkraft.ntnu.no

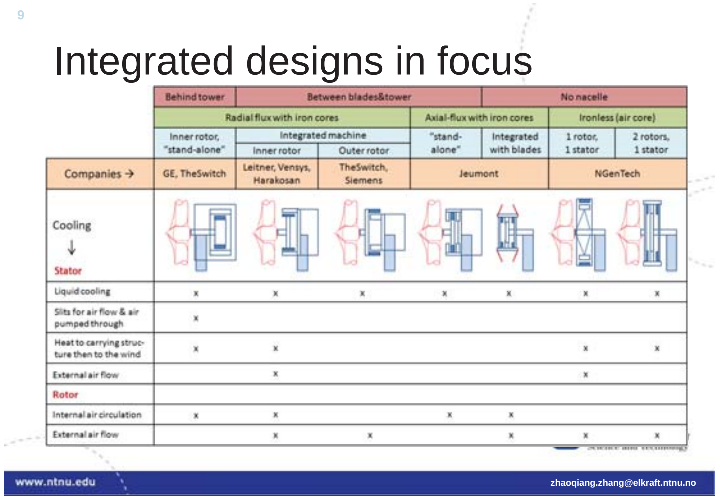
9
Integrated designs in focus
Behind tower
Between blades&tower
No nacelle
Radial flux with iron cores
Axial-flux with iron cores
Ironless (air core)
Inner rotor, "stand-alone"
Integrated machine
Inner rotor
Outer rotor
"stand-alone"
Integrated with blades
1 rotor, 1 stator
2 rotors, 1 stator
Companies →
GE, TheSwitch
Leitner, Vensys, Harakosan
TheSwitch, Siemens
Jeumont
NGenTech
Cooling
Stator
Liquid cooling
Slits for air flow & air pumped through
Heat to carrying structure then to the wind
External air flow
Rotor
Internal air circulation
External air flow
www.ntnu.edu
zhaoqiang.zhang@elkraft.ntnu.no

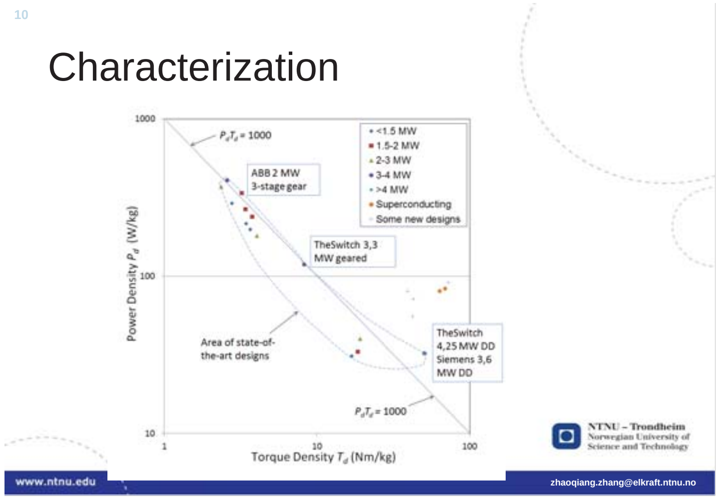
10
Characterization
Power Density P_d (W/kg)
Torque Density T_d (Nm/kg)
P_dT_d = 1000
ABB 2 MW 3-stage gear
TheSwitch 3,3 MW geared
Area of state-of-the-art designs
TheSwitch 4,25 MW DD Siemens 3,6 MW DD
<1.5 MW
1.5-2 MW
2-3 MW
3-4 MW
>4 MW
Superconducting
Some new designs
NTNU – Trondheim
Norwegian University of Science and Technology
www.ntnu.edu
zhaoqiang.zhang@elkraft.ntnu.no

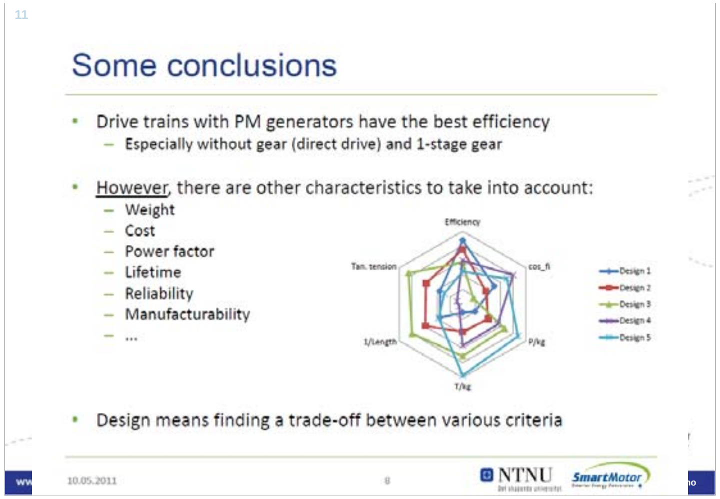
11
Some conclusions
Drive trains with PM generators have the best efficiency
Especially without gear (direct drive) and 1-stage gear
However, there are other characteristics to take into account:
Weight
Cost
Power factor
Lifetime
Reliability
Manufacturability
…
Efficiency
Tan. tension
cos_fi
1/Length
P/kg
T/kg
Design 1
Design 2
Design 3
Design 4
Design 5
Design means finding a trade-off between various criteria
10.05.2011
NTNU
SmartMotor

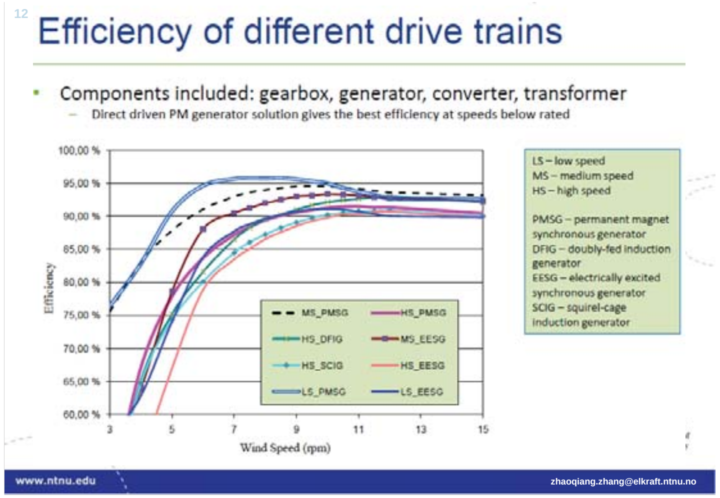
12
Efficiency of different drive trains
Components included: gearbox, generator, converter, transformer
Direct driven PM generator solution gives the best efficiency at speeds below rated
Efficiency
Wind Speed (rpm)
MS_PMSG
HS_PMSG
HS_DFIG
MS_EESG
HS_SCIG
HS_EESG
LS_PMSG
LS_EESG
LS – low speed
MS – medium speed
HS – high speed
PMSG – permanent magnet synchronous generator
DFIG – doubly-fed induction generator
EESG – electrically excited synchronous generator
SCIG – squirel-cage induction generator
www.ntnu.edu
zhaoqiang.zhang@elkraft.ntnu.no

13

Estimated weight for DD PM generators

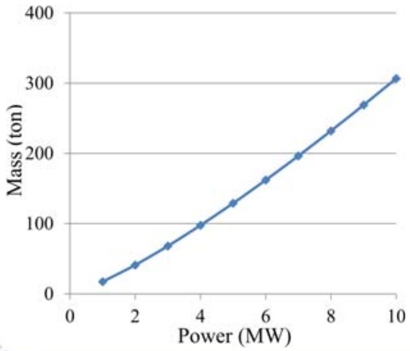

14

Direct driven generators are comming,

- but are they in the focus of commercial manufacturers?

15

“Secret” design from Siemens Januar 2010

16

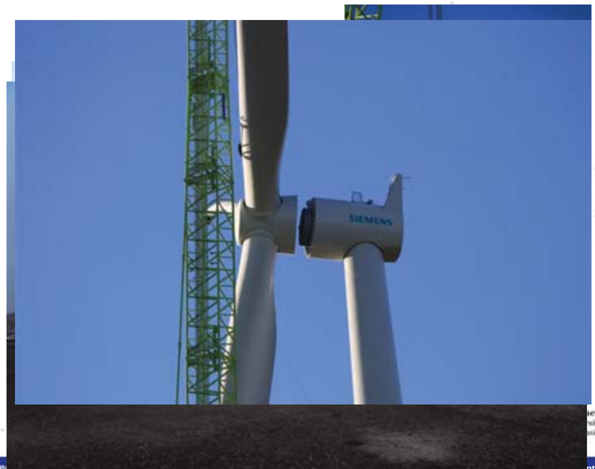

17

Expectations

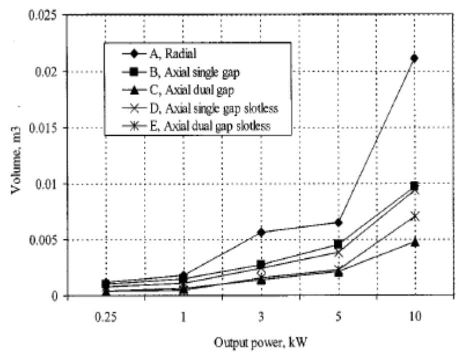

18

Multiple disc axially magnetized machines for wind applications?

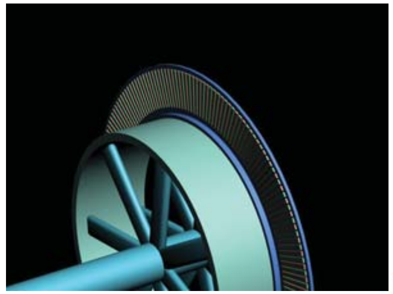

19

Compact designs - 3 times the power to volume ratio

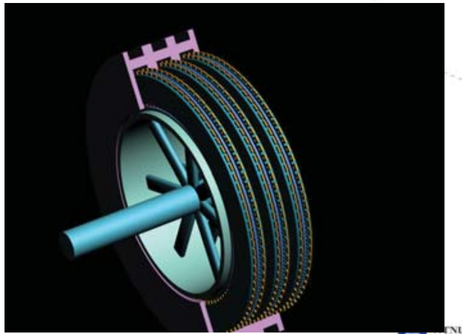

20

What about SWAY?

21

Main Features, Generator

SWAY TURBINE

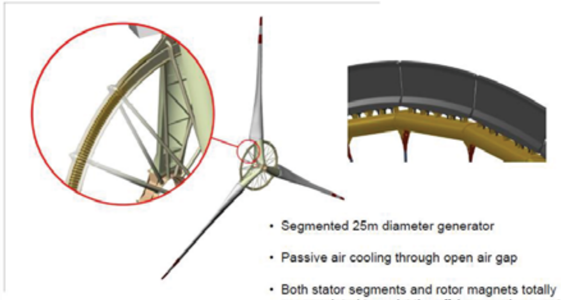

- Segmented 25m diameter generator
- Passive air cooling through open air gap
- Both stator segments and rotor magnets totally encapsulated to resist the offshore environment

22

23

Torque calculation:

$$T = \begin{cases} \frac{\sqrt{2}}{8} k_{w1} k_{le} m n_s I_{ph\_s} N_1 B_{p1} D_o^2 (1-\sigma^2), & AFPMSG \\ \frac{1}{\sqrt{2}} k_{w1} k_{le} m n_s I_{ph\_s} N_1 B_{p1} l D_a, & RFPMSG \end{cases}$$

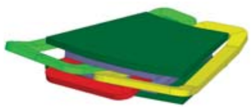

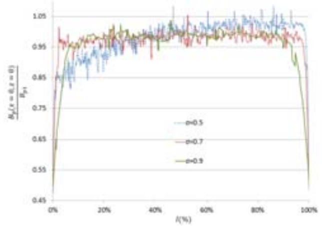

24

Modeling (3)- rotor sizing

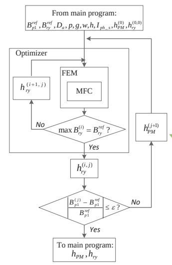

total number of poles

$$p = qmp_{se}$$

thickness of permanent magnet

$$h_{PM}^{(j+1)} = h_{PM}^{(j)}\left(1 - \frac{B_{p1}^{(j)} - B_{p1}^{(ref)}}{B_{p1}^{ref}}\right)$$

25

Test setup

1 stage, 48 pole, 23.2kW

	backEMF	Inductance
Calculation	78V	1.94mH
Measurement	82.3V	1.8mH

26

Simulation results(1)

- Parametric study
- Free variables
  - Outer diameter
  - Pole numbers
  - Fundamental flux density in the airgap
  - ratio of PM width over pole pitch
- Constrains (see specification)
- Objective: mass, efficiency, and cost

27

Simulation results (2)

- *The plots of efficiency only correspond to the designs that give lowest active mass*
- The first point on the left side of each curve shows the first feasible design as the outer diameter grows with a step of 2 m.

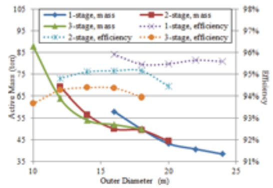

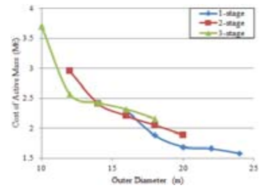

28

Simulation results (3)

- Proper cooling plays vital role in the investigated type of machine.
- Higher current density leads to the thinner winding and smaller air gap. Consequently the permanent magnets do not need to be thick, and the cost is reduced.
- It is not free to cool the winding in the two surfaces that are vertical to the shaft because of the increased air gap.
- The empty space after removing the coils for segmentation and the end coil region provide an operational room for better cooling.

29

Magnetic vibration challenges

- Maxwell's stress tensor:

$$\boxed{\begin{aligned} f_r &= \frac{1}{2\mu_0}({B_r}^2 - {B_t}^2) \\ f_t &= \frac{1}{\mu_0}(B_r B_t) \end{aligned}}$$

- Magnetic flux density distribution is computed using time-stepping FE analysis
- Radial magnetic force density wave:

$$\boxed{f_r(\theta, t) = f_{r,max}\cos(m\theta - k\omega t)}$$

- The dominant vibration mode is the lowest spatial harmonic in radial force density distribution.
- The lowest mode of vibration is 4 for the prototype machine.

30

Prototype generator

- 120slot/116pole
- Single-layer concentrated windings
- Nominal speed around 50 rpm

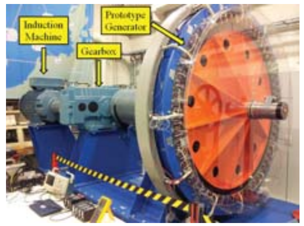

31

Magnetic simulations

- Time-stepping FE analysis

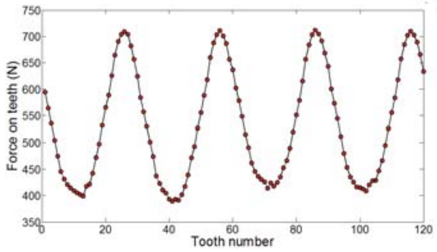

32

Structural analysis

- Modal analysis
- Static force analysis

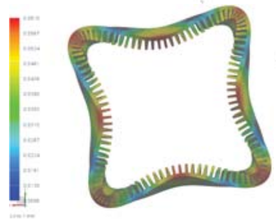

33

Experimental work

- Four accelerometers

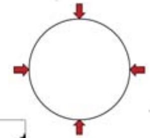

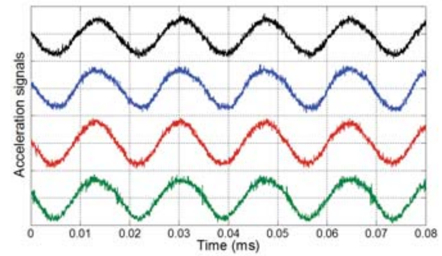

34

Multiple Airgap Machine

- 120slot/112pole double-stator single-rotor PM machine

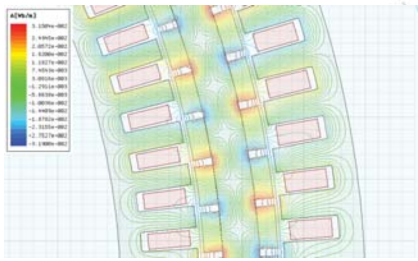

magnetic rotor yoke

35

Multiple Airgap Machine

- 120slot/112pole double-stator single-rotor PM machine

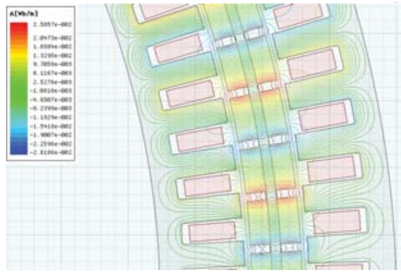

non-magnetic rotor yoke

36

Publications in 2013

- Influence of Slot Harmonics on Radial Magnetic Forces in Low-Speed PM Machine with Concentrated windings, *ICEMS 2013, Korea*.
- Analysis of a PM Wind Generator with Concentrated Windings in Eccentricity Conditions, *ICEMS 2013, Korea*.
- Influence of Pole and Slot Combinations on Magnetic Forces and Vibration in Low-Speed PM Wind Generators, *under review, IEEE Transactions on Magnetics*.

- Slot Harmonic Effect on Radial Magnetic Forces in Low-Speed PM Machine with Concentrated windings, *to be submitted to IEEE Transactions on Industry Applications*.
- Effects of Loading on Radial Magnetic Forces in Low-Speed Permanent Magnet Machine with Concentrated Windings, *to be submitted to IEEE Transactions on Magnetics*.

ZephIR Lidar

TURBINE MOUNTED LIDAR

Necessity is the mother of invention:
Nacelle mounted lidar for measurement of turbine performance

Matt Smith – 22nd January 2014

ZephIR DM

Contents

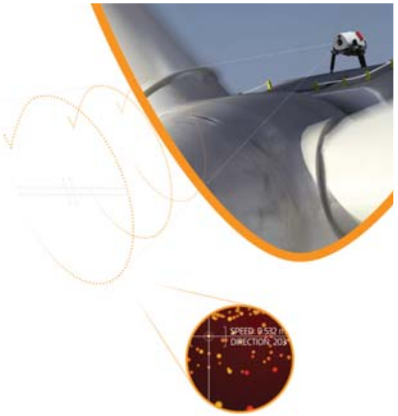

ZephIR DM

Apology

As much as possible I have tried to make this presentation about turbine mounted lidar in general.

The presentation template I have used is for ZephIR DM because certain images and diagrams are embedded within this

Certain benefits of turbine mounted lidar do relate specifically to using continuous wave lidar; ZephIR is the one that I know best

HOW DOES A LIDAR MEASURE WIND SPEED?

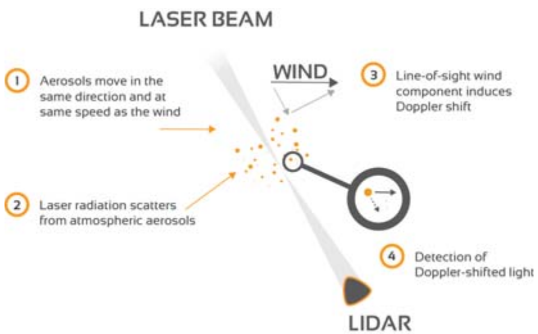

2003 - A WORLD FIRST

2003 - TRIAL

2.3 MW Nordex N90 turbine in Germany (90m hub height)
Single staring beam lidar system (CW) – Single Line of Sight (LoS) measurement
Turbine aligned it roughly into the wind
Single Beam - no measurements of wind yaw misalignment or wind shear or wind veer

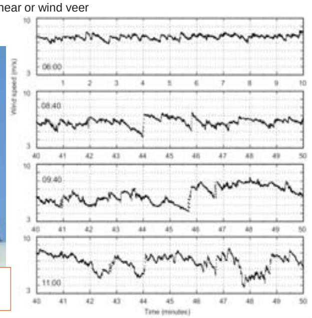

- Good estimate of approaching wind speed
- Simple gust warning

NACELLE MOUNTED - SIDELINED

GROUND BASED LIDAR DEVELOPED

- The nacelle mounted application was interesting but the market was not there
- Ground based lidar started being developed and addressed accuracy and reliability for remote resource assessment
- Adoption increased , competition entered the market and lidar remote sensing begins
- Validations completed onshore and offshore and over time the confidence grows

NACELLE MOUNTED - RESTART

GROUND BASED LIDAR DEPLOYED ON TURBINES

- Ground based production units, mounted on a frame to allow positioning and attachment of the lidar on a nacelle roof
- The mounting tended to be bespoke and difficult
- Much of this work was behind closed doors and explored the accuracy, benefit and reliability of the systems

I'd like to personally offer my thanks to Riso/DTU during this time for publicly exploring and publishing results of nacelle based applications of lidar

NACELLE MOUNTED – BASIC ACCURACY

THE WIND IS NO LONGER PERPENDICULAR (GROUND BASED) AND IS BLOWING TOWARDS THE LIDAR

- Measurements in a high-specification wind tunnel confirm very close agreement over a wide velocity range
- This is the accuracy of a single Line of Sight measurement

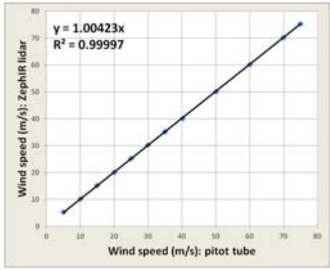

Credit:
"HTF number 049-2009-3 - Integration of wind LIDAR's in wind turbines for improved productivity and control",
a Danish National Advanced Technology Foundation's (DNATF) Project.

Reference:
A T Pedersen, B F Montes, J E Pedersen, M Harris, and T Mikkelsen,
"Demonstration of short-range wind lidar in a high-performance wind tunnel",
EWEA conf. PO78, Copenhagen (2012).

NACELLE MOUNTED – SOME RESULTS

THE BENEFITS OF LIDAR ON TURBINES:

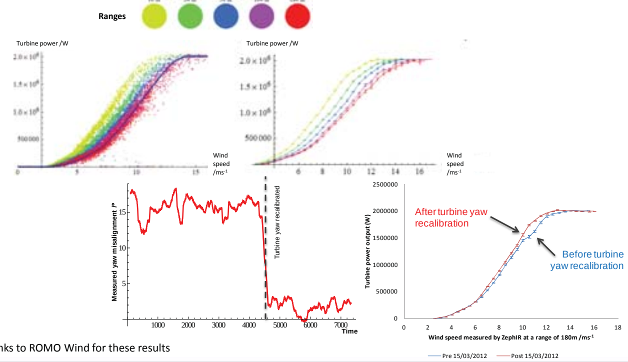

Thanks to ROMO Wind for these results

NACELLE MOUNTED – SPECIFIC PRODUCTS

LIDAR DEPLOYED ON TURBINES

- **Low System Mass.** the lidars must be light enough to allow, ideally, 2 man installation.
- **Small size.** small enough to allow it to be maneuvered through internal turbine spaces and hatches. Meeting this requirement typically allows the turbine's internal crane to be used for deployment, ideally designed to allow passage through hatches of aperture 0.55 x 0.55 m2.
- **Easy handling** and protection during installation. Adequate handles, padding, connections and rugged construction are needed.
- **Adaptable and flexible mounting arrangements.** This allows mounting on a variety of turbine roof shapes and at various heights. Often tripod arrangements, with independently adjustable legs, are a good solution. The ZephIR DM has carbon fibre tripod legs, and can be mounted at heights up to 1.5 m from the roof.
- **Adequate alignment procedures.** The ability to align the centreline of the lidar with the turbine axis is important where yaw alignment checks are to be performed.

NACELLE MOUNTED – SPECIFIC PRODUCTS

LIDAR DEPLOYED ON TURBINES

- ZephIR DM Offers:
  - Hub height and rotor equivalent horizontal wind speeds
  - Wind yaw alignment relative to turbine
  - Vertical wind shear
  - Wind veer (variation of wind direction with height)
  - TI and other turbulence measures
  - Wind field complexity
  - Turbine wakes and effects of complex terrain

BENEFITS OFFSHORE

ASSESSING/OPTIMISING TURBINE PERFORMANCE

- Traditional and IEC accepted methodologies can be expensive offshore
- Deeper water with floating wind turbines could see this further complicated
- What will warranties be based on?

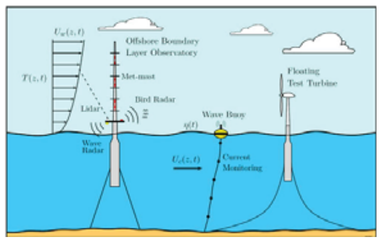

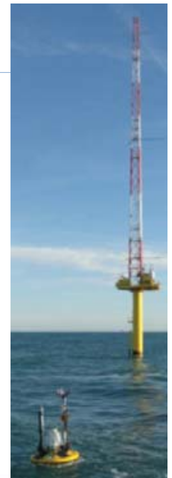

ZEPHIR DM– OFFSHORE?

THE FOLLOWING FEATURES ARE IMPLEMENTED FOR ONSHORE TURBINES:

- **Real-time inclination and roll.** The nacelle roof rolls and tilts due to inherent machine resonances as well as wind flow variations. The lidar itself is also subjected to wind loading, and the roof can flex accordingly. These influences cause the lidar beam to move in space. The coordinates of the lidar probe positions change, so different parts of the incoming wind field are probed. this can introduce additional measurement uncertainties, especially at longer ranges, where a small angular change in inclination can translate into significant changes in height.
- The ZephIR DM uses real-time inclination and roll measurement, accurate to 0.1°, and incorporates these measurements in the calculation of the derived wind field quantities accordingly. Such a capability will be particularly important on floating turbines.
- **Motion compensation.** In a similar way that nacelle angle changes can impact measurement uncertainty, nacelle motion, especially fore-aft velocity, can have an impact on lidar measurements. Without measurement of such motion, the lidar will be measuring the wind speed relative to the (moving) lidar, not the wind speed relative to the ground. The ZephIR DM has an inbuilt accelerometer that measures its motion in real-time and optionally corrects the measured LOS speeds

WOULD THIS HAVE FURTHER BENEFIT FOR FLOATING TURBINES?

MOVEMENT OF TURBINE NACELLES

RECORDED FROM ZEPHIR DM DEPLOYMENT ONSHORE

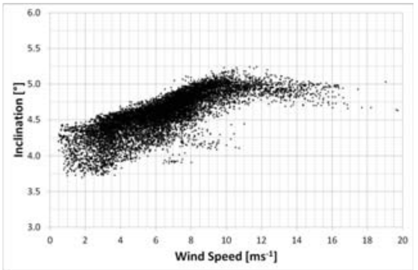

NACELLE MOUNTED – ROTOR EQUIVALENT

ROTOR EQUIVALENT WIND SPEEDS

The RE wind speed (u_{RE}) [6] concept was formalized in IEC 21400-12-1 CD. It aims for a more accurate measurement of the amount of energy in the wind, especially for larger rotor area (A) wind turbines. With these rotors sampling greater cross sections of wind flow, the effects of wind speed variation with height, and wind speed direction variation with height, become more significant. The RE formula in the standard incorporates these effects, but requires a knowledge of the horizontal wind speed u_i and direction θ_{wi} relative to the direction at hub height, at multiple (≥3) heights over the rotor disk.

$$u_{RE} = \sqrt[3]{\frac{1}{A}\sum_{i=1}^{N}(u_i \cos\theta_{wi})^3 \Delta A_i}$$

- where ΔA_i is the area of the ith slice of the rotor, and N is the number of slices over the rotor disk.

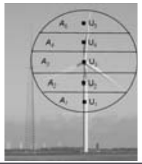

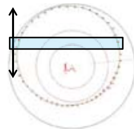

NACELLE MOUNTED – ROTOR EQUIVALENT

Nacelle-mounted ZephIR DM vertical wind profile (left) and vertical wind veer (θwi) from a single 24 hour period on a non-complex site in the UK. Each coloured line represents a 10 minute-averaged measurement. 2 MW turbine, rotor diameter 90 m, hub height 75 m

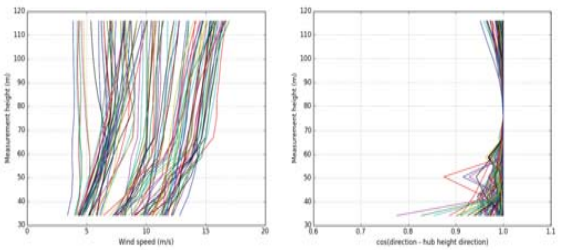

Vertical wind shear and TI. Both these quantities are influenced by atmospheric stability, and can have a significant effect on turbine performance. This is reflected in power curve measurements. Unless account of these effects is included, power curves will have larger uncertainties

DEEP AND DEEPER WATER

WHAT DOES NACELLE MOUNTED LIDAR OFFER?

- Onshore: We are seeing nacelle mounted lidar being used for optimisation and performance measurements.
- Offshore: There is no realistic turbine performance measurement option.
- Deeper water: Nacelle mounted lidar offers
  - turbine manufacturers the ability to articulate products performance
  - operators the ability to measure individual turbine performance. There is no alternative...

New Rotor Concepts for Future Offshore Wind Farms

Özlem Ceyhan and Francesco Grasso
ceyhan@ecn.nl
grasso@ecn.nl

Trondheim, Norway
22.01.2014

www.ecn.nl

EERA Deepwind 2014, 11th Deep Sea Offshore Wind Conference, Trondheim, Norway, 22-24 January 2014

ECN Your energy. Our passion.

Outline

- Introduction and Motivation
- Purpose of the Work
- Method
  - Rotor concepts studied
  - Hornsrev as reference wind farm
  - Analysis Conditions and Assumptions
- Results
  - Wind turbine level
  - Wind turbine level – With ECN airfoils
  - Wind turbine level overall
  - Wind farm level
  - Wind farm level – Effect of airfoils
- Conclusions and discussions

ECN

Introduction and Motivation

Plans to increase the offshore wind capacity enormously: EC 2008, Offshore wind should increase 30-40 times by 2020 and 100 times 2030* (www.ewea.org).

Continuous growth in the sizes of the wind turbines (not necessarily the capacity!)

Vestas V164 8MW prototype

ECN

Introduction and Motivation

Plans to increase the offshore wind capacity enormously: EC 2008, Offshore wind should increase 30-40 times by 2020 and 100 times 2030* (www.ewea.org).

Continuous growth in the sizes of the wind turbines (not necessarily the capacity!)

Vestas V164 8MW prototype

Image: Courtesy of Official Vestas Linkedin page&Albert Winnemuller

ECN

Purpose of the Work

- Reflect the current design trends in rotor design by a parametrical conceptual study
- Evaluate the rotor designs including their performance in Offshore farm environment
- Evaluate ECN's airfoils for chosen concepts in farm operation
- Include as realistic information for a farm operation as possible
- Possibility of bringing a different perspective to rotor designs for farm operations.

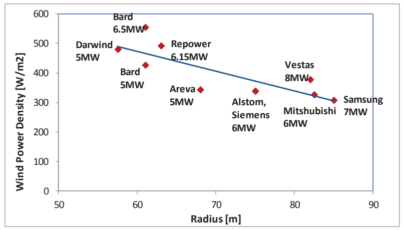

ECN

Method

ECN

Method

- INNWIND.EU 10MW RWT
- Parametrical study for Rotor design ← Reduced power density from 400W/m² to 300W/m²
- Include ECN Airfoils
- Evaluate the results in WT level
- Replace the turbines in Hornsrev with Studied Rotors
- Evaluate the results in WF level

Rotor Concepts and Parameters (1/7)

RWT 10MW

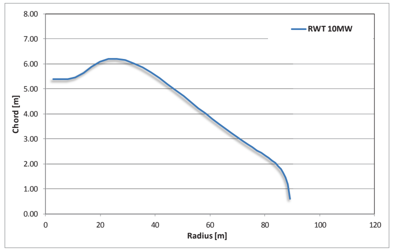

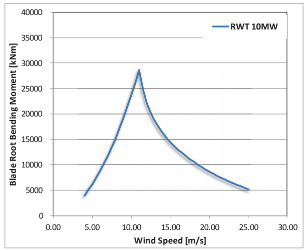

Rotor Concepts and Parameters (2/7)

RWT 10MW | UPSCALE

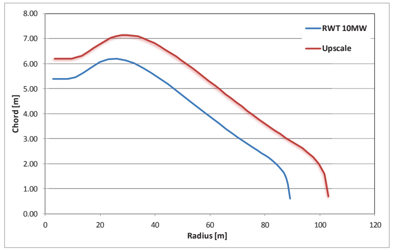

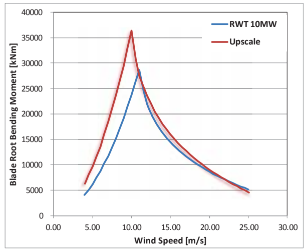

Upscaled by keeping c/r distribution constant for r/R.

Rotor Concepts and Parameters (3/7)

RWT 10MW | UPSCALE | LOW SOLIDITY

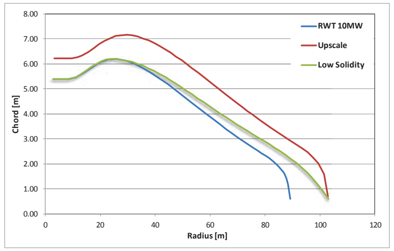

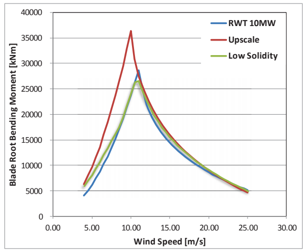

Solidity $\left(\sigma = \frac{Bc}{2\pi r}\right)$ *is decreased by averaging the chord lenght between Upscale and RWT, BRBM is reduced to RWT*

Rotor Concepts and Parameters (4/7)

RWT 10MW | UPSCALE | LOW SOLIDITY | UPSCALE PS

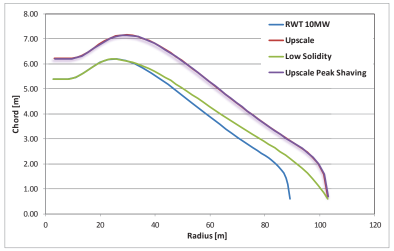

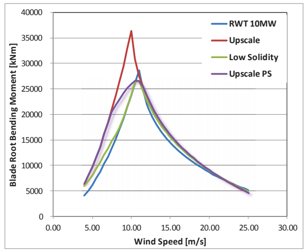

Rotor Concepts and Parameters (5/7)

RWT 10MW | UPSCALE | LOW SOLIDITY | UPSCALE PS | HIGHER LAMBDA

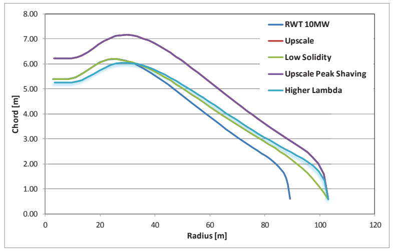

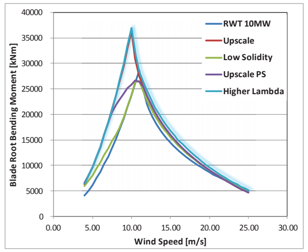

RPM is equal to RWT, lambda is increased to (aerodynamic) optimum lambda.

ECN

Rotor Concepts and Parameters (6/7)

RWT 10MW | UPSCALE | LOW SOLIDITY | UPSCALE PS | HIGHER LAMBDA | HIGHER RPM

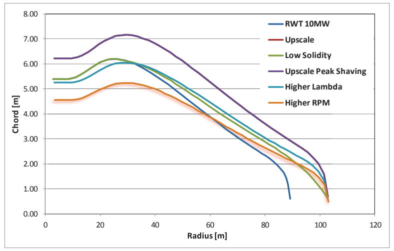

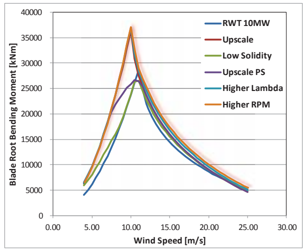

RPM is increased, tip speed is also increased. Chord is reduced proportionally.

ECN

Rotor Concepts and Parameters (7/7)

RWT 10MW | UPSCALE | LOW SOLIDITY | UPSCALE PS | HIGHER LAMBDA | HIGHER RPM | HIGHER RPM PS

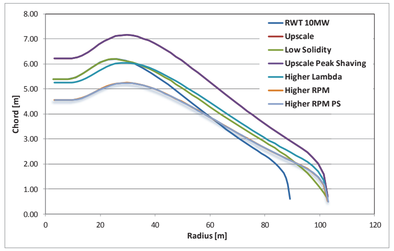

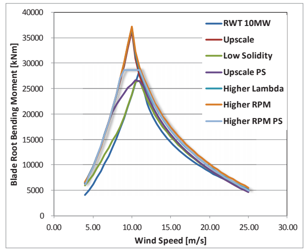

ECN

Horns Rev as Reference Wind Farm

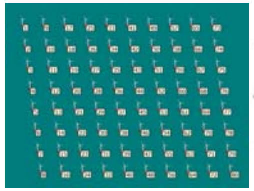

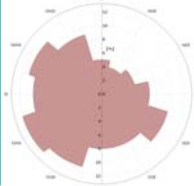

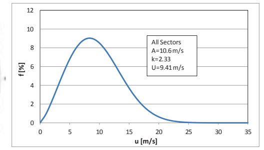

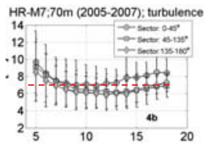

- ***Wind data is from 2000.01 to 2003.12. Measured at 62m. Undisturbed. Provided by Kurt Hansen (DTU) on 08.01.2014***

- ***Turbulence intensity graph is taken from*** *'Hansen K. et all "The impact of turbulence intensity and atmospheric stability on power deficits due to wind turbine wakes at Horns Rev wind farm", Wind Energy Special Issue: Upwind, Volume 15, Issue 1, pages 183-196, January 2012'*

ECN

Analysis Conditions and Assumptions

Wind Turbine Level Analysis

- Rotor analysis are performed with BOT software
  - *ECN's state-of-the-art BEM based rotor design and optimisation tool*
- Steady state analysis are performed.
- Structural design or analysis are not included.
- All parameters are kept the same for all rotors except the ones that are changed.

Wind Farm Level Analysis

- Farmflow software is used.
  - *Parabolized NS Eqns*
  - *WTs are modelled with actuator disc*
  - *Wake is modelled with free wake method*
  - *Modified k-ε model is implemented.*
- Wind turbine locations are kept as original.
- Wind conditions are assumed to be the same at new hub height (119m).
- Analysis are performed for every 30 degrees of wind direction.
- Turbulence intensity = 0.07

ECN

Analysis Conditions and Assumptions

Wind Turbine Level Analysis

- Rotor analysis are performed with BOT software
  - *ECN's state-of-the-art BEM based rotor design and optimisation tool*
- Steady state analysis are performed.
- Structural design or analysis are not included.
- All parameters are kept the same for all rotors except the ones that are changed.

Wind Farm Level Analysis

- Farmflow software is used.
  - *Parabolized NS Eqns*
  - *WTs are modelled with actuator disc*
  - *Wake is modelled with a free wake method*
  - *Modified k-ε model is implemented.*
- Wind turbine locations are kept as original.
- Wind conditions are assumed to be the same at new hub height (119m).
- Analysis are performed for every 30 degrees of wind direction.
- Turbulence intensity = 0.07

ECN

RESULTS

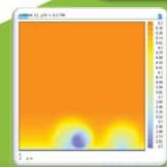

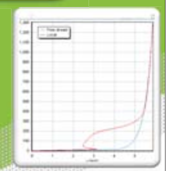

Wind Turbine Level

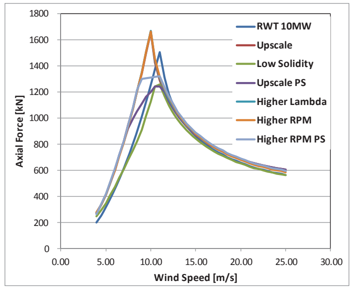

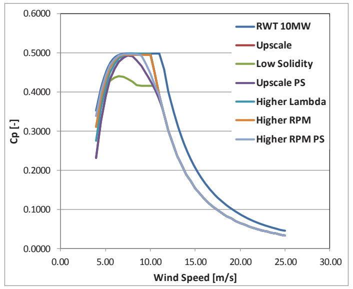

Wind Turbine Level – With ECN Airfoils

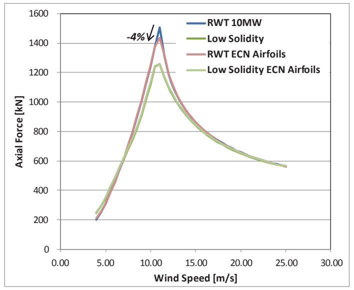

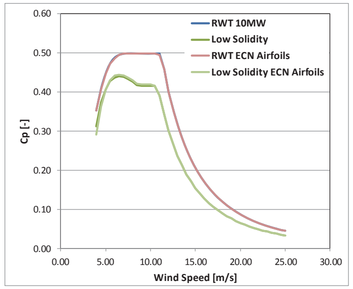

Wind Turbine Level Overall

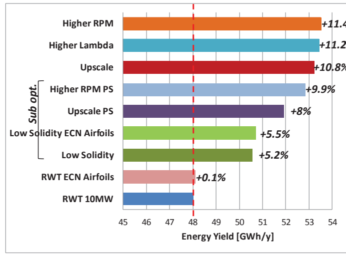

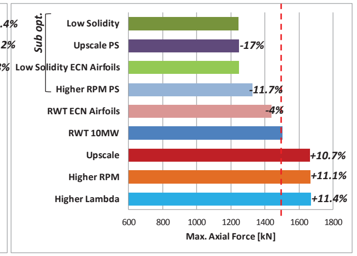

Wind Farm Level

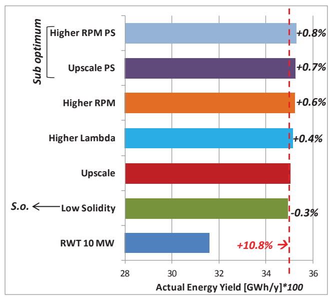

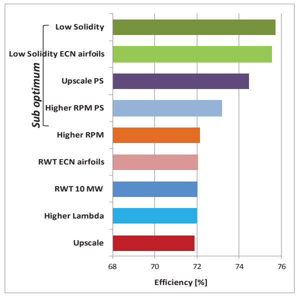

Wind Farm Level – Effect of Airfoils

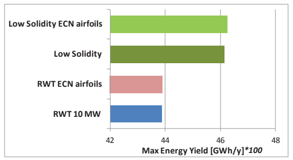

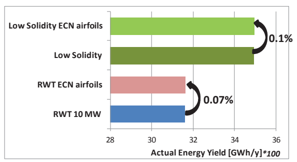

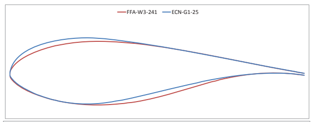

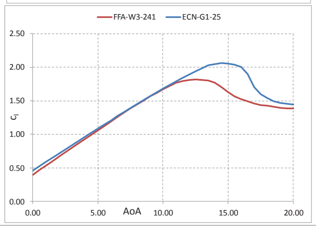

Conclusions and Discussion

- Design trends in large rotors for offshore wind farms are evaluated by a parametrical study.
- Concepts are evaluated in a wind farm environment.
- These results are highly dependent on the chosen farm parameters. Nevertheless, they still indicate the potential of the integral design for future wind farms.
- Preliminary results for the current ECN airfoils do not lead to a large gain in farm power output. However the latest studies are aiming to help to reduce the wake losses and to improve the structural efficiency of the blade.

Most important Conclusion:

Airfoil design, turbine design and control, wind farm design and farm control should be done integrally in order to operate an offshore wind farm in most optimum conditions for the reduction of CoE.

EPSRC
Engineering and Physical Sciences Research Council

Multi Rotor Systems for Large Unit Capacities Offshore

EERA Deepwind January 2014

Design of Multi Rotor System

OWES

5MW system comprising 16, 312 kW wind turbines

The Case for Multi Rotor Systems

- **Scaling laws** – total rotors and drive trains of the multi rotor system will have much less weight and cost of blades, hub and drive train of a single equivalent turbine
- **Standardisation** – systems larger than 20 MW will be realised with more rotors not larger rotors. Thus there is opportunity to gain very substantial cost and reliability advantages of standardisation of rotor and drive train components in stable serial production at a size comfortably within industry experience
- **Maintenance** – the multi-rotor system will have in effect almost no unscheduled maintenance. Single turbine faults will usually compromise only a few percent of capacity, reducing urgency to find favourable weather windows for remedial action.

Why Multi-Rotors?

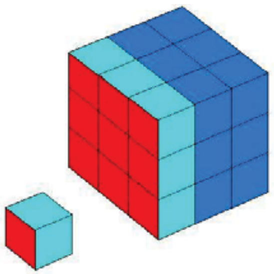

National Geographic 1976

The Multi-Rotor Argument

Equal area: $D^2 = nd^2$

Mass of large rotor: $M = kD^3$

Mass of small rotor: $m = kd^3$

The mass ratio is: $R = n\left\{\frac{d}{D}\right\}^3$

$$R = \frac{nm}{M} = \frac{1}{\sqrt{n}}$$

100 rotor, multi-rotor system has 1/10th of weight and cost of rotors and drive trains compared to a single equivalent large rotor!

Upscaling Challenges

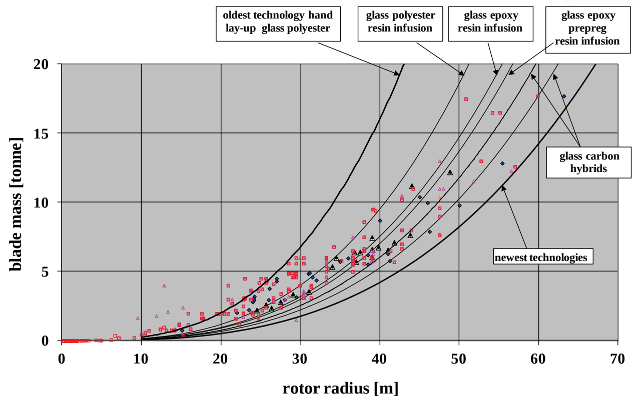

Upscaling Challenges

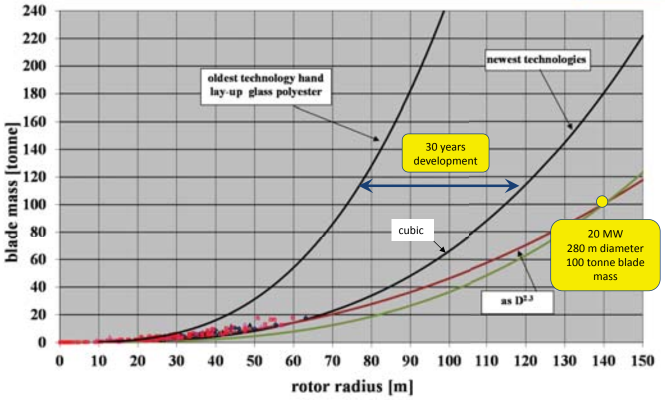

Upscaling the easy way!

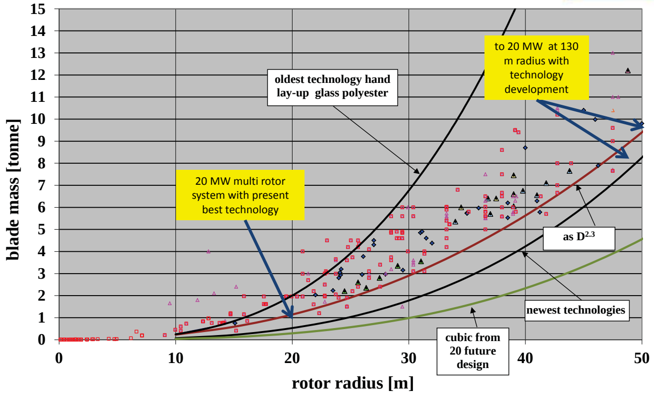

Design of Multi Rotor System

- Define multi rotor system layout
- Create a system model to determine design driving loads
- Define a reduced set of load cases
- Conduct load calculations

The main objective in modeling multi rotor system loads is to facilitate the development of a suitable design of support structure (CRES). When candidate support structures have evolved, the overall aerodynamic interference of structure and rotors will be assessed (NTUA).

Innwind.eu - Partners Roles

SU - Technical coordination, concept design, load calculation using:

GLGH - Bladed for 45 rotors.

CRES – support structure and yaw system design

NTUA – validation of aerodynamics: rotor interaction, structure blockage.

Multi Rotor System Definition

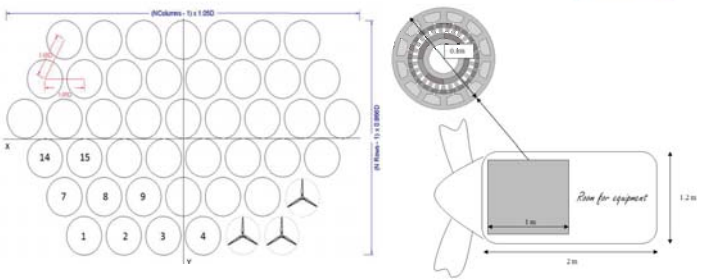

- 45 rotors each of 41 m diameter and of 444 kW rated output power comprising a net rated capacity of 20 MW
- Rotors on a triangular lattice arrangement with minimum spacing of 5% of diameter
- Variable speed, pitch regulated with direct drive PMG power conversion

Multi rotor system concept

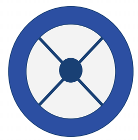

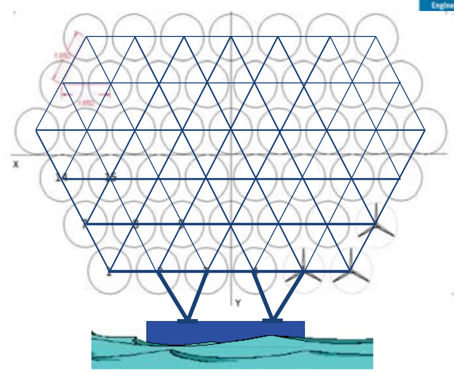

Reduced load case set

- Loads prediction using GH Bladed adapted for 45 rotors on a single structure
- Design load cases (DLC) and load calculations broadly in conformance with IEC 61400-1 (2005) and GL2003

  a) 1.2 fatigue loads – normal turbulence model (NTM)
  b) 1.3 ultimate loads –extreme turbulence model (ETM)
  c) 6.1 ultimate loads idling in 50 year gust
  d) 6.2 ultimate loads idling with grid loss in 50 year gust (large yaw errors considered but reduced safety factor compared to 6.1)

- A few other load cases are being considered – fault cases affecting a single rotor are considered unimportant for the multi-rotor system design

Ultimate loads comparison – rotor thrust loading

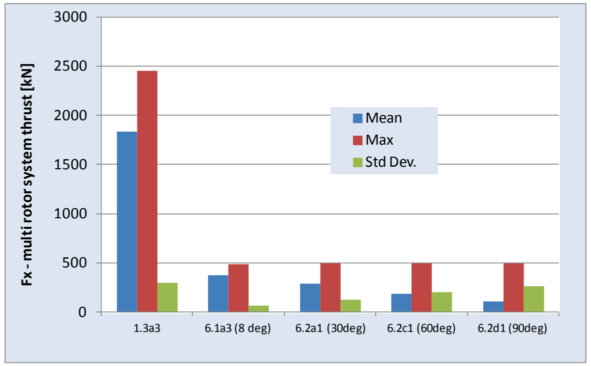

Rotor Centre Thrust – DLC 1.3 a3

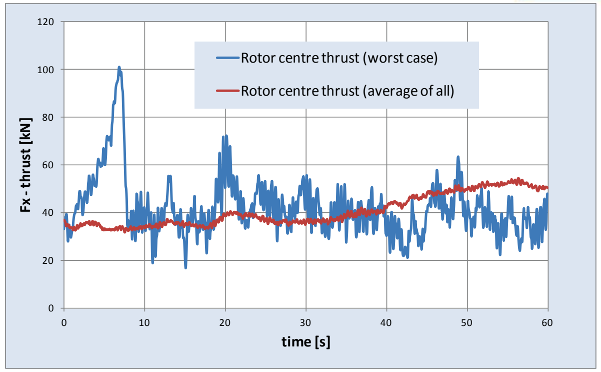

Ultimate loads comparison – rotor thrust loading

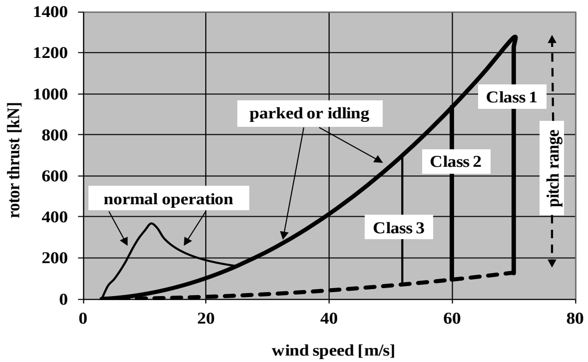

Comparison with 20 MW single rotor

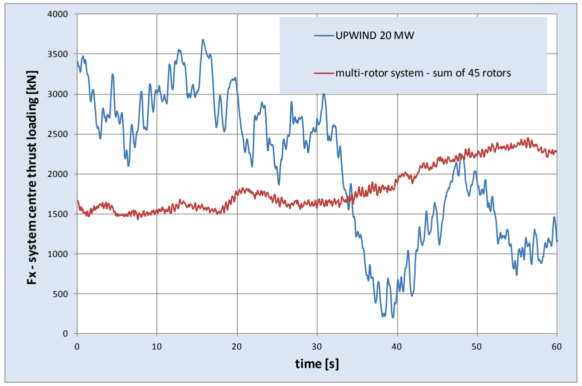

Comparison with 20 MW single rotor

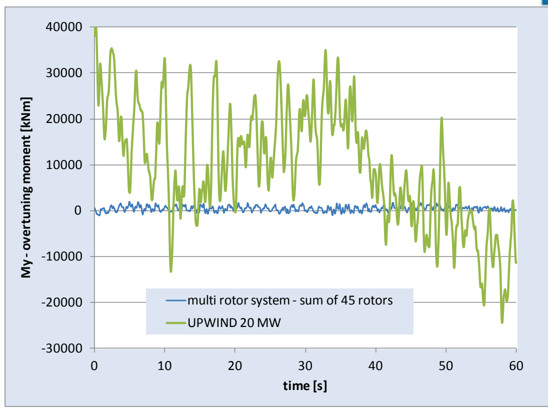

Multi rotor system loads summary comments

- **ULTIMATE LOADING** - DLC 1.3 in the sub case of operation in turbulent wind around rated wind speed leads to maximum ultimate thrust loading on the multi rotor system
- **FAULTS** - In the multi-rotor system each individual rotor is assumed to be designed in compliance with IEC, Class 1A. Thus fault cases such as blade stuck in pitch or pitch runaway fault may result in design driving loads for the individual rotor. It is assumed however that single rotor fault cases will have no significant impact on design driving loads of the multi rotor support structure
- **DYNAMIC LOADS** - The random blade azimuth relationships between the rotors of a multi rotor system appear to result in very large reductions in dynamic loading of the support structure as compared to large single rotors of equivalent net capacity
- **FURTHER COMPARISONS** - More extensive load comparisons will be made with 2 X 10 MW DTU reference turbines and 4 x 5 MW commercial wind turbines as the 20 MW single turbine is very speculative technology at present.

Structure Optimisation – stress distribution (CRES)

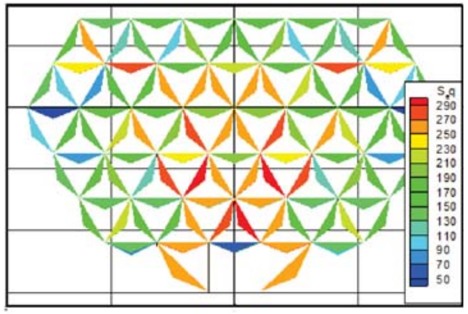

Tube stress [Mpa] for designing extreme load IEC Class 1

Structure mass within 3000 t

Structure Mass Comparisons

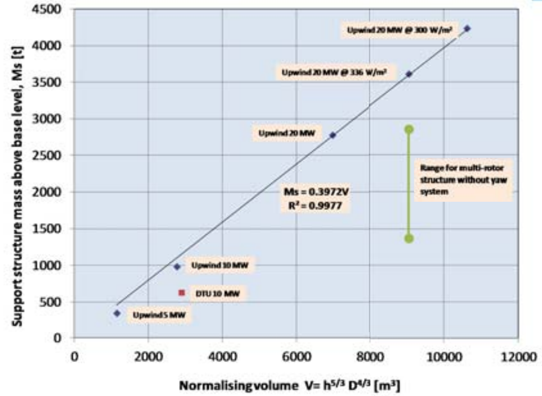

Electrical design – turbine interconnection

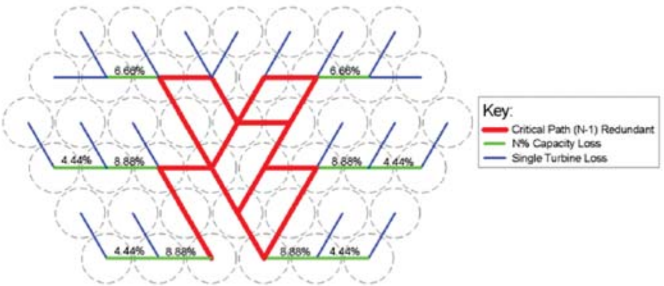

Aerodynamic evaluation of a 7 rotor set (NTUA)

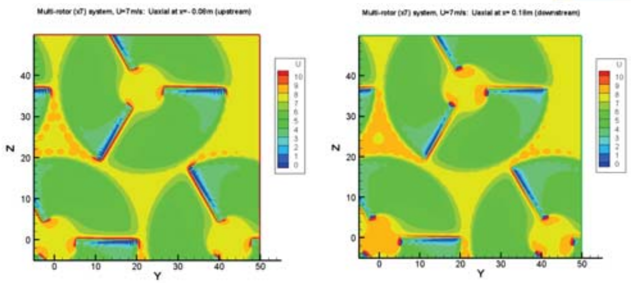

Snapshots of axial flow contours upstream and downstream a 7 rotor system operating at 7m/s wind speed.

Aerodynamic evaluation – 7 rotor set

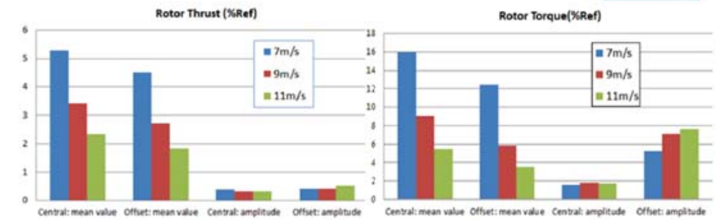

Increase in rotor thrust and torque as % of the (reference) isolated rotor performance at three wind speeds for the 7 rotor configuration. The mean values and amplitudes are provided separately for the central and offset rotors

Energy Capture Comparison

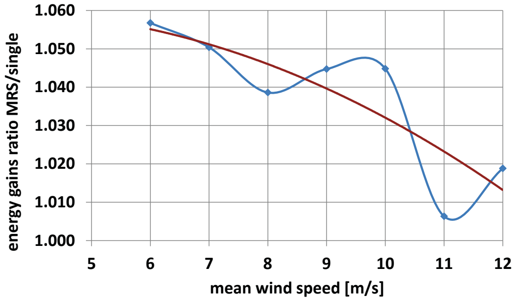

This is based on dynamic power predictions using Bladed for both single rotor and multi rotor system, 600 second record with 3 turbulence seeds and results averaged. The ratio is the ratio of the gains of each over steady state at the mean wind speed of the record.

Status and conclusions January 2014

- Concept design well developed
- Load specification and calculations near completion
- Much reduced structure loading from rotors compared to an equivalent single turbine
- Optimised support structure mass is determined as ~ 2700t, somewhat less than an equivalent single 20 MW turbine ~ 3500t
- Aerodynamic evaluation in progress
- Energy capture evaluation in progress

Acknowledgements

- Edwin BOT (ECN)
- Kurt Hansen (DTU)

The present work has been partially supported by the FP7 European project INNWIND.EU (project no. 308974).

www.innwind.eu

Thank you!

ceyhan@ecn.nl
grasso@ecn.nl

Future Work

- Perform the same analysis with relatively increased distances between the wind turbines
- Design new airfoil families per concept, taking into account these results and performance in farm in general.
- Re-evaluate the rotor designs for site-specific conditions together with new airfoils.
- Putting the analysis results into ECN's cost models for the financial results
- Performing similar study for another wind farm with wind measurements at higher altitudes.
- Looking into details in rotor design.

Rotor Concepts and Parameters (1/8)

Concept name →	(1.)RWT	(2.)Upscale, (3.)Low Solidity, (4.)Upscale PS	(5.)Higher Lambda	(6.)Higher RPM, (7.)Higher RPM PS
Capacity [MW]	10	10	10	10
Tip speed	89.64	89.64	103.55	113.54
Lambda	7.50	7.50	8.66	9.50
rpm	9.60	8.31	9.60	10.53
radius	89.166	103	103	103
Power density	400.36	300.04	300.04	300.04

For the rest of the concepts ECN airfoils are applied to (1.), (3.);
(8.) RWT ECN Airfoils *(Power output is equal to RWT, loads are reduced)*
(9.) Low Solidity ECN Airfoils *(BRBM are equal)*

Effect of Airfoils – Looking back

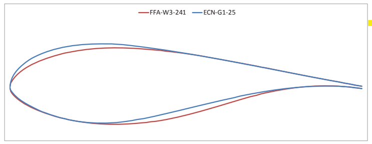

Structural properties

	FFA-W3-241	ECN-G1-25
area	0.14020	**0.13970**
slen	2.11800	**2.13000**
skin Ixx/t	0.01350	**0.01360**
centroid Xc	0.38100	**0.36700**

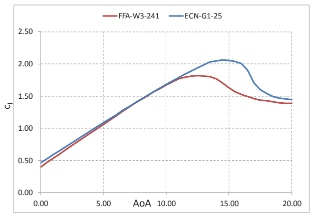

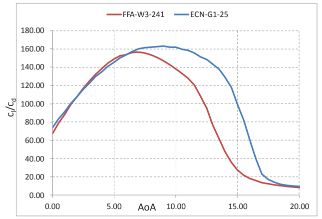

A2) New turbine and generator technology

DeepWind-from idea to 5 MW concept, Uwe Scmidt Paulsen,
Technical University of Denmark

Dynamic analysis of a floating vertical axis wind turbine during emergency shutdown through mechanical brake and hydrodynamic brake, Kai Wang, NTNU

Concept design verification of a semi-submersible floating wind turbine using coupled simulations, Fons Huijs, GustoMSC

DeepWind-from idea to 5 MW concept

DeepWind'2014-11th Deep Sea Offshore Wind R&D Conference
22-24 January 2014 Trondheim, No

Uwe Schmidt Paulsen[a]
uwpa@dtu.dk

[b] Helge Aa. Madsen, Per H. Nielsen,Knud A. Kragh
[c] Ismet Baran,Jesper H. Hattel
[d] Ewen Ritchie, Krisztina Leban
[e] Harald Svenden
[f] Petter A. Berthelsen

[a,b] DTU Department of Wind Energy, Frederiksborgvej 399 Dk-4000 Roskilde Denmark
[c] DTU Department of Mechanical Engineering, Produktionstorvet Building 425 Dk-2800 Lyngby Denmark
[d] Aalborg University, Department of Energy Technology, Pontoppidanstræde 101, DK-9220, Aalborg East Denmark
[e] Sintef Energy Research Box 4761 Sluppen, NO-7465 Trondheim, Norway
[f] Marine Technology Centre MARINTEK, Otto Nielsens veg 10, NO-7052 Trondheim, Norway

DTU Wind Energy
Department of Wind Energy

DeepWind
Contents

- DeepWind Concept
- 5 MW design
- Optimization process results
- Conclusion

  – Controller part: grid compliance

DeepWind
Contents

- DeepWind Concept
- Baseline 5 MW design
- Results from Optimization process
- Conclusion

DeepWind
The Concept

- No pitch, no yaw system
- Floating and rotating tube as a spar buoy
- C.O.G. very low – counter weight at bottom of tube
- Safety system

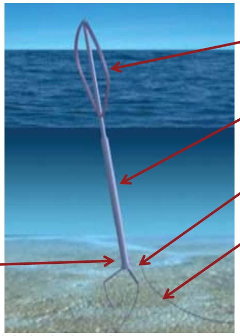

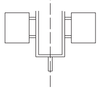

- Light weight rotor with pulltruded blades, prevailing loads from aerodynamics
- Long slender and rotating underwater tube with little friction
- Torque absorption system
- Mooring system

DeepWind
Concept- Generator configurations

- The Generator is at the bottom end of the tube; several configuration are possible to convert the energy
- Robust integrated bearing technology
- Three selected to be investigated first:
  1. Generator fixed on the torque arms, shaft rotating with the tower
  2. Generator inside the structure and rotating with the tower. Shaft fixed to the torque arms
  3. Generator fixed on the sea bed and tower. The tower is fixed on the bottom (not floating).

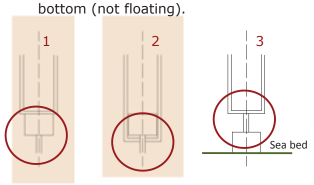

DeepWind
Contents

- DeepWind Concept
- Baseline 5 MW design
- Results from Optimization process
- Conclusion

DeepWind
1 st BaseLine 5 MW Design Floater

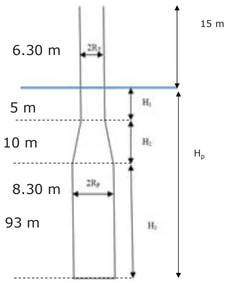

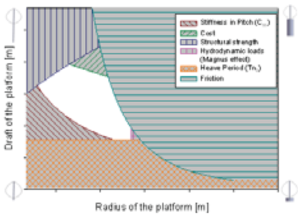

- Design space limitations

Hywind site:
~5000 tons mass
~ 35/60 sec natural periods in yaw/surge

DeepWind
BaseLine 5 MW Design Blades

- Blade length 200 m
- Blade chord 5 m constant over length
- Blades pulltruded, sectionized GRP
- NACA 0018 and NACA 0025 profiles

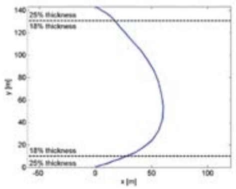

DeepWind
5 MW Design Rotor

Geometry

Rotor radius (R_0)	[m]	60.5
H / ($2R_0$)	[-]	1.18
Solidity (σ = Nc / R_0)	[-]	0.165
Swept Area (S_{ref})	[m²]	11996

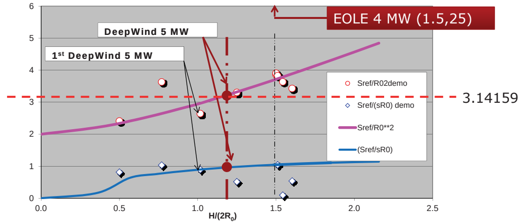

DeepWind
Load cases

- Deterministic flow with Power law wind shear
- Airy waves
- Sea current 0-0.7 m/s

	H_s [m]	T_s [s]	Current [m/s]
Sea state 0	0	0	0
Sea state 1	4	9	0.35 for $V_0 < 14$ m/s, 0.7 for $V_0 > 14$ m/s
Sea state 2	9	13.2	0.35 for $V_0 < 14$ m/s, 0.7 for $V_0 > 14$ m/s
Sea state 3	14	16	0.35 for $V_0 < 14$ m/s, 0.7 for $V_0 > 14$ m/s

- Water depth 200 m
- Site along Norwegian coast
- Met-ocean data, hindcast©DHI and WF

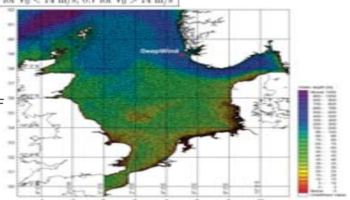

DeepWind
Contents

DeepWind
BaseLine 5 MW Design Performance

Performance

Rated power	[kW]	5000*
Rated rotational speed	[rpm]	5.73*
Rated wind speed	[m/s]	14
Cut in wind speed	[m/s]	5
Cut out wind speed	[m/s]	25

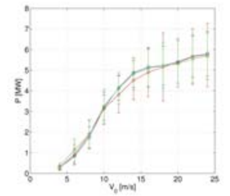

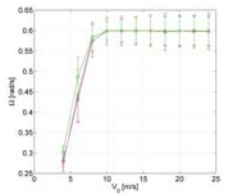

DeepWind

Floater performance at Sea states: 0.35 -0.7 m/s Current

- Pitch

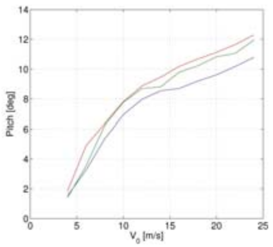

- Roll
  - Magnus forces change with current

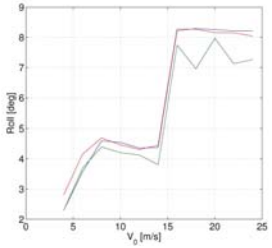

DeepWind

Constant blade chord with different profile thickness

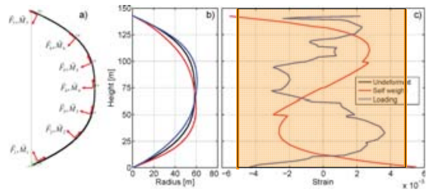

- Blade weight from ~ 157 Ton to ~ 45 Ton per blade
- 5000 µm/m limit: complex strain distribution but in control
- Less bending moments and tension during operation
- Potential for less costly pulltruded blades

DeepWind

Generator

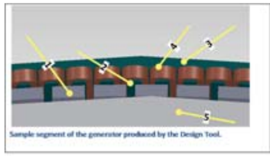

Sample segment of the generator produced by the Design Tool.

Legend:

1) Permanent magnet
2) Stator tooth
3) Stator back iron
4) Winding coil
5) Rotor back iron

3D sketch of the active parts of the 6 MW DeepWind Generator.

Dimension	Value [mm]
Outside Diameter	5811
Inside diameter	5346
Length O/A	2648

DeepWind

Magnetic Bearing

- A controlled magnetic bearing was chosen for study in a test rig
- necessary to control the forces generated by the bearing(relationship between the magnetic force and the distance is in unstable equilibrium
- DSP based control system is proposed, using appropriate sensors and a controlled power supply for each direction unstable equilibrium

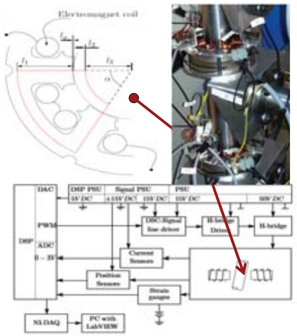

DeepWind

Baseline 5 MW Electrical system

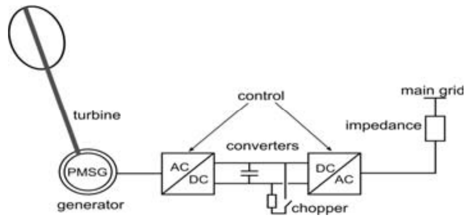

General diagram of the power transfer system.

DeepWind

Special control challenges with Deepwind

- All active turbine control via generator torque (no pitch control)
- Large 2p variations in aerodynamic torque
- Stator is not fixed,

generator speed = rotor – stator

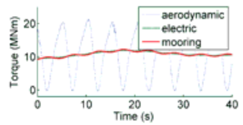

2p damping with notch filter and PI controller

DTU

DeepWind
Fault ride-though capability

- Crucial for grid code compliance
- Illustrates interesting coupling between controls, turbine and mooring dynamics

ALT 1: De-loading system
Absorb excess energy in rotation of the turbine by reducing generator torque

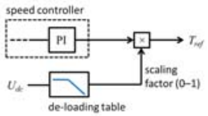

ALT 2: DC chopper system
Dump excess energy via switched resistor in DC link

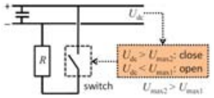

DTU

DeepWind
Simulations – fault ride-through

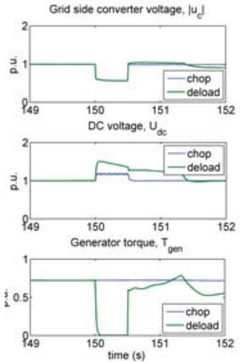

500 ms voltage dip in the grid, propagated to converter terminals

Resulting DC link voltage increase needs to be limited, to avoid damage and allow ride-through
Chopper ✓ OK
De-loading × Not working very well

Generator torque unaffected with chopper system, drastically reduced with de-loading system

DTU

DeepWind
Turbine response to grid fault

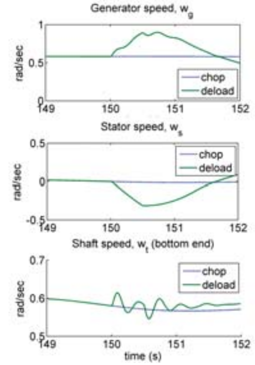

Chopper system:
Turbine completely unaffected by the fault

De-loading system:
Generator torque rapidly reduced
→ Rotor (turbine) and stator (mooring system) acceleration in opposite directions
→ Severe stress on mooring system
→ Shaft vibrations in turbine

The de-loading scheme does not work with Deepwind's non-fixed stator

But interesting illustration of the coupling between turbine/generator/mooring/controls

DTU

DeepWind
Conclusion

- Demonstration of a optimized rotor design
  - √Stall controlled wind turbine
  - √Pultruded sectionized GRF blades 2 profile sections
  - √2 Blades with~95 T total weight, ~3½x less weight than 1st baseline 5MW design
  - √Less bending moments and tension during operation
  - √Potential for less costly pulltruded blades in terms of power capture
- Use of moderate thick airfoils of laminar flow family with smaller CD_0 good C_P and favourable rigidity
- Suite available for designing deep sea underwater, new radial flux synchronous generator module
- Utilizing magnetic bearings for generator module as option
- Generator and Controller implemented in global model
- Floater optimized for most dominant variables
- Grid compliance

DTU

DeepWind
Video from Ocean lab testing

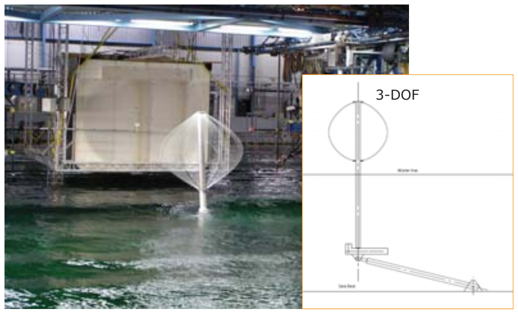

DTU

DeepWind

NTNU
Norwegian University of Science and Technology

Dynamic analysis of a floating vertical axis wind turbine under emergency shutdown using hydrodynamic brake

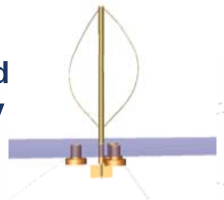

Kai Wang, Martin O.L. Hansen and Torgeir Moan

WP6 of NOWITECH
Centre for Ships and Ocean Structures (CeSOS)
The Norwegian University of Science and Technology (NTNU)

EERA DeepWind' 2014 ,Trondheim, January 22, 2014

Outline

- Background and objective
- Modeling and simulation tool
- Torque estimation of the hydrodynamic brake
- Analysis results of emergency shutdown by using the hydrodynamic brake
- Concluding remarks
- Future work

Background

- Increasing interest in floating vertical axis wind turbines
  - DeepWind Concept
  - VertiWind Concept
  - Aerogenerator X Concept

Vertical floating concepts

Courtesy of DeepWind Project

Courtesy of Marc Cahay

Courtesy of Wind Power Limited & Grimshaw

- DeepWind Concept
  - 5 MW, European project - FP7
  - Rotor Height 129.56 m
  - Rotor Radius 63.77 m
- VertiWind Concept
  - 2 MW in France
  - Rotor Height 105 m
- Aerogenerator X Concept
  - 10 MW in UK
  - Maximum Height 130 m

Background

- Increasing interest in floating vertical axis wind turbines
  - DeepWind Concept
  - VertiWind Concept
  - Aerogenerator X Concept
  - Novel concept proposed in OMAE 2013

A novel concept:
- 5-MW VAWT
- Darrieus rotor
- Semi-submersible floater
- Mooring lines

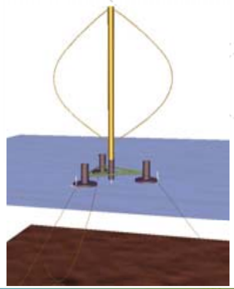

Wang, K., Moan, T., and Hansen, M.O.L. A method for modeling of floating vertical axis wind turbine. in Proceedings of the 32th International Conference on Ocean, Offshore and Arctic Engineering. 2013. Nantes, France: paper no: OMAE2013-10289.

Background

- Increasing interest in floating vertical axis wind turbines
- Distinctive features of FVAWT compared with FHAWT

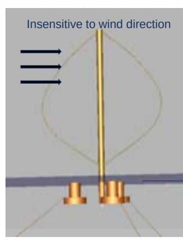

HAWT Components
1. Blade Pitch system
2. Yaw system
3. Gear box
4. Generator

VAWT Components
1. Gear box
2. Generator

Easy access to drivetrain
Reduce O&M costs

Difficult access to drivetrain
Increase O&M cost

Background

- ► Increasing interest in floating vertical axis wind turbines
- ► Distinctive features of FVAWTs compared with FHAWTs
- ► Drawbacks of the FVAWTs
  - ❖ Aerodynamic torque ripple resulting in cyclic loading on drive train and structures
  - ❖ Emergency shutdown situation

    Scenario: grid loss, loss of generator torque,

    failure of mechanical brake (possible happen in cold weather), stormy weather

    Measure: aerobrake (Spoilers)

Background

- ► Increasing interest in floating vertical axis wind turbines
- ► Distinctive features of FVAWTs compared with FHAWTs
- ► Drawbacks of the FVAWTs
  - ❖ Aerodynamic torque ripple resulting in cyclic loading on drive train and structures
  - ❖ Emergency shutdown situation

    Scenario: grid loss, loss of generator torque,

    failure of mechanical brake (possible happen in cold weather), stormy weather

    Measure: aerobrake (Spoilers)
- ► An economic and efficient braking system is preferred

Objectives

- ► Propose a novel hydrodynamic brake
- ► Establish a numerical model of the hydrodynamic brake
- ► Integrate the brake model with the coupled model of the floating vertical axis floating turbine
- ► Evaluate the effect of the hydrodynamic brake
- ► Dynamic analysis of the floating vertical axis wind turbine with the hydrodynamic brake during shutdown situation

A floating vertical axis wind turbine with hydrodynamic brake

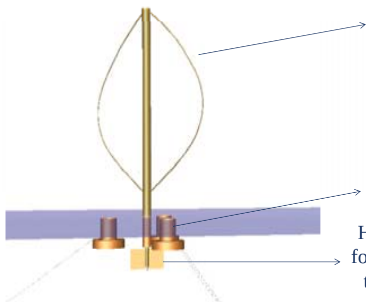

5 MW DeepWind rotor

OC4 semi-submersible

Hydrodynamic brake: four flat plates attached to the centre column

Modeling of the floating vertical axis wind turbine

RIFLEX wind turbine
Structural analysis of slender, flexible beams
(Mooring lines, tower and blades)

SIMO
Motion analysis of floating structure (rigid floater)

+

Aerodynamic loads provided through Dynamic Link Library (DLL)

=

Fully coupled model

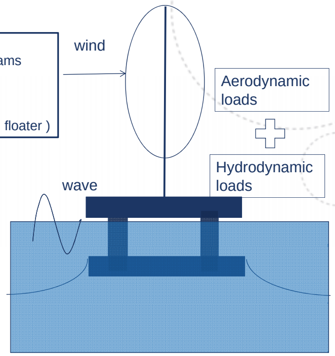

Modeling of the hydrodynamic brake

- ➢ Preliminary design of hydrodynamic brake
- ➢ Modeling as a slender beam
- ➢ Hydrodynamic coefficients
- ➢ Determination of the torque from drag force on the plate

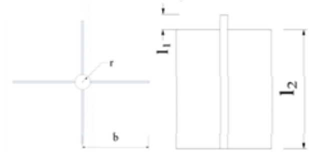

	Hydrobrake I		Hydrobrake II	
	Colomn	Plate	Colomn	Plate
Raduis/Width (m)	1.5	11	2	16
Length (m)	38.494	36	30.494	28
Thickness (m)	0.02	0.083[a]	0.02	0.083[b]
Weight (N)	551509.2	3506517.8	583500.1	4765248.1
Bouyancy (N)	2736013.9	1321983.8	3853160.8	1495577.7

[a] Sum of the hollow thickness and plate thickness of 0.014 m
[b] Sum of the hollow thickness and plate thickness of 0.017 m

Modeling of the hydrodynamic brake

- Preliminary design of hydrodynamic brake
- Modeling as a slender beam
- Hydrodynamic coefficients
- Determination of the torque from drag force on the plate

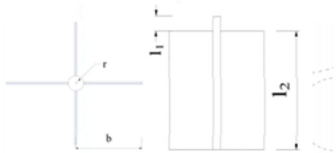

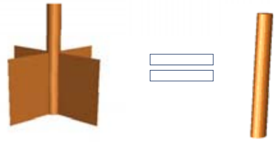

NOWITECH Norwegian Research Centre for Offshore Wind Technology

Modeling of the hydrodynamic brake (1)

- Preliminary design of hydrodynamic brake
- Modeling as a slender beam
- Hydrodynamic coefficients
- Determination of the torque from drag force on the plate

Added mass

$m_A^{hor}=\rho(1-(r/b)^2+(r/b)^4)\pi b^2 l_2$

$m_A^{ver} = \rho C_A^{ver} \pi r^2 l_2$

Drag coefficient

Cd= 1.9

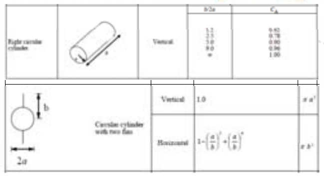

(1) Det Norske Veritas, ENVIRONMENTAL CONDITIONS AND ENVIRONMENTAL LOADS, Tech. Rep., DNV-RP-C205 (2007).

NOWITECH Norwegian Research Centre for Offshore Wind Technology

Modeling of the hydrodynamic brake (1)

- Preliminary design of hydrodynamic brake
- Modeling as a slender beam
- Hydrodynamic coefficients
- Determination of the torque from drag force on the plate

CFD simulation:
- ❖ 2D sliding mesh model
- ❖ first-order upwind
- ❖ absolute velocity formulation
- ❖ renormalized Group (RNG) k-ε turbulence model
- ❖ standard wall function for near-wall treatment
- ❖ grid mesh
  135900 inner region
  24640 outer region
- ❖ time step 0.1 s

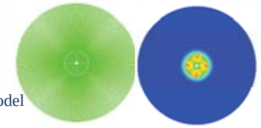

Brake I

$$T_q = -20229\omega^3 + 125338\omega^2 - 30925\omega + 2680.2$$

Brake II

$$T_q = 123523\omega^3 + 21286\omega^2 + 9917.4\omega + 19.624$$

NOWITECH Norwegian Research Centre for Offshore Wind Technology

Simulation tool: Simo-Riflex-DMS

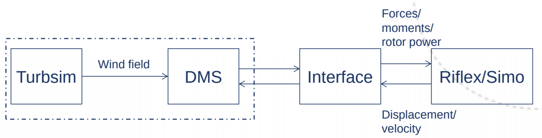

Dynamics of fully coupled model

❖ Aerodynamics

Double Multiple-Streamtube model (DMS) and BL dynamic stall model.

❖ Structural dynamics

The structural dynamics of the rotor, mooring lines and brake is calculated by the nonlinear finite element solver in RIFLEX (developed by MARINTEK).

❖ Hydrodynamics

The floater motion is simulated according to linear hydrodynamic theory plus viscous term of the Morison formula in SIMO.

❖ Wind turbine control

A PI controller is designed for generator torque.

NOWITECH Norwegian Research Centre for Offshore Wind Technology

Environmental and shutdown conditions

	Uw (m/s)	Hs (m)	Tp (s)	Turb. Model	Fault Configuration	Sim. Length
LC 1	8	2.55	9.86	NTM	A, B, C, D	2800
LC 2	10	2.88	9.98	NTM	A, B, C, D	2800
LC 3	14	3.62	10.29	NTM	A, B, C, D	2800
LC 4	18	4.44	10.66	NTM	A, B, C, D	2800
LC 5	22	5.32	11.06	NTM	A, B, C, D	2800
LC 6	25	6.02	11.38	NTM	A, B, C, D	2800

A) The original FVAWT without hydrodynamic brake and no fault happen
B) The FVAWT with hydrodynamic brake I and no fault happen
C) The FVAWT with hydrodynamic brake I and fault happen followed by free rotation
D) The FVAWT with hydrodynamic brake II and fault happen followed by shutdown

The accidence of grid loss was assumed to happen at time TF = 1200 s
The hydrodynamic brake was connected to the rotating shaft to initiate the shutdown process by a short time delay TD = 1 s.

NOWITECH Norwegian Research Centre for Offshore Wind Technology

Effect of the hydrodynamic brake I

A selection of results:

- Surge motion
- Roll motion
- Pitch motion

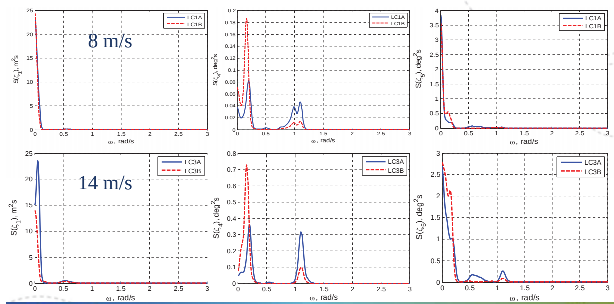

NOWITECH Norwegian Research Centre for Offshore Wind Technology

Effect of the hydrodynamic brake I

A selection of results:

➢ Mooring line tension

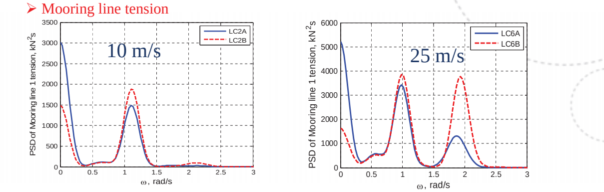

- The brake could significantly reduce the mooring tension response from the wind excitation, whereas it makes larger peak at higher frequencies.
- Besides the peak at the 2P frequency, another peak at the higher frequency was found and it should be induced by the eigenfrequency of the blade.
- With the increase of wind speed, the peak induced by structural eigenfrequency is more apparent.

Analysis of emergency shutdown by using the hydrodynamic brake I

Time history of rotational speed for different wind speed after fault occurs at TF=1200 s by using brake I

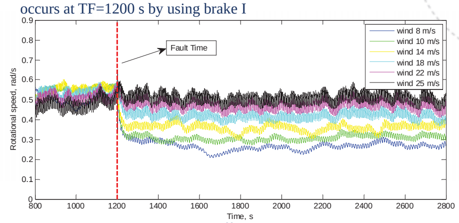

- Once the hydrodynamic brake takes effect to counter the aerodynamic torque, the rotation speed varies depending on the balance of aerodynamic torque and hydrodynamic torque
- The brake I does not give enough torque to stop the rotation, but it could avoid the overspeed of the rotor.

Analysis of emergency shutdown by using the hydrodynamic brake I

Global motion

fault configuration B vs. fault configuration C

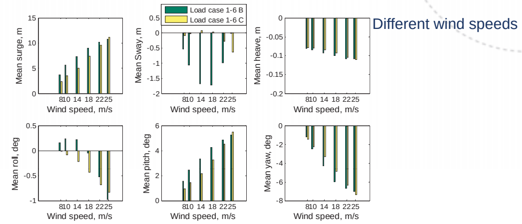

- The global motion of the platform shows better performance, which contributed from the decreasing rotational speed after the hydrodynamic brake initiates.
- Surge and pitch motion can get much more advantages while the sway and roll motions have got both good and bad effects from different load case.

Analysis of emergency shutdown by using the hydrodynamic brake I

➢ Pitch motion

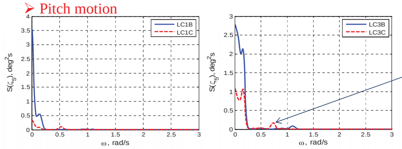

- The less wind speed, the more pitch motion reduced.
- The peak at the 2P frequency was still presented, but the 2P frequency was reduced to a lower value

➢ Fore-aft and Side-side bending moment of shaft base

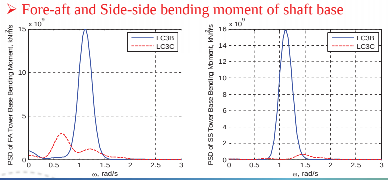

The initiation of the brake with the rotating shaft of the wind turbine together could mitigate the 2P effect and then the wave frequency excitation dominates the response of FA tower base bending moment

Shutdown process by using the hydrodynamic brake II and mechanical brake

Global platform motion, bending moment and mooring line tension

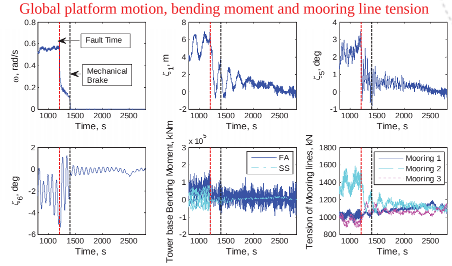

Load case 2D
V=10 m/s

Fault occurs at TF=1200 s followed by using brake II and by using mechanical brake at 1400s

Concluding remarks

- An integrated model of a floating vertical axis wind with a hydrodynamic brake was established to carry out the non-linear time domain simulation
- The effect of the hydrodynamic brake on the FVAWT was evaluated by comparing the FVAWT with the hydrodynamic brake I to the original FVAWT
- A series of promising results indicate the merit of the hydrodynamic brake used during emergency shutdown
- Combing a mechanical brake with a larger hydrodynamic brake, the shutdown could be successfully achieved.
- The application of hydrodynamic brake is expected to be efficient and promising for the emergency shutdown and reduce the platform motion and structural loads.

Future work

A more efficient brake is more attractive and promising.

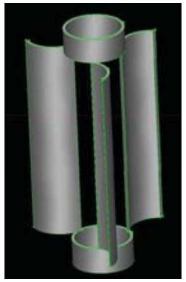

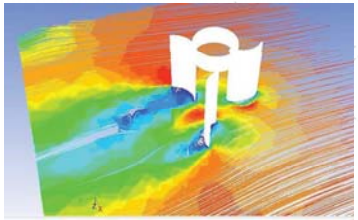

http://www.cd3wd.com/cd3wd_40/ap/Optimization_and_CFD_analysis_of_wind-powered_water_pump_system.html

Thank you for your attention!

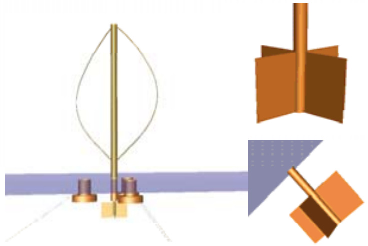

NOWITECH Norwegian Research Centre for Offshore Wind Technology

Concept design verification of a semi-submersible floating wind turbine using coupled simulations

Fons Huijs
EERA DeepWind'2014, Trondheim, 22 January 2014

GustoMSC

GustoMSC

Presentation outline

- Tri-Floater design
- Simulation approach
- Software and numerical model
- Simulation results
- Conclusions

GustoMSC

Tri-Floater design

Wind turbine	NREL 5MW
Hub height above SWL	90 m
Control system	ECN
Radius to column centre	36.0 m
Column width	8.0 m
Design draft	13.2 m
Air gap to deck structure	12.0 m
Displacement	3627 t
Catenary mooring lines	3 x 750 m
Chain diameter	100 mm

GustoMSC

Tri-Floater design

		operational			survival
		rated	above rated	cut-out	parked
significant wave height	[m]	4.5	4.5	6.5	9.4
wave peak period	[s]	7.5 – 10	7.5 – 10	9 – 12	11 – 14
wind velocity at hub	[m/s]	11.4	14.0	25.0	42.7
current velocity	[m/s]	0 – 0.6	0 – 0.6	0 – 0.6	0 – 1.2

Operational inclination	≤ 10 deg
Operational nacelle acceleration	≤ 3 m/s^2
Safety factor mooring line	≥ 1.7

GustoMSC

Simulation approach

- Verify design requirements motions and mooring loads
- Concept design stage, so minimized computational effort
- Simulation duration: 1 hour
- Weibull distribution fitted to 50 % highest extremes
- Expected maxima determined for 3 hours by extrapolation
- Time step and seed dependency studied

GustoMSC

Software and numerical model

- AQWA (Ansys)
  - Hydrodynamics (1st and 2nd order)
  - Mooring
- PHATAS (ECN)
  - Rotor aerodynamics
  - Rotor and tower structural dynamics
  - Drive-train and control systems
- Benchmarked with OC3 spar
- Hydrodynamic model validated with model tests

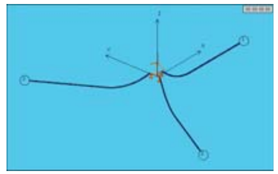

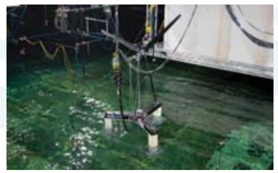

GustoMSC

Software and numerical model

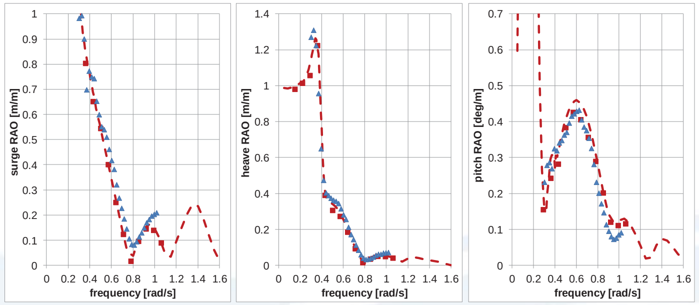

- Frequency domain motion analysis
- Coupled simulations in regular waves
- Model test in white noise

GustoMSC

Simulation results

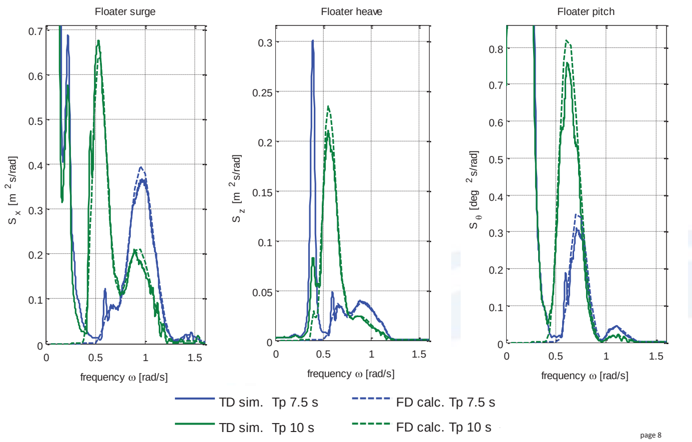

GustoMSC

Simulation results

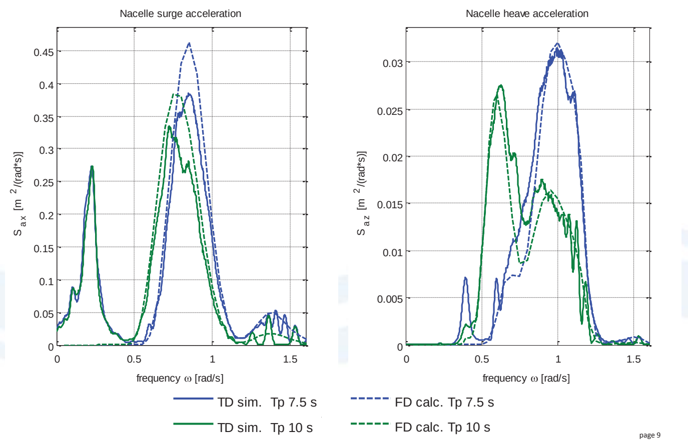

GustoMSC

Simulation results

	operational			survival
	rated	above rated	cut-out	parked
floater inclination [deg]				
mean	**3.5**	2.9	1.7	3.4
3-hour extreme (90%)	7.4	**8.5**	6.1	11.1
nacelle hor. acceler. [m/s²]				
mean	**0.7**	0.6	0.6	0.8
3-hour extreme (90%)	2.4	2.5	**3.0**	3.1

GustoMSC

Conclusions

- Tri-Floater fulfills design criteria
- Low frequency motions are dominant
- Wave frequency motions are well predicted by uncoupled frequency domain motion analysis
- Such analysis is useful to assess global floater motions in early design stages and optimize the floater design
- Coupled simulations are however indispensible in later design stages

Your Partner

www.GustoMSC.com

GustoMSC

B1) Grid connection

Power system integration of offshore wind farms, Tobias Hennig, Fraunhofer IWES

The Impact of Active Power Losses on the Wind Energy Exploitation of the North Sea, Hossein Farahmand, SINTEF Energi AS

Dynamic Series Compensation for the Reinforcement of Network Connections with High Wind Penetration, Juan Nambo-Martinez, Strathclyde University

Transient interaction between wind turbine transformer and the collection grid of offshore wind farms, Andrzej Holdyk, SINTEF Energy Research

Power System Integration of Offshore Wind Farms:

Challenges Towards Horizon 2020

Tobias Hennig, M.Sc.
Fraunhofer IWES

Agenda

- What is EERA JP Wind?
- Power system integration challenges towards 2020
- Example projects:
  - Fraunhofer IWES
  - Other projects (EERA)
- What is EERA SP4 doing towards Horizon 2020
  - The Horizon 2020 call for projects
  - EERA SP4 project proposals

EERA Objectives

- Preparing pre-competitive research laying a scientific foundation for cost effective wind power production and integration.
- **O1: Wind power plant capabilities:** Enable wind power plants to provide services and to offer characteristics similar to conventional power plants.
- **O2: Grid planning and operation:** Sustainable enlargement of the transmission capacity and enhancement of the utilisation of the grids to allow large-scale deployment of wind energy technology
- **O3: Wind energy and power management:** Tools and business models (markets) to allow economic wind power utilisation

Ambition of the Joint Programme

- The EERA vision for the joint programme on wind energy is:
  - to provide the strategic leadership for the scientific–technical medium to long term research to support the EII and the Technology Roadmap's activities on wind energy and
  - on basis of this, to initiate, coordinate and perform the necessary scientific research.
- The vision calls for all the EERA participants and associates:
  - to align their research in wind energy topics which influence the use and deployment of wind energy and
  - Perform coordinated and structured research in medium to long-term programmes with shared research facilities.

Structure of the Joint Program

- The joint program comprises the following 5 sub-programs:
  - **Wind Conditions:** coordinated by DTU in Denmark.
  - **Aerodynamics:** coordinated by ECN in the Netherlands.
  - **Offshore Wind Energy:** Coordinated by SINTEF in Norway.
  - **Grid Integration:** coordinated by FhG IWES in Germany.
  - **Research Facilities:** coordinated by CENER in Spain.

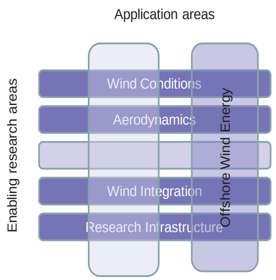

POWER SYSTEM: INTEGRATION CHALLENGES TOWARDS 2020

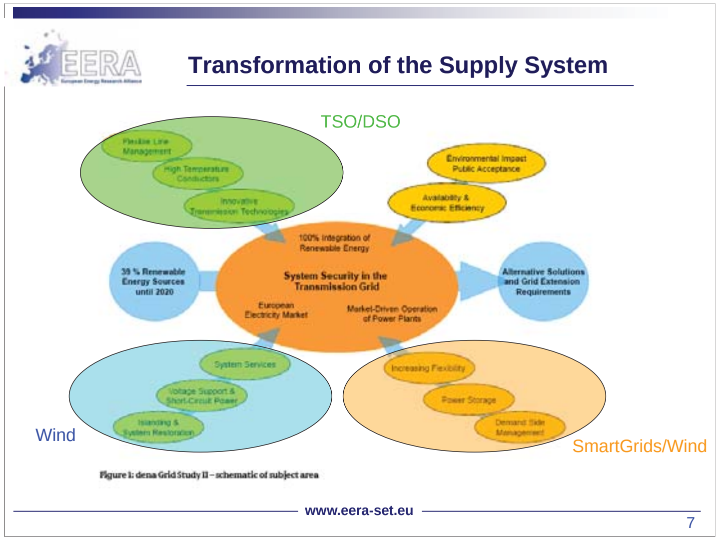
EERA
Transformation of the Supply System
TSO/DSO
Flexible Line Management
High Temperature Conductors
Innovative Transmission Technologies
Environmental Impact Public Acceptance
Availability & Economic Efficiency
100% Integration of Renewable Energy
39 % Renewable Energy Sources until 2020
System Security in the Transmission Grid
European Electricity Market
Market-Driven Operation of Power Plants
Alternative Solutions and Grid Extension Requirements
System Services
Voltage Support & Short-Circuit Power
Islanding & System Restoration
Increasing Flexibility
Power Storage
Demand Side Management
Wind
SmartGrids/Wind
Figure 1: dena Grid Study II – schematic of subject area
www.eera-set.eu
7

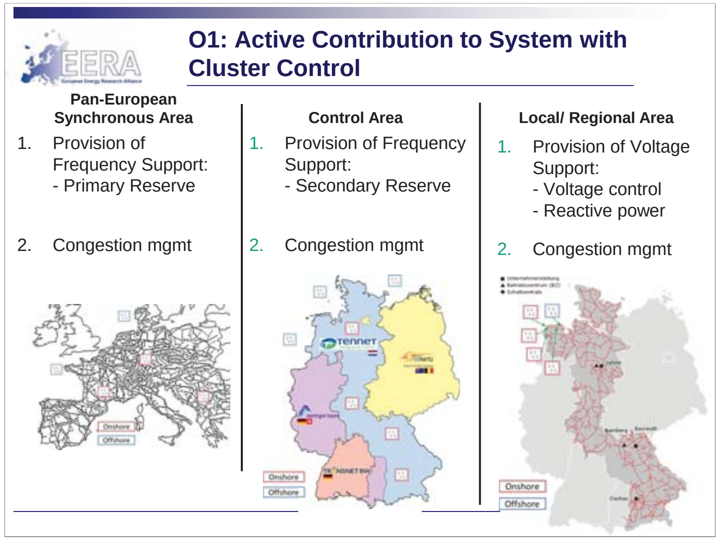
EERA
O1: Active Contribution to System with Cluster Control
Pan-European Synchronous Area
1. Provision of Frequency Support: - Primary Reserve
2. Congestion mgmt
Control Area
1. Provision of Frequency Support: - Secondary Reserve
2. Congestion mgmt
Local/ Regional Area
1. Provision of Voltage Support: - Voltage control - Reactive power
2. Congestion mgmt
Onshore
Offshore
TenneT
Onshore
Offshore
Onshore
Offshore

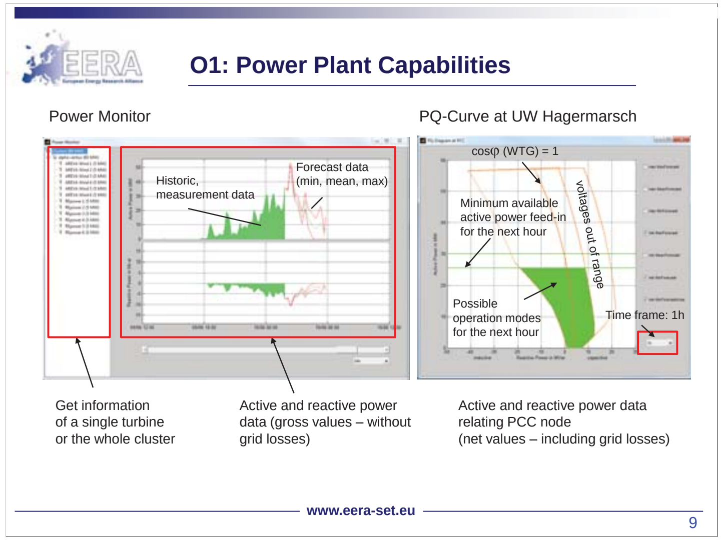
EERA
O1: Power Plant Capabilities
Power Monitor
PQ-Curve at UW Hagermarsch
Historic, measurement data
Forecast data (min, mean, max)
cosφ (WTG) = 1
Minimum available active power feed-in for the next hour
voltages out of range
Possible operation modes for the next hour
Time frame: 1h
Get information of a single turbine or the whole cluster
Active and reactive power data (gross values – without grid losses)
Active and reactive power data relating PCC node (net values – including grid losses)
www.eera-set.eu
9

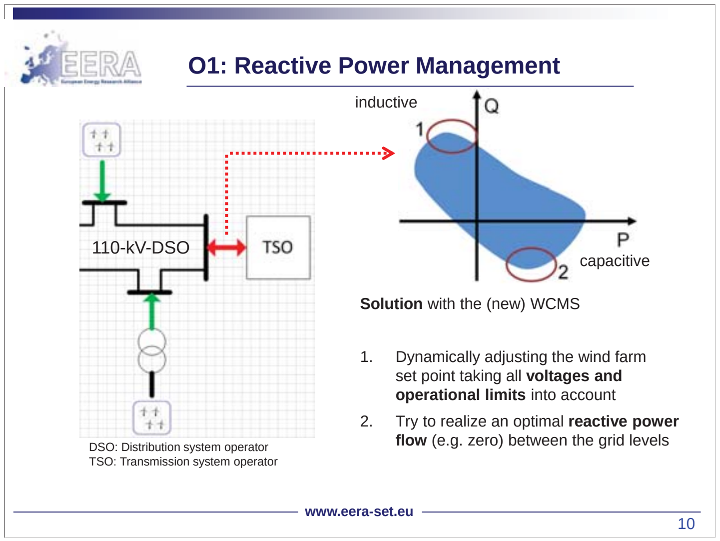
EERA
O1: Reactive Power Management
inductive
Q
1
P
2
capacitive
110-kV-DSO
TSO
Solution with the (new) WCMS
1. Dynamically adjusting the wind farm set point taking all voltages and operational limits into account
2. Try to realize an optimal reactive power flow (e.g. zero) between the grid levels
DSO: Distribution system operator
TSO: Transmission system operator
www.eera-set.eu
10

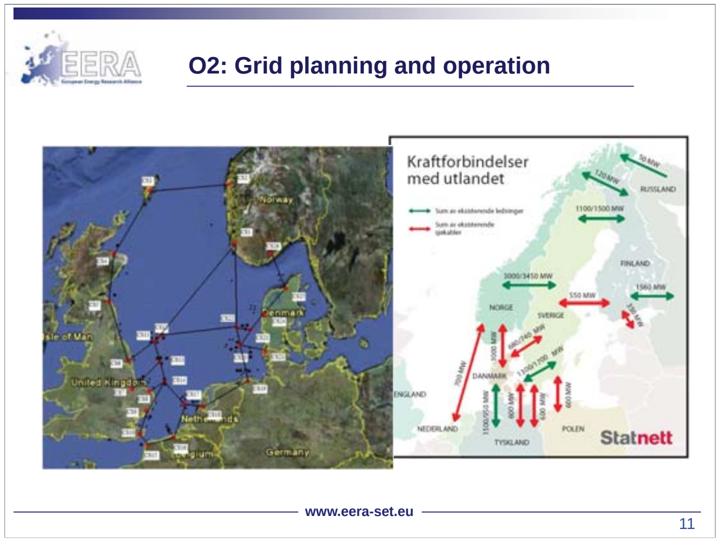
EERA
O2: Grid planning and operation
Norway
Denmark
Isle of Man
United Kingdom
Netherlands
Belgium
Germany
Kraftforbindelser med utlandet
RUSSLAND
FINLAND
NORGE
SVERIGE
DANMARK
ENGLAND
NEDERLAND
TYSKLAND
POLEN
Statnett
www.eera-set.eu
11

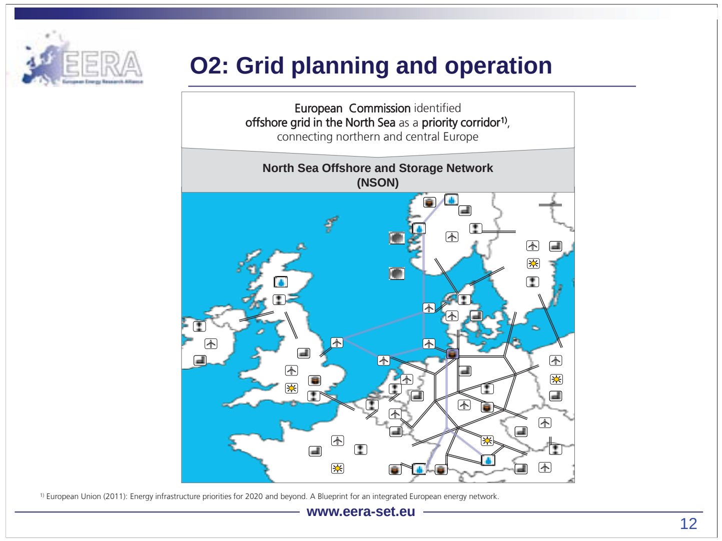
EERA
O2: Grid planning and operation
European Commission identified offshore grid in the North Sea as a priority corridor[1], connecting northern and central Europe
North Sea Offshore and Storage Network (NSON)
[1] European Union (2011): Energy infrastructure priorities for 2020 and beyond. A Blueprint for an integrated European energy network.
www.eera-set.eu
12

O2: Active Support of Grid Operation

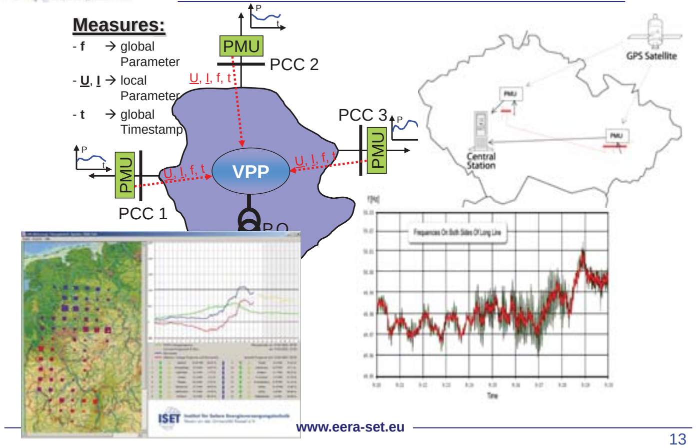

O3: Wind energy and power management

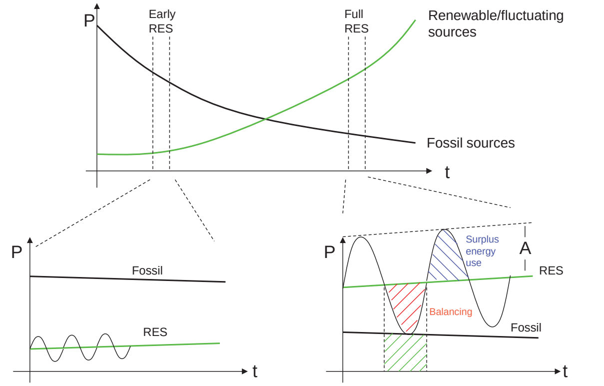

At the threshold for the age of transmission & storage

O3: Wind energy and power management

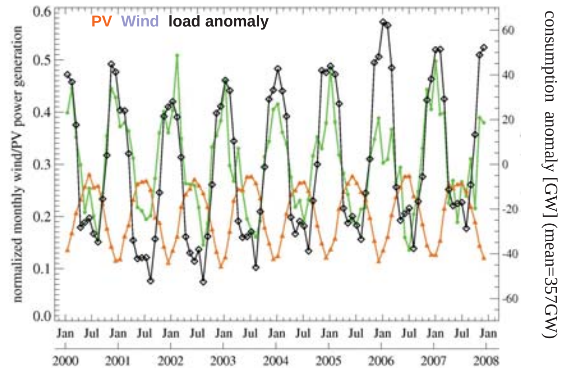

Seasonal load anomaly compared to wind and solar

O3: Wind energy and power management

➢Fluctuation of monthly residual load (RES-consumption) in a 100% renewables scenario

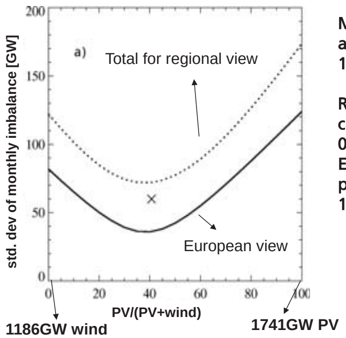

Max. reqiuired average transmission capacity: 15 GW (in D) – Max. >>>

Required storage capacity: 0,5% - 8% of average European electricity demand per year 16-260 TWh/a

Challenges

- **C:** Provision/support of system services (frequency, voltage, islanding, black start)
  R: Superior control mechanisms, VPP
- **C:** Sustainable grid extension/expansion and grid planning
  R: Models and planning tools including wind (&RES) generation
- **C:** Reliable grid (system) operation considering millions of individual generators
  R: close co-operation of TSO/DSO, generation, and trading, new operating mechanisms supported by advanced monitoring and dynamic security assessment
- **C:** balance large fluctuations in rage of x0 TWh
  R: forecast tools (minutes to months) and simulation of RES-development scenarios considering all RES and demand sectors

EXAMPLE PROJECTS

Example projects

- IMOWEN
  - Integration of large amount of wind energy using intelligent local operation and control
- EERA-DTOC
  - Design Tool for Offshore Wind Farm Clusters
  - Ancillary Service Analysis will be presented at DeepWind
- NSON
  - North Sea Offshore and Storage Network

IMOWEN

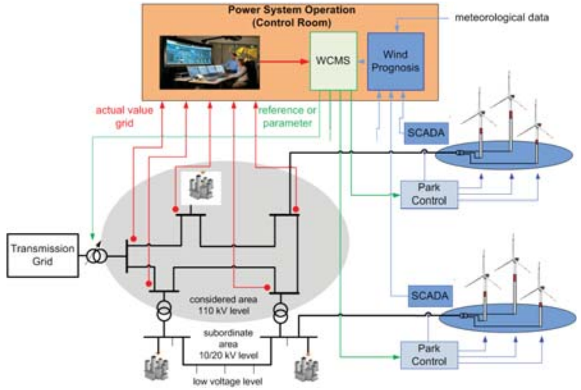

IMOWEN

- Typical 110-kV DSO district
- High penetration of wind
- Double-busbar topology, highly meshed, 7 TSO feeders, underlayed MV grid
- Cluster based on controllable wind parks with decent electrical distance

	Generation	Load	Reactive power handover in Mvar	Theoretical Controlling range (inductive and capacitive) in Mvar	Relative Possibilities
Szenario A	100 %	100 %	640 (ind.)	170	0.27
Szenario B	100 %	40 %	550 (ind.)	170	0.31
Szenario C	60 %	100 %	340 (ind.)	100	0.29
Szenario D	60 %	40 %	220 (ind.)	100	0.45
Szenario E	30 %	100 %	120 (ind.)	50	0.42
Szenario F	30 %	40 %	10 (cap.)	50	5.0

NSON

European Commission identified offshore grid in the North Sea as a priority corridor[1], connecting northern and central Europe

North Sea Offshore and Storage Network (NSON)

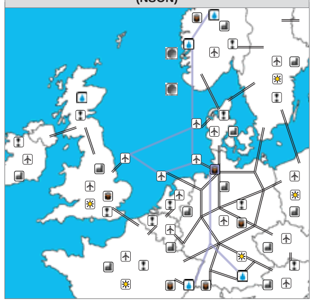

NSON initiative is determined to tackle challenges of an offshore grid in the North Sea as a combined effort of Univ. of Strathclyde, SINTEF and Fraunhofer IWES in a pre-project and feasibility phase

Objectives of the NSON initiative's pre-project and feasibility phase:

- Analyzing and evaluating different market and grid design concepts of a NSON and their socio-economic cost-benefit allocation
- Evaluating potential of offshore storage systems in a NSON
- Examining effects of a NSON on European supply system
- Assessing repercussions on onshore grid infrastructure
- Developing reusable mathematic optimization methods for transmission grid planning and operation

[1] European Union (2011): Energy infrastructure priorities for 2020 and beyond. A Blueprint for an integrated European energy network.

NSON

Technical topics for offshore power system planning:

- Portability of conventional planning rules
- Planning guidelines for DC systems
- Fulfillment of reliability and redundcy requirements
- Feedback on investment costs
- Modular expansion stages
- Optimize grid under consideration of evolving technologies and market releases of components

WHAT IS EERA SP4 DOING TOWARDS HORIZON 2020

The Horizon 2020 call for projects

- EU major challenges is to make its energy system:
  - Clean,secure and efficient, while…
  - ensuring EU industrial leadership in low-carbon energy technologies.
- Call H2020-LCE-2014/2015 aims at:
  - developing and accelerating the time to market of affordable, cost-effective and resource-efficient technology solutions
  - to decarbonise the energy system in a sustainable way
  - to secure energy supply
  - to complete the energy internal market in line with the objectives of the SET-Plan

EERA SP4 project proposals

- EERA SP4 will address various projects:
  - 4 to LCE2 → 2014
  - 1 to LCE5 → 2015
  - 1 to LCE5 → 2015
- For LCE2 (this year) is preparing:
  - 2 regarding control strategies: 1 at WF level and 1 at WT level
  - 2 regarding innovative substructures
  - 2 regarding material development
  - Proposal will be presented in April 2014

EERA SP4 project proposals

- For LCE5 and 6 (next year) are two pre-proposals:
  - North Sea Offshore and Storage Network (NSON) “phase one” proposal
  - Minimization of curative re-dispatch improving preventive methods based Wind Cluster Management Infrastructure

Nationally funded NSON projects part of a pre-project/ feasibility phase – H2020 NSON project on European level next step towards realization

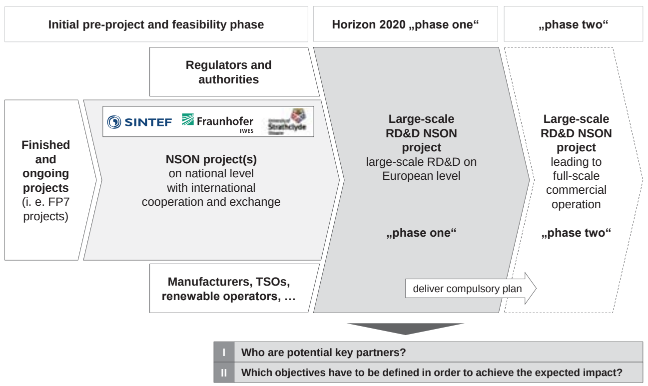

North Sea Offshore and Storage Network (NSON) proposal

- **Addressing:** LCE5 - Innovation and technologies for the deployment of meshed off-shore grids
- **Deadline:** 03/03/2015

Expected impact:

- **Accelerating** the **deployment** of **meshed HVDC off-shore grids**, with particular emphasis on Northern Seas partner countries, **before 2020**
- Ensuring that the **technology** will be **ready for deployment** in other regions in Europe for all transnational corridors defined in the trans-European energy infrastructure regulation, or be **compatible** (plug-and-play) **with** other **upcoming technologies** (e.g. ocean energy, solar energy, geothermal energy, etc. as soon as these technologies are ready for similar capacities)
- Ensuring **plug-and-play compatibility of all relevant equipment** of the key suppliers
- **Preparing** for **corresponding priority infrastructure** projects identified under the trans-European energy infrastructure regulation
- **Facilitating** the efficient **connection** of **off-shore wind resources to on-shore loads** and with other available generation **resources for balancing**, covering the main Northern Seas partner countries

Minimization of curative re-dispatch improving preventive methods

- **Addressing:** LCE6 - Transmission grid and wholesale market
- **Deadline:** 03/03/2015

Expected impact:

- To develop:
  - a) methodology to reduce the utilization of the curative methods;
  - b) manager system allows for mitigative actions of wind power plants and controllable power system components prior to an incident.
- Applying a continuous coordination process ? intelligent mgmt system.
- Usage of high resolution probabilistic forecast data for intermittent renewable energy resources.
- Usage of additional Information provided by the WCMS to the TSO

THANK YOU FOR YOUR ATTENTION.

EERA DeepWind'2014 Deep Sea Offshore Wind R&D Conference, Trondheim, 22-24 January 2014

The Impact of Active Power Losses on the Wind Energy Exploitation of the North Sea

Hossein Farahmand, Leif Warland, Daniel Huertas-Hernando
SINTEF Energy Research,

Hossein.Farahmand@sintef.no
Leif.Warland@sintef.no
daniel.h.hernando@sintef.no

Outline

- Propose an approach based on linearized active power losses
- Compare the linearized approach with iterative approach and AC optimal power flow using IEEE 9-bus case study
- Study the effect of active power losses on the study case including the Nordic system and Germany

Assumptions for DC power flow approximation

- Reactive power is neglecting ($Q_{ij} \approx 0$)
- Ignore line resistance ($Z_{ij}=R_{ij}+jX_{ij} \approx jX_{ij}$)
- Flat voltage profile, all voltage magnitudes are equal to 1 per unit ($V_i \approx V_j \approx 1$)
- Linearized: $\cos\theta \approx 1$, $\sin\theta \approx \theta$ (small θ)

Incorporation of power losses

- Active power loss at transmission line "*ij*":

$$P_{loss} = r_{ij} \cdot I_{ij}^2 \approx r_{ij} \cdot \frac{(\theta_i - \theta_j)^2}{x_{ij}^2}$$

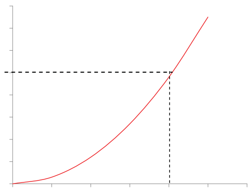

- Active power losses are proportional to the **square** of the flow through the transmission line

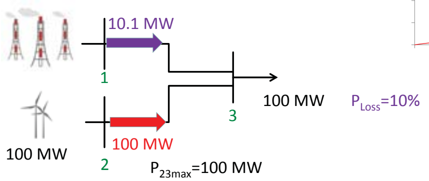

Linearized power losses

- We compared two approaches
  - Iterative approach to consider losses
  - Our approach to incorporate linearized power losses in DC Optimal Power Flow
- AC Optimal Power Flow (AC-OPF) → benchmark

Iterative approach

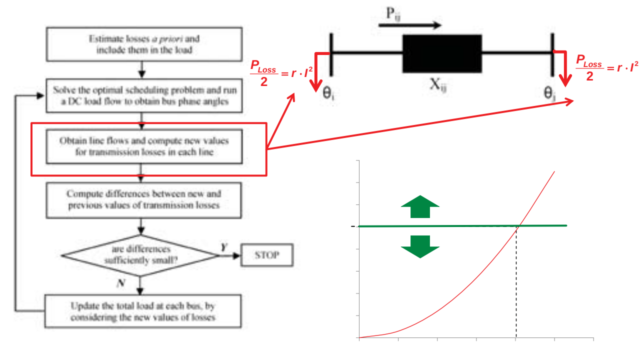

The optimisation problem is updated at each iteration with new information about the **value** of the losses

Proposed Approach

We linearize losses around operating point

$$P_L \approx a + b\Delta\theta = -\frac{r\Delta\theta_0^2}{x^2} + 2\frac{r\Delta\theta_0}{x^2}\Delta\theta$$

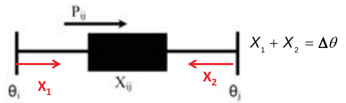

$$P_L \approx -\frac{r\Delta\theta_0^2}{x^2} + 2\frac{r\Delta\theta_0}{x^2}(x_1 + x_2)$$

This approach provides the feedback from active power losses to the optimisation routine → The optimisation problem can evaluate the trade-off between generation costs and transmission losses to find an optimum solution.

Iterative process to update coefficients of linearized losses

- Using the value of Δθ from previous step, a new linearized function of branch losses can be found → a,b can be updated

$$P_L \approx a + b\Delta\theta = -\frac{r\Delta\theta_0^2}{x^2} + 2\frac{r\Delta\theta_0}{x^2}\Delta\theta$$

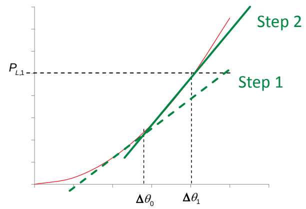

9-bus case study

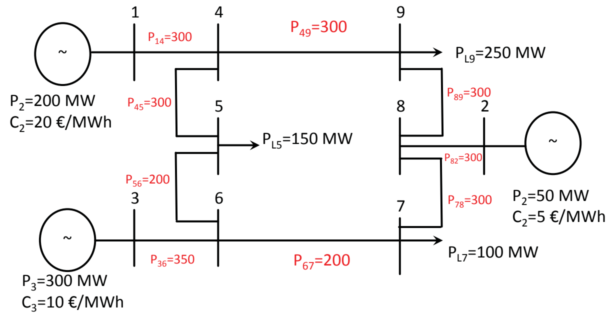

Cost comparison

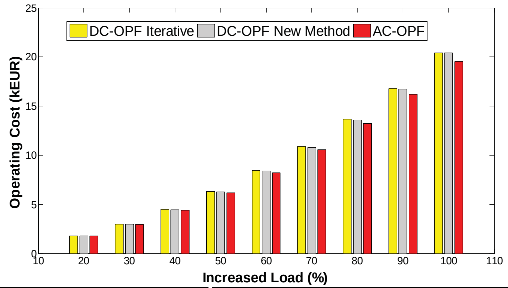

Approaches	Cumulative Operating Cost kEUR
AC-OPF	83.05
Linearized loss	85.46
DC-OPF	85.77

Approaches	Average Generation		
	G1 (20 €/kWh)	G2(5 €/kWh)	G3(10 €/kWh)
AC-OPF	107.8	50	147.06
Linearized loss	107	50	152.67
DC-OPF	109.89	50	150.58

Loss comparison

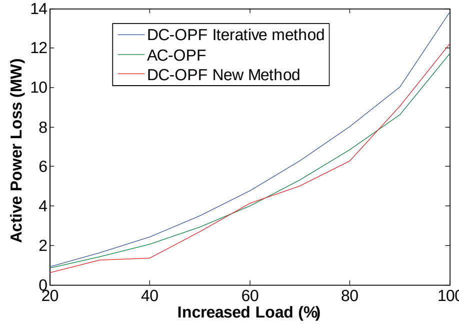

Error	Cumulative error in loss calculation (MW)
|(DCOPF)-(ACOPF)|	**17.31**
|(linear loss)-(ACOPF)|	**7.41**

Warm start problem

Our optimisation problem:

minimize $F(x) = \underline{C}x$

Subject to:

$\underline{b}_{low} \leq \underline{Ax} \leq \underline{b}$

$\underline{x}_{lb} \leq \underline{x} \leq \underline{x}_{ub}$

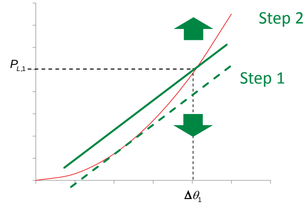

In order to use warm start functionality we cannot update "**A**" matrix →only "a" value in linearized function of branch losses can be updated

$$P_L \approx a + b\Delta\theta = -\frac{r\Delta\theta_0^2}{x^2} + 2\frac{r\Delta\theta_0}{x^2}\Delta\theta$$

Warm start problem (fixed slope)

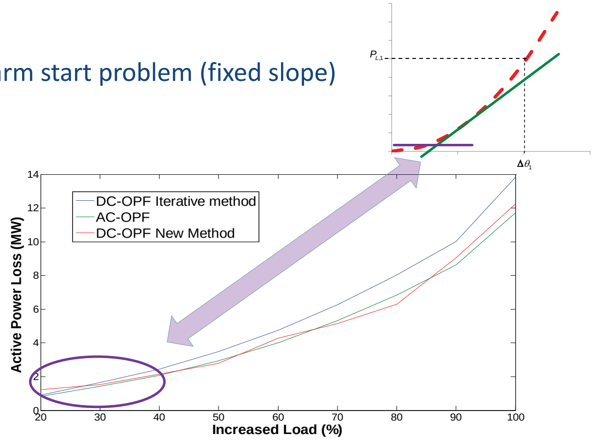

Combination of fixed value of losses and linearized losses with fixed slope

Approaches	Cumulative Operating Cost kEUR
AC-OPF	83.05
Linearized loss	85.46
Combined method	85.56
Fixed slope	85.61
DC-OPF	85.77

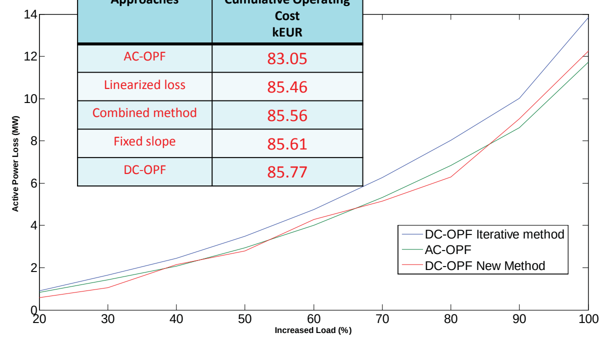

PSST Model (Flow-Based Market Model)

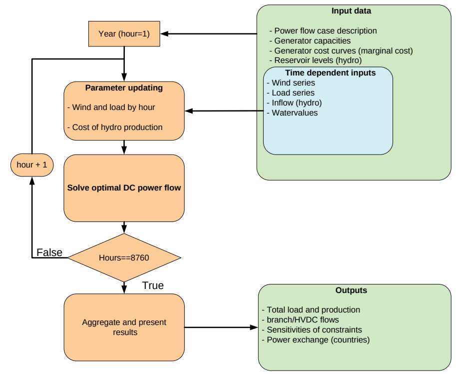

M. Korpås, L. Warland, J. O. G. Tande, K. Uhlen, K. Purchala, and, S. Wagemans, "Grid Modelling and Power System Data," SINTEF Energy Research, TradeWind EU project, Tech. Rep. D3.2, Dec. 2007.

Nordic system & Germany in 2030

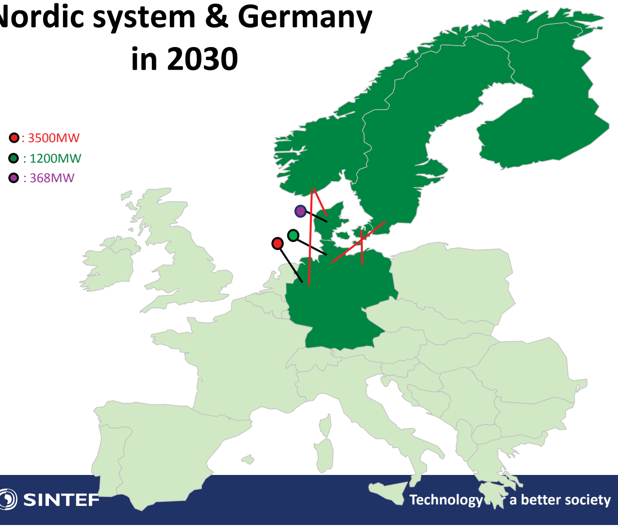

Offshore Wind Production

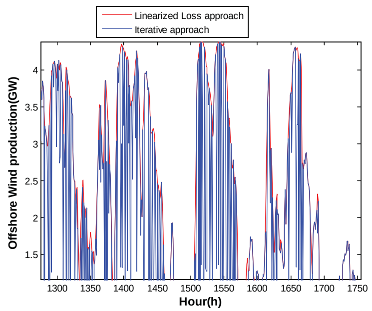

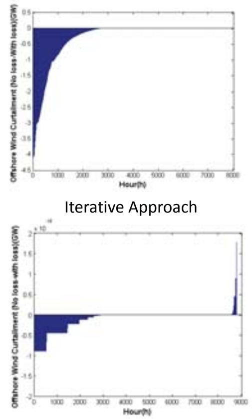

Approaches	Annual operating cost (bn Euro)
No Loss	41.43
Linearized loss	43.41
Iterative	44.46

The effect of power losses on exchange power across NorGer link (Loss percentage =3.5%)

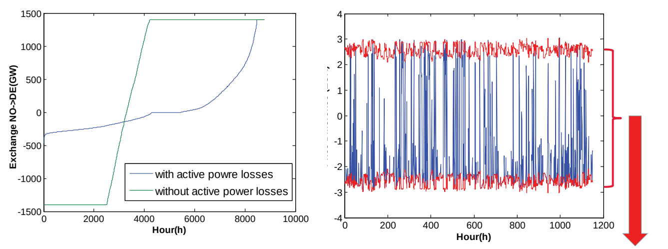

Jaehnert, Stefan; Wolfgang, Ove; Farahmand, Hossein; Völler, Steve; Huertas-Hernando, Daniel.(2013) Transmission expansion planning in Northern Europe in 2030—Methodology and analyses. *Energy Policy.*

Concluding Remark

- New methodology to include active power losses is proposed→ linearized loss curve
- This approach provides the feedback from active power losses to the optimisation routine
- Including losses may reduce the utilisation of offshore wind, therefore it is important to let the optimisation routine to evaluate the trade-off between generation costs and transmission losses to find an optimum solution
- Including power losses reduce the power exchange on HVDC link because the price difference at both ends of HVDC link should be sufficient to cover the losses on the link

Dynamic Series Compensation for the Reinforcement of Network Connections with High Wind Penetration

Juan Carlos Nambo-Martinez
Kamila Nieradzinska
Olimpo Anaya-Lara

EERA Deepwind 2014
23 January 2014, Trondheim, Norway

Content

Government Targets

Scottish Targets -

- **80% of power from Renewables by 2020**
- Interim target of 31% by 2011
- Currently at 25% (2008 figure)
- 20% of primary energy by 2020
- **Emission reduction target of 80% by 2050**
- Interim target of 42% by 2020

UK Targets –

- **32% of power form renewables by 2020**
- Currently at 7%
- 15% of primary energy by 2015
- **Emission reduction target of 80% by 2050**

SCOTTISH DEVELOPMENT INTERNATIONAL

Scotland's Market Strength in Onshore Wind

Country		Operational	Under Construction	Consented	In Planning
Scotland	MW Capacity	2267	976	1824	4040
	No of Turbines	1304	478	760	1613
England	MW Capacity	805	91	1363	1546
	No of Turbines	675	53	576	629
Wales	MW Capacity	350	27	145	964
	No of Turbines	449	14	62	404
Northern Ireland	MW Capacity	309	30	234	737
	No of Turbines	217	12	105	307
UK Total	**MW Capacity**	**3732**	**1124**	**3566**	**7287**
	No of Turbines	**2645**	**557**	**1503**	**2953**
	Percentage of Scottish MW against UK total	**61%**	**87%**	**51%**	**55%**

Offshore Wind Current Status

UK now has more installed capacity than the rest of the world combined as the 300MW Thanet project went online on September 2010

Current Capacity	Under Construction	With Planning Permission	In Pipeline	Total
3,653MW	1,152MW	2,620MW	43,238MW	50,663MW

Rest of the world installed capacity = 1,762MW

The **UK is the largest market in the world for offshore** wind and will remain so for the foreseeable future.

Major turbine manufacturers who have announced that they will set in in the UK include – Siemens, GE Energy, Gamesa and Mitsubishi Heavy Industries

UK ROUND 3 OFFSHORE WIND SITES - 32GW

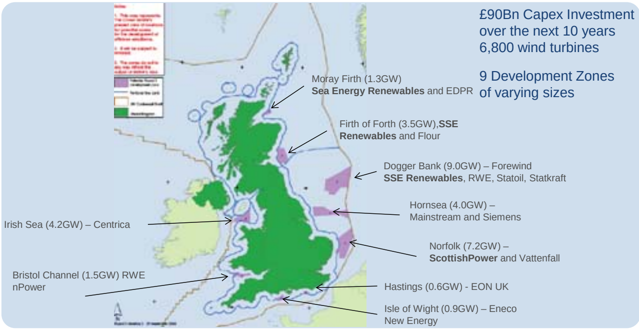

Grid availability and reliability

Total Capacity 25GW

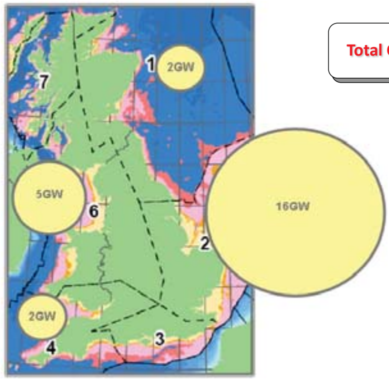

Geographical Distribution of RD 3 Offshore Wind

nationalgrid
The power of action

Grid reinforcements – Scotland to England

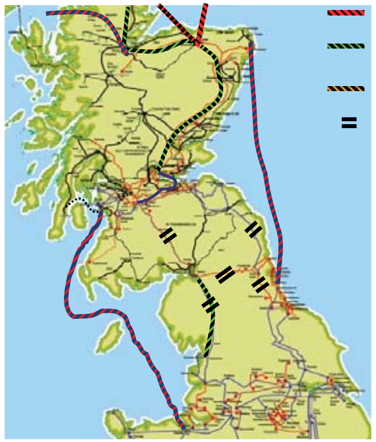

HVDC circuit

Re-conductor or re-insulate existing double circuit overhead line route

Full re-build or new build double circuit overhead line route

Series compensation (equipment located at terminal substations)

Seeking to develop wide area monitor and control to enable:-

1) Maximise stability limits
2) Use Thyristor control on series compensation to maximise thermal transfers.

nationalgrid
The power of action

Enabling Renewable Energy -The Grid

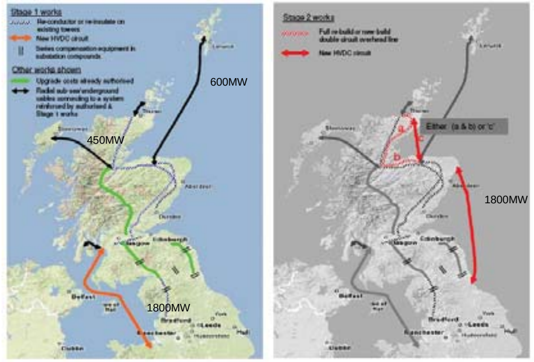

Energy Networks Strategy Group

£3.5Bn Capex Investment over the next 10 years

Simplified dynamic model

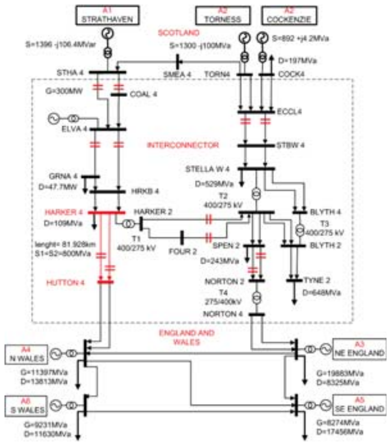

Series compensation

Series Compensation (SC) basically consist in connecting a Capacitor in series to a transmission line to cancel a portion of the reactive line impedance and thereby to increase its transmittable power capacity.

$$P = \frac{VsVr}{X_{eff}} \sin\delta$$

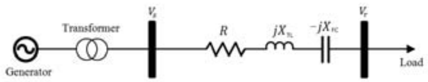

$$X_{eff} = X_{TL} - X_{SC}$$

The relation between the reactances of the transmission line and the series compensator is given by the series compensation ratio k, where,

$$k = \frac{X_{SC}}{X_{TL}}$$

Thus, the effective reactance and active power in terms of the series compensation ratio are:

$$X_{eff} = X_{TL}(1-k) \qquad P = \frac{V_s V_r}{X_{TL}(1-k)} \sin\delta$$

Dynamic Series Compensation: Thyristor Controlled Series Capacitor (TCSC)

A TCSC is a device which can behave as a variable capacitor or inductor, providing a range of variable reactance.

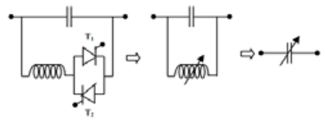

It is basically a fixed capacitor in parallel connection with an inductor. With a proper control of the antiparallel thyristors the inductor can vary its effective inductance and as such the TCSC can be controlled to behave as a variable inductor or as a variable capacitor.

$$X_{LC} = \frac{X_L X_C}{X_L + X_C}$$

Considering the end voltages and the impedance of the transmission line constant, the plot δ vs P for different k is shown below

$$P = \frac{V_s V_r}{X_{TL}(1-k)} \sin\delta$$

P_{MAX} occurs at δ = 90°

Where,

Sin90° = 1

Which means that,

$$P_{MAX} = \frac{V_s V_r}{X_{TL}(1-k)}$$

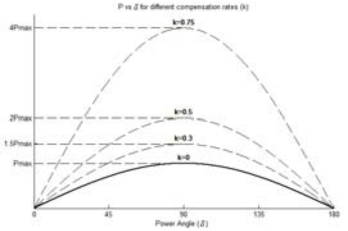

Series Compensation Ratio (k)	Maximum Active Power transference capability in terms of P_{MAX}
0	P_{MAX}
0.33	$1.5P_{MAX}$
0.5	$2P_{MAX}$
0.75	$4P_{MAX}$

Thyristor Controlled Series Capacitors (TCSC) capabilities

- **Upgrade of the Power Transmission capabilities of the path**
- **Damping of Power Oscillations**
- Improvement of the System Stability
- Reduction of System Losses
- Improvement of Voltage Profile at both Ends of the line
- Optimization of Power Flow between Parallel Lines
- Dynamic Power Flow Control
- Mitigation of Subsynchronous Resonance

Case studies

- Circuit 1. Double AC transmission circuit
- Circuit 2. Single AC transmission circuit // HVDC
- Circuit 3. Single AC transmission circuit with dynamic series compensation (TCSC) // HVDC
- Circuit 4. Double AC transmission circuit // HVDC
- Circuit 5. Double AC transmission circuit with dynamic series compensation (TCSC) // HVDC

Circuit 1. Double AC transmission circuit: The Harker-Hutton GB transmission path

Provides the parameters at which the transmission path between Harker-Hutton is operating

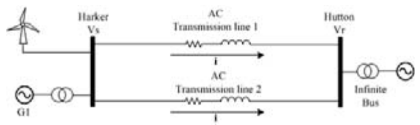

- The power injected to each transmission line at Harker is S=800+j120 MVA

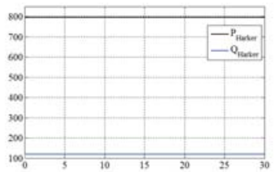

Power transmitted through each AC line

- The power delivered by both lines at Hutton is 1550 + j155 MVA

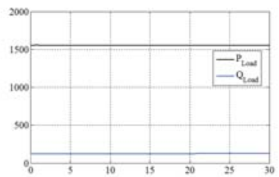

- The power angle generated between the Harker-Hutton transmission path $\delta_{H\text{-}H}$=7.49 degrees

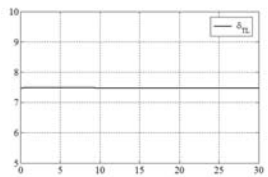

- The voltages at the receiving ends are V_s=0.98 pu and V_r =0.96 pu

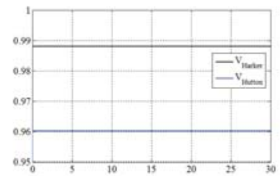

Single Parallel AC-DC Circuits

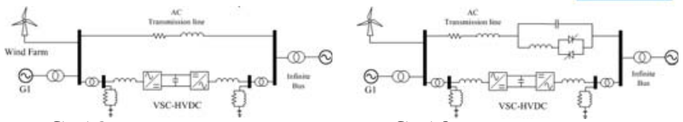

Circuit 2 Circuit 3

• Power injected at the Sending End: 2.4GW (50% of increase with respect to Circuit 1)

• Under normal conditions it is desired that the HVDC link transmits 1.2GW and the leftover 1.2GW are transmitted by the AC line

• Both HVDC and TCSC start operating at t=2s

• The HVDC link is taken out of operation at t=15s

•The signals obtained by the simulation of Circuit 2 are displayed by the dotted lines, while the signals from Circuit 3 are displayed as full lines

- 0s < t < 2s
  - Both the HVDC link and the TCSC are not operating

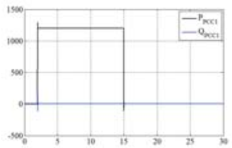

  - All the power is flowing through the AC transmission lines

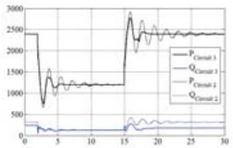

  - The TCSC provides a minimum compensation reactance of 15% (4.15Ω) which produces $X_{Equivalent}$ to decrease to 20.85Ω

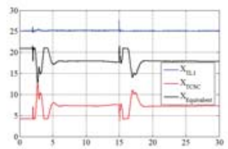

o Enhancements of Circuit 3 with respect to Circuit 2

▪ Reactive Power consumed at the Sending End: 350MVar in Circuit 2, 250MVar in Circuit 3

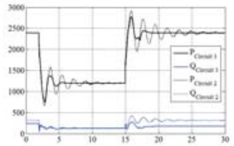

▪ Power Angle Harker-Hutton ($\delta_{H\text{-}H}$): 22.5^0 in Circuit 2, 18.5^0 in Circuit 3

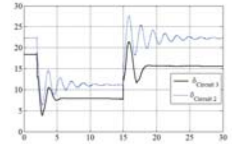

▪ Voltage profile at the Sending End: 0.982 in Circuit 2, 0.987 in Circuit 3

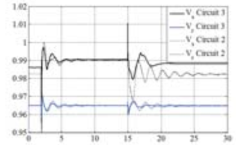

- 2s < t < 15s
  - At t=2s both HVDC and TCSC start to operate
  - The HVDC immediately demands 1.2GW from the Sending End

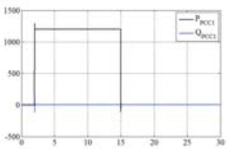

  - Power oscillations with a frequency close to 0.6Hz occur at the AC side of the circuit
  - In Circuit 2 the Power Oscillations last for about 10 seconds (2s<t<12s)
  - In Circuit 3 the TCSC damping action is noticeable from the first Power Swing
  - The TCSC brings the system to a steady state after 4 seconds (at t=6s)

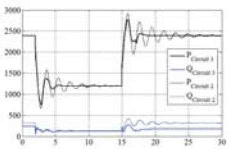

  - After the system reaches the steady state at t=6s, the TCSC sets its capacitive reactance at 8.3Ω which means 33% of Reactive Series Compensation

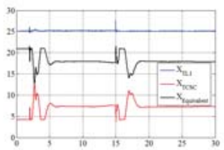

Conclusions

TCSCs allows for the increase in the power capabilities of a transmission line while the end voltages and the power angle of the transmission line remain close to the original values

TCSCs are capable to damp power oscillations and with this to improve the interaction between an AC-DC parallel circuits

Future Work

Future works includes an analysis of parallel AC-DC circuits compensated by dynamic series compensation, where the HVDC converters provide AC voltage Control at the Point of Common Coupling (PCC).

Where it is expected that the AC voltage control obtained with the HVDC links provides an additional improvement in the power capabilities of a transmission line to the one obtained with the use of TCSCs.

University of Strathclyde Glasgow

Transient interaction between wind turbine transformers and the collection grid of offshore wind farms

Andrzej Holdyk
SINTEF Energy Research
Deep Wind 2014, 23 January 2014

Outline

- Project description
- Interaction between components
- Electrical resonance
- Resonance overvoltages
- Example: Energization of a radial
- Summary

PhD project

- This presentation is mostly based on results from Ph.D. project:
  - Technical University of Denmark
  - PhD project title: Compatibility of Electrical Main Components in Wind Turbines, EMC Wind
  - Duration: 2010:2013
  - PhD thesis: Interaction between components in wind farms.

What is transient interaction?

- In 1979, WG 12-07 (Transformers): "Resonance Behavior of High-Voltage Transformers"
  - resonance phenomenon is not a matter of a passive structure (transformer) alone
  - an active structure providing various sources of oscillating voltages needed
  - transformer resonance very difficult to occur and needs:
    - its winding's natural frequency and excitation frequency coincide
    - amplitude of excitation voltage is sufficiently large and of appropriate duration
- 2013: Cigré Working Group A2/C4.39: Electrical Transient Interaction between Transformers and the Power System
  - 'Transformers suffer dielectric failure even with good insulation coordination studies and well-accepted insulation design practices'.
- Investigation in OWF still needed

Electrical resonance

- Excitation of an electric system containing inductances and capacitances results in oscillations -> natural frequency
$$f = \frac{1}{2 \cdot \pi \cdot \sqrt{L \cdot C}}$$
- Resonance when periodic source has frequency similar to the circuit's natural frequency
- High amplification of voltage/current due to energy exchange between electric and magnetic field
- Depending on connection: series or parallel resonances

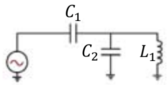

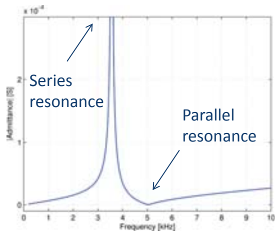

Resonance overvoltages

- Stationary resonance – stationary source of excitation
- Transient resonance – aperiodic excitation:
  - Two or more natural frequencies need to be present, i.e. network must contain at least two adjacent parts having similar resonance frequency:
$$\frac{1}{\sqrt{L_1 \cdot C_1}} = \frac{1}{\sqrt{L_2 \cdot C_2}}$$
  - The two network parts have large difference in characteristic impedance, $Z_0 = \sqrt{\frac{L}{C}}$
$$\sqrt{\frac{L_1}{C_1}} \ll \sqrt{\frac{L_2}{C_2}}$$
  - The source of the oscillation must come from the part of network characterized by the low characteristic impedance

Resonance overvoltage example

- The conditions might fulfilled for cable-transformer system
- Cable resonance frequency depends on length
- High overvoltages might occur on transformer terminals
- Important for Offshore Wind Farms, which contain large amount of cables and transformers
- Example might resemble energization of a radial

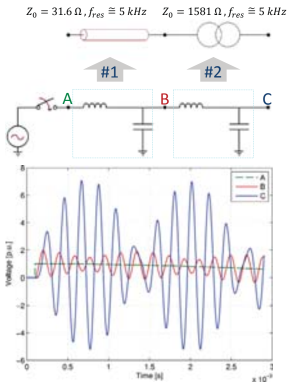

Sources of oscillations in OWF

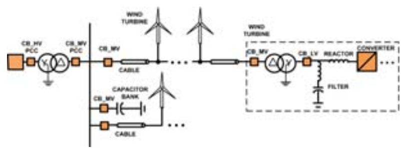

- Main sources of oscillations
  - External grid
  - Circuit breakers (HV, MV, LV) -> switching
  - Converter
  - Faults

Example: energization of a radial

- External grid / park transformer -> X/R
- 3-phase submarine cable: 50 mm^2
  - 4 sections of 400 m
  - J.Marti models in ATP
- Wind turbines
  - 100 kVA transformer
    - Wide band model
    - Admittance matrix measurements
    - sFRA commercial device
    - Admittance matrix approximated with VF
    - Passivity enforced
    - Included in ATP-EMTP as a lumped parameter network
    - LV terminals left open

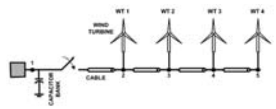

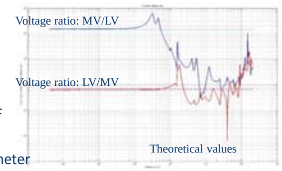

Example: energization of a radial

- Close breaker poles
- Voltage oscillation due to wave reflectio
- $f = \frac{1}{4\tau}, f = \frac{2n-1}{4l\sqrt{LC}} = \frac{2n-1}{4l} \cdot v = \frac{2n-1}{4\tau}$

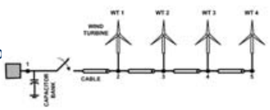

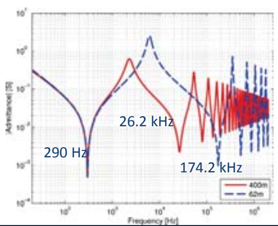

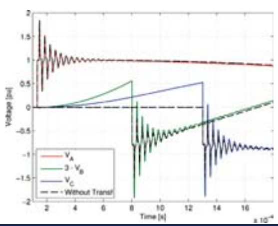

Example of resonance excitation in OWF

- Voltage oscillations visible at terminals of all wind turbines
- The same frequency at all turbines
- Driving-point admittace at WT 4 and PSD of a surge waveforms at phase A

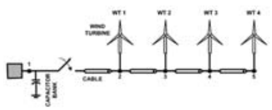

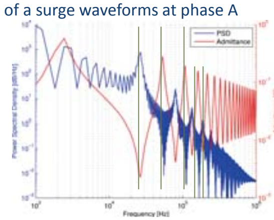

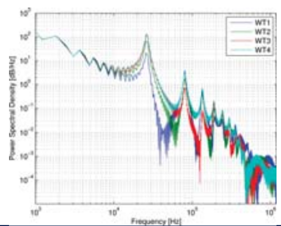

Example: resonance overvoltages

- Oscillation frequency matches resonance frequency of transformer
- Large overvoltage at LV terminals of transformer
- Magnitude depends also on loading

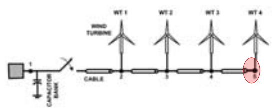

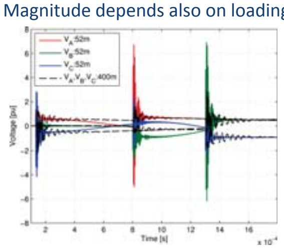

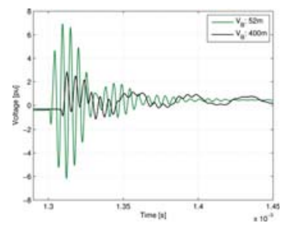

Influence of point of discontinuity for wave

- Cables of different cross sections
- Different cross-sections = different characteristic impedance Z_0
- Point of discontinuity = additional reflections
- Short cable lengths between point of discontinuity = higher frequencies
- Might increase maximum overvoltage above 2 p.u.

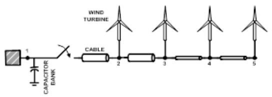

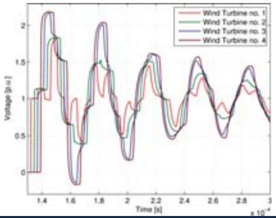

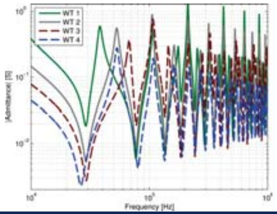

Influence of line bifurcation

- Subsections (branches) of strings often in large OWF
- Line bifurcation introduces additional reflections due to characteristic impedance missmatch
- Increases number of higher frequency oscillations
- Might cause maximum overvoltages > 2 p.u.

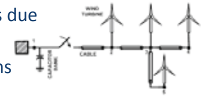

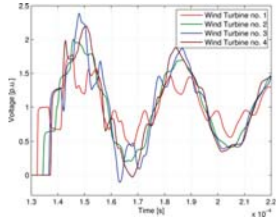

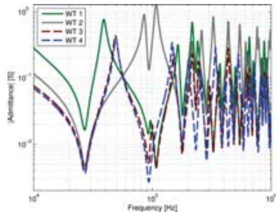

Example of OWF with complex topology

- Modern large OWF
- 111 x 3.6 MW wind turbines
- 12 strings
- 400 MW
- Cable cross-sections: (500, 240, 150 mm^2)
- Model:
  - ATP-EMTP
  - Frequency dependent cable model
  - Transformers based on SC and OC tests with additional capacitances

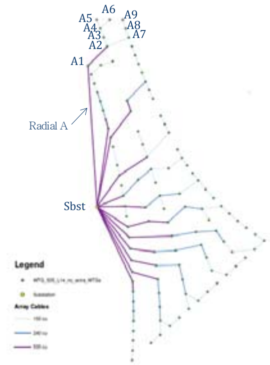

Reflections vs. transformer voltage ratio

- Voltage ratio (high to low) of several wind turbine transformers
  - Calculated from short circuit measurements
  - TR7 and TR8 -> dry type
  - TR10 – TR12 -> liquid insulated
  - High voltage amplification above approx. 200kHz
- Oscillations in string corresponding!

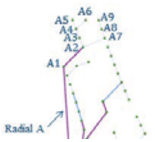

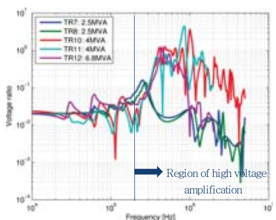

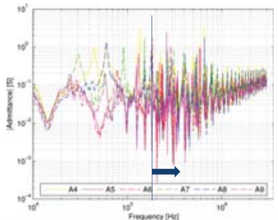

Summary

- Voltage oscillations of appropriate frequency and duration might excite transformer resonance
- Transient interaction important in OWF due to large amount of cables and transformers
- Line bifurcation and point of discontinuity for voltage wave introduce high frequency oscillations
- These oscillations are in the region of high amplification in voltage transfer of liquid insulated wind turbine transformers
- This might lead to resonant overvoltages at LV side of WT transformers
- This phenomenon depends on specific design of an OWF

The end

- Thank you for your attention.

Transient interaction between wind turbine transformers and the collection grid of offshore wind farms

Andrzej Holdyk
SINTEF Energy Research
Deep Wind 2014, 23 January 2014

Outline

- Project description
- Interaction between components
- Electrical resonance
- Resonance overvoltages
- Example: Energization of a radial
- Summary

PhD project

- This presentation is mostly based on results from Ph.D. project:
  - Technical University of Denmark
  - PhD project title: Compatibility of Electrical Main Components in Wind Turbines, EMC Wind
  - Duration: 2010:2013
  - PhD thesis: Interaction between components in wind farms.

What is transient interaction?

- In 1979, WG 12-07 (Transformers): "Resonance Behavior of High-Voltage Transformers"
  - resonance phenomenon is not a matter of a passive structure (transformer) alone
  - an active structure providing various sources of oscillating voltages needed
  - transformer resonance very difficult to occur and needs:
    - its winding's natural frequency and excitation frequency coincide
    - amplitude of excitation voltage is sufficiently large and of appropriate duration
- 2013: Cigré Working Group A2/C4.39: Electrical Transient Interaction between Transformers and the Power System
  - 'Transformers suffer dielectric failure even with good insulation coordination studies and well-accepted insulation design practices'.
- Investigation in OWF still needed

Electrical resonance

- Excitation of an electric system containing inductances and capacitances results in oscillations -> natural frequency

$$f = \frac{1}{2 \cdot \pi \cdot \sqrt{L \cdot C}}$$

- Resonance when periodic source has frequency similar to the circuit's natural frequency
- High amplification of voltage/current due to energy exchange between electric and magnetic field
- Depending on connection: series or parallel resonances

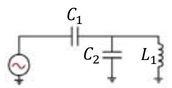

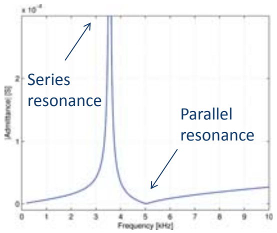

Resonance overvoltages

- Stationary resonance – stationary source of excitation
- Transient resonance – aperiodic excitation:
  - Two or more natural frequencies need to be present, i.e. network must contain at least two adjacent parts having similar resonance frequency:

$$\frac{1}{\sqrt{L_1 \cdot C_1}} = \frac{1}{\sqrt{L_2 \cdot C_2}}$$

  - The two network parts have large difference in characteristic impedance, $Z_0 = \sqrt{\frac{L}{C}}$

$$\sqrt{\frac{L_1}{C_1}} \ll \sqrt{\frac{L_2}{C_2}}$$

  - The source of the oscillation must come from the part of network characterized by the low characteristic impedance

Resonance overvoltage example

- The conditions might fulfilled for cable-transformer system
- Cable resonance frequency depends on length
- High overvoltages might occur on transformer terminals
- Important for Offshore Wind Farms, which contain large amount of cables and transformers
- Example might resemble energization of a radial

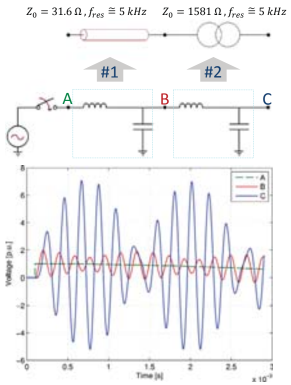

Sources of oscillations in OWF

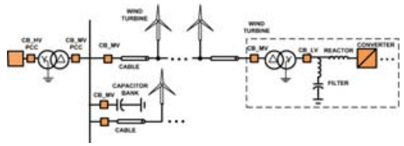

- Main sources of oscillations
  - External grid
  - Circuit breakers (HV, MV, LV) -> switching
  - Converter
  - Faults

Example: energization of a radial

- External grid / park transformer -> X/R
- 3-phase submarine cable: 50 mm²
  - 4 sections of 400 m
  - J.Marti models in ATP
- Wind turbines
  - 100 kVA transformer
    - Wide band model
    - Admittance matrix measurements
    - sFRA commercial device
    - Admittance matrix approximated with VF
    - Passivity enforced
    - Included in ATP-EMTP as a lumped parameter network
    - LV terminals left open

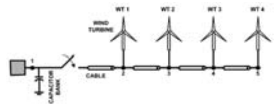

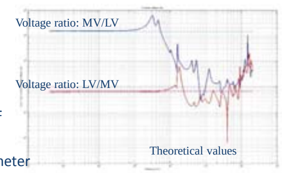

Example: energization of a radial

- Close breaker poles
- Voltage oscillation due to wave reflectio
- $f = \frac{1}{4\tau}, f = \frac{2n-1}{4l\sqrt{LC}} = \frac{2n-1}{4l} \cdot v = \frac{2n-1}{4\tau}$

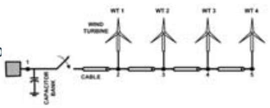

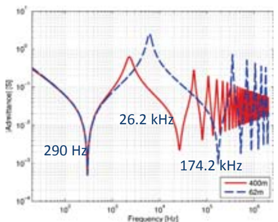

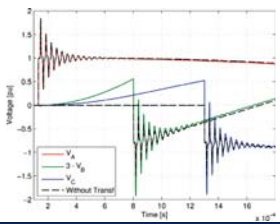

Example of resonance excitation in OWF

- Voltage oscillations visible at terminals of all wind turbines
- The same frequency at all turbines
- Driving-point admittace at WT 4 and PSD of a surge waveforms at phase A

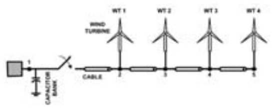

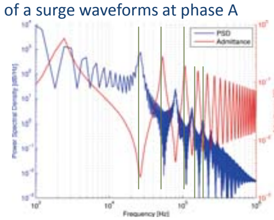

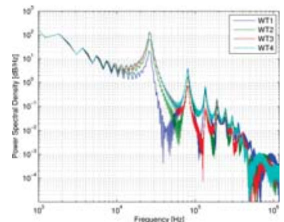

Example: resonance overvoltages

- Oscillation frequency matches resonance frequency of transformer
- Large overvoltage at LV terminals of transformer
- Magnitude depends also on loading

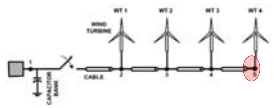

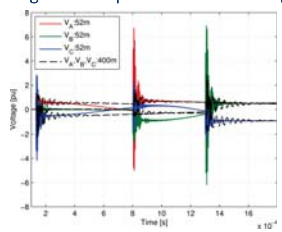

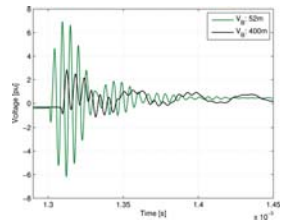

Influence of point of discontinuity for wave

- Cables of different cross sections
- Different cross-sections = different characteristic impedance Z_0
- Point of discontinuity = additional reflections
- Short cable lengths between point of dicontinuity = higher frequencies
- Might increase maximum overvoltage above 2 p.u.

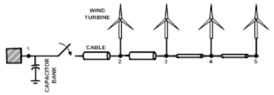

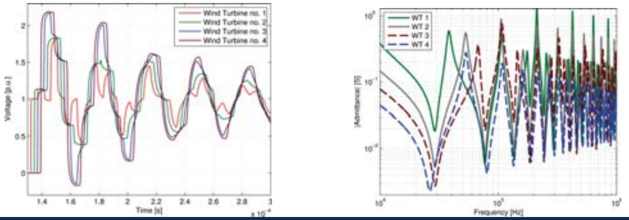

Influence of line bifurcation

- Subsections (branches) of strings often in large OWF
- Line bifurcation introduces additional reflections due to characteristic impedance missmatch
- Increases number of higher frequency oscillations
- Might cause maximum overvoltages > 2 p.u.

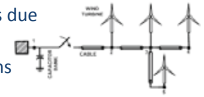

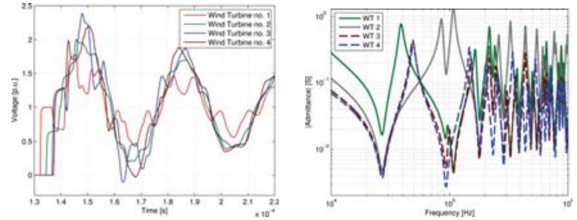

Example of OWF with complex topology

- Modern large OWF
- 111 x 3.6 MW wind turbines
- 12 strings
- 400 MW
- Cable cross-sections: (500, 240, 150 mm²)
- Model:
  - ATP-EMTP
  - Frequency dependent cable model
  - Transformers based on SC and OC tests with additional capacitances

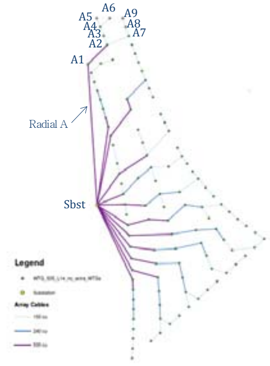

Reflections vs. transformer voltage ratio

- Voltage ratio (high to low) of several wind turbine transformers
  - Calculated from short circuit measurements
  - TR7 and TR8 -> dry type
  - TR10 – TR12 -> liquid insulated
  - High voltage amplification above approx. 200kHz
- Oscillations in string corresponding!

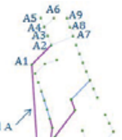

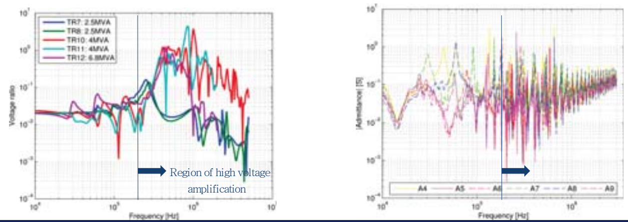

Summary

- Voltage oscillations of appropriate frequency and duration might excite transformer resonance
- Transient interaction important in OWF due to large amount of cables and transformers
- Line bifurcation and point of discontinuity for voltage wave introduce high frequency oscillations
- These oscillations are in the region of high amplification in voltage transfer of liquid insulated wind turbine transformers
- This might lead to resonant overvoltages at LV side of WT transformers
- This phenomenon depends on specific design of an OWF

The end

- Thank you for your attention.

B2) Grid connection

Experimental verification of a voltage droop control for grid integration of offshore wind farms using multi-terminal HVDC, Raymundo E. Torres-Olguin, SINTEF Energi AS

Ancillary Services Analysis of an Offshore Wind Farm Cluster - Technical Integration Steps of an Simulation Tool, Tobias Hennig, Fraunhofer IWES

Sub-sea cable technology, Hallvard Faremo, SINTEF Energy Research

Experimental verification of a voltage droop control for grid integration of offshore wind farms using a multi-terminal HVDC

Raymundo E. Torres-Olguin[a], Atle R. Årdal[a], Hanne Støylen[b] , Atsede G. Endegnanew[a], Kjell Ljøkelsøy[a], and John Olav Tande[a]

[a]Sintef Energy Research
[b]NTNU dept. of Electrical Power Engineering

Outline

- ❑ Introduction
- ❑ Reference system
- ❑ Scaled experimental platform
- ❑ Voltage droop control
- ❑ Laboratory case studies
- ❑ Conclusions

Objective

This work presents a **lab-scale implementation** of a **voltage droop control** for **a multi-terminal HVDC system** connecting an **offshore wind farm**.

Introduction

- ❑ In the near future, the construction of an **offshore electrical grid** is expected in **Europe**. The objective of such a transmission framework is to facilitate large-scale integration of **renewable energy** and to improve the **European power market**.
- ❑ It is widely recognized that for long-distance bulk-power delivery, **HVDC** transmission is more economically attractive than HVAC transmission

- ❑ **A multi-terminal HVDC** system presents many challenges: **protection, control, and operation issues**.
- ❑ One of the most critical issues is the **voltage control and power balance**

From http://www.friendsofthesupergrid.eu/

Introduction

Several **methodologies to balance the power and control the voltage** have been studied in the literature

- ❑ Master-slave control
- ❑ Voltage-margin control
- ❑ Voltage-droop control

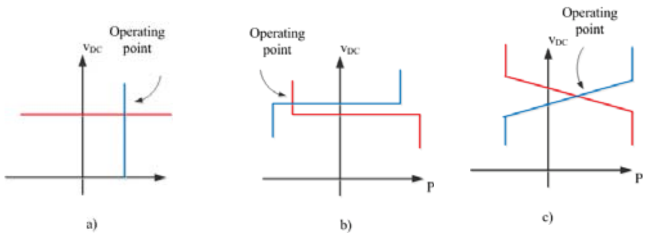

Reference system

- ❑ **Multi-terminal HVDC** system composed by **four terminals** which aims to represent the future power HVDC in the North Sea; Norway, Germany and UK are inter-connected together with an **offshore wind farm.**
- ❑ It is considered that the **three onshore** grids have a nominal voltage of **400 kV**.
- ❑ **HVDC system** is rated at **± 320 kV** and a **1200 MW offshore wind farm** is considered.

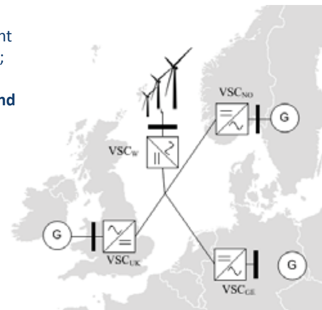

Scaled experimental platform

- The set consists of **four 60 kVA VSCs** .
- **The wind farm** is emulated using a motor drive and a **55 kVA induction motor/generator-set.**
- **The strong grids** are represented by the laboratory 400 V supply.
- A **independent grid** is emulated using a **17 kVA synchronous generator**.
- The **DC line emulator** consists of variable **series resistors** to vary the length of the emulated cable.

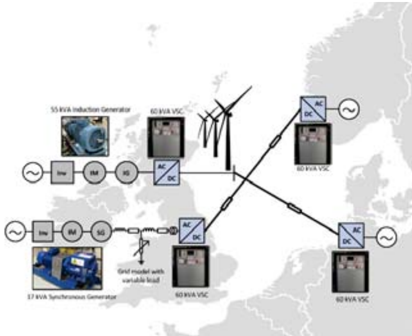

SINTEF/NTNU smart grid lab

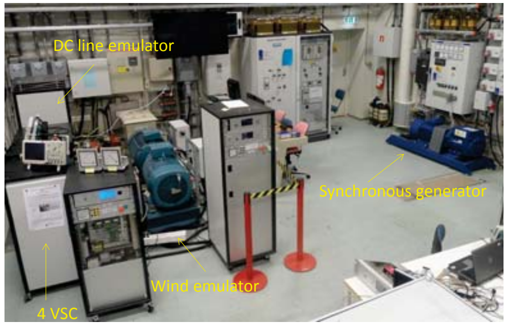

Scaled experimental platform

- The control system runs on a processor system that is embedded in **FPGA (Field-Programmable Gate Arrays).**
- For adjusting the settings, the converter is equipped with a **CAN interface** which enable receiving, sending, and controlling reference remotely.
- The droop voltage control is achieved by using the **Labview programming environment**

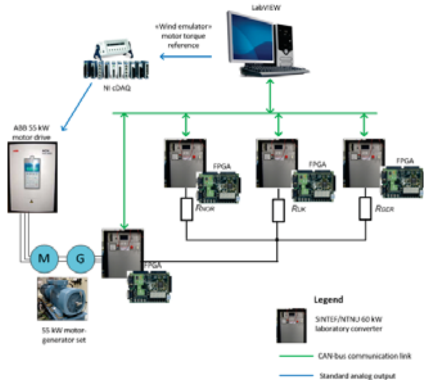

Voltage droop control

The voltage droop controller is **a proportional control law** that **regulates the DC voltage** and **provides power sharing** between the different power converters.

The mathematical expression for voltage droop control is given by

$$V_{DC} = V_0 - \rho\,(P_{DC} - P_0)$$

ρ Droop constant
V_0, P_0 Voltage and power set points

DC voltage droop characteristic.

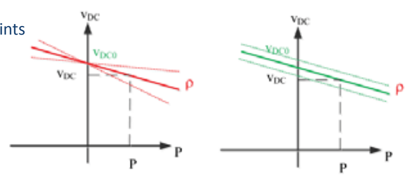

Laboratory case studies

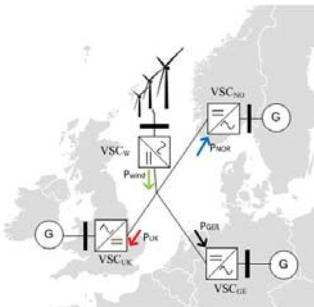

Case 1: wind variations

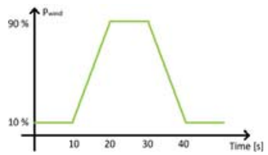

Case 2: Disconnection of two terminals

Case 1a: Varying wind – equal droop constants

- Converters **share equally the power** since the droop constants and set-points are equal
- Norway is absorbing slightly less wind power since the resistance is higher due to longer cable length

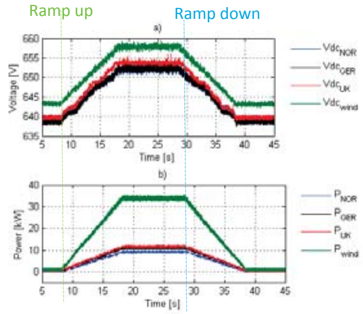

Case 1b: Varying wind – different droop constants

- Droop constants:
  - Germany: 40 power pu/voltage pu
  - Norway: 20 power pu/voltage pu
  - UK: 10 power pu/voltage pu
- The **powers are distributed proportionally** to the **droop constants**
- The droop constant should reflect the ability of the onshore grid to absorb or provide additional power to the DC-grid

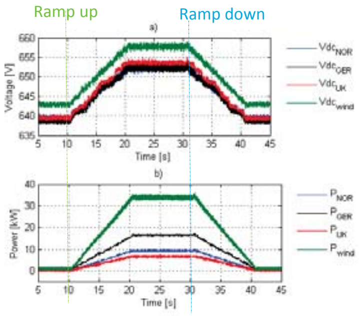

Case 1c: Varying wind – different power set-points

- Droop constants all equal (=20)
- Power set-points are different: - 0.5 pu (Norway), 0.25 pu (Germany) and 0.25 pu (UK).
- Now, **Norway exports power towards both UK and Germany**
- Since droop-constants are equal, the additional wind production is shared equally among the three countries similar to case 1a

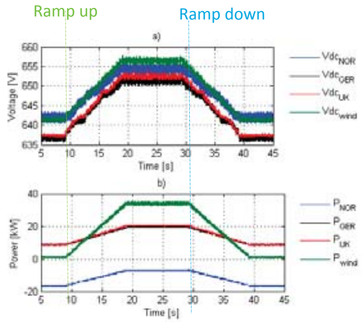

Case 2: Sudden disconnection of two converters

- Initially all countries are absorbing the same wind power. All droop constants are equal
- At t=0.7 Norway is disconnected
  - **The wind power initially absorbed by Norway is shared equally between Germany and UK**
- At t=1.7 UK is disconnected
  - **Germany is now absorbing all wind power**

System response is stable and with no overshoot against these severe events

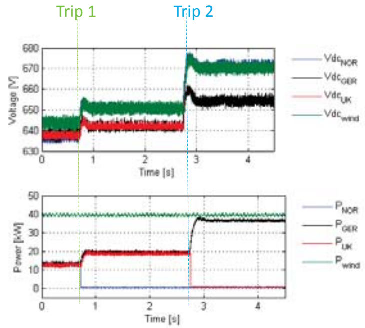

Conclusions

- The overall goal has been to implement a voltage droop control in a down scaled model of a multi-terminal VSC-HVDC grid.
- Two scenarios have been used to test the performance of the droop-control and evaluate the stability of the system: variation in wind power production, and loss of two terminals during full wind production.
- The implemented system was able to ensure that the voltage stays within its steady state limits and to reach a stable operation point after the above disturbances were applied. Moreover, the system is able to tolerate the loss of one or two terminals. It can be concluded that the voltage-droop control scheme has been successfully implemented in this laboratory model.
- ***Future work:*** **Secondary control, frequency reserve exchange, and DC protection and fault handling.**

Thanks for the attention

Picture by John Olav Tande

Fraunhofer IWES

EERA DeepWind'2014 – Session B2: Grid Connection

Ancillary Services Analysis of an Offshore Wind Farm Cluster – Technical Integration Steps of a Simulation Tool

M.Sc. Tobias Hennig, Fraunhofer IWES – Kassel, January, 20th 2012

Content

EERA-DTOC Project[1]

The **EERA (European Energy Research Alliance)** partners are pooling their resources in support of the Strategic Energy Technology plan (SET plan) of the European Commission. Some partners of the Joint Programme on Wind Energy have state-of-the-art software models in **single and multiple wake**, **energy yield** and **electrical models**. Then, the concept of the **EERA's Design Tool for Offshore Wind Farm Clusters (EERA-DTOC)** project is thus to **combine their expertise** in a common **integrated software tool** for the optimised design of offshore wind farms and wind farm clusters acting as wind power plants (WPP).

The project has defined the following Objectives:

- Integrate existing atmospheric and wake models from single wind farm to cluster scale
- Predict energy yield precisely through simulation
- Interconnection optimization for grid and offshore wind power plant system service
- Validation of the newly integrated existing models based on wind farm observations

Kriegers Flak Study Case[2][3]

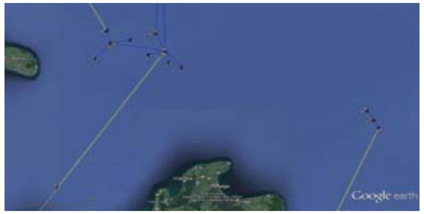

- Layout done by optimization tool (Net-Op), data include
  - Conenction points
  - Cable length
  - Applied technology (AC/DC)
  - Transmission capacity

Wind Cluster Management System I

- geographically distributed wind farms aggregated to clusters
  - Differ in size depending on considered service
  - Span over one or more voltage levels
- Provide grid supporting functionality
- Coordinated manner
- Considering grid structure
- forecast data with different temporal resolutions
- Applications:
  - Field test in portugal
  - Park controller including forecast (alphaventus)
  - Coordinated reactive power supply including **short-term forecast** and transformer **tap-changer control** in **meshed distribution grids** with **multiple feeders**

Wind Cluster Management System II

Pan-European Synchronous Area

1. Provision of Frequency Support:
   - Primary Reserve
2. Congestion mgmt

Control Area

1. Provision of Frequency Support:
   - Secondary Reserve
2. Congestion mgmt

Local/ Regional Area

1. Provision of Voltage Support:
   - Voltage control
   - Reactive power
2. Congestion mgmt

Wind Cluster Management System III

Power Monitor

PQ-Curve at UW Hagermarsch

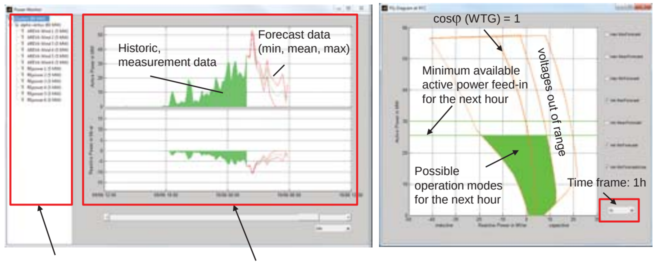

Get information of a single turbine or the whole cluster

Active and reactive power data (gross values – without grid losses)

Active and reactive power data relating PCC node (net values – including grid losses)

Wind Cluster Management System IV

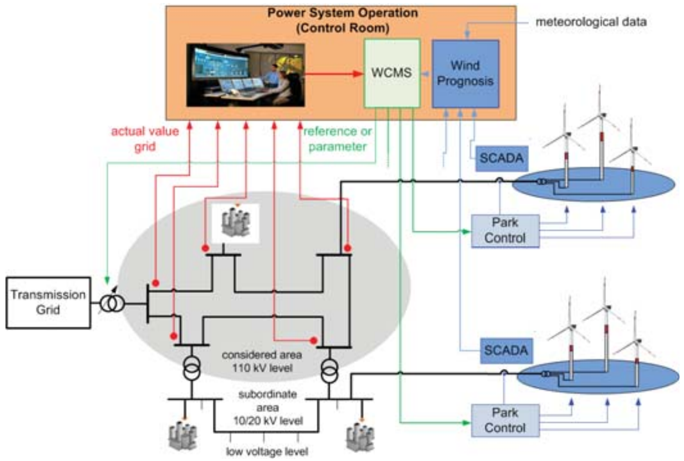

HVDC Technology Integration

- major impact is evoked by representing and respecting HVDC technology during the calculation process
- VSC-HVDC systems are the preferred technology for offshore grids
  - Voltage control
  - Islanding operation
- CSC-HVDC systems manageable if the grid is strong enough
  - e.g. meshed connection to onshore nodes
- Critical size in terms of power → switching losses VSC still higher than CSC
- Both technologies considered and implemented

CSC-HVDC Load Flow Model[4]

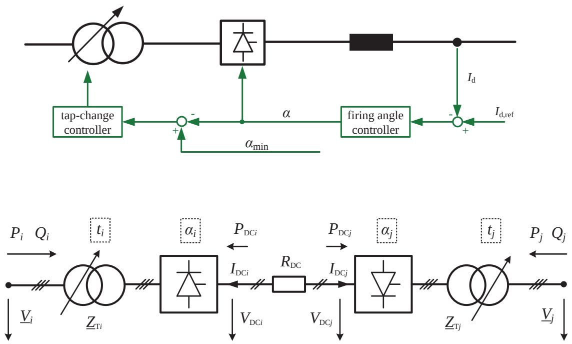

VSC-HVDC Load Flow Model[4]

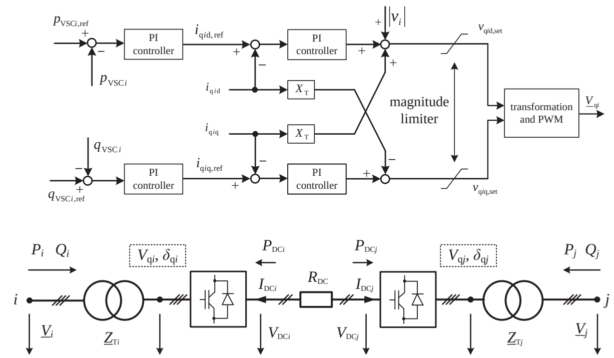

Modified Newton-Raphson Load Flow Algorithm I [4]

$$\begin{pmatrix}\Delta\vec{V}_{AC}\\ \Delta\vec{\delta}_{AC}\end{pmatrix} = \mathbf{J}_{AC}\cdot\begin{pmatrix}-\Delta\vec{P}_{AC}\\ -\Delta\vec{Q}_{AC}\end{pmatrix}$$

$$\begin{pmatrix}\Delta\vec{V}_{AC}\\ \Delta\vec{\delta}_{AC}\\ \Delta\vec{V}_{q}\\ \Delta\vec{\delta}_{q}\end{pmatrix} = \begin{bmatrix}\mathbf{J}_{AC}+\mathbf{J}_{UL} & \mathbf{J}_{UR}\\ \mathbf{J}_{LL} & \mathbf{J}_{LR}\end{bmatrix}^{-1}\cdot\begin{pmatrix}-\Delta\vec{P}_{AC}\\ -\Delta\vec{Q}_{AC}\\ -\Delta\vec{f}_{VSC}\end{pmatrix}$$

Modified Newton-Raphson Load Flow Algorithm II [4]

	Converter at node i
Active power	Master (set-point compliance) $\Delta f_{\mathrm{VSC1}} = P_{\mathrm{VSC}i,\mathrm{iter}} - P_{\mathrm{VSC}i,\mathrm{ref}}$
Reactive Power	Specified reactive power provision $\Delta f_{\mathrm{VSC3}} = Q_{\mathrm{VSC}i,\mathrm{iter}} - Q_{\mathrm{VSC}i,\mathrm{ref}}$
$\mathbf{J}_{\mathrm{UL}}$	$\partial P_{\mathrm{VSC}i}/\partial V_i, \partial P_{\mathrm{VSC}i}/\partial \delta_i, \partial Q_{\mathrm{VSC}i}/\partial V_i, \partial Q_{\mathrm{VSC}i}/\partial \delta_i$
$\mathbf{J}_{\mathrm{UR}}$	$\partial P_{\mathrm{VSC}i}/\partial V_{qi}, \partial P_{\mathrm{VSC}i}/\partial \delta_{qi}, \partial Q_{\mathrm{VSC}i}/\partial V_{qi}, \partial Q_{\mathrm{VSC}i}/\partial \delta_{qi}$
$\mathbf{J}_{\mathrm{LL}}$	$\partial \Delta f_{\mathrm{VSC1}}/\partial V_i, \partial \Delta f_{\mathrm{VSC1}}/\partial \delta_i, \partial \Delta f_{\mathrm{VSC3}}/\partial V_i, \partial \Delta f_{\mathrm{VSC3}}/\partial \delta_i$
$\mathbf{J}_{\mathrm{LR}}$	$\partial \Delta f_{\mathrm{VSC1}}/\partial V_{qi}, \partial \Delta f_{\mathrm{VSC1}}/\partial \delta_{qi}, \partial \Delta f_{\mathrm{VSC3}}/\partial V_{qi}, \partial \Delta f_{\mathrm{VSC3}}/\partial \delta_{qi}$

Fraunhofer IWES

Modified Newton-Raphson Load Flow Algorithm III [4]

Converter at node j
Slave (balancing mode) $\Delta f_{\mathrm{VSC2}} = P_{\mathrm{VSC}i,\mathrm{iter}} + P_{\mathrm{VSC}j,\mathrm{iter}} - R_{\mathrm{DC}} I_{\mathrm{DC}}^2$
Voltage control $\Delta f_{\mathrm{VSC4}} = V_{j,\mathrm{iter}} - V_{j,\mathrm{ref}}$
$\partial P_{\mathrm{VSC}j}/\partial V_j, \partial P_{\mathrm{VSC}j}/\partial \delta_j, \partial Q_{\mathrm{VSC}j}/\partial V_j, \partial Q_{\mathrm{VSC}j}/\partial \delta_j$
$\partial P_{\mathrm{VSC}j}/\partial V_{qj}, \partial P_{\mathrm{VSC}j}/\partial \delta_{qj}, \partial Q_{\mathrm{VSC}j}/\partial V_{qj}, \partial Q_{\mathrm{VSC}j}/\partial \delta_{qj}$
$\partial \Delta f_{\mathrm{VSC2}}/\partial V_i, \partial \Delta f_{\mathrm{VSC2}}/\partial \delta_i, \partial \Delta f_{\mathrm{VSC2}}/\partial V_j, \partial \Delta f_{\mathrm{VSC2}}/\partial \delta_j, \partial \Delta f_{\mathrm{VSC4}}/\partial V_j$
$\partial \Delta f_{\mathrm{VSC2}}/\partial V_{qi}, \partial \Delta f_{\mathrm{VSC2}}/\partial \delta_{qi}, \partial \Delta f_{\mathrm{VSC2}}/\partial V_{qj}, \partial \Delta f_{\mathrm{VSC2}}/\partial \delta_{qj}, \partial \Delta f_{\mathrm{VSC4}}/\partial V_{qj}$

Fraunhofer IWES

Control Mode Selection

- Scanning for swing bus (slacks) in synchronous areas
- Slack Mode Operation of HVDC
- Set-point allocation due to demand or reserve restrictions
- **Offshore grid operational control needs to be coordinated with ancillary service provision**

Fraunhofer IWES

Ancillary Services Analysis I

Category	Service	Description
Frequency Support	Reserve	Frequency Restoration Reserve (Secondary Reserve)
		Replacement Reserve (Minute Reserve)
	Balancing Power	Balancing power supply
Voltage Support	Reactive power contribution to onshore nodes	Reactive power provision of the cluster (if connected with AC) or by HVDC links to onshore nodes
System Management	Congestion Management	Maximum load flow into the grid due to congestions on land

Fraunhofer IWES

Ancillary Services Analysis II [5][6]

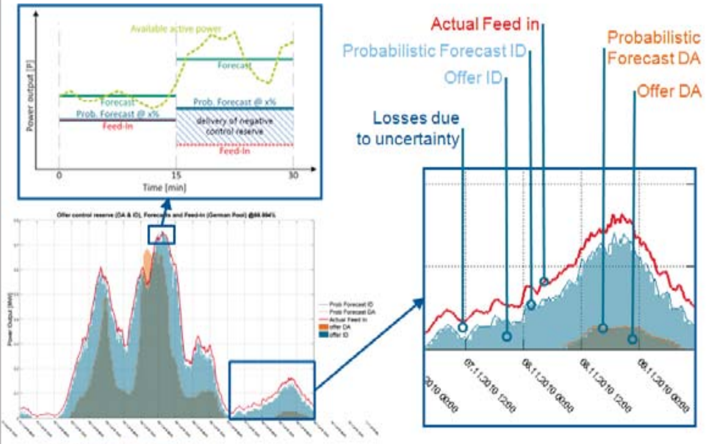

Source: Malte Jansen – Fraunhofer IWES

Fraunhofer IWES

Reserve and Balancing Power Provision

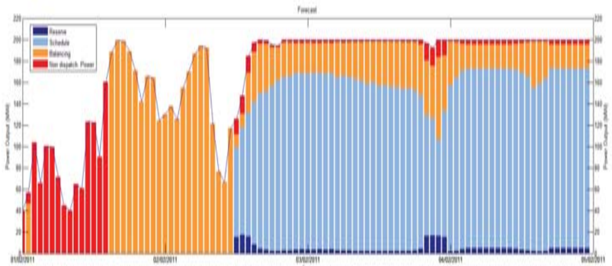

- Dark blue: day ahead forecast, probability 99.5 %, → possible reserve
- Light blue: day ahead forecast, probability 90 %, → schedule
- Orange: 1h forecast, probability 99.5 %, → balancing power (intraday)
- Red: non-dispatchable power → losses due to forecast uncertainties, security requirements

Fraunhofer IWES

Remarks and Outlook

- Results provided are technical solutions
- No procurement or market rules considered
- Coupling with market rules need to be investigated (see next slide)
- Optimization of voltage selection/ transformer placement, reflect cost in:
  - Necessary transformers
  - Insulation material of cables
  - Need for platform space due to insulation distances
- Modular expansion stages → optimization on time perspective
  - Evolving technologies (DC breakers, new converter…)
  - Market releases
- Reliability analysis and design of AC/DC systems

Virtual Power Plant (VPP) vs. Wind Farm Cluster (WFC)

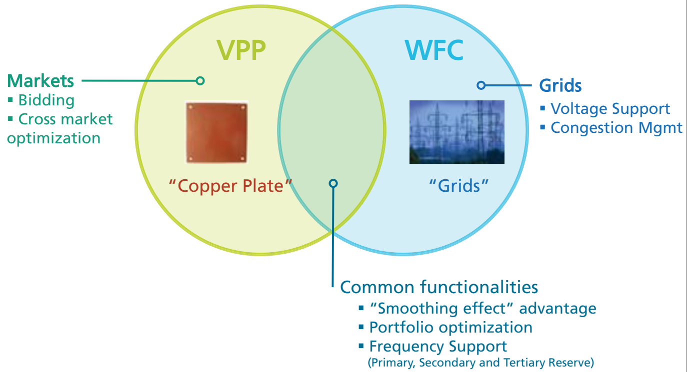

References and Acknowledgement

[1] www.eera-dtoc.com

[2] Svendson, H. G. Planning Tool for Clustering and Optimised Grid Connection of Offshore Wind Farms, presented at EERA DeepWind’2013, Trondheim, 2013.

[3] Svendson, H. G. "Report on tools and results from a case study (D2.3)", EERA-DTOC Project Deliverable D2.3. February 2013.

[4] Panosyan, A. Modeling of Advanced Power Transmission System Controllers, PhD thesis Leibniz University Hannover, 2010.

[5] Jansen, M.; Speckmann, M.; et al. Impact of Control reserve Provision of Wind Farms on Regulating Power Costs and Balancing Energy Prices. EWEA Event 2012. Copenhagen, 2012.

[6] Jansen, M.; Speckmann, M. Wind turbine participation on Control Reserve Markets. EWEA Conference 2013. Vienna: EWEA, 2013.

The research leading to these results has received funding from the European Union Seventh Framwork Programme.

EERA DTOC project FP7-ENERGY-2011-1/ n°282797

EERA DeepWind'2014

Sub-sea Cable Technology

Hallvard Faremo
SINTEF Energy Research

Brief presentation of:

Wind Farm Cable R&D project

High Voltage Subsea Cables Networking the North Sea

Application for a KMB project within the Research Council of Norway

- Project content
- Education (PhD / MSc)
- Scientific equipment
- Financing
- Research Partners

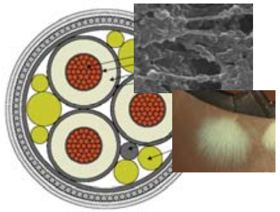

High Voltage Subsea Cables Networking the North Sea

Key words: Long operation times, Flexible designs, Qualification and test methods, HVDC/AC

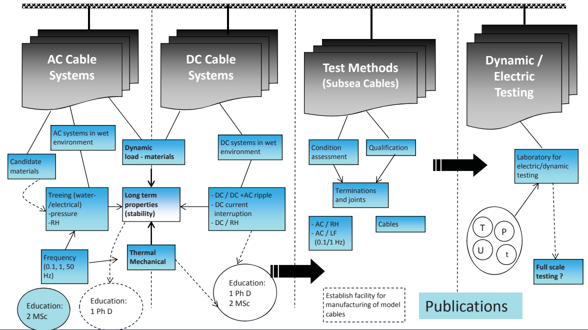

Project Content

1. AC cable systems
2. DC cable systems
3. Test methods
4. Dynamic / electrical testing (prototypes)
5. Education (NTNU)

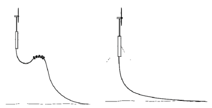

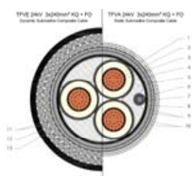

AC Cable Systems

- Polymeric AC cables have been in use for decades in subsea environment
- In general the service experience is good
- Under some service conditions water treeing has caused premature failures
- Dynamic high voltage cables have now been in service for some years
- A PhD student (NTNU) is working with partial discharge questions

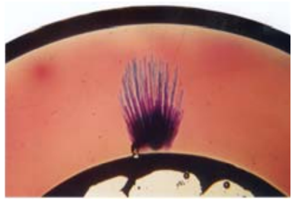

Water treeing in a 24 kV XLPE cable

DC Cable Systems

- Polymeric HVDC cables have been installed for more than a decade in Norway (The Troll Cables)
- The subsea HVDC cables are all water tight constructions (lead sheathed)
- Water treeing at DC stresses are not commonly expected to be a problem
- However, voltage ripple do exist in HVDC systems
- A PhD student (NTNU) is working with questions related to moisture ingress in XLPE insulation

Polymer HVDC cables

Combined AC and DC Stresses

- As HVDC systems have some percent ripple – an AC voltage stress will occur in HVDC cables
- This will not cause any damage under dry conditions
- Combined AC and DC stress may cause rapid water tree initiation and growth if the water barrier has been compromised

Electrical treeing due to rapid water tree growth under combined AC and DC stresses

Combined AC and DC Stressing - Water tree analysis

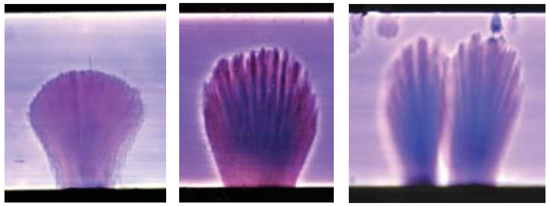

2 weeks 4 weeks 8 weeks

25 kV/mm DC + 2.5 kV/mm AC 5 kHz_{peak}

Dynamic / Electrical Testing

- Dynamic testing of high voltage cables have been performed for many years
- No electric stressing is usually applied under the dynamic tests

Marintek – Dynamic test rigs

Dynamic / Electric Testing

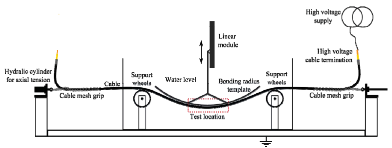

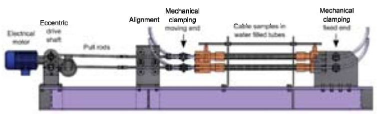

- Two different test rigs for combined dynamic and electrical testing have been developed
- Bending rig
- Axial strain rig

Dynamic / Electrical Testing

- Tests have been performed in both test rigs
- More than 3 million dynamic cycles have been applied to XLPE cables
- AC stressing according to CENELEC standard have been used (both 50 and 500 Hz)
- The results show an increased number of water trees when the XLPE cable insulation is exposed to combined dynamic and electrical stress
- The water tree lengths; however, do not increase
- Hence, as long as the dynamic stresses are kept at reasonable levels, no severe increased degradation is observed when the XLPE cable is aged under combined dynamic and electrical stresses

Summary

- The project was established in 2009
- Two test rigs for combined dynamic and electrical stressing of cable insulation ave been built
- Long term tests have been performed in both test rigs
- Dynamic stressing at reasonable values (around 1 % elongation) do not result in detrimental ageing phenomena
- Combined HVDC and AC ripple has shown to result in enhanced ageing if moisture has penetrated the moisture barrier
- Two PhD students have been working in this project
- Several MSc students have also participated in the project

Pressure Testing – not part of this presentation

This presentation do not present results when testing in SINTEF's high pressure vessels. All tests presented is performed at ambient pressure

SINTEF Technology for a better society 13

Thank you for your attention

Questions?

SINTEF Technology for a better society 14

SINTEF

Technology for a better society

SINTEF Technology for a better society 15

B3) Power system integration

Active damping of DC voltage oscillations in multiterminal HVDC systems,
Salvatore D'Arco, SINTEF Energy Research

Analysis and Design of a LCL DC/DC converter for Offshore Wind Turbines,
Rene A. Barrera, PhD Student NTNU

Fault Ride Through Enhancement of Multi Technology Offshore Wind Farms,
Arshad, Ali, University of Strathclyde

Reliability of power electronic converters for offshore wind turbines,
Magnar Hernes, SINTEF Energy Research

EERA DeepWind'2014
Trondheim, Norway, 23 January 2014

Active Damping of DC Voltage Oscillations in Multi-Terminal HVDC Systems

Salvatore D'Arco SINTEF Energy Research
Jon Are Suul SINTEF Energy Research & NTNU

Introduction

- Cable connections in HVDC systems are characterized by substantial capacitance and inductance
- The dc side of an HVDC system can exhibit not well damped oscillatory behaviours as a reaction to changes of the system conditions
- Resistance is in general responsible for dampening of oscillations in physical circuits but this generates losses and conflicts with efficiency goals (Passive Damping)
- Damping of oscillations in power electronics can be also integrated in the control (Active Damping)

AC Active Damping

- Active damping is common in power electronics systems sensitive to oscillations
  - Grid connected converters with LCL filters
- The principle is to add to the output voltage a component in counterphase with the oscillations in order to force a damping (similar to noise cancelling headphones)
- Oscillations are isolated with high pass filtering

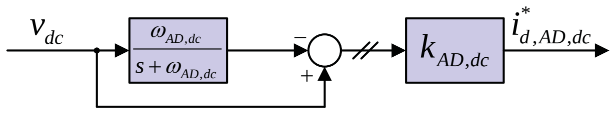

Reference model for HVDC terminal

- Rated power: 1200MW
- Rated Voltage AC: 220 kV
- Line length: 200 km
- Line resistance: 0.011 Ω /km
- Line capacitance: 0.19 μF/km
- Line inductance: 2.6 mH/km
- Bus capacitance: 8.2 mF
- Worst case configuration

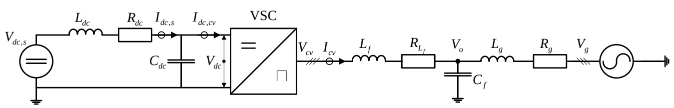

Overview Control Scheme

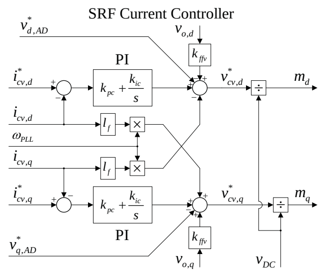

Current controller

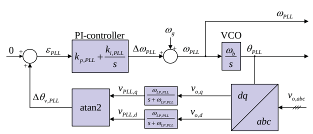

PLL

DC Active Damping

- The concept and the implementation of the DC Active Damping is similar to the AC Active Damping
  - The oscillations in the dc voltage are isolated by high pass filtering the measured voltage on the dc bus
  - A counterphase component is added to the reference current for the current controller
  - The damping effect is lossless and can be tuned by the gain and the filtering frequency

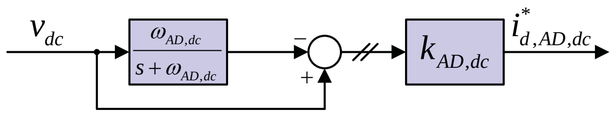

ProOfGrids

Small signal modelling

- A small signal linearized system is derived in the dq frame (17 th order)

$$\Delta\dot{\mathbf{x}} = \mathbf{A}\cdot\Delta\mathbf{x} + \mathbf{B}\cdot\Delta\mathbf{u}$$

$$\mathbf{x} = \begin{bmatrix} v_{o,d} & v_{o,q} & i_{l,d} & i_{l,q} & \gamma_d & \gamma_q & i_{o,d} & i_{o,q} & \varphi_d & \varphi_q & v_{PLL,d} & v_{PLL,q} & \varepsilon_{PLL} & \delta\theta_{PLL} & v_{dc} & i_{dc} & \rho \end{bmatrix}^T$$

$$\mathbf{u} = \begin{bmatrix} i^*_{l,q} & i^*_{l,d} & v_{dc,s} & \hat{v}_g & \omega_g \end{bmatrix}^T$$

ProOfGrids

Small signal modelling

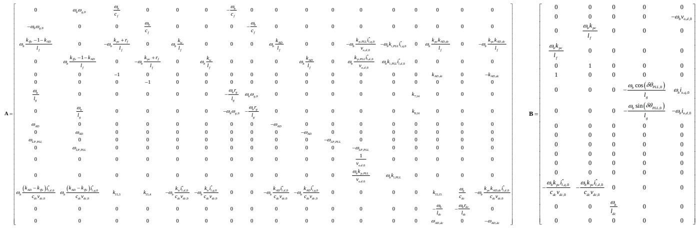

A B

ProOfGrids

Example of oscillatory behaviour without active damping

- Response to a step change in the id reference of 0.1 pu
- Very good match between the linearized and the non linear model

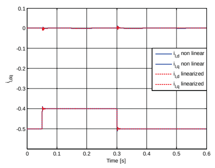

DQ CURRENT

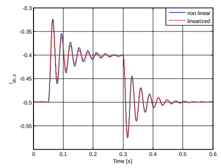

DC LINE CURRENT

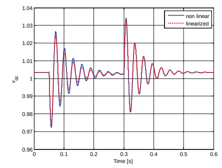

DC LINE VOLTAGE

ProOfGrids

DQ Current

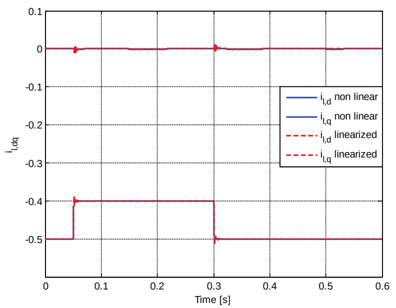

ProOfGrids

DC Line Current

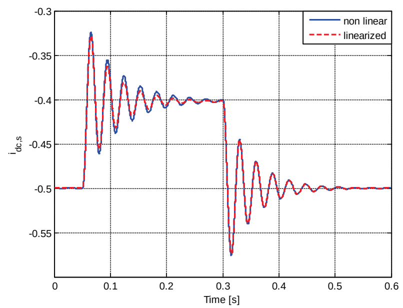

ProOfGrids

DC Line Voltage

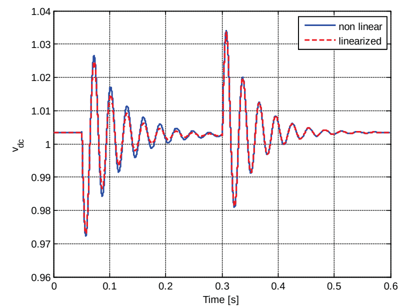

ProOfGrids

Effect of active damping on dc voltage oscillations

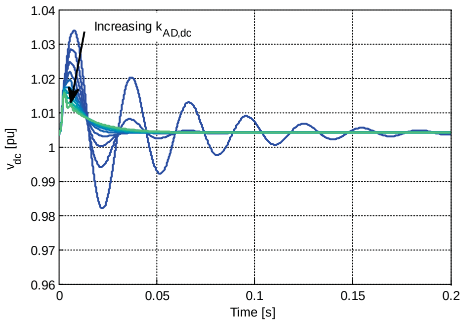

ProOfGrids

Root locus for Active Damping gain sweep

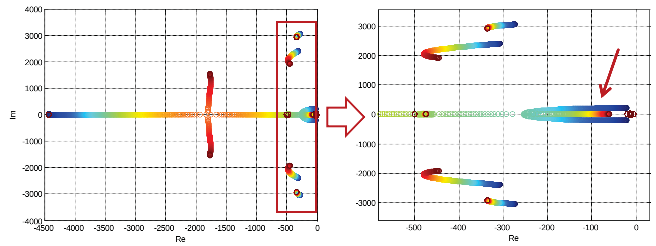

ProOfGrids

Pole parametric sensitivity

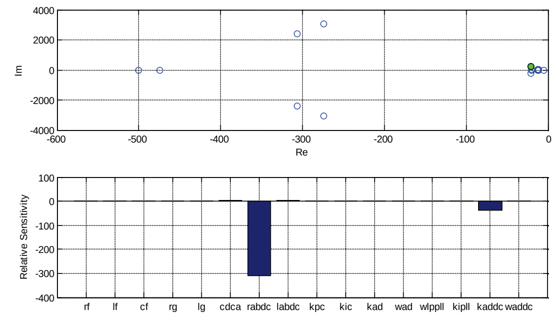

ProOfGrids

Example of behaviour with active damping

- Response to a step change in the id reference of 0.1 pu
- Very good match between the linearized and the non linear model

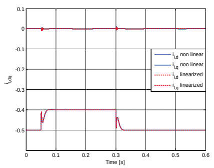

DQ CURRENT

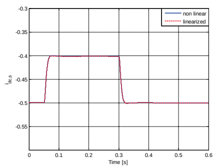

DC LINE CURRENT

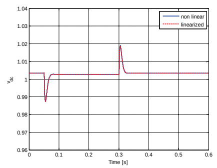

DC LINE VOLTAGE

ProOfGrids

DQ Current

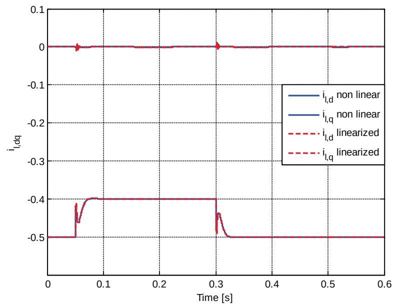

ProOfGrids

DC Line Current

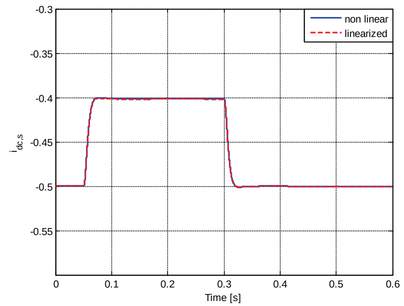

ProOfGrids

DC Line Voltage

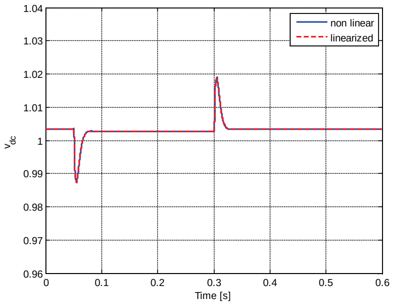

ProOfGrids

Example of oscillatory behaviour with active damping

- Response to a step change in the id reference of 0.1 pu
- Very good match between the linearized and the non linear model

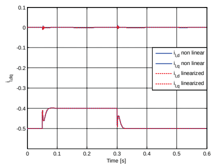

DQ CURRENT

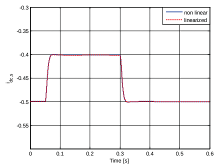

DC LINE CURRENT

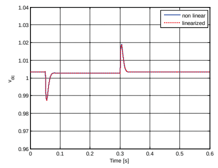

DC LINE VOLTAGE

ProOfGrids

Example of oscillatory behaviour without active damping

- Response to a step change in the id reference of 0.1 pu
- Very good match between the linearized and the non linear model

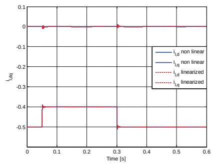

DQ CURRENT

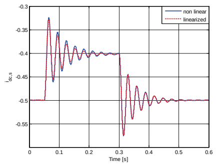

DC LINE CURRENT

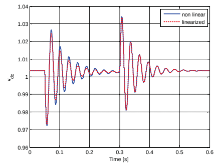

DC LINE VOLTAGE

ProOfGrids

Conclusions

- Changes in operating conditions can trigger oscillations on the dc side of HVDC systems due to the relatively large capacitance and inductance of the cable connections
- An active damping scheme has been proposed and its operation demonstrated on a sample case
- The active damping can effectively reduce the oscillatory behaviours.

ProOfGrids

Questions?

This activity is supported by the project:
Protection and Fault Handling in **Of**fshore HVDC **Grids**
contact: salvatore.darco@sintef.no

ProOfGrids Protection and Fault Handling in Offshore HVDC Grids

1

ANALYSIS AND DESIGN OF AN AC/DC CONVERTER FOR OFFSHORE WIND TURBINES

René Alexander Barrera Cárdenas
Marta Molinas

NOWITECH
Norwegian Research Centre for Offshore Wind Technology

NTNU – Trondheim
Norwegian University of Science and Technology

2

NTNU – Trondheim
Norwegian University of Science and Technology

Outline:

1. Introduction
2. Parameters of design
3. Methodology for evaluation of Performance indicators
4. Main results
5. Conclusions

3

Offshore Wind turbine challenges

Optimal design targeting two objectives

1. Maximize efficiency (η): Reduce power losses. Less conversion stages.
2. Maximize power density (ρ) of conversion system: Minimize weight/Size for a given power. Increase the Frequency.

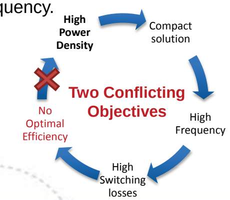

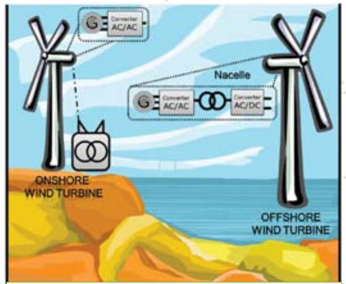

Assumption: DC Grid is more convenient for offshore wind farms [MEYER]
New WECS architectures for offshore applications. Design taken into account all stages of the system.

4

Wind Energy conversion System

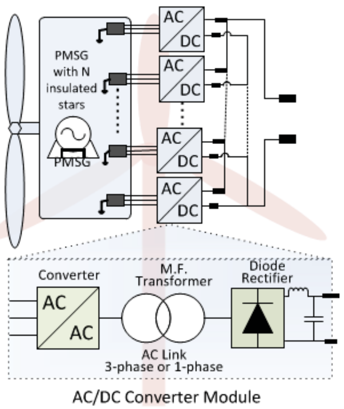

Modular Power converter with N sub-modules.

Current source operation
➔ series connection

Voltage source operation
➔ parallel connection

NTNU – Trondheim
Norwegian University of Science and Technology

5

Parameters of design

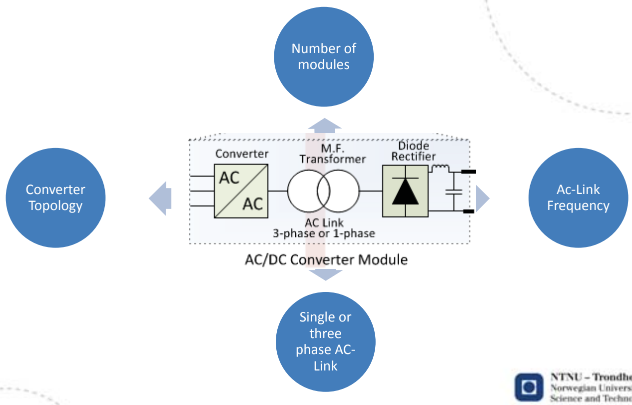

NTNU – Trondheim
Norwegian University of Science and Technology

6

Parameters of design – Converter topology

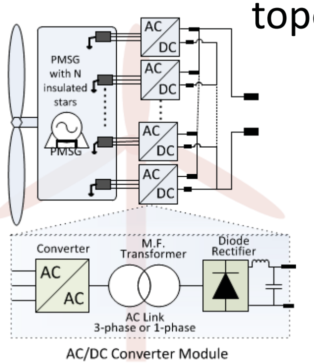

AC-LINK	Converter Topology (AC/AC)		
3 phase Sinusoidal waveform	B2B Back-to-Back	IMC Indirect Matrix Converter [Holtsmark]	DMC Direct Matrix Converter [Holtsmark]
Squared waveform	B2B-3p Back-to-Back with 3-phase output	B2B-1p Back-to-Back with 1-phase output	RMC Reduced Matrix Converter [Garces]

*Holtsmark and Molinas, "Matrix converter efficiency in a high frequency link offshore WECS," in IECON 2011.
**A. Garces. "Design, Operation and control of series connected power converters for offshore wind parks". Thesis for the Degree of Doctor of Philosophy. NTNU 2012.

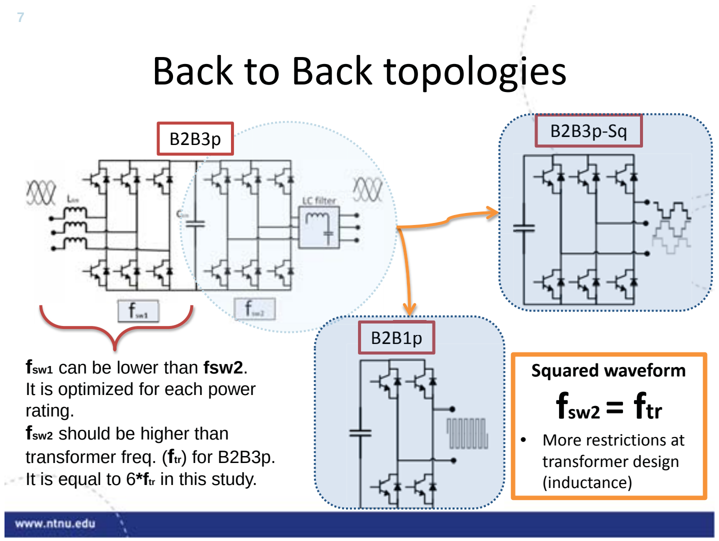
7
Back to Back topologies
B2B3p
B2B3p-Sq
B2B1p
LC filter
f_{sw1} can be lower than fsw2.
It is optimized for each power rating.
f_{sw2} should be higher than transformer freq. (f_{tr}) for B2B3p.
It is equal to 6*f_{tr} in this study.
Squared waveform
$f_{sw2} = f_{tr}$
More restrictions at transformer design (inductance)
www.ntnu.edu

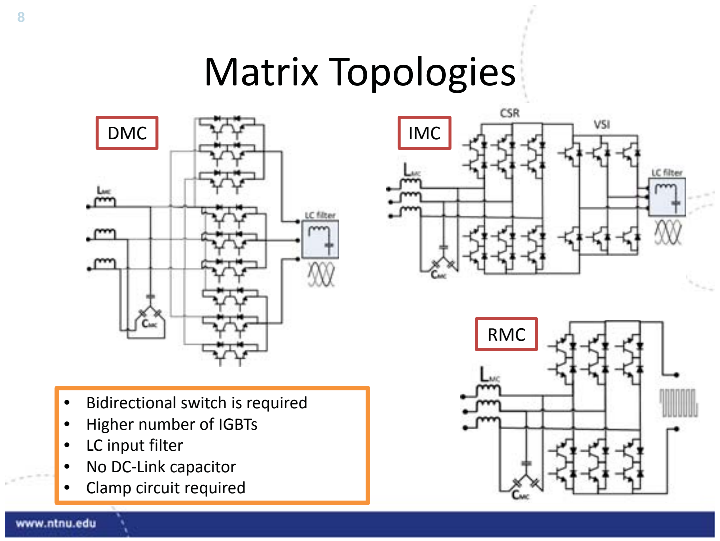
8
Matrix Topologies
DMC
IMC
RMC
CSR
VSI
LC filter
Bidirectional switch is required
Higher number of IGBTs
LC input filter
No DC-Link capacitor
Clamp circuit required
www.ntnu.edu

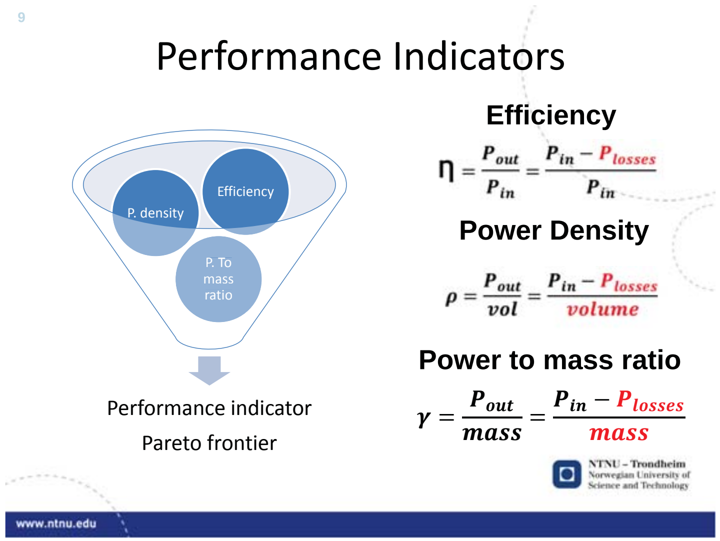
9
Performance Indicators
P. density
Efficiency
P. To mass ratio
Performance indicator
Pareto frontier
Efficiency
$\eta = \frac{P_{out}}{P_{in}} = \frac{P_{in} - P_{losses}}{P_{in}}$
Power Density
$\rho = \frac{P_{out}}{vol} = \frac{P_{in} - P_{losses}}{volume}$
Power to mass ratio
$\gamma = \frac{P_{out}}{mass} = \frac{P_{in} - P_{losses}}{mass}$
NTNU – Trondheim
Norwegian University of Science and Technology
www.ntnu.edu

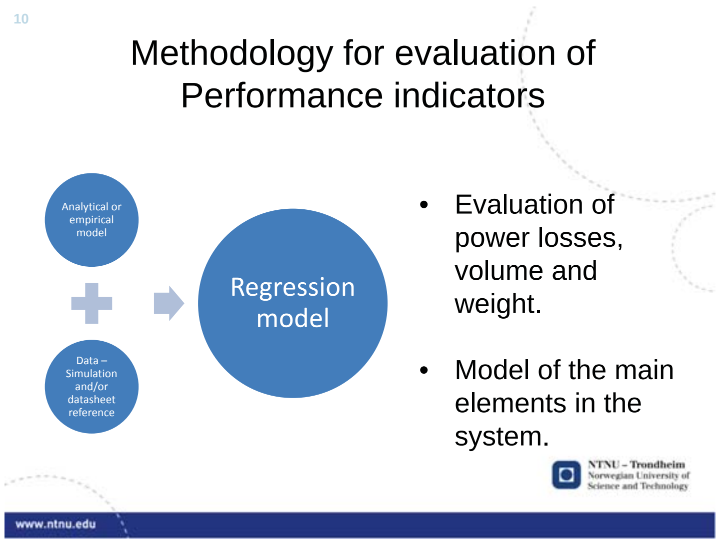
10
Methodology for evaluation of Performance indicators
Analytical or empirical model
Data – Simulation and/or datasheet reference
Regression model
Evaluation of power losses, volume and weight.
Model of the main elements in the system.
NTNU – Trondheim
Norwegian University of Science and Technology
www.ntnu.edu

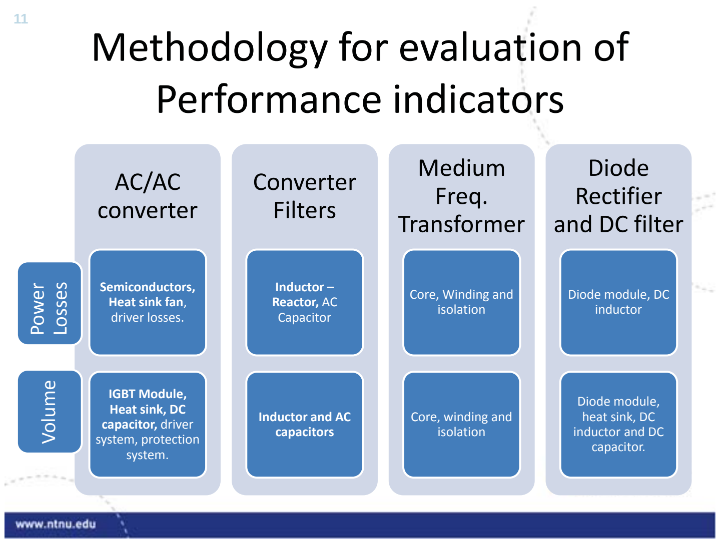
11
Methodology for evaluation of Performance indicators
AC/AC converter
Converter Filters
Medium Freq. Transformer
Diode Rectifier and DC filter
Power Losses
Volume
Semiconductors, Heat sink fan, driver losses.
Inductor – Reactor, AC Capacitor
Core, Winding and isolation
Diode module, DC inductor
IGBT Module, Heat sink, DC capacitor, driver system, protection system.
Inductor and AC capacitors
Core, winding and isolation
Diode module, heat sink, DC inductor and DC capacitor.
www.ntnu.edu

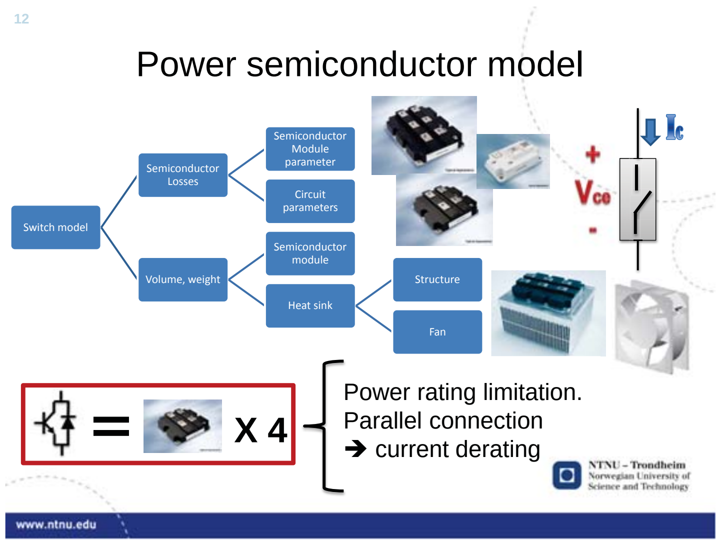
12
Power semiconductor model
Switch model
Semiconductor Losses
Volume, weight
Semiconductor Module parameter
Circuit parameters
Semiconductor module
Heat sink
Structure
Fan
Ic
Vce
X 4
Power rating limitation.
Parallel connection
➔ current derating
NTNU – Trondheim
Norwegian University of Science and Technology
www.ntnu.edu

13

Power semiconductor model

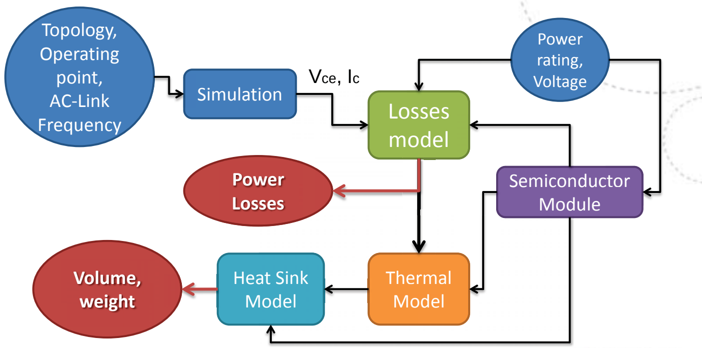

NTNU – Trondheim
Norwegian University of Science and Technology

14

Parameter variation of semiconductor module

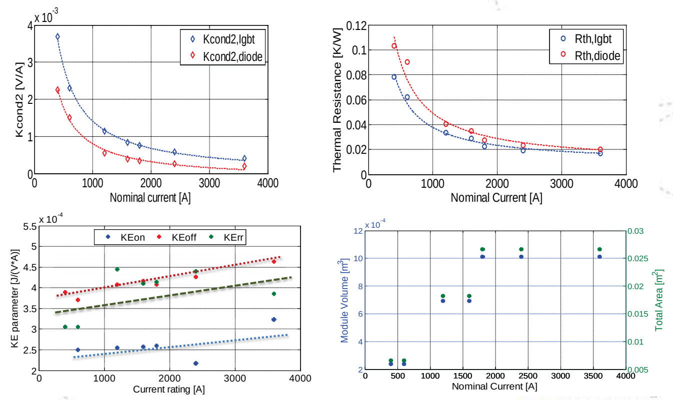

15

Parameters and Design Constraints

Parameter	Value
Total Power	10 [MW]
Input Voltage	690[V]
Output DC Voltage	33 [kV]
Generator Frequency	50[Hz]
DC-Link Voltage ripple	1%
Current Input ripple	20%
Current Output ripple	20%
Generator Power factor	0.9
Magnetic material	Metglas alloy 2605SA1
Max. DT Transformer	70 K
AC-Link Freq. [kHz]	[0.2, 10]
Power x module [MW]	[0.2, 10]

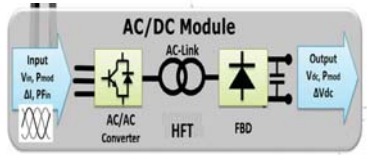

Device	Reference
Ref. Inductor (filters)	Siemens 4EU and 4ET
Ref. DC-link Capacitor	EPCOS MKP DC B256XX
Ref. AC-Capacitor	EPCOS MKP AC B2536XX
IGBT Module	Infineon IGBT4 FZXXR17HP4
DIODE Module	Infineon IGBT3 DDXXS33HE3
Heat Sink	Bonded Fin - DAU series BF
Axial FAN – Heat sink	Semikron SKF 3-230 series

16

B2B – Selection of f_{sw1}

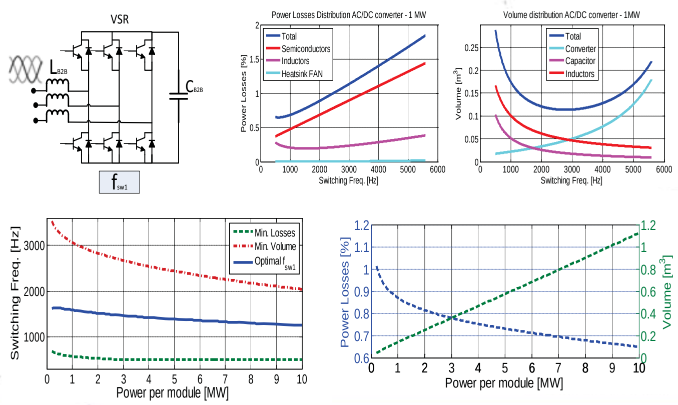

17

Efficiency

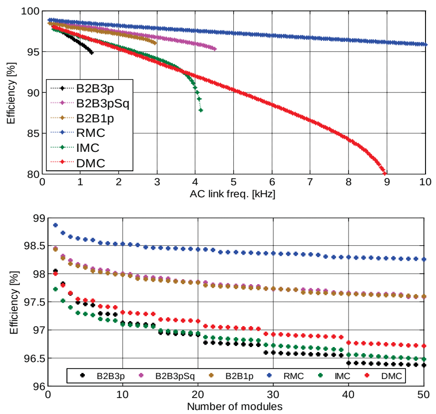

The slope is less steep in solutions based on squared waveform in the AC-Link.

The RMC solutions are the most efficient for any number of modules or AC-link frequency.

Solutions based on matrix topologies present less variation in efficiency when increase in the number of modules

NTNU – Trondheim
Norwegian University of Science and Technology

18

Power Density

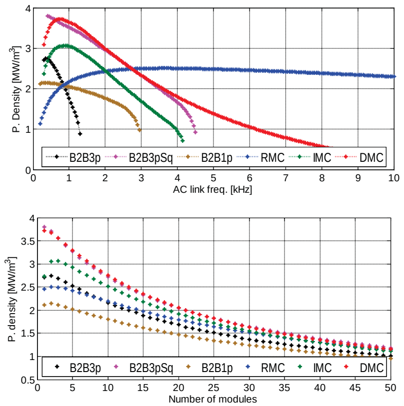

- Similar maximum values are obtained with DMC and B2B3pSq topologies.
- B2B3pSq ➔ 400 to 600 Hz
- DMC ➔ 700 to 1000 Hz

- Low number of modules present the highest power density in all solution, however there is an optimum number of modules for each topology.

NTNU – Trondheim
Norwegian University of Science and Technology

19

Power to mass ratio

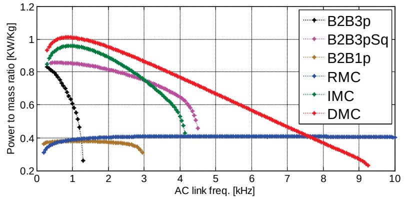

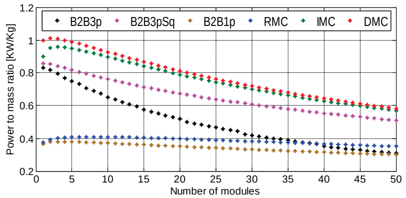

- DMC and IMC solutions present the maximum values of Power to mass ratio.
- For RMC solution the maximum values are obtained at high freq.
- The optimal number of modules for max. P. to mass ratio is higher than the case of max. power density.
- An increase in the number of modules is less drastic in RMC and B2B1p solutions.

NTNU – Trondheim
Norwegian University of Science and Technology

20

Pareto surface

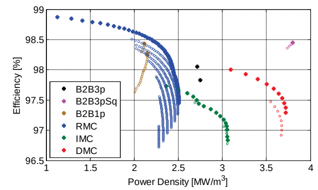

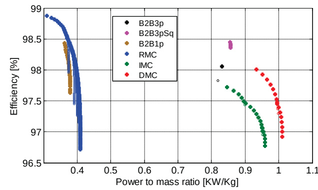

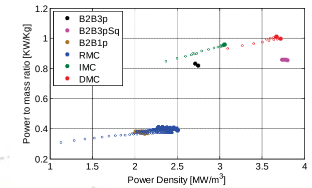

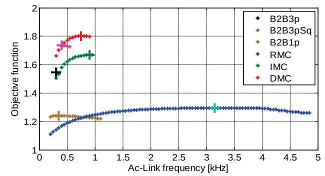

21

Conclusions

- WECS based on DMC and B2B3pSq topologies will lead the best trade-off between efficiency and power density in range of AC-Link frequencies from 200[Hz] to 3[KHz].
- RMC topology has better performance when AC-link frequency is required to be above 3[kHz].

22

NOWITECH
Norwegian Research Centre for Offshore Wind Technology

Thanks for your attention

Rene Barrera-Cardenas and Marta Molinas
(rene.barrera, marta.molinas) @elkraft.ntnu.no
Department of Electric Power Engineering

NTNU – Trondheim
Norwegian University of Science and Technology

23

Power semiconductor - Conduction losses

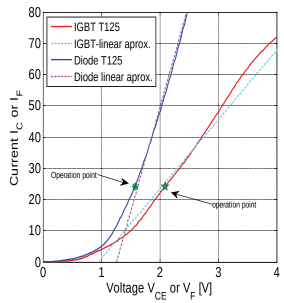

$$P_{cond} = \frac{1}{T}\int_{t_0}^{t_0+T} V_{ce}(t)\cdot I_c(t)\cdot dt\,;$$

$$V_{ce}(t) = K_{cond1} + K_{cond2}\cdot I_c(t)$$

$$P_{cond} = \frac{1}{T}\int_{t_0}^{t_0+T} (K_{cond1} + K_{cond2}\cdot I_c(t))\cdot I_c(t)\cdot dt$$

$$P_{cond} = \frac{1}{T}\int_{t_0}^{t_0+T} K_{cond1}\cdot I_c(t) + K_{cond2}\cdot I_c(t)^2\cdot dt$$

$$\boxed{P_{cond} = K_{cond1}\cdot I_{c(avg)} + K_{cond2}\cdot I_{c(rms)}^{\;2}}$$

24

Power semiconductor - Switching losses

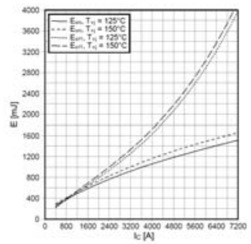

$$P_{sw} = \frac{1}{T}\sum_{T} E_{on} + E_{off} + E_{rr}$$

$$E_{sw} = E(I_c)\frac{V_{ce}}{V_{test}}$$

$$E_{sw} = \frac{E_{test}}{V_{test}\cdot I_{test}} V_{ce(t^*)}\cdot I_{c(t^*)}$$

$$\boxed{P_{sw} = K_E\cdot V_{ce_{(avg)}}\cdot I_{c_{(avg)}}\cdot fun_{sw}(f_{sw}, f_0, mod)}$$

$$fun_{sw} = \sum_{i=0:3} K_{sw,i}\cdot\left(\frac{f_{sw}}{f_0}\right)$$

$K_{sw,i}$ depends on the converter topology and the modulation strategy

25

Heat sink volume

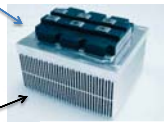

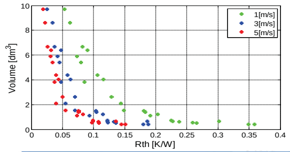

Heat sink volume dependents of thermal resistance. Based on Datasheet information.

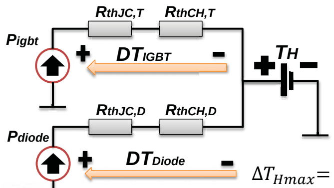

$$Vol_{HS} = \frac{K_{HS}}{R_{\theta sa}} = \frac{K_{HS}}{\Delta T_{Hmax}} P_{loss}$$

ΔT_{Hmax} based on worst case assumption in thermal design.

$$\Delta T_{Hmax} = K_{SFT} \cdot T_{jmax} - T_{amb} - max\{R_{th,igbt} \cdot P_{igbt}\ ;\ R_{th,diode} \cdot P_{diode},\}$$

26

Example: Capacitor Volume (1)

1. Selecting type and technology

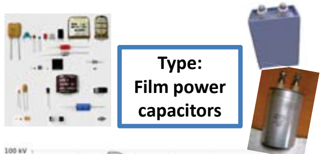

Type: Film power capacitors

Technology?

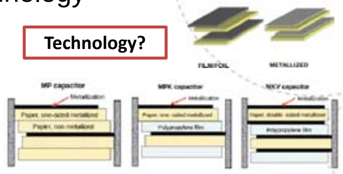

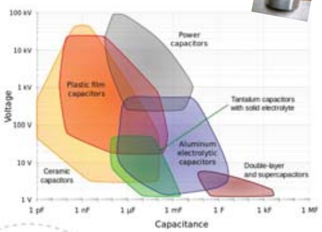

Source: http://en.wikipedia.org/wiki/Types_of_capacitor

Suggestion of the manufacturer for the type of application

TDK

EPCOS

Power Capacitors for Wind Power Generation

Technology: **MKP**

DC series | AC Series

27

Example: Capacitor Volume (2)

2. Obtaining the model

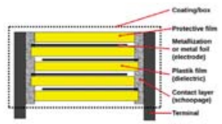

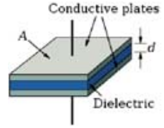

$$C \approx \frac{\epsilon \cdot A}{d}$$

$$E_{stored} = \frac{1}{2} C \cdot V^2$$

The breakdown voltage (*Vb*) is defined by the separation of the electrodes and dielectric strength.

$$V \propto V_b \propto d$$

$$volume \propto A \cdot d$$

$$E_{stored} \propto \frac{\epsilon \cdot A}{d} d^2 \propto A \cdot d$$

$$volume \propto E_{stored} \propto C \cdot V^2$$

NTNU – Trondheim Norwegian University of Science and Technology

28

Example: Capacitor Volume (3)

3. Regression model

$$vol = (K_{11} \cdot C + K_{10})(K_{22}V^2 + K_{21}V + K_{20})$$

$$vol = K_1(V) \cdot C + K_0(V)$$

K_0 and K_1 depends of application voltage

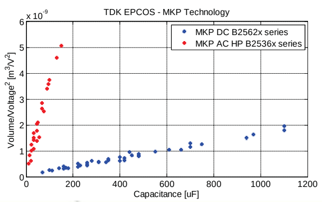

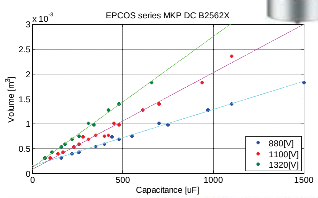

29

Magnetic components losses

- Core Losses → based on Steinmetz equation

$$P_{core} = K_{core} \cdot Vol_{core} \cdot f^{\alpha_c} \cdot B^{\beta_c}$$

highly dependent of magnetic material, volume and waveform voltage

- Copper Losses → losses of all windings

$$P_{cu} = \sum_{i=1}^{nw} K_{cu(i)} \frac{\rho_{cu} N_{(i)} MLT_{(i)}}{A_{w(i)}} I_i^2 (1 + THD^2)$$

K_δ as a function of frequency, winding design (layers, conductor)

NTNU – Trondheim Norwegian University of Science and Technology

30

Transformer volume and losses

Design process aims to minimize the volume of the transformer taking into account some assumptions.

- Type transformer structure
  - dry shell-type transformers
  - optimal set of relative dimensions***
- Temperature rise
  - α Power losses
  - α 1 / (surface area)
- Power rating
  - each winding carry the same current density

1-phase*

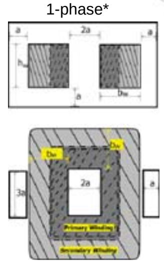

Transformer Superior view

3-phase**

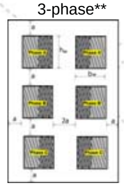

Front view

*S. Meier, et al. "Design Considerations for Medium-Frequency Power Transformers in Offshore Wind Farms." IEEE 2010.
** T. Mclyman. "Transformer and Inductor Design Handbook." CRC Press 2004.
***N. Mohan, T. M. Undeland, and W. P. Robbins, Power Electronics: Converters, Applications, and Design, 3rd ed. Wiley, Oct. 2002

31

Transformer volume and losses

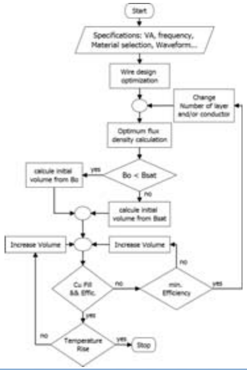

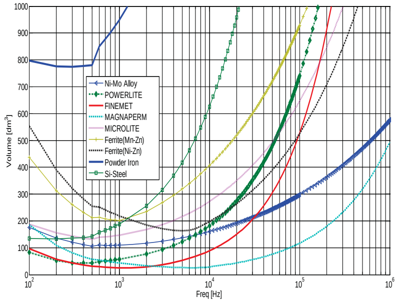

Example: Single-phase transformer volume
S= 100 [KVA] V = 1 [KV]

*Optimum flux density calculation based on W. G. Hurley, W. H. Wolfle, and J. G. Breslin, "Optimized transformer design: inclusive of high-frequency effects," IEEE Transactions on Power Electronics, vol. 13, no. 4, pp. 651–659, Jul. 1998.
**Wire design based on Litz wire structure: http://www.elektrisola.com/litz-wire/technical-data/formulas.html

32

Transformer volume

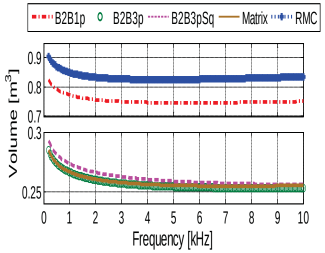

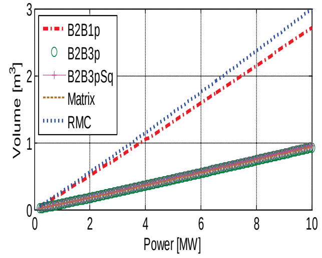

a) Volume dependence frequency and power = 3[MVA].
b) Volume dependence power and frequency = 1[kHz].

NTNU – Trondheim Norwegian University of Science and Technology

33

High Frequency Transformer

Electric model of High Frequency transformer. Parameters obtained from the design procedure*.

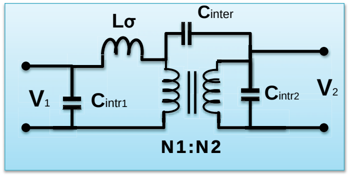

Example. Transformer 690V/3.3kV, 625kW

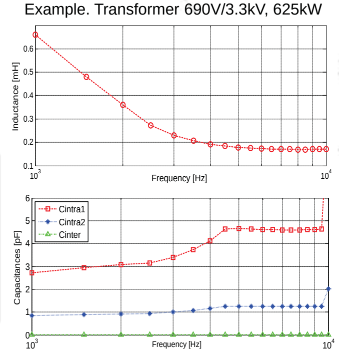

*S. Meier, et al. "Design Considerations for Medium-Frequency Power Transformers in Offshore Wind Farms." IEEE 2010.

34

DC link Capacitor

Proportional model in order to estimate the capacitor volume from the reference capacitor.*

$$Vol_{Cap} = \frac{C}{C_{ref}} \left(\frac{V_{DC}}{V_{ref}}\right)^2 \cdot Vol_{ref}$$

- The capacitance is designed in order to limit the DC voltage ripple*.

$$C \propto \frac{I_{rms}}{V_{DC} f_{sw}}$$

*M. Preindl and S. Bolognani, "Optimized design of two and three level full-scale voltage source converters for multi-MW wind power plants at different voltage levels," in IECON 2011.

35

Filters

The Inductance is designed in order to limit the current ripple*,**.

$$L_{B2B} \propto \frac{V_{DC}}{I_{rms} f_{sw}} \qquad L_{MC} \propto \frac{V_{LL}^2}{f_{sw} \cdot P} \qquad C_{MC} \propto \frac{P}{f_{sw} \cdot V_{LL}^2}$$

Proportional model in order to estimate the Inductor volume* and losses from the reference Inductor.

$$Vol_{induc.} = K_{ind} \cdot \left(L_{filter} \cdot I^2\right)^{3/4}$$

$$P_{loss\_L} = \left(P_{cuRef} + P_{coreRef} \cdot \left(\frac{f_{ref}}{f}\right)^{\frac{(7\alpha-2)}{(12\beta-\alpha)}}\right) \cdot \left(\frac{Vol_{ind.}}{Vol_{Ref}}\right)$$

*M. Preindl and S. Bolognani, "Optimized design of two and three level full-scale voltage source converters for multi-MW wind power plants at different voltage levels," in IECON 2011.
**M. hamouda, F. Fnaiech, and K. Al-Haddad, "Input filter design for SVM Dual-Bridge matrix converters," in 2006 IEEE International Symposium on Industrial Electronics, vol. 2. IEEE, Jul. 2006.

36

AC/AC Converter - Topologies

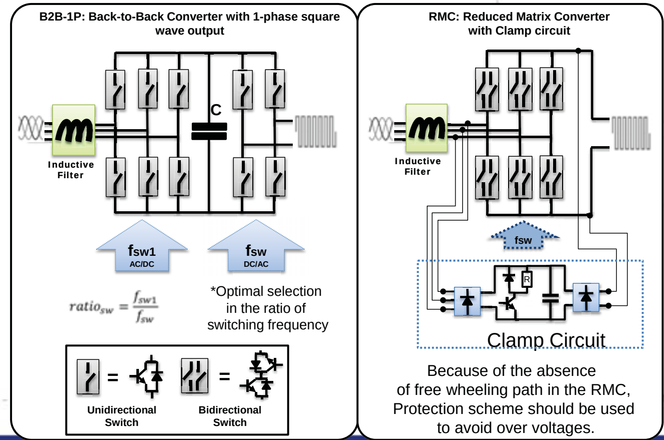

Fault ride-through enhancement of multi-technology offshore wind farms

Arshad Ali
Fan Zhang
Olimpo Anaya-Lara

EERA Deepwind 2014
23 January 2014, Trondheim, Norway

Outline of presentation

- Background
- Problem description
- Modelling
- FRT control for DFIG
- FRT control for DFIG and FRC-WT
- Conclusions

Government Targets

Scottish Targets -

- **80% of power from Renewables by 2020**
- Interim target of 31% by 2011
- Currently at 25% (2008 figure)
- 20% of primary energy by 2020
- **Emission reduction target of 80% by 2050**
- Interim target of 42% by 2020

UK Targets –

- **32% of power form renewables by 2020**
- Currently at 7%
- 15% of primary energy by 2015
- **Emission reduction target 80%** by 2050

UK ROUND 3 OFFSHORE WIND SITES - 32GW

£90Bn Capex Investment over the next 10 years

6,800 wind turbines

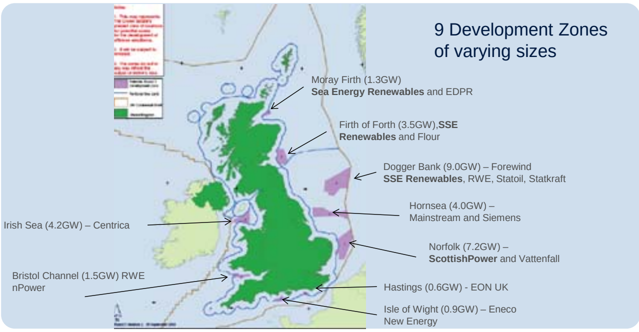

Fault Ride-Through Capability

- Large-capacity wind farms must remain connected to the network even in the event of faults in the high-voltage network
- FRT requirements are different from country to country

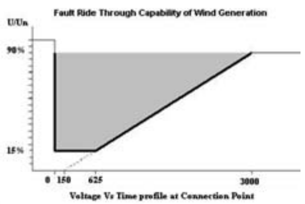

»**Voltage characteristic for Eire 'ride through' requirement**

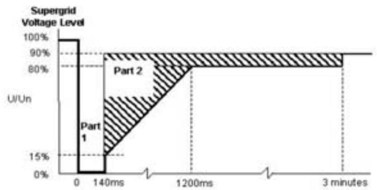

»**Voltage characteristic for GB 'ride through' requirement**

5

FRT depends on turbine concept

- FRT capability varies by different wind turbine concept
- Major wind turbine concepts in the market
  - ➢ (a) fixed speed wind turbine: high damping, low efficiency
  - ➢ (b) DFIG wind turbine: partially coupled to grid, low damping, low FRT capability
  - ➢ (c) PMG wind turbine: totally decoupled from grid, high FRT capability.

DFIG dominates current wind turbine market

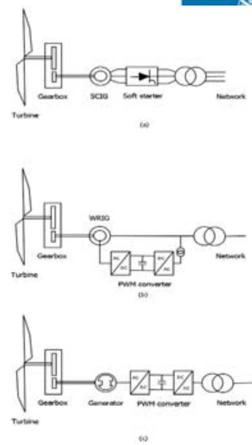

Doubly-fed induction generator (DFIG)

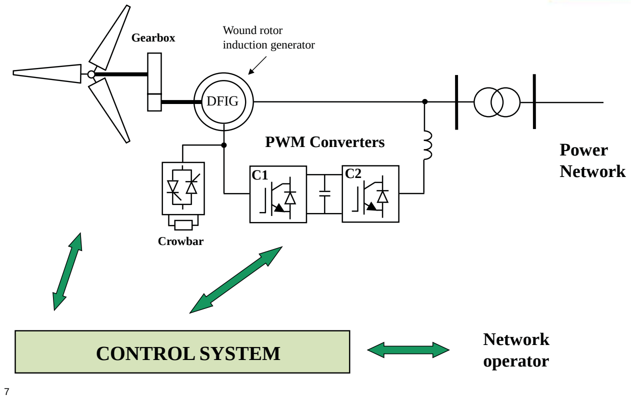

Voltage sags and FRT solutions

- Voltage sags can be typical classified based on the cause, e.g.:
  - Fault related
  - Large induction motor start
  - Large induction motor re-acceleration
- DFIG-FRT problem solutions may be:
  - Modification of conventional controller
  - Active crowbar control
  - Application of dynamic breaking resistors

FRT Issues – holistic approach needed

- Mechanical
  - Consistent operation, no protection triggered
  - Loads alleviation
- Electrical
  - High voltage/current protection
  - Reactive power support
  - Stable torque generation to avoid wind turbine rotor speed-up

DFIG control during fault – crowbar with variable resistance

- Advantages
  - Wind turbine stays connected during grid fault
  - Wind turbine keeps generating power during grid fault
  - Rotor speed acceleration and drive-train oscillation are prevented
- Limitations
  - Fault level: the power generation is not possible under extremely low grid voltage
  - High power loss during fault

Crowbar with variable resistance

- During grid fault, converters are blocked, DFIG operates in SCIG mode. DFIG torque is calculated as:

$$T = \frac{3}{2}\frac{p_f R_r I_r^2}{s\omega_s}$$

- Applying Kirchhoff's current law to SCIG equivalent circuit, The torque is expressed as

$$T = \frac{3}{2}\frac{p_f R_r V_s^2}{s\omega_s\left[\left(R_s + \frac{R_r}{s}\right)^2 + (L_s + L_r)^2\right]}$$

- Torque is expressed in terms of rotor resistance

Crowbar with variable resistance – T/Slip curve

- Torque-slip curve of induction machine changes under different rotor resistance and grid voltage

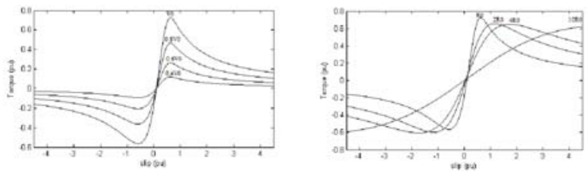

- By controlling the rotor resistance, reference torque can be produced under certain grid voltage

Implementation

- Switching by grid voltage level
- Normal operation: external resistor bypassed
- Fault case: IGBT switched to connect variable resistor to DFIG rotor

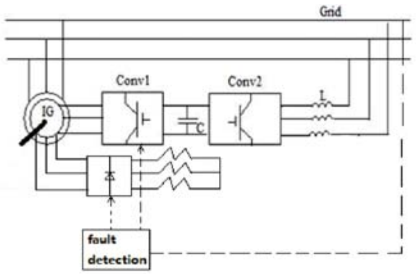

Control implementation – Flow Chart

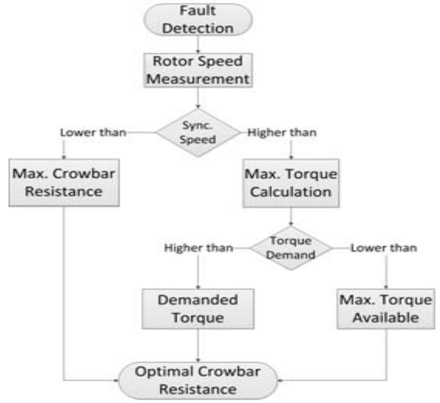

Test model construction

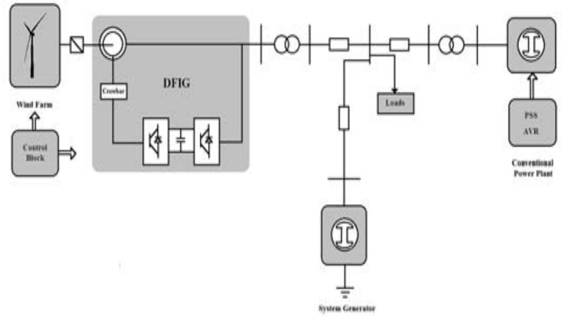

Model construction (const)

- Wind Turbine Model
  - Dynamic model of rotor, tower and drive-train
- DFIG Model
  - Induction machine model
  - DFIG controller in d-q frame
- Grid Model
  - Generic network model comprising wind farm, conventional power plant with AVR, PSS and etc, Local Grid

Simulation results

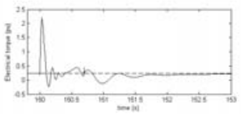

Electrical torque

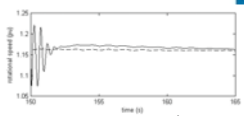

Rotor speed

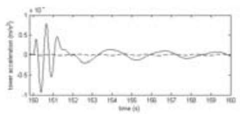

Tower acceleration

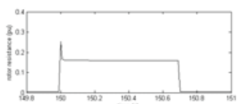

Rotor resistance

Solid line: with normal crowbar protection

Dashed line: with variable resistance crowbar control

Fully-Rated Converter-based wind turbine

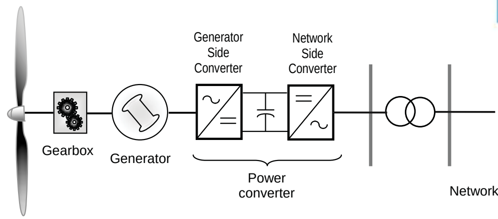

- Uses either an induction generator or a synchronous generator (it can either be an electrically excited synchronous generator or a permanent magnet machine.
- The converter completely decouples the generator from the network, enabling variable-speed operation.
- The rating of the power converter in this wind turbine corresponds to the rated power of the generator.

Block Diagram of Proposed System

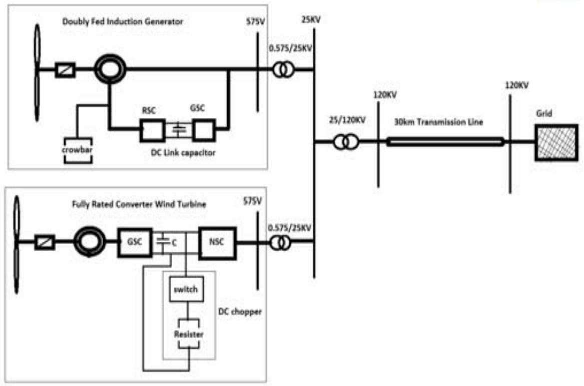

Results

Without Protection **After applying Protection**

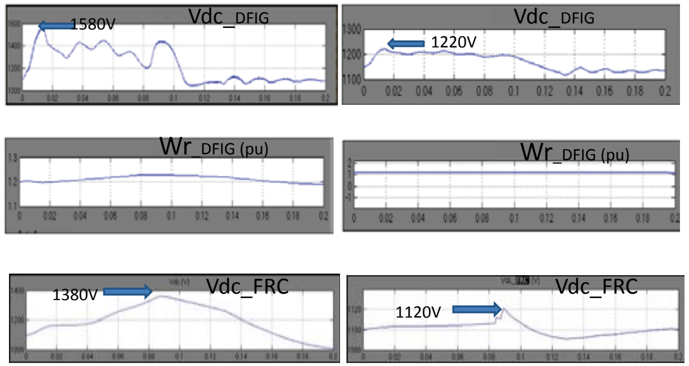

Conclusions

- ❑The multi technology wind farm eliminate the need of STATCOM at the point of common coupling (PCC).
- ❑Proposed strategy is applied to multi-technology wind farm to eliminate current and voltage transients during grid faults.
- ❑The DC link voltage and high rotor currents are controlled within limits after applying the protection scheme.

University of Strathclyde Glasgow

Reliability of power electronic converters for offshore wind turbines

A main topic in the research project:
"Power Electronics for Reliable and Energy Efficient Renewable Energy Systems"
Short name: **OPE**
Duration: 2009-2014
Financing: The Research Council of Norway and three industry partners
Web: www.sintef.no/OPE

Magnar Hernes SINTEF Energy Research
Magnar.Hernes@sintef.no

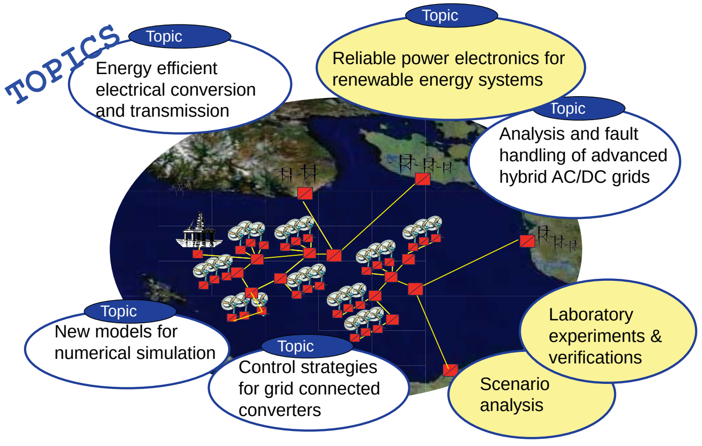

Reliable and Energy Efficient Renewable Energy Systems

Power electronics for wind farm power conversion

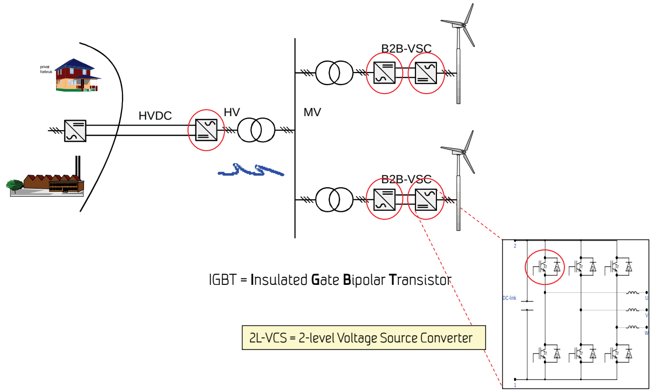

Converter topologies for MV and HV applications

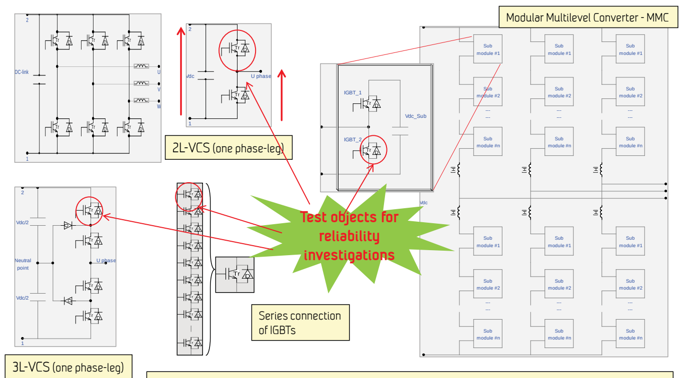

Due to voltage limitation of single IGBTs, MV and HV converters need more complex topologies and/ or series connection of IGBTs

Reliability of power semiconductors - Failure modes

- Spontaneous failures due to overloads
  - Related to power semiconductor chips
  - Thermal overload and overvoltage
  - Exceeding V/I safe operating area for the device
- Failures triggered by external environment
  - E.g. intrusion of humidity
  - E.g. cosmic radiation
- Failures due to aging or exhaustion
  - Mechanical and electrical termination of the chips
  - Packaging and encapsulation

Project focus

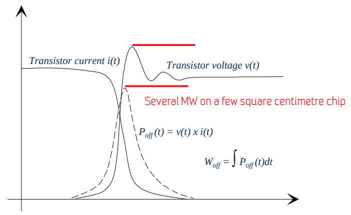

Typical turn-off behaviour for a controllable power semiconductor

- Mostly chip related:
  - Spontaneous failures
  - Cosmic radiation
- Mostly related to packaging
  - Ageing or exhaustion
  - Intrusion of humidity in chip insulation

IGBT packaging

- Mainly two technologies
  - Planar bonded modules
  - Press-pack housing
- Both can contain both IGBT chips and antiparallel free-wheeling diodes

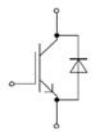

- A 750A/ **6500V** IGBT module from Infineon

- An 1800A/ **4500V** press-pack IGBT from Westcode

Planar bonded IGBT modules

- Main failure mechanisms:
  - Bond wire lift off
  - Solder layer disconnect
- Thorough investigations and publications

$N_f = K \cdot \Delta T_j^{\beta_1} \cdot e^{\left(\frac{\beta_2}{T_j+273}\right)} \cdot t_{on}^{\beta_3} \cdot I^{\beta_4} \cdot V^{\beta_5} \cdot D^{\beta_6}$ (T_j=T_{low} in °C)

- Failure mode
  - ➢ **Failure to break**

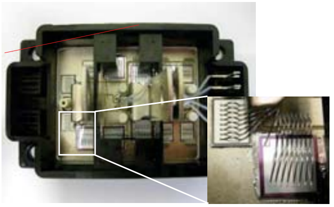

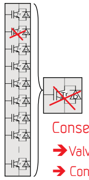

Consequence:
➔ Valve failure
➔ Converter failure

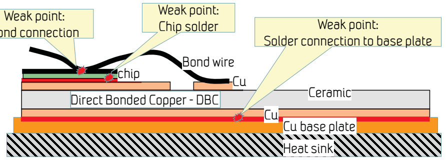

Life time curves – no of cycles to failure

Experience data from modules:

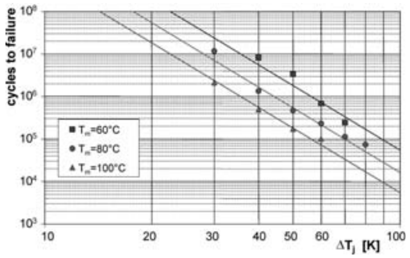

Lifetime dependent on:

- ΔT
- T_{max}
- dT/dt
- t_{on}
- I_{Load}
- control strategy
- and more….

Press-pack IGBTs

- Failure mechanisms:
  - *Limited knowledge*
- Few publications on failure mechanisms and reliability
- Failure mode
  - ➢ **Expected failure to short**

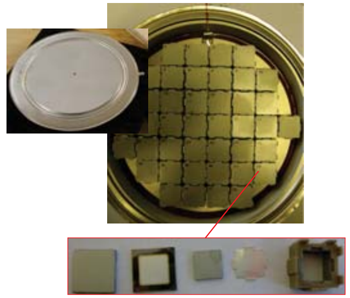

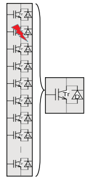

Consequence:
➔ Valve still functional
➔ Reduced voltage margins to failure

Main focus on reliability of press-pack IGBTs in the OPE project

- The OPE project prioritized reliability of press pack devices for the following reasons:
  - Limited published information regarding failure mechanisms and power cycling life time
  - Press-pack devices are very relevant in medium voltage wind power applications due to series connection capabilities (fail-to short-circuit)
  - Special power cycling stress condition for wind power converters (wind fluctuations, low motor side frequency etc.)
- Then we need to know:
  - Load profiles for the application, e.g. power cycling due to wind fluctuations
  - Stress levels related to grid side and generator side load conditions (power frequency, cos φ etc.)
  - Stress levels related to the converter power circuit and controls (topology, switching frequency etc)
- Theoretical work
- Experimental work

Case study: A medium voltage PWM 3L-NPC VSC for 3.3 kV AC

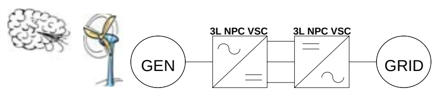

- DC link voltage ~ 5 kV
- 3.3 kVac (LL voltage)
- Switching frequency ~ 1500 Hz +/-
- 5 MVA (connected to a 3.6 MW wind turbine gen.)
- IGBT: Press-pack 1800 A/4500 V

Test Cell for mapping switching characteristics of HV IGBTs

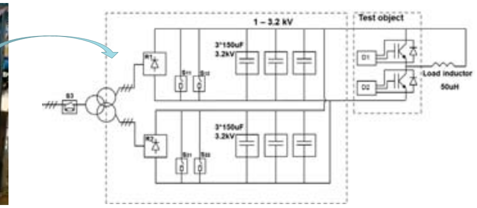

- Present Test Cell with 0-5 kV DC-link
- Planned to be extended to 10kV

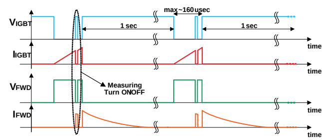

- "Double-pulse" waveform for measuring IGT turn-on and turn off waveform
- External liquid (silicon oil) heating/cooling circuit for temperature control (5- 50 °C)

Turn-off waveforms with DC-link 2800V and turn-off current 1800A

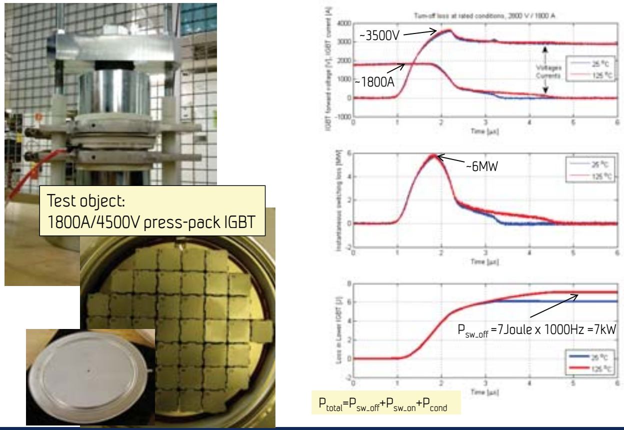

Power Cycling Tester for life-time testing of high-power IGBTs (2000 A)

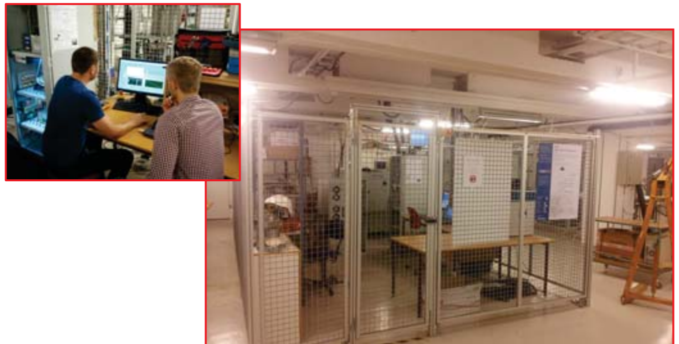

Project investment of ~1MNOK.
Developed in cooperation with Chemnitz University of Technology

Operation of the Power Cycling Tester

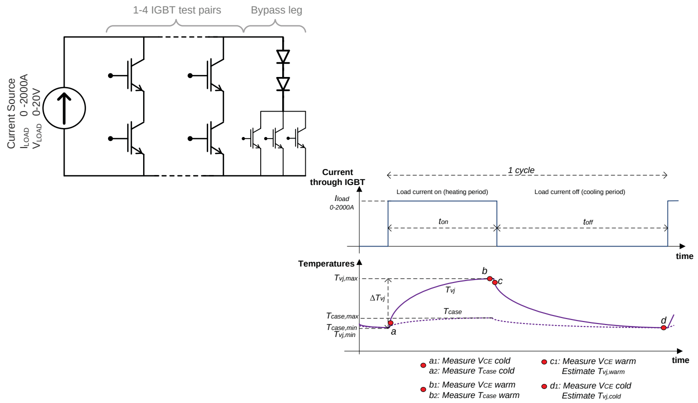

OPE Power Cycling Tester – Control screen

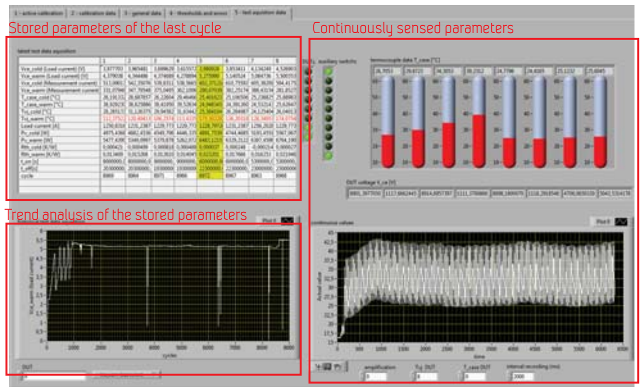

Plot from measurement of planar bonded modules

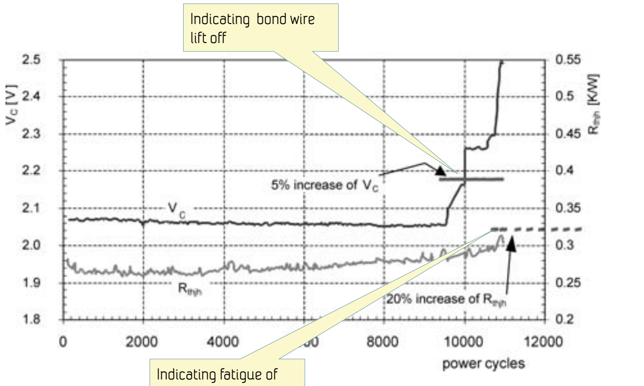

From Chemnitz University of Technology

Power Cycling Tester with 4x modules + 4x press packs

Modelling press-pack IGBT for stress analysis
Work by PhD student Tilo Poller at Chemnitz University of Technology

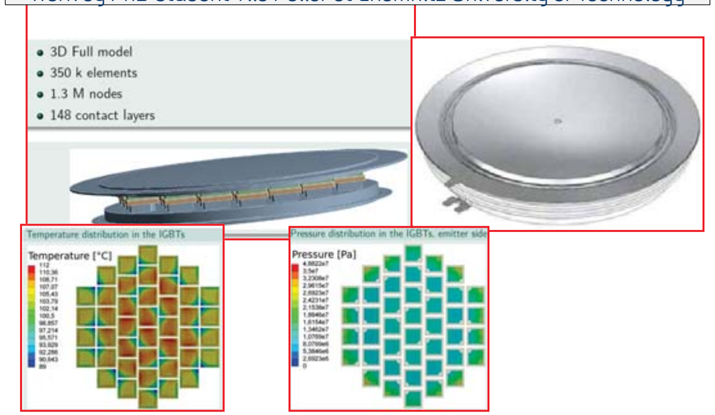

Simulation model of (PSCAD) of PWM Voltage Source Converter

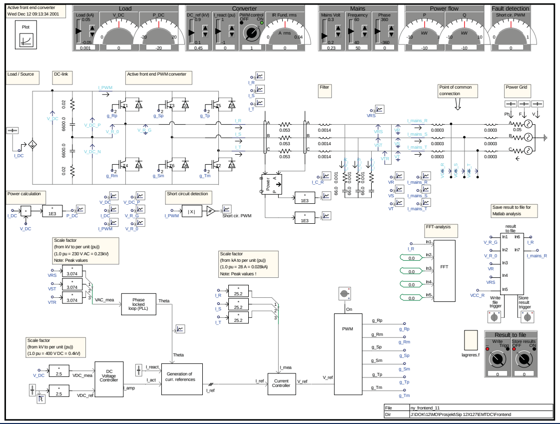

IGBT loss calculator in PSCAD with thermal network add-on

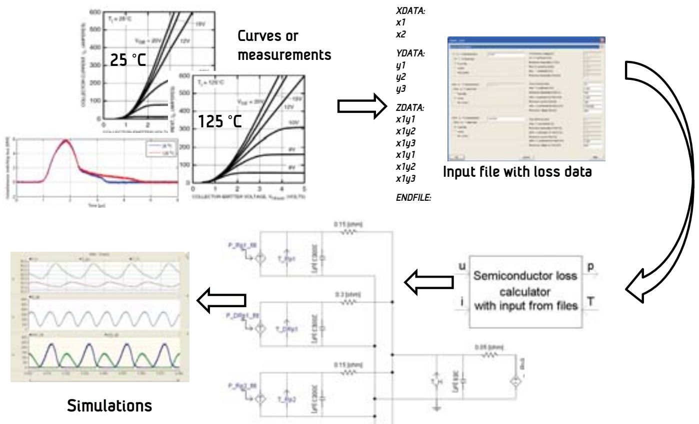

Simulated load dependent swings of IGBT hotspot temperature

Motive:

- Combine laboratory measurements with numerical simulations to estimate efficiency and lifetime of power semiconductors

Simulated temperature swings affected by:

- Switching frequency
- Line-side and generator side power frequency, cos φ etc,
- Filter ripple current
- Wind fluctuations
- ..and more

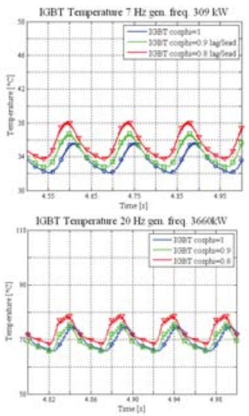

Methodology for power cycling lifetime estimation

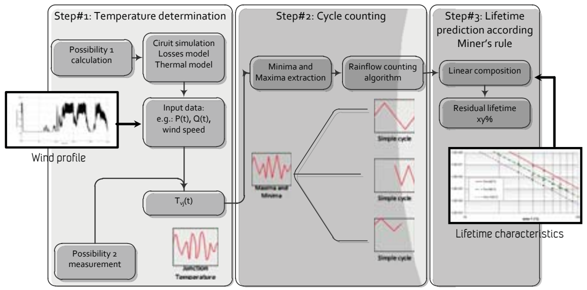

TABLE VI SUMMARY OF LIFETIME CONSUMPTION

device	$\sum LRN$	$\sum LR$	LR	Lifetime
	[p.u]	[p.u.]	[p.u.]	[years]
IGBT, CGe	0.039	0.0719	0.111	17.8
IGBT, CGr	0.047	0.057	0.104	19.3
Diode, CGe	0.083	1.244	1.327	1.51
Diode, CGr	0.016	0	0.016	122

Example:
If not oversized lifetime for the generator side diode can be very short!

Planned continuing activities on converter reliability

- Completion of the reliability work in the OPE project (deadline 30th June 2014)
  - Continue power cycling of IGBTs
    - Press-packs and modules
    - Power Cycling of single chips (master student work)
  - Post processing of result
  - Final reporting and publications
- Develop a new research project for continuation of converter reliability topics
  - Together with colleagues at Chemnitz University of Technology
  - Start-up spring 2015
  - Exploit results and ideas from OPE
  - Address VSC converter applications for HV collecting and transmission systems
  - Power cycling capabilities assuming various converter topologies and AC/DC systems
  - New methods for condition monitoring, predicting rest life-time etc.

Thank you for your attention !

B4) Power system integration

Design and Optimisation of Offshore Grids in Baltic Sea for Scenario Year 2030,
Vin Cent Tai, NTNU

Operation of power electronic converters in offshore wind farms as virtual synchronous machines, Jon Are Suul, SINTEF Energy Research

The Future of HVDC, Yiannis Antoniou, University of Strathclyde

North-Sea Offshore Network – NSON, Magnus Korpås, SINTEF Energy Research

NTNU – Trondheim
Norwegian University of Science and Technology

Design and Optimisation of Offshore Grids in Baltic Sea for Scenario Year 2030

Vin Cent Tai & Kjetil Uhlen

Norwegian University of Science and Technology

EERA Deepwind'2014
Trondheim, Norway
22 – 24 / Jan / 2013

NTNU – Trondheim
Norwegian University of Science and Technology

Outline

NTNU – Trondheim
Norwegian University of Science and Technology

Offshore Grid Design

Objective

OffshoreDC project [1] WP-5:

- Find an optimal grid structure taking into account:
  - Wind power variations
  - Stochastic power prices
  - On- and offshore load and generation scenarios
- Use formal optimization for a structured approach to finding good grid layouts
  - Huge number of possible grid structures
  - Combinatorial problem solved efficiently by optimization tools
- Results:
  - Which cables to build & capacity on the cables
  - Gives valuable decision support, but:
  - Must be combined with market/network model in an iterative procedure

[1] www.offshoredc.dk

NTNU – Trondheim
Norwegian University of Science and Technology

Offshore Grid Design

Design Flow Chart

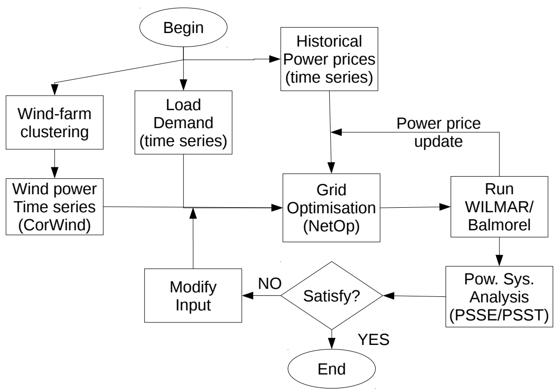

NTNU – Trondheim
Norwegian University of Science and Technology

Case Study : Baltic Sea 2030

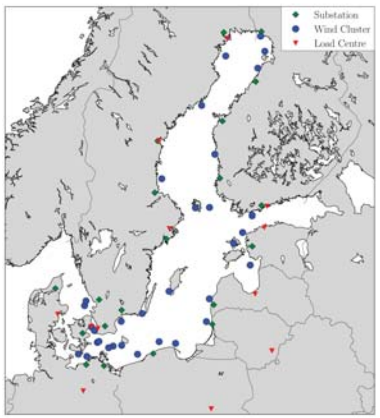

- **Problem :** How to connect the wind farms to the onshore grids?
  - # of offshore windfarms : 97
  - # of onshore substations : 18
  - # of market areas : 12
  - # of combinations = $2^{N(N-1)/2}$
- To reduce the # of combinations:
  - Windfarms owned by the same country
  - Geographical size ± 100km
  - Cluster size ± 2000MW
- Results : Total windfarm clusters = 32

NTNU – Trondheim
Norwegian University of Science and Technology

Design Inputs

Objective Function

Network Optimisation Tool : NetOp [1]

- Mixed Integer Linear Programming (MILP Problem)
- Objective function:

$$min\left(C_{Tot}^{branch}+C_{Tot}^{node}+C_{Tot}^{geno}\right)$$

[1] H.G.Svendsen (2013). Planning tool for clustering and optimised grid connection of offshore wind farms. Energy Procedia 35, pp. 297 – 306.

Design Inputs

Wind Power Model

Table 1: Total installed wind power capacity for each country by 2030 [1].

#	Country	Installed Capacity [MW]
1	Germany	4737
2	Denmark	3334
3	Sweden	8413
4	Finland	5433
5	Poland	500
6	Estonia	2602
7	Lithuania	1000
8	Latvia	1100

Assumption: The wind power generation profile is the same across the Baltic sea. **(Not realistic!!)**

Current Model:
- Wind power time series data for wind farms in the Krigersflak area [2].
- Aggregate wind power output of the wind farms and normalise it against the total capacity of the wind farms:

$$W_{profile}(t)=\frac{\sum_{n=i}P_{wf,i}(t)}{\sum_{n=i}P_{wf,i}^{max}}$$

Next step: Use *CorWind* [3] model.

[1] N. Cutululis (N.A). TWENTIES Deliverable 16.1: Offshore wind power data, unpublished.
[2] H.G.Svendsen (2013). Planning tool for clustering and optimised grid connection of offshore wind farms. Energy Procedia 35, pp. 297 – 306.
[3] P. Sorensen et al., (2009). Power fluctuation from large wind farms – Final report.

Table 2 : Wind clusters and their corresponding onshore connection points. The wind clusters are connected radially to the connection points closest to them as initial *NetOp* input.

#	Country	Cluster Name	Capacity [MW]	Latitude	Longitude	Connection Point	Case
1	DE	DE-1	1780	54.8115	14.1094	Lubmin	2
2	DE	DE-2	1800	54.8135	13.7852	Lubmin	2
3	DE	DE-3	1090	54.4579	12.2551	Bentwisch	2
4	DK	DK-1	890	54.5510	11.6587	Bjaerverskov	2
5	DK	DK-2	180	55.6520	12.5810	Bjaerveskov	2
6	DK	DK-3	1980	55.0298	12.9970	Bjaerveskov	2
7	DK	DK-4	160	54.9080	14.7035	Bjaerveskov	2
8	DK	DK-5	150	56.5000	12.0950	Trige	2
9	FI	FI-1	2440	65.6558	24.4852	Isohara	1
10	FI	FI-2	1220	65.2093	24.7811	Isohara	1
11	FI	FI-3	490	64.7023	24.2873	Pyhajoki	1
12	FI	FI-4	620	61.9607	21.2616	Rauma	1
13	FI	FI-5	10	60.1340	20.8890	Rauma	1
14	FI	FI-6	160	59.8590	23.8880	Espoo	1
15	FI	FI-7	500	60.1170	19.9000	Rauma	1

Table 2 : (continued..)

#	Country	Cluster Name	Capacity [MW]	Latitude	Longitude	Connection Point	Case
16	SE	SE-1	1420	56.6831	12.1947	Breared	2
17	SE	SE-2	600	55.8781	14.6704	Hemsjo	2
18	SE	SE-3	920	55.0700	13.1030	Hurva	2
19	SE	SE-4	1300	55.5110	12.7790	Hurva	2
20	SE	SE-5	1600	56.1899	16.1460	Hemsjo	2
21	SE	SE-6	550	57.0576	18.0397	Hemsjo	2
22	SE	SE-7	1010	61.1328	17.5281	Stockholm	1
23	SE	SE-8	920	63.5470	20.3350	Sundsvall	1
24	SE	SE-9	60	65.0700	22.0300	Svartbyn	1
25	PO	PO-1	180	54.9914	18.4973	Slupsk	2
26	PO	PO-2	230	55.0601	17.3409	Slupsk	2
27	PO	PO-3	90	54.5461	15.8235	Slupsk	2
28	EE	EE-1	1580	59.2572	23.2171	Lihula	1
29	EE	EE-2	520	58.0541	23.7503	Lihula	1
30	EE	EE-3	500	58.8670	22.5830	Lihula	1
31	LV	LV-1	1000	55.8687	20.6711	Grobina	2
32	LT	LT-1	1100	56.7656	20.8797	Klaipeda	2

Design Inputs

Load Model

Table 3 : Annual demand of each price area in 2030.

#	Price Area	Load Demand [GWh]	Case study
1	DK1	23347	1
2	DK2	15735	1
3	DE	581128	1
4	PO	165344	1
5	FI	90922	2
6	LI	10922	1
7	LT	8699	1
8	EE	10921	1
9	SE1	12461	2
10	SE2	14631	2
11	SE3	90392	2
12	SE4	25693	1

$$L_{p.area}^{2030}=L_{p.area}^{2012}\times\frac{L_{country}^{2030}}{L_{country}^{2012}}$$

Note:

$L_{p.area}^{2012}$, $L_{country}^{2012}$ Extracted from time series data from *ENTSO-E*

$L_{country}^{2030}$ Forecast data from [1]

Assumption: The load consumption pattern of each price area does not vary too much from 2012's pattern.

[1] S.Uski-Joutsenvuo and N. Helisto. Initializing network simulations for case studies of offshore wind power and offshore DC grid integration in the power system of Northern Europe. 12Th Wind Integration Workshop, 22-24 Oct 2013, London, UK.

Design Inputs

Generator Model

- Generators other than wind power generators are modelled as power prices in the relevant price areas.

Assumptions:
- Transmission capacity within each country is unlimited.
- Cost of generation is not affected by wind power.
- Maximum power generation (exclude wind) is as high as the total demand of the respective price area.

Power prices :
- 2012 time series data is used.
- Sweden, Finland, & Estonia (www.nordpoolspot.com)
- Germany (www.eex.com)
- Poland (www.pse-operator.pl)
- Latvia & Lithuania (assume the same as Estonia's)

Preliminary Results

Case Studies

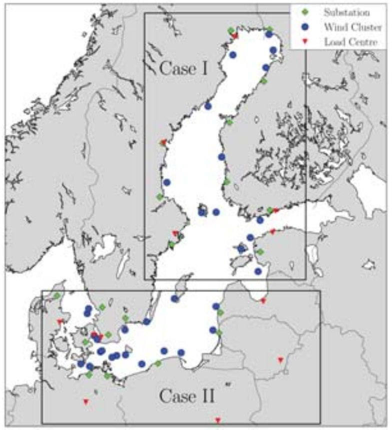

Preliminary Results
Case I

NTNU – Trondheim
Norwegian University of Science and Technology

- SE1 – SE3 :
  - WFs – substations:
    - Radial Connections
    - Direct DC > 70 km
- Northern FI:
  - WFs – substations:
    - AC lines ≤ 70 km
- Southern FI & EE:
  - Offshore connection point 307 collects power from WFs 208 (1580 MW capacity) & 211 (10 MW capacity).
  - Most power flows to FI. Mean flows:
    - 211 → 307 : 540 MW
    - 208 → 307 : 4 MW
    - 307 → 104 : 520 MW
- Wind power in EE (103 → 305):
  - Total 660 MW from WFs 211, 212 and 213.

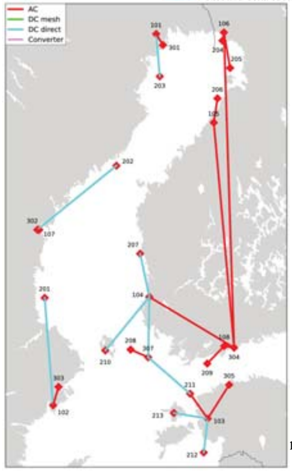

Preliminary Results
Case I

NTNU – Trondheim
Norwegian University of Science and Technology

Table 4 : Key results for case I.

from node 3	to node	Branch type	Distance (km)	# of cables	Capacity (MW)	mean flow (MW) 1 → 2	mean flow (MW) 1 ← 2
201	102	3	236	2	1010	460	0
202	107	3	202	1	920	420	0
203	101	3	78	1	60	30	0
204	106	1	15	4	2440	1100	0
205	106	1	66	2	1220	560	0
206	105	1	46	1	480	220	0
207	104	3	92	1	620	280	0
209	108	1	53	1	160	70	0
210	104	3	149	1	500	230	0
211	103	1	69	1	390	240	40
212	103	3	78	1	520	240	0
213	103	3	78	1	500	230	0
102	303	1	43	0	10000	440	0

Branch type: 1 = AC, 2 = DC mesh, 3 = DC direct, 4 = Converter

Preliminary Results
Case I

NTNU – Trondheim
Norwegian University of Science and Technology

Table 4 : (continued.)

from node	to node	Branch type	Distance (km)	# of cables	Capacity (MW)	mean flow (MW) 1 → 2	mean flow (MW) 1 ← 2
107	302	1	4	0	10000	400	0
101	301	1	23	0	10000	20	0
106	304	1	627	0	10000	1650	0
105	304	1	461	0	10000	220	0
104	304	1	212	0	10000	990	20
108	304	1	22	0	10000	70	0
103	305	1	90	0	10000	660	10
208	307	1	42	1	10	4	0
211	307	3	123	2	1900	540	30
307	104	3	130	2	1840	520	30

Note: Node 307 is the offshore node suggested by NetOp.

Preliminary Results
Case II

NTNU – Trondheim
Norwegian University of Science and Technology

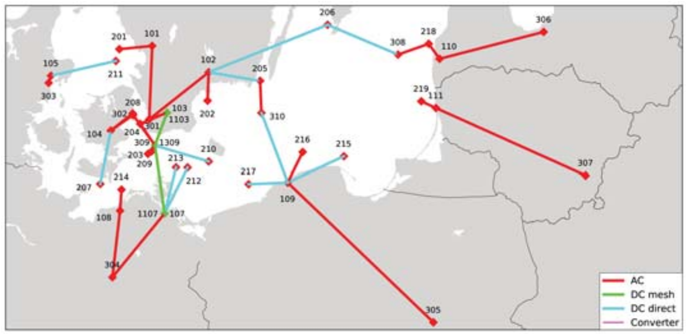

Preliminary Results
Case I

NTNU – Trondheim
Norwegian University of Science and Technology

- SE4, DK1 and DE are connected at point 309.
- 103 → 309 (AC cable): 540 MW mean flow
- Wind power from WFs 203, 204, 208, 209 and 210 are collected at offshore node 309.
- 309 → 107 (4 DC cables): 2680 MW
- 3-terminal HVDC connects 103, 309, 107. Power transfer 900 MW from 103 to 107.

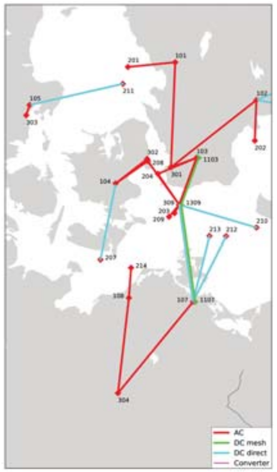

Preliminary Results
Case II

NTNU – Trondheim
Norwegian University of Science and Technology

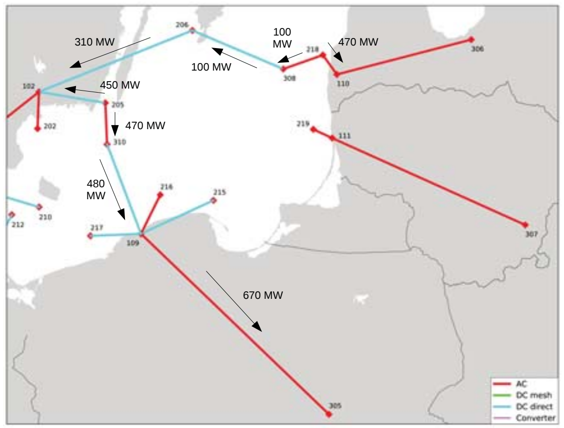

NTNU – Trondheim
Norwegian University of Science and Technology

Preliminary Results

Case II

Table 5 : Key results for case II.

from node	to node	Branch type	Distance (km)	# of cables	Capacity (MW)	mean flow (MW) 1 → 2	mean flow (MW) 1 ← 2
201	101	1	57	3	1422	640	0
202	102	1	50	1	604	270	0
204	103	1	51	1	593	210	220
205	102	3	91	1	895	450	100
206	102	3	220	1	810	310	30
207	104	3	97	1	884	400	0
208	104	1	48	1	689	220	310
211	105	3	115	1	147	70	0
212	107	3	93	2	1778	800	0
213	107	3	86	2	1793	810	0
214	108	1	39	2	1084	490	0
215	109	3	112	1	183	80	0
216	109	1	61	1	231	100	0

Branch type: 1 = AC, 2 = DC mesh, 3 = DC direct, 4 = Converter

NTNU – Trondheim
Norwegian University of Science and Technology

Preliminary Results

Case I

Table 5 : (continued.)

from node	to node	Branch type	Distance (km)	# of cables	Capacity (MW)	mean flow (MW) 1 → 2	mean flow (MW) 1 ← 2
217	109	3	72	1	90	40	0
218	110	1	32	2	830	470	12
219	111	1	28	2	1000	450	0
101	301	1	128	0	10000	940	300
102	301	1	133	0	10000	960	100
103	301	1	34	0	10000	150	1490
104	302	1	49	0	10000	510	220
105	303	1	13	0	10000	60	0
107	304	1	153	0	10000	5270	390
108	304	1	125	0	10000	820	330
109	305	1	377	0	10000	670	100
110	306	1	185	0	10000	470	12
111	307	1	293	0	10000	450	0

Branch type: 1 = AC, 2 = DC mesh, 3 = DC direct, 4 = Converter

NTNU – Trondheim
Norwegian University of Science and Technology

Preliminary Results

Case II

Table 5 : (continued.)

from node	to node	Branch type	Distance (km)	# of cables	Capacity (MW)	mean flow (MW) 1 → 2	mean flow (MW) 1 ← 2
203	309	1	12	2	920	420	0
204	309	1	47	1	700	620	20
205	310	1	56	1	700	470	110
206	308	3	131	1	270	70	100
208	309	1	67	1	700	350	180
209	309	1	20	3	1970	890	0
210	309	3	101	1	160	70	0
218	308	1	56	1	270	100	70
309	103	1	62	1	700	60	540
309	107	3	124	4	3650	2680	70
310	109	3	133	1	700	480	110

Note : 308 – 310 are offshore nodes resulted from the optimisation.

Branch type: 1 = AC, 2 = DC mesh, 3 = DC direct, 4 = Converter

NTNU – Trondheim
Norwegian University of Science and Technology

Preliminary Results

Case II

Table 5 : (continued.)

from node	to node	Branch type	Distance (km)	# of cables	Capacity (MW)	mean flow (MW) 1 → 2	mean flow (MW) 1 ← 2
1309	1103	2	62	1	1000	70	900
1309	1107	2	124	1	1000	900	70
1103	103	4	0.0	2	1020	60	910
1107	107	4	0.0	1	1000	900	70

Branch type: 1 = AC, 2 = DC mesh, 3 = DC direct, 4 = Converter

NTNU – Trondheim
Norwegian University of Science and Technology

Future Work

- Re-run the cases I & II with *CorWind* models.
- “Close the loop”:
  - Evaluate the technical feasibility of the grids
  - Investigate the how the grids will impact on the power market

NTNU – Trondheim
Norwegian University of Science and Technology

Thanks!!

EERA DeepWind'2014
Trondheim, Norway, 23 January 2014

Operation of Power Electronic Converters in Offshore Wind Farms as Virtual Synchronous Machines

Salvatore D'Arco*
salvatore.darco@sintef.no

Jon Are Suul*†
Jon.A.Suul@sintef.no

*SINTEF Energy Research, Norway
†Norwegian University of Science and Technology, Norway

Outline

- Power Electronics Converters in Offshore Wind Farms
- Introduction to Virtual Synchronous Machines (VSM)
  - Implementation
  - Comparison to other inertia emulation schemes
- VSM application in HVDC-connected Offshore Wind Farms
- Conclusions

HVDC Connected Offshore Wind Farms

- Long distances to shore
  - Point-to-point HVDC connection to shore
    - Grid side and offshore HVDC converters
  - Internal AC collection grid with converter interface to wind turbines
    - Full-scale back-to-back converter
    - Doubly Fed Induction Generators – rotor converter

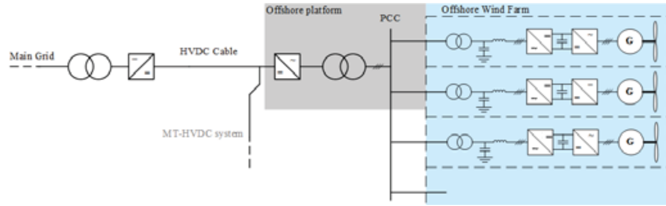

Conventional HVDC Control – Offshore

- Offshore Wind Farm converter:
  - Operates as a frequency master
    - Determines voltage and frequency of local AC collection grid
  - Wind turbine converters are synchronized to the voltage generated by the HVDC converter
- No physical inertia in the offshore grid

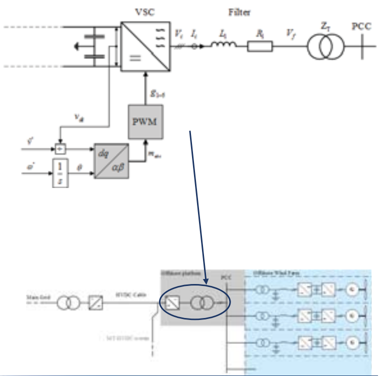

Conventional HVDC Control – Onshore

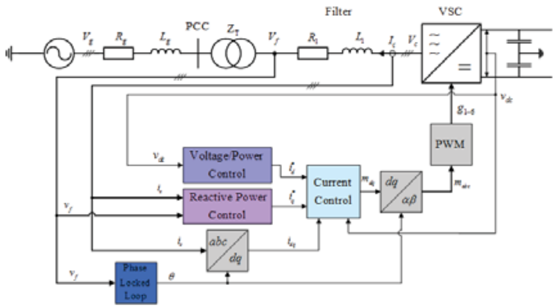

- Synchronized to onshore power system by Phase Locked Loop (PLL)
  - Depends on a relatively strong grid with rotating inertia
- Islanded operation or black-start requires change of control system

Virtual Synchronous Machines

- Power Electronic converters controlled to emulate traditional synchronous machines
  - Emulates inertia and damping
  - Parameters are not limited by physical design constraints
- Will operate in the grid in a similar way as traditional Synchronous Machines
  - Self-synchronization by power-balance effect
    - Does not depend on PLL
  - Allows for stand alone and/or parallel operation as well as connection to a strong grid
- Several possible implementations

VSM Implementation

- Based on synchronous machine swing equation
  - Reduced order approximation of the inertia and damping of a traditional synchronous machine
  - Provides a frequency and phase angle reference that can be used to control the converter
- Reactive power controller can provide voltage amplitude reference

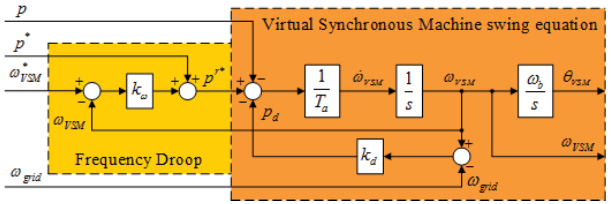

Overview of VSM-based control scheme

- Inertia emulation and reactive power control gives phase angle references and voltage amplitude reference
  - Used for cascaded voltage and current controllers
    - Protections and controller saturations can be explicitly included
    - Tuning may be complex, especially for low switching frequency

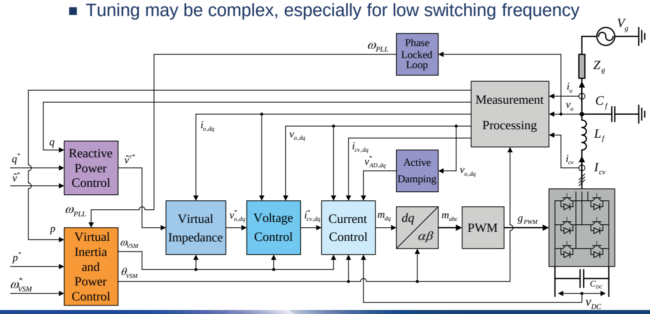

VSM and Inertia Emulation

- Inertia emulation is becoming a possible requirement for modern wind farms
  - Most implementations are based on sensing of the grid frequency

$$\Delta P = k_H \frac{df_{grid}}{dt}$$

  - Will contribute to improve power system dynamic response and stability but depends on a stable grid frequency detection
    - Usually based on frequency tracking by PLL or similar techniques
    - Depends on dominant presence of traditional synchronous machines
  - There is no real inertia emulated in the control system
    - Only the power response of an equivalent inertia is emulated
- A Virtual Synchronous Machine can provide the same virtual inertia without depending on a strong grid
- The energy requirements for Inertia Emulation is the same

VSM applications in offshore wind farms - I

- Grid side HVDC Converter
  - Providing Virtual Inertia and damping to the AC system
  - Allows for stand-alone and black-start capability with the same control system as for grid connected operation

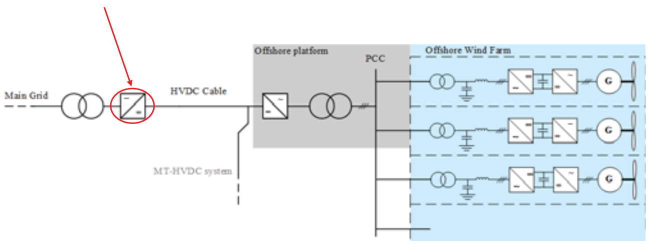

VSM applications in offshore wind farms - II

- Offshore HVDC Converter
  - VSM provides frequency and voltage regulation
    - Wind turbine converters will synchronize to the virtual inertia of the VSM
  - Allows for simple parallel connection and load sharing
    - Wind farms with multiple HVDC connections

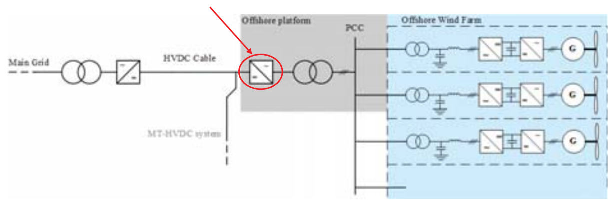

Wind farm with multiple HVDC connections

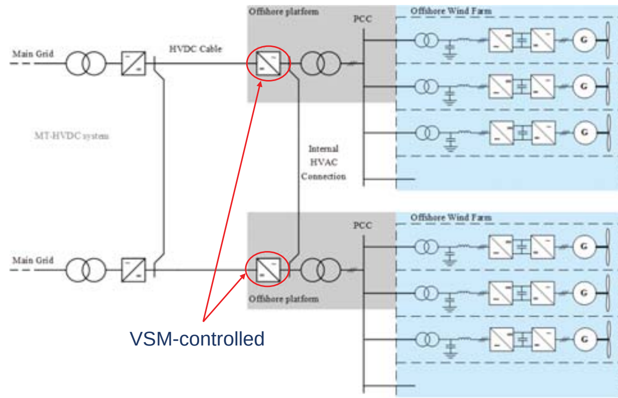

VSM applications in offshore wind farms - IIi

- Each wind turbine converter can be controlled like a VSM
  - Equivalent to large number of synchronous generators operated in parallel
  - Not a preferable solution in short term

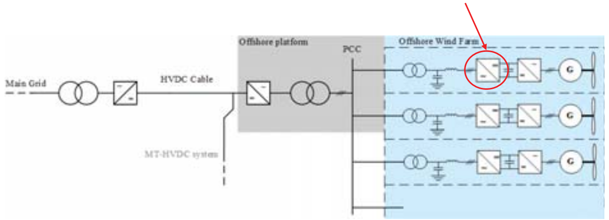

Simulation example

- VSM in a HVDC configuration
- Simulation starting from perturbed initial condition
  - First second shows transient response with perturbed initial conditions of the system states
- Step of power reference at 1.5 s
  - No fast transients are excited
- Smooth over-damped response
  - Significantly more damped response than for a traditional synchronous machine
  - Damping coefficient can be higher than for design of a practical machine

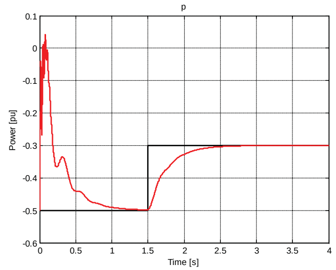

Conclusions

- The Virtual Synchronous Machines is a new and promising concept for control of power electronic converters in power systems
  - Emulation of inertia and damping are common to all VSM implementations
  - Based on the same self synchronization effect as a traditional Synchronous Machine and do not depend on PLL
  - Does not have the same limitations of applicability as simple schemes for inertia emulation
- Relevant applications in offshore wind farms
  - Virtual Inertia in grid-side HVDC stations
  - Control of HVDC stations in isolated AC collection grids
    - Simple parallel operation of multiple converter stations
    - The same control can be used for various operation modes

Questions?

This work was supported by the project:
Power Electronics for Reliable and Energy Efficient Renewable Energy Systems - "Offshore Power Electronics" http://sintef.no/OPE

Classification of VSM Implementations

	Voltage vector reference Direct PWM	Voltage vector reference Cascaded Control	Current vector reference	Power Reference
Full order SM model.	Possible	Possible	VISMA	Not relevant
Reduced order SM model	VISMA	Possible	VISMA	Not relevant
Swing Equation	Syncronverter	In literature	In literature	Not relevant
Inertia emulation with power from grid voltage.	Not relevant	Not relevant	Possible	EU VSYNC project

Research Opportunities for better integration of Offshore wind farms using HVDC links

(The Future of HVDC)

William Ross MEng
Ioannis Antoniou MSC
Research Students
University of Strathclyde

Outline of Presentation

- **Annual Report Outcomes**
- **Where next**
- **Why HVDC**
- **Multi Terminal HVDC**
- **HVDC Converter Technology**
- **Earlier VSC Technologies**
- **Modular Multilevel Converters**
- **Offshore DC Grid Connection**
- **Protection Requirements**
- **Issues for further integration**
- **Conclusions**

Some Annual Report Outcomes

- Annual Electrical power demand increased from just over 117,200 TWh to 153,600 TWh between 2000 and 2010 (an increase of ~30%) (U.S. Energy Information Administration, 2013).
- Greater pressure placed on development of sustainable energy sources with targets being set and some financial support/rewards in place
- Often necessitates long distance transmission
- Average distance of off-shore wind farms continues to increase
  - 2011 being 23.4km and that in 2012 being 29km from shore (EWEA 2011, 2012)
  - announced projects for installations up to 200km from shore

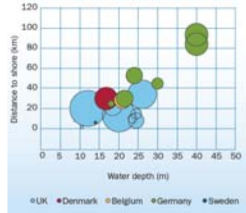

(EWEA 2012 annual report)

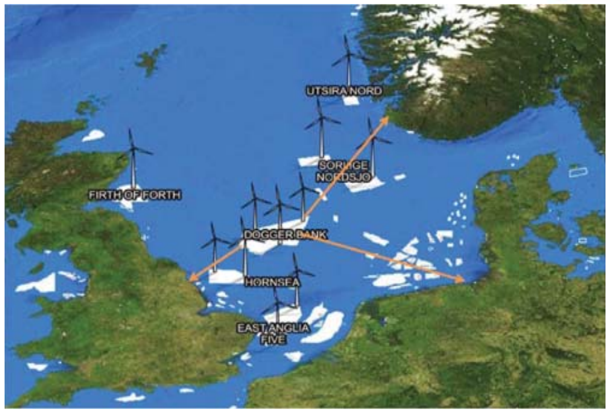

Where Next?

- Increasing wind penetration leading to a growing impact of wind farms on their networks
- Greater need for adoption of HVDC transmission in connection of large offshore wind farms and control of power injected onto the grid
- Use of HVDC to allows control of Voltage and reactive power injected into the grid with asynchronous connection between different AC grids
- Adoption of multi terminal HVDC connection to allow better power flow management amongst a number of interconnected grids instead of simply point to point connection

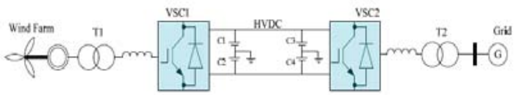

Multi-Terminal HVDC

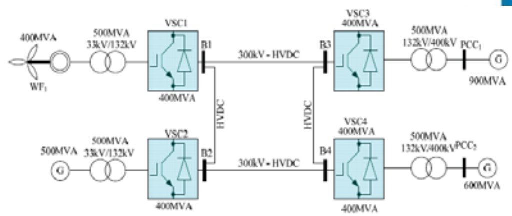

- Allows better power management in event of severe faults in localised parts of the grid that would leave many without power using point to point connection
- Boost Electricity economy for countries with large renewables potential
- Needs better standardisation of grid code requirements across Europe

Why HVDC

Offshore wind energy projects are becoming more attractive, but a number of technological challenges still need to be resolved.

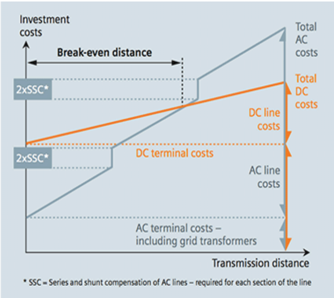

http://electrical-engineering-portal.com/download-center/books-and-guides/siemens-basics-of-energy/power-td-solutions

- Large amounts of reactive power required in HVAC to feed the capacitive charging current of the cables.
- For 1 GW of offshore wind farms and distances greater than 80 km the preferable way of transferring power to onshore is HVDC.
- There are a number of upcoming HVDC projects, especially in China
- Predominantly Thyristor based systems ~ 600kV, 6400MW
- Several IGBT based systems planned in Europe (mostly ABB)

HVDC Converter Technology

Line Commutated Converters

- Line Commutated Converters used for HVDC projects since 1950's.
- Use SCRs as the switching device, a method that lacks gate turn-off capability. The AC current needs to become zero in order to switch off.
- Not suitable for connection with weak AC networks. They need reactive power compensation in order to be functional.

Voltage Source Converters

- VSCs use self commutating devices such as IGBTs and GTOs that have voltage ratings close to 6.5kV
- Unlike LCCs , they provide rapid, independent control of active and reactive power.
- By using Pulse Width Modulation any phase angle or magnitude can be constructed
- Lower filtering requirements, thus improving the overall converter footprint.
- Black-start capability and no restriction on multiple infeeds

Earlier VSC Technologies

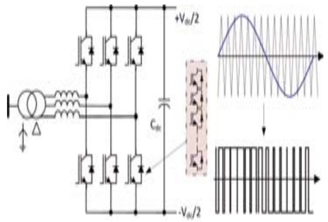

Two level half bridge VSC

- Two level and three level VSCs started become popular during the early 1990's
- High voltage IGBT devices allow the inverter output to be switched between the positive and negative DC poles (0.5Vdc) and (-0.5Vdc)
- The output voltage consists of series rectangular pulses with controllable width, thus making it possible to control the frequency, phase and magnitude.
- AC filters are used to eliminate the large harmonic content, but are reduced compared with LCC technology.

Modular Multilevel Converters

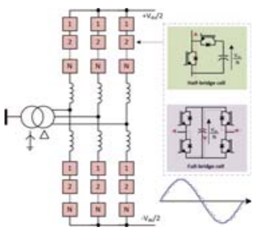

3 Phase Modular Multi Level Converter

- Earlier VSC designs were unable to meet the voltage requirements for HVDC due to low IGBT ratings.
- A series combination of sub-modules allows scaling to required HV levels
- The capacitor of each cell can accommodate a fraction of the DC link voltage.
- With the use of stepped modulation, intermediate voltage levels could be synthesized.
- The use of MMC results in improvements in power quality, filtering requirements and lower switching losses

Sub Module Topologies for MMC

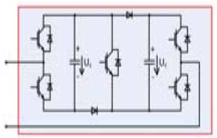

Clamp-Double sub-module
http://www.ptd.siemens.de/TransBayCable__HVDC_PLUS_Presentation.pdf

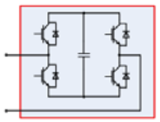

Full Bridge MMC sub-module
http://www.ptd.siemens.de/TransBayCable__HVDC_PLUS_Presentation.pdf

- Full Bridge sub-modules have been proposed instead of half-bridge. They provide the capability of DC-side fault protection.
- Conduction losses are larger due to additional semiconductor devices in the conduction path.
- The use of Clamp-Double sub-modules doubles the voltage capability of the converter compared with other arrangements.
- Can turn off DC pole to pole faults and has lower switching losses than the full bridge sub-module.

Offshore DC Grid connection

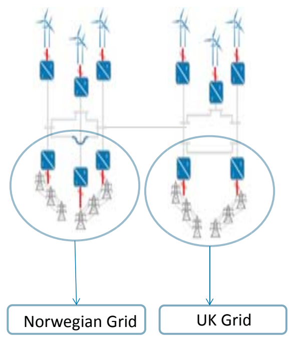

- Existing VSC HVDC connections are point-to-point.
- Considerations have been made for Multi Terminal DC connections (MTDC)
- They will be capable of bringing together geographically dispersed wind farms
- Offering transmission path for offshore wind power to the markets.
- Sophisticated control strategies need to be implemented for power sharing between the converters during normal operation as well as during faulty conditions.

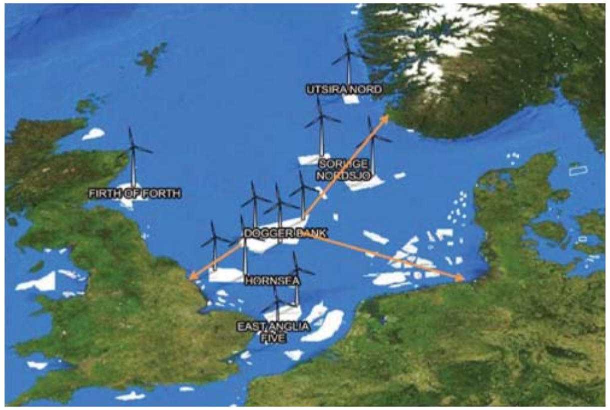

Protection issues for MTDC

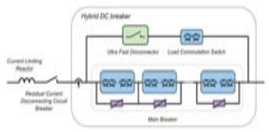

Hybrid HVDC Breaker.
http://new.abb.com/about/hvdc-grid

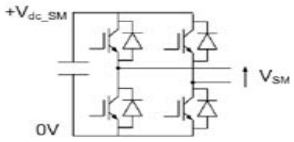

Full Bridge MMC sub-module
http://new.abb.com/about/hvdc-grid

- HVDC offshore grids consist of multi terminal converter arrangement which are regarded as a cost effective way to connect large offshore projects to onshore networks.
- DC to ground faults in a meshed HVDC grid could be isolated with the use of multiple protection zones, thus increasing the reliability of the overall system.
- In DC Grids a fault would lead to a rapid increase in fault current and a voltage dip would appear in the system.
- DC Breaker technology currently developing could be proven a reliable choice to selective fault clearing .
- Alternatively, use full bridge sub-modules with fault blocking capability.

Summary

- Ever rising electricity demand is fuelling a growth in renewables
- Increasing wind penetration leading to a growing impact of wind farms on their networks
- Advances in power electronic devices and their improved controllability are making the adoption of larger scale wind derived energy plausible on existing AC networks
- R&D to further develop wind power plant models and control strategies to demonstrate and validate their ability to provide ancillary services and support system security
- We shall be working in this area over the next 3 years, looking at topics and technologies outlined hoping to provide a solution to make offshore wind easier to integrate with AC networks with better network support.

Thank You

Questions?

University of Strathclyde Glasgow

Deepwind 2014, Trondheim, Norway

NSON

North Sea Offshore and Storage Network

An RD&D project/program Initiative

Dr. Magnus Korpås, SINTEF Energi
Research Director, Energy Systems

EERP University of Strathclyde Engineering · Fraunhofer IWES · SINTEF

Content

- The idea
- Related Frameworks and Initiatives
- The need for NSON
- The Gain
- Timing R&D&D to make it happen
- The Berlin Model for R&D&D
- NSON Project - and Pre project

EERP University of Strathclyde Engineering · Fraunhofer IWES · SINTEF

EERP University of Strathclyde Engineering · Fraunhofer IWES · SINTEF

The idea

- One common planning of NSON
- Requires harmonization at several levels of national interaction
  - Technology
  - Regulation
  - Market Design
  - Policy

Level	NO	DE	UK
Technology	Harmonised	Harmonised	Harmonised
Cost-benefit sharing			
Politics			

← Not harmonised →
(All countries need to change something at all three levels)

- Due to long construction times there is time for research – to make NSON better without delaying implementation
- We pursue the proposed Berlin Model for R&D&D cooperation to ensure speed and volume

"nothing new under the sun"

Related Frameworks and Initiatives

- SET Plan
- A Single European Electricity Market
- EU "North Sea Power Wheel"
- NSCOGI
- ENTSO-E Regional Group North Sea
- DE, UK & NO Transmission system expansion studies
- EERA JP WIND & SmartGrids
- TPWind
- FP7/IEE: TWENTIES & Offshorwind & Tradewind & …

OffshoreGrid
TradeWind
Twenties

The need for NSON

- Harvesting offshore wind
- Connect national energy markets to enhance security, stabilize prices and increase cost efficiency
- Provide large scale hydro balancing power to markets with high penetration of variable renewable production
- Implementing deep-water pump storage plant to balance fluctuations
- Electrification of oil and gas installations to reduce GHG emissions

Common initiative is needed to make it happen - under current national schemes it will not

EERP Strathclyde · Fraunhofer · SINTEF

EERP University of Strathclyde Engineering · Fraunhofer IWES · SINTEF

The Gain

- Significant Lower Overall Socio Economic Cost
  - Supported by several FP7/IEE, national and NSCOGI analysis
  - Several studies support that a common undertaking, with shared costs among the different stakeholders over a long timeframe, will be considerably cheaper than a case by case approach. The overall cost will be minimized and future industrial initiatives in the region (such as more wind, ocean energy, oil and gas) would see a relatively lower marginal integration cost.
- Industrial Innovation Opportunity
  - Meshed subsea high voltage DC transmission system technology
  - A first mover in implementing a multi national regulation, policy and market design
  - European Market for rebuilding transmission infrastructure estimated at 104 billion €
  - Will ensure Europe's industrial lead globally

Timing R&D&D to make it happen

- Plans for interconnections , offshore wind park connections and multi terminal demos are moving – not room for more looking towards 2020
- Projects beyond 2020 are just sketches
- Gives an opportunity for an R&D&D Program that provide decision support for investments beyond 2020 by developing and/or testing
  - Economic consequences of national vs multi-national approach for offshore grid planning, including interaction with the grid on land
  - The role of an extensive offshore grid in balancing fluctuating renewables
  - Alternative policy and regulation framework, including cost-benefit sharing models for grid investments and market structures
  - Technology needs and possibilities beyond what is available today

NSCOGI December 3rd 2012:
The Ministers recognise the value of this regional cooperation between all the parties needed to bring about investment in cross-border infrastructure. They have therefore asked the network operators, ENTSO-E, ACER and national regulators to continue working with the Government authorities and the European Commission to assess pathways towards possible future grid configurations for the North Seas area, using a range of generation and demand scenarios, and develop proposals to address the regulatory, market and planning barriers.

The Berlin Model for R&D&D

- Proposed at a German SET-Plan conference in Berlin in March 2012
- Suggests a variable geometry, bottom-up approach to organizing large RD&D as an alternative to the existing instruments (FPX, ERANET, ERANET+, PPP, P2P etc)
- It allows a few especially motivated countries with a strong common interest to take on a research/innovation challenge as a coordinated effort with a minimum of "red tape"

NSON Project focus

P1: Energy meteorology, scenario definition and generation
P2: Technology design
P3: Offshore grid planning and operation
P4: Energy storage analysis
P5: Policy and regulation
P6: Environmental and societal aspects

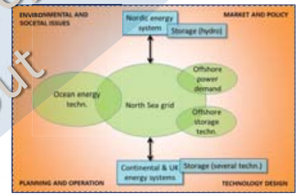

Pre project focus - Norway

Level	NO	DE	UK
Technology	Harmonized	Harmonized	Harmonized
Cost-benefit sharing			
Politics			
Not harmonised (All countries need to change something at all three levels)			

- **Technology perspectives** – NO/DE/UK parties contributing according to expertise (in network or storage technologies)
- **Cost-benefit sharing models and methodologies** - (main section) each party can contribute with own models, but addressing different/complementary components
- **Policy drivers** – all parties contibuting national perspective

-→ Establishing a Strategic Research Agenda for NSON
Concluding with a case for a bigger project to tackle the challenges
- All NSCOGI Countries
- Industrial Innovation – Demo's
- Active Government Involvement

Thank You for Your Attention

C1) Met-ocean conditions

Using the NORSEWInD lidar array for observing hub-height winds in the North Sea,
Charlotte Bay Hasager, DTU Wind Energy

Results and conclusions of a floating Lidar offshore test, Julia Gottschall, Fraunhofer IWES

Metocean analysis of a low-level coastal jet off the Norwegian coast,
Konstantinos Christakos, Polytec R&D

Air-Sea Interaction Influenced by Swell Waves, Mostafa Bakhoday Paskyabi,
Geophysical Institute, University of Bergen

2007 - 2013

Using the NORSEWInD lidar array for observing hub-height winds in the North Sea

Charlotte Bay Hasager, DTU Wind Energy
Detlef Stein, DNV GL
Michael Courtney, DTU Wind Energy
Alfredo Peña, DTU Wind Energy
Torben Mikkelsen, DTU Wind Energy
Matthew Stickland, University of Strathclyde
Andrew Oldroyd, Oldbaum Services

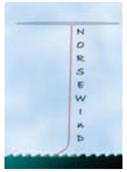

EERA DeepWind 2014
11th Deep Sea Offshore Wind R&D Conference

Trondheim, 22 - 24 January 2014

NORSEWInD in brief

Northern Seas Wind Index database project (2008-2012)

Coordination of Oldbaum Services for a consortium of 20 partners.

The budget of €7.9 million with €3.9million from EC FP7.

Offshore wind development is becoming increasingly expensive as developers move to deeper waters. Recent met masts have demanded prices upwards of €15million.

Motivation for alternatives: LIDARs on platforms.

LIDAR data has been acquired, collated, quality controlled and analysed.

This represents the largest single purpose wind LIDAR dataset in the industry worldwide.

NORSEWInD provides offshore wind atlases of the North, Irish and Baltic Seas based on mesoscale modelling and satellite images.

2

Content

- Study area
- Pre deployment lidar tests
- Deployment of lidars at offshore platforms
- Post deployment lidar tests
- Flow distortion at platforms
- Selected results
- Summary

3

Measurement locations in the North Sea

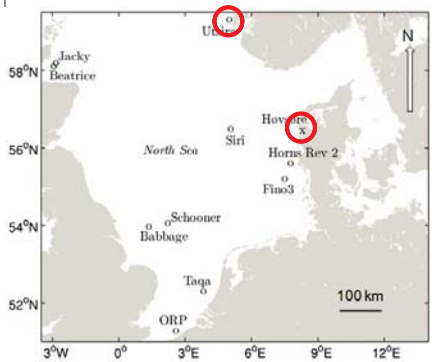

In collaboration with industries:

DONG energy
Statoil Hydro ASA
TAQA
Shell UK
Talisman Energy
Kinsale Energy
SSE
3E
Scottish Enterprise
Scottish and Southern Renewables

4

Pre and post deployment lidar tests at Høvsøre

5

Høvsøre illustration of set up

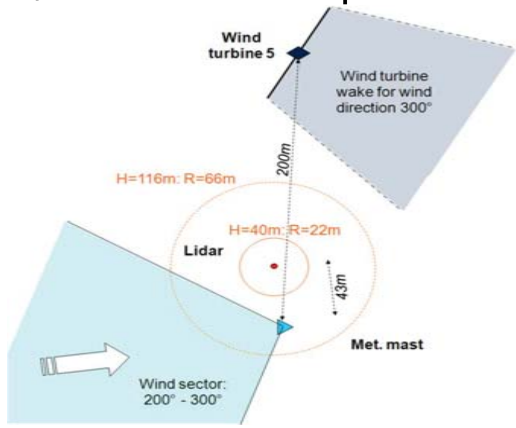

6

“NORSEWInD standard”

Data quality acceptance levels for NORSEWInD lidar systems. *u* stands for wind speed.

Parameter	Criteria	Ranges (Height and Speed)
Absolute error	<0.5 ms^{-1} for 2 < u < 16 ms^{-1} Within 5% above 16 ms^{-1} Not more than 10% of data to exceed those values	All valid data
Data availability	Assessed case by case Environmental conditions dependency	All valid data
Linear regression Slope	Slope between 0.98 and 1.01 <0.015 variation in slope between u-ranges (b) and (c)	Heights from 60 to 116 m u-ranges: (a) 4–16 ms^{-1}, (b) 4–8 ms^{-1}, (c) 8–12 ms^{-1}
Linear regression Correlation coefficent (R^2)	>0.98	Heights from 60 to 116m u-ranges: (a) 4–16 ms^{-1}, (b) 4–8 ms^{-1}, (c) 8–12 ms^{-1}

Measurement wind speed at cup vs. lidar

The vertical lines indicate the 4, 8 and 12 ms^{-1} levels.

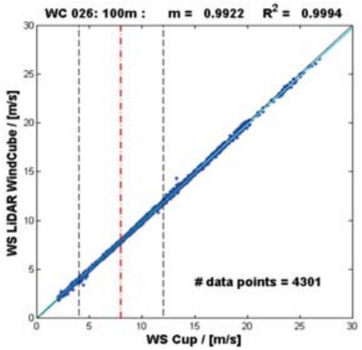

Pre-deployment test results

Linear correlation slope and R^2 for the wind speeds in the range from 4 to 16 ms^{-1} at four heights.

Lidar	Slope at 116 m 100 m 80 m 60 m	R^2 at 116 m 100 m 80 m 60 m
1	0,991 0,976 0,977 0,948	0,999 0,976 0,974 0,915
2	0,988 0,992 0,991 0,993	0,999 0,999 0,998 0,998
3	0,993 0,997 0,997 1,000	0,998 0,998 0,998 0,997
4	0,996 0,999 0,998 0,998	0,999 0,999 0,999 0,998
5	0,985 0,993 0,992 0,993	0,999 0,998 0,998 0,997
6	0,983 0,986 0,986 0,990	0,996 0,996 0,996 0,995
7	0,978 0,983 0,984 0,992	0,994 0,994 0,995 0,995
8	0,976 0,980 0,977 0,989	0,995 0,996 0,996 0,995

Lidars 1-5 are WindCube and 6-8 are ZephIR

Offshore platforms used for deployment

Offshore installation schematic rig / platform

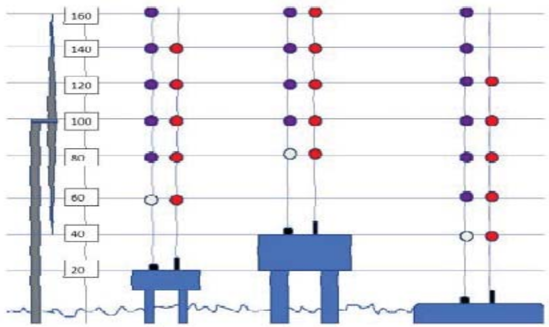

Red dots ZephIR, Blue dots WindCube

Offshore measurement heights

The lidar deployment height and observational heights are listed in meter above mean sea level. WC is WindCube, ZP is ZephIR.

Platform	Babbage	Beatrice	Fino3	HornsRev2	Jacky	ORP	Schooner	Siri	Taqa	Utsira
Lidar type	ZP	ZP	ZP	WC	WC	WC	WC	WC	WC	WC
Height	42	42.5	26	26	28	30	36	45	30	26
1	60	52.5	51	66	60	70	76	85	70	67
2	80	75.5	71	86	80	90	92	*105*	90	80
3	*100*	90.5	91	*106*	*100*	*110*	*99*	125	*110*	*100*
4	130	*105.5*	*101*	126	116	130	102	145	130	120
5	160		130	146	130	150	107	161	150	140
6			160	166	160	170	116	175	170	160
7				196	200	190	126	205	190	180
8				226	250	210	152	245	210	200
9				256	300	230	182	295	230	250
10				286			216	345	250	300

Offshore measurement periods

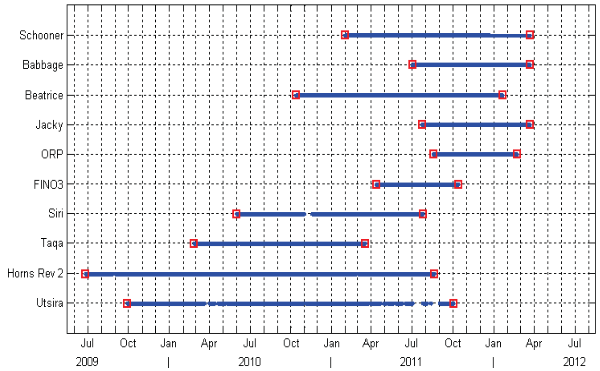

CNR and data availability offshore

The carrier-to-noise ratio (CNR) as a function of observations height above installation.

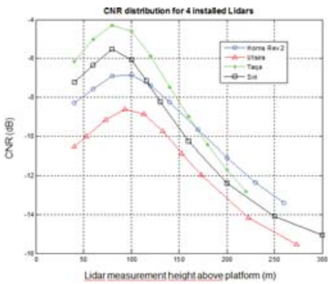

The average data availability as a function of observations height above installation.

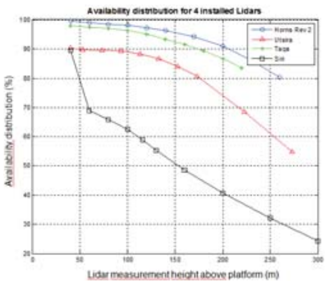

Data availability

System and data availability in % and hours are listed during the offshore deployment. The values are for observations at around 100 m AMSL.

Lidar	System Availability in %	Operational Hours	Data Availability in %	Data Hours
Utsira	85	14,995	81	12,075
Horns Rev 2	98	18,433	98	18,019
Taqa	99	9120	97	8870
Siri	95	9585	85	8178
Fino3	98	4304	88	3778
ORP	100	792	73	581
Jacky	97	5622	93	5228
Beatrice	86	9597	85	8154
Babbage	99	6255	97	6070
Schooner	86	8583	76	6538
Total		87,286		77,491

Around 12 years data in total

Post deployment test results

Linear correlation slope and R^2 for the wind speeds in the range from 4 to 16 ms^{-1} at four heights.

Lidar	Time	Slope at 116 m 100 m 80 m 60 m	R^2 at 116 m 100 m 80 m 60 m	N
	Pre	0,988 0,992 0,991 0,993	0,999 0,999 0,998 0,998	3,606
2	Post	0,991 0,997 0,993 0,992	0,999 0,998 0,998 0,997	3,659
	Diff.	0,003 0,005 0,002 −0,001	0,000 −0,001 0,000 −0,001	-
	Pre	0,996 0,999 0,998 0,998	0,999 0,999 0,999 0,998	5,065
4	Post	0,989 0,994 0,989 0,999	0,998 0,998 0,998 0,997	3,510
	Diff.	−0,007 −0,005 −0,009 0,001	−0,001 −0,001 −0,001 −0,001	-
	Pre	0,985 0,993 0,992 0,993	0,999 0,998 0,998 0,997	991
5	Post	0,983 0,987 0,984 0,992	0,999 0,999 0,998 0,998	2,791
	Diff.	−0,002 −0,005 −0,008 −0,001	0,000 0,000 0,001 0,001	-
	Pre	0,976 0,980 0,977 0,989	0,995 0,996 0,996 0,995	1,547
8	Post	0,960 0,971 0,970 0,979	0,993 0,994 0,995 0,995	1,206
	Diff.	−0,016 −0,009 −0,007 −0,010	−0,002 −0,002 −0,001 0,000	-

Flow distortion analysis for rigs / platforms

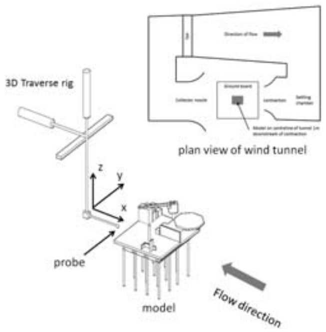

Wind tunnel experiments

CFD modelling

Wind tunnel and CFD results

Platform	Rign Height (m)	Lidarm Height (m)	Height above Lidar in m (Height Normalized by Rig Height): Wind Tunnel Point u	CFD Results Point u	CFD Results Point θ	CFD Results Lidar u	CFD Results Lidar θ	Height AMSL for 2.5% Free-Stream: CFD Results Lidar u	CFD Results Lidar θ
Babbage	42	42	33 (0.8)					75	
Beatrice	62	42.5	64 (1.0)	30 (0.5)	>64 (1.0)	34 (0.5)	59.5(1.0)	76.5	102
HornRev 2	26	26	30 (1.2)	44 (1.7)	57 (2.2)	25 (1.0)	55 (2.1)	50	80
Jacky	28	28		20 (0.7)	19 (0.7)	10 (0.4)	18 (0.6)	38	46
Schooner	38	36.25	24 (0.6)	24 (0.6)	35 (0.9)	9 (0.2)	24 (0.6)	39	54
Taqa	31.4	30	37 (1.2)	30 (1.0)	36 (1.1)	33 (1.1)	27 (0.9)	63	57
Utsira	26	26		108 (4.2)	192 (7.4)	150 (5.8)	300 (11.5)	176	326

Selected results from lidar observations

All NORSEWInD wind lidars were able to observe winds at 100 m and higher. Most of them were pulsed lidars (WindCubes). For those the availability of data decreases with height.

In order to maximize the amount of data we decided to estimate the wind shear from the two closest wind speed observations to the 100 m height.

Wind shear (shear exponent α of the power law)

$$\frac{u_1}{u_2} = \left(\frac{z_1}{z_2}\right)^{\alpha}$$

$$\alpha = \frac{z}{u}\left(\frac{du}{dz}\right) \approx \frac{z}{u}\left(\frac{\Delta u}{\Delta z}\right)$$

$$\alpha = \frac{\Phi_m}{\ln\left(\frac{z}{z_0}\right) - \psi_m}$$

Normalized distribution of α-values around 100m

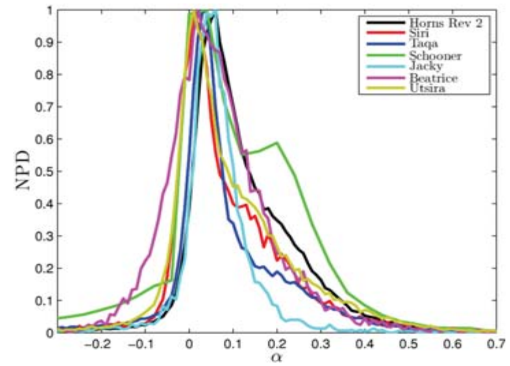

α-'roses' at Horns Rev 2 and Taqa around 100m

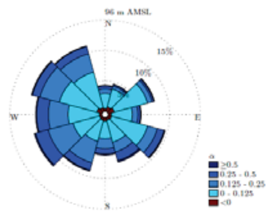

Horns Rev 2

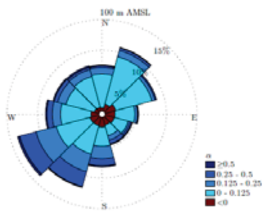

Taqa

α-variation diurnal and seasonal at Horns Rev 2

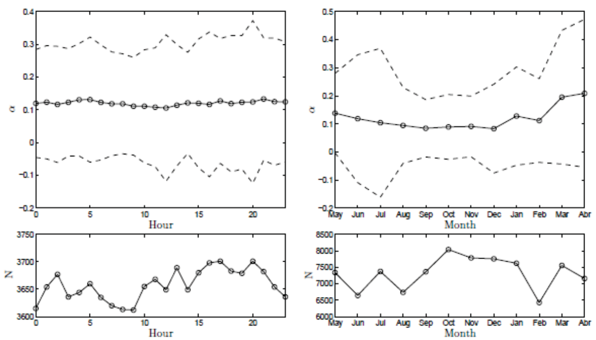

Summary

- ✓ First comprehensive project to demonstrate use of lidars offshore
- ✓ Pre and post deployment results were relatively good
- --- notice this was for more than two years of observations offshore
- ✓ System availability was acceptable
- ✓ Further development in lidars since 2008 – this improve data availability and increase system reliability
- ✓ Wind shear data observed near hub-height at several nodes in the North Sea (also analysed from several met masts)
- ✓ Lidar wind data in database are now available for further research
- ✓ Bankable?

Results and conclusions of a floating Lidar offshore test

J. Gottschall, G. Wolken-Möhlmann, Th. Viergutz, B. Lange

[Fraunhofer IWES Wind Lidar Buoy next to FINO1 met. mast]

EERA DeepWind'2014 Conference, 22-24 January 2014, Trondheim, Norway

Fraunhofer IWES

Overview

- Introduction
  - … Floating Lidar
- Fraunhofer IWES Wind Lidar Buoy
- Offshore test next to FINO1 met. mast
  - … Setup
  - … Results
  - … Conclusions
- Summary

Fraunhofer IWES

Overview

- Introduction
  - … Floating Lidar
- Fraunhofer IWES Wind Lidar Buoy
- Offshore test next to FINO1 met. mast
  - … Setup
  - … Results
  - … Conclusions
- Summary

Fraunhofer IWES

Introduction → Floating Lidar

- Floating-lidar system offer a great potential to assess offshore wind resources,
  and are a cost-effective and flexible alternative to offshore meteorological (met.) masts.
- Development of suitable (for an application in the offshore wind industry optimized) systems has made considerable progress during the last few years –
- Realisations vary in adapted lidar technology, buoy concepts, data handling, power supply, …

  as well as in the consideration of motion effects on the recorded data.

[Selected floating-lidar systems – © system manufactureres / providers]

Fraunhofer IWES

Overview

- Introduction
  - … Floating Lidar
- Fraunhofer IWES Wind Lidar Buoy
- Offshore test next to FINO1 met. mast
  - … Setup
  - … Results
  - … Conclusions
- Summary

Fraunhofer IWES

Fraunhofer IWES Wind Lidar Buoy

- Developed within the R&D project 'Offshore Messboje' (funded by BMU, 2011-13), prototype completed in spring 2013
- Floating-lidar system integrating a Windcube® v2 lidar device in an adapted marine buoy ('Leuchtfeuertonne' LT81)
- Buoy dimensions: 7.2 m height, 2.55 m diameter, 4.7 t weight
- Encapsulated lidar device in custom-made housing
- Autonomous power system based on three micro-wind turbines, solar panels, AGM battery banks for energy storage
- Motion-correction algorithm developed by Fraunhofer IWES implemented as part of post-processing

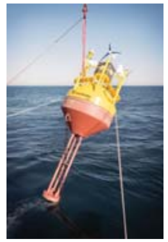

© Fraunhofer IWES, Photograph: Caspar Sessler

Fraunhofer IWES

Overview

- Introduction
  - … Floating Lidar
- Fraunhofer IWES Wind Lidar Buoy
- Offshore test next to FINO1 met. mast
  - … Setup
  - … Results
  - … Conclusions
- Summary

Offshore test next to FINO1 – Setup

© Fraunhofer IWES, Photograph: Caspar Sessler

- Offshore test from 2 Aug – 6 Oct 2013 in 450 m distance (NW direction) to FINO1 met. mast (German North Sea, 45 km offshore)
- Representative offshore conditions: 30 m water depth, yearly-averaged wind speed of 9.9 m/s at 100 m height, mean wind direction SW, sea currents governed by tides
- Floating-lidar system was installed together with bottom-based AWAC system for recording of sea conditions
- Basic procedure of testing (verification / accuracy assessment): comparison of wind data (horizontal 10-min-mean wind speed, wind direction, turbulence intensity) measured by floating-lidar device with data from reference sensors of met. mast (cup anemometers, wind vanes)

Overview

- Introduction
  - … Floating Lidar
- Fraunhofer IWES Wind Lidar Buoy
- Offshore test next to FINO1 met. mast
  - … Setup
  - … Results
  - … Conclusions
- Summary

Offshore test next to FINO1 – Results

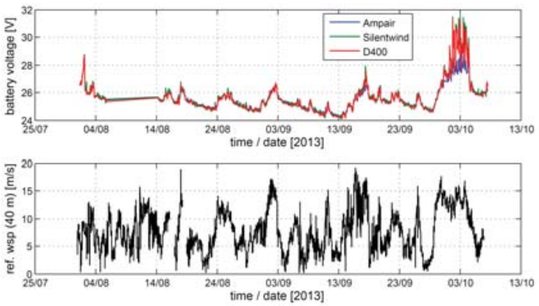

[Transmitted status data (voltages of battery banks assigned to micro-wind turbines) in relation to reference wind conditions.]

Offshore test next to FINO1 – Results

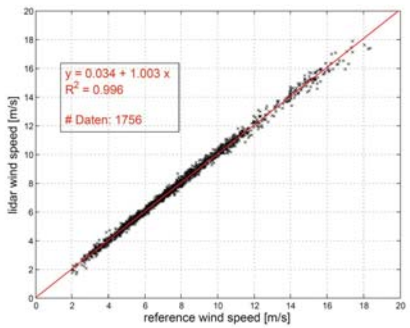

[Correlation between measured 10-min-mean (horizontal) wind speeds from floating-lidar device and cup anemometers at 100 m measurement height.]

→ very good correlation for uncorrected (!) data

Offshore test next to FINO1 – Results

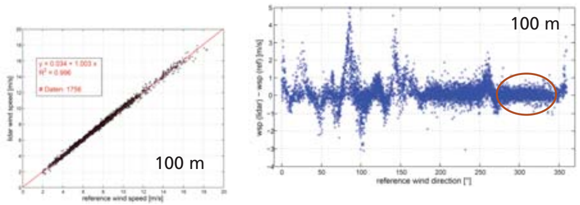

Correlation results (for measured wind speeds) are obtained for…

- limited wind direction sector and
- top height of meteorological mast.

80 m

Offshore test next to FINO1 – Results

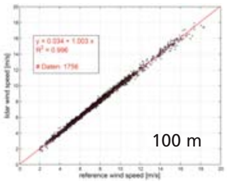

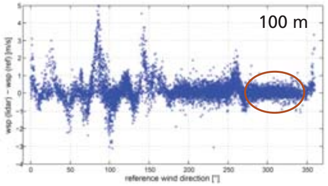

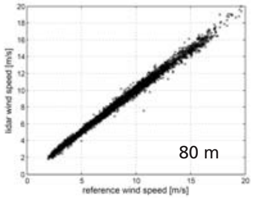

Correlation results (for measured wind speeds) are obtained for…

- limited wind direction sector and
- top height of meteorological mast

Offshore test next to FINO1 – Results

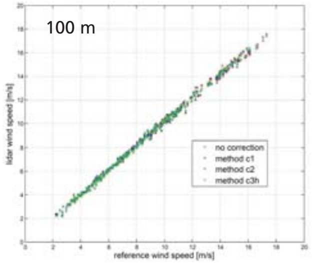

Application of motion correction (for limited dataset) further improves the correlation between wind measurements from floating-lidar device and reference cup anemometer.

	#data	m [-]	C [m/s]	R^2	k [-]	R^2
no correction	375	1.0039	0.0538	0.9969	1.0092	0.9968
method c1	375	1.0138	- 0.0013	0.9970	1.0137	0.9970
method c2	375	1.0061	0.0241	0.9979	1.0085	0.9978
method c3h	375	1.0170	- 0.0880	0.9978	1.0083	0.9977

Applied linear models:
$y = mx + C$
$y = kx$

Offshore test next to FINO1 – Results

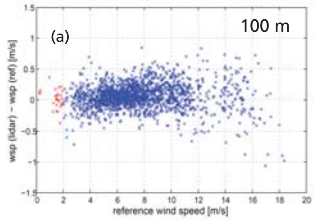

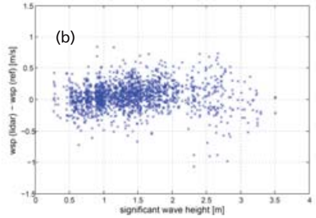

[Deviation in measured 10-min-mean wind speeds from floating lidar* and cup anemometer versus
(a) reference wind speed values and
(b) simultaneously recorded (30-min-mean) significant wave height]

* again uncorrected

Offshore test next to FINO1 – Results

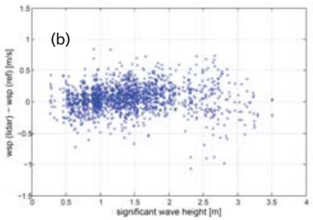

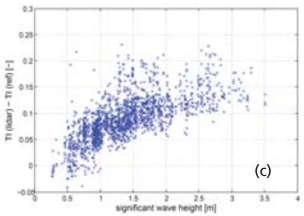

[← (c) Deviation in measured Turbulence Intensity (TI) values versus significant wave height …]

Offshore test next to FINO1 – Results

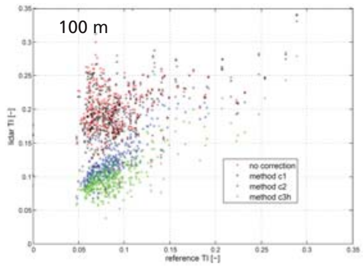

Application of motion correction (for limited dataset) significantly improves the correlation between TI values based on measurements from floating-lidar device and reference cup anemometer.

	#data	m [-]	C [m/s]	R^2	k [-]	R^2
no correction	375	(linear regression not applicable)				
method c1	375	(linear regression not applicable)				
method c2	375	0.922	0.042	0.703	1.314	0.556
method c3h	375	0.651	0.042	0.582	1.049	0.332

Offshore test next to FINO1 – Results

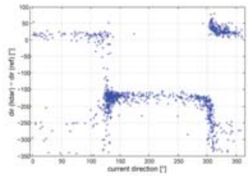

[← Deviation in measured (10-min-mean) wind directions versus current direction …]

Offshore test next to FINO1 – Results

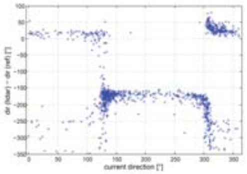

[← Deviation in measured (10-min-mean) wind directions versus current direction …]

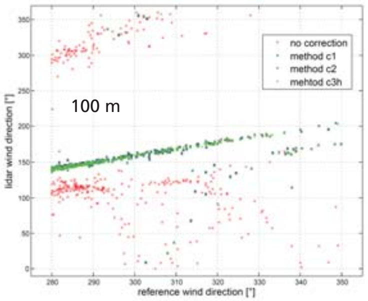

Yaw correction basically solves the wind-direction confusion in the measurements of the floating-lidar device.

Fraunhofer IWES

Overview

- Introduction
  - … Floating Lidar
- Fraunhofer IWES Wind Lidar Buoy
- Offshore test next to FINO1 met. mast
  - … Setup
  - … Results
  - … Conclusions
- Summary

Fraunhofer IWES

Offshore test next to FINO1 – Conclusions

– Results of floating-lidar offshore test (for Fraunhofer IWES Wind Lidar Buoy) are largely in line with the acceptance criteria for KPIs defined in *Carbon Trust OWA roadmap for the commercial acceptance of floating LIDAR technology* (published Nov. 2013).

– Further analysis (e.g. sensibility study with respect to different external parameters, investigation of motion correction on different levels) extremely helpful to assess the performance of the floating-lidar device under test in more detail → and necessary to estimate the complete uncertainty budget for the final application.

– Further work on Recommended Practices for the use of floating-lidar systems is scheduled within IEA Task 32 WP 1.5 (our results and conclusions will be an input to this work).

Fraunhofer IWES

Overview

- Introduction
  - … Floating Lidar
- Fraunhofer IWES Wind Lidar Buoy
- Offshore test next to FINO1 met. mast
  - … Setup
  - … Results
  - … Conclusions
- Summary

Fraunhofer IWES

Summary

– Introduction of the Fraunhofer IWES Wind Lidar Buoy as a compact floating-lidar concept with an encapsulated (well-protected) lidar device, a reliable power supply strategy, and an efficient (in-house developed) motion correction algorithm.

– Wind speed measurements show very good correlation with reference data from FINO1 met. mast (in nine-weeks trial from August to October 2013), wind direction and Turbulence Intensity data require motion correction.

– System availability close to 100% (98%) – definition of post-processed data availability depends on needed motion data and applied correction.

– Further work on the Fraunhofer IWES Wind Lidar Buoy is in progress – a second offshore test with a modified prototype is planned for the first half of 2014.

Fraunhofer IWES

Thank you for listening.*

* The work presented has been funded by the Federal Ministry for the Environment, Nature Conservationd and Nuclear Safety (BMU).

Fraunhofer IWES

Further reading

Hasager *et al.* 2013, Remote Sensing, open access journal, online

Peña *et al.* 2012, Offshore vertical wind shear, DTU Wind Energy report, online

Database available for research

Contact Andy Oldroyd at Oldbaum Services

NORSEWInD
NORTHERN SEAS WIND INDEX DATABASE

Home About Partners Publications Work Packets Database Contact

MetOcean analysis of a low-level coastal jet off the Norwegian coast.

EERA DeepWind'2014 Deep Sea Offshore Wind R&D Conference, Trondheim, 22 - 24 January 2014

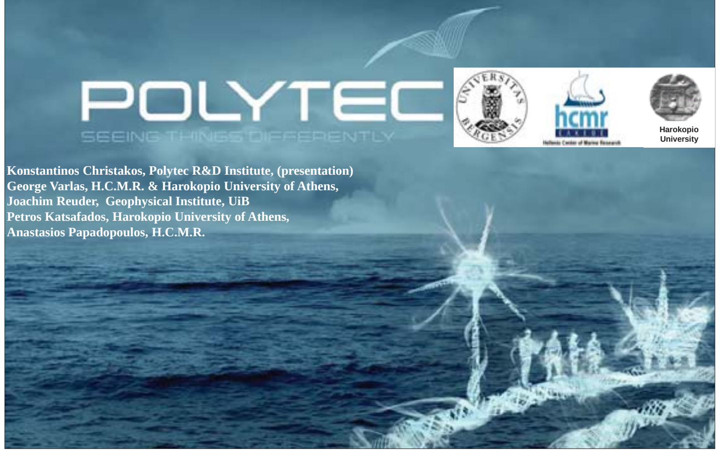

Konstantinos Christakos, Polytec R&D Institute, (presentation)
George Varlas, H.C.M.R. & Harokopio University of Athens,
Joachim Reuder, Geophysical Institute, UiB
Petros Katsafados, Harokopio University of Athens,
Anastasios Papadopoulos, H.C.M.R.

Low level coastal jet

Low-level coastal jet (LLCJ) is a high speed air flow which occur along some coastlines.

Atmospheric conditions that lead to LLCJ:

- A well-mixed, cool and moist MABL which is capped by an inversion.
- Maximum of sea level pressure gradient close to the coast

The low level wind speeds increase and lead to a coastal jet.

- The presence of coastal mountains can keep the air flow parallel to the coastline.

Source: https://www.meted.ucar.edu/mesoprim/coastaljets/

Important for offshore constructions and operations

- High offshore wind speeds (greater than 18 m/s)
- High waves
- Strong vertical wind shear.

Width of the LLCJ is usually between 20 and 40 km

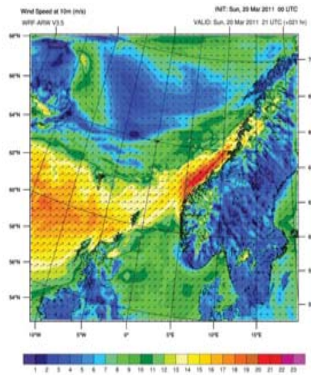

Source: https://www.meted.ucar.edu/mesoprim/coastaljets/

Case study:
Low Level Coastal Jet at Havsul region
20.03.2011

Study area: Havsul region

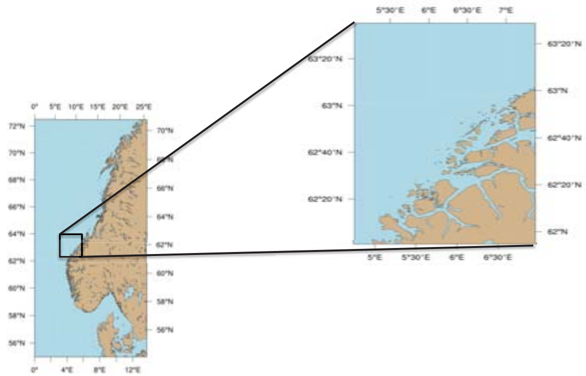

Synoptic Meteorological conditions 18:00 UTC, 20.03.2011

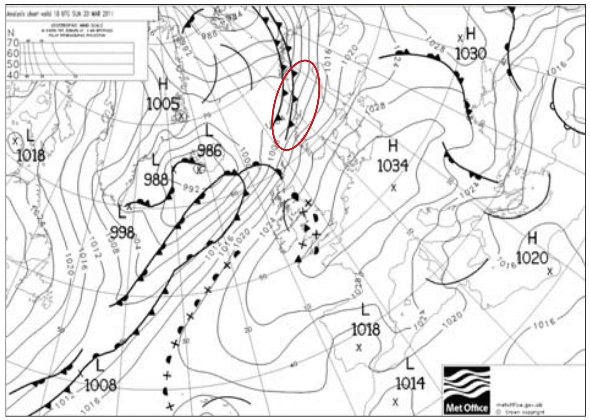

Synoptic Meteorological conditions, 20.03.2011

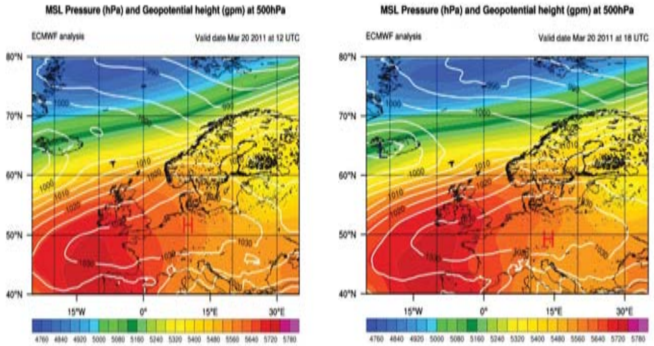

Observations: Low level coastal jet at Havsul region 20.03.2011

Satellite Observation 21:00 UTC, 20.03.2011

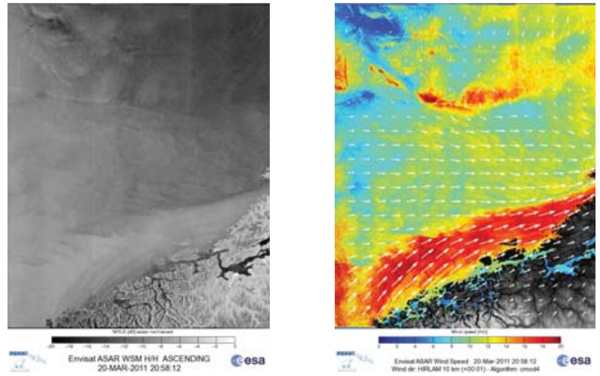

Source: Konstantinos Christakos, Characterization of the coastal marine atmospheric boundary layer for wind energy applications, Bergen Open Research Archive (BORA), June 2013, URI: http://hdl.handle.net/1956/7186

Observations at Ona (20.03.2011 – 21.03.2011)

Wind speed: 12 to 26 m/s

Turbulence Intensity: 5 % - 12 %

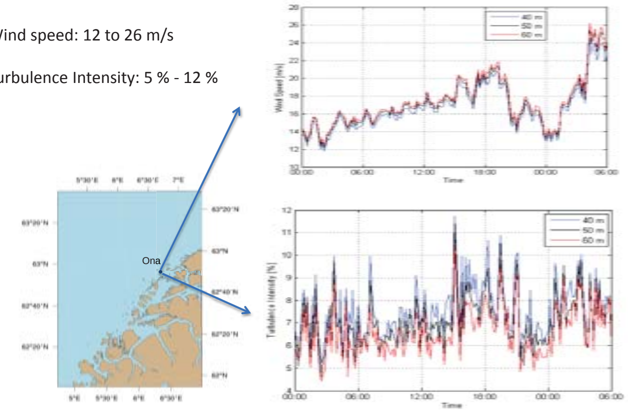

Source: Konstantinos Christakos, Characterization of the coastal marine atmospheric boundary layer for wind energy applications, Bergen Open Research Archive (BORA), June 2013, URI: http://hdl.handle.net/1956/7186

Simulation: Low level coastal jet at Havsul region 20.03.2011

Model - Set up

- WRF-ARW V3.5
- Non- Hydrostastic
- 2-way nesting
- Simulation period: 2011 March 20 at 00UTC to 21 at 06UTC

2 simulations:

- 3 Domains : 9x9, 3x3, 1x1 km
- 4 Domains: 9x9, 3x3, 1x1, 1/3x1/3 km

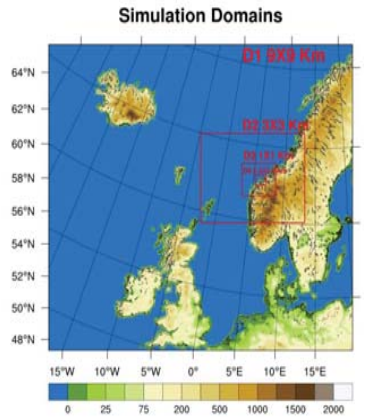

Obs. and WRF (D3 & D4) at 60 m

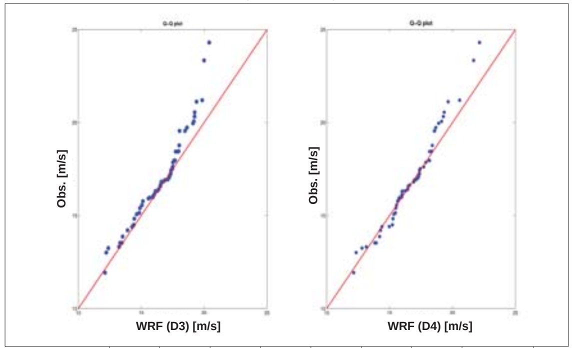

	Min	Max	Median	Mean	Q1	Q3	Std	Mean Error
Obs. [m/s]	11.93	26.21	16.76	17.03	15.34	18.44	2.59	-
WRF (D3) [m/s]	12.12	20.40	16.60	16.48	14.88	17.78	2.02	0.55
WRF (D4) [m/s]	12.15	22.15	16.91	16.77	15.49	18.21	2.08	0.26

WRF simulation of LLCJ
21:00 UTC 20.03.2011

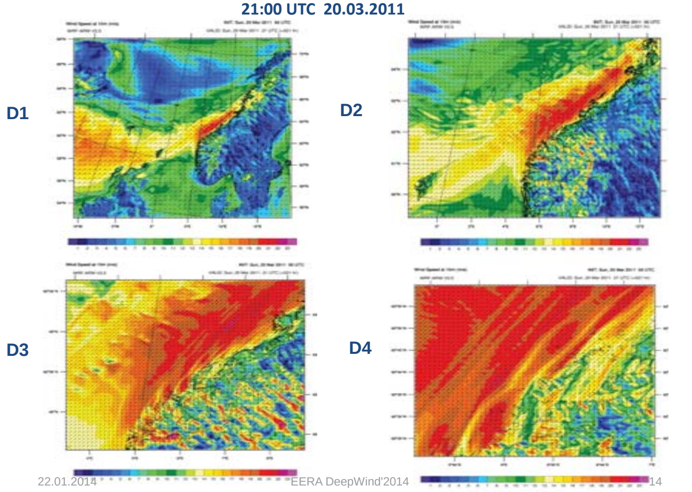

Cross section of wind speed

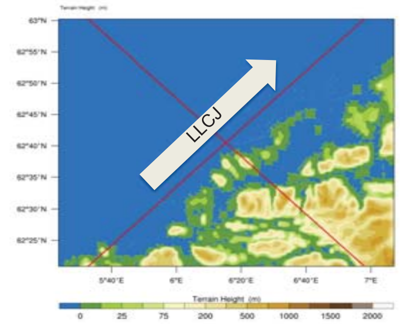

Cross section of wind speed normal to LLCJ

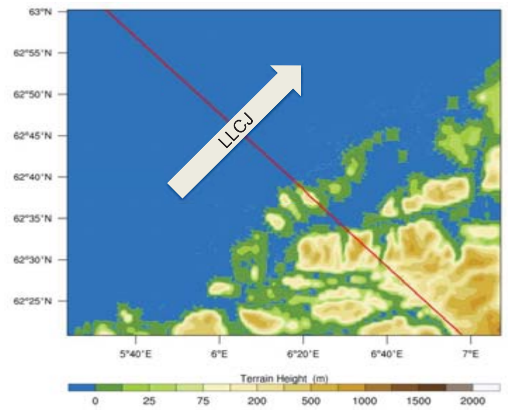

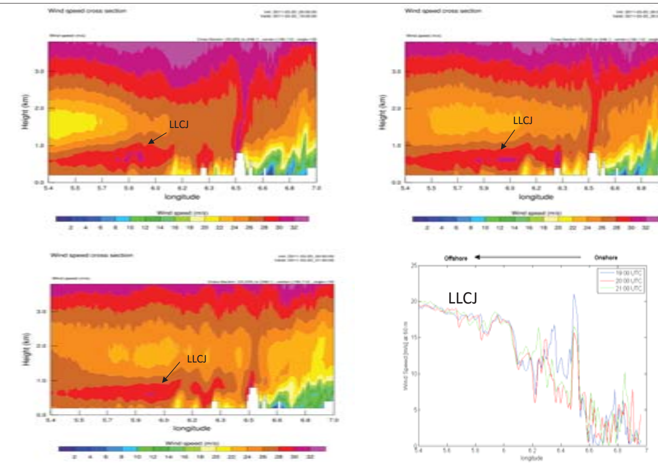

LLCJ width: approx. 30-40 km

Cross section of wind speed parallel to the LLCJ

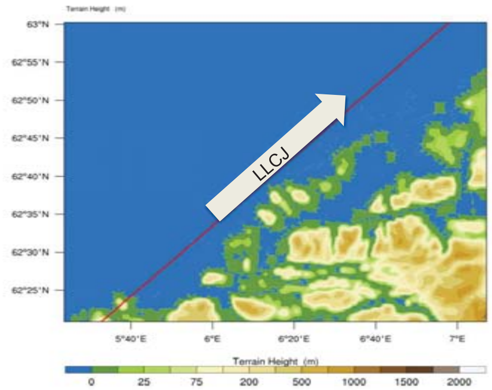

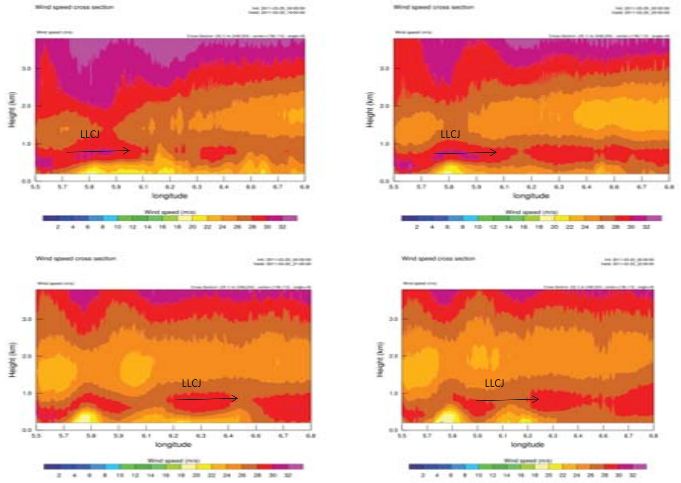

Wind Speed at 100 m

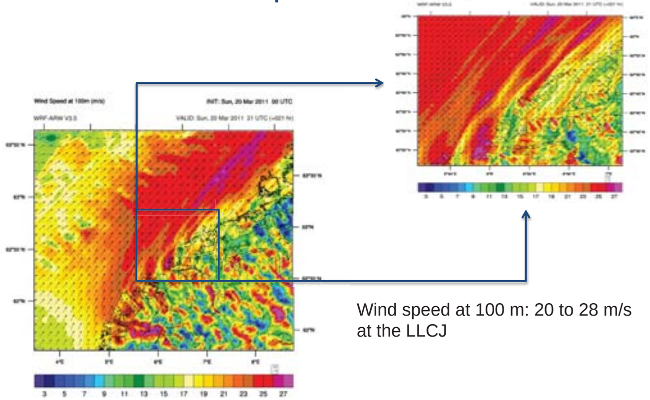

Wind speed at 100 m: 20 to 28 m/s at the LLCJ

Wind shear over the rotor disk during LLCJ

Wind power exponent:

$$\frac{U_2}{U_1} = \left(\frac{z_2}{z_1}\right)^{\alpha}$$

z_1= 60 m
z_2= 120 m
α > 0.10, neutral-stable conditions.

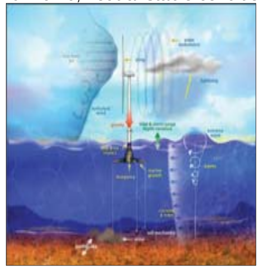

Source: http://www.ieawind.org/GWEC_PDF/GWEC%20Annex23.pdf

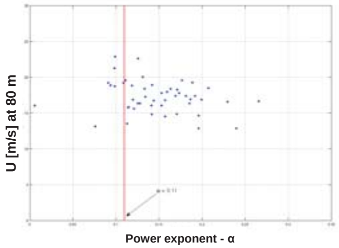

Stability class	Boundary layer properties	Hub-height wind speed	Wind shear
Strongly stable	Highest shear in swept-area, nocturnal LLJ may be present, little turbulence except just below the LLJ	Strong, especially at night	Highest: $\alpha > 0.3$
Stable	High wind shear in swept-area, low amount of turbulence unless a nocturnal LLJ is present	Strong, especially at night	High: $0.2 < \alpha < 0.3$
Near-neutral	Logarithmic wind profile	Generally strongest	Moderate: $0.1 < \alpha < 0.2$

Source: Wharton S and Lundquist J K (2012) Atmospheric stability affects wind turbine power collection, Environ. Res. Lett. 7

Summary

Case study of LLCJ, 20.03.2011 at Havsul region:

- The width of LLCJ: approx. 30 - 40 km
- Observed wind speeds: 12 to 26 m/s
- Observed Turbulence Intensity: 5 % - 12 %
- WRF model performs well (D3 and D4)
- Vertical wind shear– α > 0.10

Thanks for your attention

Air-Sea Interaction Influenced by Swell Waves

Mostafa Bakhoday Paskyabi
Geophysical Institute, University of Bergen, Norway
Mostafa.Bakhoday@gfi.uib.no
and
S. Zieger, A.D. Jenkins, A. Babanin, M. Ghantous, and D. Chalikhov, I. Fer
Swinburne University, Melbourne, Australia, Norway

Wind and Wave energy distribution in period

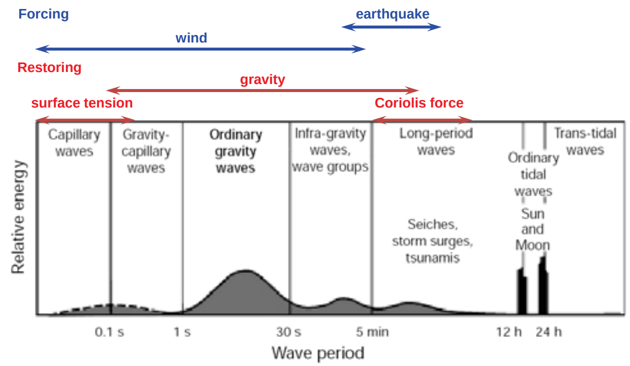

Outline

- Wave processes in the Atmospheric Boundary Layer (ABL)
- Wave-current interaction
- Wave-turbulence interaction.

Wave Processes in ABL

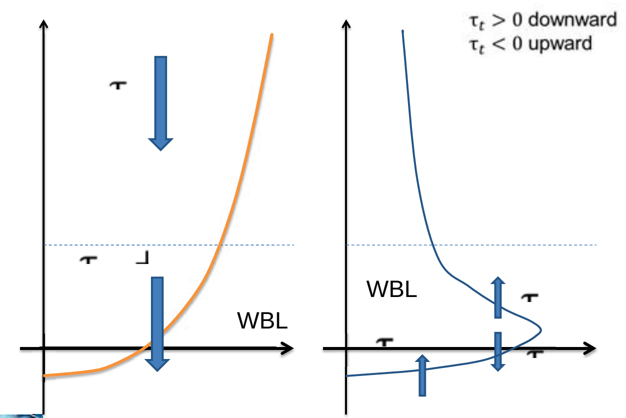

The air-sea fluxes

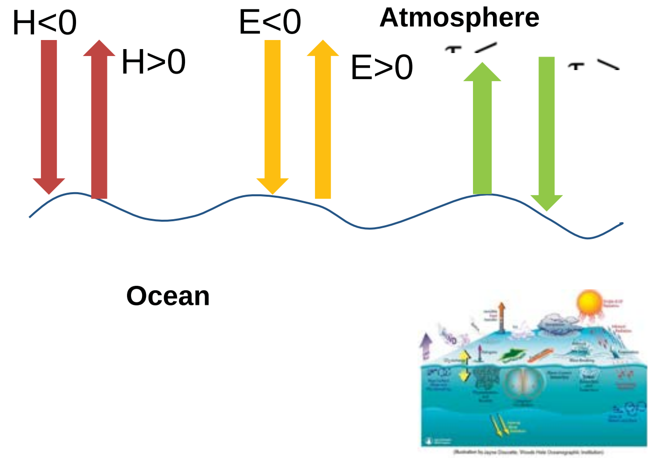

Analysis: Momentum

To account wave effects on momentum and energy equations, we decompose velocity and pressure in mean, wave, and turbulence components

$$\mathbf{u} = \bar{\mathbf{u}} + \tilde{\mathbf{u}} + \mathbf{u}',$$

$$p = \bar{p} + \tilde{p} + p'$$

Temporal scale for seperation

$$T \gg \tilde{t} \gg t'$$

Analysis: Momentum

$$\frac{\partial \bar{u}}{\partial t} = -\frac{1}{\rho}\frac{\partial}{\partial z}\left[K_m \frac{\partial \bar{u}}{\partial z} + \tau_{wx}\right],$$

$$\frac{\partial \bar{v}}{\partial t} = -\frac{1}{\rho}\frac{\partial}{\partial z}\left[K_m \frac{\partial \bar{v}}{\partial z} + \tau_{wy}\right],$$

wave-induced stress

Over the sea, the total wind stress can be made up as vector sum of shear stress, τ_s, and wave–induced stress, τ_w.

$$\tau = \tau_v + \tau_t + \tau_w.$$

Analysis: Momentum

Following Janssen 1991, the wave–dependent total wind velocity is given by

$$U_{10}^{w}(z) = \frac{u_*}{\kappa}\left[\ln\left(\frac{z+z_1}{z_0+z_1}\right) - \psi_m\right].$$

where z_1 is the wave stress contribution in the effective roughness ($z_e = z0 + z_1$).

The wave stress is expressed as

$$\tau_w = \rho_w \int_0^{2\pi}\int_0^{\infty} \sigma S_{in}(\sigma,\theta) d\sigma d\theta, \quad |\theta_{wind} - \theta| \le \pi/2,$$

where θ_{wind} is the wind direction, θ and σ denote the direction and the angular frequency, respectively. The wind energy input source term is expressed as

$$S_{in}(\sigma,\theta) = \sigma \frac{\rho_a}{\rho_w}\left[\frac{1.2}{\kappa^2}\epsilon \ln^4(\epsilon)\right]\left(\frac{u_* \cos(\theta)}{c_p}\right) E(\sigma,\theta) = \beta_w E(\sigma,\theta),$$

with

$$\epsilon = \left(\frac{u_* \cos(\theta)}{c_p}\right)^2 \left(\frac{g\kappa^2 z_e}{u_*^2}\right) \exp\left(\frac{\kappa c_p}{u_* \cos\theta}\right).$$

$$z_e = \frac{z_0}{\sqrt{1 - c_0 \tau_w/\tau}} \text{ and } z_0 = \frac{\beta_0 u_*}{g\sqrt{1 - c_0\tau_w/\tau}}.$$

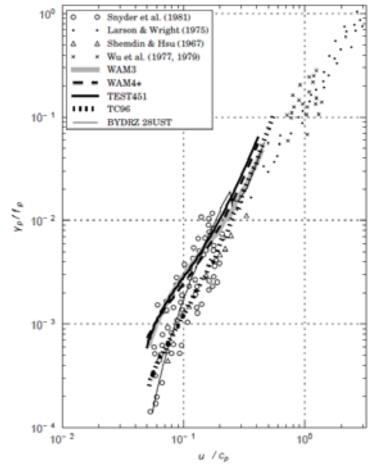

Fig. 1. (a) first picture.

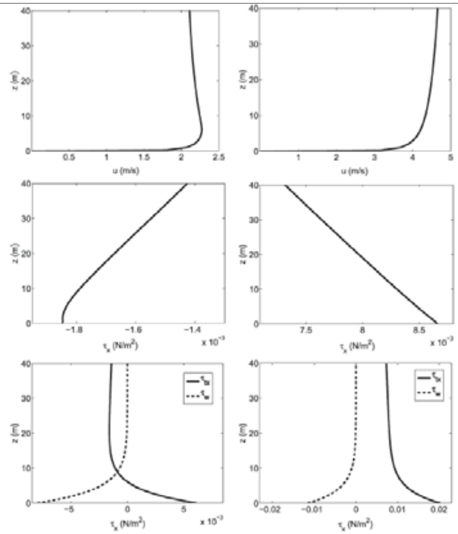

$$\tau_w = \tau_w(0)\exp^{-z/h_i}$$

Belceheer et al 2008

Analysis: momentum flux

the direction change of total stress change within wave ages ragend Between 0-0.2.

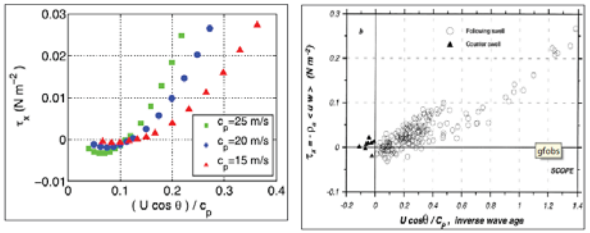

Grachev & Friall 2001

Analysis: Drag Coeffecient

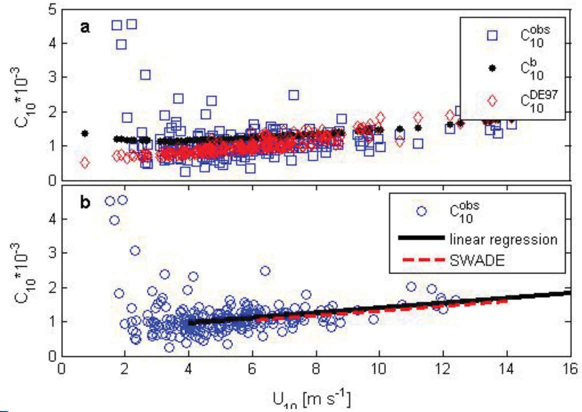

Bakhoday etal 2013

Analysis: TKE

In the presence of gravity waves

$$\frac{\partial e}{\partial t} = -\overline{u'w'}\frac{\partial \bar u}{\partial z} \overbrace{-\overline{\tilde u\tilde w}\frac{\partial \bar u}{\partial z}}^{1} + \frac{\partial}{\partial z}\left[\frac{1}{\rho}\overline{w'p'} + \overline{e'w'}\right] \overbrace{-\frac{1}{\rho}\frac{\partial \overline{\tilde w\tilde p}}{\partial z}}^{2} - \varepsilon = 0,$$

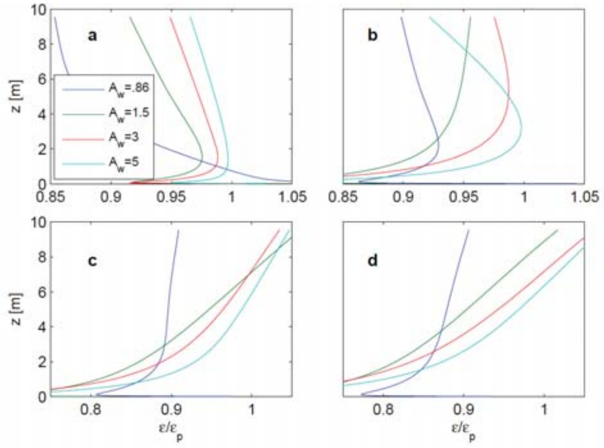

Aw is inverse of wave age

Wave-ocean processes

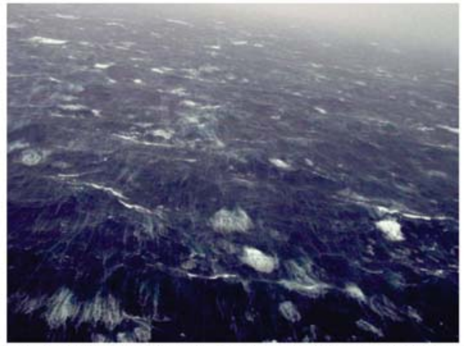

Photograph of sea-surface and breaking waves in Hurricane Isabel taken from a low-level flight during the CBLAST field campaign (Black et al. 2007).

Wave parameters

$$\mathbf{U}_s(z) = 4\pi\int_\theta\int_f f\mathbf{k}E(f,\theta)e^{-2k|z|}\,df\,d\theta,$$

$$\rho_w \nu_t \frac{\partial \mathbf{U}}{\partial z} = \vec\tau^{\,surf}_{mod},$$

$$\mathbf{F}_{ds} = -4\pi\int_f\int_\theta f S_{ds}(f,\theta)\hat{\mathbf{k}}ke^{-2k|z|}\,d\theta\,df,$$

where

$$\vec\tau^{\,surf}_{mod} = \tau_{tot} - 2\pi\rho_w\int_f\int_\theta \hat{\mathbf{k}} f S_{in}(f,\theta)\,d\theta\,df.$$

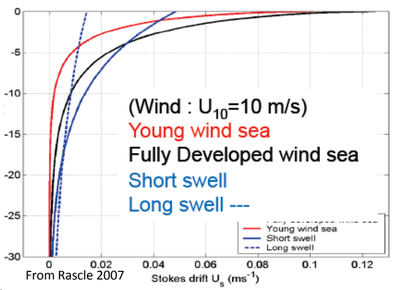

From Rascle 2007

Wave Current Interaction

In the non–steady case, the (quasi) Eulerian mean currents are governed by the wave–modified momentum equations:

$$\frac{\partial \mathbf{u}}{\partial t} = -f_{cor}\hat z \times \mathbf{u} + \mathbf{F}_{CSF} - \frac{\partial}{\partial z}\underbrace{\overline{\mathbf{u}'w'}}_{1} - \frac{1}{\rho_0}\nabla p^* + \underbrace{\mathbf{u}_s \times (\nabla \times \mathbf{u})}_{2} + \mathbf{F}_{ds}(z),$$

Background Fig. From S. Monismith

From Bakhoday-Paskyabi & Fer a2013

Wave turbulence interactions

- By simplifying motion equations:

$$\frac{\partial u}{\partial t} = -\frac{\partial(\overline{u'w'})}{\partial z} + f_{cor}(v + v_s) + F_x,$$

$$\frac{\partial v}{\partial t} = -\frac{\partial(\overline{v'w'})}{\partial z} - f_{cor}(u + u_s) + F_y,$$

$$\frac{\partial e}{\partial t} = -\left(\overline{u'w'}\frac{\partial U}{\partial z} + \overline{v'w'}\frac{\partial V}{\partial z}\right) + \overline{b'w'} - \frac{\partial}{\partial z}\left(\overline{ew'} + \frac{1}{\rho_0}\overline{P'w'}\right) - \varepsilon.$$

From Bakhoday-Paskyabi & Fer b 2013

Wave turbulence interactions

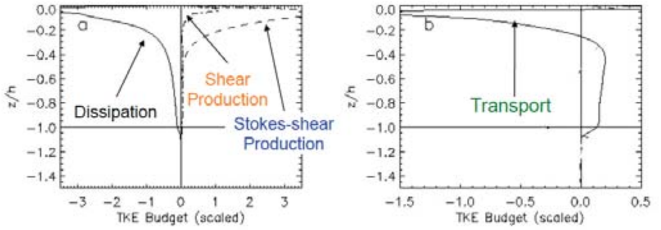

The k model

$$\overbrace{\frac{\partial k}{\partial t}}^{1} = \overbrace{\frac{\tau}{\rho_0}\cdot\frac{\partial \mathbf{u}}{\partial z}}^{2} + \overbrace{\frac{\tau}{\rho_0}\cdot\frac{\partial \mathbf{u}_s}{\partial z}}^{3} + \overbrace{\frac{g}{\rho_0}\overline{b'w'}}^{4} - \varepsilon + \overbrace{\frac{\partial}{\partial z}\left[\frac{\nu_t}{\sigma_k}\frac{\partial k}{\partial z}\right]}^{5} - \overbrace{\frac{\partial \mathbf{F}}{\partial z}}^{6},$$

Grant & Belcher (2009)

From Bakhoday-Paskyabi & A. Jenkins 2013

Comparisons with measurements

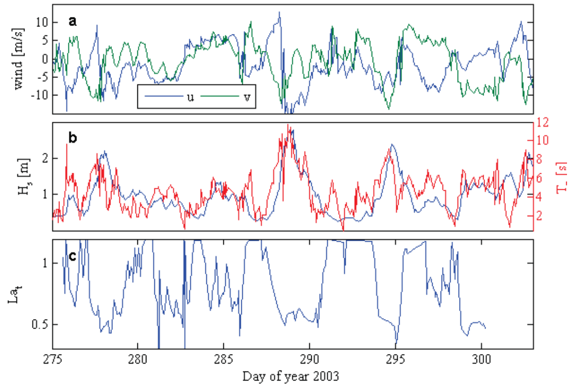

Data extracted from Kukula etal 2010

From Bakhoday-Paskyabi & A. Jenkins 2013

Comparisons with measurements

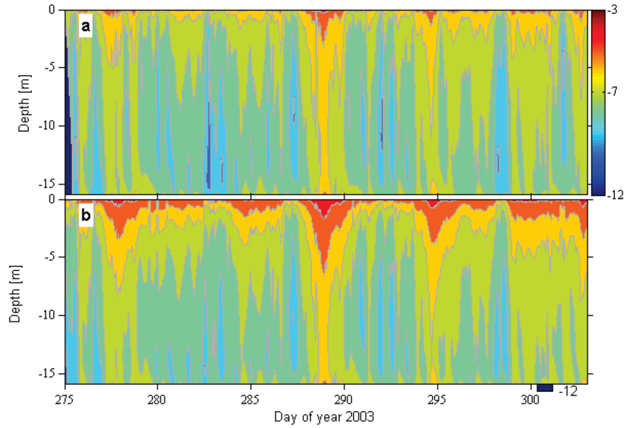

From Bakhoday-Paskyabi & Fer 2013

Comparisons with measurements

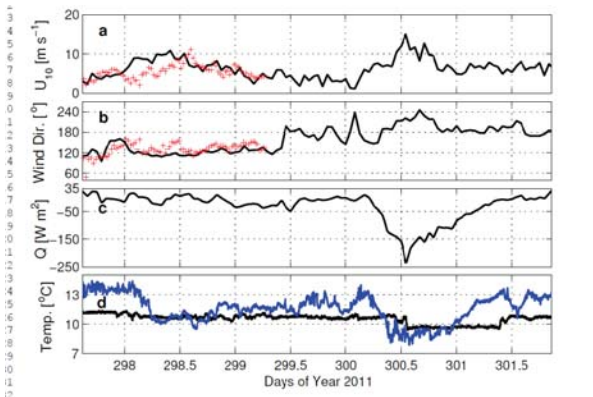

Fig. 2 Time series of (a) wind speed at 10 m height, U_{10}, from Vigra station (solid line), and from WS buoy (plus makers), (b) wind direction at 10 m height from Vigra station (solid line), and from WS buoy (plus markers), (c) total surface heat flux, and (d) water and air temperature at air-sea interface (black and blue solid lines, respectively) for the duration of the experiment on October 25 to 30 2011.

From Bakhoday-Paskyabi & Fer 2013

Comparisons with measurements

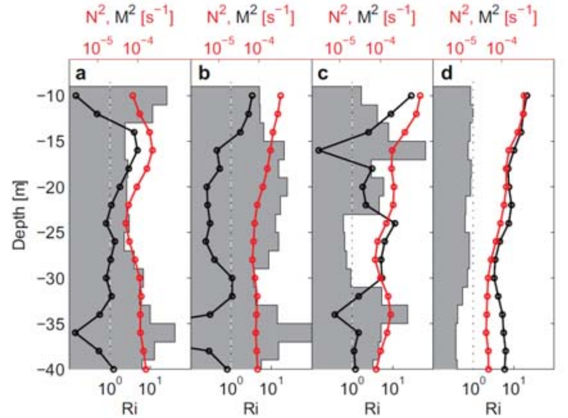

Fig. 11 Time averaged vertical profiles of squared shear M^2 (black solid lines), squared buoyancy N^2 (red solid lines), and $Ri = N^2/M^2$ (gray): (a) periods between 297.5 and 297.8, (b) between 299.4 and 299.9, (c) between 300.35 and 300.4, and (d) between 301.8 and 302.

From Bakhoday-Paskyabi & Fer 2013

Comparisons with measurements

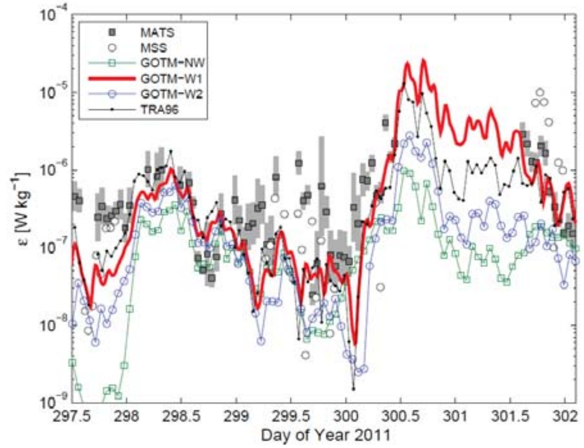

From Bakhoday-Paskyabi & Fer 2013

Comparisons with measurements

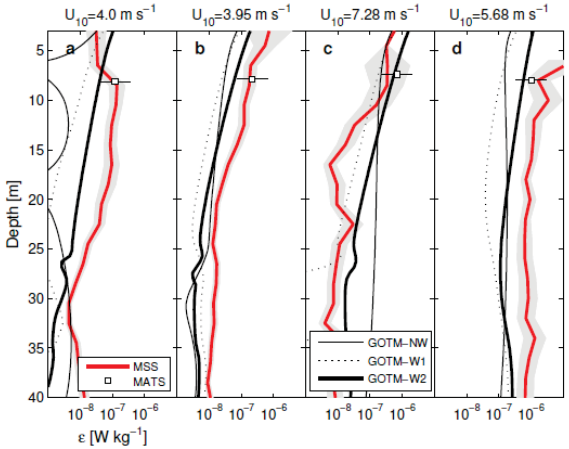

Conclusions:

1. Wave modified momentum and energy equations in both ABL and OBL,
2. Modified MY and k-epsilon models,
3. Wave induced momentum parameterization
4. Wave-current interaction,
5. Wave turbulence interaction (Wave-swell interaction)

Future works

1. Model-observation comparison with Marstein measured turbulence data acquired during November 2012 and 2013
2. Modification of 3D model,
3. Developing parameterizations using accessible data and theories.

References

Kukula eta al 2010, Rapid Mixed Layer Deepening by the Combination of Langmuir and Shear Instabilities: A Case Study,

Grant, A. L. M. and Belcher, S. E. (2009)*Characteristics of Langmuir Turbulence in the Ocean Mixed Layer.* Journal of Physical Oceanography, 39 (8). pp. 1871-1887. ISSN 0022-3670 doi: 10.1175/2009JPO4119.1,

A. A. GRACHEV, C. W. FAIRALL, (2001) Upward Momentum Transfer in the Marine Boundary Layer,

M. Bakhoday-Paskyabi et al, (2013) The influence of surface gravity waves on the injection of turbulence in the upper ocean,

M. Bakhoday-Paskyabi et al, (2013), Turbulence structure in the upper ocean: a comparative study of observations and modelling Ocean Dynamics.

C2) Met-ocean conditions

Wave refraction analyses at the western coast of Norway for offshore applications, Ole Henrik Segtnan, Polytec R&D Institute

Improving Gap Flow Simulations near Coastal Areas of Continental Portugal, Paulo Costa, LNEG

Wave driven wind and the effect on offshore wind turbine performance, Siri Kalvig, StormGeo/University of Stavanger

Wave refraction analyses at the coast of Norway for offshore applications

POLYTEC
SEEING THINGS DIFFERENTLY

Ole Henrik Segtnan, Polytec R&D Institute

January 22 2014 EERA DeepWind'2014

OBJECTIVES

Introduction: what is wave refraction?
why study wave refraction?

Methods: how to calculate wave propagation paths?

Application: effect of current induced refraction on rays reaching the coastal regions off Norway

WAVE REFRACTION

Change in propagation direction due to a change in its transmission medium

Current and depth induced refraction

RELATION TO OFFSHORE WIND ENERGY

Wave load: where will wave energy propagate?

Wave load: winds and waves misaligned, bending moment of the mast increases (Tarp-Johansen et al., 2009; Seidel, 2010).

METHODS - ASSUMPTIONS

Linear wave theory

Relative change in water depth over wavelength is small

Relative change in current velocity over wavelength and period is small

No temporal variations in current velocity

METHODS – RAY CURVATURE (MATHIESEN, 1987)

$$\kappa = \frac{\boldsymbol{\mu}_z \cdot \left(\frac{d\mathbf{r}}{dt} \times \frac{d^2\mathbf{r}}{dt^2} \right)}{\left| \frac{d\mathbf{r}}{dt} \right|^3}$$

WAVE REFRACTION: COAST OF NORWAY

Depth induced refraction: Long waves, the topography affects the wave speed

H ~ 20 m (T ~8s)

Application to coastal area off Norway: only current induced refraction will be relevant

POLYTEC

EXAMPLE – NO CURRENTS

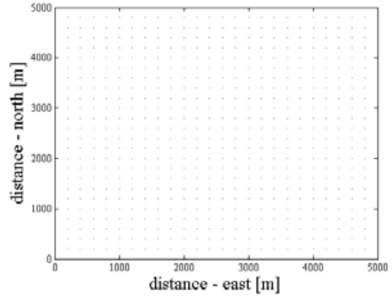

POLYTEC

EXAMPLE – NO CURRENTS

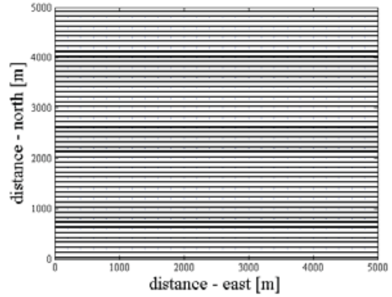

POLYTEC

EXAMPLE - VORTEX

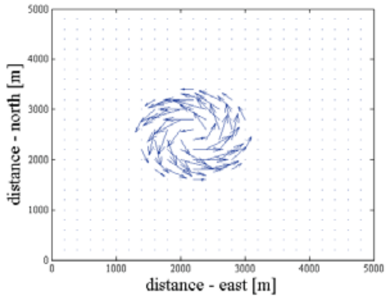

POLYTEC

EXAMPLE - VORTEX

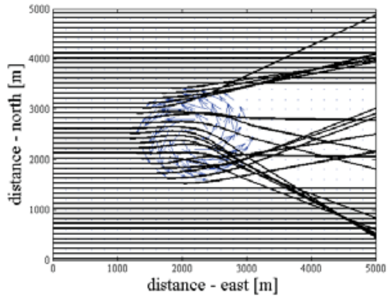

POLYTEC

SURFACE VELOCITY

NorKyst800 (Albretsen et al., 2011)

Operational ocean model (Meterological inst., IMR, NIVA)

800 spatial m resolution

Daily averages since July 2012

POLYTEC

APPLICATION

For each current field: offshore wave propagation from 180° to 360°

Rays determined by eddies

All flow fields are representative for any wave propagation direction.

STUDY AREA AND SELECTED REGIONS

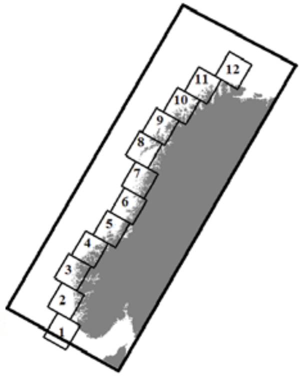

RAY DISTRIBUTIONS

RAY DISTRIBUTION

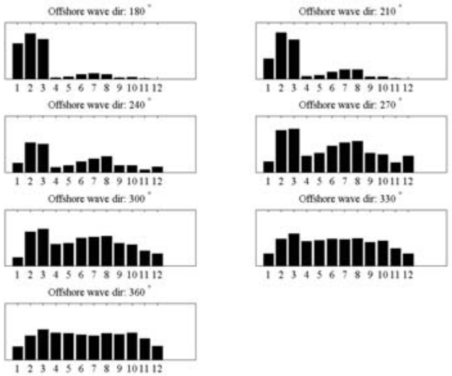

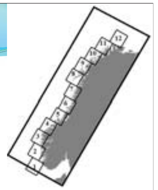

DEVIATION DISTRIBUTION- NORTHERLY WINDS

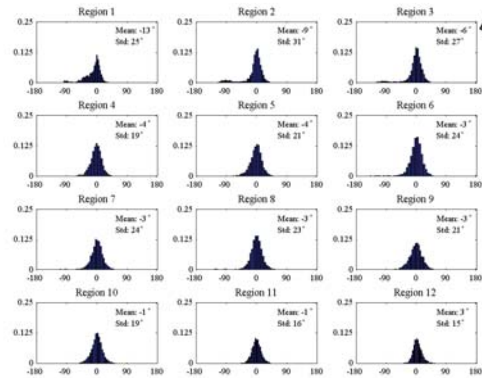

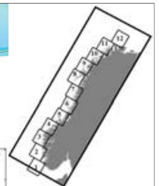

DEVIATION DISTRIBUTION- WESTERLY WINDS

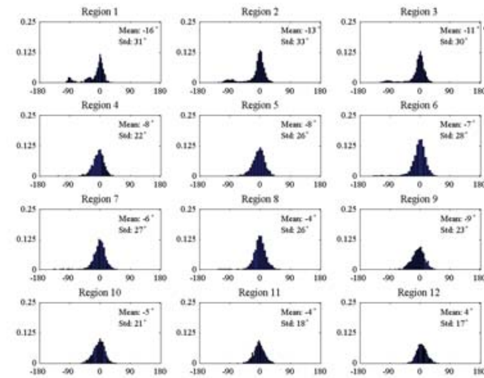

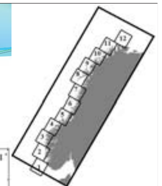

DEVIATION DISTRIBUTION- SOUTHERLY WINDS

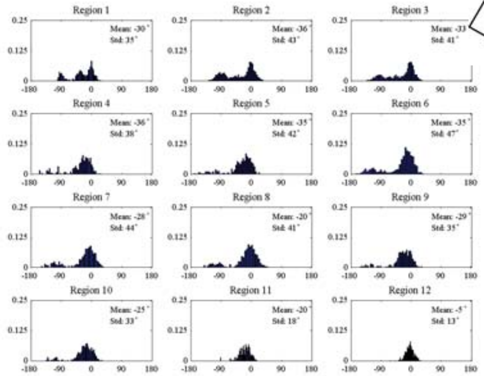

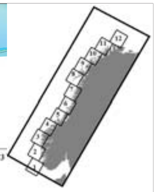

CONCLUSIONS

Southerly and westerly winds:

Convergence of wave energy at southwstern part of Norway

South of Lopphavet: Wave and wind are misaligned

Refraction effects may result in increased bending moment

Thanks for your attention

Improving Gap Flow Simulations Near Coastal Areas of Continental Portugal

11th Deep Sea Offshore Wind R&D Conference Trondheim, 22-24 January 2014

Section Met Ocean Conditions

paulo.costa@lneg.pt antonio.couto@lneg.pt raquel.marujo@lneg.pt ana.estanqueiro@lneg.pt
amouche@cls.fr

Gap Flows

- Gap flows are locally generated wind currents that spread abruptly to the ocean, triggered by non-linear atmospheric phenomena.
- Its intensity and spreading may bring several impacts near coastal areas in particularly where offshore wind parks can be deployed.

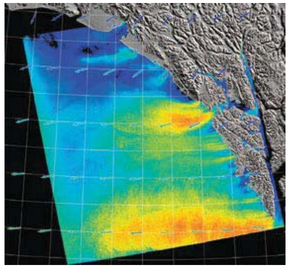

Gap Flows

- Modelling this phenomena is still a challenge from the meteorological point of view since models still not reproduce efficiently way gap flows, especially, the ones occurring very near the coasts.
- A high resolution satellite SAR image is nowadays the "*best observational spatial wind tool*" to detect the phenomena in action

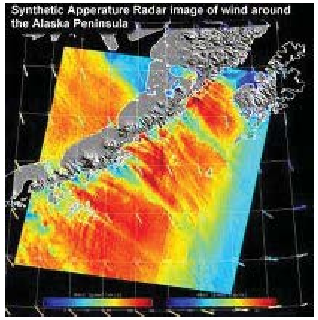

Gap Flows in Portugal

- At 9th December 2010 strong gap flows were identified along some western coastal regions of Continental Portugal
- This region contains several promising sea areas with high sustainable wind resource for offshore wind park's deployment

Gap Flows in Portugal

The phenomena in action…

This "zoomed" SAR image on day, 9th December 2010 @ ~ 22:30h shows the gap flows (surface).

"red zones" wind speeds ~ 20 to 30m/s

"green zones" – vicinity ~ 10 to 13 m/s

"blue zones" -around ~ 3 to 6 m/s

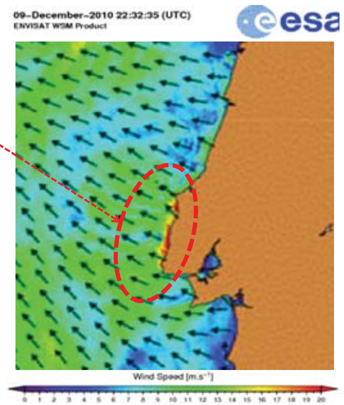

Gap Flows in Portugal

LNEG operates three anemometric masts in the region. At that day & time, observed mean wind speed and direction was:

IN01 (sensor height 10m):
~ 9.86 m/s ; ~ 90º

IN33 (sensor height 10m):
~ 8.76 m/s ; 65º

IN166 (sensor height 21m):
~ ? m/s ; ?º
(data with -9999 error code)

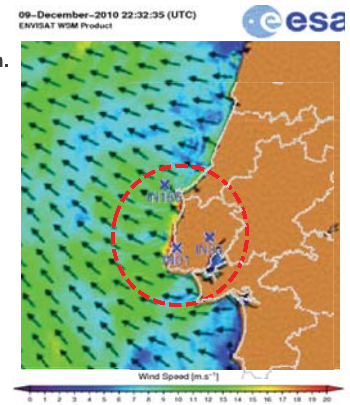

Gap Flow Simulation

Simulation tasks:

- **To set up a high resolution mesoscale simulation with the WRF model for the case study day (09.12.2010);**
- **To use the 3D-VAR data assimilation technique;**
- **To compare model's results with and without data assimilation and to validate the simulated wind flow with LNEG's anemometric masts**

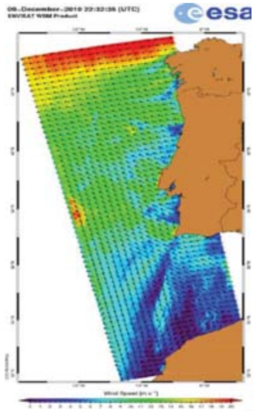

Assimilation advantages

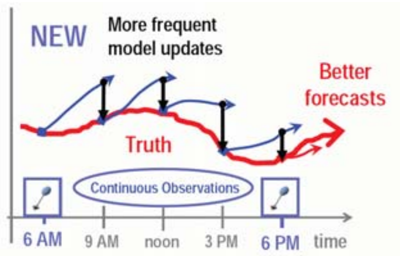

- **Assimilation of observations will reduce error forecasts**
- **Reducing error forecasts means getting better forecasts!**

3D-VAR assimilation

A "BLUE" method ...

"Best Linear Unbiased Estimate"

≅ Kalman Filter

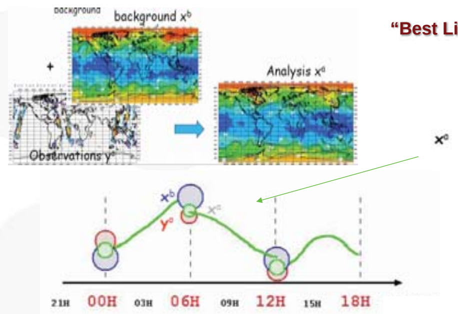

$x^a = x^b + dx$
$ = x^b + K(y^o - H(x^b))$

Gain $K = BH^T(HBH^T + R)^{-1}$

Inovation $d = y^o - H(x^b)$

Backgroud error covariance matrix $B \rightarrow \overline{x'x'^T} \approx A\overline{(x^{t2} - x^{t1})(x^{t2} - x^{t1})^T}$ **Mean forecasts @12h - @00h**

Gap Flow Simulation

Setup WRF model …

As a background "run"

- Three domains covering the area under study; 50x50km ; 10x10km and 2x2km;
- Historical initial and boundary conditions from GFS forecast model @ 0.5x0.5º, ingested every three hours;
- Running period:

1 day - 1200h 09-12-2010 to 1200h 10-12-2010

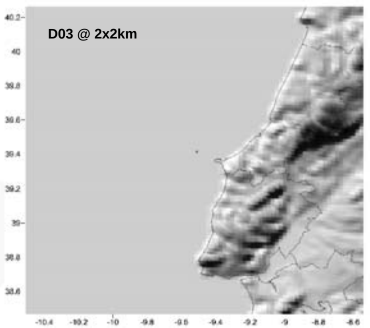

Gap Flow Simulation

Setup WRF model …

Assimilation "run" - 3D-VAR

- Assimilated "SAR" wind data image at **21h** (09-12-2010) @ all model domains;
- Assimilated surface synoptic data at **12h, 18h and 21h** from LPPT Lisbon station *(T,Hr,P,U,V)*
- Assimilated IN01 & IN33 at **12h, 18h** and **21h**;
- Validation: IN01 & IN33 *(daily period)*

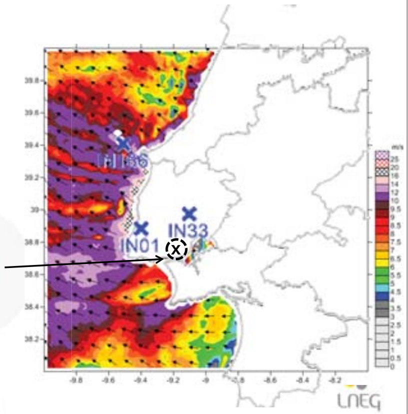

WRF forecasted results (2x2km) – (surface) @ **2200h** 09-12-2010

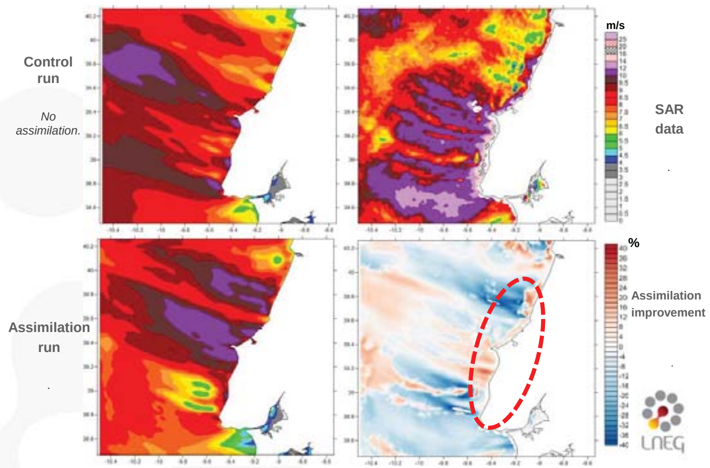

WRF forecasted results (2x2km) – (surface)

from 1200h 09-12-2010 to 1200h 10-12-2010

Wind speed comparison (m/s) @ IN01 (h=10m)

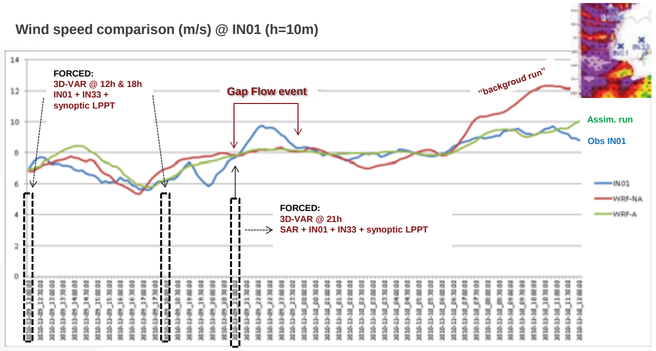

Correl –NA (%)	Correl – A (%)
77.22	83.19

wind speed (m/s) @ 22h		
WRF-NA	WRF-A	Obs
8.18	8.21	9.60

Mean wind speed (m/s)		
WRF-NA	WRF-A	Obs
8.29	7.98	7.83

Results

- **Observational assimilated data slightly improved WRF forecasted estimates in IN01 place - very near to the coast.**
- **SAR image helped in the description of the phenomena - with positive (30%) and negative (-35%) impacts when compared with "background run". The origins of the phenomena are being studied and further simulations are being conducted in order to improve its performance.**
- **Other similar coastal phenomena cases will be investigated and, if possible, on other countries' offshore wind deployment areas.**

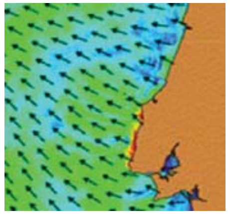

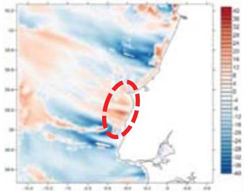

Thank you!

Improving Gap Flow Simulations Near Coastal Areas of Continental Portugal

11th Deep Sea Offshore Wind R&D Conference
Trondheim, 22-24 January 2014

Section Met Ocean Conditions

Paulo Costa
paulo.costa@lneg.pt

Ana Estanqueiro
ana.estanqueiro@lneg.pt

Wave influenced wind and the effect on offshore wind turbine performance

Siri Kalvig[a], Eirik Manger[b], Bjørn Hjertager[c], Jasna B. Jakobsen[c]

[a]StormGeo AS, Nordre Nøstekaien 1, 5011 Bergen, Norway
[b]Acona Flow technology AS, Uniongt. 18, 3732 Skien, Norway
[c]University of Stavanger,4036 Stavanger, Norway

Introduction

StormGeo
Control in a changing environment

- Motivation
- Wave influenced wind
- Wind turbine performance
- Method, WIWTS
- Results
- Conclusions & comments

StormGeo
Control in a changing environment

Motivation

StormGeo
Control in a changing environment

Statoil's Hywind Norway, Photo; Lene Eliassen

http://www.sorenlarsen.co.nz

- Will wave influenced wind at an offshore wind site result in different wind shear and more turbulence than expected ?
- And if so, how will this affect the turbines?

Wave influensed wind

StormGeo
Control in a changing environment

Wind sea and swell influences the atmosphere different!

Wind sea - waves generated by local wind
Swell - long period waves generated by distant storms

Most common is a mixture of wind sea and swell, and this makes the picture even more complicated.

Method – wave generation

StormGeo
Control in a changing environment

Need to simulate wave movements!

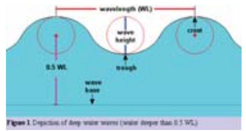

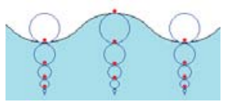

From: Grand Valley State University, http://faculty.gvsu.edu/videticp/waves.htm

Need a new boundary condition that take into account the sinusoidal movement of the "ground".

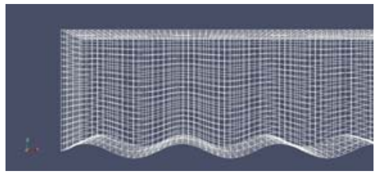

Method – wave generation

Need to simulate wave movements!

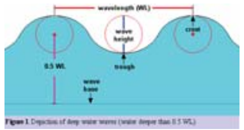

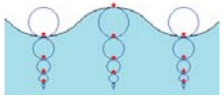

From: Grand Valley State University, http://faculty.gvsu.edu/videticp/waves.htm

Need a new boundary condition that take into account the sinusoidal movement of the "ground".

Solution:
Transient OpenFOAM simulation with pimpleDyMFoam. New boundary condition implemented with mesh transformations.

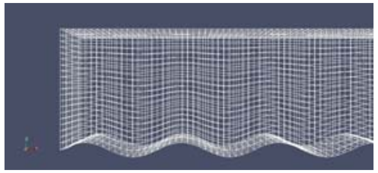

Wave influenced wind

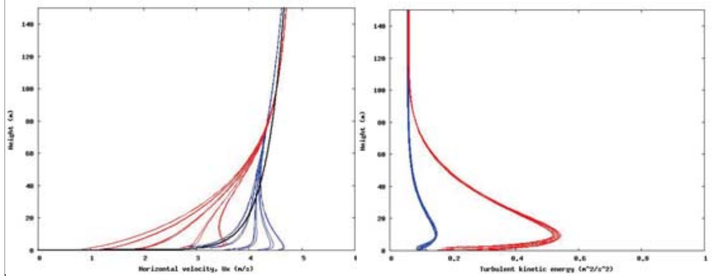

Domain: 1200m x 25 m x 400 m
Logarithmic wind at inlet with U_{100m} =5 m/s, z_0=0.0002 m, U*=0.15 m/s. Wave with C=12,5 m/s, L=100 m, a=1,6 m

In general:

The wind speed profile and the turbulent kinetic energy pattern far above the waves will be different depending on the wave state and wave direction.

Method - Actuator line method in SOWFA

Actuator line method of Sørensen and Shen used in the Simulator for Offshore Wind Farm Applications SOWFA

Method - Actuator line method in SOWFA

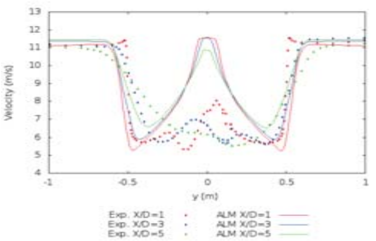

Testing the model:
Blind test1: NORCOWE & NOWITECH organized a wind turbine blind test in 2011-2012

Tip speed ratios		Experiment	FRM	Deviation	ALM	Deviation
3	C_P	0.12	0.23	91.6 %	0.17	43.3 %
	C_T	0.40	0.46	15.0 %	0.34	- 15.3 %
6	C_P	0.45	0.46	2.2 %	0.45	0.8 %
	C_T	0.92	0.85	- 7.6 %	0.86	- 6.7 %
10	C_P	0.20	0.16	- 20.0 %	0.04	- 80.1 %
	C_T	1.17	1.03	- 12.0 %	0.88	- 24.4 %

Table 1: Power coefficient (Cp) and thrust coefficient (C_T) from FRM and ALM simulations for different tip speed ratios (λ) are compared with experimental values.

Method - Actuator line method in SOWFA

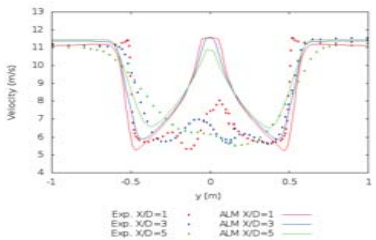

Testing the model:
Blind test1: NORCOWE & NOWITECH organized a wind turbine blind test in 2011-2012

Tip speed ratios		Experiment	FRM	Deviation	ALM	Deviation
3	C_P	0.12	0.23	91.6 %	0.17	43.3 %
	C_T	0.40	0.46	15.0 %	0.34	- 15.3 %
6	C_P	0.45	0.46	2.2 %	0.45	0.8 %
	C_T	0.92	0.85	- 7.6 %	0.86	- 6.7 %
10	C_P	0.20	0.16	- 20.0 %	0.04	- 80.1 %
	C_T	1.17	1.03	- 12.0 %	0.88	- 24.4 %

Table 1: Power coefficient (Cp) and thrust coefficient (C_T) from FRM and ALM simulations for different tip speed ratios (λ) are compared with experimental values.

Method – combined set up - WIWTS

Wave simulations are combined with the actuator line simulations of SOWFA

Wave Influenced Wind Turbine Simulation
WIWTS

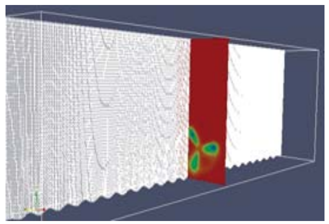

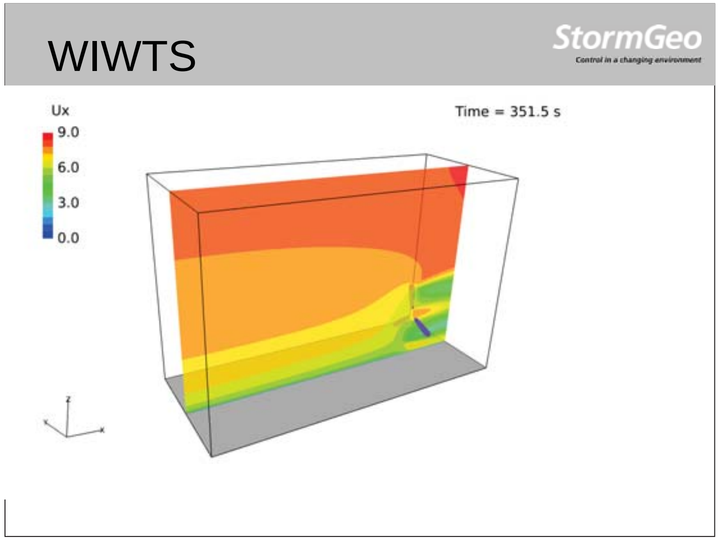
WIWTS
StormGeo
Ux
9.0
6.0
3.0
0.0
Time = 351.5 s

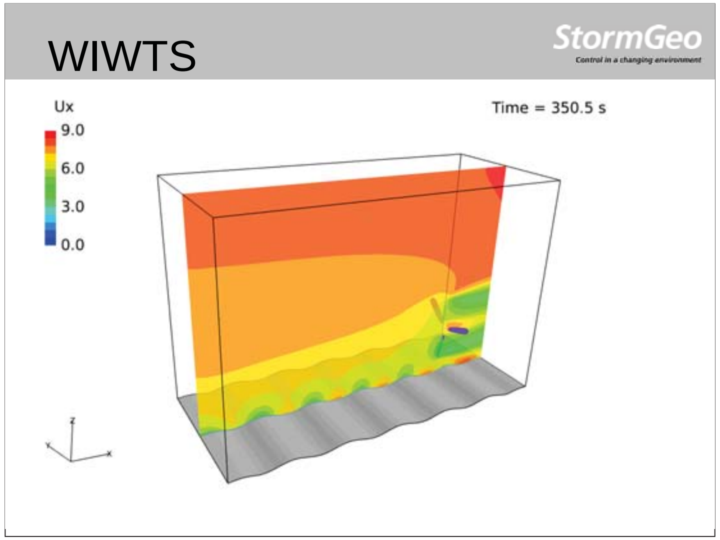
WIWTS
StormGeo
Ux
9.0
6.0
3.0
0.0
Time = 350.5 s

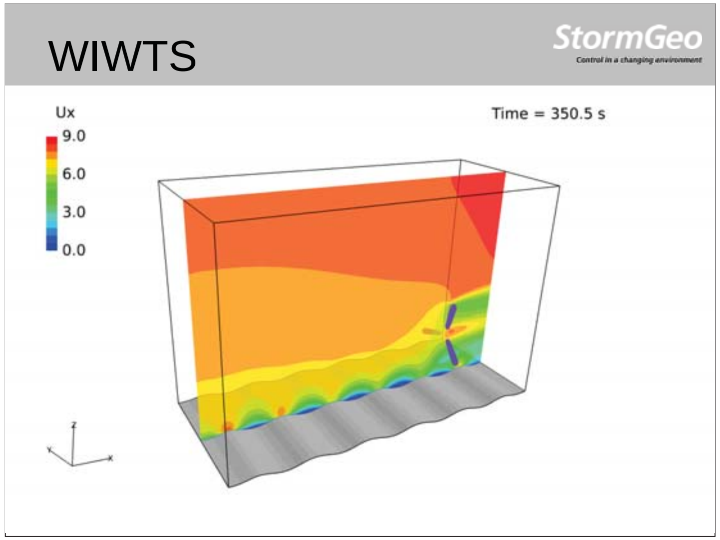
WIWTS
StormGeo
Ux
9.0
6.0
3.0
0.0
Time = 350.5 s

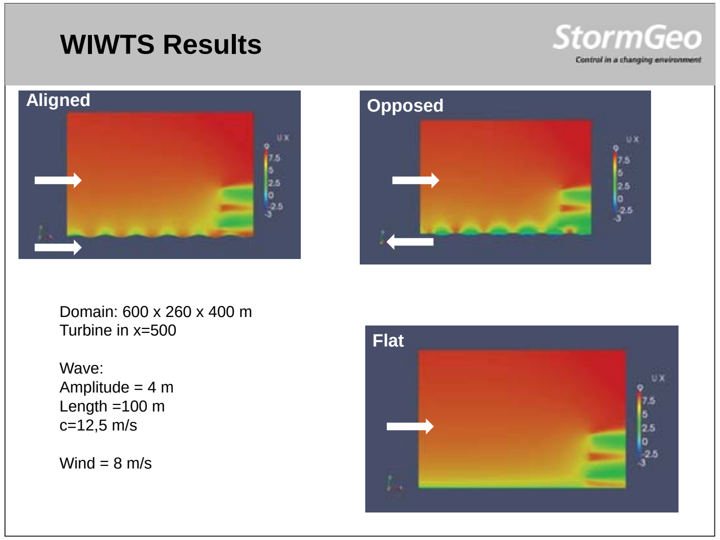
WIWTS Results
StormGeo
Aligned
Opposed
Flat
Domain: 600 x 260 x 400 m
Turbine in x=500
Wave:
Amplitude = 4 m
Length =100 m
c=12,5 m/s
Wind = 8 m/s

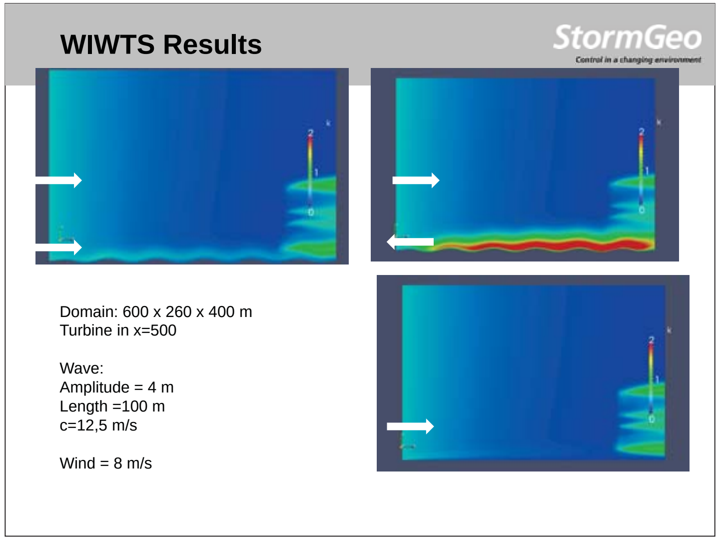
WIWTS Results
StormGeo
Domain: 600 x 260 x 400 m
Turbine in x=500
Wave:
Amplitude = 4 m
Length =100 m
c=12,5 m/s
Wind = 8 m/s

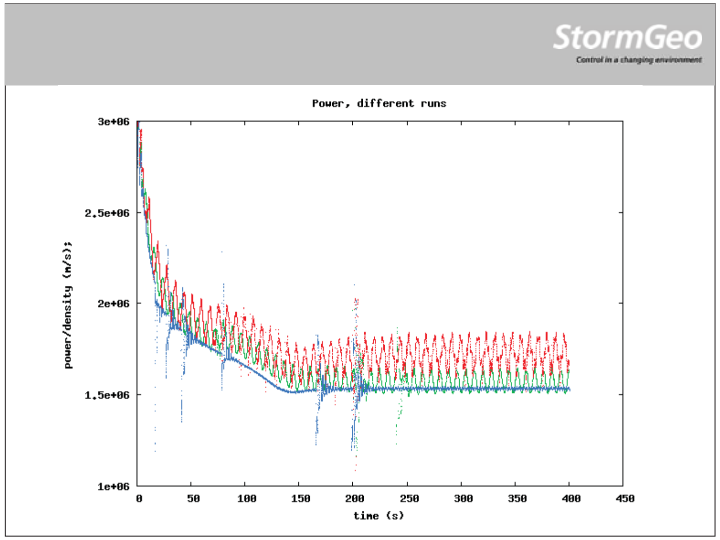
StormGeo
Power, different runs
3e+06
2.5e+06
2e+06
1.5e+06
1e+06
0
50
100
150
200
250
300
350
400
450
time (s)

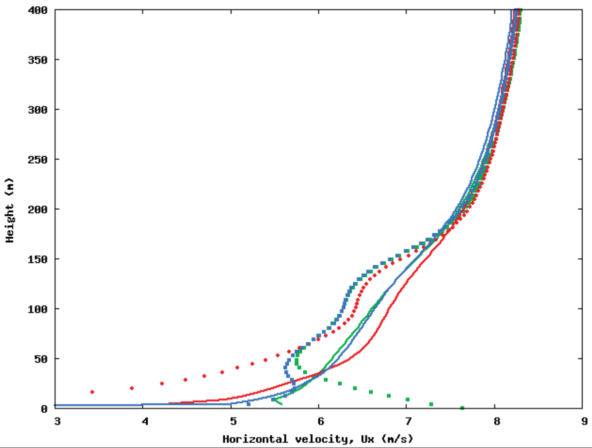

Line, x=437 m
Point, x=469 m

T = 200 sec

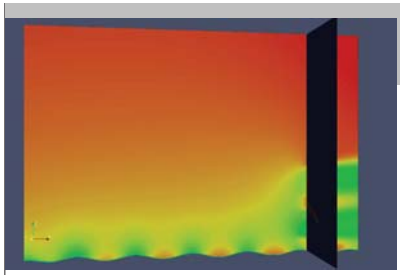

365 sec – position over wave aligned situation

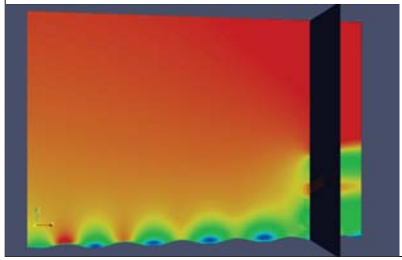

365 sec – position over wave opposed situation

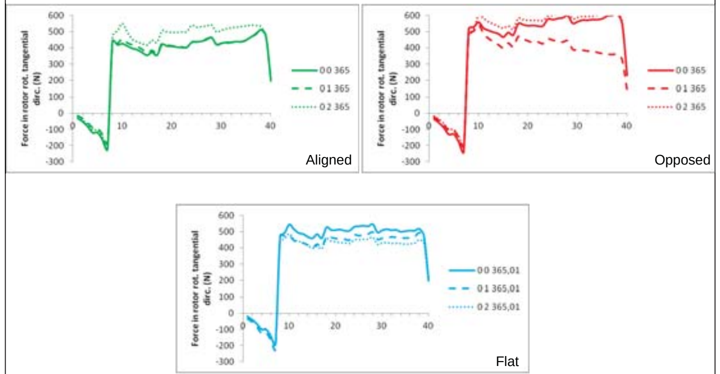

StormGeo/UiS/NORCOWE project:
Coupled meso scale atmosphere model with wave model

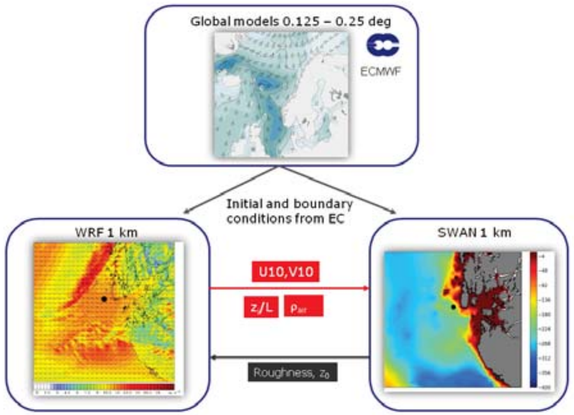

waveAmplitude	4.0 m
waveSpeed	12.5 m/s
waveLength	100.0 m
waveAmplitude	2.0 m
waveSpeed	-6.24 m/s
waveLength	25.0 m

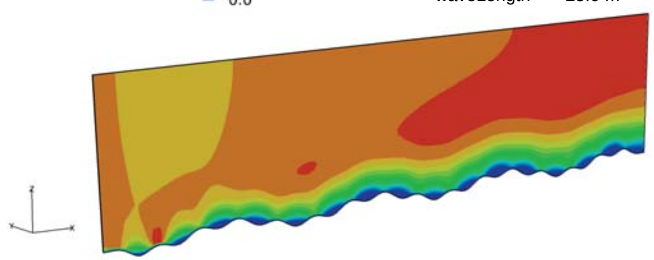

Summary

✓ Wave-wind simulations with openFOAM is ongoing PhD work at University of Stavanger, StormGeo and Norcowe.

✓ A new set up: Wave influenced wind turbine simulations – **WIWTS**. The actuator line part of SOWFA are slightly changed and coupled with the wave simulations.

✓ The flow response over the waves are very different for cases where the wind is aligned with the wave propagation and wind opposing the wave.

✓A low level speed up in the lowest meters for wind aligned with a fast moving wave. The profiles over the waves are not logarithmic. Turbulent kinetic energy is slightly higher for wind opposing the wave than wind aligned with the wave.

✓ A case study of a large fast moving swell, with amplitude 4 m, shows implications for both power production and loads. Problem with the grid size. The domain should be higher and longer. Grid independency was not completely reached.

✓ Future work: Simulate more realistic waves. Link result to metocean statistics in order to reveal if interesting situations will occur often enough in order to be of any significance to power harvest and load considerations.

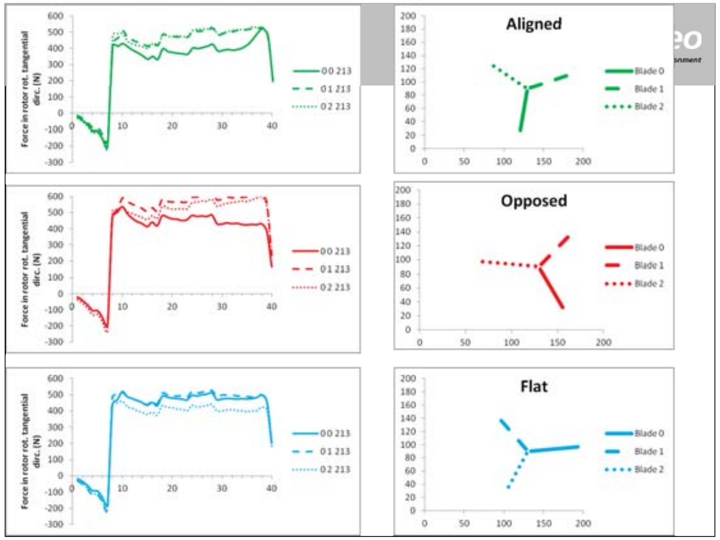

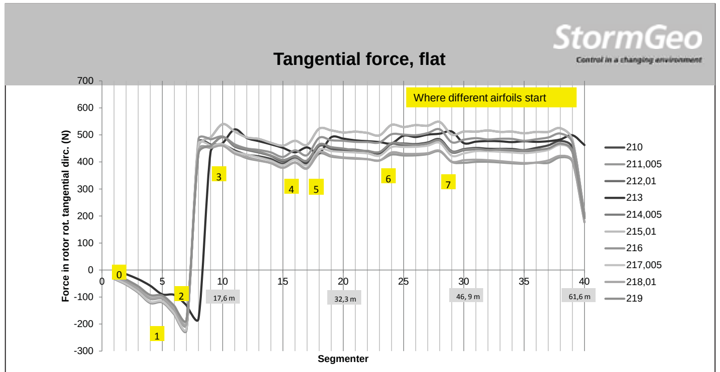

Viser bare hvor på en av force kurvene de forskjellige airfoilene "slår" inn. Tror vi kan si at mesteparten av "hoppene" I kurven relateres til endring av airfoilegenskaper…?

NEK IEC 61400-1;
Wind turbines - part 1; Design requirements

NEK IEC 61400-3;
Wind turbines - part3: Design requirements for offshore wind turbines

NS-EN 1991-1-4;
Eurocode 1: Actions on structures - Part 1-4: General actions - Wind actions

- Only log profile or power law is used
- Only neutral stratification
- Charnock relation to some extend used when calculating turbulent intensity
- Turbine classes on shore is used offshore
- 33 design load cases versus 22 for onshore
- No hydrodynamic influence or wave influence on rotor-narcelle assembly or wind flow

There is a gap between "best knowledge" (science) and "best practice" (codes, standards) and there is a need for improved guidance on the impact atmospheric stability and wave-wind interaction in the MABL can have on the offshore wind industry

Kalvig, Gudmestad & Winther: Exploring the gap between 'best knowledge' and 'best practice' in boundary layer meteorology for offshore wind energy, Wind Energy, published online: 30 JAN 2013, doi: 10.1002/we.1572

✓A new set up: Wave influenced wind turbine simulations – **WIWTS**. The actuator line part of SOWFA are slightly changed and coupled with the wave s

✓A case study of a large wave with amplitude 4 m shows implications for both power production and loads.

✓Problem with the grid size. The domain should be higher and longer. Grid independency was not completely reached.

Future work: Simulate more realistic waves. Link result to metocean statistics in order to reveal if interesting situations will occur often enough in order to be of

StormGeo
Control in a changing environment

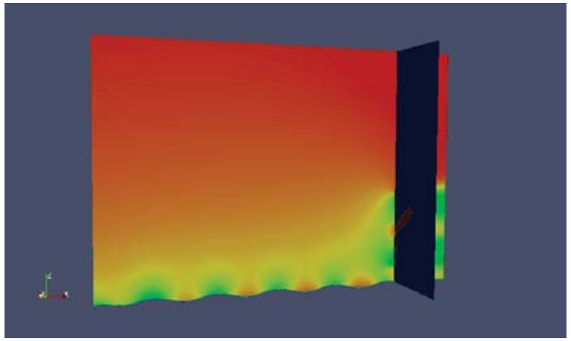

213 sec – position over wave aligned situation

D) Operations & maintenance

Fatigue Reliability-Based Inspection and Maintenance Planning of Gearbox Components in Wind Turbine Drivetrains, Amir Nejad, NTNU

Cost-Benefit Evaluation of Remote Inspection of Offshore Wind Farms by Simulating the Operation and Maintenance Phase, Øyvind Netland, NTNU

The effects of using multi-parameter wave criteria for accessing wind turbines in strategic maintenance and logistics models for offshore wind farms,
Iver Bakken Sperstad, SINTEF Energi AS

NTNU
Norwegian University of Science and Technology

EERA DeepWind'2014
11'th Deep Sea Offshore Wind R&D Conference

Fatigue Reliability-Based Inspection and Maintenance Planning of Gearbox Components in Wind Turbine Drivetrains

Amir R. Nejad[1], Yi Guo[2], Zhen Gao[1], Torgeir Moan[1]

[1]Norwegian Research Centre for Offshore Wind Technology (Nowitech) and Centre for Ships and Ocean Structures (CeSOS), NTNU

[2]National Wind Technology Centre (NWTC), National Renewable Energy Laboratory (NREL), USA

CeSOS – Centre for Ships and Ocean Structures

Outline

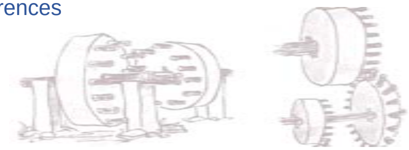

NOWITECH Norwegian Research Centre for Offshore Wind Technology

Introduction

Maintenance, in general terms, is classified into [1]:

- **Corrective** actions.

The corrective action is taken when the failure of components is occurred and the system is partly broken down.

- Precautionary- or **preventive** - actions.

The preventive maintenance action is on routine schedule to repair or replace components before they fail [2].

NOWITECH Norwegian Research Centre for Offshore Wind Technology

Introduction

- **Preventive** maintenance in Wind Turbines:

The preventive maintenance of wind turbine gearboxes is often carried <u>every 6 months</u> for each wind turbine, normally within a day, and a major check-up is performed <u>every 3 years</u> [3].

- What is included in gearbox routine inspection?

Oil sampling for particle counting, oil filter checking, observing the possible oil leakage from housing or pipes and identifying any unusual noise from the gearbox [3]. The oil sampling even in offshore wind turbines equipped with condition monitoring systems is often offline.

NOWITECH Norwegian Research Centre for Offshore Wind Technology

Introduction

If the result indicates high debris in the oil, unusual noise or leakage, further internal visual inspection by other means such as **endoprobe** or **fiberscope** with camera is then performed [3].

In the endoprobe or fiberscope inspection, the maintenance inspector should examine all gears and bearings, one by one in order to find the source of noise or debris in the oil. <u>Any knowledge of impending failure can reduce cost dramatically and can help the maintenance team to plan</u>. [4]

NOWITECH Norwegian Research Centre for Offshore Wind Technology

Objectives

The main aim of this paper is:

To propose a method for developing the "**<u>vulnerability map</u>**" which can be used for maintenance team to identify the components with lower reliability.

This map is developed based on the fatigue damage of gears and bearings.

NOWITECH Norwegian Research Centre for Offshore Wind Technology

7

Model: 750 kW NREL Drivetrain

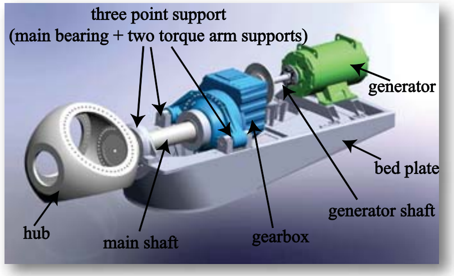

8

Model: 750 kW NREL Gearbox Topology

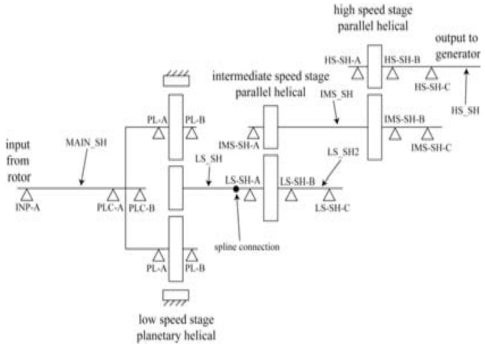

9

Methodology : decoupled approach

Step I:

NREL dynamometer test bench.

Torque time series

10

Methodology : decoupled approach

Step II:

Torque time series are applied on Gearbox MBS model.

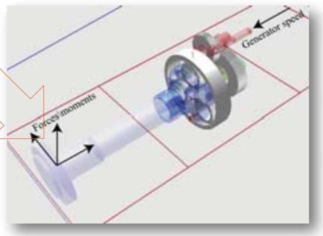

Gearbox multibody dynamic (MBS) model

Step III:

Loads on gears and bearings are measured.

11

Methodology

We rank the gears and bearings based on their fatigue damage.

Rated Wind Speed

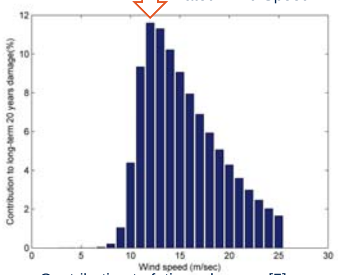

Contribution to fatigue damage [5]

12

Methodology

Gear Fatigue Damage (gear tooth root):

$$D = \frac{N_T}{K_c}\int_0^\infty s^m \cdot f(s)\cdot ds = \frac{N_T}{K_c}\left\{A^m \cdot \Gamma\left(1+\frac{m}{B}\right)\right\}$$

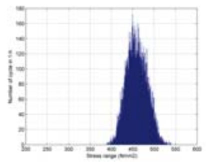

Bearing Fatigue Damage:

$$D = \frac{v_{P0}.T}{L_{10}.C^a}\cdot A^a \cdot \Gamma\left(1+\frac{a}{B}\right)$$

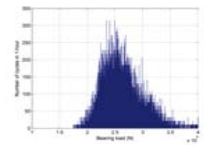

Load Duration Distribution (LDD) method is used for cycle counting [5].

Results

Gear Fatigue Damage (gear tooth root):

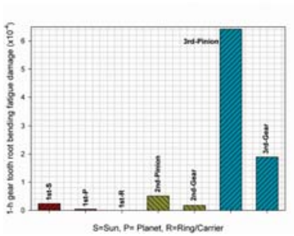

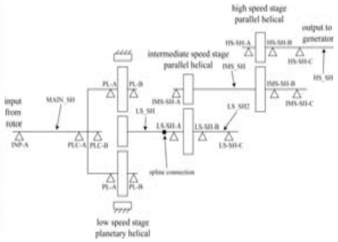

Results

Bearing Fatigue Damage:

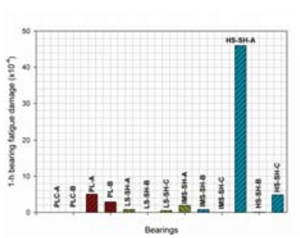

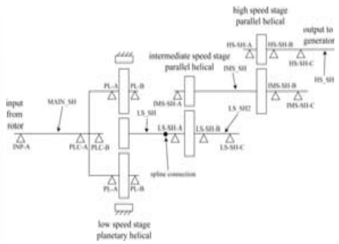

Results

Rank	Gear or Bearing	Name	*Damage* x 10^{-4}
1	Bearing	HS-SH-A	46.00
2	Gear	3rd Pinion	6.423
3	Bearing	PL-A	5.064
4	Bearing	HS-SH-C	4.846
5	Bearing	PL-B	2.921
6	Bearing	IMS-SH-A	1.954
7	Gear	3rd Gear	1.893
8	Bearing	LS-SH-A	0.812
9	Bearing	IMS-SH-B	0.777
10	Gear	2nd Pinion	0.509
11	Bearing	LS-SH-C	0.507
12	Gear	1st Sun Gear	0.241
13	Gear	2nd Gear	0.171
14	Bearing	HS-SH-B	0.096
15	Gear	1st Planet Gear	0.039
16	Bearing	IMS-SH-C	0.021
17	Bearing	LS-SH-B	0.020
18	Gear	1st Ring Gear	0.004
19	Bearing	PLC-A	0.000
20	Bearing	PLC-B	0.000

Results

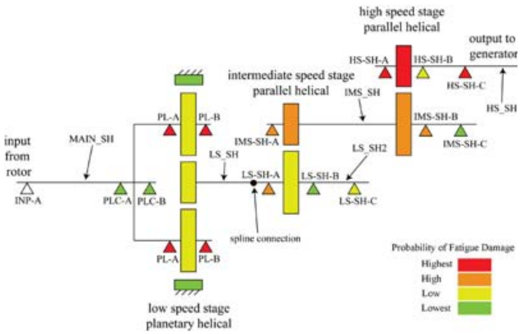

Vulnerability map of 750 kW NREL GRC gearbox

Results

Good agreement with ReliaWind project [6,7]. Failure modes identifed through FMEA includes:

1)Planetary gear failure.

2)High speed shaft bearing failure.

3)Planetary bearing failure.

4)Intermediate shaft bearing failure.

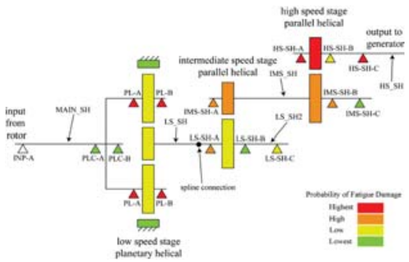

Vulnerability map of 750 kW NREL GRC gearbox

Summary

- ✓ An inspection and maintenance planning map “vulnerability map” based on the fatigue damage of gears and bearings is presented.
- ✓ The procedure for calculating the short-term fatigue damage for gears and bearings is described and exemplified for the NREL GRC 750 kW gearbox.
- ✓ This maintenance map can be used for maintenance planning and inspection of components during routine preventive maintenance inspections.

Advantages:

- Reducing the maintenance time.
- Focusing on those with higher probability of failure.
- It can also be used for condition monitoring system, interpreting the field data and searching the source of problem within those with higher probability of damage.

19

References

[1] Pintelon L., Parodi-Herz A. Maintenance: an evolutionary perspective. In : Kobbacy K. A. H., Murthy D. N. P. editors. Complex system maintenance handbook. Springer, 2008.
[2] Marquez F. P. G., Tobias A. M., Perez J. M. P., Papaelias M. Condition monitoring of wind turbines: techniques and methods. Renewable Energy 2012; 46: 169-178.
[3] Hockley C. J. Wind turbine maintenance and typical research questions. Procedia CIRP 2013; 11: 284-286.
[4] Butterfield S., Sheng S., Oyague F. Wind energy's new role in supplying the world's energy: what role will structural health monitoring play? National Renewable Energy Laboratory; NREL/CP-500-46180:2009, USA.
[5] Nejad A. R., Gao Z., Moan T. On long-term fatigue damage and reliability analysis of gears under wind loads in offshore wind turbine drivetrains, International Journal of Fatigue, in press, 2014, (DOI: http://dx.doi.org/10.1016/j.ijfatigue.2013.11.023).
[6] ReliaWind. Whole system reliability model. Report no. D.2.0.4.a. 2011. Available online at: http://www.reliawind.eu/files/file-inline/110318_Reliawind_DeliverableD.2.0.4aWhole_SystemReliabilityModel_Summary.pdf .
[7] Tavner P. Offshore wind turbine reliability, availability and maintenance. IET, 2012.

For more details, the reader is encouraged to review the paper associated with this presentation in “Energy Procedia”, June 2014.

20

Thank you for your attention!

NTNU
Norwegian University of Science and Technology

Cost-benefit evaluation of remote inspection of offshore wind farms by simulating the operation and maintenance phase

EERA DeepWind 2014
24th January 2014

Øyvind Netland, Iver Bakken Sperstad, Matthias Hofmann & Amund Skavhaug

Outline

- O&M of Offshore Wind Turbines
- Remote Inspection
- Simulations
- Results
- Conclusions

O&M of Offshore Wind Farms

- High cost compared to on land.
- Access to the turbines are:
  - Expensive.
  - Time consuming.
  - Not possible in harsh weather.
- Reduction in «offshore work» can reduce the cost.

Remote Inspection Concept

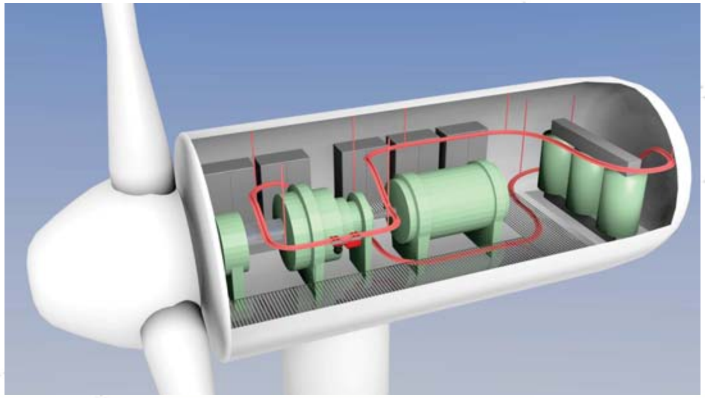

Remote Inspection Prototype

- A prototype has been developed.
- Have been tested in a series of experiments that compare remote and manned inspections.
- Results have shown that with this early prototype, remote inspections have performed almost as good as manned inspections.

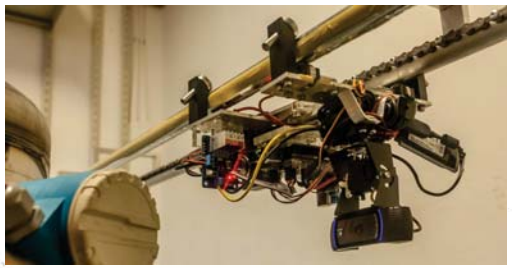

Simulations

- Simulations performed with the NOWIcob tool.
- Wind farm size, possible failures, vessels and maintenance personnel were the same for all simulations.
- Three cases were defined:

	Base	Condition monitoring	Remote inspection
Corrective maintenance	Yes	Yes	Yes
Condition-based maintenance		Yes	Yes
Pre-inspecions	Manned	Manned	Remote
False alarms		Manned	Remote

- Three variants of the remote inspection case were tested:
  1. Five times higher investment cost of the system.
  2. The remote inspection system fails five times as often.
  3. Remote inspection failures cause the turbine to stop.

Condition Monitoring vs Remote Inspection

7

- To rely on corrective maintenance alone, as the base case, is not a viable strategy.
- Remote inspections had better availability than condition monitoring.
- Cost of energy is also better, but due to the additional investment cost and cost of replacement robots the improvement over condition monitoring is smaller than for availability.
- The difference between the two cases are larger for electricity-based availability than time-based.

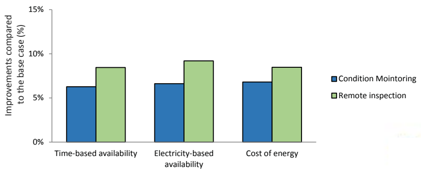

Pessimistic Variants

8

- Five time increase in investment cost or failure rate are highly exaggerated values, thus a large effect is expected.
- The availability is still higher than for condition monitoring, larger effect on the cost of energy.
- It seems as keeping the remote inspection system reliable is important.

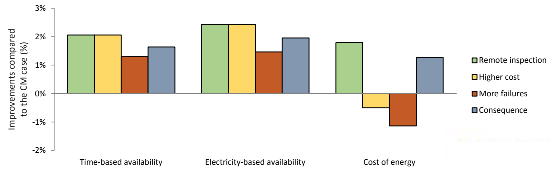

Conclusions

9

- The results show an economic benefit to remote inspections.
- The effect seems robust for the case variants that were tested.

10

Questions?

NTNU
Norwegian University of Science and Technology

NOWITECH
Norwegian Research Centre for Offshore Wind Technology

The effects of using multi-parameter wave criteria for accessing wind turbines in strategic maintenance and logistics models for offshore wind farms

Iver Bakken Sperstad, Elin E Halvorsen-Weare, Matthias Hofmann, Lars Magne Nonås, Magnus Stålhane, MingKang Wu

SINTEF Energy Research

Trondheim, 24 January 2014

Acknowledgements

Elin E Halvorsen-Weare: MARINTEK (Maritime transport systems)
SINTEF Information and Communication Technology
Matthias Hofmann: SINTEF Energy Research
Lars Magne Nonås: MARINTEK (Maritime transport systems)
Magnus Stålhane: MARINTEK (Maritime transport systems)
NTNU, Department of Industrial Economics and Technology Management
MingKang Wu: MARINTEK (Ship Technology)

FAROFF

NOWITECH Norwegian Research Centre for Offshore Wind Technology

Outline

"The effects of using multi-parameter wave criteria for accessing wind turbines in strategic maintenance and logistics models for offshore wind farms"

- Motivation – accessibility
- Multi-parameter wave criteria
- The effects in a strategic maintenance and logistics models
- Conclusions

Motivation – accessibility

Motivation – accessibility

Motivation – accessibility

Traditional access criterion: Limiting significant wave height (Hs)

Low limiting Hs → low accessibility → low availability of the wind turbines

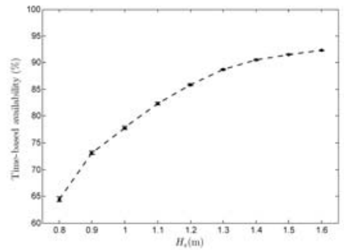

Motivation – accessibility

Traditional access criterion: Limiting significant wave height (Hs)
Low limiting Hs → low accessibility → low availability of the wind turbines

Strategic maintenance and logistics models as decision support tools:
- Wants to know what vessels to use
- Wants to use vessels with high accessibility
- Needs to know the value of the limiting Hs

Is a single limiting Hs good enough?

Other weather parameters:
- Wave period
- Relative wave heading
- Current
- Wind speed
- Wind direction
- Visibility
- Swell
- …

Methodology of the work

1. Numerical analysis to calculate multi-parameter wave criteria (including also wave heading and peak wave period)
2. Estimate possible corresponding measures of a single limiting Hs
3. Compare multi-parameter and single-parameter wave criteria for a simulation model
   - NOWIcob: Simulates maintenance activities and related logistics to estimate O&M costs and analyse O&M strategies
4. Compare multi-parameter and single-parameter wave criteria for a optimisation model
   - Finds the optimal vessel fleet size and mix, minimizing O&M costs

Objective of the work

What question are we asking?
- *Not* how a given vessel performs in absolute terms
- *Not* how the performance of a given vessel compares with the numbers stated for its limiting significant wave height
- *But* what are the effects of using multi-parameter vs single-parameter wave criteria in strategic maintenance and logistics models
  - How can modelling approaches be compared?
  - Does it matter which approach one uses?
  - Is there any added value of more complex modelling?

Numerical analysis to calculate wave criteria

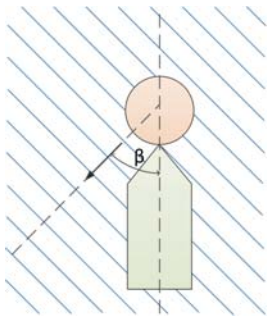

- Crew transfer vessel with bow fender
- Wave conditions:
  - Significant wave height
  - Peak wave period
  - Relative wave heading
- Also modelled: Motion-compensated gangway

Multi-parameter wave criteria

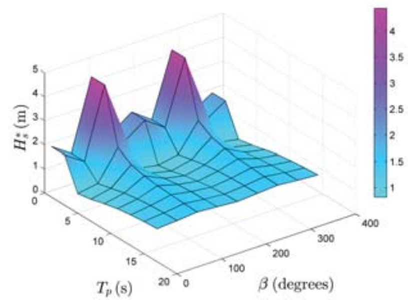

Corresponding single-parameter wave criteria

Possible measures of a single limiting significant wave height:

a) Weighted average
b) Most probable wave conditions
c) Most typical wave conditions
d) Equal average accessibility
e) Most restrictive/limiting value

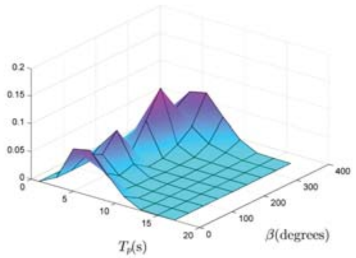

Corresponding single-parameter wave criteria

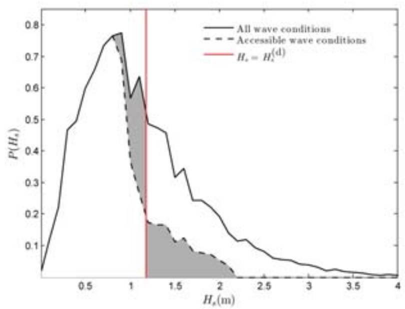

Corresponding single-parameter wave criteria

Possible measures of a single limiting significant wave height:

a) Weighted average
b) Most probable wave conditions
c) Most typical wave conditions
d) Equal average accessibility
e) Most restrictive/limiting value

Corresponding single-parameter wave criteria

Possible measures of a single limiting significant wave height:

a) Weighted average	1.513 m
b) Most probable wave conditions	1.11 m
c) Most typical wave conditions	1.030 m
d) Equal average accessibility	1.160 m
e) Most restrictive/limiting value	0.82 m

Reference case for simulation and optimisation models

- Weather time series with wind speed, peak wave period, wave heading and relative wave height
- Wind farm with 80 turbines 50 km from onshore maintenance base
- Corresponding single-parameter wave criteria
- Vessel fleet fixed to 3 crew transfer vessels for simulation model
- Optimisation model finds the optimal vessel fleet

Comparison for the simulation model – availability

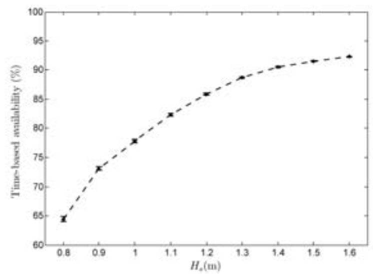

Comparison for the simulation model – availability

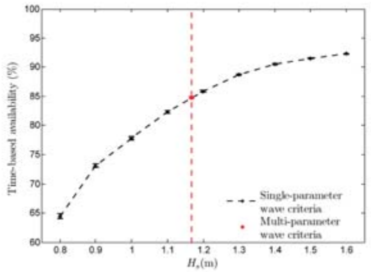

Comparison for the simulation model – availability

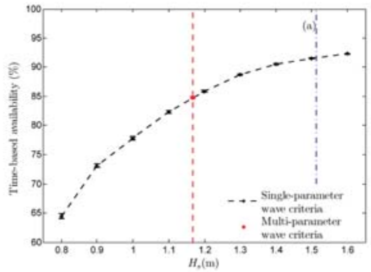

Comparison for the simulation model – availability

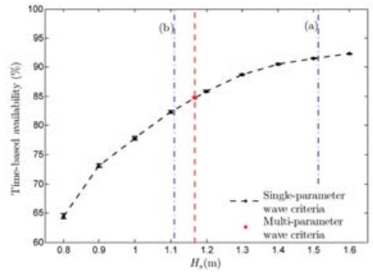

Comparison for the simulation model – availability

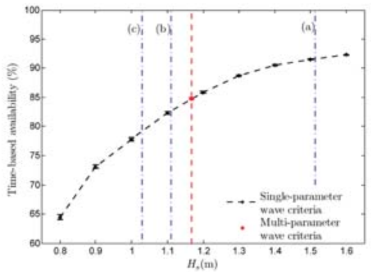

Comparison for the simulation model – availability

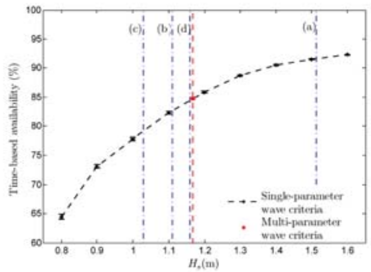

Comparison for the simulation model – availability

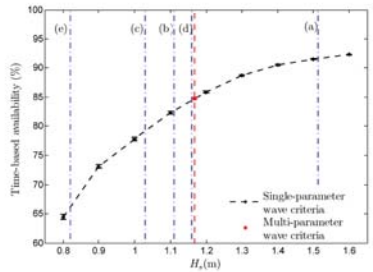

Corresponding single-parameter wave criteria

Possible measures of a single limiting significant wave height:

a) Weighted average 1.513 m
b) Most probable wave conditions 1.11 m
c) Most typical wave conditions 1.030 m
d) Equal average accessibility 1.160 m
e) Most restrictive/limiting value 0.82 m

Corresponding single-parameter wave criteria

Possible measures of a single limiting significant wave height:

a) Weighted average 1.5 m
b) Most probable wave conditions 1.1 m
c) Most typical wave conditions 1.0 m
d) Equal average accessibility 1.2 m
e) Most restrictive/limiting value 0.8 m

Comparison for the simulation model – availability

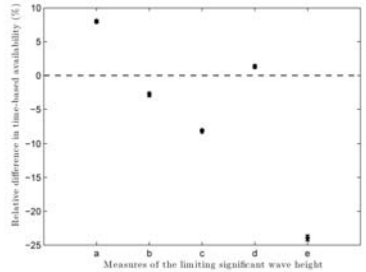

Comparison for the simulation model – O&M costs

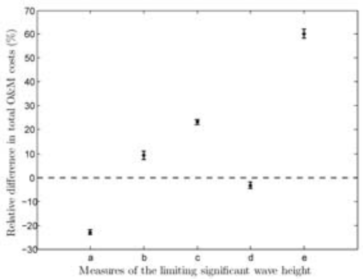

Comparison for the optimisation model

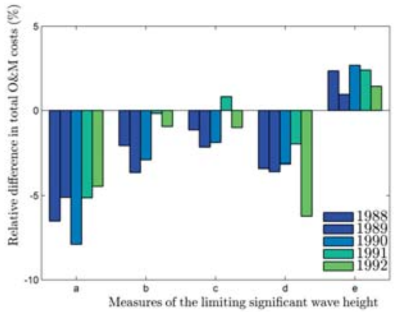

Conclusions

- Demonstrated how one may use multi-parameter weather criteria in comparing vessel concepts with strategic maintenance and logistics models
- The difference between multi-parameter and single-parameter wave criteria may be relatively small
- This requires that the single limiting Hs is chosen carefully
- Information from multi-parameter wave criteria and wave conditions useful

- If a single limiting Hs can be used to represent the wave criteria, how is it found?
- Would a single limiting Hs apply for all locations?

SINTEF

Technology for a better society

E1) Installation and sub-structures

Experimental Studies and numerical Modelling of structural Behavior of a Scaled Modular TLP Structure for Offshore Wind turbines, Frank Adam, GICON

Tension-Leg-Buoy Platforms for Offshore Wind Turbines, Tor Anders Nygaard, IFE

A preliminary comparison on the dynamics of a floating vertical axis wind turbine on three different floating support structures, Michael Borg, Cranfield University

Modelling challenges in simulating the coupled motion of a semi-submersible floating vertical axis wind turbine, R. Antonutti, EDF R&D – IDCORE

Tension-Leg-Buoy (TLB) Platforms for Offshore Wind Turbines

EERA DeepWind'2014 Deep Sea Offshore Wind R&D Conference, Trondheim, 22 - 24 January 2014


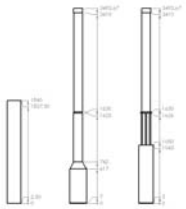


Tor Anders Nygaard, Institute for Energy Technology (IFE), Norway
Anders Myhr, NMBU(UMB)

Outline

- Introduction: Life Cycle Greenhouse Gas (GHG) emissions and cost drivers for offshore wind turbine platforms
- The simulation tool 3DFloat for analysis and optimization
- TLB application example, 75m water depth
- MARINET wave tank test at IFREMER, Brest, France, January 2013, and comparison with simulations
- Conclusions and outlook

GHG emissons per kWh

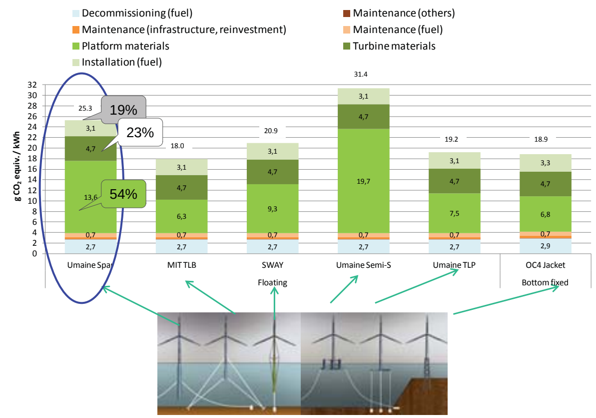

Raadal, H. L., Vold, B. I., Myhr, A. and Nygaard, T. A. (2014). GHG emissions and energy performance of offshore wind power. Renewable Energy, 2014, Vol. 66, 314-324

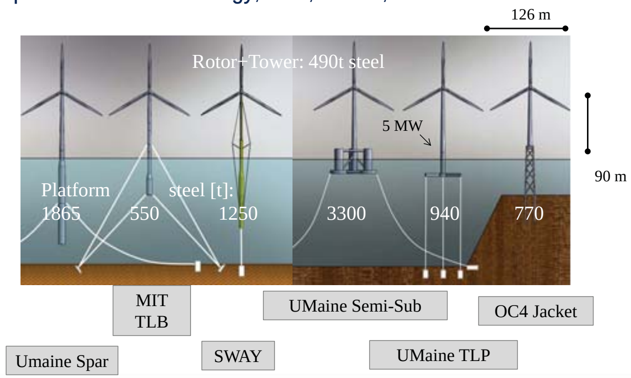

3DFloat Simulation Tool

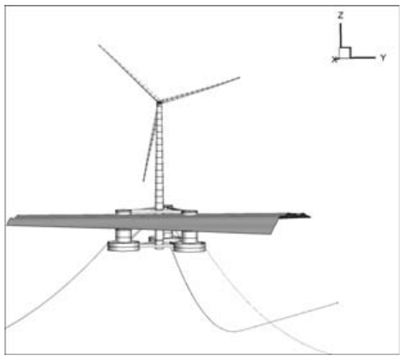

- General nonlinear Finite-Element Model
- Engineering models for aerodynamics, hydro-dynamics and control systems
- Verified (code-to-code) for Spar-Buoy, Jacket and Semi-Submersible (IEA OC3/OC4)
- Validation against experiments ongoing for Tension-Leg-Buoy and Semisubmersible platforms (MARINET)

TLB History

- First application presented by Prof. Sclavounos, MIT in 2005 as the MIT Double Taut Leg.
- The TLB has been developed at MIT in a commercial project.
- The TLB has been used for optimization studies and experiments at UMB.

Butterfield, S, Musial, W, Jonkman, J and Sclavounos, P (2005)."Engineering Challenges for Floating Offshore Wind Turbines". *Proc 2005 Copenhagen Offshore Wind Conference*, Copenhagen, Denmark, October 26–28, 2005

TLB Application Example

- NREL 5MW 126m rotor, hub height 90m
- Draft 50m, water depth 75m
- Mooring line axial stiffness governed by eigen frequencies
- Buoyancy governed by requirement on taut mooring lines
- Survival: 30m wave height, parked rotor fully exposed to steady wind wind of 62m/s.
- Deplacement 3000t, Excess buoyancy 1900E4 N
- Anchor uplift peak: 1800E4 N
- Steel mass: Floater 455t, Tower/nacelle 666t, Anchors 190t

Myhr, A. and Nygaard, T. A. (2012). *Load Reductions and Optimizations on Tension-Leg-Buoy Offshore Wind Turbine Platforms.* International Offshore and Polar Engineering Conference (ISOPE), 2012.

MARINET: Marine Renewables Infrastructure Network for Emerging Energy Technologies

http://www.fp7-marinet.eu/

- Co-financed by the EC, MARINET offers periods of free-of-charge access to world-class R&D facilities and conducts joint activities in parallel to standardise testing, improve testing capabilities and enhance training and networking.

IFREMER Deep Sea Water Wave Tank, Brest, France

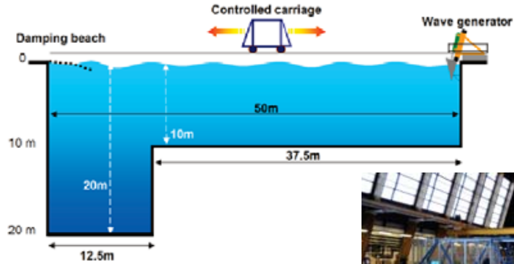

Platforms, scale 1:40

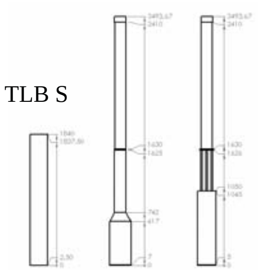

Mooring system

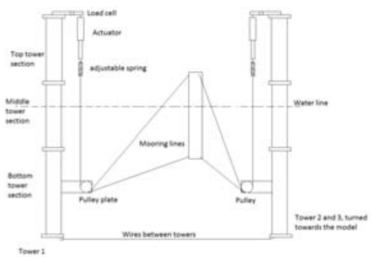

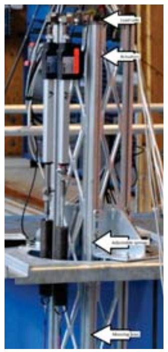

Load cases (presented in full scale)

- Decay tests: Heave,Surge/Pitch
- Regular waves: 10 cases
  1. Periods 6s – 16s
  2. Wave heights 6m – 20m
- Irregular waves: 3 cases

	Hs	Tp	Gamma
1	11.2	19.2	1.05
2	5.2	10	2.87
3	11.2	16	2.9

Heave Decay Test Results, Model Scale

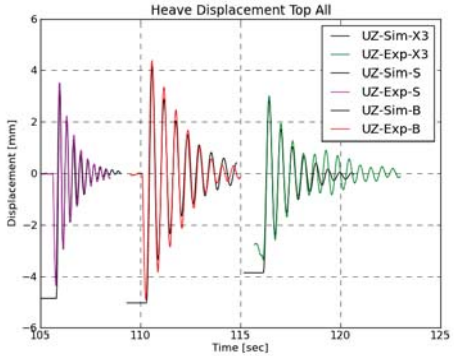

Matches first part of decay well

X3 experiment disturbed by other mode

Heave eigen frequencies are 2.9, 1.7 and 1.7 Hz for S, B and X3 respectively

Pitch/Surge Decay Test, Model Scale

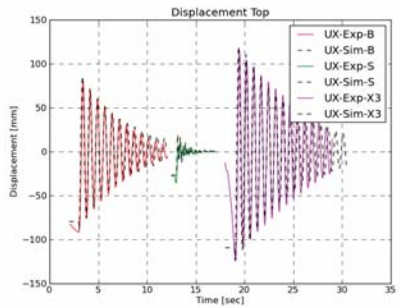

Period of S and B are OK

X3 period 3% longer in computation

Damping matches well
For B and X3.

Damping in experiment for S is erratic and difficult to interpret

Pitch/Surge eigen frequencies are 2.34, 1.35 and 1.35 Hz for S, B and X3 respectively

LC9, Regular Waves: H = 5.2m, T = 10s in Full Scale
Sensitivity Study on Added Mass, Cm = 1.6 – 2.0

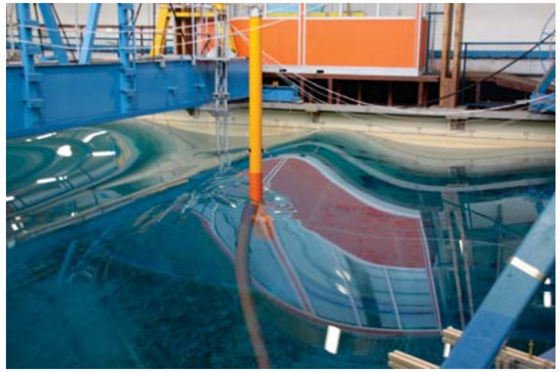

Tower Top Pitch Angle

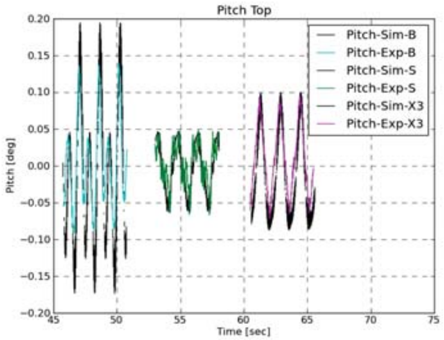

- Good agreement despite small angles
- TLB B (left) responds both at wave frequency, and twice the wave frequency (close to pitch/surge eigen frequency).

Tower Top Displacements

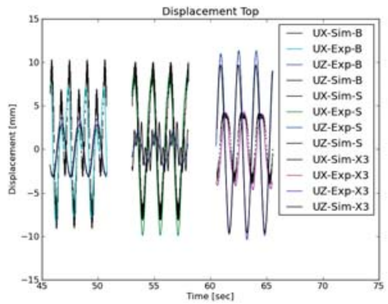

Good agreement, except for TLB S in heave (middle of figure):
Experiment (Blue): First order response.
Computations (Black): Also component 5x wave frequency, close to heave eigen frequency.

Heave resonant response found in the experiment, start of LC 26

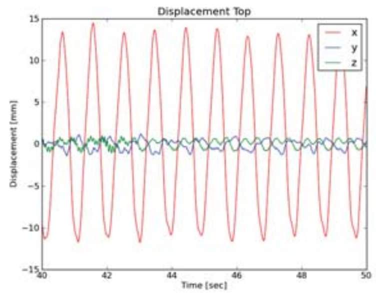

Vertical component at heave eigen frequency is damped out.

One possible explanation is the friction in the pulleys in the experiment. The friction hystereis in the mooring lines was measured to be 1N, at a mooring line tension of 200N

Lower Mooring Lines Tension

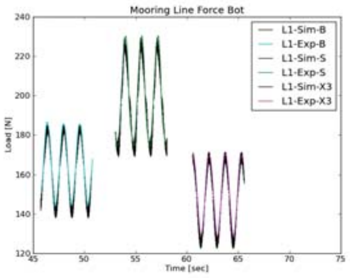

Good agreement

30.01.2014

Upper Mooring Lines Tension

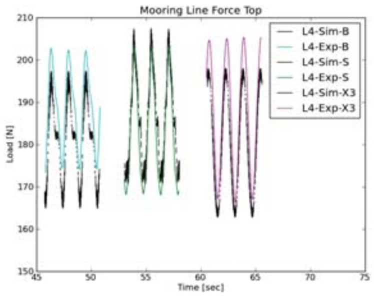

Mean tension offsets, but amplitudes match well

30.01.2014

Irregular(lines) and regular (dots) Wave Cases, Tower Top Horizontal Displacement RAOs, Model Scale

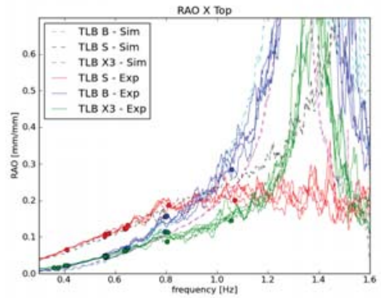

Good agreement for B

Higher response towards resonance for S and X3 in computations

Results in region above 1 Hz are sensitive to friction

30.01.2014

Conclusions, experiment

- Time series for decay tests, regular- and irregular wave cases have been measured for three different 1:40 scale models of Tension-Leg-Buoys.
- Preliminary computations show good agreements for the regular load cases, except heave resonant response for TLB S in the simulation.
- The irrgular wave cases show good agreement for low frequencies, and significant differences for frequencies around pitch/surge and heave resonance
- The differnces between experiment and simulation may be due to friction in the pulleys in the experiment
- The X3 space-frame reduced anchor loads 10 %, not enough to justify the increased complexity of this floater.

30.01.2014

Conclusions, experiment, outlook

- Next step: We are currently implementing node hysteresis damping in 3DFloat, to take into account the friction in the pulleys in the experiment
- The data set should be of interest for validation of computational tools for offshore wind turbines. The raw time series will be open after our publication of the results.

30.01.2014

Outlook for TLB

- Next step is better modeling of the anchors in different types of soil
- IFE and the Norwegian Geotechnical Institute (NGI) has just started discussions about implementation of anchor «super-elements» in 3DFloat
- The TLB is a candidate for filling the gap between bottom-fixed foundations (up to 50m depth) and the Spar-Buoy (100m and deeper), at sites with restrictions on footprint and adequate soil conditions

30.01.2014

Acknowledgements

- EU FP7 MARINET funded wave tank time, on-site support and part of the travel costs
- NOWITECH/IFE funded direct costs for building the test equipment
- UMB funded parts of the test equipment
- Thanks to the staff at IFREMER for two interesting, intensive and fun weeks.

30.01.2014

Thank you for your attention !

30.01.2014

Extra slides

30.01.2014

Summary, GHG emissions

- For the six conceptual design examples in the study, the resulting GHG emissions are in the range18 - 31g CO2-equivalents per kWh.
- To put this in perspective: Coal is around 1000g/kWh
- The Energy Payback Time is in the range 1.6 to 2.7 years
- Major drivers are substructure (steel) mass, installation/decommisioning and maintenance
- For a large-scale deployment of offshore wind turbines, substructures with low steel mass should be of interest

30.01.2014

Tension-Leg-Buoy, IFREMER, Brest

- Platforms: (rotor represented by clump mass), 1:40, intended to support NREL 5MW rotor in full scale
  1. Simple straight tubular floater («Simple»)
  2. Baseline floater including conical section («TLB B»)
  3. Load reduction by transparent structure in the wave action zone («X3»)
- Load cases
  1. Decay tests
  2. Regular waves
  3. Irregular waves
- Sensors
  1. Wave elevation, front and side of model
  2. Mooring line tension
  3. Motion of platform

30.01.2014

Coefficients for computations

1. Morison normal drag coefficient of 1.0 chosen from KC and Re (Sarpkaya experiments)
2. Morison axial drag coefficient set to 0.5 for bottom end cap, and 0.5 for top end cap (X3).
3. Morison axial and normal added mass chosen to match heave and pitch/surge eigen periods respectively
4. Structural damping in the mooring lines and horizontal and vertical linear damping chosen to match the decay in the free-decay tests

30.01.2014

Documentation of results

- Design and fabrication of equipment: Master Thesis of Anders Spæren, UMB (in Norwegian).
- Experiment and model geometry: Journal article by PhD candidate Anders Myhr and Tor Anders Nygaard (supervisor). Ongoing internal review
- Experiment and comparisons with 3DFloat computations: Journal article by PhD candidate Anders Myhr and Tor Anders Nygaard. Ongoing internal review
- Time series of results will be available after publication of the articles

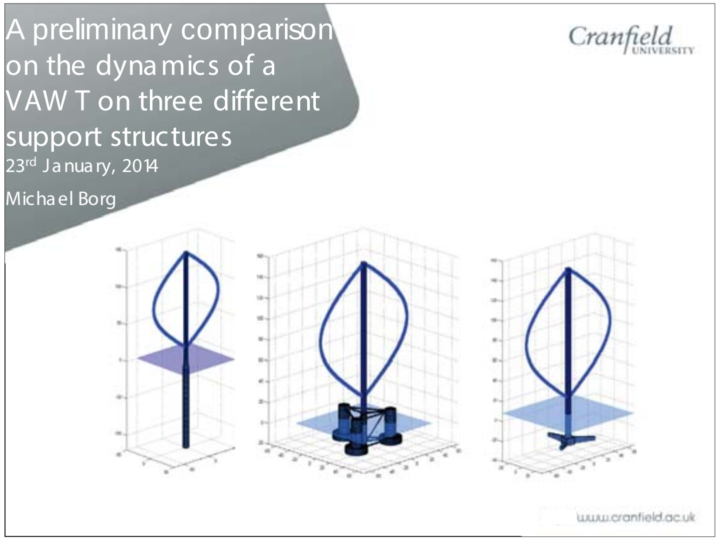
A preliminary comparison on the dynamics of a VAWT on three different support structures
23rd January, 2014
Michael Borg
Cranfield UNIVERSITY
www.cranfield.ac.uk

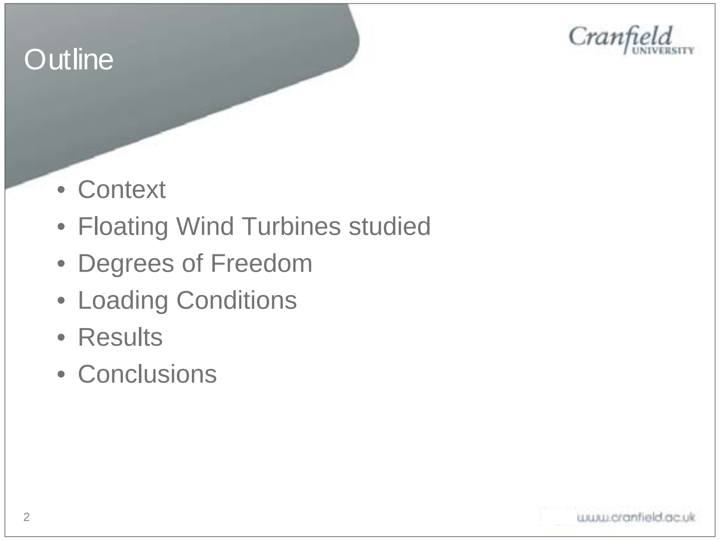
Outline
Cranfield UNIVERSITY
• Context
• Floating Wind Turbines studied
• Degrees of Freedom
• Loading Conditions
• Results
• Conclusions
2
www.cranfield.ac.uk

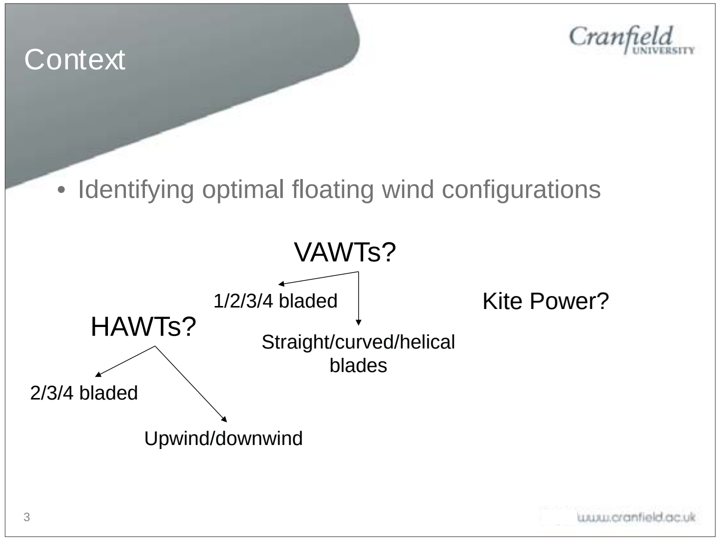
Context
Cranfield UNIVERSITY
• Identifying optimal floating wind configurations
VAWTs?
1/2/3/4 bladed
Straight/curved/helical blades
Kite Power?
HAWTs?
2/3/4 bladed
Upwind/downwind
3
www.cranfield.ac.uk

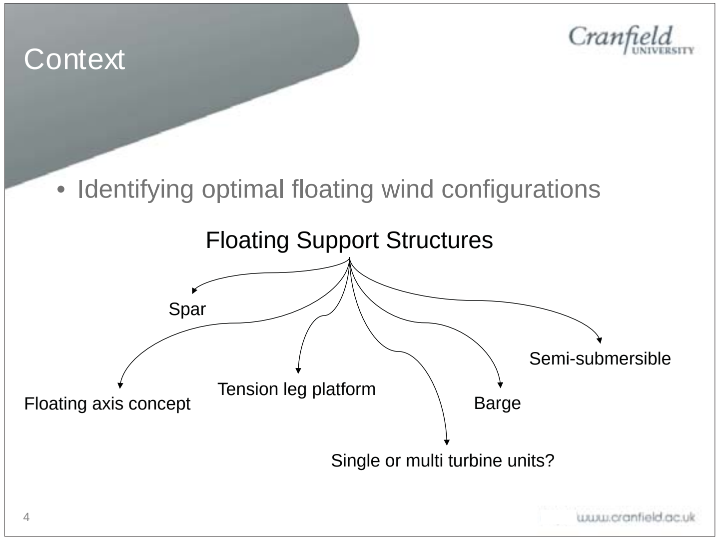
Context
Cranfield UNIVERSITY
• Identifying optimal floating wind configurations
Floating Support Structures
Spar
Semi-submersible
Floating axis concept
Tension leg platform
Barge
Single or multi turbine units?
4
www.cranfield.ac.uk

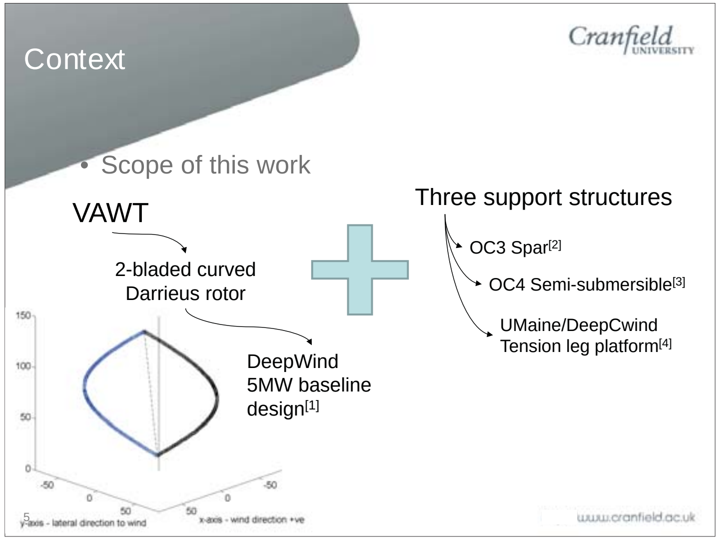
Context
Cranfield UNIVERSITY
• Scope of this work
VAWT
2-bladed curved Darrieus rotor
DeepWind 5MW baseline design[1]
Three support structures
OC3 Spar[2]
OC4 Semi-submersible[3]
UMaine/DeepCwind Tension leg platform[4]
y-axis - lateral direction to wind
x-axis - wind direction +ve
5
www.cranfield.ac.uk

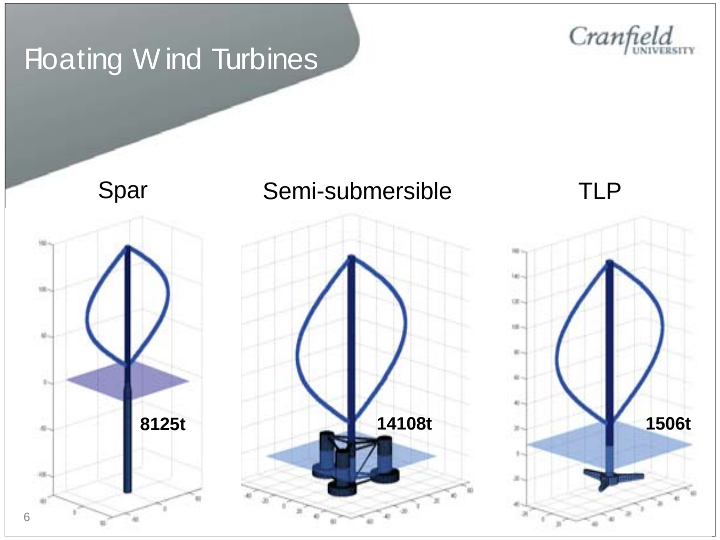
Floating Wind Turbines
Cranfield UNIVERSITY
Spar
Semi-submersible
TLP
8125t
14108t
1506t
6

Numerical Tool

Cranfield UNIVERSITY

- FloVAWT in development at Cranfield University

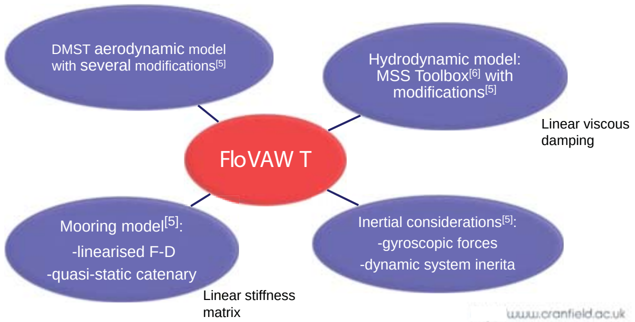

Degrees of Freedom Issues

Cranfield UNIVERSITY

- Aerodynamic forces excitation of platform
- HAWT: relatively steady thrust + torque in roll
- VAWT: oscillatory surge, sway, roll, pitch, yaw loads

Degrees of Freedom Issues

Cranfield UNIVERSITY

- Spar
  - Mooring system yaw stiffness
    - Not sufficient→ Yaw DOF disabled

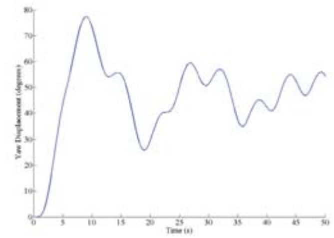

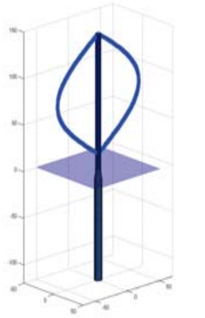

Degrees of Freedom Issues

Cranfield UNIVERSITY

- TLP
  - Mooring system surge/sway stiffness
    - Unstable behaviour
      →surge & sway disabled

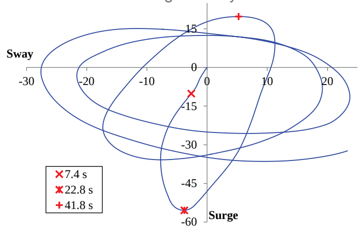

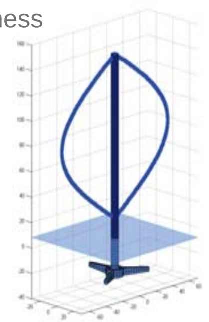

Degrees of Freedom Issues

Cranfield UNIVERSITY

- Semi-submersible
  - No problems!

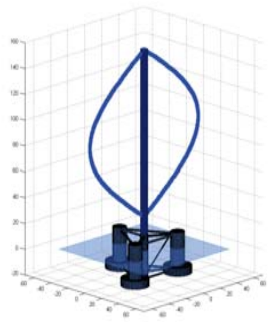

Load Cases

Cranfield UNIVERSITY

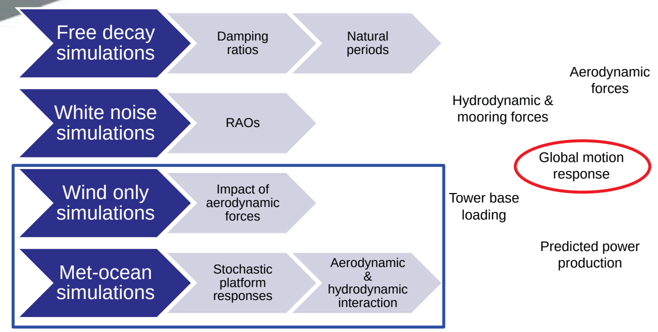

Load Cases 3 & 4

Cranfield UNIVERSITY

Load Case	Wind Speed (m/s)	Hs (m)/Tp (s), LC4
x.1	5 (BR)	2.1/9.74
x.2	9 (BR)	2.88/9.98
x.3	14 (R)	3.62/10.29
x.4	18 (AR)	5.32/11.06
x.5	25 (AR)	6.02/11.38

Results
Wind Only

Cranfield UNIVERSITY

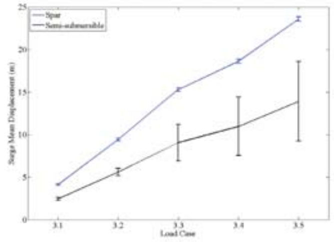

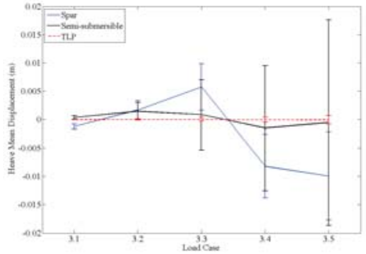

Results Wind Only

Cranfield UNIVERSITY

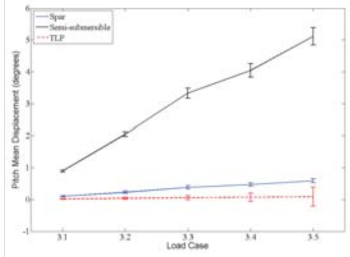

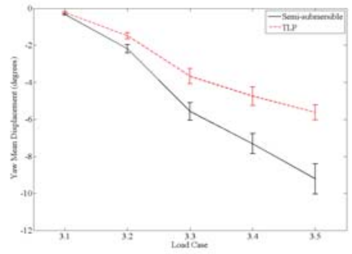

Results
Met-ocean

Cranfield UNIVERSITY

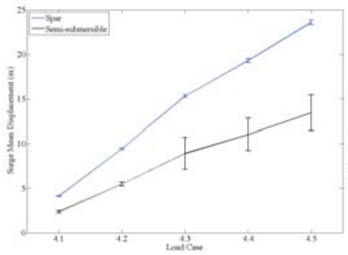

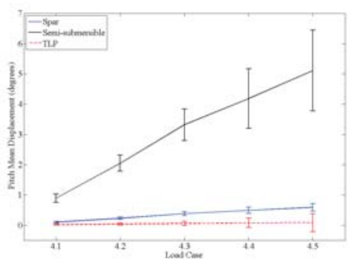

Results
Wind Only vs. Met-ocean

Cranfield UNIVERSITY

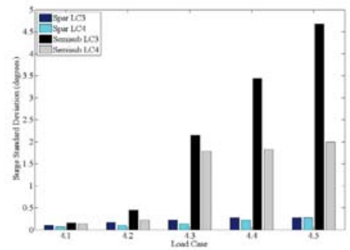

Results
Wind Only vs. Met-ocean

Cranfield UNIVERSITY

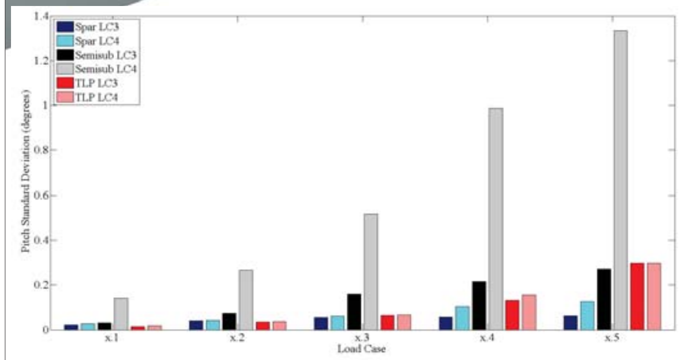

Conclusions

- Three floating VAWT configurations
- Differences in mooring systems required HAWT vs. VAWT
- Wind-only & met-ocean responses

FUTURE WORK

- Frequency response analyses
- More expansive load cases
- Use DeepWind optimised design

Thank you for attention

Questions?

References

[1] Vita, L. (2011), *Offshore floating vertical axis wind turbines with rotating platform (Ph.D. thesis), Technical University of Denmark, Roskilde, Denmark.*

[2] Jonkman, J. and Musial, W. (2010), *Offshore Code Comparison (OC3) for IEA Task 23 Offshore Wind Technology and Deployment, NREL/TP-5000-48191, NREL, Colorado*

[3] Robertson, A., Jonkman, J., Musial, W., Vorpahl, F. and Popko, W. (2013), "Offshore Code Comparison Collaboration, Continuation: Phase II Results of a Floating Semisubmersible Wind System", *EWEA Offshore 2013, 19-21 November, 2013, Frankfurt, Germany.*

[4] Stewart, G. M., Lackner, M., Robertson, A., Jonkman, J. and Goupee, A. J. (2012), "Calibration and Validation of a FAST Floating Wind Turbine Model of the DeepCwind Scaled Tension-Leg Platform", *22nd International Offshore and Polar Engineering Conference, 17-22 June, 2012, Rhodes, Greece, ISOPE*

[5] Collu, M., Borg, M., Shires, A., Rizzo, N. F. and Lupi, E. (2014), "Further progresses on the development of a coupled model of dynamics for floating offshore VAWTs", *ASME 33rd International Conference on Ocean, Offshore and Arctic Engineering, 8-13 June 2014, San Francisco, USA.*

[6] Fossen, T. I. and Perez, T. , *MSS. Marine Systems Simulator (2010), available at: http://www.marinecontrol.org*

VAWT Definition

Rotor height, root-to-root (m)	129.56
Rotor radius (m)	63.74
Chord (m)	7.45
Airfoil section	NACA0018
Total mass, including tower and generator (kg)	844226
Centre of gravity, from tower base (m)	67.4
Rated power (MW)	5.0
Rated wind speed at 79.78m above MSL (m/s)	14
Rated rotational speed (rpm)	5.26

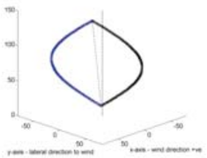

FOWT Definitions

	Spar	Semi-sub	TLP
Draft, from keel (m)	120	20	30
Mass (tonnes)	8125.2	14108	1505.8
Centre of Gravity (CG), from keel (m)	45.37	11.07	64.1
Radius of gyration about CG , roll (m)	30.11	30.59	66.88
Radius of gyration about CG, pitch (m)	29.01	29.97	64.13
Radius of gyration about CG, yaw (m)	8.83	29.91	19.85

Load Cases

		Initial conditions			Simulation Length (s)			Time step (s)
		Spar	Semi-sub	TLP	Spar	Semi-sub	TLP	
LC1.1	Surge	+12m	+12m	N/A	1200	1200	N/A	0.1
LC1.2	Heave	+6m	+6m	+0.35m	150	150	50	0.1
LC1.3	Pitch	+5deg	+8deg	+0.5deg	300	300	50	0.1
LC1.4	Yaw	N/A	+8deg	+15deg	N/A	900	200	0.1

	No.of wave components	Length (s)	Time step (s)
LC2.1	800	3600	0.1

MODELLING CHALLENGES IN SIMULATING THE COUPLED MOTION OF A SEMI-SUBMERSIBLE FLOATING VAWT

Raffaello Antonutti (EDF R&D – IDCORE)
Christophe Peyrard (EDF R&D)
Nicolas Relun (EDF R&D)

EERA DeepWind'2014, 11th Deep Sea Offshore Wind R&D Conference, 22-24 January 2014, Trondheim, Norway

SUMMARY

- The VertiWind project
- Coupled dynamic simulation methodology
- Viscous damping modelling study
- Coupled hydro-aerodynamic study
- Conclusions
- Future work

THE VERTIWIND PROJECT

CONTEXT

- Onshore reduced scale turbine model
- VertiFloat: Onshore full scale turbine prototype
- VertiWind: Offshore full scale turbine prototype
- INFLOW: Design optimisation & supply chain
- VertiMED: 26 MW floating offshore windfarm

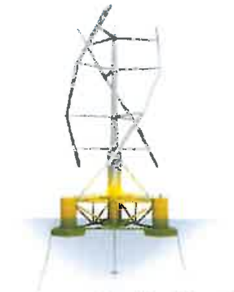

© EDF EN / Technip / Nenuphar

THE VERTIWIND PROJECT

PARTNERS AND FUNDING

Project partners:

- **Technip**
  Project leader. Substructure, mooring and installation design + procurement
- **Nénuphar**
  VAWT design + procurement
- **EDF EN**
  Pilot site utility client. Definition of maintenance strategy
- Seal Engineering
- Bureau Veritas
- Oceanide
- IFP EN
- Arts & Métiers
- USTV

Governmental funding:

ADEME
Agence de l'environnement et de la maîtrise de l'énergie
(Agency for the environment and management of energy)

THE VERTIWIND PROJECT

TECHNOLOGY

- Bespoke VAWT design
- Direct drive 2MW permanent magnet generator
- Column-stabilised semisubmersible platform
- Catenary moorings

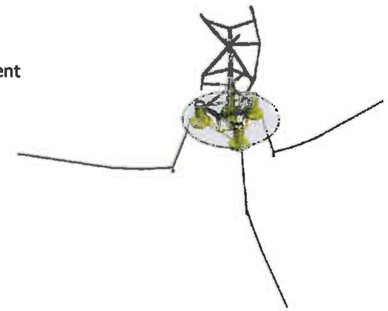

© EDF EN / Technip / Nenuphar

COUPLED DYNAMIC SIMULATION METHODOLOGY

GENERAL

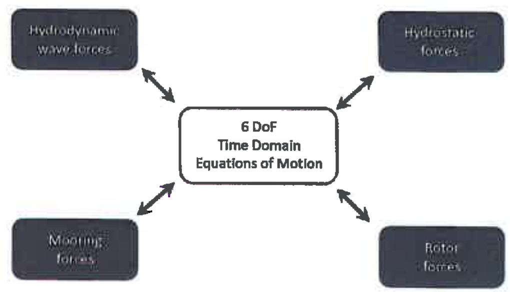

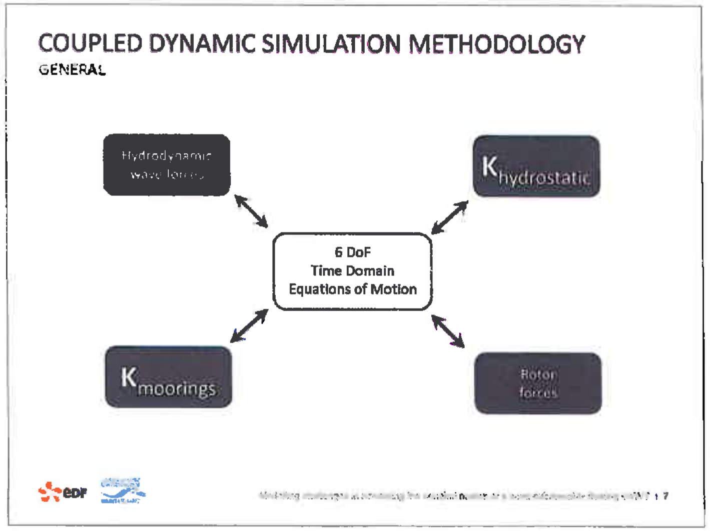
COUPLED DYNAMIC SIMULATION METHODOLOGY
GENERAL
Hydrodynamic wave forces
K hydrostatic
6 DoF
Time Domain
Equations of Motion
K moorings
Rotor forces
EDF

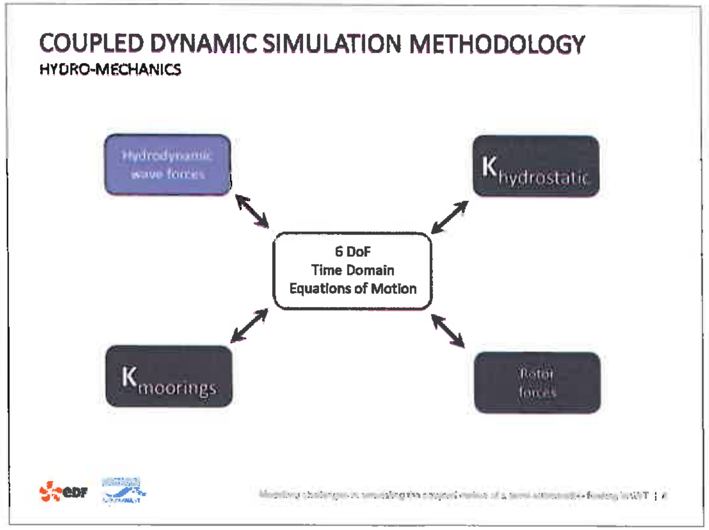
COUPLED DYNAMIC SIMULATION METHODOLOGY
HYDRO-MECHANICS
Hydrodynamic wave forces
K hydrostatic
6 DoF
Time Domain
Equations of Motion
K moorings
Rotor forces
EDF

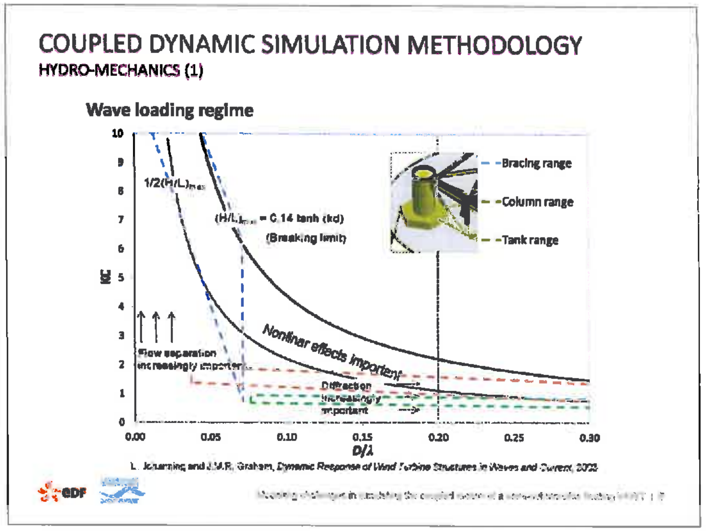
COUPLED DYNAMIC SIMULATION METHODOLOGY
HYDRO-MECHANICS (1)
Wave loading regime
Bracing range
Column range
Tank range
(Breaking limit)
Nonlinear effects important
Flow separation
Diffraction
D/λ
EDF

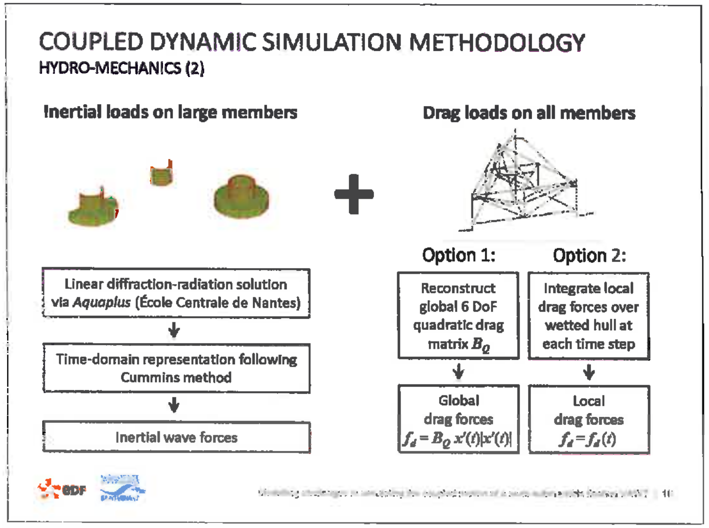
COUPLED DYNAMIC SIMULATION METHODOLOGY
HYDRO-MECHANICS (2)
Inertial loads on large members
Drag loads on all members
Linear diffraction-radiation solution via Aquaplus (École Centrale de Nantes)
Time-domain representation following Cummins method
Inertial wave forces
Option 1:
Reconstruct global 6 DoF quadratic drag matrix B_Q
Global drag forces $f_d = B_Q\,x'(t)|x'(t)|$
Option 2:
Integrate local drag forces over wetted hull at each time step
Local drag forces $f_d = f_d(t)$
EDF

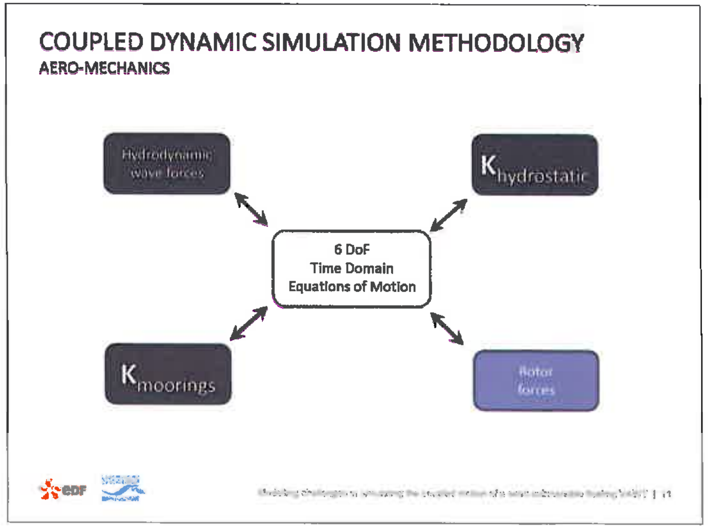
COUPLED DYNAMIC SIMULATION METHODOLOGY
AERO-MECHANICS
Hydrodynamic wave forces
K hydrostatic
6 DoF
Time Domain
Equations of Motion
K moorings
Rotor forces
EDF

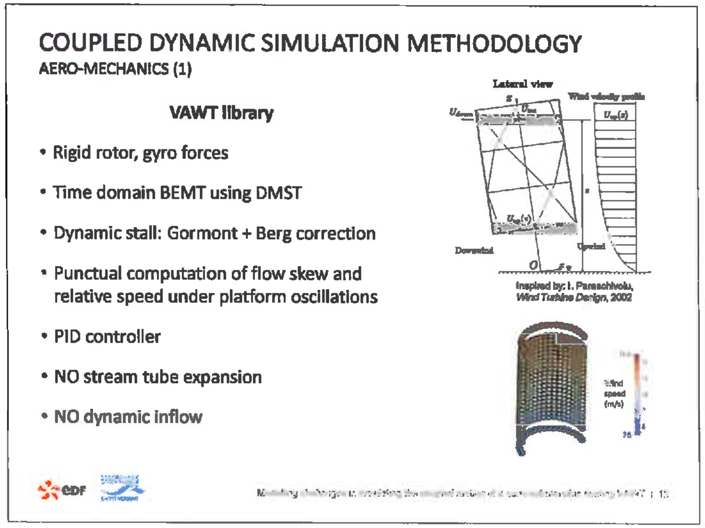
COUPLED DYNAMIC SIMULATION METHODOLOGY
AERO-MECHANICS (1)
VAWT library
Rigid rotor, gyro forces
Time domain BEMT using DMST
Dynamic stall: Gormont + Berg correction
Punctual computation of flow skew and relative speed under platform oscillations
PID controller
NO stream tube expansion
NO dynamic inflow
Lateral view
Wind velocity profile
Downwind
Upwind
Inspired by: I. Paraschivoiu, Wind Turbine Design, 2002
EDF

COUPLED DYNAMIC SIMULATION METHODOLOGY
AERO-MECHANICS (2)

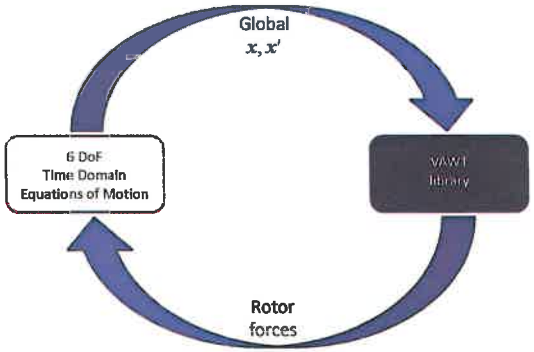

VISCOUS DAMPING MODELLING STUDY
MODELLING OPTIONS

a) Quadratic viscous damping matrix B_Q

$$f_d = B_Q\, x'(t)\, |x'(t)|$$

b) Integration of drag forces over wet hull

$$f_d = \sum_{n=1}^{N_{cylinder}} \int_{Span} \tilde{f}_{cyl}\, ds + \sum_{n=1}^{N_{plate}} f_{plate}$$

Using relative flow speed with linear wave kinematics

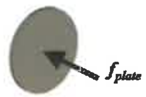

VISCOUS DAMPING MODELLING STUDY
SIMULATION RESULTS (PARKED ROTOR)

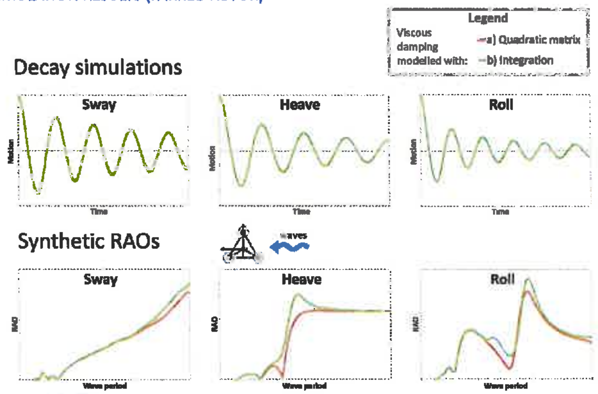

COUPLED HYDRO-AERODYNAMIC STUDY
ENVIRONMENTAL/OPERATIONAL CONDITIONS (1)

a) **Waves + standstill**
V_w = 0 m/s
Turbine parked

b) **Waves + spinning (reference case)**
V_w = 0 m/s
Turbine spinning at same speed as c) and d)

c) **Waves + collinear wind**
V_w = 80% cut-out wind speed
Turbine operating at prescribed speed

d) **Waves + cross wind**
V_w = 80% cut-out wind speed
Turbine operating at prescribed speed

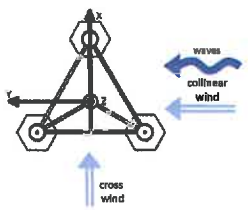

COUPLED HYDRO-AERODYNAMIC STUDY
ENVIRONMENTAL/OPERATIONAL CONDITIONS (2)

a) **Waves + standstill**
V_w = 0 m/s
Turbine parked
} Blade Element Theory only

b) **Waves + spinning (reference case)**
V_w = 0 m/s
Turbine spinning at same speed as c) and d)
} BEMT, TSR → ∞

c) **Waves + collinear wind**
V_w = 80% cut-out wind speed
Turbine operating at prescribed speed
} BEMT, Low TSR

d) **Waves + cross wind**
V_w = 80% cut-out wind speed
Turbine operating at prescribed speed
} BEMT, Low TSR

COUPLED HYDRO-AERODYNAMIC STUDY
SIMULATION RESULTS

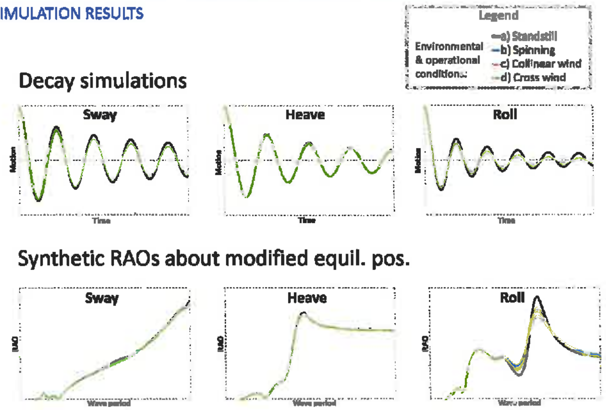

CONCLUSIONS

Viscous hydro damping

Global quadratic matrix representation $\boldsymbol{B}_Q$:

- fits well experimental decay tests BUT
- does not explain extra motion response in resonance band

⇩

integration of drag forces over wetted hull allows to include viscous excitation

Aero-hydrodynamic coupling

Operating VAWT rotor provides aerodynamic damping:

- significant for roll & pitch
- function of TSR
- relatively insensitive to wind direction relative to motion

FUTURE WORK

- Further improvements of BEMT solver (including validation)
- Turbulent, unsteady wind input
- Rotor elasticity
- Nonlinear hydrostatics
- Nonlinear potential hydrodynamics
- Dynamic moorings model

ACKNOWLEDGEMENTS

Supervision:

Prof. David Ingram (Uni. Edinburgh)

Prof. Atilla Incecik (Uni. Strathclyde)

Dr. Lars Johanning (Uni. Exeter)

Funding:

energy technologies institute

ADEME

E2) Installation and sub-structures

Offshore wind R&D at NREL, Senu Sirnivas, NREL

Ringing and impulsive excitation of offshore wind turbines from steep and breaking waves on intermediate depth. Results from the Wave Loads project, Henrik Bredmose, DTU Wind Energy

Damping of wind turbine tower vibrations by means of stroke amplifying brace concepts, Mark Brodersen, DTU

NREL

DOE Advanced Technology Demonstration Projects

Deepwind 2014

Senu Sirnivas

January 23, 2014

NREL is a national laboratory of the U.S. Department of Energy, Office of Energy Efficiency and Renewable Energy, operated by the Alliance for Sustainable Energy, LLC.

Outline

- **DOE**
  - o Objectives
  - o Offshore wind demonstration projects
- **Overview - 7 projects**
  - o 4 fixed foundation
  - o 3 floating foundation

20% Wind Energy (54-GW from Offshore)

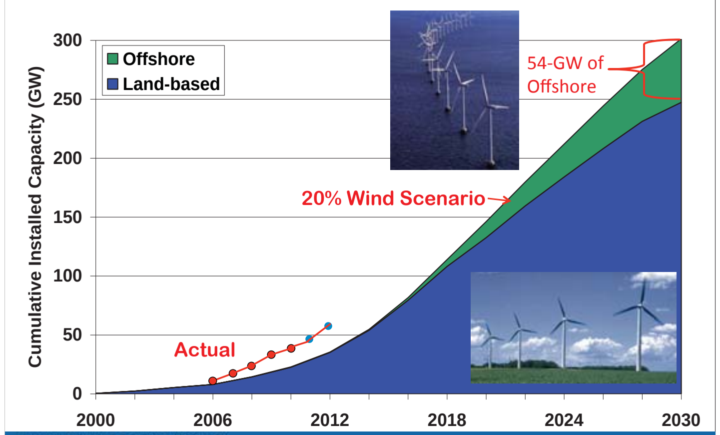

DOE FOA 410

Demonstrate Next Generation Technology

Advanced Technology Demonstration Projects

$168M DOE 5 Years

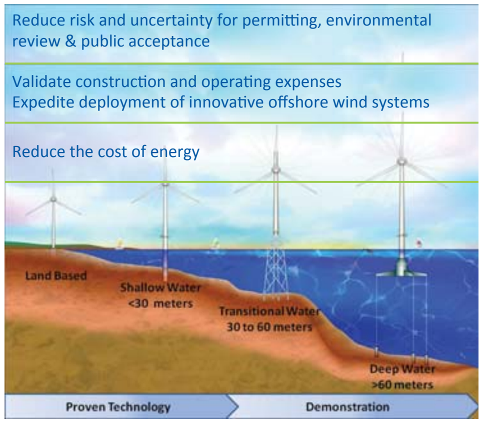

DOE FOA 410

2012
- DOE 410 funding opportunity
- Many applicants (~ 30)
- 12 selected for oral presentation

2013
- 7 projects awarded
- $1M applicant + $4M DOE per project
- Develop 50% FEED

2014 - 2018
- Down select to 3 projects
- $47M applicant + $47M DOE per project
- 100% FEED, fabrication, and deployment

Offshore Wind Potential (Over 4000GW)

No Projects have yet been installed in The United States

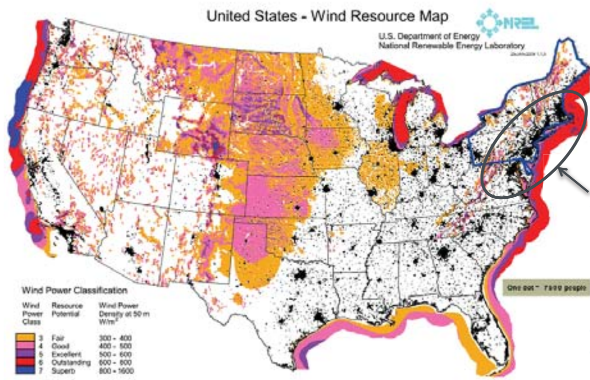

55 million people in NE

18% of US population

Highest electricity costs

Regional Technology Barriers

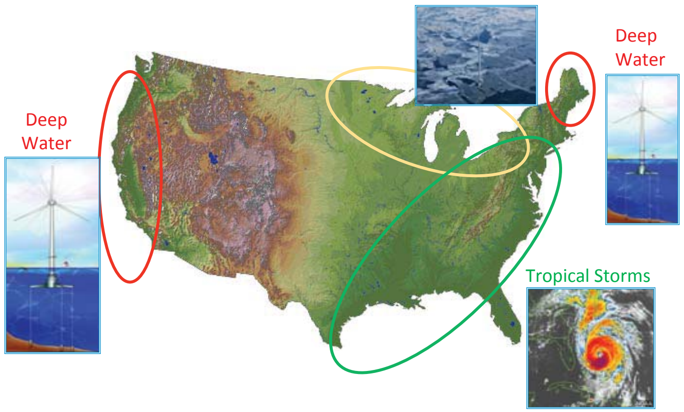

DOE FOA 410 Demonstration Projects

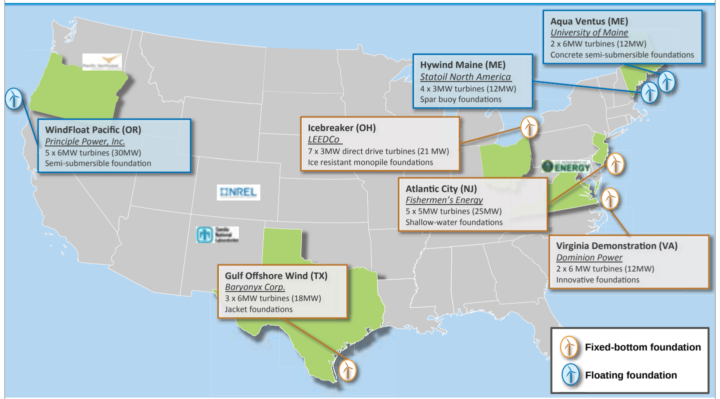

DOE's ATD FOAs will bring next generation of technology to U.S

Projects announced in Dec 2012 will receive $4M for initial planning and design phases. Three will be selected to complete the follow-on design and deployment phases by 2017.

GoWind – Baryonyx

Project Highlights:
- Oil & Gas experience and Ormonde wind farm (30 Jacketed REpower 5MW)
- Mix of a power purchase agreement, merchant market sales and an agreement with an industrial user.
- 9-month LIDAR campaign for resource assessment

Innovations:
- Jacket foundation design
- Blimp tethered to buoy for wind measurement

Installation:
- Retrofit an existing jack-up or other vessel

Team Partners:
- Offshore Design Engineering, ODE, Keppel AmFELS

Site Characteristics	
Location	Texas, State Waters
Number of Turbines	3
Turbine	6 MW, Direct Drive
Foundation Type	Jacket
Depth	18 m (54 ft)
Distance from Shore	8 km (5 miles)

VOWTAP - Dominion

Project Highlights:
- Alstom Haliade 150 wind turbine
  - Large LM 73.5-m GloBlade
  - PureTorque system
- Leveraged Carbon Trust Offshore Wind Accelerator (IBGS foundation – Hornsea Metmast)

Innovations:
- Innovative foundation and installation methods
- Offshore-specific wind turbine with advanced control
- Integrated system design for hurricane survivability

Installation:
- Heavy lift vessel

Team Partners:
- DMME, Alstom, NREL, KBR, Virg. Coastal Energy Research Consortium, Newport News Shipbuilding, TETRA TECH

Site Characteristics	
Location	Virginia, Federal Waters
Number of Turbines	2
Turbine	6 MW, PMDD
Foundation Type	Jacket
Depth	?
Distance from Shore	?

Atlantic City Windfarm – Fisherman's Energy

Project Highlights:
- Unique need to balance conflicting goals of key stakeholders (NJBPU and USDOE)
- Demonstrating validity of LIDAR and OSW

Innovations:
- Shallow-water foundations

Team Partners:
- XEMC, Keystone, Mott MacDonald, NREL, Weeks Marine, Marmon Utilities, DCO Energy, ABS

Site Characteristics	
Location	New Jersey, State Waters
Number of Turbines	5
Turbine	Darwind 5MW
Foundation Type	?
Depth	?
Distance from Shore	4.5 km (2.8 miles)

Icebreaker - LEEDCo

Project Highlights:
- Adapted from monopile concept well-proven in North Sea
- Designed to withstand harsh winters
- Integrates innovative technology for Lake Erie soil conditions
- Creates an artificial reef

Innovations:
- Design to withstand ice conditions

Team Partners:
- Siemens, DNV GL, Green Giraffe, Ariel Ventures, Freshwater Wind, Bayer Materials, NREL, CWRU, ode, OCC/COWI, Eranti Engineering, GLWN, McMahon DeGulis, Environ, PNNL, PMC

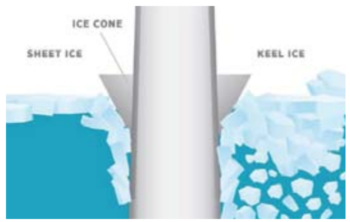

Site Characteristics	
Location	Great Lakes, State Waters
Number of Turbines	6
Turbine	3 MW
Foundation Type	Adapted monopile
Depth	18 m (60 ft)
Distance from Shore	11 km (7 miles)

WindFloat Pacific Project – Principle Power

Project Highlights:
- Project builds off single smaller turbine project off Portugal
- Only project in the Pacific
- Quayside construction and assembly
- Power Purchaser: Jordan Cove

Innovations:
- Floating semi-submersible foundation with moveable ballast
- Virtual MET towers using LIDAR
- Potential for modular construction

Installation:
- Pre-lay of moorings and setting of anchors
- Fully assembled turbine and platform towed to site

Team Partners:
- Houston Offshore Engineering, PNNL, NREL, Jordan Cove Energy

Site Characteristics	
Location	Oregon, Federal Waters
Number of Turbines	5
Turbine	6 MW, Direct Drive
Foundation Type	Floating, Semi-Sub
Depth	365 m (1,200 ft)
Distance from Shore	28 km (17 miles)

Hywind - Statoil

Project Highlights:
- Project builds off single smaller turbine project off Norway
- Conventional technology, used in a new way
- Beneficial motion characteristics

Innovations:
- Optimized design – larger turbine, lighter substructure with reduced draught
- Blade pitch control to dampen out motion

Installation:
- Simple and safe construction, assembly, and installation

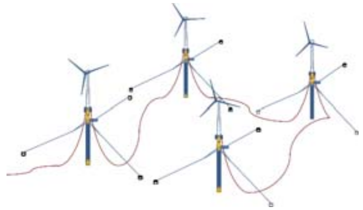

Site Characteristics	
Location	Gulf of Maine, Federal Waters
Number of Turbines	4
Turbine	3 MW
Foundation Type	Floating, Spar
Depth	145 m (475 ft)
Distance from Shore	22 km (14 miles)

Aqua Ventus I – University of Maine

Project Highlights:
- Build upon VolturnUS 1:8 scaled prototype experience
- First installed U.S scaled floating wind turbine

Innovations:
- Concrete semi-submersible
- Composites

Team Partners:
- Iberdrola, Technip, ABS, NREL, FYLIN, AWS Truepower, CIANBRO, University of Massachusetts, Maine Maritime Academy, ERSHINGS, Goldwind, Senergy, HDR/DTA

Site Characteristics	
Location	Maine, State Waters
Number of Turbines	2
Turbine	6 MW, Direct Drive
Foundation Type	Floating, Semi-Sub
Depth	?
Distance from Shore	?

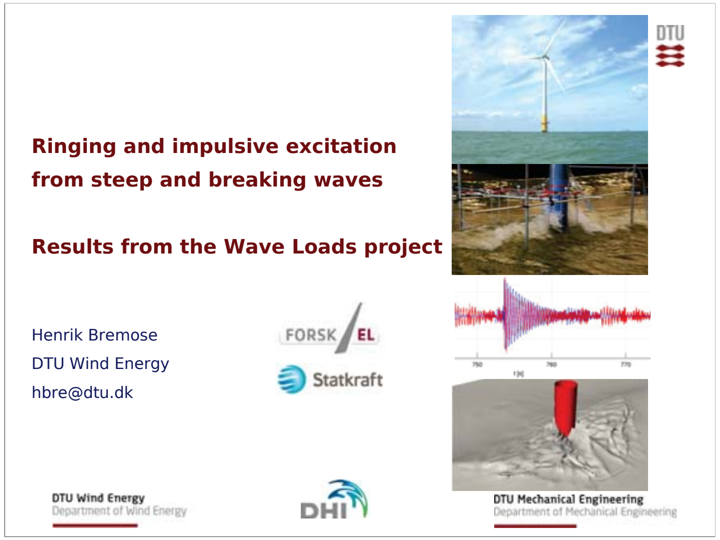
Ringing and impulsive excitation from steep and breaking waves
Results from the Wave Loads project
Henrik Bremose
DTU Wind Energy
hbre@dtu.dk
FORSK EL
Statkraft
DTU Wind Energy
Department of Wind Energy
DHI
DTU Mechanical Engineering
Department of Mechanical Engineering

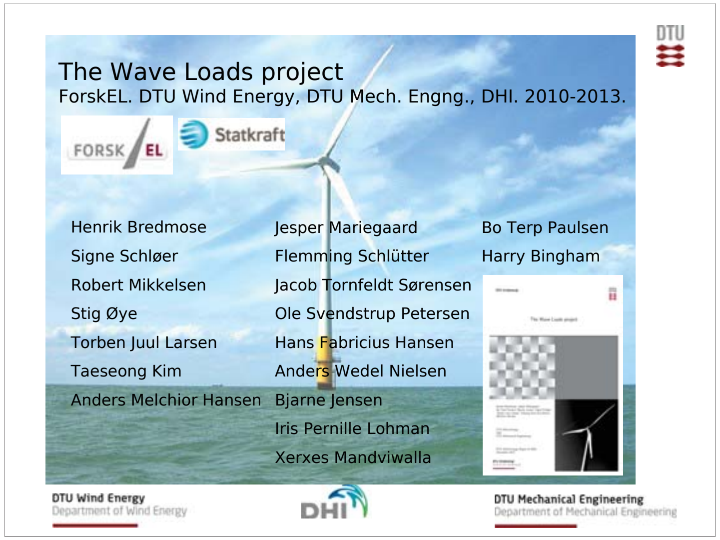
The Wave Loads project
ForskEL. DTU Wind Energy, DTU Mech. Engng., DHI. 2010-2013.
FORSK EL
Statkraft
Henrik Bredmose
Signe Schløer
Robert Mikkelsen
Stig Øye
Torben Juul Larsen
Taeseong Kim
Anders Melchior Hansen
Jesper Mariegaard
Flemming Schlütter
Jacob Tornfeldt Sørensen
Ole Svendstrup Petersen
Hans Fabricius Hansen
Anders Wedel Nielsen
Bjarne Jensen
Iris Pernille Lohman
Xerxes Mandviwalla
Bo Terp Paulsen
Harry Bingham
DTU Wind Energy
Department of Wind Energy
DHI
DTU Mechanical Engineering
Department of Mechanical Engineering

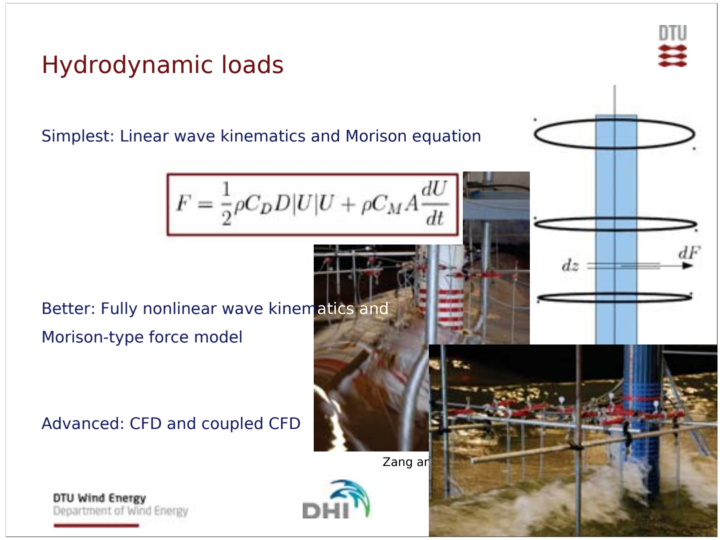
Hydrodynamic loads
Simplest: Linear wave kinematics and Morison equation
$F = \frac{1}{2}\rho C_D D|U|U + \rho C_M A \frac{dU}{dt}$
dz
dF
Better: Fully nonlinear wave kinematics and Morison-type force model
Advanced: CFD and coupled CFD
DTU Wind Energy
Department of Wind Energy
DHI

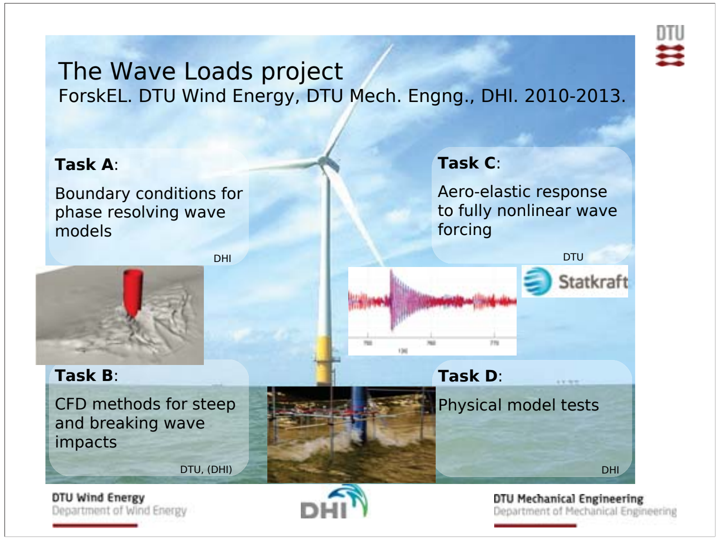
The Wave Loads project
ForskEL. DTU Wind Energy, DTU Mech. Engng., DHI. 2010-2013.
Task A:
Boundary conditions for phase resolving wave models
DHI
Task C:
Aero-elastic response to fully nonlinear wave forcing
DTU
Statkraft
Task B:
CFD methods for steep and breaking wave impacts
DTU, (DHI)
Task D:
Physical model tests
DHI
DTU Wind Energy
Department of Wind Energy
DHI
DTU Mechanical Engineering
Department of Mechanical Engineering

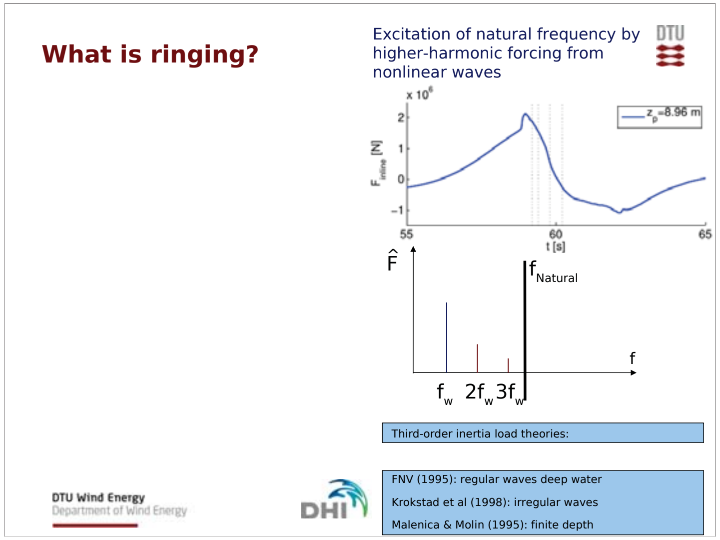
What is ringing?
Excitation of natural frequency by higher-harmonic forcing from nonlinear waves
x 10^6
z_p=-8.96 m
F_{inline} [N]
t [s]
$\hat{F}$
$f_{Natural}$
f
f_w $2f_w$ $3f_w$
Third-order inertia load theories:
FNV (1995): regular waves deep water
Krokstad et al (1998): irregular waves
Malenica & Molin (1995): finite depth
DTU Wind Energy
Department of Wind Energy
DHI

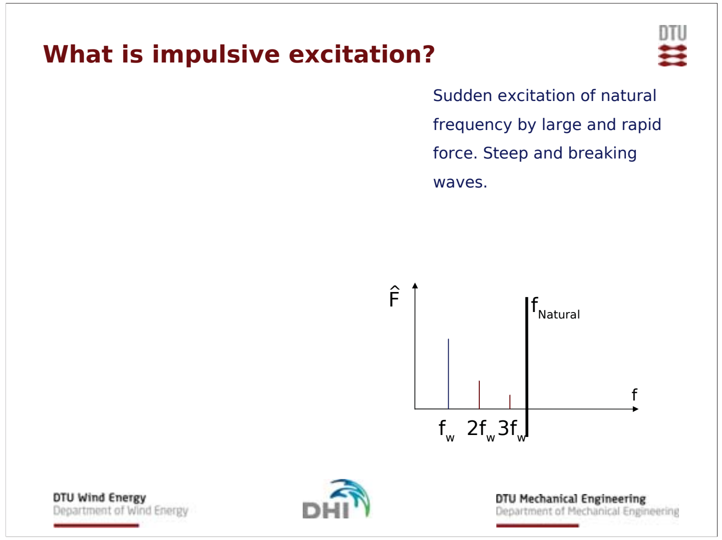
What is impulsive excitation?
Sudden excitation of natural frequency by large and rapid force. Steep and breaking waves.
$\hat{F}$
$f_{Natural}$
f
f_w $2f_w$ $3f_w$
DTU Wind Energy
Department of Wind Energy
DHI
DTU Mechanical Engineering
Department of Mechanical Engineering

Study of nonlinear wave load effects

Response calculations with Flex5 aero-elastic model, NREL 5MW turbine

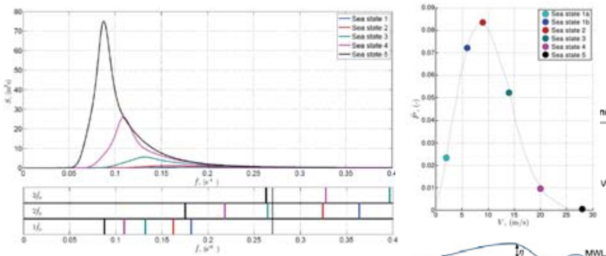

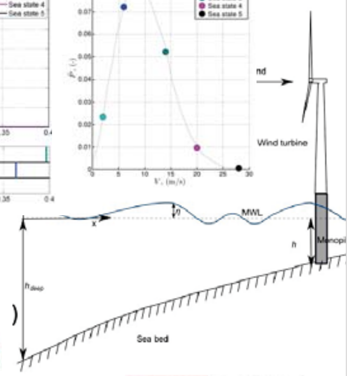

Signe Schløer (2013)

Statkraft

Kinematics from a fully nonlinear potential flow solver

'OceanWave3D', Engsig-Karup et al (2009)

Allan Engsig-Karup, Harry Bingham and Ole Lindberg

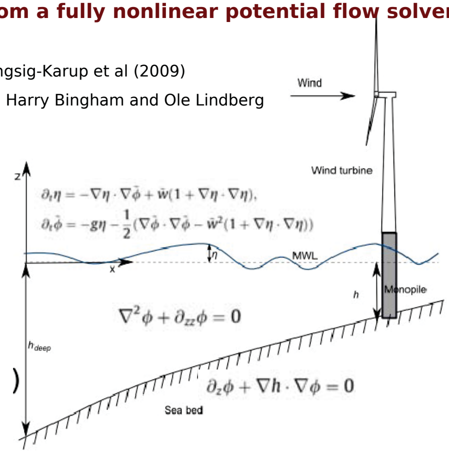

$$\partial_t \eta = -\nabla\eta \cdot \nabla\tilde{\phi} + \tilde{w}(1 + \nabla\eta\cdot\nabla\eta),$$
$$\partial_t \tilde{\phi} = -g\eta - \frac{1}{2}(\nabla\tilde{\phi}\cdot\nabla\tilde{\phi} - \tilde{w}^2(1+\nabla\eta\cdot\nabla\eta))$$
$$\nabla^2\phi + \partial_{zz}\phi = 0$$
$$\partial_z\phi + \nabla h \cdot \nabla\phi = 0$$

From kinematics to distributed force

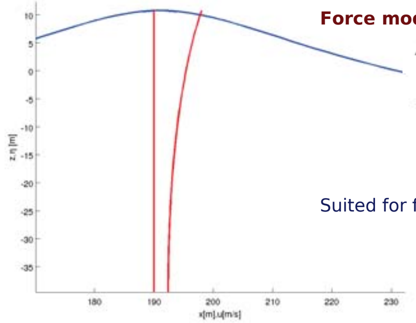

Force model (Rainey 1989, 1995)

$$F_{\text{surface}} = -\tfrac{1}{2}\rho_w \mathscr{A} c_m \eta_x (u - \dot{X})^2$$
$$f(t,z) = \rho_w \mathscr{A} c_m (\dot{u} - \ddot{X}) + \rho_w A \dot{u} + \rho_w \mathscr{A} c_m w_z (u - \dot{X}) + \tfrac{1}{2}\rho_w c_D D (u - \dot{X})|u - \dot{X}|$$

Suited for fully nonlinear kinematics

Response in bottom of tower

Fully nonlinear waves versus linear waves

$H_s = 9.4$ m, $T_p = 14.2$ s, $W = 5$ m/s

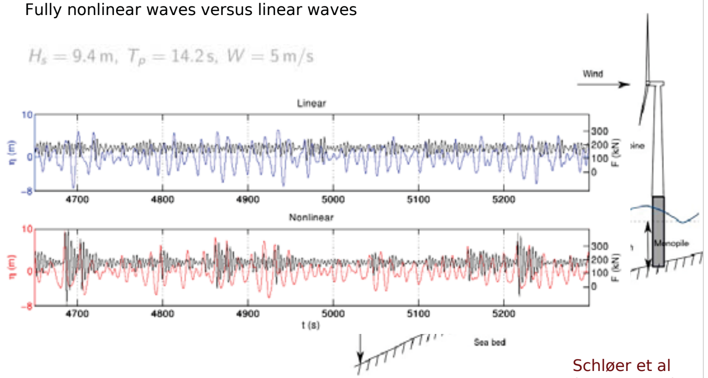

Schløer et al (OMAE 2012)

Static load analysis, h=30m

crest elevations

force peaks depth integrated force

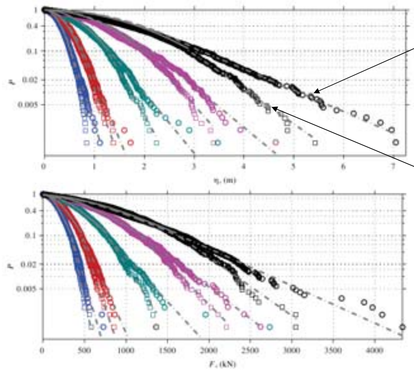

nonlinear

linear

Results of aero-elastic computations

Tower response – largest sea state

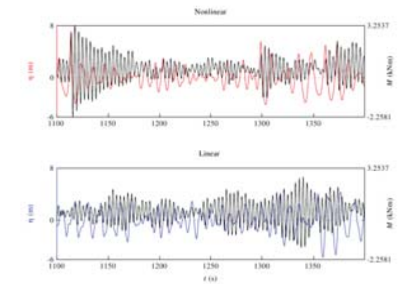

Figure 44: Nonlinear and linear surface elevation for the largest sea state and the corresponding moment in the bottom of the tower, $H_s = 6.76$m, $T_p = 11.41$s, $V = 28$m/s and $I_r = 0.13$

Linear waves can also excite the tower

Results of aero-elastic computations
Monopile response – largest sea state

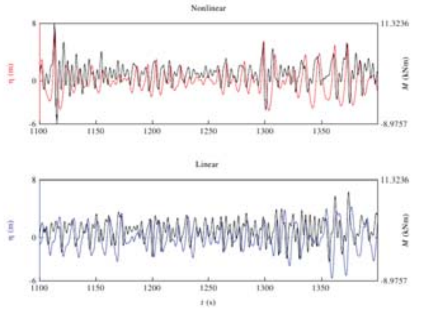

Figure 45: Nonlinear and linear surface elevation for the largest sea state and the corresponding moment in the bottom of the monopile, $H_s = 6.76$m, $T_p = 11.41$s, $V = 28$m/s and $I_t = 0.13$

Vibrations less visible – occur on top of the wave loads

Quantify fatigue effect

Equivalent load

$$L_{eq} = \left(\sum_i \frac{N_{s,i}(S_i)^m}{N_{eq}}\right)^{\frac{1}{m}}$$

Accumulated equivalent load

$$L_{eq,acc} = \left(\sum_j L_{eq,j}^m \frac{T_j}{T}\right)^{\frac{1}{m}}$$

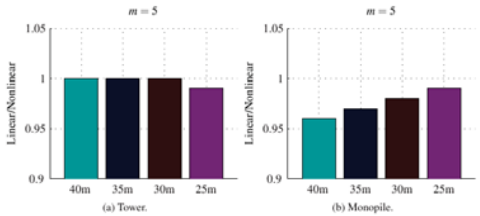

Tower effect occur at 25m – wave nonlinearity is stronger for smaller depth

Monopile effect is largest at 40m, where it gives 4% larger equivalent loads.

Quantify fatigue effect

Equivalent load

$$L_{eq} = \left(\sum \frac{N_{s,i}(S_i)^m}{N}\right)^{\frac{1}{m}}$$

Accumulated equivalent load

$$L_{eq,acc} = \left(\sum L_{eq,j}^m \frac{T_j}{T}\right)^{\frac{1}{m}}$$

Conclusion of present study:

Wave nonlinearity not critical for *equivalent fatigue loads*.

But 4% in equivalent load corresponds to 18% in *fatigue damage*

More investigations with more sea states included needed

Inclusion of diffraction needed

Nonlinearity seems more important for ULS than for FLS

Hence ULS study is needed

Tower effect occur at 25m – wave nonlinearity is stronger for smaller depth

Monopile effect is largest at 40m, where it gives 4% larger equivalent loads.

The Wave Loads project

ForskEL. DTU Wind Energy, DTU Mech. Engng., DHI. 2010-2013.

Task A:
Boundary conditions for phase resolving wave models
DHI

Task C:
Aero-elastic response to fully nonlinear wave forcing
DTU

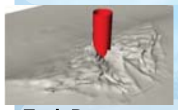

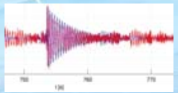

Task B:
CFD methods for steep and breaking wave impacts
DTU, (DHI)

Task D:
Physical model tests
DHI

The OpenFOAM® CFD solver

Open source CFD toolbox
Vast attention during last 3 years

This study: interFoam solver
- 3D incompressible Navier-Stokes
- two phases (water and air)
- VOF treatment of free surface

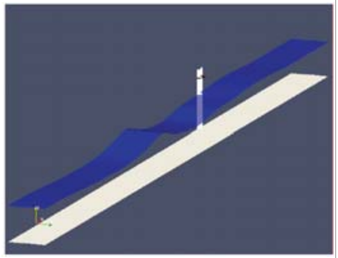

Waves2foam wave generation toolbox has been developed and validated
(Niels Gjøl Jacobsen
PhD thesis 2011; Paper in Int. J. Num. Meth. Fluids)

Platform height of 8.96m

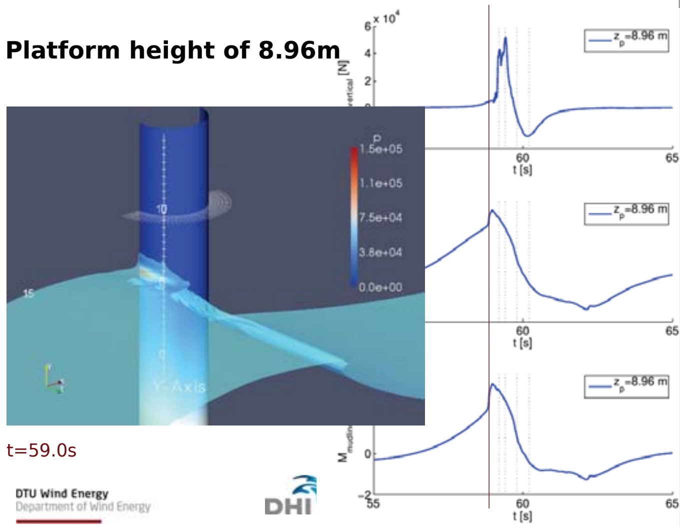

t=59.0s

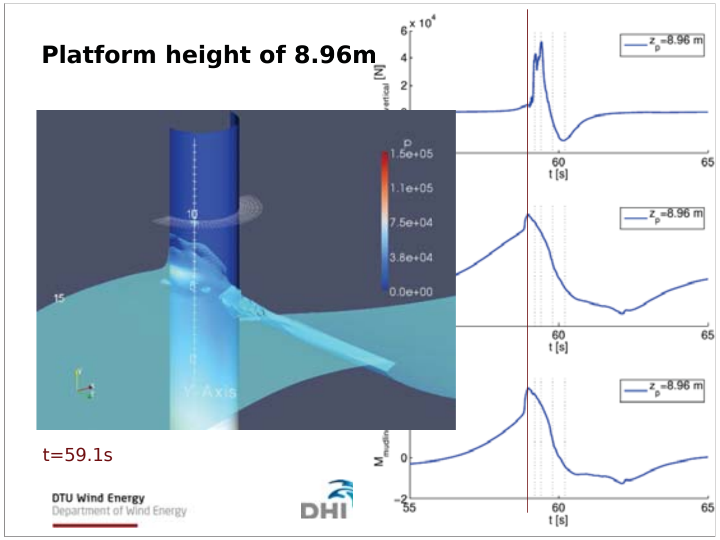
Platform height of 8.96m
t=59.1s
DTU Wind Energy
Department of Wind Energy
DHI

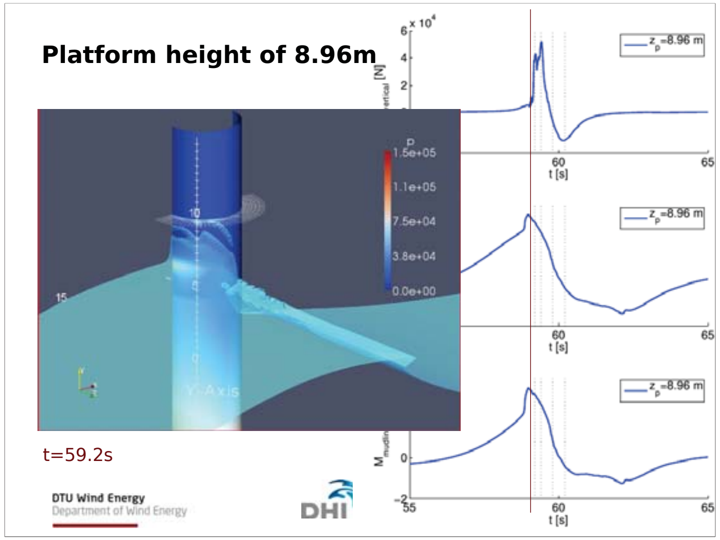
Platform height of 8.96m
t=59.2s
DTU Wind Energy
Department of Wind Energy
DHI

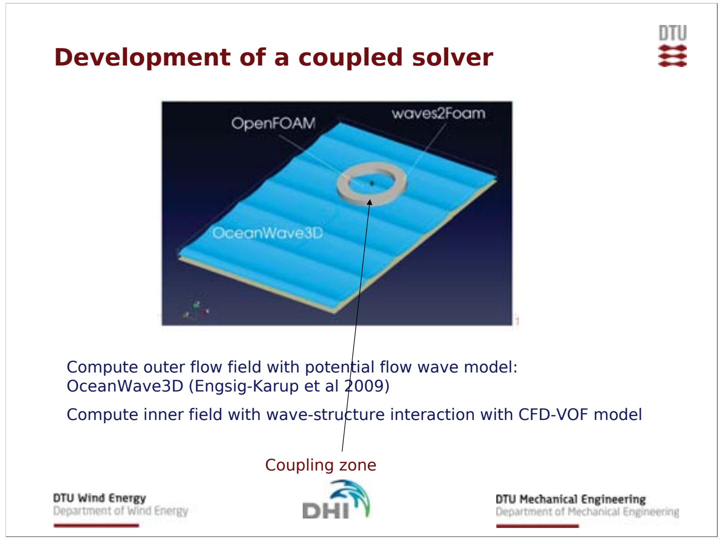
Development of a coupled solver
OpenFOAM
waves2Foam
OceanWave3D
Compute outer flow field with potential flow wave model:
OceanWave3D (Engsig-Karup et al 2009)
Compute inner field with wave-structure interaction with CFD-VOF model
Coupling zone
DTU Wind Energy
Department of Wind Energy
DHI
DTU Mechanical Engineering
Department of Mechanical Engineering

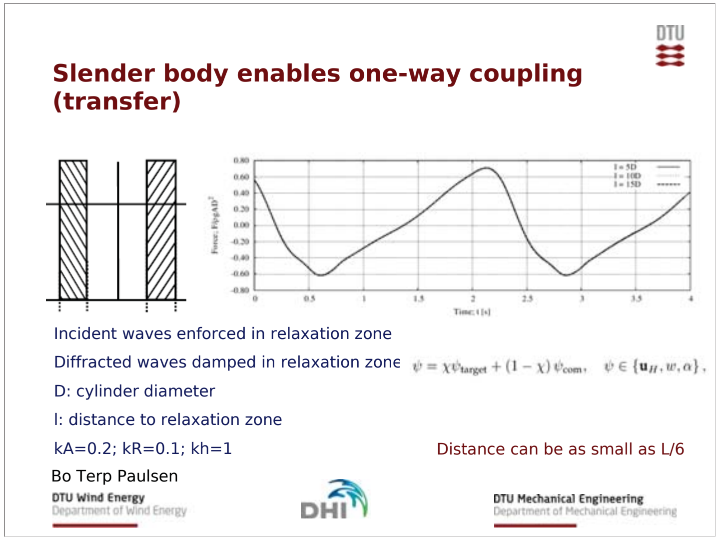
Slender body enables one-way coupling (transfer)
Incident waves enforced in relaxation zone
Diffracted waves damped in relaxation zone
$\psi = \chi\psi_{target} + (1-\chi)\psi_{com}, \quad \psi \in \{\mathbf{u}_H, w, \alpha\}$,
D: cylinder diameter
l: distance to relaxation zone
kA=0.2; kR=0.1; kh=1
Distance can be as small as L/6
Bo Terp Paulsen
DTU Wind Energy
Department of Wind Energy
DHI
DTU Mechanical Engineering
Department of Mechanical Engineering

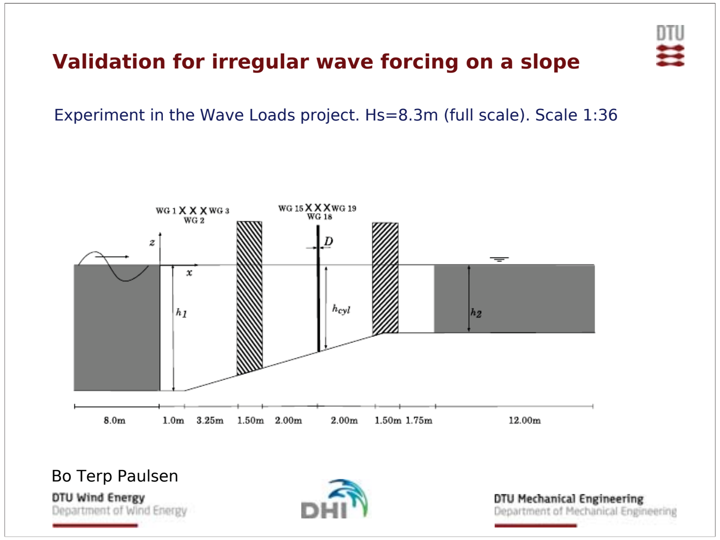
Validation for irregular wave forcing on a slope
Experiment in the Wave Loads project. Hs=8.3m (full scale). Scale 1:36
Bo Terp Paulsen
DTU Wind Energy
Department of Wind Energy
DHI
DTU Mechanical Engineering
Department of Mechanical Engineering

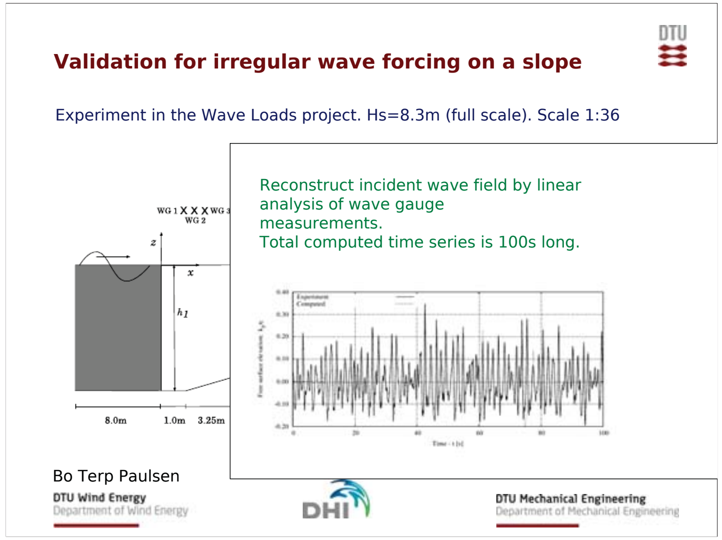
Validation for irregular wave forcing on a slope
Experiment in the Wave Loads project. Hs=8.3m (full scale). Scale 1:36
Reconstruct incident wave field by linear analysis of wave gauge measurements.
Total computed time series is 100s long.
Bo Terp Paulsen
DTU Wind Energy
Department of Wind Energy
DHI
DTU Mechanical Engineering
Department of Mechanical Engineering

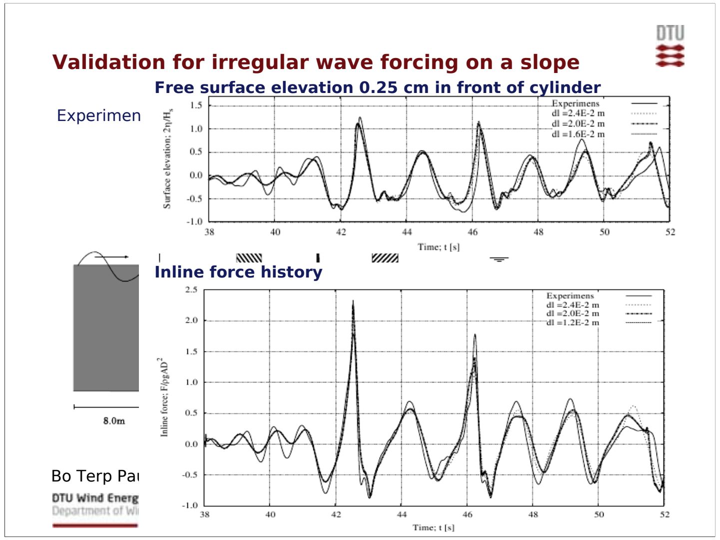
DTU
Validation for irregular wave forcing on a slope
Free surface elevation 0.25 cm in front of cylinder
Experimen
Experimens
dl =2.4E-2 m
dl =2.0E-2 m
dl =1.6E-2 m
Time; t [s]
Inline force history
Experimens
dl =2.4E-2 m
dl =2.0E-2 m
dl =1.2E-2 m
Time; t [s]
8.0m
Bo Terp Pau
DTU Wind Energ

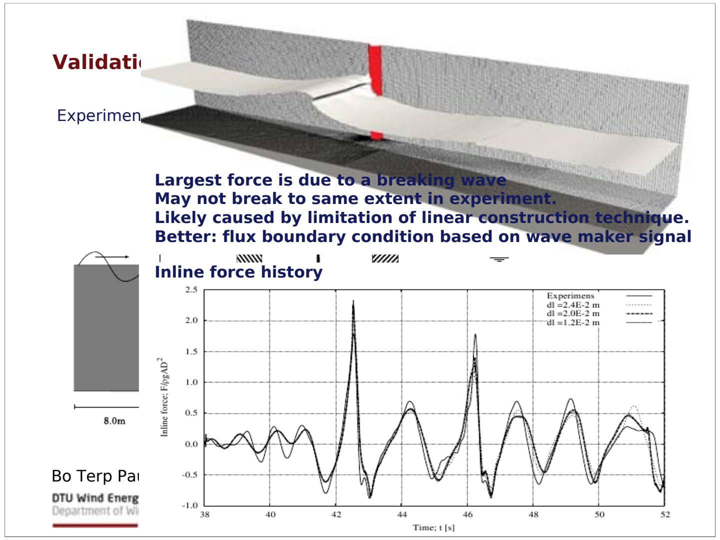
Validati
Experimen
Largest force is due to a breaking wave
May not break to same extent in experiment.
Likely caused by limitation of linear construction technique.
Better: flux boundary condition based on wave maker signal
Inline force history
Experimens
dl =2.4E-2 m
dl =2.0E-2 m
dl =1.2E-2 m
Time; t [s]
8.0m
Bo Terp Pau
DTU Wind Energ

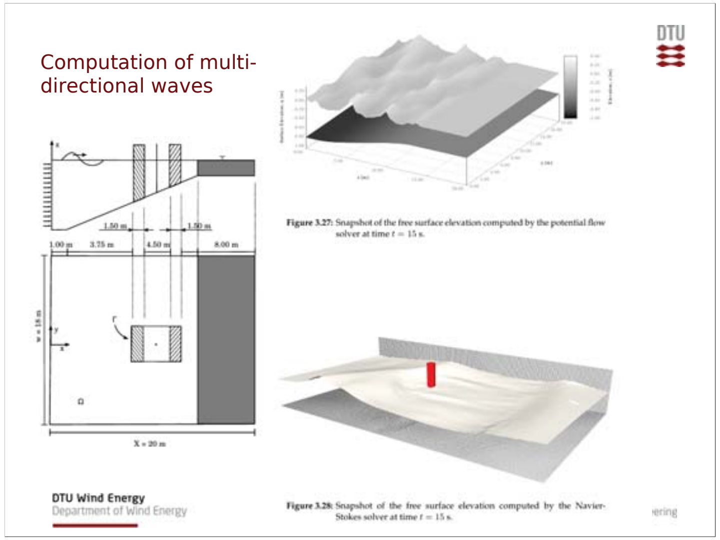
DTU
Computation of multi-directional waves
Figure 3.27: Snapshot of the free surface elevation computed by the potential flow solver at time t = 15 s.
Figure 3.28: Snapshot of the free surface elevation computed by the Navier-Stokes solver at time t = 15 s.
X = 20 m
DTU Wind Energy
Department of Wind Energy

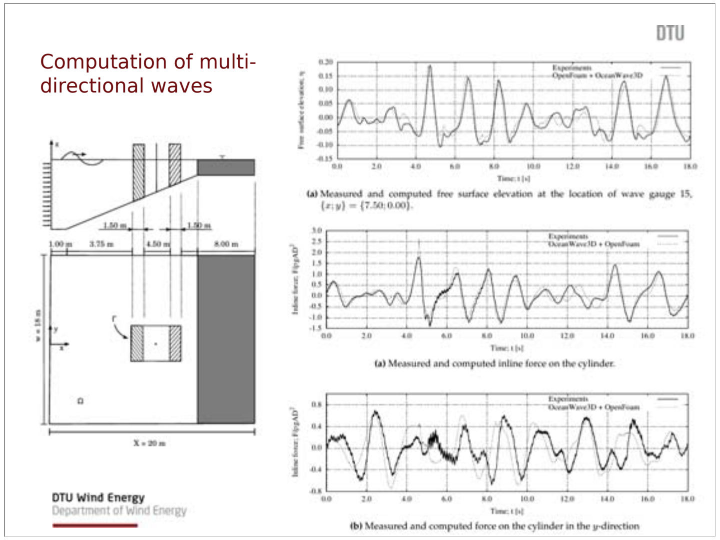
DTU
Computation of multi-directional waves
(a) Measured and computed free surface elevation at the location of wave gauge 15, (x; y) = (7.50; 0.00).
(a) Measured and computed inline force on the cylinder.
(b) Measured and computed force on the cylinder in the y-direction
X = 20 m
DTU Wind Energy
Department of Wind Energy

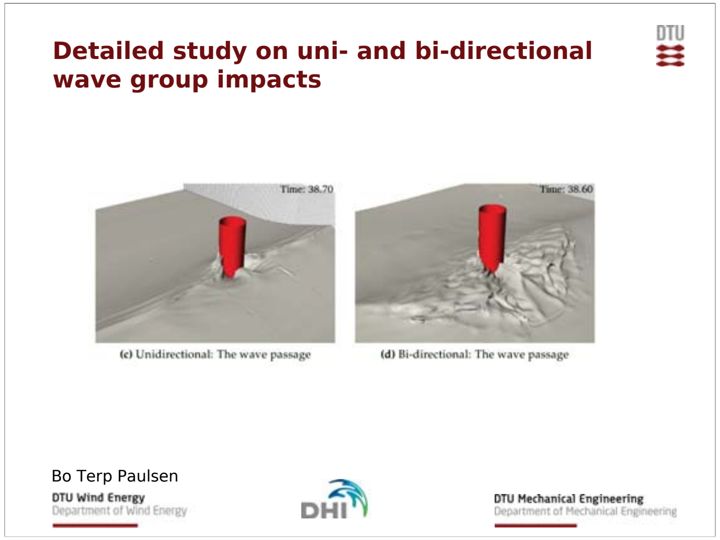
DTU
Detailed study on uni- and bi-directional wave group impacts
Time: 38.70
Time: 38.60
(c) Unidirectional: The wave passage
(d) Bi-directional: The wave passage
Bo Terp Paulsen
DTU Wind Energy
Department of Wind Energy
DHI
DTU Mechanical Engineering
Department of Mechanical Engineering

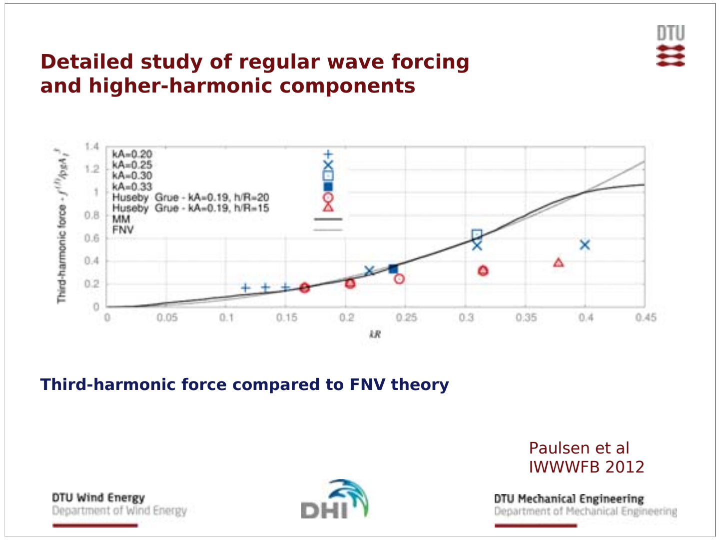
DTU
Detailed study of regular wave forcing and higher-harmonic components
kA=0.20
kA=0.25
kA=0.30
kA=0.33
Huseby Grue - kA=0.19, h/R=20
Huseby Grue - kA=0.19, h/R=15
MM
FNV
kR
Third-harmonic force compared to FNV theory
Paulsen et al
IWWWFB 2012
DTU Wind Energy
Department of Wind Energy
DHI
DTU Mechanical Engineering
Department of Mechanical Engineering

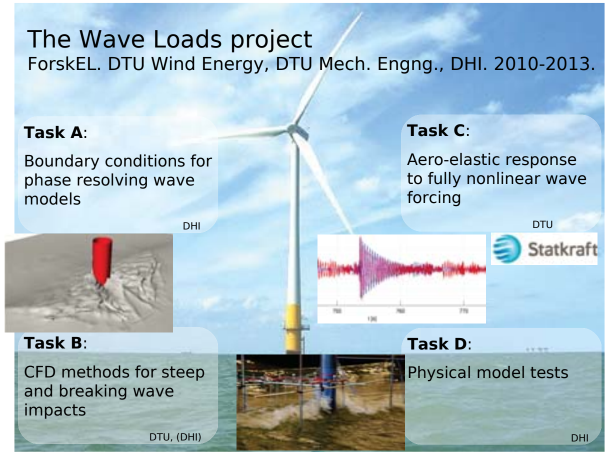

DTU Wind Energy
Department of Wind Energy

DTU Mechanical Engineering
Department of Mechanical Engineering

Physical model test with a flexible cylinder at DHI

Bredmose et al OMAE 2013

Inspiration from de Ridder et al OMAE 2011

Pipe properties

Target values from NREL 5MW reference WT

tuning to get 1st and 2nd scaled nat frequencies

	Lab scale (1:80)	Prototype scale
D_{outer}	7.5 cm	6.0 m
Wall thickness	1.8 mm	0.144 m
EI (estimated)	1026 Nm^2	$4.20\cdot10^{10}$ Nm^2
ζ (estimated)	0.017	0.017
Density	0.64 kg/m	$4.20\cdot10^3$kg/m
height	200 cm	160 m
m_1	1.786 kg	$937\cdot10^3$kg
m_2	1.784 kg	$936\cdot10^3$kg
h_1	160.75 cm	128.6 m
h_2	108.75 cm	87.0 m
f_1	2.5 Hz	0.28 Hz
f_2	18 Hz	2.0 Hz
f_3	50 Hz	5.6 Hz

TABLE 1. Data for flexible pipe. Prototype values are indicated just for reference.

DTU Wind Energy
Department of Wind Energy

Instrumentation

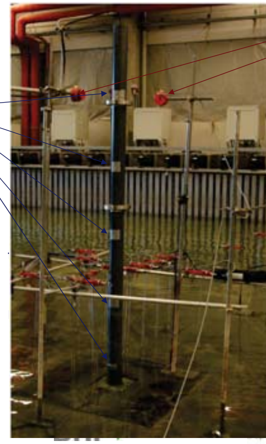

DTU Wind Energy
Department of Wind Energy

Mechanical Engineering
Department of Mechanical Engineering

Example of measurement

h=40.8m; Hs=8.3m; Tp=12.6s

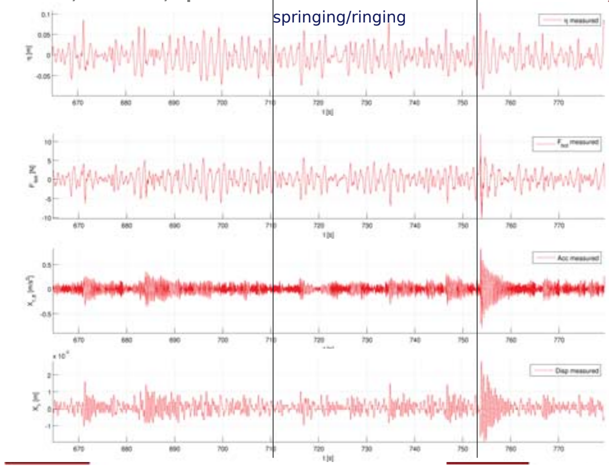

Which waves give the largest accelerations?

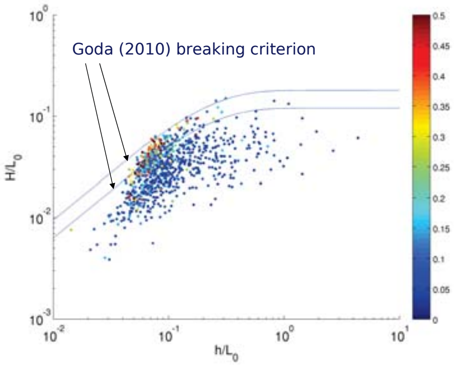

See also Hansen et al (OMAE 2012)

DTU Wind Energy
Department of Wind Energy

DTU Mechanical Engineering
Department of Mechanical Engineering

Which waves give the largest accelerations?

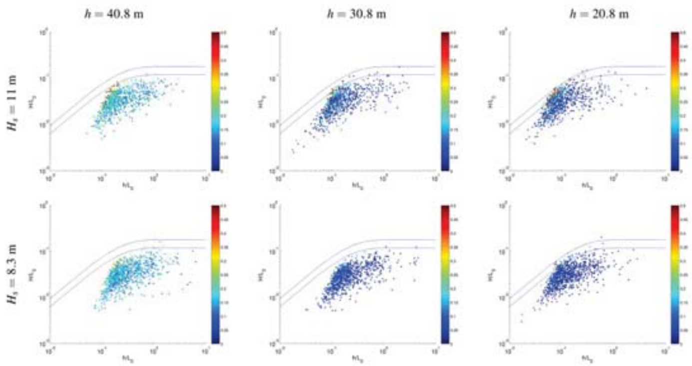

Deeper water: larger bulk accelerations. DEPTH AND ARM

Shallow water: larger extreme accelerations. NONLINEARITY AND BREAKING

DTU Wind Energy
Department of Wind Energy

DTU Mechanical Engineering
Department of Mechanical Engineering

Numerical reproduction of experiments

Linear wave detection

Nonlinear wave transformation

OceanWave3D (Engsig-Karup et al 2009)

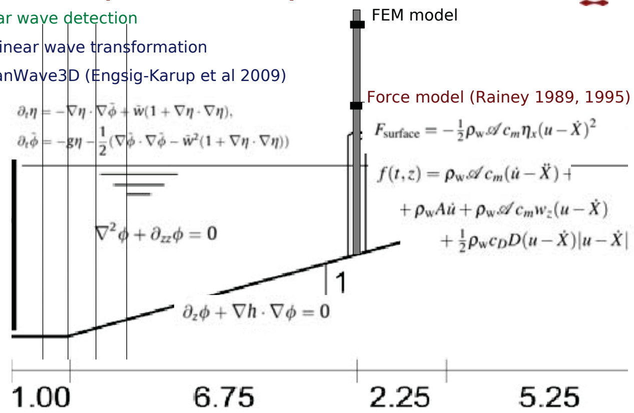

Response, h=40.8 m

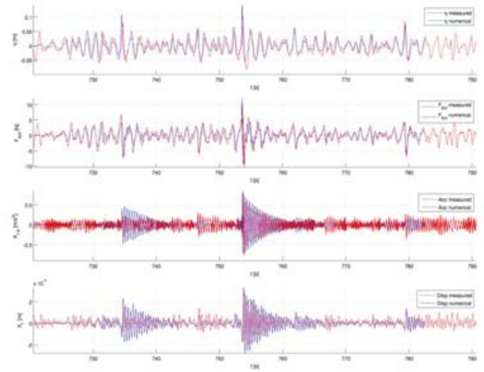

Response, h=20.8 m

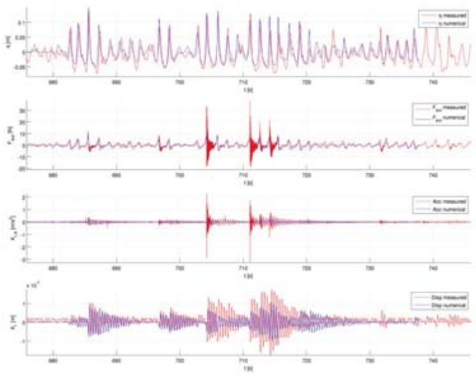

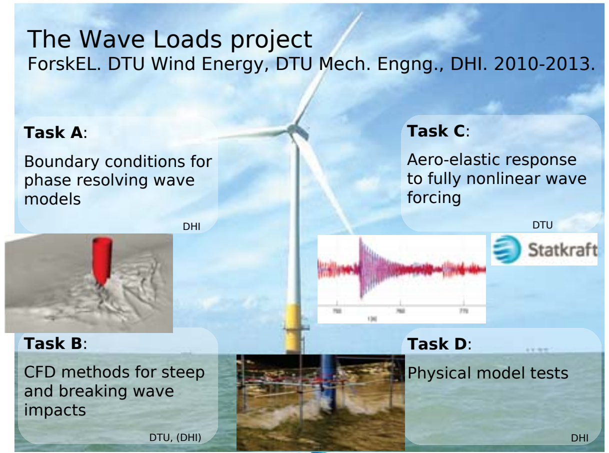

Damping of Wind Turbine Tower Vibrations by a stroke amplifying brace concept

Mark L. Brodersen & Jan Høgsberg

Department of Mechanical Engineering
Technical University of Denmark
mlai@dtu.dk

EERA Deepwind
January 22-24 2014

Outline

Motivation

Implementation of dampers

Numerical models

Results

Damping of Wind Turbine Tower Vibrations
Mark L. Brodersen

Offshore wind turbine tower vibrations

- Wind-wave misalignment
  - Larger wind turbine and deeper waters

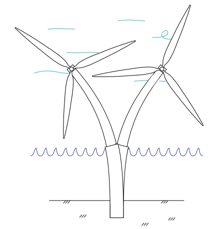

Damping of Wind Turbine Tower Vibrations
Mark L. Brodersen

Offshore wind turbine tower vibrations

- Wind-wave misalignment
  - Larger wind turbine and deeper waters
- Resonant dampers

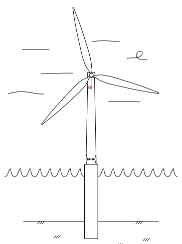

Damping of Wind Turbine Tower Vibrations
Mark L. Brodersen

Offshore wind turbine tower vibrations

- Wind-wave misalignment
  - Larger wind turbine and deeper waters
- Resonant dampers
- Dampers inside the tower

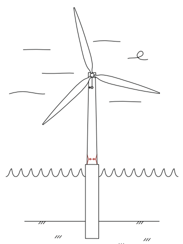

Damping of Wind Turbine Tower Vibrations
Mark L. Brodersen

Criteria for effective damping

- Damper stroke
  - Activation of damper
  - Damper force

$$E_d = \dot{u}_d f_d$$

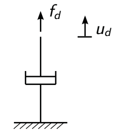

Damping of Wind Turbine Tower Vibrations
Mark L. Brodersen

Criteria for effective damping

- Damper stroke
  - Activation of damper
  - Damper force

$$E_d = \dot{u}_d f_d$$

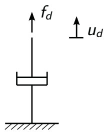

- Attainable damping
  - Given by the change in frequency

$$\zeta_{max} \simeq \frac{\omega_\infty - \omega_0}{\omega_\infty + \omega_0}$$

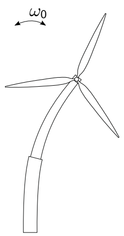

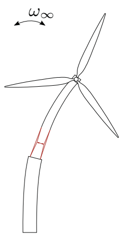

Criteria for effective damping

- Tuning of dampers
  - Viscous dampers with damping parameter c

$$f_d = c\dot{u}_d$$

  - Tuning for maximum damping

$$c_{opt} \simeq 2\frac{\omega_\infty - \omega_0}{\sum_k^N \gamma_k^2}$$

γ is the damper stroke with respect to mode $\mathbf{u}_0$ for unit modal mass $\mathbf{u}_0^T \mathbf{M} \mathbf{u}_0 = 1$

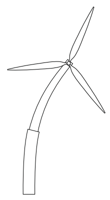

Damping of Wind Turbine Tower Vibrations
Mark L. Brodersen
Motivation
Offshore wind turbine tower vibrations
Implementation of dampers
Criteria for effective damping
Tower modes
Brace concepts
Numerical models
Beam model and HAWC2 model
Results
Damper stroke
Attainable damping
Damper force
Free decay
Outlook

Tower modes

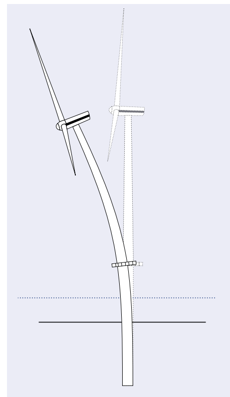

For-aft mode

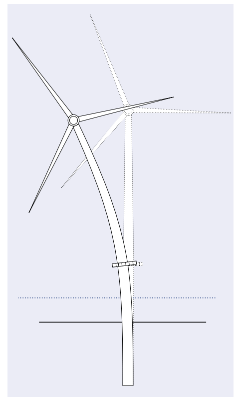

Side-to-side mode

Damping of Wind Turbine Tower Vibrations
Mark L. Brodersen
Motivation
Offshore wind turbine tower vibrations
Implementation of dampers
Criteria for effective damping
Tower modes
Brace concepts
Numerical models
Beam model and HAWC2 model
Results
Damper stroke
Attainable damping
Damper force
Free decay
Outlook

Brace concepts

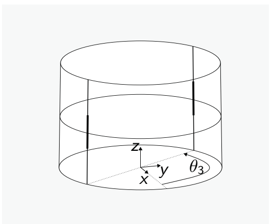

Curvature-brace

Damping of Wind Turbine Tower Vibrations
Mark L. Brodersen
Motivation
Offshore wind turbine tower vibrations
Implementation of dampers
Criteria for effective damping
Tower modes
Brace concepts
Numerical models
Beam model and HAWC2 model
Results
Damper stroke
Attainable damping
Damper force
Free decay
Outlook

Brace concepts

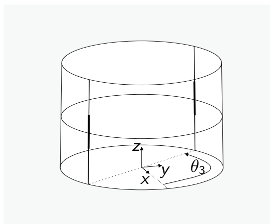

Curvature-brace

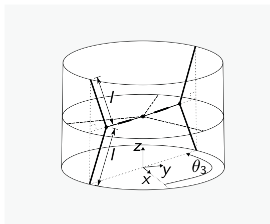

Curvature-toggle-brace

Damping of Wind Turbine Tower Vibrations
Mark L. Brodersen
Motivation
Offshore wind turbine tower vibrations
Implementation of dampers
Criteria for effective damping
Tower modes
Brace concepts
Numerical models
Beam model and HAWC2 model
Results
Damper stroke
Attainable damping
Damper force
Free decay
Outlook

Brace concepts

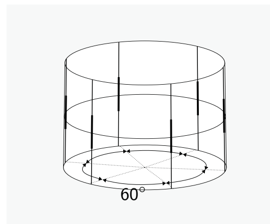

Curvature-brace

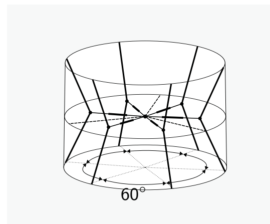

Curvature-toggle-brace

Damping of Wind Turbine Tower Vibrations
Mark L. Brodersen
Motivation
Offshore wind turbine tower vibrations
Implementation of dampers
Criteria for effective damping
Tower modes
Brace concepts
Numerical models
Beam model and HAWC2 model
Results
Damper stroke
Attainable damping
Damper force
Free decay
Outlook

Numerical models

- Linear beam model
  - Wind turbine at standstill
  - Linear Winkler type spring model
  - Lumped inertia
  - Stiffness matrix derived from complementary energy

Numerical models

Damping of Wind Turbine Tower Vibrations
Mark L. Brodersen
Motivation
Offshore wind turbine tower vibrations
Implementation of dampers
Criteria for effective damping
Tower modes
Brace concepts
Numerical models
Beam model and HAWC2 model
Results
Damper stroke
Attainable damping
Damper force
Free decay
Outlook

- Linear beam model
  - Wind turbine at standstill
  - Linear Winkler type spring model
  - Lumped inertia
  - Stiffness matrix derived from complementary energy
- HAWC2
  - Blade element momentum theory
  - Multi-body formulation
  - Control via Dynamic Link Library (dll) interface
  - External system

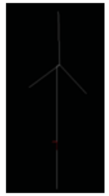

Numerical models

Damping of Wind Turbine Tower Vibrations
Mark L. Brodersen
Motivation
Offshore wind turbine tower vibrations
Implementation of dampers
Criteria for effective damping
Tower modes
Brace concepts
Numerical models
Beam model and HAWC2 model
Results
Damper stroke
Attainable damping
Damper force
Free decay
Outlook

- Linear beam model
  - Wind turbine at standstill
  - Linear Winkler type spring model
  - Lumped inertia
  - Stiffness matrix derived from complementary energy
- HAWC2
  - Blade element momentum theory
  - Multi-body formulation
  - Control via Dynamic Link Library (dll) interface
  - External system
- Offshore Code Comparison Collaboration
  - NREL reference turbine + monopile in 20 m water

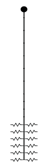

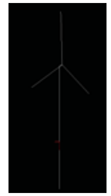

Displacement of damper

Damping of Wind Turbine Tower Vibrations
Mark L. Brodersen
Motivation
Offshore wind turbine tower vibrations
Implementation of dampers
Criteria for effective damping
Tower modes
Brace concepts
Numerical models
Beam model and HAWC2 model
Results
Damper stroke
Attainable damping
Damper force
Free decay
Outlook

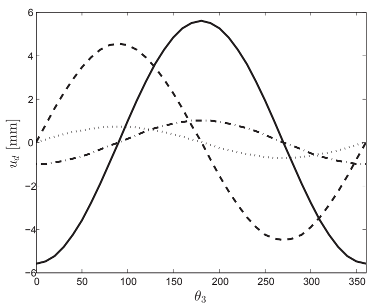

u_d for the curvature brace with respect to the fore-aft mode (dotted) and the side-to-side mode (dash-dotted) and u_d for the curvature-toggle-brace with respect to the fore-aft mode (dashed) and the side-to-side mode (solid)

Displacement of damper

Damping of Wind Turbine Tower Vibrations
Mark L. Brodersen
Motivation
Offshore wind turbine tower vibrations
Implementation of dampers
Criteria for effective damping
Tower modes
Brace concepts
Numerical models
Beam model and HAWC2 model
Results
Damper stroke
Attainable damping
Damper force
Free decay
Outlook

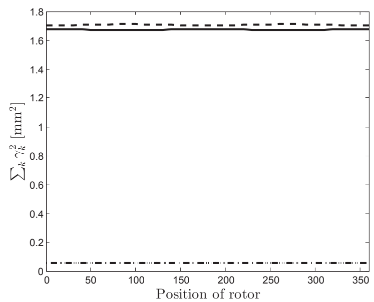

γ^2 for the curvature brace with respect to the fore-aft mode (dotted) and the side-to-side mode (dash-dotted) and γ^2 for the curvature-toggle-brace with respect to the fore-aft mode (dashed) and the side-to-side mode (solid)

Attainable damping

Damping of Wind Turbine Tower Vibrations
Mark L. Brodersen
Motivation
Offshore wind turbine tower vibrations
Implementation of dampers
Criteria for effective damping
Tower modes
Brace concepts
Numerical models
Beam model and HAWC2 model
Results
Damper stroke
Attainable damping
Damper force
Free decay
Outlook

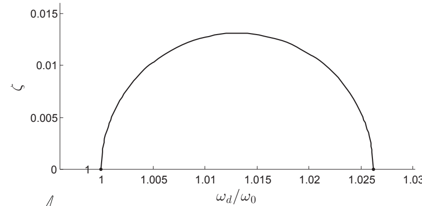

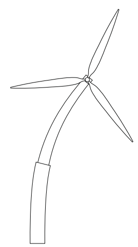

Attainable damping

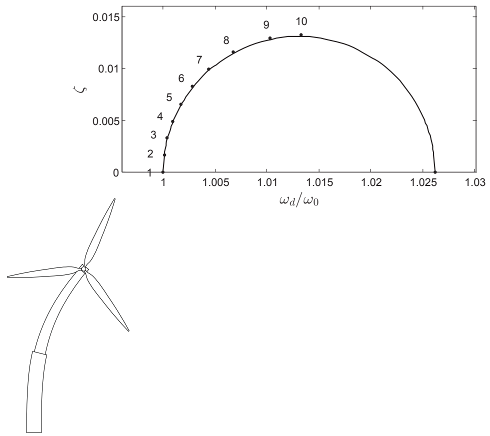

Damping of Wind Turbine Tower Vibrations

Mark L. Brodersen

- Motivation
  - Offshore wind turbine tower vibrations
- Implementation of dampers
  - Criteria for effective damping
  - Tower modes
  - Brace concepts
- Numerical models
  - Beam model and HAWC2 model
- Results
  - Damper stroke
  - Attainable damping
  - Damper force
  - Free decay
- Outlook

Attainable damping

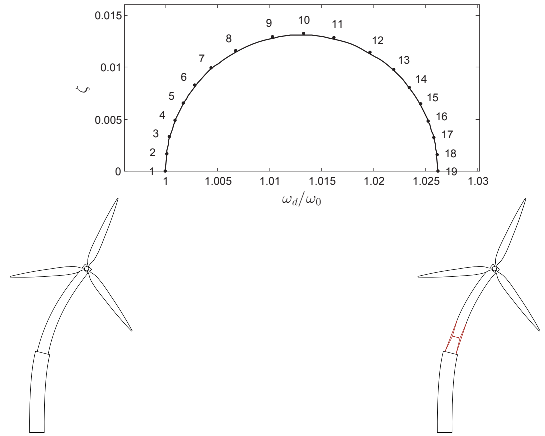

Damping of Wind Turbine Tower Vibrations
Mark L. Brodersen
Motivation
Offshore wind turbine tower vibrations
Implementation of dampers
Criteria for effective damping
Tower modes
Brace concepts
Numerical models
Beam model and HAWC2 model
Results
Damper stroke
Attainable damping
Damper force
Free decay
Outlook

Attainable damping

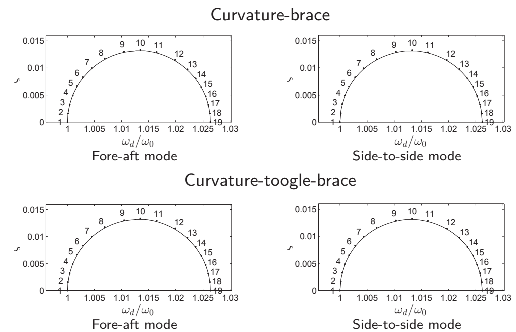

Damping of Wind Turbine Tower Vibrations
Mark L. Brodersen
Motivation
Offshore wind turbine tower vibrations
Implementation of dampers
Criteria for effective damping
Tower modes
Brace concepts
Numerical models
Beam model and HAWC2 model
Results
Damper stroke
Attainable damping
Damper force
Free decay
Outlook

Damper force

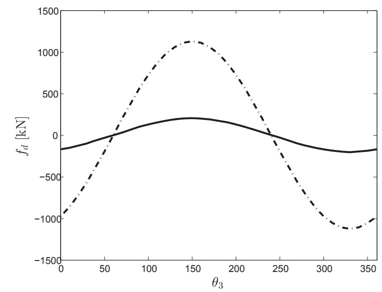

f_d for the curvature brace (dash-dotted)
and f_d for the curvature-toggle-brace (solid)

Damping of Wind Turbine Tower Vibrations
Mark L. Brodersen
Motivation
Offshore wind turbine tower vibrations
Implementation of dampers
Criteria for effective damping
Tower modes
Brace concepts
Numerical models
Beam model and HAWC2 model
Results
Damper stroke
Attainable damping
Damper force
Free decay
Outlook

Free decay

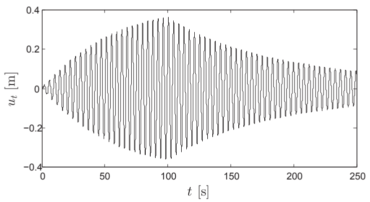

Damping of Wind Turbine Tower Vibrations
Mark L. Brodersen
Motivation
Offshore wind turbine tower vibrations
Implementation of dampers
Criteria for effective damping
Tower modes
Brace concepts
Numerical models
Beam model and HAWC2 model
Results
Damper stroke
Attainable damping
Damper force
Free decay
Outlook

Free decay

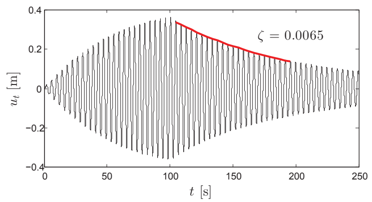

Damping of Wind Turbine Tower Vibrations
Mark L. Brodersen
Motivation
Offshore wind turbine tower vibrations
Implementation of dampers
Criteria for effective damping
Tower modes
Brace concepts
Numerical models
Beam model and HAWC2 model
Results
Damper stroke
Attainable damping
Damper force
Free decay
Outlook

Free decay

Damping of Wind Turbine Tower Vibrations
Mark L. Brodersen
Motivation
Offshore wind turbine tower vibrations
Implementation of dampers
Criteria for effective damping
Tower modes
Brace concepts
Numerical models
Beam model and HAWC2 model
Results
Damper stroke
Attainable damping
Damper force
Free decay
Outlook

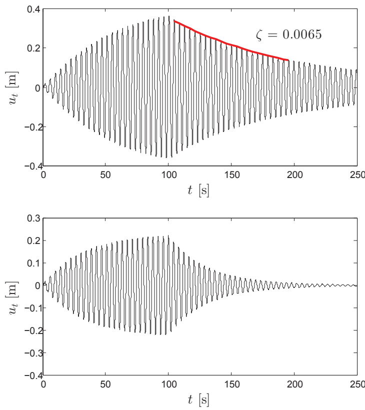

Free decay

Damping of Wind Turbine Tower Vibrations
Mark L. Brodersen
Motivation
Offshore wind turbine tower vibrations
Implementation of dampers
Criteria for effective damping
Tower modes
Brace concepts
Numerical models
Beam model and HAWC2 model
Results
Damper stroke
Attainable damping
Damper force
Free decay
Outlook

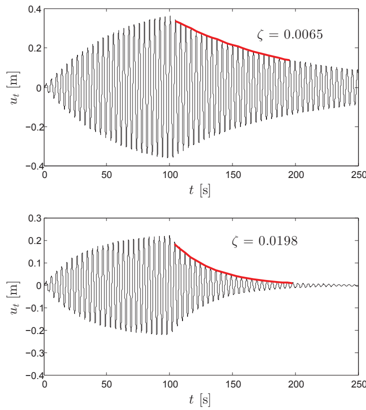

Outlook

Damping of Wind Turbine Tower Vibrations
Mark L. Brodersen
Motivation
Offshore wind turbine tower vibrations
Implementation of dampers
Criteria for effective damping
Tower modes
Brace concepts
Numerical models
Beam model and HAWC2 model
Results
Damper stroke
Attainable damping
Damper force
Free decay
Outlook

Summary

- Maximize attainable damping and damper stroke
  - Installation at the bottom of the tower
  - Stroke amplifying toggle brace
  - Attainable damping: 1.3 % critical
  - Optimum tuning independent of the orientation of the rotor
  - The same tuning can be used for both critical modes

Outlook

Damping of Wind Turbine Tower Vibrations
Mark L. Brodersen
Motivation
Offshore wind turbine tower vibrations
Implementation of dampers
Criteria for effective damping
Tower modes
Brace concepts
Numerical models
Beam model and HAWC2 model
Results
Damper stroke
Attainable damping
Damper force
Free decay
Outlook

Summary

- Maximize attainable damping and damper stroke
  - Installation at the bottom of the tower
  - Stroke amplifying toggle brace
  - Attainable damping: 1.3 % critical
  - Optimum tuning independent of the orientation of the rotor
  - The same tuning can be used for both critical modes

Ongoing work

- Physical implementation
- Experimental validation

F) Wind farm optimization

EERA-DTOC: How aerodynamic and electrical aspects come together in wind farm design, Gerard Schepers, Energy Research Center of the Netherlands

Benchmarking of Lillgrund offshore wind farm scale wake models in the EERA-DTOC project, K.S. Hansen, DTU

Variable Frequency Operation for Future Offshore Wind Farm Design: A Comparison with Conventional Wind Turbines, Ronan Meere, University College Dublin

Estimation of Possible Power in Offshore Wind Farms during Downregulation, PossPOW Project, Tuhfe Göçmen Bozkurt, DTU

EERA-DTOC: *How aerodynamic and electrical aspects come together in wind farm design*

G. Schepers, A van Garrel, E Wiggelinkhuizen, J. Pierik, E. Bot
(*ECN Wind Energy*)
Wei He (*Statoil Petroleum AS*)

Support by
FP7-ENERGY-2011-1/ n°282797

Contents

- *EERA-DTOC: Introduction*
- EERA-DTOC: Scenarios to be calculated
- EERA-DTOC: Results from a preliminary scenario calculated with ECN's tools FarmFlow and EEFARM

EERA-DTOC summary slide

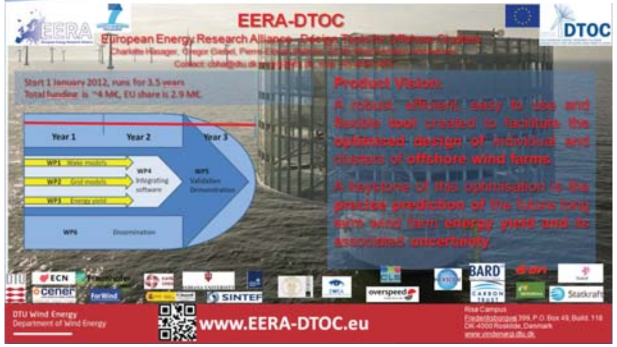

EERA-DTOC main idea

- Use and bring together existing models from the partners
- Develop open interfaces between them
- Implement a shell to integrate
- Fine-tune the wake models using dedicated measurements
- **Validate and demonstrate the final tool through likely scenarios**

Contents

- EERA-DTOC: Introduction
- *EERA-DTOC: Scenarios to be calculated*
- EERA-DTOC: Results from a preliminary scenario calculated with ECN's tools FarmFlow and EEFARM

Scenarios

- Demonstration of **INTEGRATED** design tool to verify user requirements
- Measurement data are scarce and synchronous measurement data for wind farm clusters are fully missing
  - Tools will be demonstrated on basis of likely scenarios.
- Industry is heavily involved in the definition of scenarios

Scenarios

Scenarios:
1. **Base and near future scenario**
   - *Base scenario*: Single 500 MW wind farm with 6 MW turbines,
   - *Near future scenario*:
     - Carried out in steps
       1. Single 1GW wind farm with 10 MW turbines
       2. Adding other wind farms → cluster
2. **Far future** scenario:
   - Offshore wind farm clusters including innovations, e.g. floating turbines

Scenario 1→2 reflects:
- A shift towards the future.
- Increasing complexity of the modeling problem
- A shift in target group:
  - Developers (base scenario)
  - Developers and strategic planners (far future scenario)

27-1-2014
7

Present study focusses on near future scenario

- Single 1000 MW wind farm (other wind farms will be added at later stage to form a cluster)
- 100*10 MW turbines
  - Innwind.EU 10 MW reference turbine
- 20 parallel grid lines (66 kV) connecting 5 turbines to a central sub station
- North Sea wind climate
- Distance to shore: ~125 km
- Water depth: ~40 m

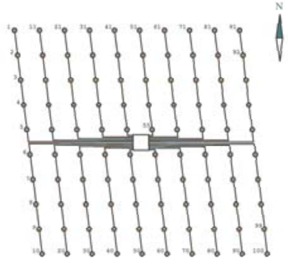

27-1-2014
8

Contents

- EERA-DTOC: Introduction
- EERA-DTOC: Scenarios to be calculated
- *EERA-DTOC: Results from a preliminary scenario calculated with ECN's tools FarmFlow and EEFARM*

'Preliminary' scenario

- Eventually the scenarios will be calculated with the final EERA-DTOC tool
- 'Preliminary' scenario calculated with a combination of ECN's aerodynamic (**FarmFlow**) and electrical tool (**EEFARM**)
  - Demonstrates value of **INTEGRATED** electrical-aerodynamic tool
  - Near future scenario, starting with 10D distance between the turbines (low aerodynamic losses versus high electrical losses and high costs for electrical infrastructure)
    - Decrease distance
      - Higher aerodynamic losses can be balanced versus lower electrical losses and lower costs for electrical infrastructure

27-1-2014
10

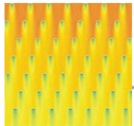

What is FARMFLOW?

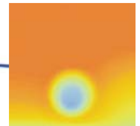

- Calculates:
  - Losses and added turbulence due to wakes
  - Annual energy production (AEP)
- The model is based on UPMWAKE [1])/WAKEFARM
  - Modified by ECN since 1993
  - Extensively validated with results from ECN's research farms and measurements from EU projects (e.g. ENDOW, Upwind, EERA-DTOC)

[1]) Crespo et al. 1988

11

FARMFLOW: Theory and the Model description

- Solves the Parabolized Navier-Stokes equation
- Turbines modelled as actuator disc, prescribed by C_{Dax}
- Wake modelled with a k-ε turbulence model

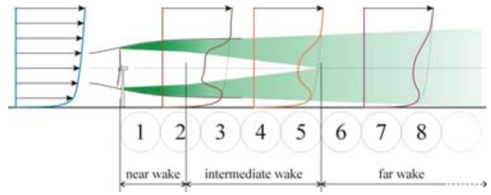

12

FARMFLOW: Advanced Model Properties

DTOC

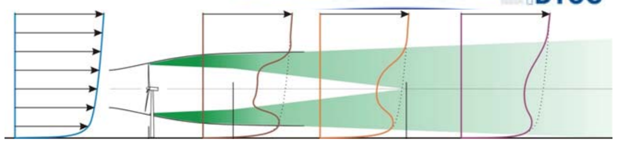

- Parabolisation: Fast, but how to solve the near wake where axial pressure gradients are significant?
- Solution:
  - Prescribe axial pressure gradients from free vortex wake method!
    - Fast database approach
    - Wake interaction fully modeled including the effect of a non-zero pressure gradient and retaining the (fast) parabolisation
- Adjusted k-ε turbulence model parameters in near wake to account for actuator disc assumption, based on:
  - Measurements from ECN's research farms and Horns Rev farm
  - Detailed wake measurements in TUDelft wind tunnel underway *)

*) Lorenzo Lignaroli, TUDelft, personal communication

What is EEFARM?

ECN

DTOC

- Program to study and optimise the electrical performance of wind farms.
- Program is used to determine the:
  - Energy production,
  - Electrical losses,
  - Component failure losses
  - Price of the produced electric power

EeFarm-II linked to FarmFlow!

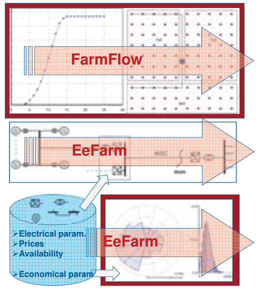

Aerodynamic power:
$P_{WT1} \ldots P_{WTN} = f\,(Vw, Vdir)$

Investments
P_{loss}
P_{fail}
per component

Levelized Production Costs

Reminder: Lay-out of 1GW farm

DTOC

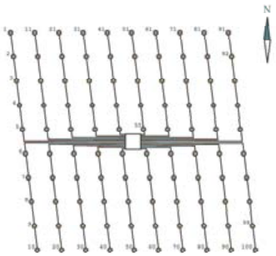

- 100 INNWIND.EU reference turbines of 10 MW
- Inter turbine distance is a variable between 3.6 and 10 D
- 20 parallel grid lines connecting 5 turbines to central substation

Annual Energy Production per row

DTOC

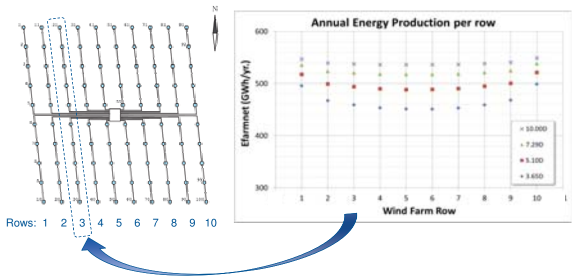

Main results

DTOC

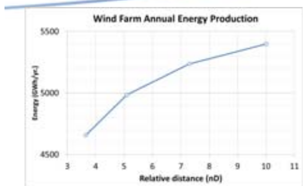

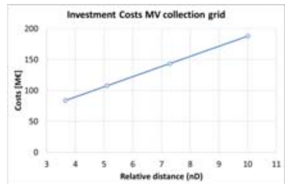

Net energy farm production (including aerodynamic **and** electrical losses)
- **Increase** with distance
- Increase **levels off** with distance

Investment costs of electrical infrastructure
- **Linear increase** with distance

Conclusions and Outlook

- Within the EERA-DTOC project a wind farm design tool is developed which combines existing wake models with electrical grid models
- The integrated tool is demonstrated on basis of likely scenarios
- A sequence of scenarios is defined ranging from a base scenario to a far future scenario with a near future scenario in between

Conclusions and Outlook, ctd

- The near future scenario has been calculated with a combination of ECN's aerodynamic tool FarmFlow and the electrical tool EEFARM
- The net energy yield increases with distance but the increase becomes less with distance
- The investment costs of the electrical infrastructure increase linearly with distance

Conclusions and Outlook, ctd

- The near future scenario has been calculated with a combination of ECN's aerodynamic tool FarmFlow and the electrical tool EEFARM
- An increase from 3.6 to 10 rotor diameters is earned back in 1.5 years with an energy price of 0.1 Euro/kWh
- First results from an overall cost model (using the energy yield and investments costs of the present study) indicate a decrease in COE when distance is increased from 3.5 to 10 rotor diameters but decrease becomes less with distance
- Work on a cost model which includes the actual FarmFlow/EEFARM parameters (energy yield and investment costs) is underway at ECN based on the former OWECOP model [1]

[1] S.A. Herman Probabolistic Cost model for analysis of offshore wind energy, costs and potential, ECN-I-02-007, 2002, Energy Research Centre of the Netherlands, ECN

Thank you very much for your attention

Benchmarking of Lillgrund offshore wind farm scale wake models

Kurt S. Hansen
Senior Scientist
DTU Wind Energy – Fluid Mechanics

Support by

Outline

- Motivation;
- Participants;
- Wind farm location, layout and challenges;
- Wake models;
- Benchmark flow cases;
- Results;
- Conclusion;
- Acknowledgement.

Motivation

- The wake modeling part of the EERA - DTOC (Design Tool for Offshore wind farm Clusters) project is to improve the fundamental understanding of wind turbine wakes and modeling.
- Many different types of wind farm wake models that have been developed during the last three decades.
- Two benchmark campaigns have been organized on the existing wind farm wake models available within the project.
- First benchmark deals with regular 8 x 10 turbines layout and medium internal spacing (7 – 10 D);
- The present benchmark represents an irregular layout of 48 wind turbines - with small internal spacing (3.3 – 4.3 - 7 D).

Participants

- E. Maguire, Vattenfall AB;
- P.-E. Rethoré, DTU Wind Energy;
- S. Ott, DTU Wind Energy;
- T.Göçmen, DTU Wind Energy;
- A. Penã, DTU Wind Energy;
- J.Prospathopoulos, CRES, Greece;
- G.Scheepers, ECN, The Netherlands;
- T. Young, RES-LTD, United Kingdom;
- J.Rodrigo, CENER, Spain.

Benchmark test case: Lillgrund offshore wind farm

Site Description:

- The Lillgrund offshore wind farm is located in Öresund, the body of water between Malmö, Sweden and Copenhagen, Denmark.
- Owner: Vattenfall AB – 100%
- The farm consists of 48 Siemens SWT-2.3-93 wind turbines, each producing a rated power of 2.3 MW with a rotor diameter of 93 m and a hub height of 65 m.
- The turbines are arranged in a dense array with separation of 3.3 rotor diameters (D) within a row and 4.3 D between the rows.

Lillgrund offshore wind farm, located Between Sweden & Denmark

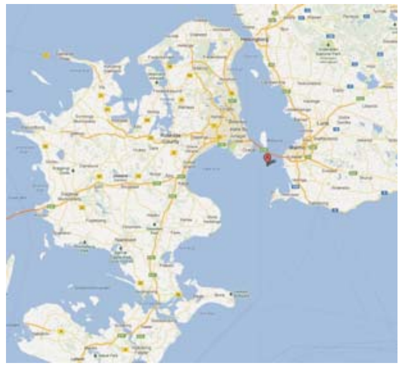

Location of Lillgrund offshore wind farm.

Layout of the Lillgrund offshore wind farm (Dahlberg, 2009).

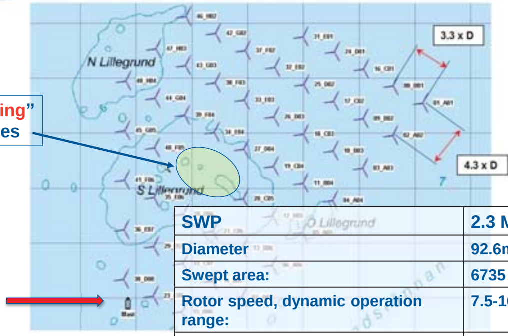

SWP	2.3 MW
Diameter	92.6m
Swept area:	6735 m^2
Rotor speed, dynamic operation range:	7.5-16 rpm
Hub height:	65 m

8 Rows of turbines: NE => SW
8 Columns of turbines: SE => NW

Lillgrund; Available measurements.

- 65 m mast (wind speed, turbulence, wind direction, air temperature), period: 2003 – 2006 (before WF installation, with high quality)
- 65 m mast (wind speed, turbulence, wind direction, air temperature) with medium quality, period: 2008 – 2010.
- SCADA data from WF as 10 minute statistics (mean values and stdev from each wind turbine). Period 2008 – 2012. Signals: power, pitch, rpm, nacelle wind speed and position.

Wind Farm wake models used in the benchmark

1. **SCADA** is the processed wind farm data to be compared with the wind farm wake models;
2. **FUGA** is a linearized actuator disc eddy-viscosity CFD model for offshore wind farm wake developed by DTU;
3. **CRESflowNS** is an elliptic k-ε actuator disc CFD model tailored for offshore wake simulation developed by CRES;
4. **FarmFlow** is a parabolized k-ε actuator disc CFD model tailored for offshore wake simulation developed by ECN;
5. **GCL** is the G.C. Larsen eddy-viscosity wake model v2009 developed by DTU;
6. **NOJ** is the original N.O Jensen model;
7. **AD/Ainslie** is an eddy-viscosity wake model developed by RES-LTD.

1. Flow case

Power deficit along a row of turbines - 3.3D & 4.3 D spacing at 9 m/s;

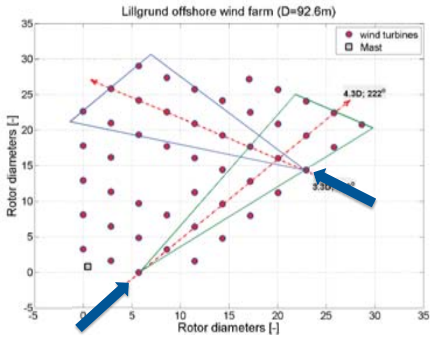

2. Flow case

Power deficit along a row of turbines - 3.3D & 4.3 D spacing – with "missing" wind turbines at 9 m/s;

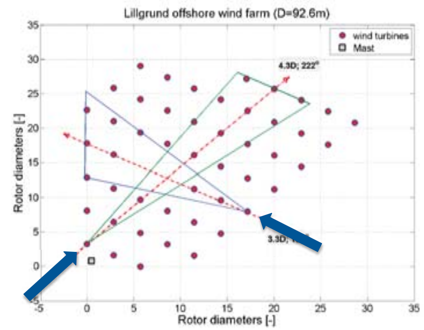

3. Flow case

1. Maximum power deficit – as function of turbulence intensity (TI) for a pair of turbines with 3.3D & 4.3 D spacing respectively;

DEMO: Δ= 5°; V_{hub}=9 m/s; spacing X D

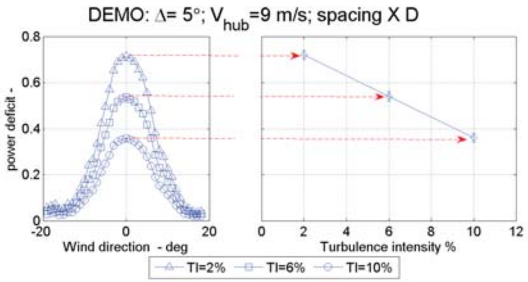

4. Flow case

Park efficiency for 0 – 360° inflow at 9 m/s & Δ=3°.

Inflow conditions:
-Wind direction (derived)
-Wind speed (derived)

Benchmark matrix

EERA-DTOC		Complete rows		Missing turbine(s)		Turbulence		Park
Institution/model		Row:3-120deg	Row:B-222deg	Row:5-120deg	Row:D-222deg	TI-3.3D	TI-4.3D	Efficiency
DTU	FUGA	1	1	1	1	1	1	1
CRES	CRESflowNS	1	1	1	1			
ECN	FarmFlow	1	1	1	1	1	1	1
DTU	GCJ-BinAve	1	1	1	1	1	1	1
DTU	GCJ-GauUnc	1	1	1	1	1	1	1
DTU	NOJ-BinAve	1	1	1	1			1
DTU	NOJ-GauUnc	1	1	1	1			1
DTU	NOJ(Penã)	1	1	1	1	1	1	1
RES-LTD	AD/Ainslie	1	1	1	1	1	1	1
CENER	GCJ-GauUnc	1	1	1	1	1	1	1
sum		10	10	10	10	7	7	9

63 simulation results have been provided from the 10 participants.

Basic definitions

Maximum deficit

Power deficit as function of inflow direction

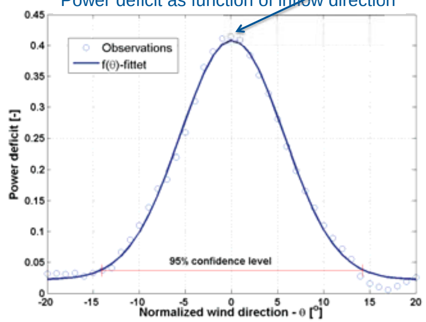

1 Flow case, 3.3 D spacing

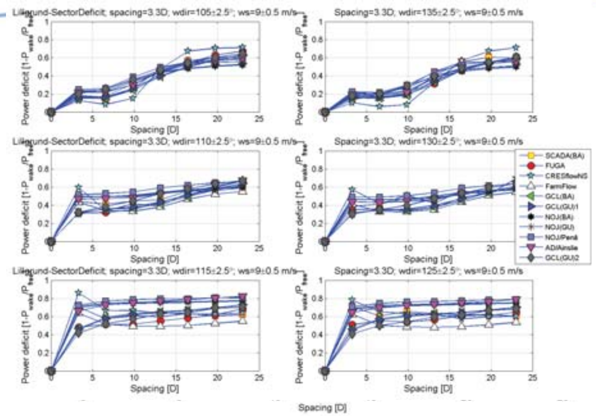

1 Flow case, 3.3 D spacing

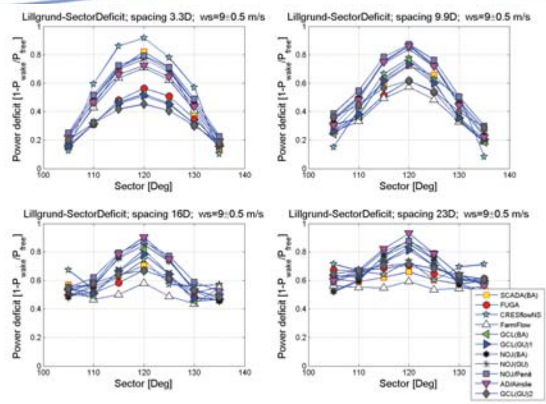

2 Flow case, 3.3 D spacing with "missing turbines"

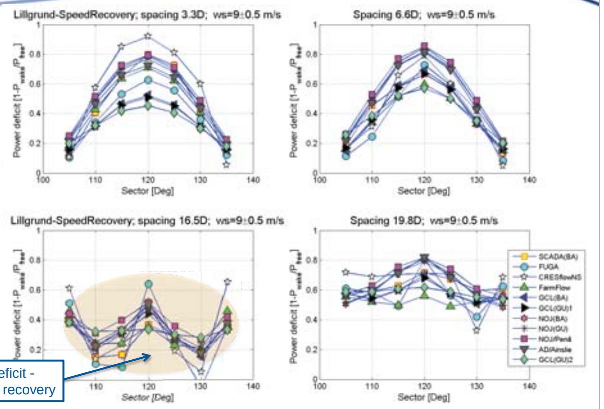

3 Flow case – turbulence dependence

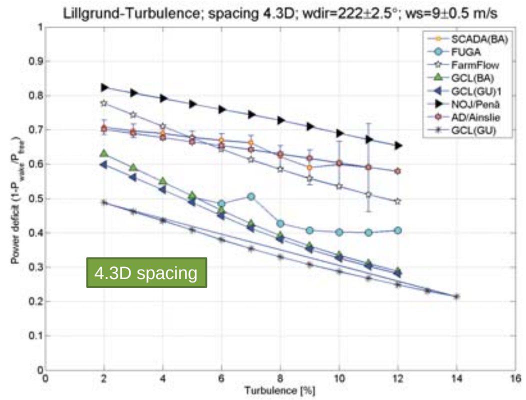

4 Flow case – park efficiency

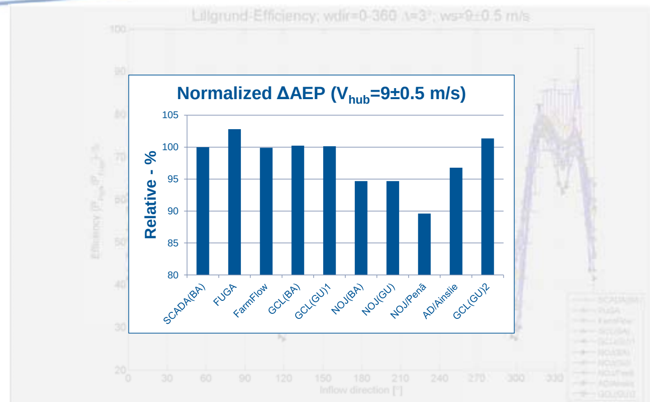

Conclusion

- Good agreement between wake model results and measurements;
- All models were able to predict the increased deficit between closely spaced turbines;
- The speed recovery was well reproduced;
- Linear relation between deficit and turbulence was well reproduced;
- Park power deficit for 0 - 360° inflow was well reproduced within 4-5% at 9 m/s;

Acknowledments

This work was supported by the EU EERA-DTOC project nr. FP7-ENERGY-2011/n 282797.

We acknowledge Vattenfall AB for having access to the SCADA data from the Lillgrund offshore wind farm.

Thank you for your attention

Variable Frequency Operation for Future Offshore Wind Farm Design: A Comparison with Conventional Wind Turbines

Dr. Ronan Meere*, Mr. Jonathan Ruddy and Dr. Terence O'Donnell

Electricity Research Centre,
University College Dublin,
Ireland.

Presentation Overview

- Introduction
- Motivation
- Variable Frequency Operation
- Modelling Power Losses of Wind Farm Components
- Results
- Conclusions

Introduction : Offshore Wind

- Offshore wind expected to contribute significantly to European targets
- Currently approx. 5 GW installed, 40 GW by 2020, 150 GW by 2030

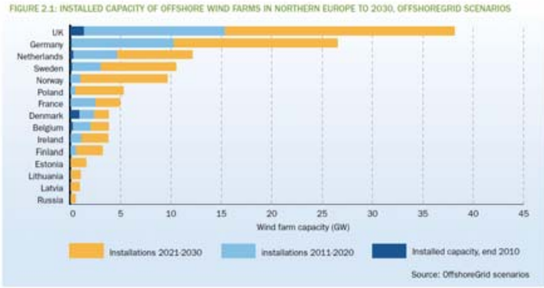

EWEA, Pure Power – Wind energy targets for 2020 and 2030, 2011 update, July 2011.

Introduction : Offshore Grid

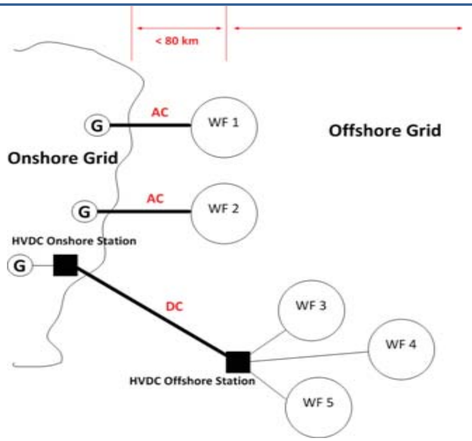

Offshore Connection Possibilities

- Converters at the turbine and at the VSC-HVDC transmission station
- AC to DC conversion just at the transmission converter level[1 2 3]

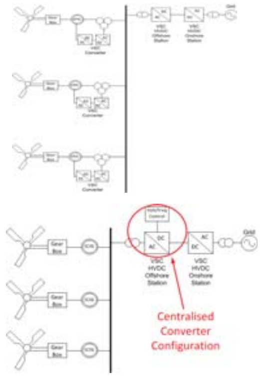

[1] R. Meere, M. O'Malley, A. Keane "*VSC-HVDC Link to Support Voltage/Frequency Fluctuations for Variable Speed Wind Turbines for Grid Connection*" IEEE PES Innovative Smart Grid Technologies (ISGT) Europe Conference, Berlin, Germany, October 14 – 17, 2012.
[2] V. Gevorgian et al. "*Variable Frequency Operation of a HVDC-VSC Interconnected Type 1 Offshore Wind Power Plant*" IEEE Power and Energy Society General Meeting July 22-26, pp 1-8, 2012.
[3] L. Trilla et al. "*Control of SCIG wind farm using a single VSC*" in Proc. 14th European Conference on Power Electronics and Applications, Aug. 30 -Sept. 1, 2011.

Motivation

- Power electronics has the highest failure rate for the wind turbine system

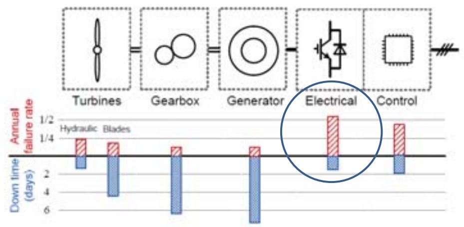

- Less power electronic converters results in greater wind farm reliability[4].

[4] B. Hahn, M. Durstewitz, K. Rohrig "*Reliability of wind turbines –Experience of 15 years with 1500 WTs*", Wind Energy: Proceedings of the Euromech Colloquium, S. 329–332, Springer-Verlag, Berlin.

Objective of the Study

- Type 4 Turbines optimise individual machines for maximum wind capture
- Variable Frequency Scheme : cluster of turbines are centrally controlled – lose up to 2% annual energy capture[2]

But…..

- Can you save with reduced power losses for variable/lower frequency operation in the wind farm ?
- Compare both variable and fixed frequency designs to see is there a difference in power loss

[2] V. Gevorgian et al. "*Variable Frequency Operation of a HVDC-VSC Interconnected Type 1 Offshore Wind Power Plant*" IEEE Power and Energy Society General Meeting July 22-26, pp 1-8, 2012

Offshore Wind and Variable Frequency

- Wind speed data is utilised to demonstrate the potential of the variable frequency approach
- Focus on wind speeds for turbine operational range at 2 sites off the west Irish coast for the years 2011/2012

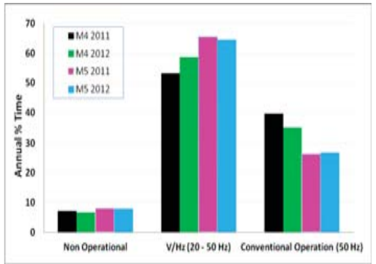

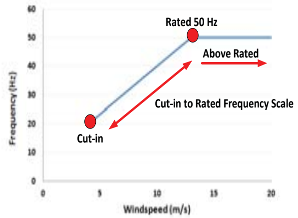

< 50 Hz Operation Impact at Farm

- The lower than rated frequency operation of the system may result in potentially lower power loss for the wind farm components - the **cables** and **transformers**

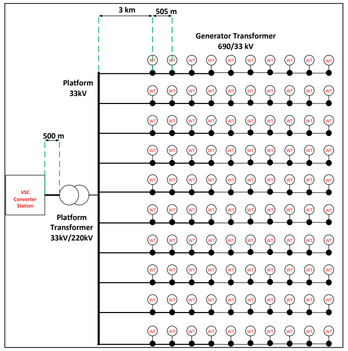

Key Losses for Wind Farm [100 (2MW)] :

- Cables
- Transformers
- Converters

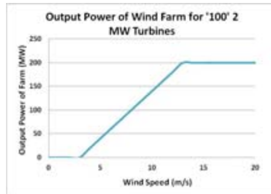

Impact: Cables

Cables:

- Charging current reduces with decreasing frequency: $Ic = 2\pi fClV$
- Decreasing V/Hz – Load current does not reduce at the same rate

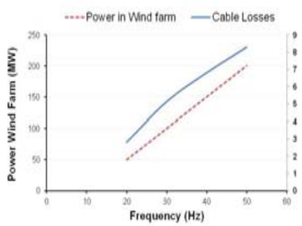

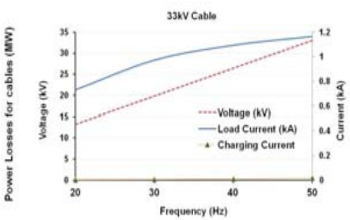

Impact: Transformers

Transformer:

- Core Losses – based on the Steinmetz Equation : $P_{core} = Kf^{\alpha} B_{pk}^{\beta}$
- Conduction Losses - I^2R winding losses (excludes AC resistance loss)

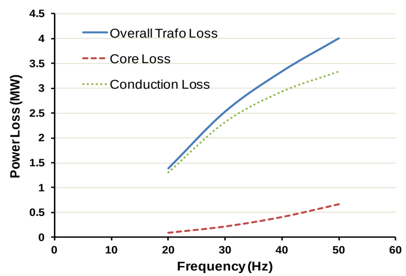

Variable vs. Fixed Frequency: Losses

FF : Fixed Frequency **VF : Variable Frequency**

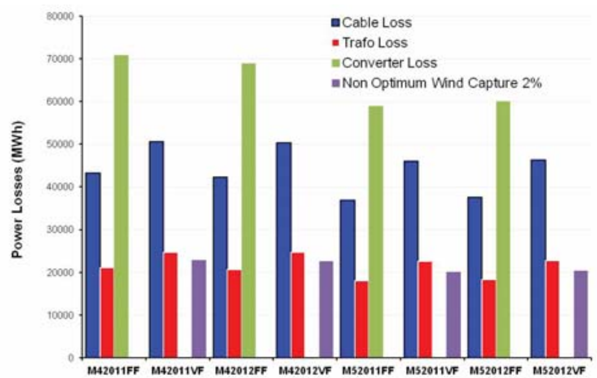

Variable vs. Fixed Frequency Results

- 2012/2011 Wind Data for 2 Irish Offshore Sites
- Variable Frequency 2.7-3.5 % **greater** total annual energy return

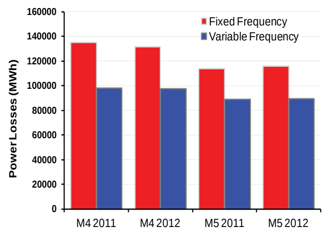

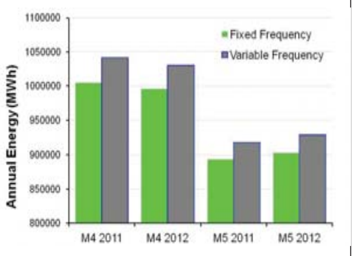

Variable vs. Fixed Frequency Results

- 2012 Mean Wind Speed Distribution for both sites
- Site specific – Site M5 is more favorable for variable frequency

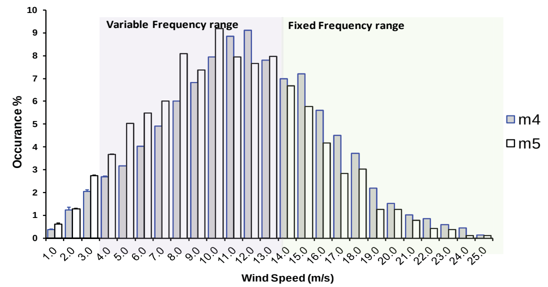

Variable vs. Fixed Frequency Results

- FF approach has 27% greater losses in terms of power loss (€) than VF

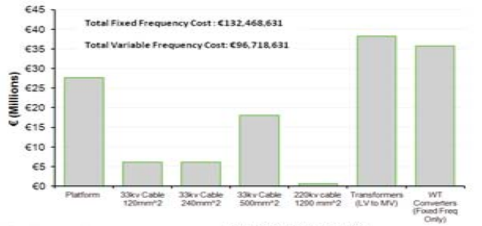

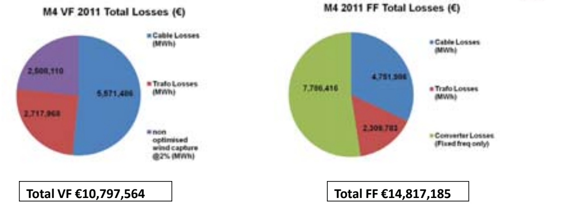

Conclusions and Future Work

- Question: Can you gain what you lost (2% Energy Capture with Variable Freq)

  Yes : Lower power loss, greater annual energy, less maintenance and lower cost

But, ……..

- Further work is needed to fully understand the non-optimum power capture calculation and also examine the impacts of wind farm layout on energy capture variation
- Reliability of power electronics will improve and costs will reduce
- This study is only opening the discussion – more detailed analysis and models are needed to further understand the potential of the approach

Thanks for your attention

Questions ?

PossPOW

Estimation of Possible Power in Offshore Wind Farms during Downregulation

Tuhfe Göçmen Bozkurt
PhD Student
DTU Wind Energy
Risø, Denmark

Co-authors: Gregor Giebel,
Pierre-Elouan Réthoré, Mahmood Mirzaei

DTU Wind Energy
Department of Wind Energy
1

Contents

PossPOW – Background & Aim of the Project

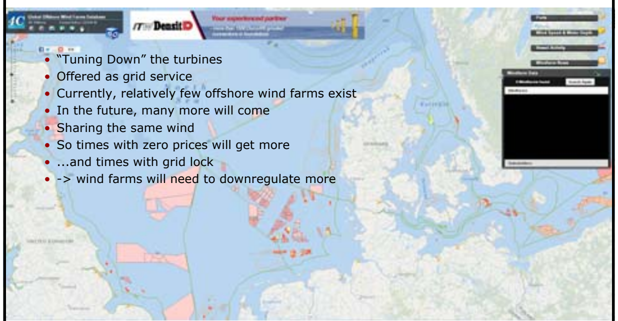

- "Tuning Down" the turbines
- Offered as grid service
- Currently, relatively few offshore wind farms exist
- In the future, many more will come
- Sharing the same wind
- So times with zero prices will get more
- ...and times with grid lock
- -> wind farms will need to downregulate more

Image source: 4C Offshore.com

PossPOW – Background & Aim of the Project

- "Reserve Power" of offshore wind farms (i.e. how much the wind farm is down-regulated) can be traded on the grid services markets
- Estimation of possible (or Available) power of a downregulated single turbine is straight-forward & widely known
- ...but when it comes to the wind farm scale:
  - $\sum Possible\ Power_{single\ turbines} > Possible\ Power_{wind\ farm}$
  - Simply because a turbine in the wake of a downregulated turbine sees more wind than usual $\longrightarrow$ decreased wake effect
- Energinet.dk, UK National Grid and other Transmission System Operators (TSOs) have no real way to determine the available power of a whole down-regulated wind farm
- *Therefore, PossPOW aims* $\longrightarrow$ verified & internationally accepted way to estimate the available power of downregulated offshore wind farms.

PossPOW – Wind Speed Estimation (Procedure)

- Nacelle Anemometer $\longrightarrow$
  - not always available + high inaccuracy
- Power Curve method $\longrightarrow$
  - no longer applicable due to downregulation
- Backward verification of wind speed

$$P = \frac{1}{2}\rho A_{rotor} C_P(\theta,\lambda) U_{eff}^3$$

- Power + rotor speed + pitch angle $\longrightarrow$ incoming wind speed

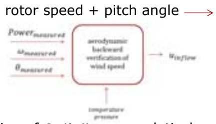

- Estimation of $C_P\ (\lambda,\theta)$ $\longrightarrow$ analytical model by Heier(1998)

$$C_P(\lambda,\theta) = c_1\left(\frac{c_2}{\lambda_i} - c_3\theta - c_4\theta^{c_5} - c_6\right) exp\left(\frac{-c_7}{\lambda_i}\right)$$

Where

$$\lambda_i = \left[\left(\frac{1}{\lambda + c_8\theta}\right) - \left(\frac{c_9}{\theta^3+1}\right)\right]^{-1}$$

Heier, S., 1998, *Grid Integration of Wind Energy Conversion Systems*, John Wiley & Sons Ltd, Chichester, UK, and Kassel University, Germany

PossPOW – Wind Speed Estimation (Procedure)

- Nacelle Anemometer $\longrightarrow$
  - not always available + high inaccuracy

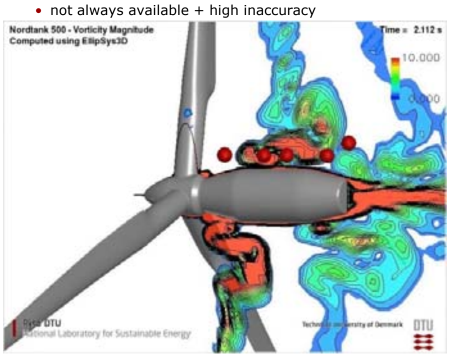

Zahle, F. and Sørensen, N. N. , 2011, Characterization of the unsteady flow in the nacelle region of a modern wind turbine. Wind Energy, 14: 271–283

PossPOW – Wind Speed Estimation (Procedure)

- Nacelle Anemometer ⟶
  - not always available + high inaccuracy
- Power Curve method ⟶
  - no longer applicable due to downregulation
- Backward verification of wind speed

$$P = \frac{1}{2}\rho A_{rotor} C_P(\theta,\lambda) U_{eff}^3$$

- Power + rotor speed + pitch angle ⟶ incoming wind speed

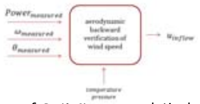

- Estimation of $C_P\ (\lambda,\theta)$ ⟶analytical model by Heier(1998)

$$C_P(\lambda,\theta) = c_1\left(\frac{c_2}{\lambda_i} - c_3\theta - c_4\theta^{c_5} - c_6\right) exp\left(\frac{-c_7}{\lambda_i}\right)$$

Where

$$\lambda_i = \left[\left(\frac{1}{\lambda + c_8\theta}\right) - \left(\frac{c_9}{\theta^3+1}\right)\right]^{-1}$$

Heier, S., 1998, *Grid Integration of Wind Energy Conversion Systems*, John Wiley & Sons Ltd, Chichester, UK, and Kassel University, Germany

PossPOW – Wind Speed Estimation (Single Turbine)

- Case Study : Horns Rev I ⟶ 80 Turbines & Vestas V80 2 MW-Offshore
  - 2 different second-wise datasets
    - Normal Operation : below cut-in to above rated wind speed

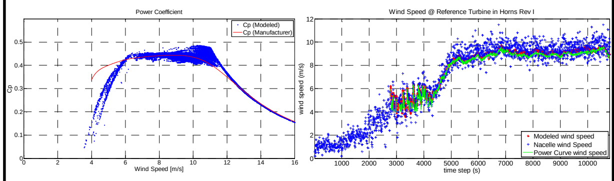

- Poor agreement in C_P for low wind speeds
- Over-estimation near transition region (control strategies)
- Nacelle anemometer seems to be measuring slightly higher

PossPOW – Wind Speed Estimation (Wind Farm)

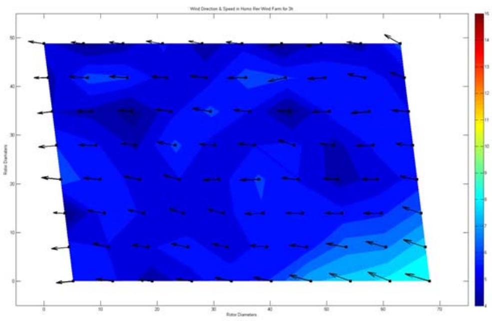

PossPOW – Wind Speed Estimation (DownRegulation)

- Downregulation: Horns Rev I Dataset

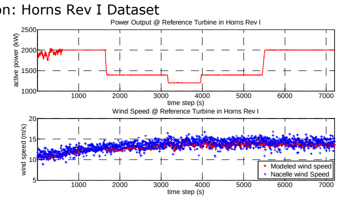

- App. 30% of downregulation
- Different control strategies applied
- Power Curve approach no longer applicable

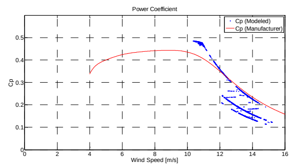

PossPOW – Wind Speed Estimation (DownRegulation)

- Downregulation: NREL 5MW[1] Simulations

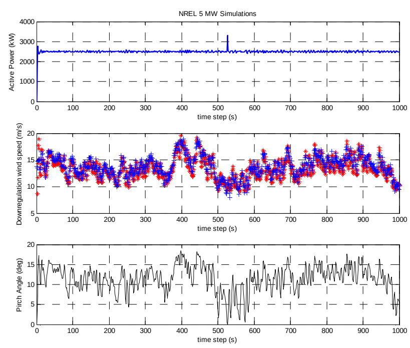

- 50% of downregulation
- Very good agreement with the simulations
- Active Pitch Control

1 Jonkman, J., Butterfield, S., Musial, S. and Scott G., Definition of a 5-MW Reference Wind Turbine for Offshore System Development. NREL/TP-500-38060 National Renewable Energy Laboratory, Golden, CO, 2007

PossPOW - Wake modelling

- After the flow speed is estimated during down regulation;
  - Wake effects are to be considered as if the turbine is operating ideally to achieve the available power
  - No wake models are to be developed
  - However, the wake models are tuned to give good average wake losses, not instantaneous ones ⟶ Real time implementation of the existing wake model(s)
    - Re-calibration of GCLarsen
- The modeled wind speed for upstream turbines, i.e. without any "reduced" wake effect will be input to the integrated wake model to obtain *Available Power* during downregulation

PossPOW - Wake model re-calibration (for real time)

- GCLarsen wake model
  - Simple and robust
  - Implemented in WindPro
  - Performs relatively well also on offshore
- 2 parameters to adjust in single wake case

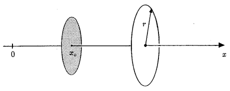

- $u_x(x,r) = -\frac{U_\infty}{9}\left(c_T A (x_0+\Delta x)^{-2}\right)^{\frac{1}{3}}\left\{r^{\frac{3}{2}}\left(3c_1^2 c_T A (x_0+\Delta x)\right)^{-\frac{1}{2}} - \left(\frac{35}{2\pi}\right)^{\frac{3}{10}}\left(3c_1^2\right)^{-\frac{1}{5}}\right\}^2$

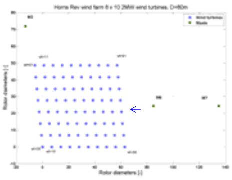

» All data filtered for wind direction 90±10˚
» Nonlinear Least Squares fitting
  - $R^2=0.96$ & $RMSE=0.41$

» Re-calibration was tested using the downregulated dataset
  - Re-calibrated model wind speed < Downregulated dataset

Larsen G. C., 1998, *A Simple Wake Calculation Procedure*, Technical Report Risø-M-2760, Risø

PossPOW - Wake model re-calibration (for real time)

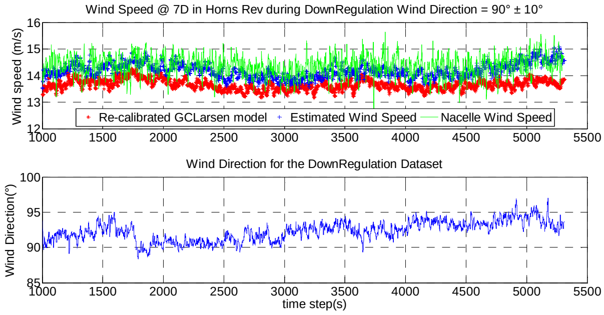

- Modeled wind Speed < Downregulated dataset as expected
- High quality data has been requested

PossPOW – Future Work

- Improve the recalibration of GCLarsen model for single wake case
  - Validation using normal operational dataset
- Re-parameterization for Wind Farm Scale
  - Dynamic factors
    - Wind direction variability ⟶ upstream turbines
    - Meandering
    - 'Sweeping' ⟶ row by row application of the model
- Consideration of other DTU Wake Models:
  - Dynamic Wake Meandering Model
  - Fuga
- The developed algorithm will be verified on some of the large offshore wind farms
  - Dedicated experiments are planned

PossPOW – Conclusion & Acknowledgements

- We are looking for a verified and accepted way to estimate the possible (or available) power of down-regulated offshore wind farms
  - Aerodynamic models for wind turbines
  - Wake modelling of large offshore wind farms
  - Stochastic model estimation & computer simulations
- First period of the project
  - ✓ *The estimation of wind speed using power, pitch & rotational speed*
- Second period
  - ✓ *Real-time implementation of the wake model(s) & finalized algorithm*
- Third period
  - ❑ *Measurements & verification of the algorithm*

- The partners of the PossPOW project are Vattenfall, Siemens, Vestas, and DONG

- PossPOW is a PSO project sponsored by Energinet, Contract ForskEL 10763

Thank you for your attention!

G1) Experimental Testing and Validation

Joint test field research – selected results from the RAVE initiative,
Michael Durstewitz, Fraunhofer IWES

Testing of towing and installation of Reinertsen self-installing concept,
Marit Reiso, Reinertsen AS

Wind turbine wake blind test; Prof Per-Åge Krogstad, NTNU

Wind Turbine Wake Experiment - Wieringermeer (WINTWEX-W),
Valerie-Marie Kumer, UiB

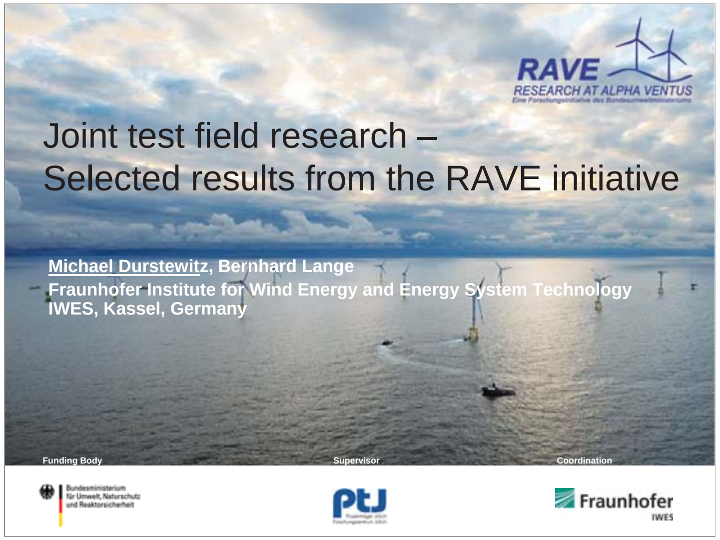
RAVE
RESEARCH AT ALPHA VENTUS
Joint test field research –
Selected results from the RAVE initiative
Michael Durstewitz, Bernhard Lange
Fraunhofer Institute for Wind Energy and Energy System Technology
IWES, Kassel, Germany
Funding Body
Supervisor
Coordination
Fraunhofer
IWES

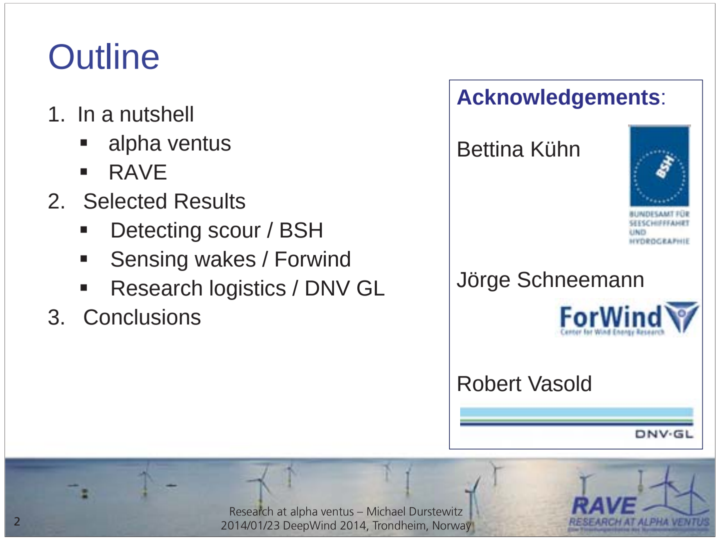
Outline
1. In a nutshell
▪ alpha ventus
▪ RAVE
2. Selected Results
▪ Detecting scour / BSH
▪ Sensing wakes / Forwind
▪ Research logistics / DNV GL
3. Conclusions
Acknowledgements:
Bettina Kühn
Jörge Schneemann
ForWind
Robert Vasold
DNV·GL
2
Research at alpha ventus – Michael Durstewitz
2014/01/23 DeepWind 2014, Trondheim, Norway
RAVE
RESEARCH AT ALPHA VENTUS

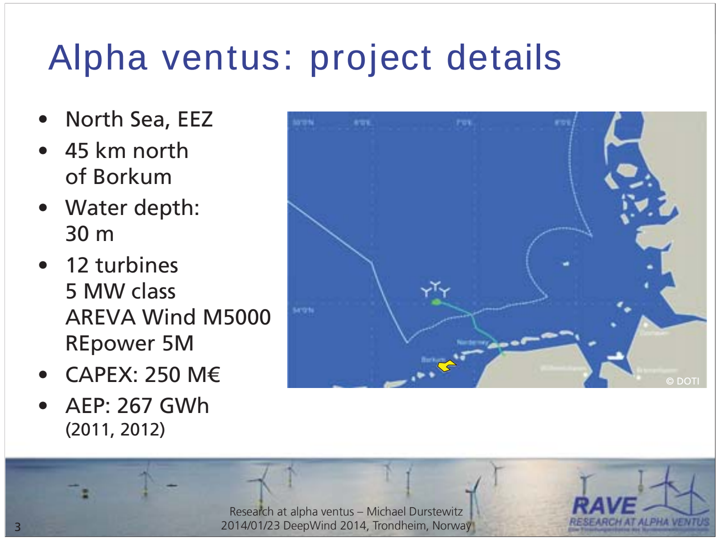
Alpha ventus: project details
• North Sea, EEZ
• 45 km north of Borkum
• Water depth: 30 m
• 12 turbines
5 MW class
AREVA Wind M5000
REpower 5M
• CAPEX: 250 M€
• AEP: 267 GWh
(2011, 2012)
© DOTI
3
Research at alpha ventus – Michael Durstewitz
2014/01/23 DeepWind 2014, Trondheim, Norway
RAVE
RESEARCH AT ALPHA VENTUS


RAVE – Research at alpha ventus
• Funded by the German Federal Environment Ministry (BMU)
• Accompanying research at the alpha ventus test site
• +30 R&D projects
• +50 mill. € support
• +50 project partners
• RAVE – Steering Committee :
Fraunhofer
AREVA
REpower
KIT
ForWind
alpha ventus
BAM
DEWI
Universität Stuttgart
4
Research at alpha ventus – Michael Durstewitz
2014/01/23 DeepWind 2014, Trondheim, Norway
RAVE
RESEARCH AT ALPHA VENTUS

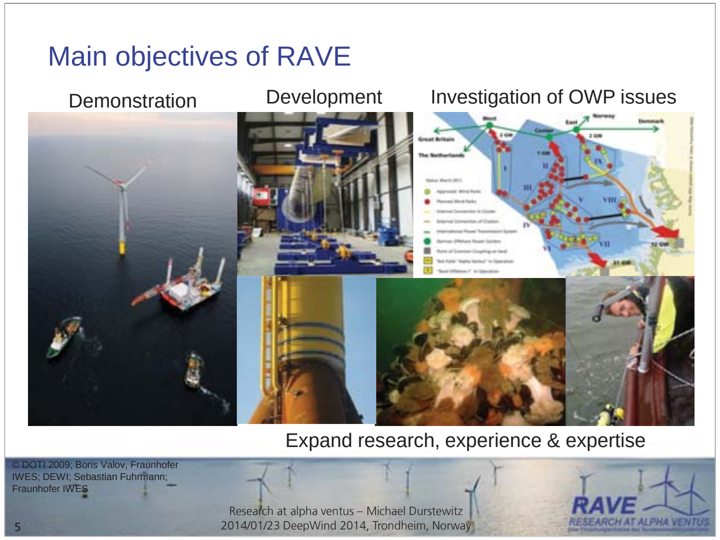
Main objectives of RAVE
Demonstration
Development
Investigation of OWP issues
Expand research, experience & expertise
© DOTI 2009; Boris Valov, Fraunhofer IWES; DEWI; Sebastian Fuhrmann; Fraunhofer IWES
5
Research at alpha ventus – Michael Durstewitz
2014/01/23 DeepWind 2014, Trondheim, Norway
RAVE
RESEARCH AT ALPHA VENTUS

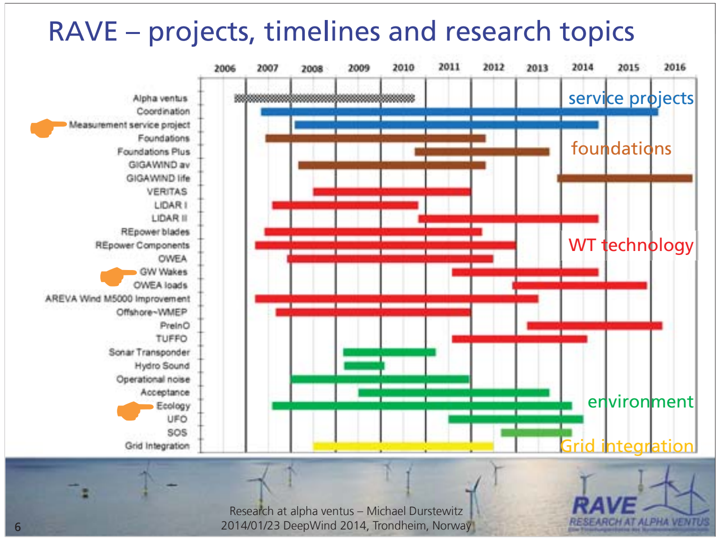
RAVE – projects, timelines and research topics
2006
2007
2008
2009
2010
2011
2012
2013
2014
2015
2016
Alpha ventus
Coordination
Measurement service project
Foundations
Foundations Plus
GIGAWIND av
GIGAWIND life
VERITAS
LIDAR I
LIDAR II
REpower blades
REpower Components
OWEA
GW Wakes
OWEA loads
AREVA Wind M5000 Improvement
Offshore-WMEP
PreInO
TUFFO
Sonar Transponder
Hydro Sound
Operational noise
Acceptance
Ecology
UFO
SOS
Grid Integration
service projects
foundations
WT technology
environment
Grid integration
6
Research at alpha ventus – Michael Durstewitz
2014/01/23 DeepWind 2014, Trondheim, Norway
RAVE
RESEARCH AT ALPHA VENTUS

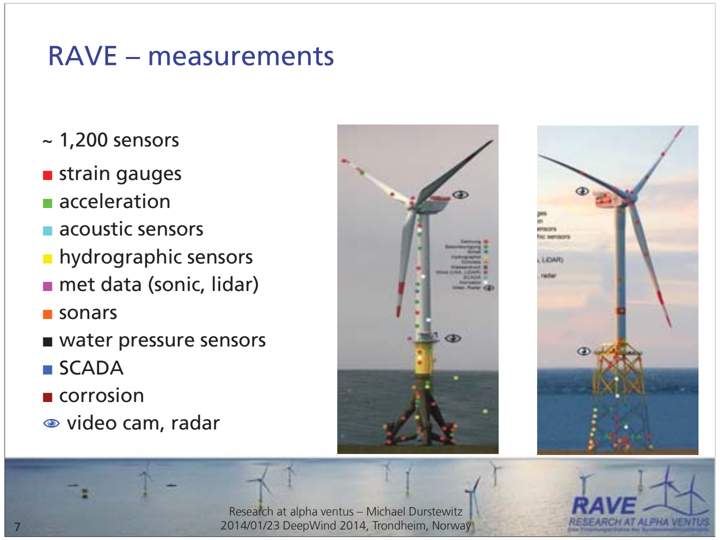
RAVE – measurements
~ 1,200 sensors
strain gauges
acceleration
acoustic sensors
hydrographic sensors
met data (sonic, lidar)
sonars
water pressure sensors
SCADA
corrosion
video cam, radar
Research at alpha ventus – Michael Durstewitz
2014/01/23 DeepWind 2014, Trondheim, Norway
RAVE
RESEARCH AT ALPHA VENTUS
7

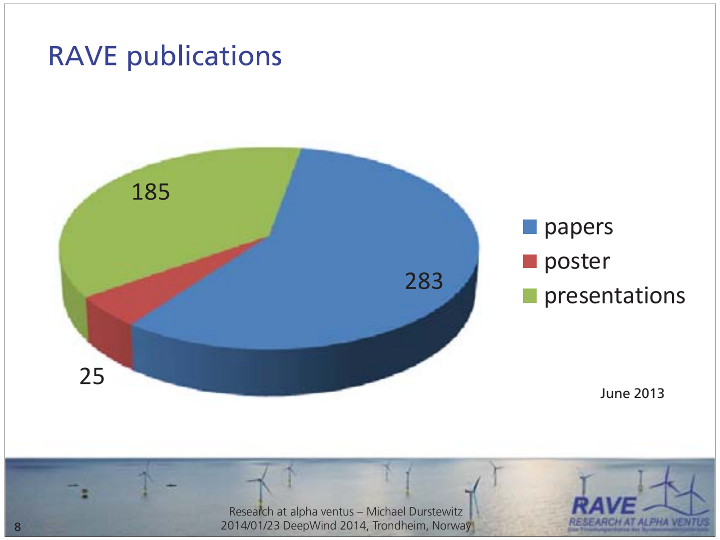
RAVE publications
185
283
25
papers
poster
presentations
June 2013
Research at alpha ventus – Michael Durstewitz
2014/01/23 DeepWind 2014, Trondheim, Norway
RAVE
RESEARCH AT ALPHA VENTUS
8

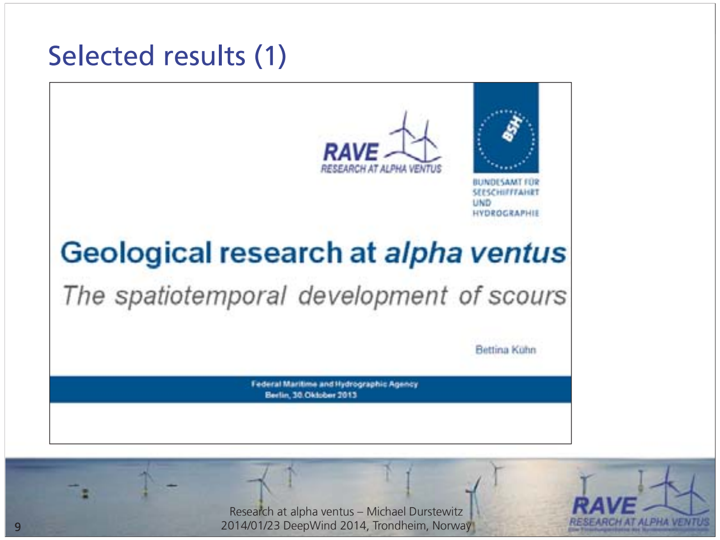
Selected results (1)
RAVE
RESEARCH AT ALPHA VENTUS
BSH
BUNDESAMT FÜR SEESCHIFFFAHRT UND HYDROGRAPHIE
Geological research at alpha ventus
The spatiotemporal development of scours
Bettina Kühn
Federal Maritime and Hydrographic Agency
Research at alpha ventus – Michael Durstewitz
2014/01/23 DeepWind 2014, Trondheim, Norway
RAVE
RESEARCH AT ALPHA VENTUS
9

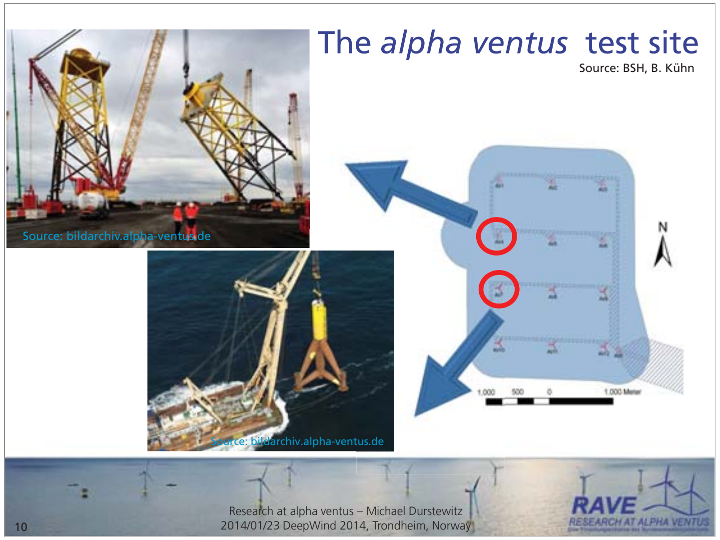
The alpha ventus test site
Source: BSH, B. Kühn
Source: bildarchiv.alpha-ventus.de
Source: bildarchiv.alpha-ventus.de
N
Research at alpha ventus – Michael Durstewitz
2014/01/23 DeepWind 2014, Trondheim, Norway
RAVE
RESEARCH AT ALPHA VENTUS
10

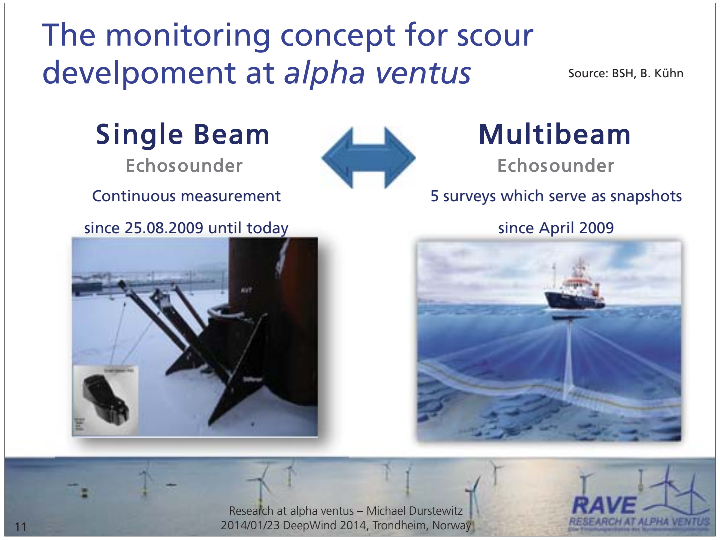
The monitoring concept for scour develpoment at alpha ventus
Source: BSH, B. Kühn
Single Beam
Echosounder
Continuous measurement
since 25.08.2009 until today
Multibeam
Echosounder
5 surveys which serve as snapshots
since April 2009
Research at alpha ventus – Michael Durstewitz
2014/01/23 DeepWind 2014, Trondheim, Norway
RAVE
RESEARCH AT ALPHA VENTUS
11

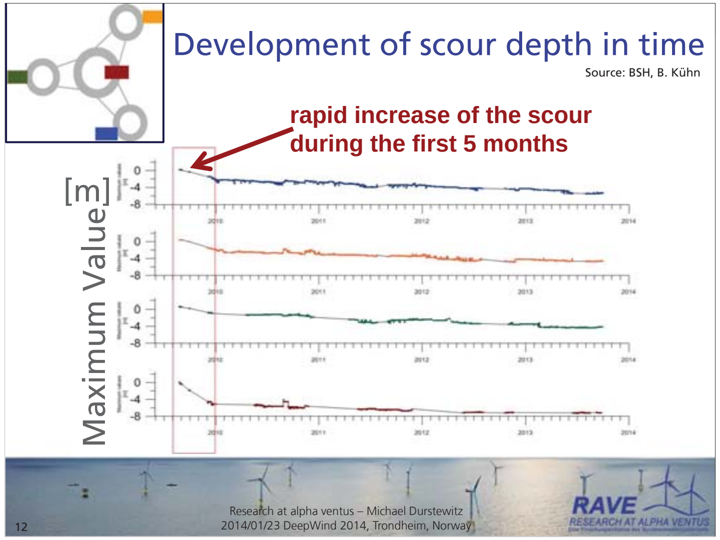
Development of scour depth in time
Source: BSH, B. Kühn
rapid increase of the scour during the first 5 months
Maximum Value [m]
0
-4
-8
Research at alpha ventus – Michael Durstewitz
2014/01/23 DeepWind 2014, Trondheim, Norway
RAVE
RESEARCH AT ALPHA VENTUS
12

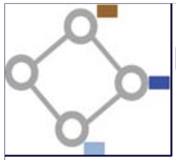

Development of scour depth in time

Source: BSH, B. Kühn

rapid increase of the scour
during the first 3 months

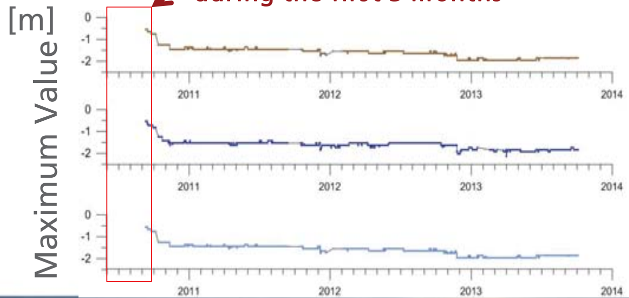

Research at alpha ventus – Michael Durstewitz
2014/01/23 DeepWind 2014, Trondheim, Norway
13

Development of the scour between 2010 and 2012

Source: BSH, B. Kühn

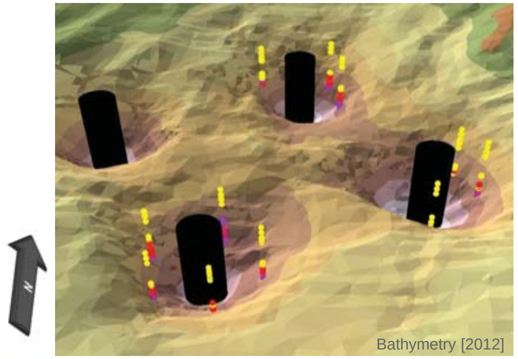

Research at alpha ventus – Michael Durstewitz
2014/01/23 DeepWind 2014, Trondheim, Norway
14

The geometry of the scour (AV4)

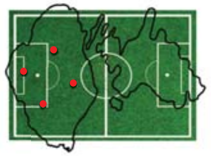

7140 m²
FIFA
standard

scour volume: 1700 m³
scour area: 2400 m²

accumulation volume: 200 m³
accumulation area: 1400 m²

Source: BSH, B. Kühn

Research at alpha ventus – Michael Durstewitz
2014/01/23 DeepWind 2014, Trondheim, Norway
15

Selected results (2)

Research at alpha ventus – Michael Durstewitz
2014/01/23 DeepWind 2014, Trondheim, Norway
16

Long range lidars in alpha ventus

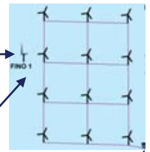

Location	Lidars
FINO 1	2 x WLS200S
Substation	1 x WLS200S

Research at alpha ventus – Michael Durstewitz
2014/01/23 DeepWind 2014, Trondheim, Norway
17

Long range lidar WindCube WLS200S V1.1

- Pulsed Doppler lidar with "all sky" scanner
- Various possible settings (pulse length, range gate length and position, averaging time,...) → lidar could be well adapted to current task
- Maximal performances (dependent on settings and atm. conditions):
  - Range: 50 – 8000 m
  - Spatial resolution: 25 m
  - Temporal resolution: 240 range gates @ 10Hz
  - Velocity resolution: 0.1 m/s
  - Positioning/ accuracy: 0.1° / 0.01°
  - Scenarios: VAD, DBS, RHI, PPI, staring, "complex trajectory"

Research at alpha ventus – Michael Durstewitz
2014/01/23 DeepWind 2014, Trondheim, Norway
18

Example of „long-range" measurements
Scan of azimuth at constant elevation

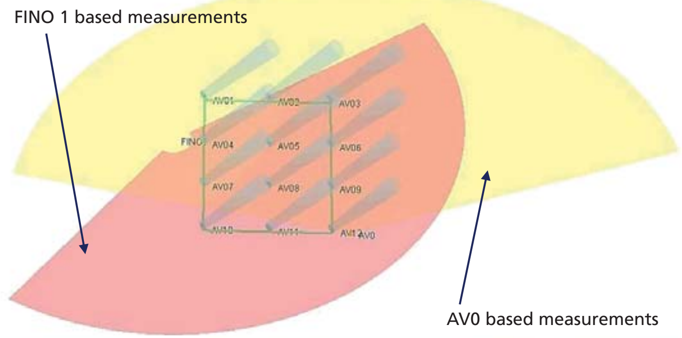

Example of „long-range" measurements
Radial wind speed at SW wind

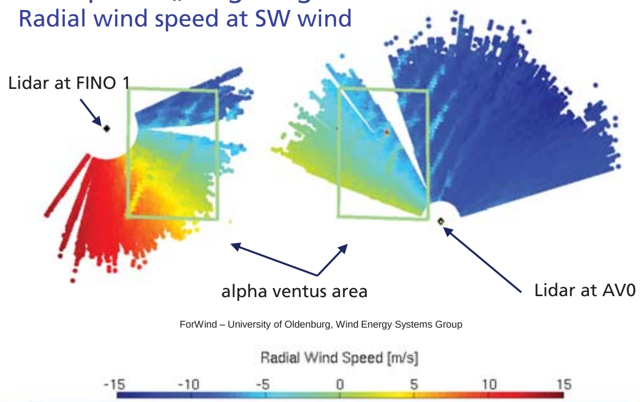

Next steps

- Coupling of data measured at FINO 1 and AV0
  - ⇒ "Dual Doppler Lidar"
- Synchronisation of two lidars on (quasi-) arbitrary 2D trajectories
  - ⇒ 2D cut of wind field
  - ⇒ "Remote met tower"
  - ⇒ Comparison to floating / ship lidar of FHG-IWES

Contact: Jörge Schneemann <joerge.schneemann@forwind.de>

Selected results (3)

Transportation of RAVE personnel

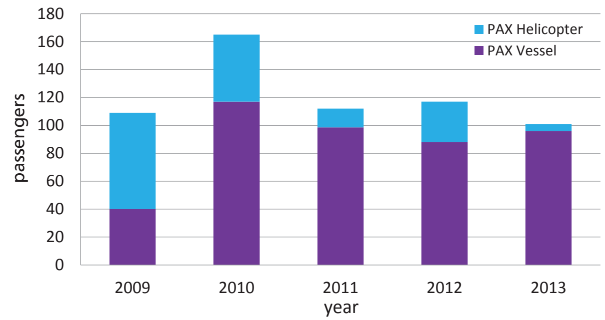

Source: DNV GL / Robert Vasold

Logistics: Main Issues and bottlenecks

- Weather and port restrictions
- PAX capacity bottlenecks
- Technical problems
- Work task priorities
- Limitations of accompanying personal
- HSE qualifications

Source: DNV GL / Robert Vasold

Summary

- Alpha ventus performs good
- Successful research cooperation
- New findings achieved
- New questions arose
- Further R&D is needed
- Increasing 3rd-party interest on data

Wind turbine Blind Test 3
Model experiments and predictions

Per-Åge Krogstad and Lar Roar Sætran
The Norwegian University of Science and Technology, Trondheim, Norway

DeepWind-2014, Trondheim 22-24 January, 2014

Background :

* Nowitech and Norcowe has about 35 PhD students together, many of these use or develop models for wind turbine performance predictions
* Full scale data bases not suited for prediction verifications
* Most multi-turbine model tests performed on very small models
* Interaction between turbines hard to predict
* How accurate are wind farm performance predictions?

Need for high quality turbine data bases for model verifications

Blind test 1 (Bergen October 2011):

* Single turbine in wind tunnel, tested with uniform inlet velocity and low turbulence intensity
* Turbine geometry specified; predict turbine performance and wake development

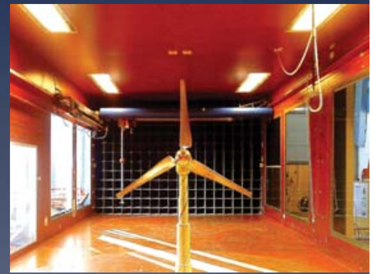

Compulsory results: C_P

10 sets of data from 8 groups

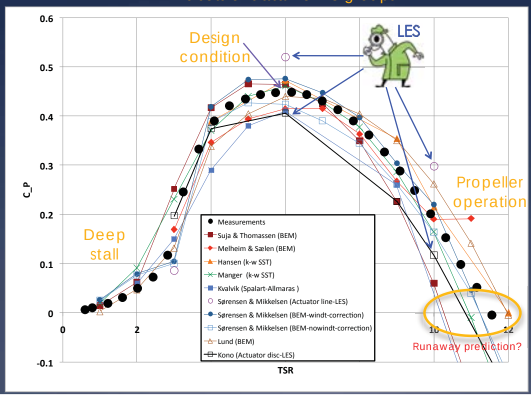

Wake data, X/D=5: Design condition; TSR = 6

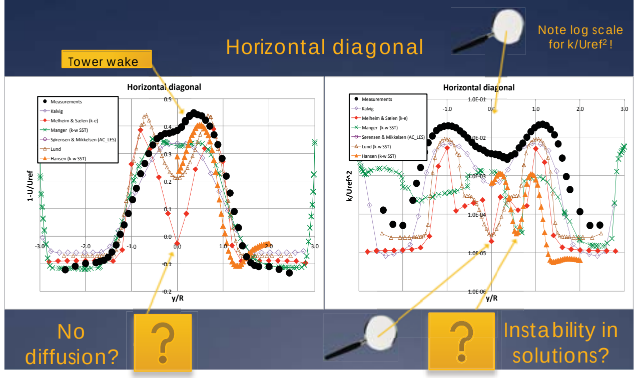

Blind test 2 (Trondheim October 2012):

* Two in-line wind turbines tested with uniform inlet velocity and low turbulence intensity
* Turbine geometry specified; predict turbine performances and wake development downstream of second turbine!

Power coefficient: C_P

9 sets of data from 8 groups

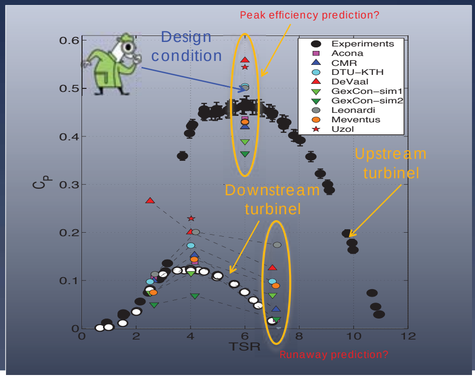

Wake data, X/D=4 downstream of T_2:

T1: design condition; TSR = 6,

T2: peak efficiency; TSR = 4

Horizontal diagonal

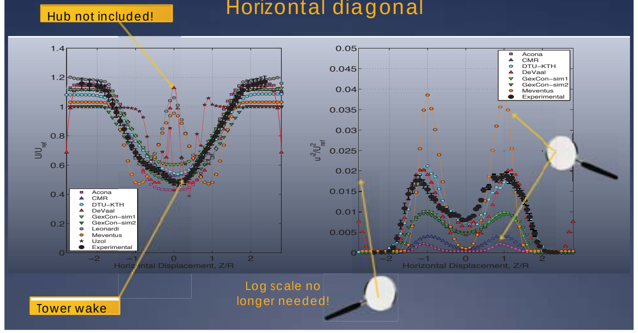

Blind test 3 (Bergen December 2013):

- Two in-line wind turbines offset sideways by approximately D/2
- Uniform flow, with 0.2 and 10% turbulence intensity
- Turbine geometry and turbulence field specified;

Predict turbine performances and wake development downstream of second turbine!

Contributors:

- Alcona Flow Technology; E. Manger (fully resolved 3D model/Fluent/k-ω SST, transient)
- CD-adapco; S. Evans & J. Ryan (Star-CCM+/k-ω SST and Realizable k-ε)
- CMR; A. Hallanger & I.Ø. Sand (Music by CMR, BEM model with hub but no tower, standard k-ε and subgrid model)
- DTU Mech. Eng. / KTH Mechanics; R. Mikkelsen, S. Sarmast, H.S. Chivaee & J.N. Sørensen (actuator line/LES)
- GexCon; M. Khalil (Flacs-wind by GexCon, actuator disk, standard k-ε, transient)

Case A, no grid: C_P & C_T

6 sets of predictions from 5 contributors

Filled symbols: Upstream turbine (T_1)
Open symbols: Downstream turbine (T_2)

Black symbols: Measurements

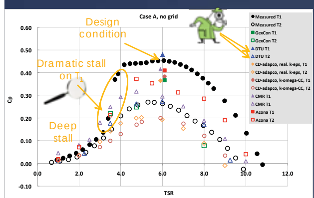

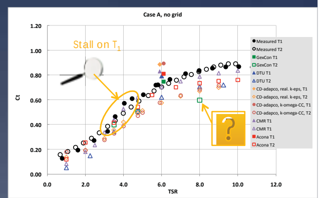

DTU has predicted C_p for both turbines extremely well.
C_T mostly underpredicted for T_2 !

Case B, with grid: C_P & C_T

5 sets of predictions from 4 contributors

Filled symbols: Upstream turbine (T_1)
Open symbols: Downstream turbine (T_2)

Black symbols: Measurements

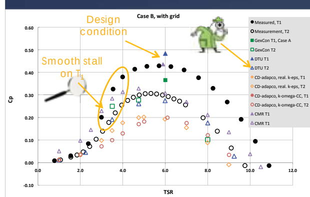

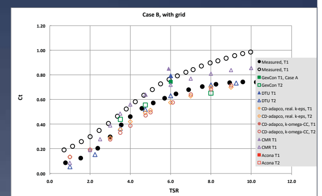

Smooth stall for T_1 and max C_p slightly reduced with turbulence
Max C_p for T_2 somewhat increased
C_T reduced for T_1 but hardly affected for T_2

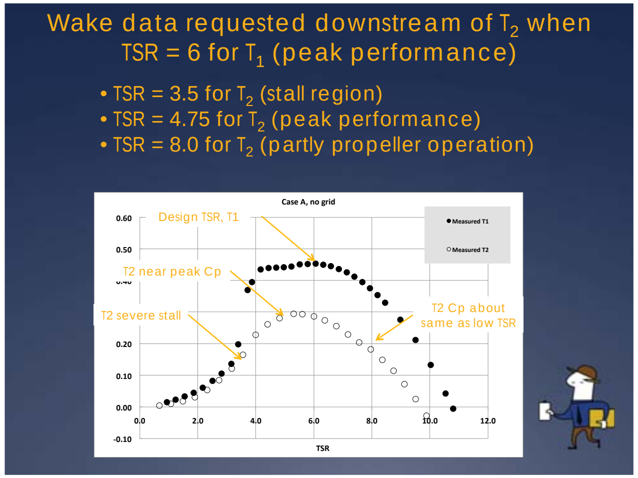

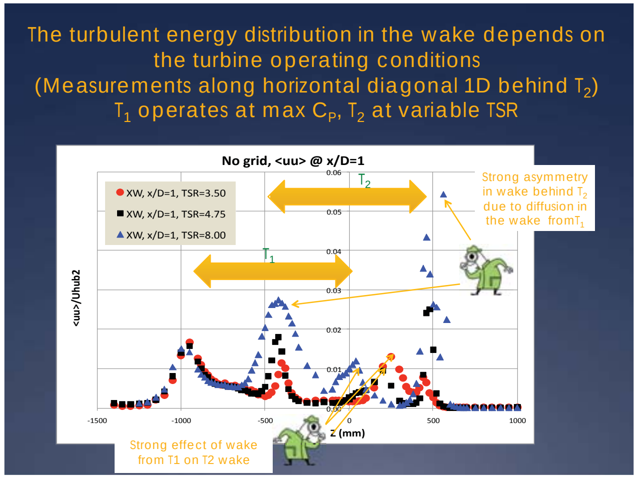

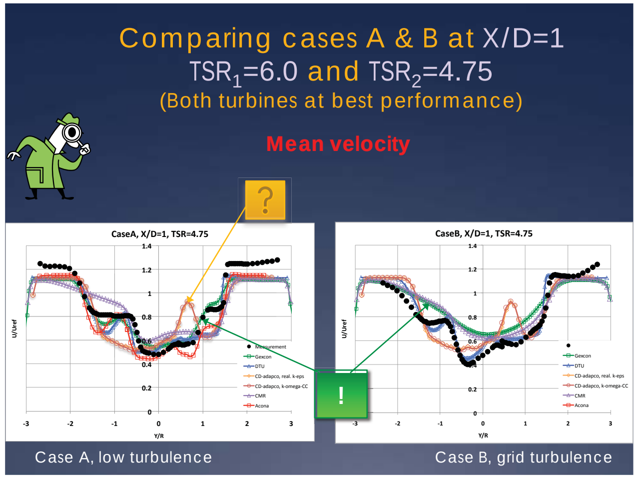

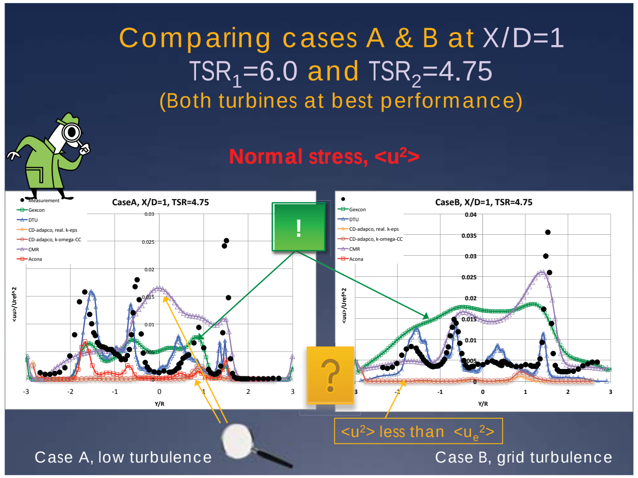

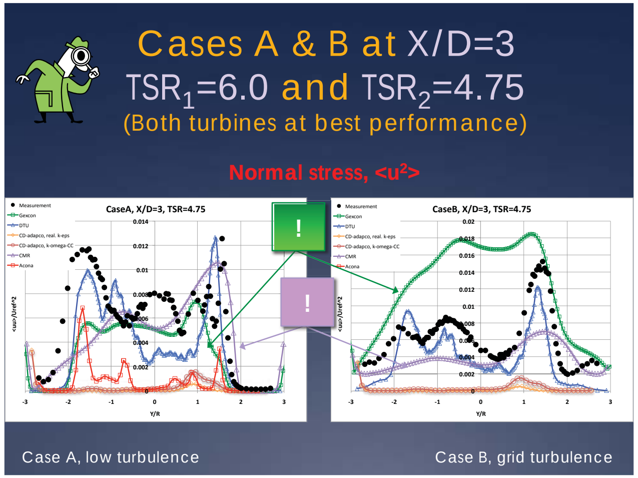

Tentative conclusions....

- The test case proved to be as challenging as we hoped for, with strong non-homogeneities in the mean velocity and multiple sharp peaks in the stress distributions.
- It is a bit surprising that there is still a significant scatter in predicting Cp and Ct of T1 at its design condition for the low turbulence case when the data has been out for 2 years.
- Some of the methods reproduced very few of the details that characterized the interactions between the two wakes.
- Some predictions showed strong sensitivities to the background turbulence while others were completely insensitive to this.
- The only Large Eddy Simulation this year proved to be very capable of reproducing all changes in the flow. Is this because LES is superior or because DTU did a good job? Another LES would have been welcome!


Thank you for your attention.
Questions?

WINTWEX-W

Wind Turbine Wake Experiment - Wieringermeer

ECN test site Wieringermeer

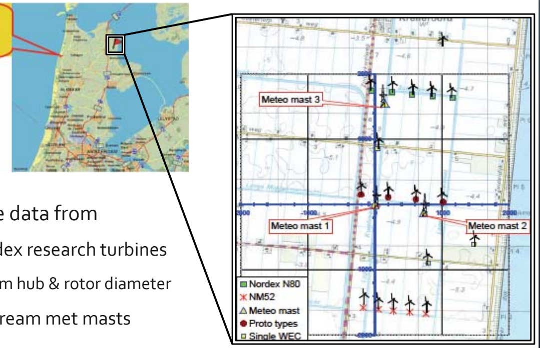

- Available data from
  - 5 Nordex research turbines
    - 80 m hub & rotor diameter
  - 6 upstream met masts

ECN test site Wieringermeer

- Met mast 3
  - 3 sonic anemometers at 52 m, 80 m and 109 m

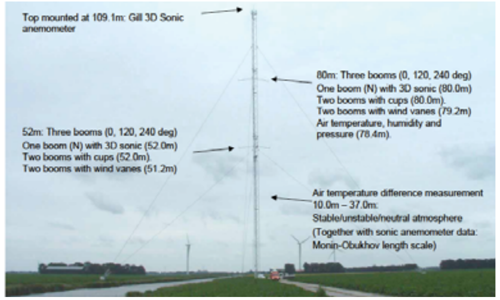

ECN test site Wieringermeer

- Analysis of 2 years met mast data (met mast 1&3)
  - Main wind direction at 71,6 m: SW
  - Most frequent wind speed at 71,6 m: 7 m/s
  - Maximum turbulence intensity at 80 m: NE

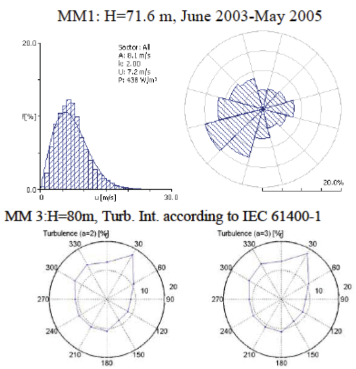

Campaign setup

- Additional measurement equipment aligned in the main wind direction (210°)
  - 1x Windcube 100s
  - 3x Windcube v1
  - 1x Windcube v2
  - 1x Zephir DM
  - 1x SUMO

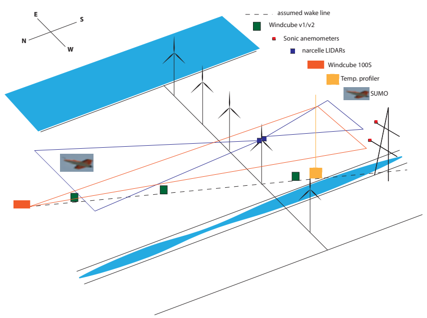

Campaign setup

- WindCube v1

Performances	
Range	40 – 200 m
Probe length	20 m
Data sampling rate	4s
Scanning cone angle	30°

Campaign setup

+ Measurement Methods

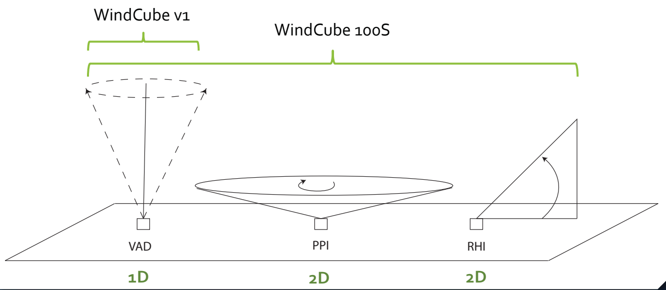

Campaign setup

+ WindCube 100S

Performances	
Range	100 – 3500 m
Probe length	50 m
Data sampling rate	1s / deg
Azimuth angle	0° - 360°
Elevation angle	-10° - 190°

Campaign Setup

+ Rotor diameter (D): 80 m
+ Distance: 973 m (12.2 D)
+ Area of interest: 2D x 10D

Type	Azimuth	Elevation	Speed	Duration
PPI	198° - 258°	2.4°	6°/sec	10 sec
PPI	258° - 198°	4.7°	6°/sec	10 sec
PPI	198° - 258°	7.1°	6°/sec	10 sec
RHI	228°	60° - 0°	6°/sec	10 sec
RHI	228°	0° - 60°	6°/sec	10 sec
RHI	228°	60° - 0°	6°/sec	10 sec
Sampling rate:				1 min

Campaign Setup

+ New scan setup

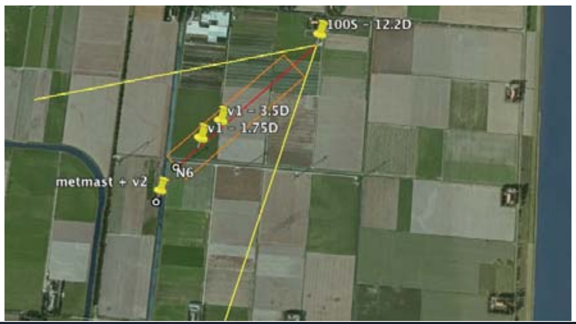

First picture

+ 60° PPI at 3° elevation with a scan speed of 6°/sec
+ 1st row wakes of 3 Nordex research turbines
+ 2nd row wakes of prototypes

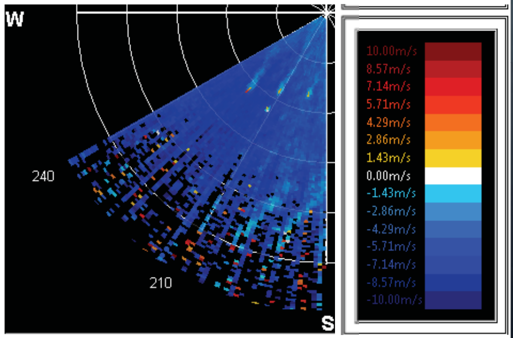

Outlook

+ Planed duration of the campaign
  + November 2013 – April 2014
+ Research aims
  + Test of WLS100S performance for wake measurements
  + Tests of different scan patterns for wake studies
  + Investigations of wake characteristics
    + Extension and persistency for different weather conditions
    + Meandering
  + Model validation studies

G2) Experimental Testing and Validation

Design of a 6-DoF Robotic Platform for Wind Tunnel Tests of Floating Wind Turbines,
Marco Belloli, Politecnico di Milano

Experimental study on wake development of floating wind turbine models,
Stanislav Rockel, ForWind, Univ Oldenburg

Floating Wind Turbines, Prof Paul Sclavounos, MIT

Numerical CFD comparison of Lillgrund employing RANS, Nikolaos Simisiroglou, WindSim AS

Design of a 6-DoF Robotic Platform for Wind Tunnel Tests of Floating Wind Turbines

Marco Belloli

Dipartimento di Meccanica Politecnico di Milano

Hexafloat: Motivation and objectives

Motivation

- Some numerical codes to to simulate FOWT dynamics is been developing from different research groups all over the world.
- These very sophisticated numerical tools require experimental data to validation
- There are a few of full scale data available and in most cases these data are not complete.

Objectives

- This work aims at proposing an approach to test scale models of FOWT complementary to wave basin testing.
- The design of a 6 degrees-of-freedom (DoF) robot, called “HexaFloat”, capable of reproducing the floating motion of a scale FOWT for wind tunnel experiments. This approach gives the chance to investigate the aerodynamics of using aeroelastic FOWT scale models in a 14mx4m civil boundaryl ayer test section

POLITECNICO DI MILANO

Hexafloat: experimental tool

An experimental tool to validate the numerical models to:

- Aero-Hydroelastic and floating codes
- Aerodynamic interaction
- Control strategies

- Known lab conditions
- Aerodynamic parameters (Reynolds Number effects)

- Real time forces measurement
[rotor, nacelle, tower, blades]
- Wake measurement
- Overall aerodynamic forces measured at the base of the tower
- Dynamic behavior parameters

POLITECNICO DI MILANO

Politecnico di Milano Wind Tunnel

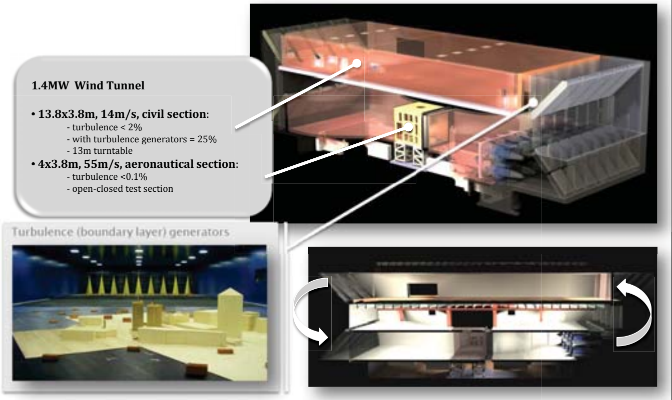

POLITECNICO DI MILANO

FOWT: HIL approach

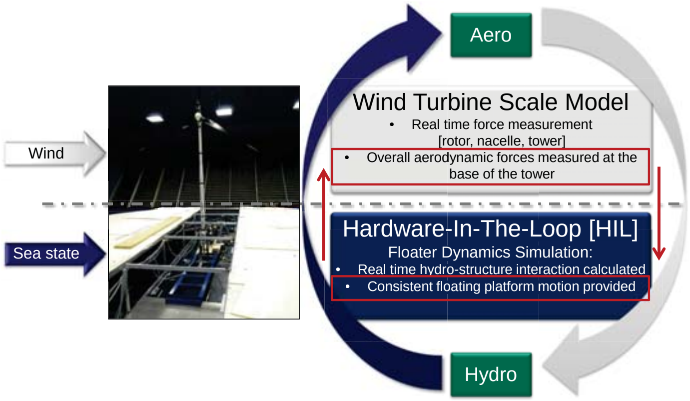

POLITECNICO DI MILANO

Robot requirements

The reference machine is the 5 MW NREL wind turbine
To define the specifications of the robot in terms of Frequencies and displacements
3 reference case have been chosen

1. MIT/NREL TLP
2. ITI Energy Barge
3. OC3-Hywind

The scale factor is 1/58, driven by the wind tunnel dimensions and BL reproduction

Froude scaling law has been adopted
Reynolds Number could be a problem → Known aerodynamics limits

POLITECNICO DI MILANO

Robot requirements

	Design		Verification	
Dof	[m]	[Hz]	[m]	[Hz]
Surge	0.5	0.7	0.01	3
Sway	0.3	0.7	0.01	3
Heave	0.25	0.7	0.01	3
	[deg]	[Hz]	[deg]	[Hz]
Roll	15	0.7	3	3
Pitch	15	0.7	3	3
Yaw	15	0.7	3	3

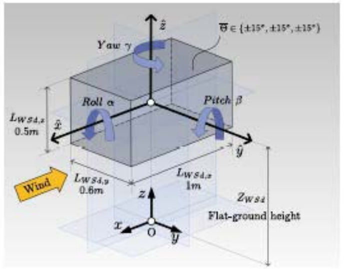

Design process: architecture

Parallel kinematic robots (PKM) have been chosen

The main peculiarities of such robots can be defined as follows:
1. High positioning accuracy
2. High load capability
3. High dynamic performances
4. Components modularity

“Hexaglide” kinematic architecture, also known as 6-PUS architecture with parallel rails.

Advantages
1. low workspace center (TCP):
2. the workspace is characterized by a predominant direction
3. the actuation is placed basically on the ground

Design process: geometric parameters

The Hexaglide robot is characterized by fixed links and parallel rails

All the other architectural details are determined through a geometric parameterization.

Constrains: orientation workspace symmetric with respect to a vertical plane, parallel to the rails and passing through the longitudinal centerline of the machine

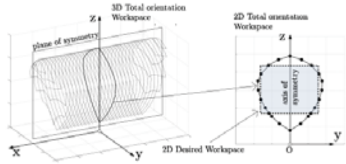

The constrains results in a disposition of the links in pairs with a symmetry with respect to the vertical-longitudinal plane or the central symmetry with respect to the vertical axis passing through the TCP.

Design process: geometric parameters

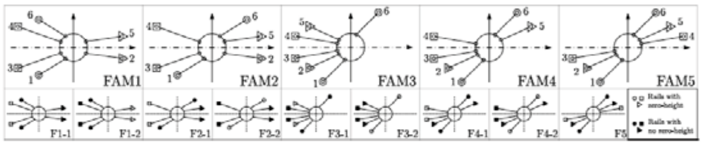

The considerations and the constrains follow in choosing FAM 1. Symmetry considerations let us define a plane 2D problem

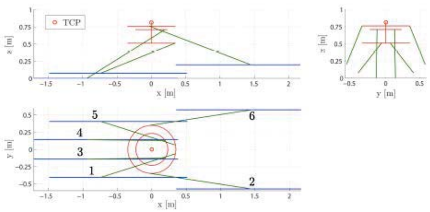

Design process: kinematic syntesis

A multi-objective optimization campaign via genetic has been used to define the dimensions of the manipulator

The target are:
1. Coverage of the workspace
2. Static forces multiplication
3. Interference between the links
4. Interference between the links and the rails
5. Longitudinal size

Two different cost functions have been defined

Thresholds have been decided in terms of maximal static force multiplication and minimal link-to-link and link-to-rail distance

Different Pareto-optimal solutions were obtained and then kineto-statically analyzed and compared.

Design process: kinematic syntesis

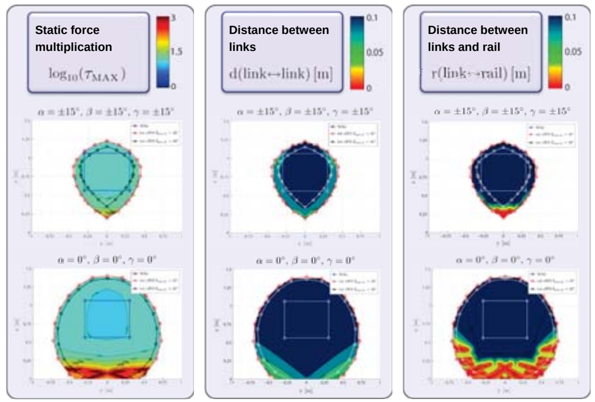

Design process: Dynamics

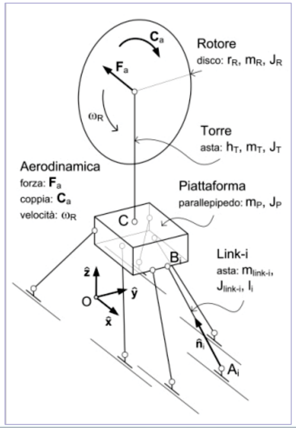

Multi-body model to solve the Dynamics To dimension the joints and the rods of the robot

We impose indipendent sinusoidal motion to each degree of freedom and then compute the forces on each element

This was useful to compare different solutions, considering also other technical issues such as mounting, management and cost-effective aspects.

Ball screw and Belt transmissions system were compared on the basis of the dynamic performances

Design process: Dynamics, results

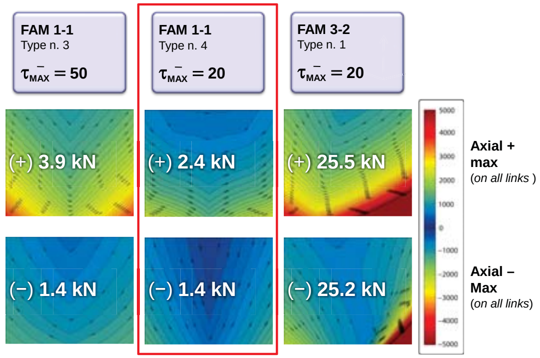

Design process: Dynamics, results

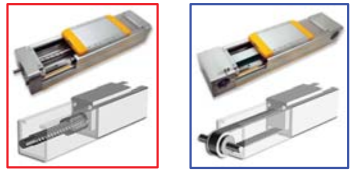

Ball screw: Thomson WH80D

Belt drive: Thomson WH120

		WM80D $p_h = 50mm$	WH120	Fam. 1-1 ind. 4
v_{max}	[m/s]	2.5	10	2.20
a_{max}	[m/s^2]	20	40	13.02
F_x	[N]	5000	5000	2308
F_y	[N]	3000	4980	709
F_z	[N]	3000	9300	764

Pareto Optimal solution

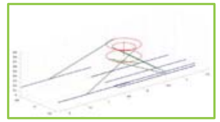

Hexapod Design: final desing

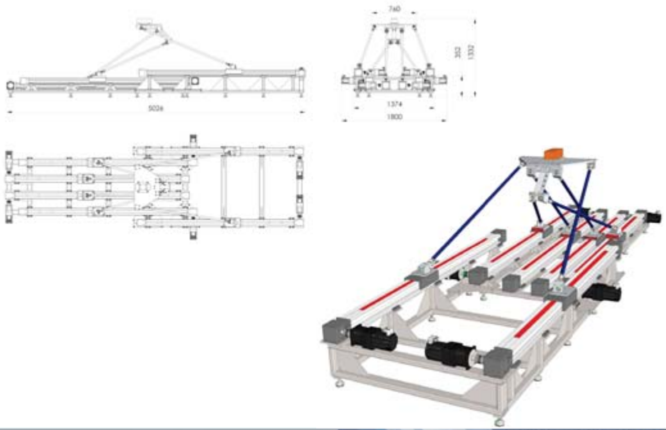

Hexapod design: installation

Hexapod design: verification

A reference case has been used to test the robot capabilities
OC3 system was performed considering the nominal operational condition
Sea-state: Jonswap spectrum, wave height Hs = 3.66m, pick-period Tp = 9.7 s

FAST simulation results scaled to 1/58

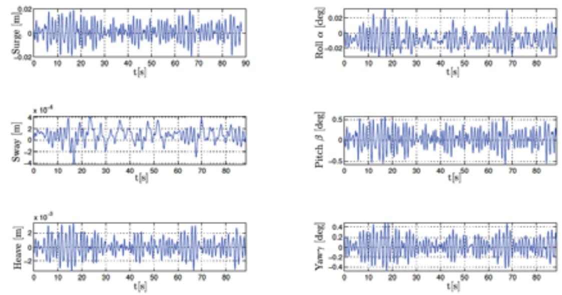

Hexapod design: verification

The selected case gives this output on the robot

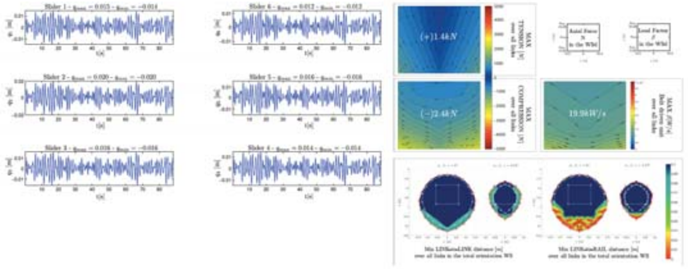

Conclusions

I. The desing process of a PKM to aerohydro simulation of FOWT has been presented
II. The machine is designed to be inserted in a HIL test bench in wind tunnel
III. A new concept PKM has been designed using Pareto Optimal kinematic and dynamic solutions
IV. Commercial components
V. Very small vertical dimensions compared to the workspace
VI. The robot will be available at the end of 2014.

POLITECNICO DI MILANO

Influence of pitch motion on the wake of floating wind turbine models

S. Rockel*[1], J. Peinke[1], R. B. Cal[2] and M. Hölling[1]

[1]ForWind, Institute of Physics - University of Oldenburg
[2]Dept. of Mechanical and Materials Engineering, Portland State University

*contact: stanislav.rockel@uni-oldenburg.de

Motivation

- tripods and monopiles feasible in shallow water

Motivation

- tripods and monopiles feasible in shallow water
- floating platforms are a solution for offshore wind energy in deep water [Henderson, 2009]

Motivation

- tripods and monopiles feasible in shallow water
- floating platforms are a solution for offshore wind energy in deep water [Henderson, 2009]
- floating platform adds dynamics to system [Jonkman, 2009; Sebastian, 2012]

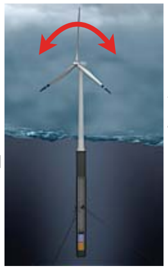

Motivation

- tripods and monopiles feasible in shallow water
- floating platforms are a solution for offshore wind energy in deep water [Henderson, 2009]
- floating platform adds dynamics to system [Jonkman, 2009; Sebastian, 2012]
- changed inflow and wake characteristics

Motivation

- tripods and monopiles feasible in shallow water
- floating platforms are a solution for offshore wind energy in deep water [Henderson, 2009]
- floating platform adds dynamics to system [Jonkman, 2009; Sebastian, 2012]
- changed inflow and wake characteristics

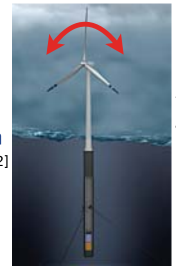

Experimental investigation of wake development

Objectives - Approach

- understand the differences between a fixed turbine and a floating turbine

Objectives - Approach

- understand the differences between a fixed turbine and a floating turbine
- wind tunnel experiments with model wind turbines using stereo particle image velocimetry (SPIV)

Objectives - Approach

- understand the differences between a fixed turbine and a floating turbine
- wind tunnel experiments with model wind turbines using stereo particle image velocimetry (SPIV)
  - simplification of floating turbine:
    1D streamwise oscillation (pitch motion)

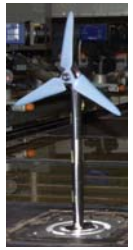

Objectives - Approach

- understand the differences between a fixed turbine and a floating turbine
- wind tunnel experiments with model wind turbines using stereo particle image velocimetry (SPIV)
  - simplification of floating turbine:
    1D streamwise oscillation (pitch motion)
- comparison of inflow and wake development
  - near wakes of up– and downstream turbines

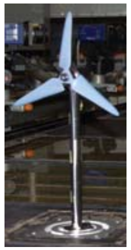

Experimental setup

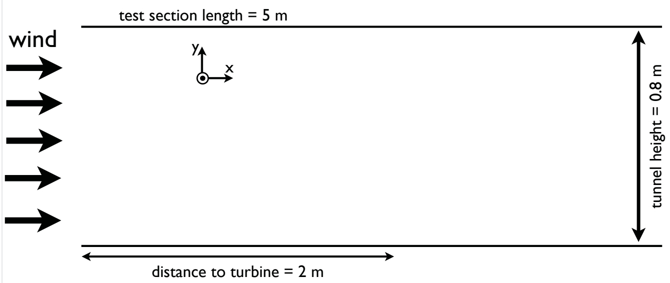

wind tunnel at Portland State Univ.

Experimental setup

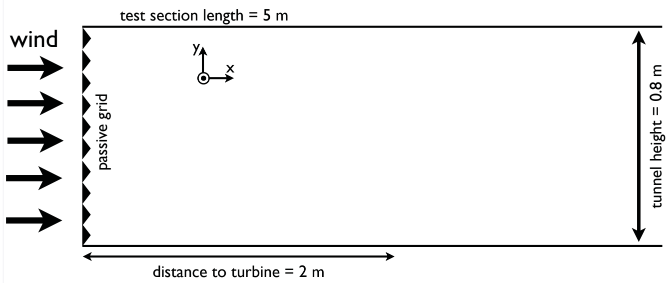

wind tunnel at Portland State Univ.

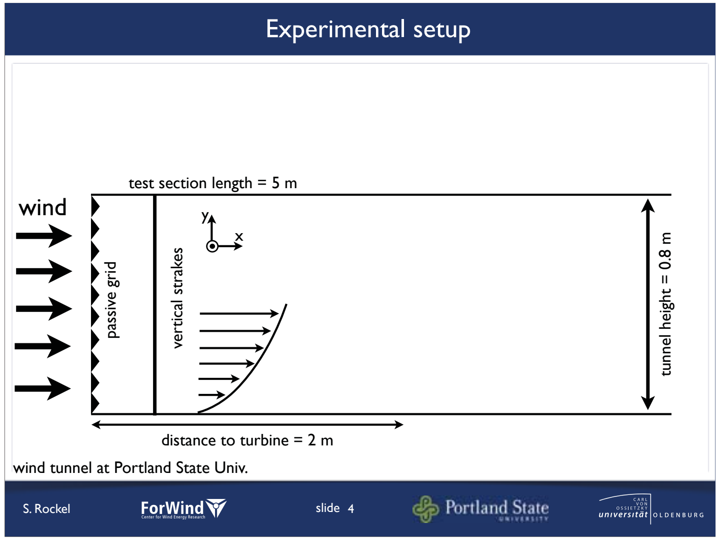
Experimental setup
test section length = 5 m
wind
passive grid
vertical strakes
y
x
tunnel height = 0.8 m
distance to turbine = 2 m
wind tunnel at Portland State Univ.
S. Rockel
ForWind
slide 4
Portland State
universität oldenburg

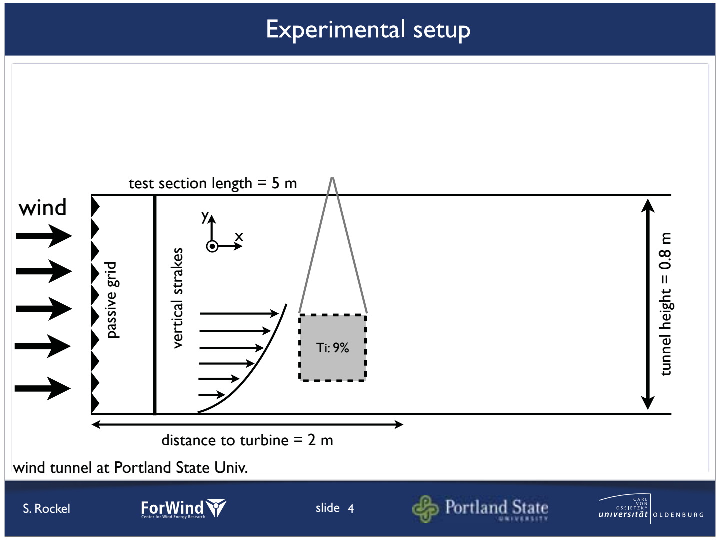
Experimental setup
test section length = 5 m
wind
passive grid
vertical strakes
y
x
Ti: 9%
tunnel height = 0.8 m
distance to turbine = 2 m
wind tunnel at Portland State Univ.
S. Rockel
ForWind
slide 4
Portland State
universität oldenburg

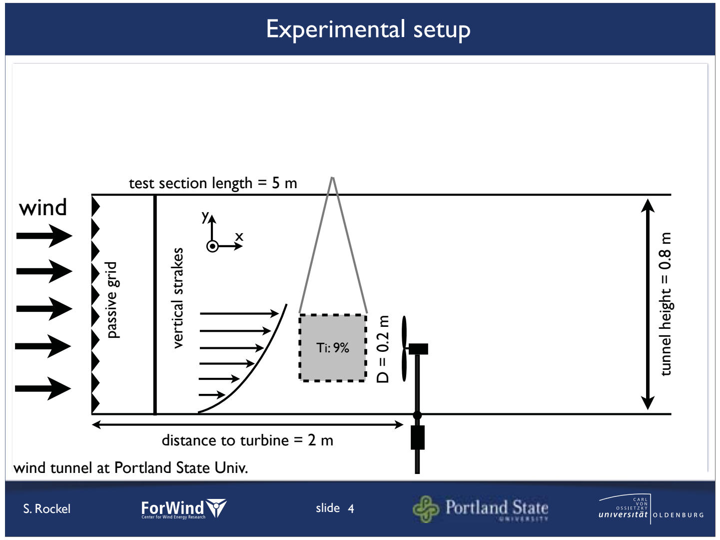
Experimental setup
test section length = 5 m
wind
passive grid
vertical strakes
y
x
Ti: 9%
D = 0.2 m
tunnel height = 0.8 m
distance to turbine = 2 m
wind tunnel at Portland State Univ.
S. Rockel
ForWind
slide 4
Portland State
universität oldenburg

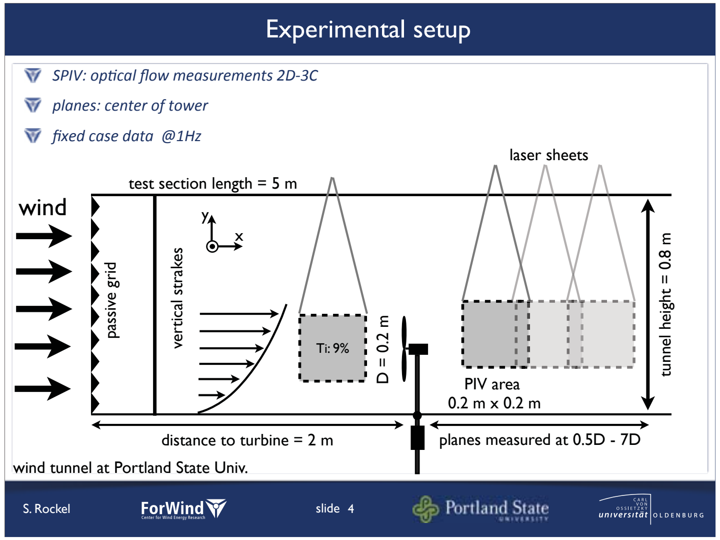
Experimental setup
SPIV: optical flow measurements 2D-3C
planes: center of tower
fixed case data @1Hz
laser sheets
test section length = 5 m
wind
passive grid
vertical strakes
y
x
Ti: 9%
D = 0.2 m
PIV area
0.2 m x 0.2 m
tunnel height = 0.8 m
distance to turbine = 2 m
planes measured at 0.5D - 7D
wind tunnel at Portland State Univ.
S. Rockel
ForWind
slide 4
Portland State
universität oldenburg

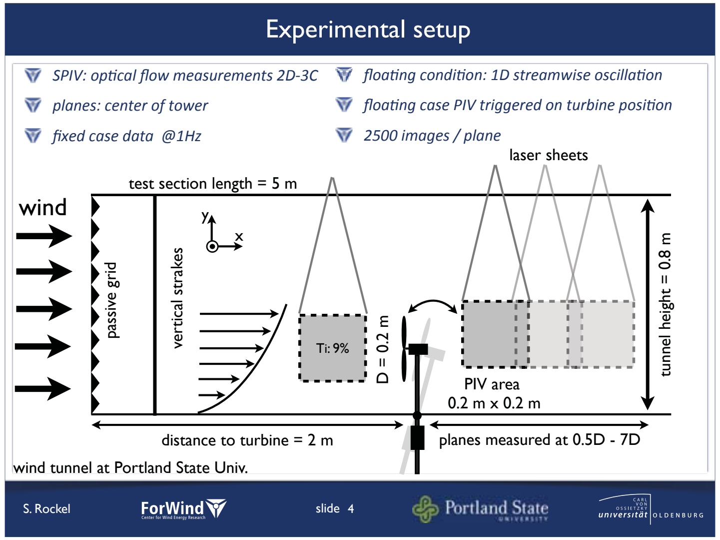
Experimental setup
SPIV: optical flow measurements 2D-3C
planes: center of tower
fixed case data @1Hz
floating condition: 1D streamwise oscillation
floating case PIV triggered on turbine position
2500 images / plane
laser sheets
test section length = 5 m
wind
passive grid
vertical strakes
y
x
Ti: 9%
D = 0.2 m
PIV area
0.2 m x 0.2 m
tunnel height = 0.8 m
distance to turbine = 2 m
planes measured at 0.5D - 7D
wind tunnel at Portland State Univ.
S. Rockel
ForWind
slide 4
Portland State
universität oldenburg

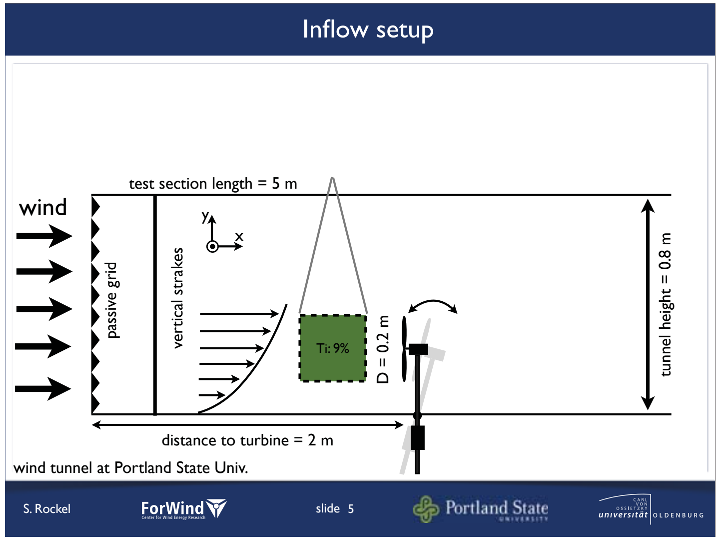
Inflow setup
test section length = 5 m
wind
passive grid
vertical strakes
y
x
Ti: 9%
D = 0.2 m
tunnel height = 0.8 m
distance to turbine = 2 m
wind tunnel at Portland State Univ.
S. Rockel
ForWind
slide 5
Portland State
universität oldenburg

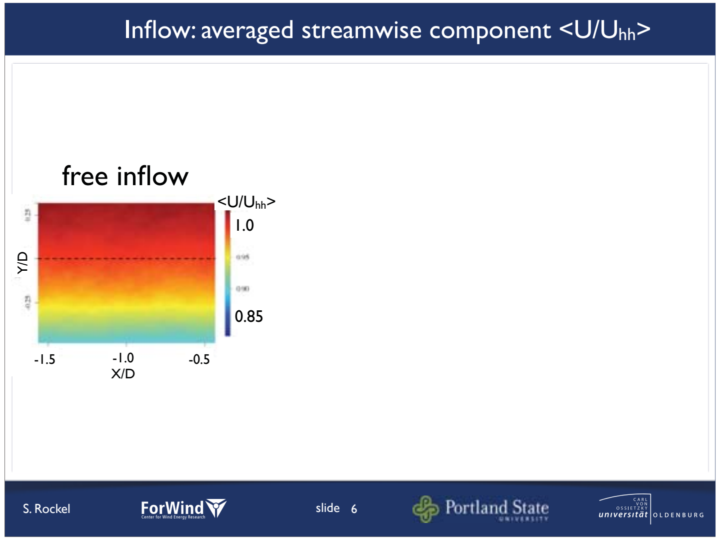
Inflow: averaged streamwise component <U/Uhh>
free inflow
<U/Uhh>
1.0
0.85
Y/D
-1.5
-1.0
-0.5
X/D
S. Rockel
ForWind
slide 6
Portland State
universität OLDENBURG

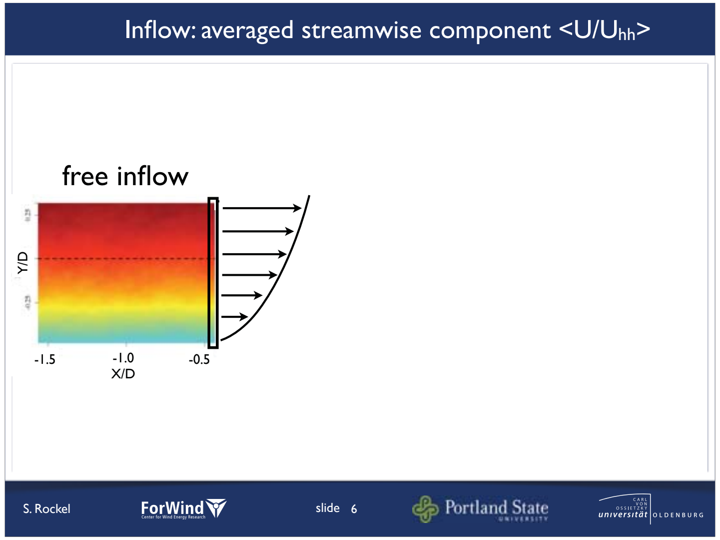
Inflow: averaged streamwise component <U/Uhh>
free inflow
Y/D
-1.5
-1.0
-0.5
X/D
S. Rockel
ForWind
slide 6
Portland State
universität OLDENBURG

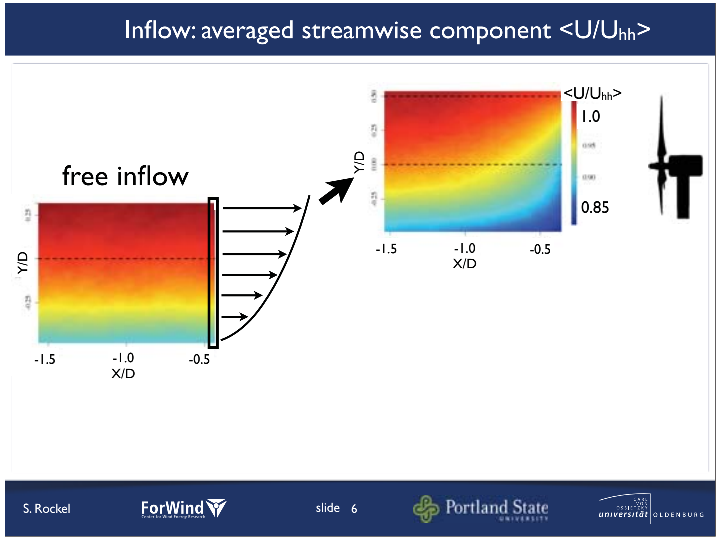
Inflow: averaged streamwise component <U/Uhh>
free inflow
<U/Uhh>
1.0
0.85
Y/D
-1.5
-1.0
-0.5
X/D
S. Rockel
ForWind
slide 6
Portland State
universität OLDENBURG

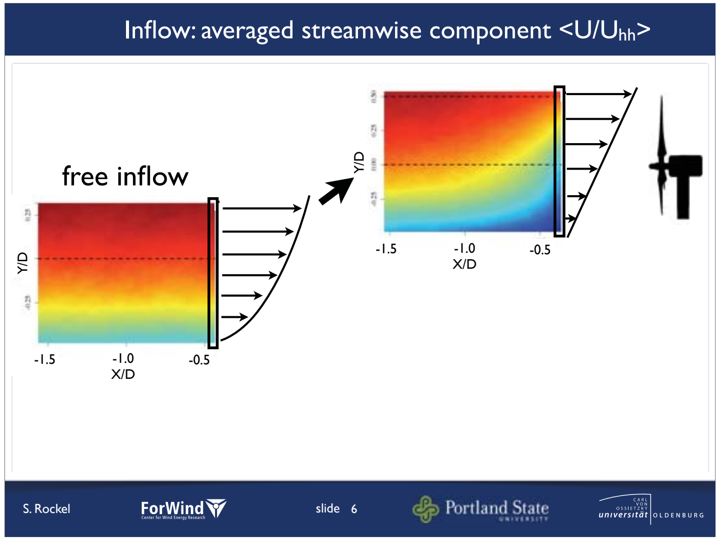
Inflow: averaged streamwise component <U/Uhh>
free inflow
Y/D
-1.5
-1.0
-0.5
X/D
S. Rockel
ForWind
slide 6
Portland State
universität OLDENBURG

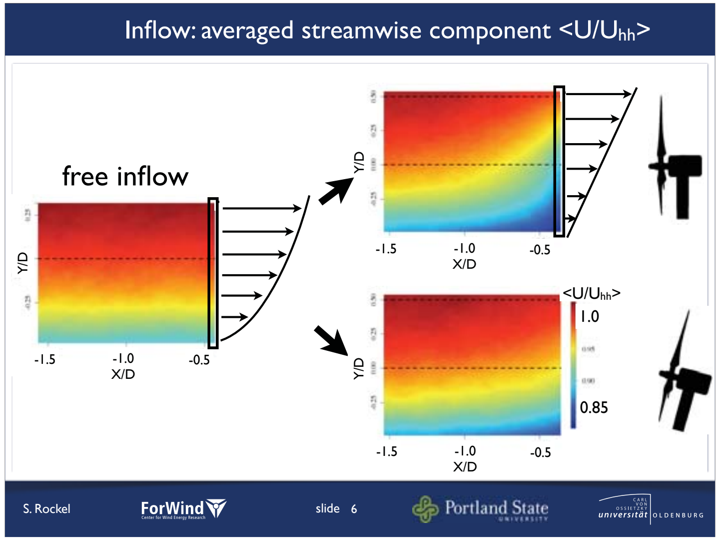
Inflow: averaged streamwise component <U/Uhh>
free inflow
<U/Uhh>
1.0
0.85
Y/D
-1.5
-1.0
-0.5
X/D
S. Rockel
ForWind
slide 6
Portland State
universität OLDENBURG

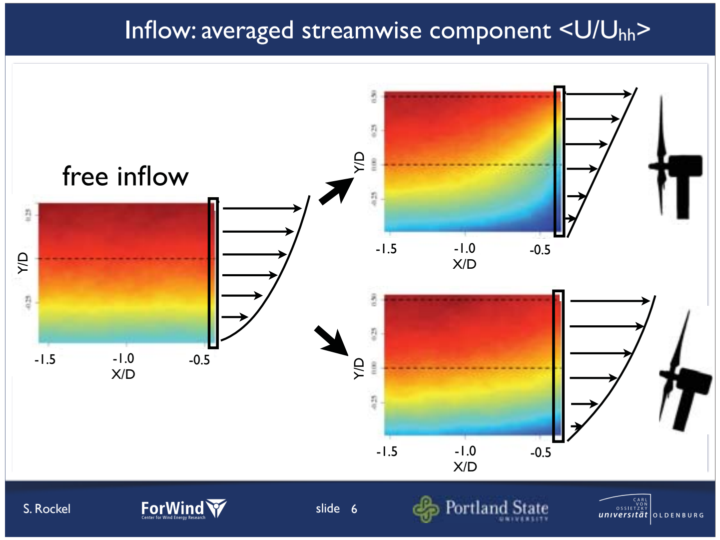
Inflow: averaged streamwise component <U/Uhh>
free inflow
Y/D
-1.5
-1.0
-0.5
X/D
S. Rockel
ForWind
slide 6
Portland State
universität OLDENBURG

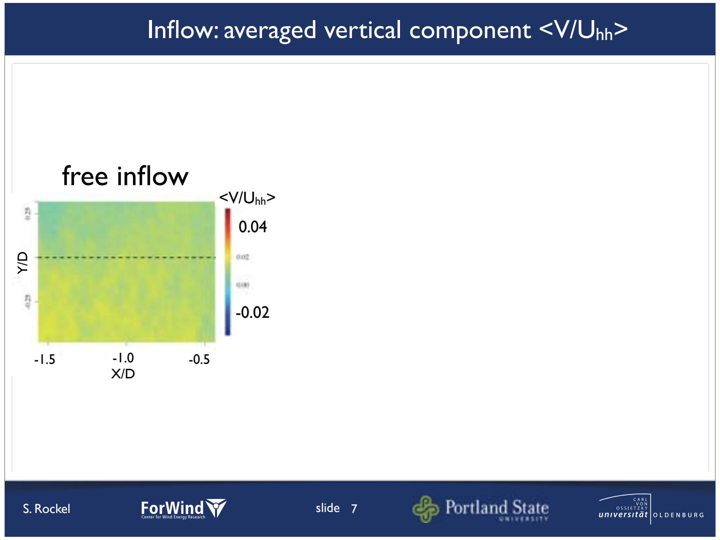
Inflow: averaged vertical component <V/U_hh>
free inflow
<V/U_hh>
0.04
-0.02
Y/D
-1.5
-1.0
X/D
-0.5
S. Rockel
ForWind
slide 7
Portland State
universität OLDENBURG

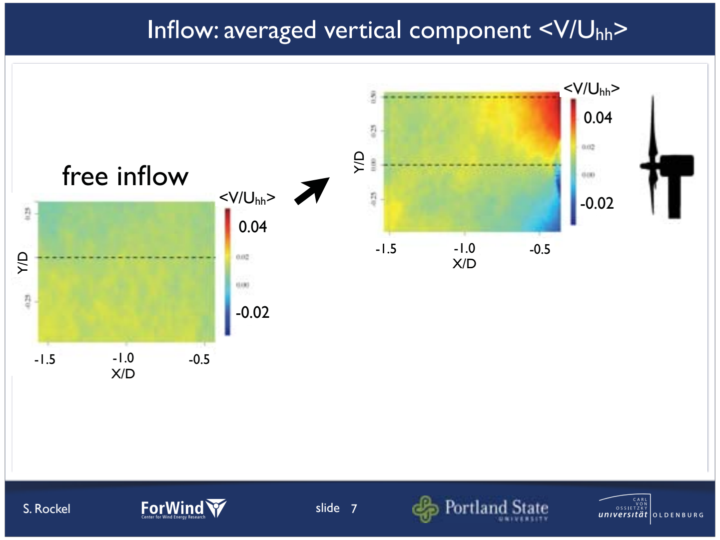
Inflow: averaged vertical component <V/U_hh>
free inflow
<V/U_hh>
0.04
-0.02
Y/D
-1.5
-1.0
X/D
-0.5
S. Rockel
ForWind
slide 7
Portland State
universität OLDENBURG

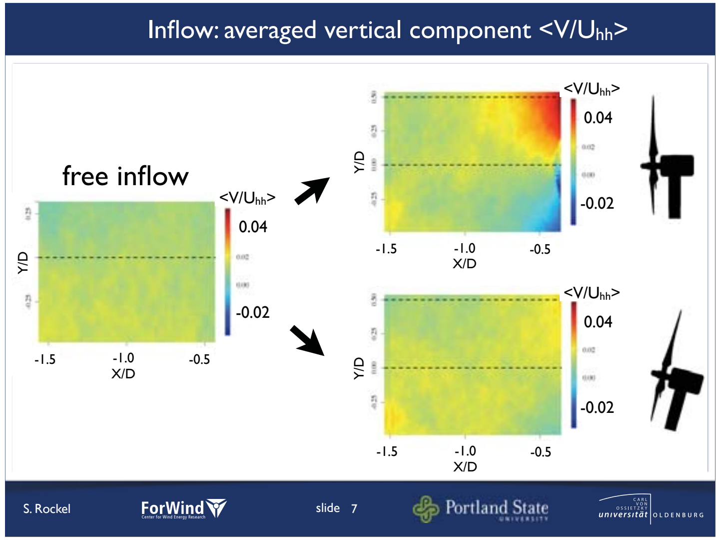
Inflow: averaged vertical component <V/U_hh>
free inflow
<V/U_hh>
0.04
-0.02
Y/D
-1.5
-1.0
X/D
-0.5
S. Rockel
ForWind
slide 7
Portland State
universität OLDENBURG

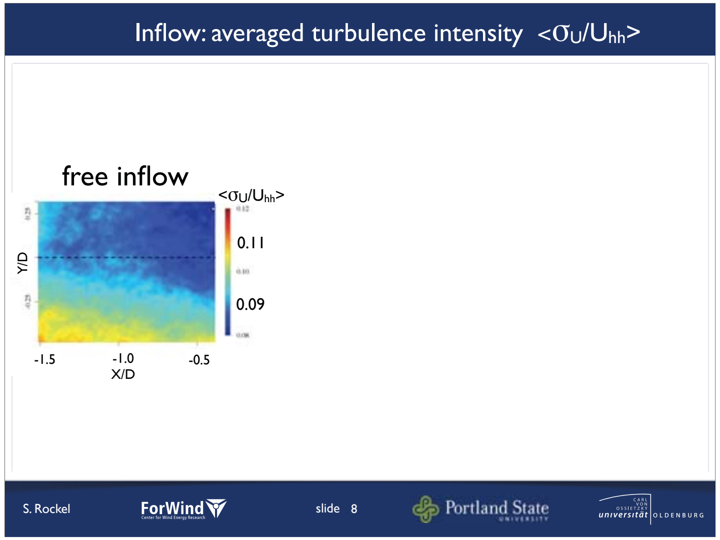
Inflow: averaged turbulence intensity <σ_U/U_hh>
free inflow
<σ_U/U_hh>
0.11
0.09
Y/D
-1.5
-1.0
X/D
-0.5
S. Rockel
ForWind
slide 8
Portland State
universität OLDENBURG

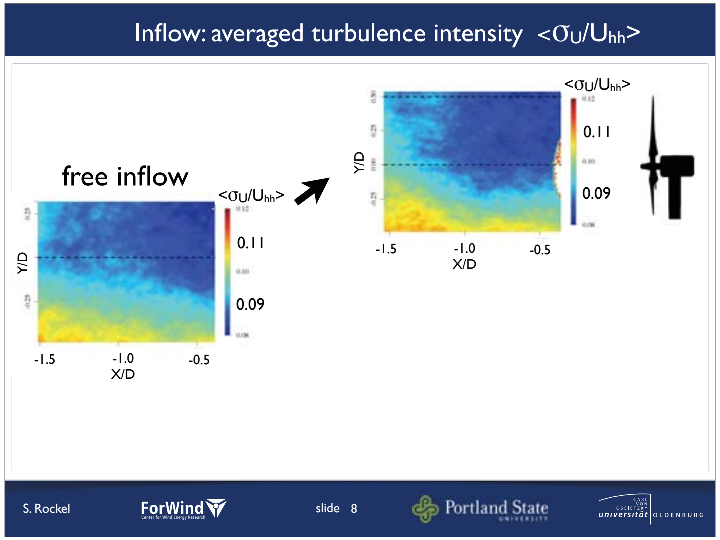
Inflow: averaged turbulence intensity <σ_U/U_hh>
free inflow
<σ_U/U_hh>
0.11
0.09
Y/D
-1.5
-1.0
X/D
-0.5
S. Rockel
ForWind
slide 8
Portland State
universität OLDENBURG

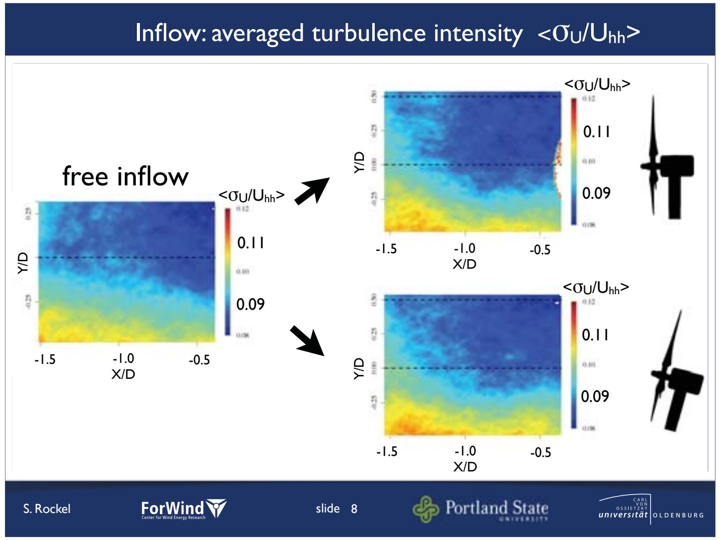
Inflow: averaged turbulence intensity <σ_U/U_hh>
free inflow
<σ_U/U_hh>
0.11
0.09
Y/D
-1.5
-1.0
X/D
-0.5
S. Rockel
ForWind
slide 8
Portland State
universität OLDENBURG

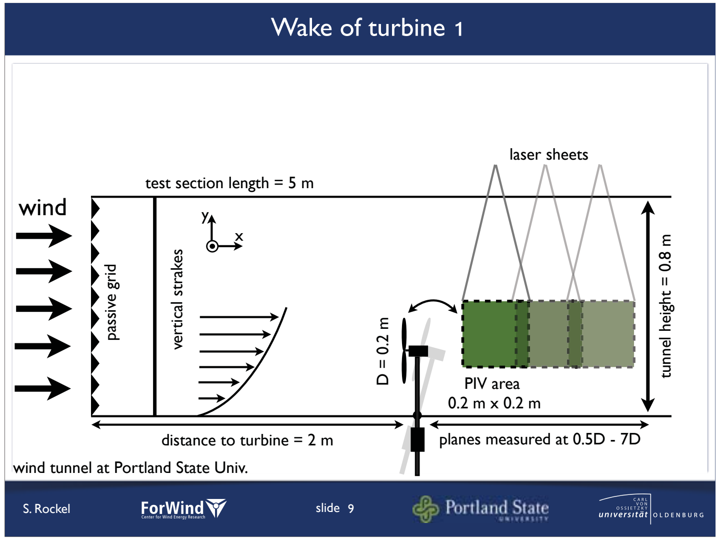
Wake of turbine 1
wind
test section length = 5 m
laser sheets
passive grid
vertical strakes
y
x
D = 0.2 m
PIV area
0.2 m x 0.2 m
tunnel height = 0.8 m
distance to turbine = 2 m
planes measured at 0.5D - 7D
wind tunnel at Portland State Univ.
S. Rockel
ForWind
slide 9
Portland State

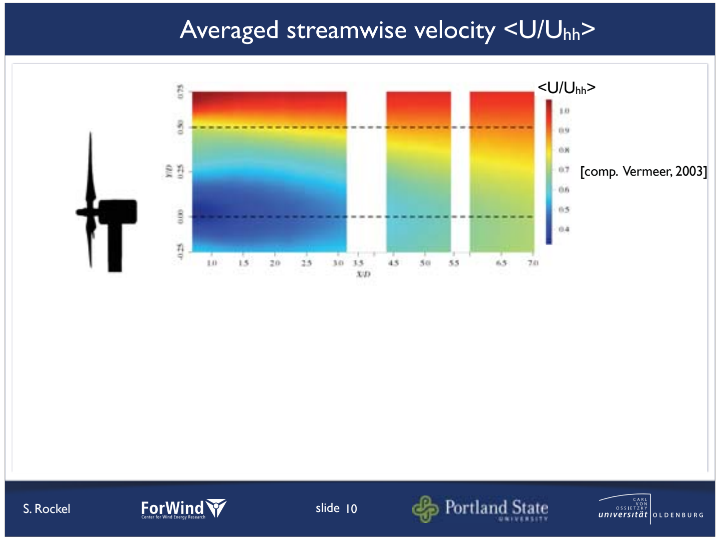
Averaged streamwise velocity <U/Uhh>
<U/Uhh>
[comp. Vermeer, 2003]
S. Rockel
ForWind
slide 10
Portland State

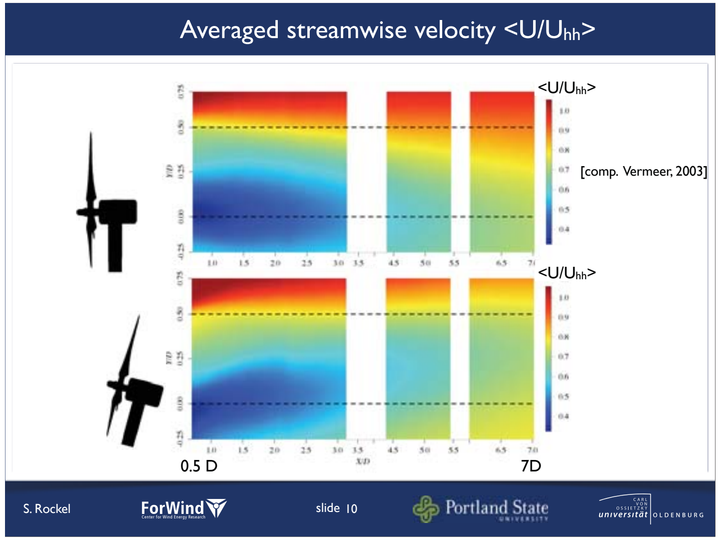
Averaged streamwise velocity <U/Uhh>
<U/Uhh>
[comp. Vermeer, 2003]
<U/Uhh>
0.5 D
7D
S. Rockel
ForWind
slide 10
Portland State

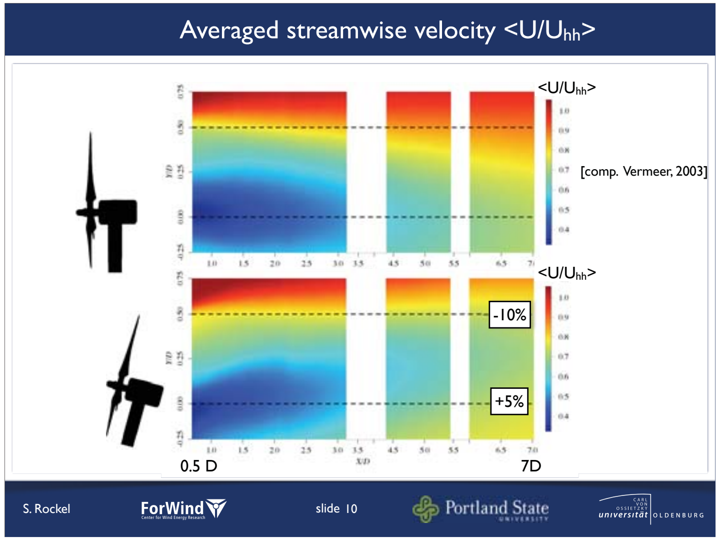
Averaged streamwise velocity <U/Uhh>
<U/Uhh>
[comp. Vermeer, 2003]
<U/Uhh>
-10%
+5%
0.5 D
7D
S. Rockel
ForWind
slide 10
Portland State

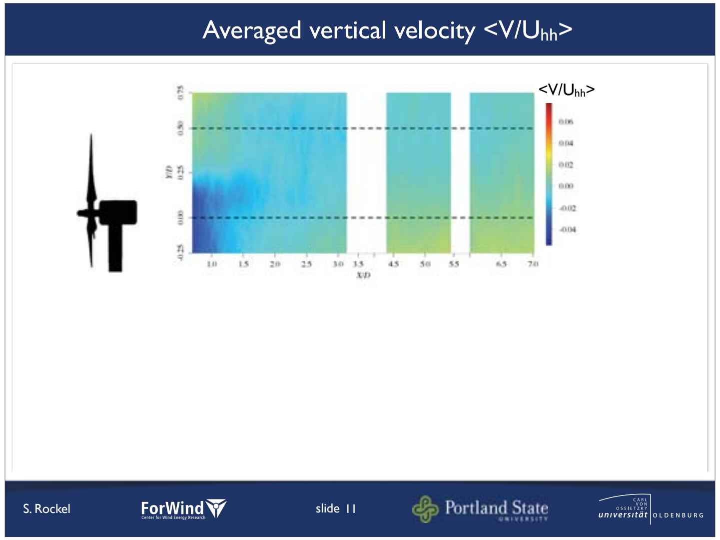
Averaged vertical velocity <V/Uhh>
<V/Uhh>
S. Rockel
ForWind
slide 11
Portland State

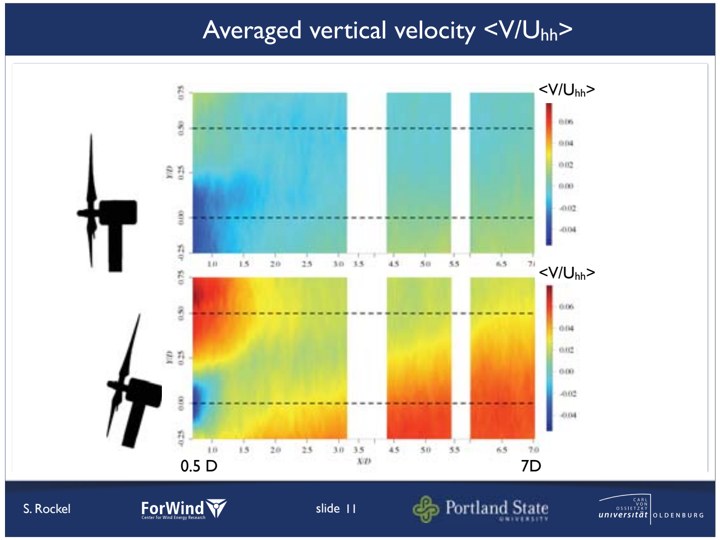
Averaged vertical velocity <V/Uhh>
<V/Uhh>
<V/Uhh>
0.5 D
7D
S. Rockel
ForWind
slide 11
Portland State

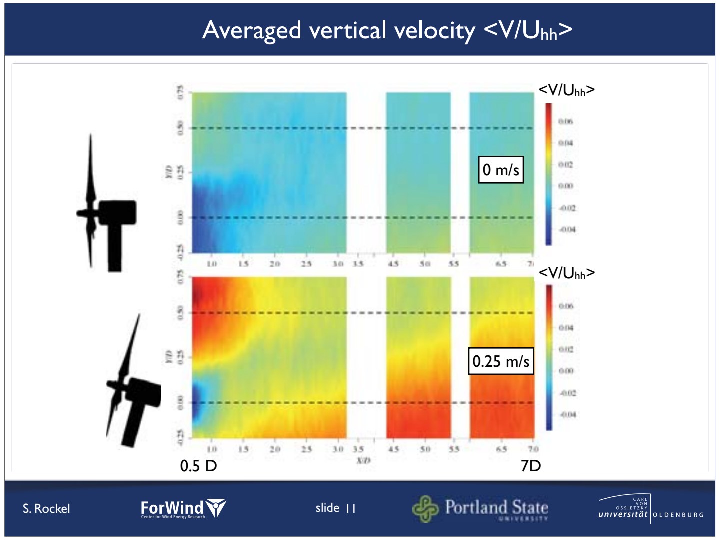
Averaged vertical velocity <V/Uhh>
<V/Uhh>
0 m/s
<V/Uhh>
0.25 m/s
0.5 D
7D
S. Rockel
ForWind
slide 11
Portland State
universität OLDENBURG

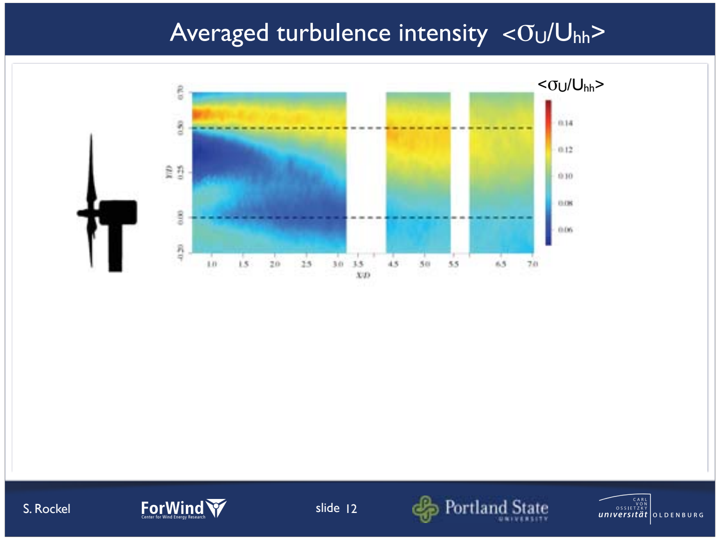
Averaged turbulence intensity <σU/Uhh>
<σU/Uhh>
S. Rockel
ForWind
slide 12
Portland State
universität OLDENBURG

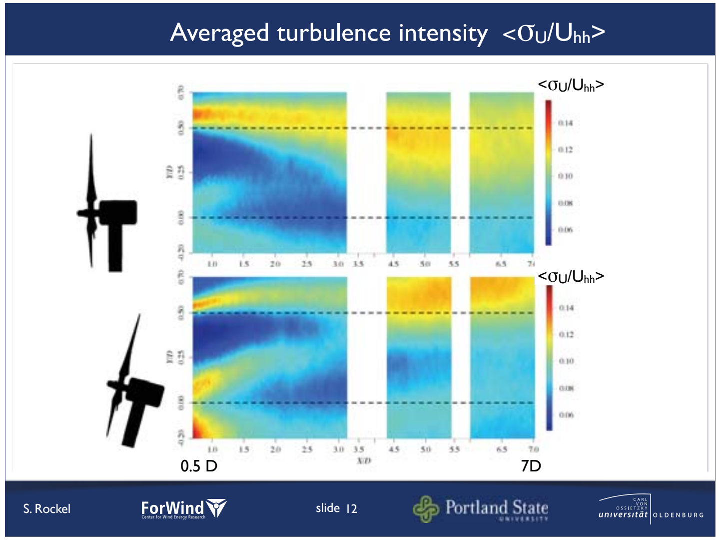
Averaged turbulence intensity <σU/Uhh>
<σU/Uhh>
<σU/Uhh>
0.5 D
7D
S. Rockel
ForWind
slide 12
Portland State
universität OLDENBURG

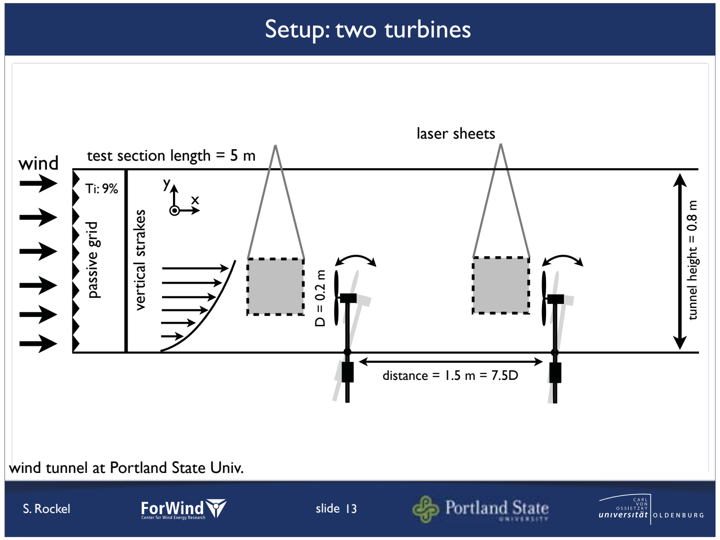
Setup: two turbines
wind
test section length = 5 m
laser sheets
Ti: 9%
passive grid
vertical strakes
D = 0.2 m
tunnel height = 0.8 m
distance = 1.5 m = 7.5D
wind tunnel at Portland State Univ.
S. Rockel
ForWind
slide 13
Portland State
universität OLDENBURG

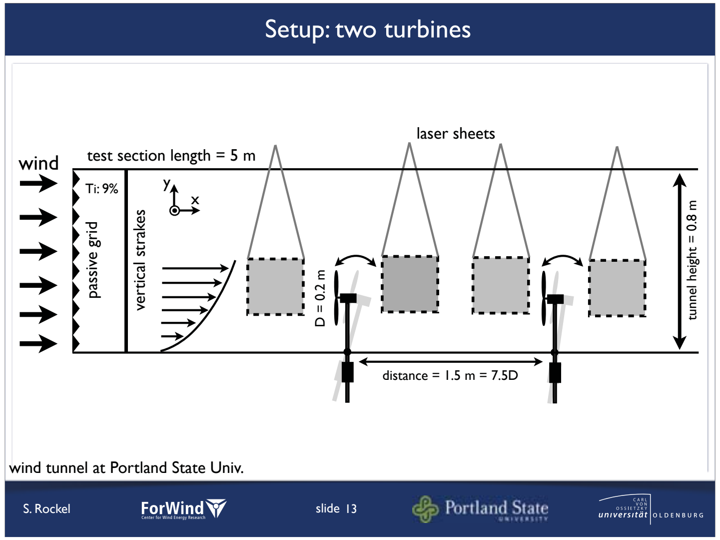
Setup: two turbines
wind
test section length = 5 m
laser sheets
Ti: 9%
passive grid
vertical strakes
D = 0.2 m
tunnel height = 0.8 m
distance = 1.5 m = 7.5D
wind tunnel at Portland State Univ.
S. Rockel
ForWind
slide 13
Portland State
universität OLDENBURG

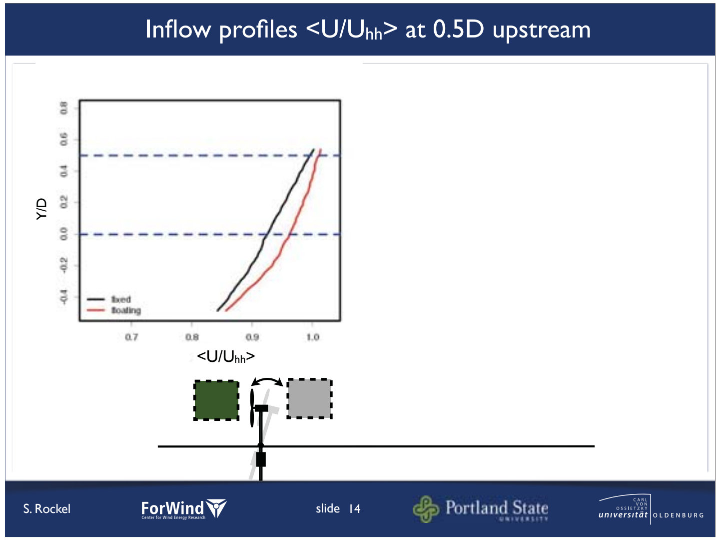
Inflow profiles <U/Uhh> at 0.5D upstream
Y/D
fixed
floating
<U/Uhh>
S. Rockel
ForWind
slide 14
Portland State
universität OLDENBURG

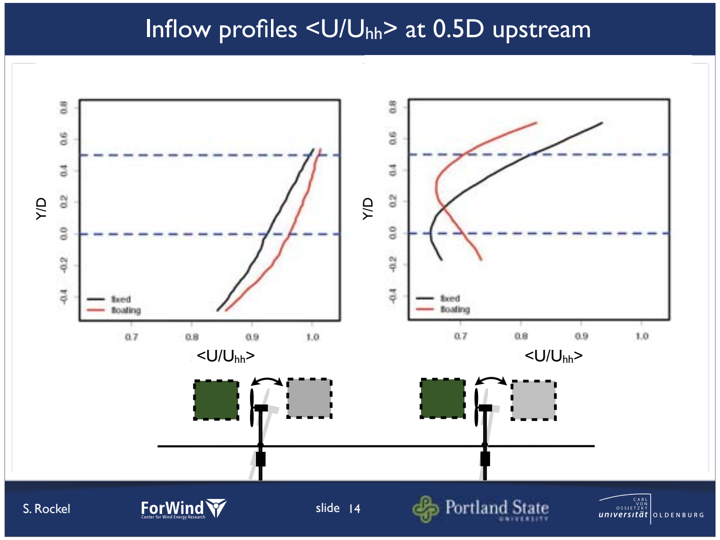

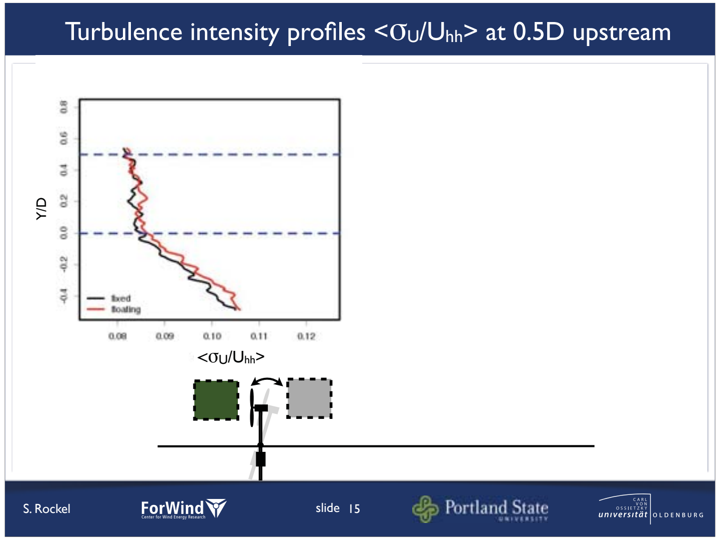

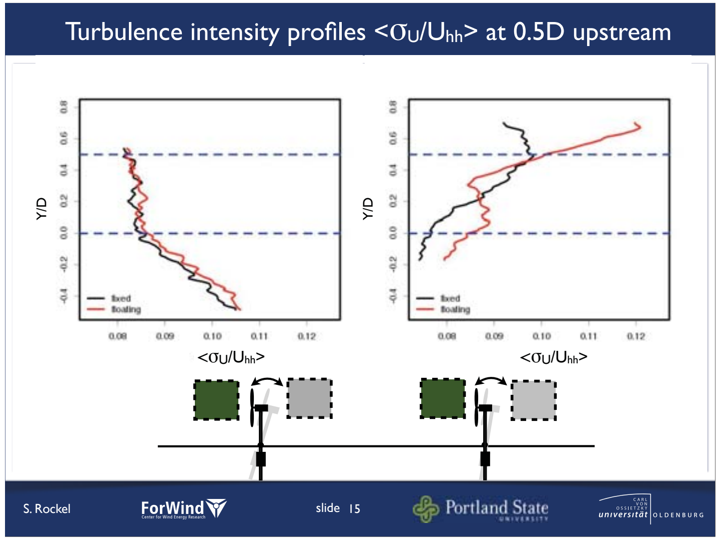

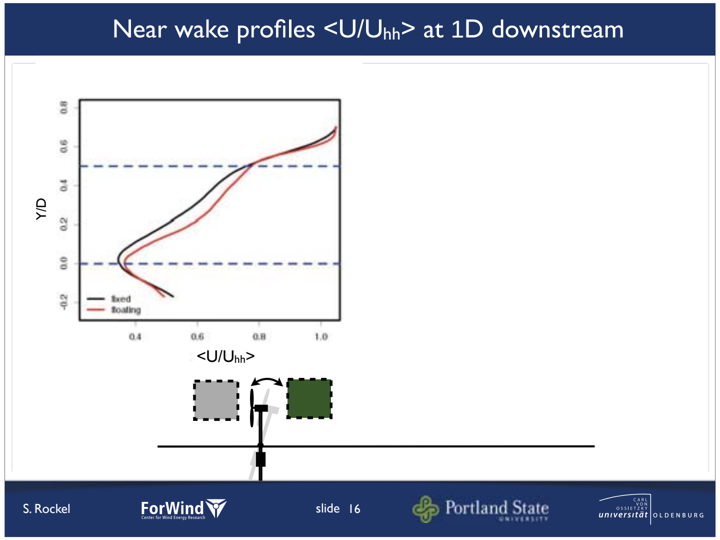

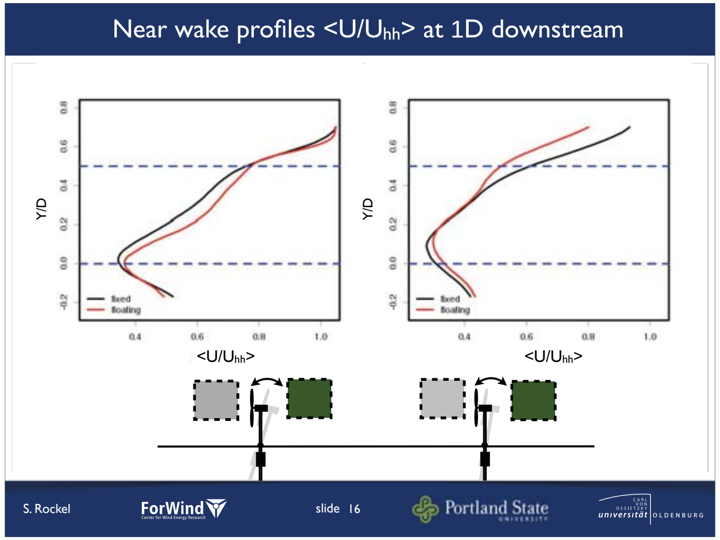

Summary & Conclusions

- Blockage changes inflow profile
- Pitch motion has strong impact on wake
  - Vertical trend in all quantities
  - Increased vertical flow
- Reduced turbulence intensity in far wake
- Changed inflow profile for downstream turbine has no influence on near wake

Thank you!

Questions?

Acknowledgements:
- Elizabeth Camp
- German Environmental Foundation

„Experimental study on influence of pitch motion on the wake of a floating wind turbine model“, Rockel et al., *Energies, submitted 2013*

spanwise velocity

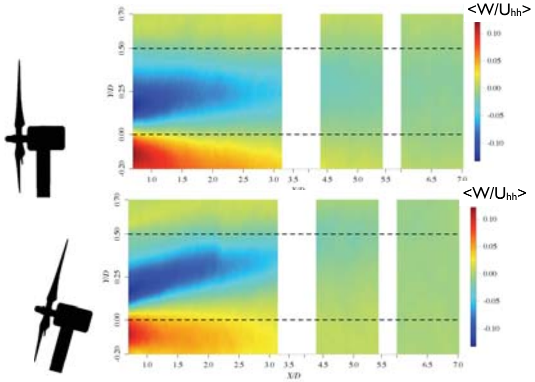

Near wake profiles $\langle V/U_{hh} \rangle$ at 1D downstream

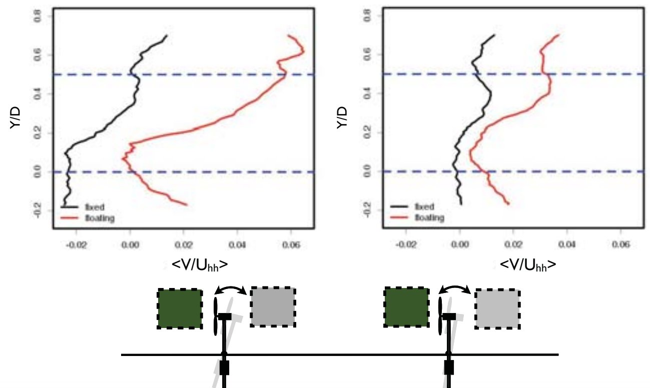

Near wake turbulence intensity $\langle \sigma_U/U_{hh} \rangle$ at 1D downstream

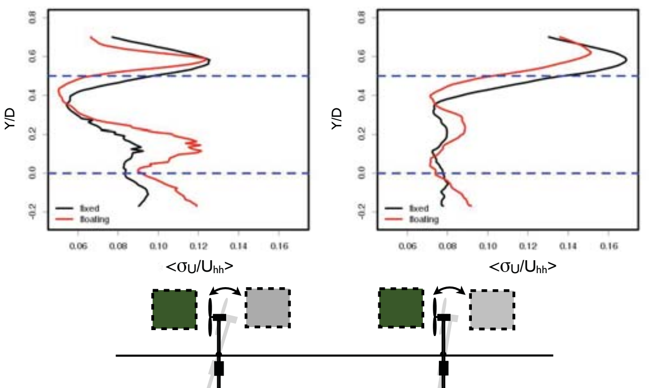

Comparison with wake models: fixed

- shape and magnitude of deficit predicted for X = 3D and 4.5D

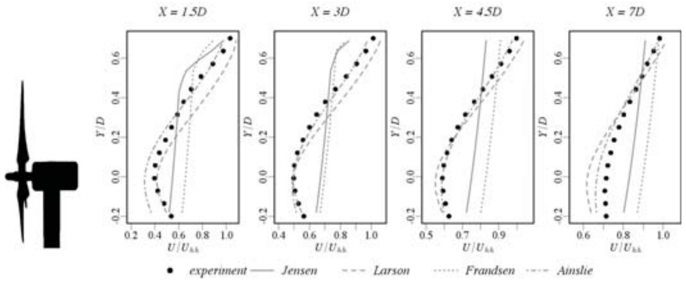

Comparison with wake models: floating

- vertical displacement NOT captured

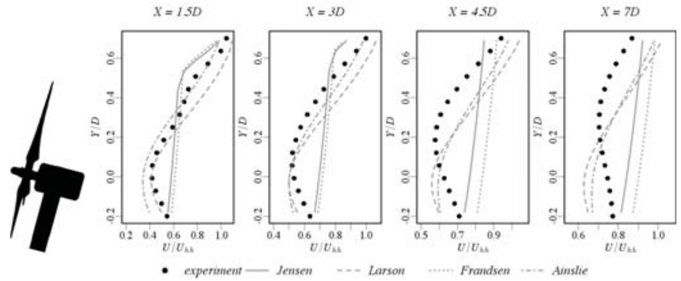

Floating Wind Turbines

Paul D. Sclavounos

Professor of Mechanical Engineering and Naval Architecture
Department of Mechanical Engineering
Massachusetts Institute of Technology

EERA DeepWind 2014, January 23th 2014, Trondheim, Norway

Floating Wind Turbines

- Vast Offshore Sites Available for Wind Resource Development
- Offshore Siting Mitigates Visual, Noise and Flicker Impact
- Coastal Assembly – Low Cost Float-out Operation
- Floater Cost Lower than Turbine Cost per Marginal MW
- Fault Tolerant Efficient Operation using Turbine Controls
- Larger Turbines on Fewer Floaters – Low O&M Costs per MW

Floating Wind Turbine Prototypes

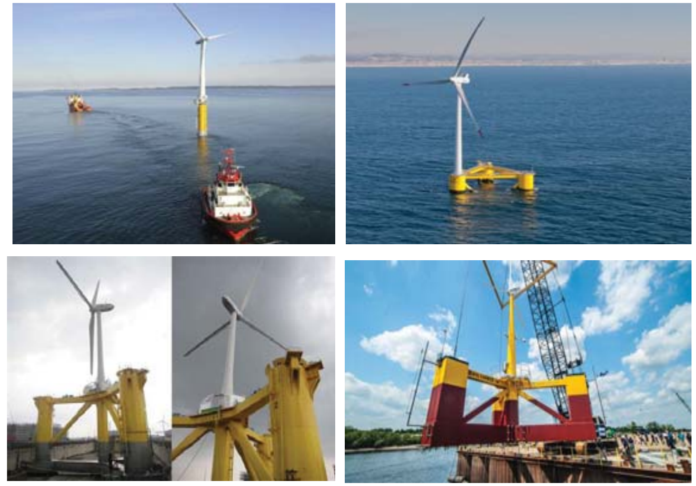

Hydrodynamics

- Frequency Domain Preliminary Design Analysis
- State-Space Formulation of Free Surface Hydrodynamics
- Generalized Morison Equation with Memory Effects
- Fluid Impulse Theory for Nonlinear Loads
- Ringing Loads
- Efficient Computation – Nonlinear Statistics

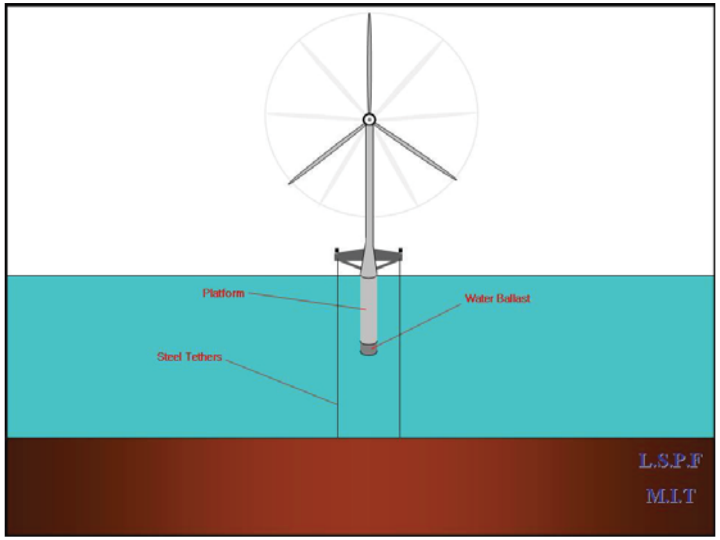

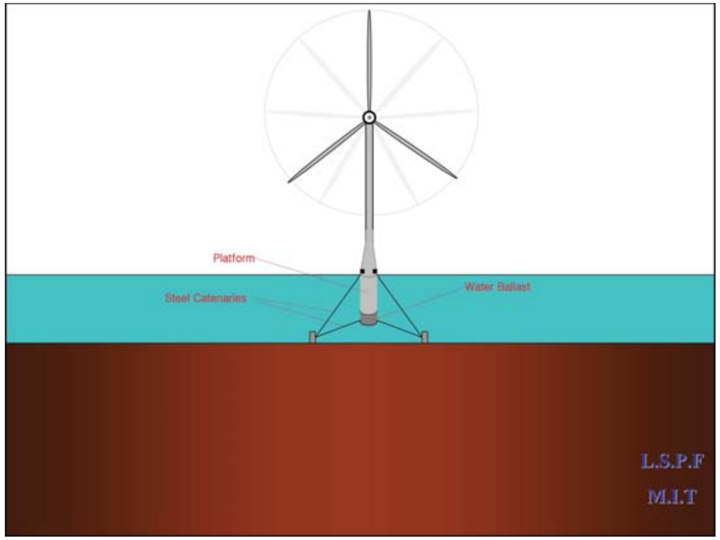

Dynamic Analysis of Floating Wind Turbines

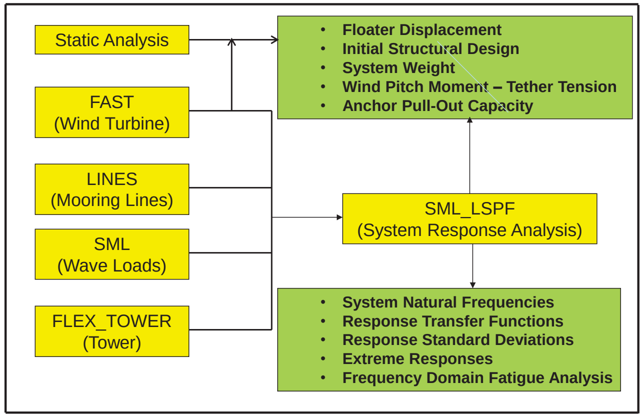

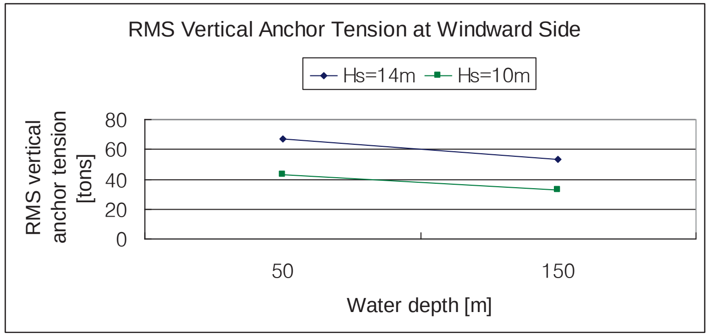

3 MW TLP Floating Wind Turbine

Wind Turbine and Floater Damping

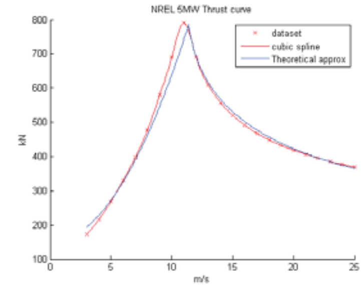

$$B_{TURBINE}(U)=\frac{dT}{dU};\quad B_{BUOY}=\frac{1}{2}\rho C_d S\sqrt{\frac{8}{\pi}}\sigma_V;$$

Damping Ratio=0.23 at U=10 m/s; Hs=6m
Damping Ratio=0.15 at U=15 m/s; Hs=6m

Nielsen et. al. (OMAE, 2006), Jonkman (Wind Energy, 2008)

Wave Energy Extraction Potential – NREL 5MW

NREL – 5 MW – TLP platform					
Buoy characteristics					
		Draft	30 m	Draft	15 m
		Radius	4.75 m	Radius	6.72 m
Depth	**Conditions**	**Additional Power** (+% of turbine power at that wind speed)			
50 m	Sig. Wave H. [m]	6	10	6	10
	Mean Period [s]	11.6	13.6	11.6	13.6
	Wind 6 m/s	+3.13%	+8.94%	+4.92%	+13.5%
	Wind 8 m/s	+2.47%	+6.73%	+3.89%	+10.2%
	Wind 10 m/s	+2.29%	+5.59%	+3.58%	+8.33%
100 m	Sig. Wave H. [m]	6	10	6	10
	Mean Period [s]	11.6	13.6	11.6	13.6
	Wind 6 m/s	+2.3%	+6.46%	+3.55%	+9.5%
	Wind 8 m/s	+1.74%	+4.83%	+2.69%	+7.11%
	Wind 10 m/s	+1.51%	+4.06%	+2.34%	+5.98%

Nonlinear Time Domain Loads

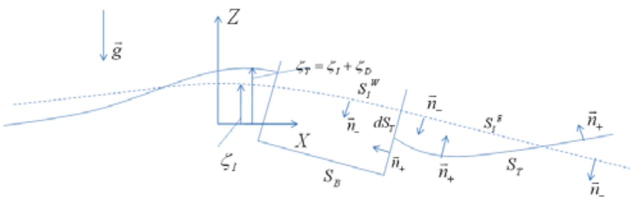

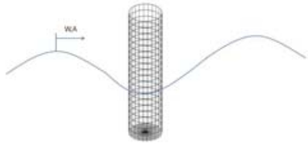

Cylinder Diameter: d
Wave Amplitude: A
Wavenumber: k

Nonlinear Fluid Impulse Hydrodynamic Force

$$\vec F(t)=\vec F_1(t)+\vec F_2(t)$$

$$\vec F_1(t)=\underbrace{-\rho g\int_{S_B^W(t)+S_I^W(t)} Z\,\vec n\,ds}_{\text{Buoyancy force}}\underbrace{-\rho\frac{d}{dt}\int_{S_B^W(t)+S_I^W(t)}\varphi_I\,\vec n\,ds}_{\text{Froude-Krylov Impulse Force}}\underbrace{-\rho\frac{d}{dt}\int_{S_B^W(t)}\varphi_D\,\vec n\,ds}_{\text{Radiation and Diffraction Body Impulse Force}}$$

$$\left.\begin{aligned}\vec F_2(t)&=-\rho\frac{d}{dt}\int_{S^E_I(t)}\varphi_D\vec n\,ds-\rho g\vec k\int_{S^E_I(t)}\zeta_D\,ds\\&\quad-\rho\frac{d}{dt}\iint_{\upsilon(t)}\left(\nabla\varphi_I+\nabla\varphi_D\right)\mathrm{sgn}\left(\zeta_D\right)d\upsilon\end{aligned}\right\}$$

Radiation and Diffraction
Free Surface Impulse Force
Slow Drift, Springing and
Ringing Loads

Sclavounos (Journal of Fluid Mechanics, 2012)

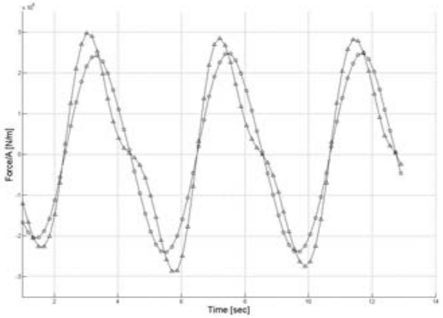

Nonlinear Surge exciting force in an ambient wave with kA=0.4 and kd=0.9. Triangles: Bernoulli Force; Circles: Body Impulse Force F_1.

Controls

- State-Space Model of Floating Wind Turbine Dynamics
- Unsteady Linear Quadratic Controller – Conjugate Control
- Energy Yield Enhancement by Blade Pitch and Torque Control
- Forecasting of Wave Elevation and Exciting Forces
- Load Mitigation and Damping at Above Rated Wind Speeds
- Energy Yield Increase by LIDAR Forecasting of Wind Speed

State-Space Model of Floater and Wind Turbine Dynamics

- Surge Equation of Motion in the Time-Domain:

$$\left[M + A_\infty\right]\ddot{\xi}(t) + \int_0^t K\left(t-\tau\right)\cdot\dot{\xi}(\tau)\,d\tau + B_V\dot{\xi} + C\xi(t) = X\left(t\right) + F_T(t,\vec{u})$$

$$K\left(s\right) = \frac{p_r s^r + p_{r-1}s^{r-1} + \cdots + p_0}{s^n + q_{n-1}s^{n-1} + \cdots + q_0}$$

- Equation of Motion of Rotor and Generator:

$$I\frac{d\Omega}{dt} = T_{Aero}(t,\vec{u}) - \eta T_{Gen}(\Omega); \quad \eta = \Omega_{Gen}/\Omega; \quad I = I_{Rotor} + \eta^2 I_{Gen}$$

- State-Space Model of System:

$$\dot{\vec{x}} = [A]\vec{x} + \vec{X} + [B_W]\vec{u}$$

Taghipour, Perez, Moan (Ocean Engineering, 2008)

15

Numerical CFD comparison of Lillgrund employing RANS

EERA DeepWind 2014

Deep sea offshore wind power
22-24 January 2014
Trondheim

Nikolaos Simisiroglou[a,b], Simon-Philippe Breton[b], Giorgio Crasto[a], Kurt Schaldemose Hansen[c], Stefan Ivanell[b]

[a] WindSim AS, Fjordgaten 15, N-3125 Tønsberg, Norway
[b] Uppsala University, Campus Gotland, Visby SE 621 67, Sweden
[c] Technical University of Denmark, Nils Koppels Alle 403, Kgs. Lyngby DK 2800, Denmark

Content

- Industrial PhD
  - WindSim AS
  - Uppsala University
- The Actuator Disc Concept
- Lillgrund
  - Lillgrund 120 Row 5 & Row 3
  - Lillrgrund 222 Row D & Row B
- Summary
- Future Study
- Aknowledgments

WindSim AS

- Established in 1993
- WindSim - World class software launched in 2003
- Ownership - Privately held company and venture backed
- Business areas
  - Software solutions, consulting services and training
    - Wind farm simulation and wind energy assessment
      - Entire wind farm lifecycle (pre/post construction)
      - Onshore and offshore

WindSim • offices and • resellers

WindSim HQ in Tønsberg, Norway

- WindSim AS has offices and reseller partners in; Argentina, Brazil, China (2), Costa Rica, Greece, Italy, India, Iran, Korea, Mexico, Norway, Serbia, Spain (2),Turkey and USA

www.windsim.com

Uppsala University Campus Gotland Wind Energy

Research

- From research on wake instabilities to simulations of complete wind farms
- Behavior of wakes and wake-turbine interactions
- Applied research on farm optimization
- Numerical Methods Actuator
  - •Actuator Disk (ACD)
  - •Actuator Line (ACL)

Education

- 1 Year Master program on campus in: Wind Power Project Management
- 11 Distance courses in Wind Power

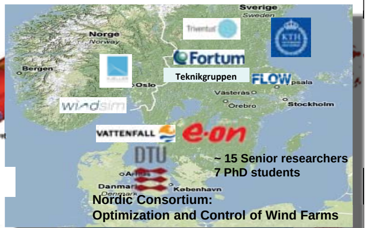

Actuator Disc Concept

The thrust, momentum sink for the axial flow, is supposed evenly distributed on the swept area (uniform pressure drop)

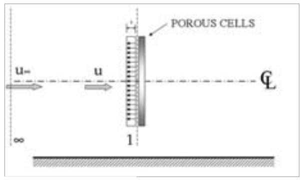

By definition axial induction factor

$$a_i = \frac{u_{\infty i} - u_{1i}}{u_{\infty i}} \quad (1)$$

Betz's theory

$$a_i = \frac{1}{2}\left(1 - \sqrt{1 - C_{T,i}}\right) \quad (2)$$

$$t_i = C_T \frac{1}{2} \rho u_\infty^2 area_i$$

$$\Rightarrow t_i = C_{T,i}(u_{1,i}) \frac{1}{2} \rho \left(\frac{u_{1,i}}{1 - a_i(u_{1,i})}\right)^2 area_i \quad (3)$$

$$T \approx \sum_i t_i$$

Uniform : $t = T / A = C_T \frac{1}{2} \rho u_\infty^2$

Polynomial : $t(r) = C_1 + C_2 r^2 + C_3 r^4$

Lillgrund Offshore Wind Farm

- Located in Øresund consisting of 48 wind turbines (Siemens SWT-2.3-93)
- The presence of shallow waters caused the layout of the wind farm to have regular array with missing turbines (recovery holes).
- Very close inter-row spacing (3.3xD and 4.3xD)

Source: Vattenfall

- The maximum peak loss occurs for the second turbine in the row and is, for inter row spacing of 4.4xD, typically 70%, and for row spacing of 3.3xD, typically 80%.(Dahlberg, 2009)
- The turbine production efficiency rate for the entire wind farm has been found to be 67% if only below rated wind speeds are considered. (Dahlberg, 2009)

Different Parameters Analysed

- Grid sensitivity study
  - D/6 (approximately 15.3 m)
  - D/8 (approximately 11.5 m)
- Main Inflow angles
  - 120 degrees, TI=7,8
  - 222 degrees , TI=5,6
  - 300 degrees , TI=6,0
- Axial thrust distributions
  - Uniform
  - Polynomial
- Turbulence closure models
  - Standard k-epsilon,
  - Modified k-epsilon
  - K-epsilon with YAP correction
  - RNG k-epsilon

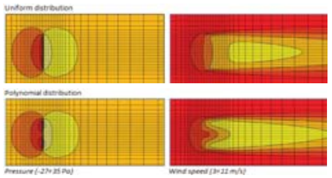

Lillgrund Row 5 120 ± 2,5 degrees

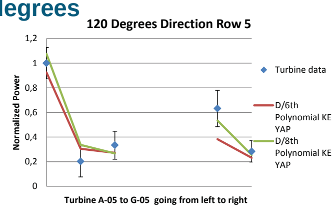

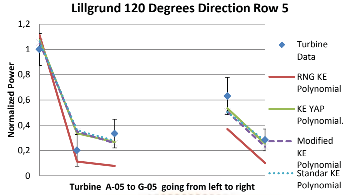

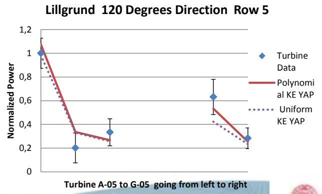

Lillgrund Row 3 120 ± 2,5 degrees

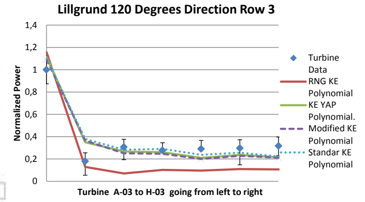

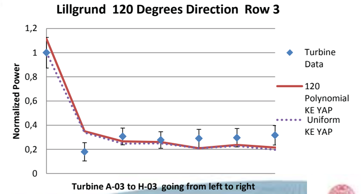

Lillgrund Row D 222 ± 2,5 degrees

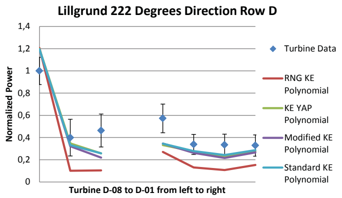

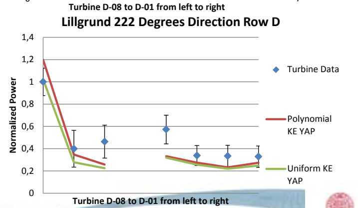

Lillgrund Row B 222 ± 2,5 degrees

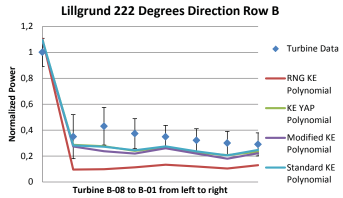

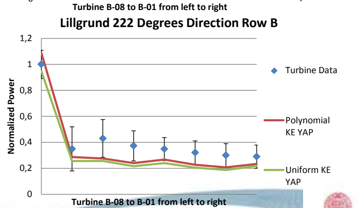

Summary

- Estimation capture the power production from wakes within the error bars of the experimental data.
- The results achieved using the higher resolution, D/8, outperform those obtained using the lower resolution simulation D/6.
- The polynomial distribution, by representing more accurately the thrust force distribution on the rotor, leads to results of higher accuracy in comparison to the uniform distribution.
- Good performance standard k-epsilon, modified k-epsilon and k-epsilon with YAP correction overestimate the power output of the second wind turbine in the row
- RNG k-epsilon captures in some cases the power production reduction in the second wind turbine but underestimates the following wind turbines of the row.

Future research

- Include additional analysis of the total amount of simulated result in further search for general trends.
- Moreover research will be directed on how to include meandering and swirl effects in the wake model used in this analysis.
- Finally studies with higher grid resolution will be conducted and comparison with analytical models and LES models will be conducted.

Acknowledgements

This research has been supported by:

The Research Council of Norway

Vattenfall Vindkraft

DeepWind 2014 – Deep sea offshore wind power, Trondheim

Poster Session

1. *Numerical simulation of a wind turbine with hydraulic transmission system, Zhiyu Jiang, NTNU*
2. *A DC-OPF Computation for Transmission Network Incorporating HVDC Transmission Systems, Phen Chiak See, NTNU*
3. *Cross-Border Transfer of Electric Power under Uncertainty: A Game of Incomplete Information, Phen Chiak See, NTNU*
4. *FSI-WT: A comprehensive design methodology for Offshore Wind Turbines, Espen Åkervik, FFI*
5. *First verification test and wake measurement results using a Ship-Lidar System, G Wolken-Möhlmann, Fraunhofer IWES*
6. *Buoy-mounted lidar provides accurate wind measurement for offshore wind farm developments*, Jan-Petter Mathisen, Fugro OCEANOR
7. *Characterization of the SUMO turbulence measurement system for wind turbine wake assessment, Line Båserud, UiB*
8. *Field Measurements of Wave Breaking Statistics Using Video Camera for Offshore Wind Application, Mostafa Bakhoday Paskyabi, UiB*
9. *Stochastic Particle Trajectories in the Wake of Large Wind Farm, Mostafa Bakhoday Paskyabi, UiB*
10. *LiDAR Measurement Campaign Sola (LIMECS), Valerie-Marie Kumer, UiB*
11. *Fatigue Reliability-Based Inspection and Maintenance Planning of Gearbox Components in Wind Turbine Drivetrains, Amir Nejad, NTNU*
12. *Engineering Critical Assessment (ECA) of Electron Beam (EB) welded flange connection of wind turbine towers, P. Noury, Luleå University of Technology*
13. *A Multiscale Wind and Power forecast system for wind farms, Adil Rasheed, SINTEF ICT*
14. *NOWITECH Reference Wind Farm, Henrik Kirkeby, SINTEF Energi AS*
15. *Actuator disk wake model in RaNS, Vitor M. M. G. Costa Gomes, Faculdade de Engenharia da Universidade do Porto*
16. *Model reduction based on CFD for wind farm layout assessment, Chad Jarvis, Christian Michelsen Research AS*
17. *Energy yield prediction of offshore wind farm clusters at the EERA-DTOC European project, E. Cantero, CENER*
18. *Sizing of Offshore Wind Localized Energy Storage, Franz LaZerte, NTNU*
19. *Unsteady aerodynamics of attached flow for a floating wind turbine, Lene Eliassen, UiS*
20. *FloVAWT: development of a coupled dynamics design tool for floating vertical axis wind turbines, Michael Borg, Cranfield University*
21. *Use of an industrial strength aeroelastic software tool educating wind turbine technology engineers, Paul E. Thomassen, Simis as*
22. *Offshore ramp forecasting using offsite data, Pål Preede Revheim, UiA*
23. *Significance of unsteady aerodynamics in floating wind turbine design, Roberts Proskovics, Univ of Strathclyde*
24. *Wind Tunnel Testing of a Floating Wind Turbine Moving in Surge and Pitch,* Jan Bartl, NTNU
25. *Sub-sea Energy Storage for Deep-sea Wind Farms*, Ole Christian Spro, SINTEF Energi AS
26. *How can more advanced failure modelling contribute to improving life-cycle cost analyses of offshore wind farms*?, Kari-Marie Høyvik Holmstrøm, University of East London
27. *Will 10 MW wind turbines bring down the operation and maintenance cost of offshore wind farms?,* Matthias Hofmann/Iver Sperstad Bakken, SINTEF Energi AS
28. *Modelling of Lillgrund wind farm: Effect of wind direction,* Balram Panjwani, SINTEF
29. *Lab-scale implementation of a multi-terminal HVDC grid connecting offshore wind farms, Raymundo Torres-Olguin, SINTEF Energi AS*

Numerical Simulation of a Wind Turbine with Hydraulic Transmission System

NTNU – Trondheim
Norwegian University of Science and Technology

Zhiyu Jiang[1,2,3], Limin Yang[4], Zhen Gao[1,2,3], Torgeir Moan,[1,2,3]

[1] Department of Marine Technology, Norwegian University of Science and Technology (NTNU), Trondheim, Norway
[2] Centre for Autonomous Marine Operations and Systems, NTNU, Trondheim, Norway
[3] Centre for Ships and Ocean Structures, NTNU, Trondheim, Norway
[4] DNV GL, Høvik, Norway

Abstract

We investigate numerical modeling and analysis of wind turbines with high-pressure hydraulic transmission machinery. A dynamic model of the hydraulic system is developed and coupled with the aeroelastic code HAWC2 through external Dynamic Link Library. The hydraulic transmission system consists of a hydraulic pump, transportation pipelines, a hydraulic motor, and check valves. By use of the Runge-Kutta-Fehlberg method with step size and error control, we solved the Ordinary Differential Equations of the hydraulic system with a time step smaller than the one used in the HAWC2 main program. Under constant and turbulent wind conditions, the performances of a land-based turbine during normal operation are presented.

Objectives

During the study, the research objectives are the following:

- To model the hydraulic transmission system by Ordinary Differential Equations
- To propose an approach for numerical simulation of hydraulic turbines

Mathematical Modeling

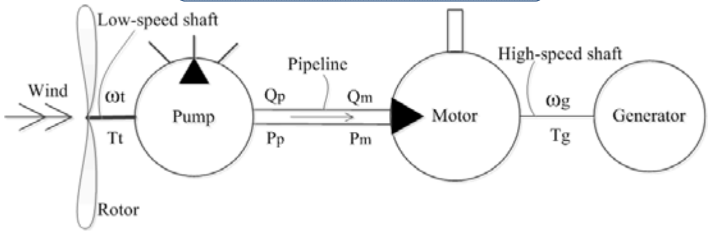

Main shaft $T_t = J_p\dot{\omega}_t + D_p(P_p - P_{low})$

Pump $\dot{P}_p = \dfrac{\beta}{V_p}[\omega_t D_p - Q_{ip}(P_p - P_{low}) - Q_{ep}P_p - Q_p]$

Motor $\dot{P}_m = \dfrac{\beta}{V_m}[Q_m - Q_{im}(P_m - P_{low}) - Q_{em}P_m - D_m\omega_g]$

Transmission line $\begin{bmatrix}\dot{Q}_{p0}\\ \dot{Q}_{m0}\end{bmatrix} = \omega_c\left[A_0\begin{bmatrix}Q_{p0}\\ Q_{m0}\end{bmatrix} + B_0\begin{bmatrix}P_p\\ P_m\end{bmatrix}\right]$ $\begin{bmatrix}\dot{Q}_{p1}\\ \dot{Q}_{m1}\end{bmatrix} = \omega_c\left[A_1\begin{bmatrix}Q_{p1}\\ Q_{m1}\end{bmatrix} + B_1\begin{bmatrix}P_p\\ P_m\end{bmatrix}\right]$

Generator $\dot{\omega}_g = \dfrac{1}{J_m + J_g}[D_m P_m - C_m\omega_g - T_g]$

Numerical Approach

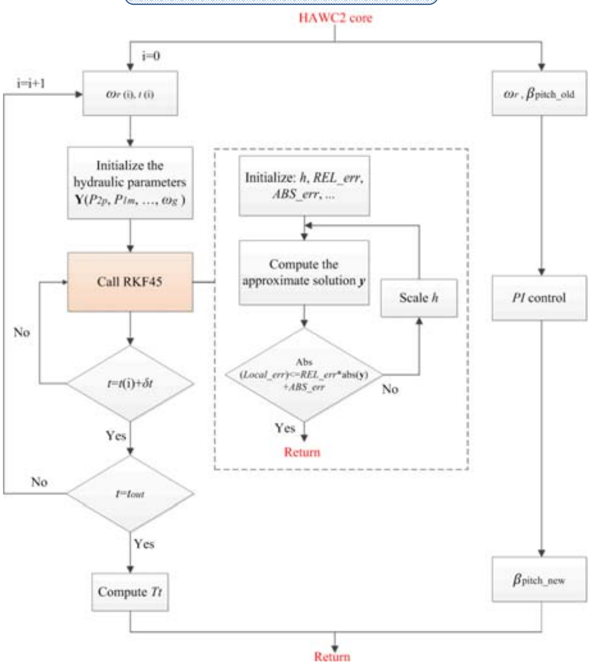

Results

Constant wind, Turbulence Intensity=0

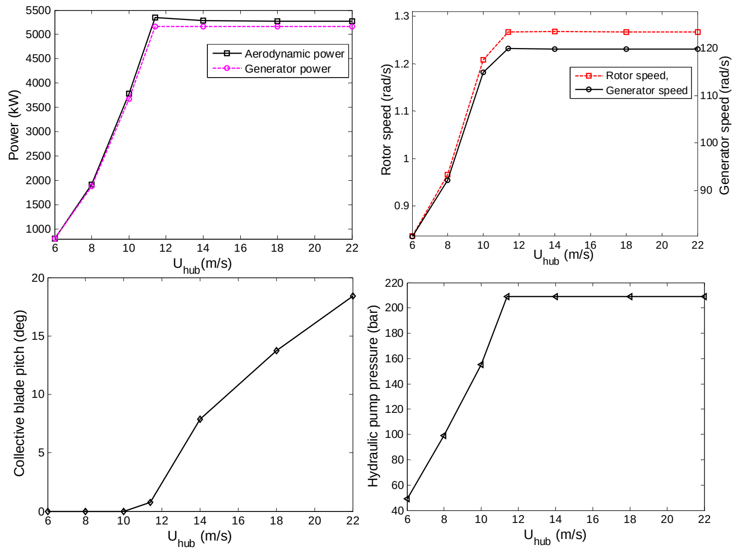

Uhub=8 m/s, Turbulent wind, Turbulence Intensity=0.23

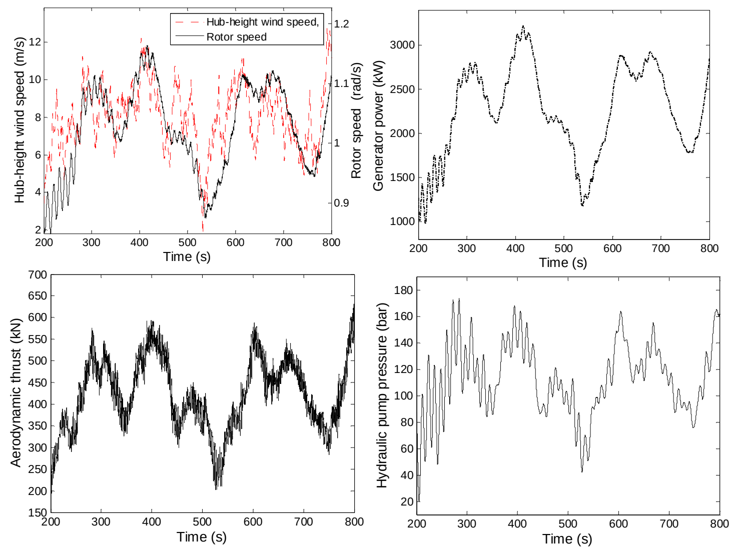

Conclusions

- The presented numerical approach is robust and efficient
- The hydraulic wind turbine has decent performance under constant and turbulent wind conditions

Acknowledgment

The authors gratefully acknowledge the financial support from the European Commission through the 7th Framework Programme (MARINA Platform—Marine Renewable Integrated Application Platform, Grant Agreement 241402).

References

1. Yang, L., Moan, T. (2011). Dynamic analysis of wave energy converter by incorporating the effect of hydraulic transmission lines, *Ocean Engineering*, 38(16) 1089-1102.
2. Skaare , B., Hornsten, B., Nielsens, F.G. (2012). *Modeling*, simulation and control of a wind turbine with a hydraulic transmission system, *Wind Energy*, 1-19.

Refer to the paper for more.

A DC-OPF Computation for Transmission Network Incorporating HVDC Transmission Systems

Phen Chiak See and Olav Bjarte Fosso

Department of Electric Power Engineering, Norwegian University of Science and Technology, 7491 Trondheim, Norway

phenchiak.see@gmail.com

This paper presents a new method for computing the Direct Current Optimal Power Flow (DC-OPF) in transmission network integrated with HVDC transmission systems. The method is called the Fictitious Aggregated Node (FAN) model. Conceptually, the method flexibly forms aggregated nodes (when computing the OPF of transmission network) by combining buses connected with the HVDC lines. After that, the modified transmission network topology is subjected to regular DC-OPF computation. The resultant power flow between buses located within the aggregated node can then be calculated based on the results derived in DC-OPF. This simplified method is fast and intuitive. Besides, it is able to cover HVDC computation in DC-OPF without significantly increasing the computation time. The method can be applied in economic studies related to expansion of inter-region transmission network. Currently, the method is applied by the authors in game theoretic studies of offshore transmission networks.

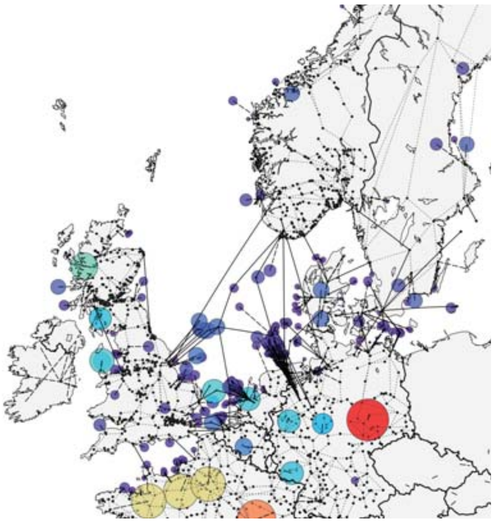

An offshore grid scenario in 2050 (Source: SINTEF).

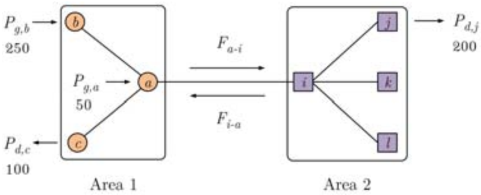

A transmission network with HVDC connecting bus a and i.

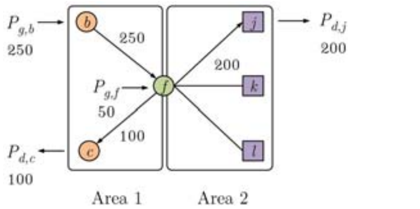

Power flow on the transmission lines computed with DC-OPF.

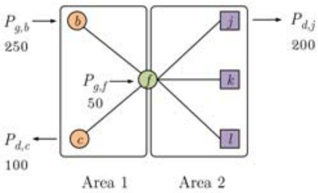

Formation of FAN. This transmission network model is called FAN model.

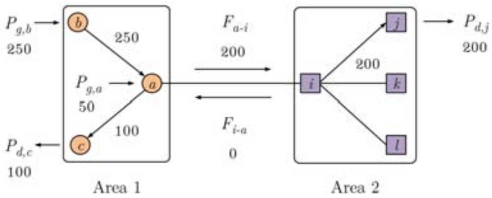

The resultant power flow on the HVDC lines.

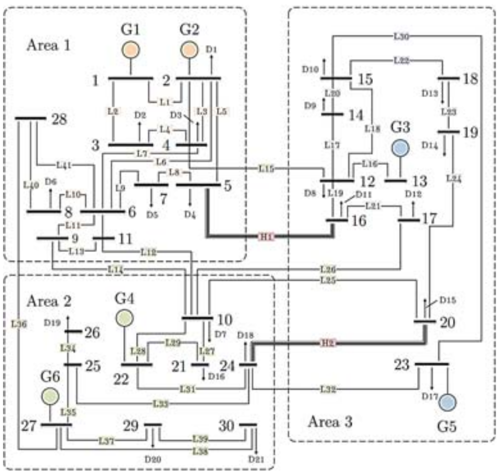

A slightly modified IEEE 30-bus test system connected with two HVDC lines.

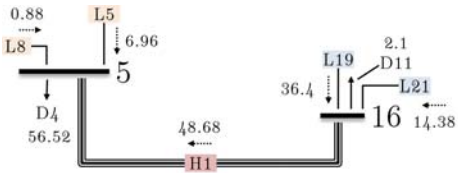

Power flow around FAN 1.

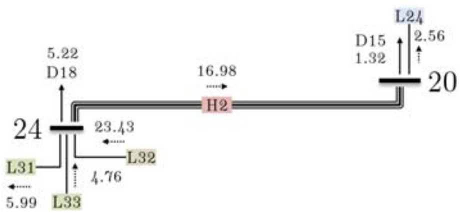

Power flow around FAN 2.

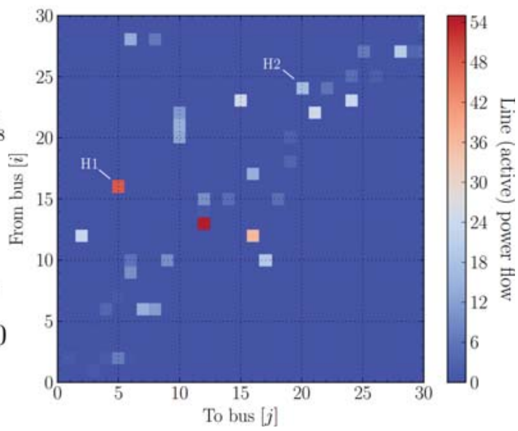

Power flow on transmission lines in the 30-bus model connected with HVDC.

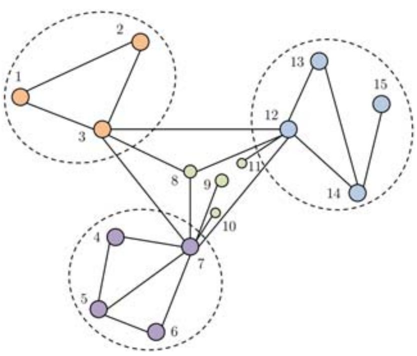

A 15-bus transmission network model connected with four wind power generators and meshed HVDC grids.

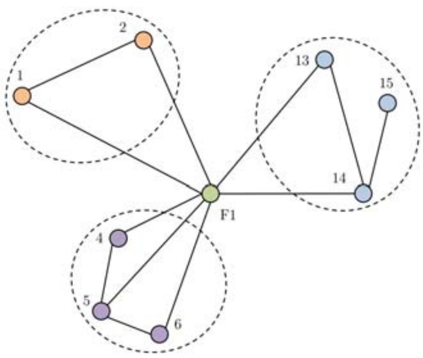

The meshed grid is aggregated as FAN. The power flow in the model is then computed with DC-OPF.

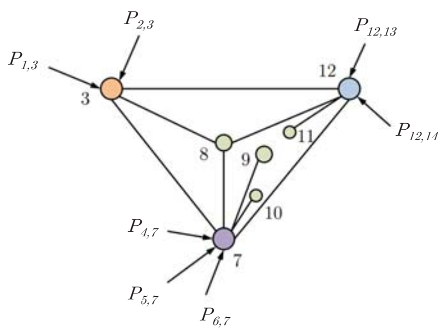

The power flow on the HVDC grid can be computed based on power balance at node 3, 12, and 7.

Cross-Border Transfer of Electric Power Under Uncertainty: A Game of Incomplete Information

Phen Chiak See and Olav Bjarte Fosso

Department of Electric Power Engineering, Norwegian University of Science and Technology,
7491 Trondheim, Norway

phenchiak.see@gmail.com

Cross-border transfer of electric power promotes collaboration in power generation between integrated electricity markets. It as well resolve grid reinforcement issues in existing transmission networks. Because of that, researchers have given higher attention to the field and have conducted various studies on the subject using technical simulation approaches. Yet, substantial works have to be done for quantifying the socioeconomic benefits of the mechanism. This paper intends to fill the gap by introducing a method for analyzing the mechanism by representing it as a game of incomplete information. The subject is modeled as Bayesian game in which the type of marginal generators located within one (or more) external market area is not known. Based on that, the Bayesian equilibrium which represent the state where all marginal generators would incline to converge is found. The authors suggest that the method is robust and can be used for quantifying the performance of a market coupling mechanism because it realistically consider all marginal generation scenarios.

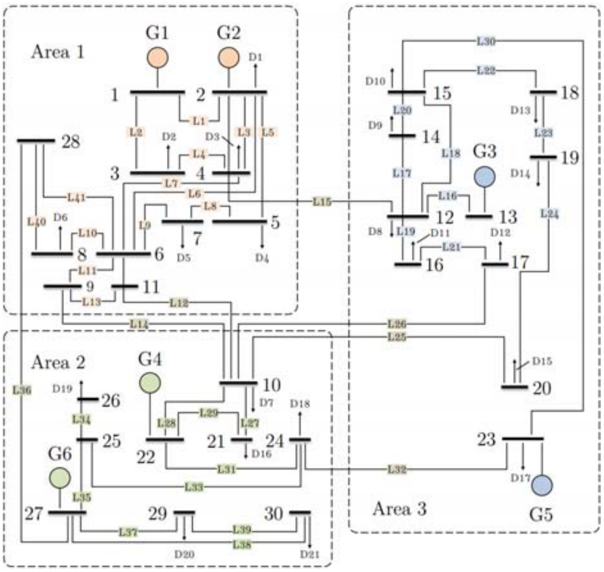

A slightly modified IEEE 30-bus test system

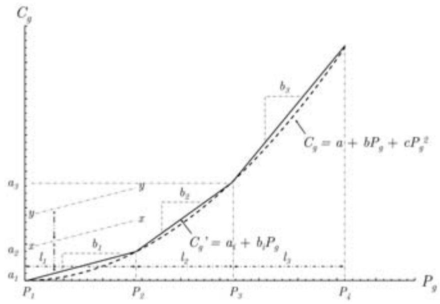

Upper piecewise approx. of generation cost.

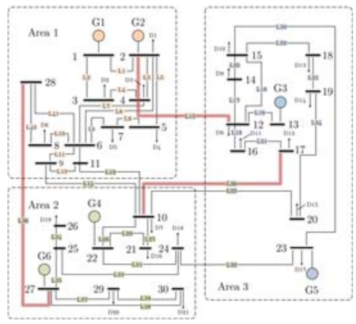

PTDF, flowgate capacity computation

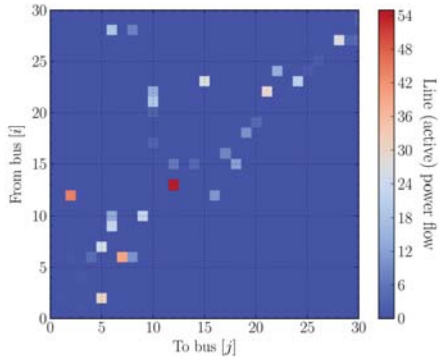

Base case power flow (DC-OPF)

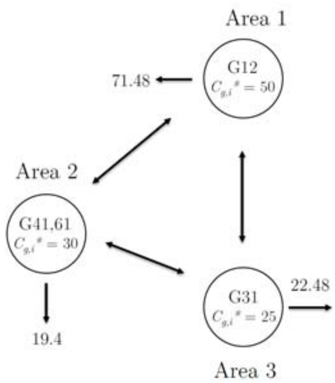

Cross-border transfer model (FBMC)

Formally, let θ_i be the type of player i in a game, and $p(\theta_{-i}|\theta_i)$ represents first order belief owned by player i towards the type of his opponent (given that the type of him is θ_i, which is known only to himself). The set of all types of player i is Θ_i and $\theta_i \in [0, 1)$ for all $\theta_i \in \Theta_i$. Under such conditions, a player would choose his action based on his types, and different actions may be assigned to different types. Based on that, he owns a strategy, s_i that maps Θ_i to A_i. Hence, $s_i : \Theta_i \to A_i$. Because Bayesian game theory suggests that the choice of a player's action follows θ_i and $p(\theta_{-i}|\theta_i)$, the expected payoff of by player i in the game becomes:

$$E[u_i(s_i|s_{-i},\theta_i)] = \sum_{\theta_i \in \Theta_{-i}} u_i(s_i, s_{-i}(\theta_i), \theta_i, \theta_{-i}) p(\theta_i|\theta_{-i}) \qquad (1)$$

where, $s_{-i}(\theta_i)$ is the strategy taken by players except player i, given that the type of player i is θ_i. A Bayesian equilibrium (BE) is the Nash equilibriums of the Bayesian game, formulated as follows.

$$E[u_i(s_i|s_{-i},\theta_i)] \geq E[u_i(s_i'|s_{-i},\theta_i)] \qquad (2)$$

Upon achieving BE, player i receives lower expected utility if he uses a strategy other than s_i (denoted by s_i'). The existence of BE is guaranteed because of the proven existence of NE.

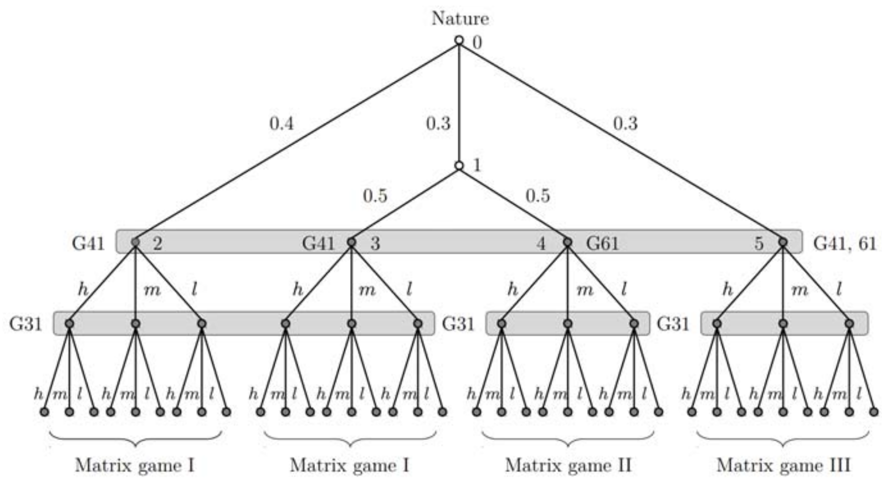

The Bayesian game in cross-border trade of electric power simulated in this work.

G31

G41

G41–G31	Low	Medium	High
Low	700, 1000	700, 800	700, 600
Medium	525, 1000	525, 800	525, 600
High	350, 1000	350, 800	350, 600

G61

G61–G31	Low	Medium	High
Low	700, 875	700, 700	700, 525
Medium	525, 875	525, 700	525, 525
High	350, 875	350, 700	350, 525

G41,61

G41–G31	Low	Medium	High
Low	1400, 466	1400, 373	1400, 592
Medium	1050, 466	1050, 373	1050, 600
High	700, 466	700, 373	700, 280

Payoff received by area 2: 910, area 3: 858

" … In order to decide what we ought to do to obtain some good or avoid some harm, it is necessary to consider not only the good or harm in itself. But also the probability that it will or will not occur, and to view geometrically the proportions all these things have when taken together … "

Arnauld and Nicole 1996, 273-4

FSI-WT: A COMPREHENSIVE DESIGN METHODOLOGY FOR WIND TURBINES

Espen Åkervik[1], Jørn Kristiansen[2], Adil Rasheed[3], Runar Holdahl[3], Trond Kvamsdal[3]
[1]Norwegian Defense Research Establishment, [2]MET Norway, [3]Applied Mathematics SINTEF ICT

A Multiscale approach to model the entire event from mesoscale meteorology, through microscale meteorology to the aerodynamics of wind turbine blades

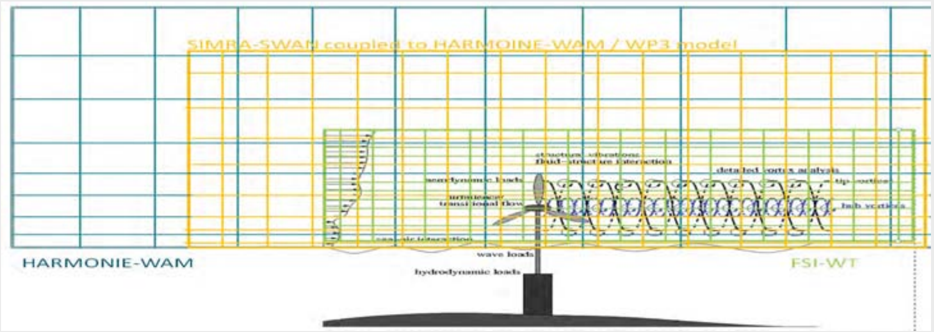

Global-Meso coupling

Isogeometric finite element code to simulate fluid-structure interaction of a rotating turbine

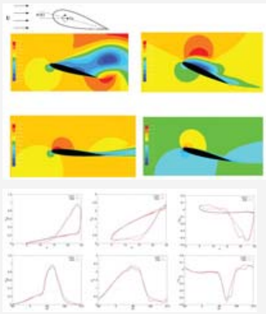

FSI of a moving 2-D airfoil
Output:: Drag, lift and moment coefficient

In progress: FSI of a single 3D blade

Planned work: FSI of a full 3D rotating turbine

Boundary conditions: Wind and Turbulence for FSI simulation

HARMONIE-WAM coupling

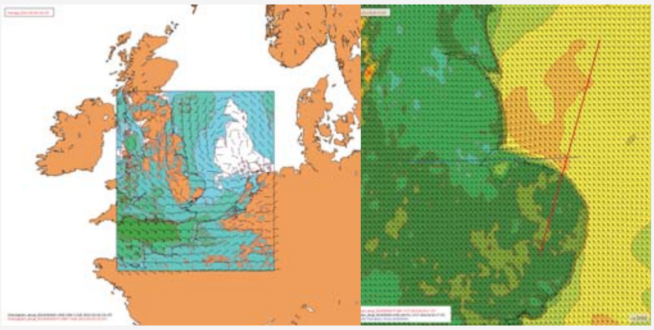

Bessaker Wind Farm

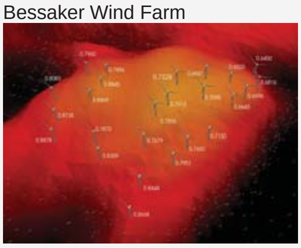

Microscale simulation of a wind farm in complex terrain
Output: Power production forecast and detailed 3D wind, temperature and turbulence field

Sheringham Shoal Wind Farm

Planned work: Microscale simulation of an offshore wind farm: Power production forecast and detailed 3D wind field

WIND ENERGY FORECAST

Improved parameterization for modeling of air-sea interaction

Near shore characterization of waves

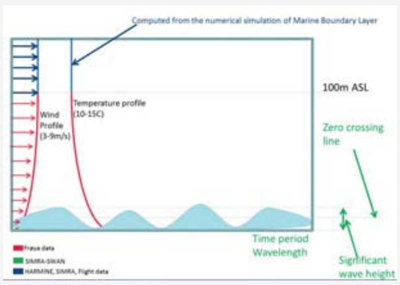

SWAN results, Meteorological data,and observation data to set up cases for detailed LES

Large Eddy Simulation to capture wave effects on turbulent boundary layers

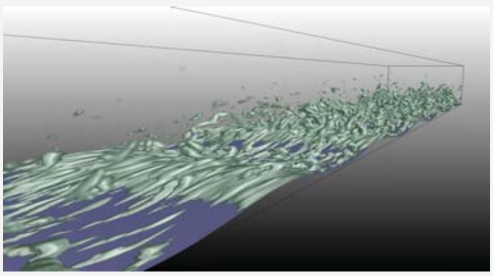

LES of turbulent flow over wavy wall

Advanced Finite Volume code on unstructured grid

Effects of waves on turbulence in atmospheric boundary layer modeled in detail

Improve parameterization of the sea-atmosphere interface in wave models

Planned work:

Include stratification effects

Two way coupling of air-sea using Volume of Fluid and/or Level Set method

The authors acknowledge the financial support from the Norwegian Research Council and the industrial partners of the FSI-WT-project (216465/E20) | Contact: espen.akervik@ffi.no, adil.rasheed@sintef.no

First verification test and wake measurement results using a Ship-LIDAR System

Fraunhofer IWES

G. Wolken-Möhlmann*, J. Gottschall and B. Lange

Fraunhofer IWES, Am Seedeich 45, 27572 Bremerhaven, Germany

*gerrit.wolken-moehlmann@iwes.fraunhofer.de

Abstract

Measuring wind offshore in deep water depths will be a future challenge. Where the sea bed installation of foundations for fixed met masts is impossible, even the mooring of floating systems are more complicated. Ship-lidar systems are an alternative solution for a number of different applications.

In this poster we describe two motion-correction methods for motion-influenced lidar measurements. The ship-lidar system will be presented as well as the first measurements carried out as part of the EERA-DTOC project. Therefore a verification of one correction algorithm will be shown as well as first results from wake measurements behind the Alpha Ventus offshore wind farm.

Measuring set-up

The ship-lidar system comprises a Leosphere WindCube V2 device, different motions-sensors (AHRS, satellite compass), a computer for data acquisition as well as equipment for power supply and wireless communication. The system is combined in a frame in order to ensure a fixed geometry, compare [1].

For the presented measurements, the system was installed on the offshore support vessel LEV TAIFUN with a length of 41.45 m. The system was located approx. 7 m above the point of rotation, whereas the roll frequency is close to f=5 s with extreme roll angles up to 20°

Figure 1: Ship-lidar installation on the LEV TAIFUN.

Figure 2: Ship-lidar measurement in proximity to offshore meteorological mast FINO1. Position of the lidar system is indicated by the red beam lines.

Motion correction algorithms

Wind-lidar measurements using line of sight (LoS) measurements in different beam orientations are solved under the assumption of homogeneity as well as constant wind velocity on each altitude, using a system of linear equations (SLE):

$$\begin{bmatrix} o_x(t_1) & \cdots & o_z(t_1) \\ \vdots & \ddots & \vdots \\ o_x(t_n) & \cdots & o_z(t_n) \end{bmatrix} \cdot \begin{pmatrix} u(h) \\ v(h) \\ w(h) \end{pmatrix} = \begin{pmatrix} v_{LoS}(t_1, h) \\ \vdots \\ v_{LoS}(t_n, h) \end{pmatrix}$$

$$=> O \cdot \vec{u} = \vec{v}_{LoS}$$

In general, these measurements can be influenced by translatory and rotatory motions, that can be considered by modifying the SLE to

$$O_{tilt} \cdot \left(\vec{u} - \vec{v}^{sys.Velocity,lt}\right) = \vec{v}^{wind}_{LoS} + O_{tilt} \cdot V^{sys.Velocity}_{ko}$$

Under the assumption of constant orientation and motion during the time period covered by the system of SLE, a simplified motion correction can be applied on the resulting wind vector from the SLE.

$$\vec{u}_{wind} = R_{yaw}(\vec{u}_{measured}) - \vec{u}_{ship}$$

Especially periodical tilting motions in the frequency range of the lidar measurement frequency, combined with additional translatory motion due to the distance from lidar to center of rotation can lead to beating effects that are not considered by the simple motion correction.

Floating lidar corrections algorithms were studied in [2] and [3].

Measurement campaigns

For the EU FP7-funded EERA-DTOC project, two measurement campaigns were performed from 27-31 August 2013 and 04-09 October 2013 comprising approx. 7.5 days in proximity to Alpha Ventus wind farm.

Goal of the measurement was the survey of wind farm wakes in different distances. In order to verify the measurement principle, data was also acquired in free inflow in proximity to FINO1.

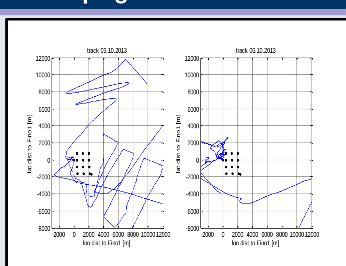

Figure 4: Plots of ship track for the second measurement campaign.

Verification of correction algorithm

For the first analysis, the simplified correction algorithm was applied on the measured data. Figure 5 shows results of uncorrected, yaw corrected (rotated) and fully corrected data for one-minute-mean values for the 5th of October 2013.

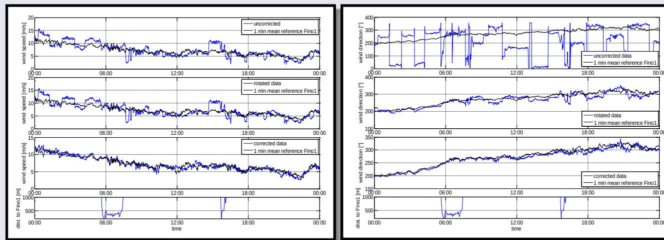

Figure 5: Comparison of wind speed and direction data between FINO1 and ship measurement for different levels of correction.

Scatter plots also show improvements between uncorrected and corrected data (see figure 6). Nevertheless the correlation of the data is not comparable to fixed lidar or lidar-buoy data [4].

A reason could be motion effects on the ship measurement that are not considered by the simplified motion correction.

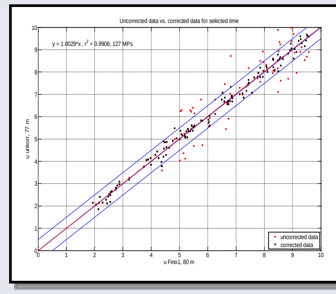

Figure 6: Scatter plot of 10-min-mean values, selected for wind direction and distance to FINO1.

Wake measurements

First wake measurements were performed with ship tracks perpendicular to the wakes, see figure 8. Results show distinct wakes for a distance of approx. 15D, see figure 7. These wakes can be identified by decreased wind speeds and increased turbulence.

For longer distances, reference wind data are necessary.

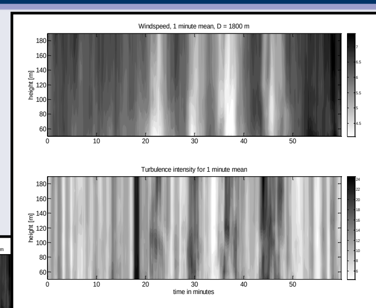

Figure 7: Plots of wind speed and turbulence intensity.

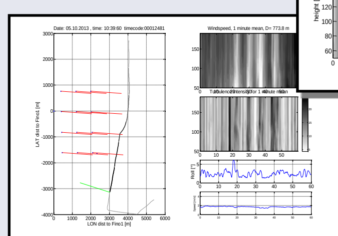

Figure 8: Overview of ship track and theoretical wind wakes.

Conclusions

First ship-based lidar measurements next to met masts FINO1 show good correlations for wind speed and direction using the simplified correction. Nevertheless it is assumed that the complete motion correction will improve the data.

Using the ship-lidar for wake measurements, wakes could be identified clearly for distances of approx. 15 rotor diameters. For longer distances, inflow reference data as well as a complete motion correction is necessary.

References

1. Ship based -lidar measurements, G. Wolken-Möhlmann et. al., *Proceedings of DEWEK 2012, Bremen*
2. Simulation of motion induced measurement errors for wind measurements using LIDAR on floating platforms, G. Wolken-Möhlmann et. al., *Proceedings of ISARS 2010, Paris, France*
3. Lidars on floating offshore platforms – about the corrections of motion-induced lidar measuremen terrors, J. Gottschall et. al., *Proceedings of EWEA conference 2012, Copenhagen*
4. Path towards bankability of floating lidar data, P. Flower, DNV-GL, *Presentation EWEA Offshore*

Acknowledgements

This research projekt was funded as part of the Seventh Framework Programme.

Reference data was provided by the DEWI (wind data) and the German Federal Maritime and Hydrographic Agency (BSH) which was acquired as part of the FINO project, funded by the German Federal Ministry for the Environment, Nature Conservation and Nuclear Safety (BMU).

SEAWATCH WIND LIDAR BUOY

A multi-purpose buoy for measuring wind profile at 10 levels from 12m up to 300m, other meteorological parameters, waves and current profile. By using the new Seawatch power system the buoy can measure the wind profile continuously for 6 months without service.

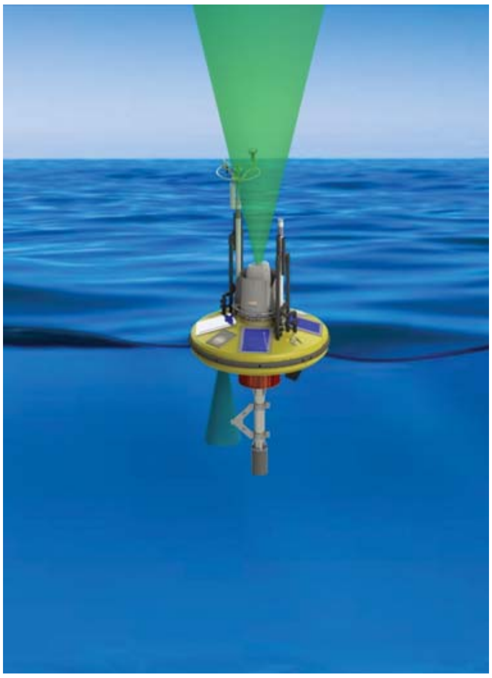

Field test Titran – Wind speed at 53m

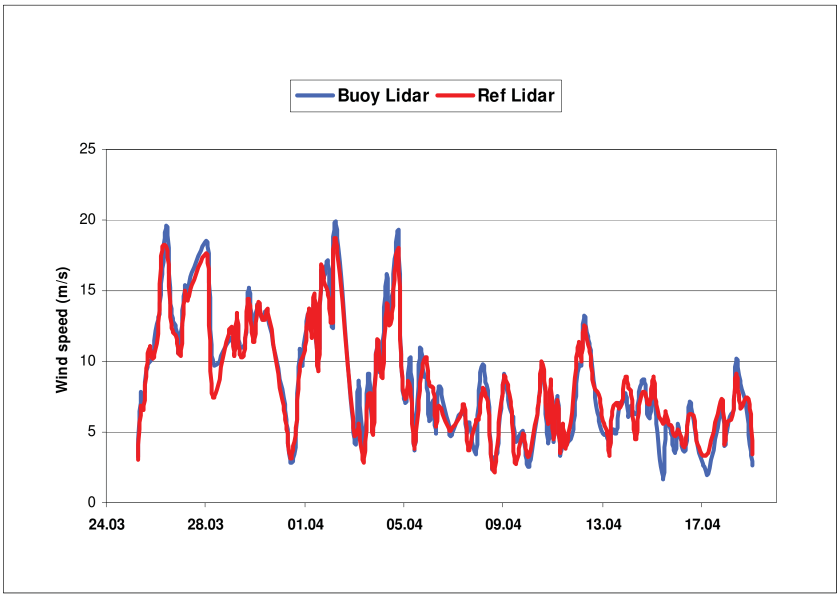

Verification test Ijmuiden Met mast

Storm Hilde Trondheimsfjord

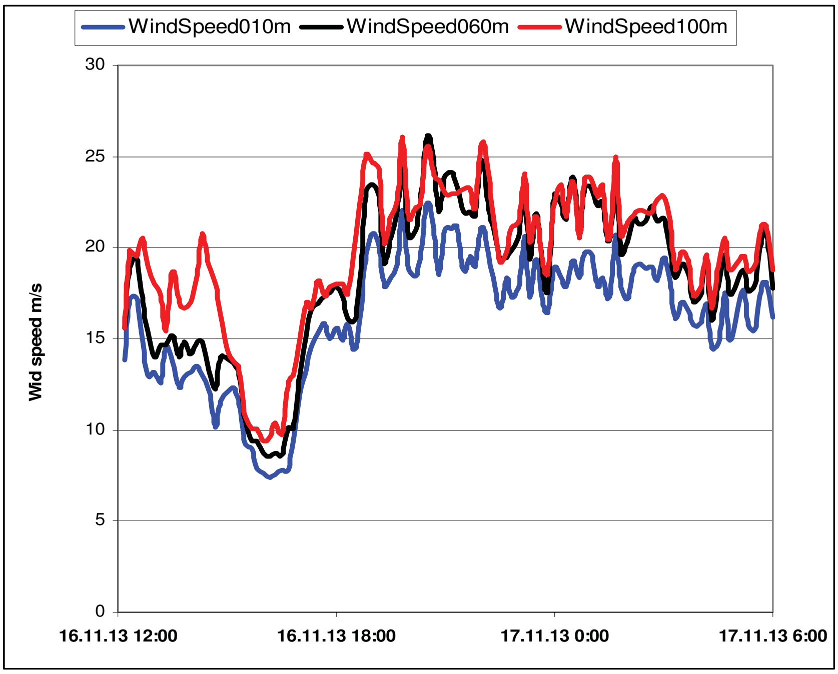

Characterization of the SUMO turbulence measurement system for wind turbine wake assessment

Line Båserud, Martin Flügge, Anak Bhandari, Joachim Reuder

Geophysical Institute, University of Bergen
Line.Baserud@gfi.uib.no

EERA DeepWind'2014, 11th Deep Sea Offshore Wind R&D Conference

The remotely piloted aircraft system (RPAS) SUMO (Small Unmanned Meteorological Observer) has recently been equipped with a miniaturized 5-hole probe turbulence sensor with a temporal resolution of 100 Hz.
Due to it's small size SUMO is well suited for operations in wind farms as it will not impose any danger to the turbines in case of a collision.
The spectral response of the 5-hole probe has been investigated through laboratory- and environmental tests.

Measurement system

The RPAS SUMO is based on the fixed-wing model aircraft FunJet. It is a small and flexible system with a take-off weight of 600 g and length and width of about 80 cm (Fig. 1). More details can be found in e.g. Reuder et al. 2009.

The 5-hole probe micro Air Data System (ADS) consists of an Air Data Computer (ADC), a 5-hole probe and corresponding pressure transducers (Fig. 1). The probe is placed in the nose of the aircraft. Output for true airspeed (TAS), angle of attack (α), angle of sideslip (β) and altitude is given based on differential pressure measurements.

The 3-dimensional wind vector is calculated from 5-hole probe measurements of the flow approaching the aircraft after correcting for aircraft movement (e.g. Lenschow 1989).

Fig 1: The SUMO system and the 5-hole probe turbulence sensor.

Achnowledgements:
The authors are greatful to Prof. Stephan Lämmlein from the University of Applied Sciences in Regensburg for giving access to the wind tunnel and to his student Sebastian Wein for performing the wind tunnel tests of the 5-hole probe. Great thanks are also going to Bjrn Nygaard and his colleagues from the Avinor team at Bergen airport Flesland for the permission to use the runway and for all help and assistance during the environmental comparison test of the SUMO system against the sonic anemometers. This work has been funded by a joint research project between Statoil AS and the Geophysical Institute at the University of Bergen as part of the Norwegian Center for Oshore wind Energy (NORCOWE).

Wind tunnel tests of the 5-hole probe

Fig 2: The setup for the laboratory tests. Left: The test setup for the ADS; Right: The horizontal stick used to create turbulence in the flow. Pictures by Sebastian Wein.

The 5-hole probe was first tested in a parallel experiment together with a hot-wire anemometer (HW). Spectra of airspeed from the two systems can be seen in Fig. 3.

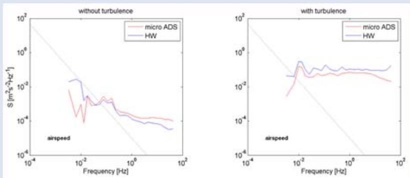

Fig 3: Spectra of airspeed from the HW and 5-hole probe parallel test.

- Both systems experience an energy shift between laminar and turbulent conditions
- The 5-hole probe react to the turbulence in a similar manner as the HW system in the relevant frequency range

The 5-hole probe was also tested with different tubing lengths between the probe and the ADC (15 cm, 30 cm and 90 cm). Spectra of TAS, α and β can be seen in (Fig. 4).

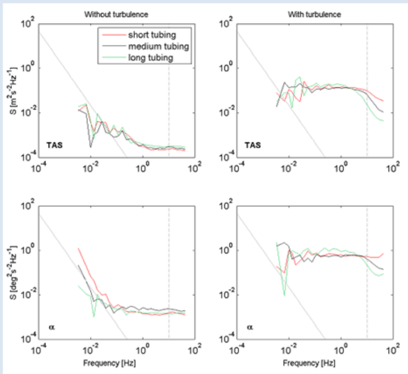

Fig 4: Spectra of TAS and α from the 5-hole probe for the different tubing lengths of 15 cm (red), 30 cm (black) and 90 cm (green).

- Little effect for laminar conditions
- With turbulence, some energy is lost for the highest frequencies
- The longer the tubing, the larger the loss by spectral damping.
- The system resolves turbulence appropriately up to a frequency of 20-30 Hz when using the shortest tubing

References:

Reuder et al, 2009: The Small Unmanned Meteorological Observer SUMO: A new tool for atmospheric boundary layer research. *Meteorologische Zeitscrift.*, **18**(2), 141-147.

Lenschow DH & Spyers-Duran P, 1989: Measurements techniques: Air motion sensing. *National Center for Atmospheric Research (NCAR) Bulletin* **23**

Environmental test of the 5-hole probe

To investigate the behavior of the 5-hole probe under atmospheric turbulence conditions, the spectral response of the u, v and w wind components from SUMO and a sonic anemometer was compared by driving with the instruments mounted on a car along the 2600 m long runway of Bergen airport Flesland (total of 12 legs with a speed of 20 or 25 m/s).

Fig 5: Setup for the test campaign at Flesland airport. From left to right: Gill R3-100 sonic anemometer, SUMO dummy with the 5-hole turbulence probe, Campbell CSAT3 sonic anemometer.

The resulting measurements of u, v, and w in the SUMO coordinate system by the 5-hole probe are shown in Fig. 6:

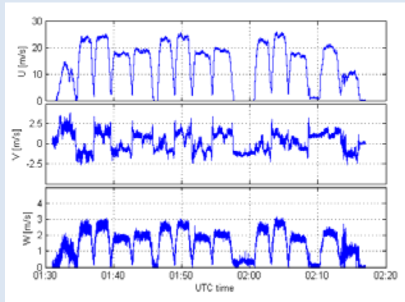

Fig 6: Time-series of u (in direction of the moving car), v (crosswind) and w (vertical) components of the measured flow vector.

First results of turbulence spectra for the u-component are presented in Fig. 7:

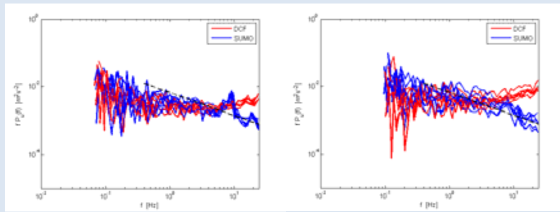

Fig 7: Spectra of the u-component for the legs with 20 m/s (left) and 25 m/s (right)

- The SUMO system measures spectra that are in general following the expected -2/3 slope expected from a Kolmogorov spectrum
- The peak at around 9 Hz is related to a vibration frequency of the SUMO mounting rod
- In the frequency range up to ca. 5 Hz, the 5-hole probe and the sonic anemometer show good agreement
- At higher frequencies the energy level of the sonic anemometer is distinctly enhanced, this can most likely be attributed to flow distortion at the edges of the mounting platform

Field Measurements of Wave Breaking Statistics Using Video Camera for Offshore Wind Application

Geofysisk institutt
Universitetet i Bergen

M Bakhoday Paskyabi, M. Flugge, V. Kumer, J. Reuder, and I.Fer
Geophysical Institute, University of Bergen, Bergen, Norway

norcowe
Norwegian Centre for Offshore Wind Energy

Introduction

Wave breaking as a widespread phenomenon all over the world oceans that interacts in a nonlinear complicated way to marine structures and provides a mechanism for exchange of momentum, heat, gas, energy, and moisture across the air-sea interface. In spite of difficulty to measure this phenomenon in the field, wave breaking in deep and shallow waters have been subjected to several theoretical, laboratory, observational, and numerical studies during the last four decades. Recent research, e.g. Sullivan et al 2009 and Nielsson 2012, has shown that waves have the ability to influence the turbulence structure in the lower marine atmospheric boundary layer and thus to increase loads and fatigue on turbine rotor blades. In addition, wave breakings will doubtless increase loads exerted on the turbine foundations and monopile structure. Investigation of wave breaking processes is therefore highly required for the development of offshore wind farms in deep water. In this study, we use a video camera mounted on a discus buoy during a 10-day deployment at the end of November 2013. The buoy will presumable be moored in the Norwegian Havsul area which is approved for offshore wind farms. This gives us first hand ability to reconstruct the sea surface waves and orbital velocities. Furthermore, we detect breakers with an image processing algorithm and track them on the observed surface. These techniques enable us to capture a broad frequency (wavenumber) range of breakers by conventional visible video techniques. The key breaking quantity extracted from the video recording is the length of breaking crest per unit area. We investigate this parameter for different sea states to estimate the amount of energy dissipated from wave field to the underlying ocean mixing. The obtained dissipation is than compared with modelled and parameterized wave energy dissipation.

➢Site: South of Bergen, 20-29 November 2013

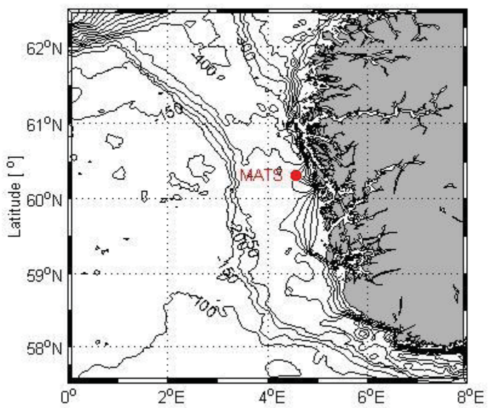

➢Instrumentaqtions

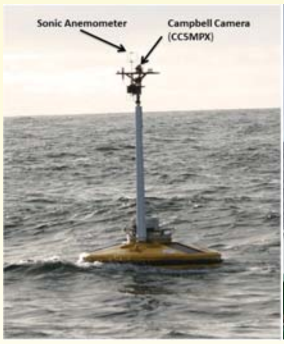

➢Atmospheric measurements

Two sonic anemometers: mounted on moving buoy abd ship,.

The bottom mounted platform was equipped with different oceanographic sensors including : Acoustic Doppler Velocitimeter (ADV), Nortek AWAC, you get a current profiler and a wave directional system in one unit, and an up-looking Aquadopp to give Burst of current.

➢Bottom fixed frame

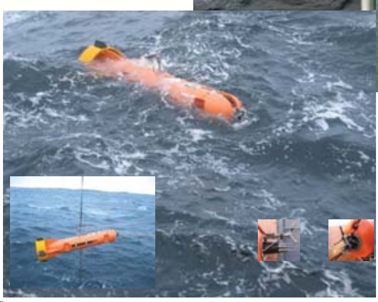

➢Microstructure Autonomous Turbulence System

Taking image at frequency 1 Hz, mounted on moving moord buoy. The camera installed in such a way pointing out towards surface with small angle below the horizontal plane. For the height of 4.5 m, It was set about 4 degree below the horizontal plane.

Here the difficulties of extracting wave breaking and sea surface wave characteristics from camera are examined. However, accurate analysis require more elaborations.

To date, Gemmrich et al. (2008) used images facquired from a video camera mounted on a floating platform to measure whitecaps passing through the field of view.

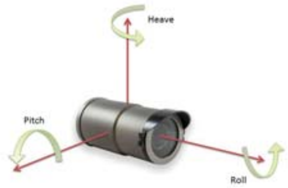

➢Langmuir Cells !?

➢Image Processing

Each sea surface images physical dimensions are calculated using a combination of camera height, camera inclination angle, calibrated lens focal length and size of the camera CCD chip. Furthermore, the effects of lens distortion are removed from . Then, we do transformation over all pixel s to real world coordinates. This allowed us to calculate the whitecaps However, there are different resource of uncertainity in camera motions and lack of tracking whitchaps' patches due to camera wave-induced motion

➢Whitecap Foam and breaking waves

One difficult stages in image processing in our application is segmentation of images into regions containing foam, active breaking, and no breaking For this means and to differentiate different regions from each other, a brightness threshold is employed. An important and key parameters here is the Philips breaking crest length per unit area that can be applied to determine wave breaking characteristics. Fig .1 Shows this quantity idealized behavior with respect to breaking crest phase velocity for different thereshold.

$$b(c)\Lambda(c)c^5 = g^2 S_{ds}(k)\,dk/dc$$

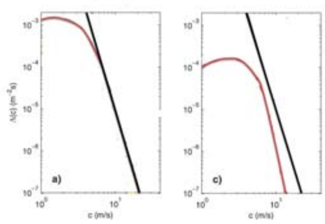

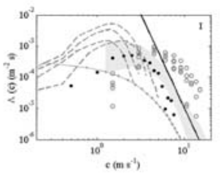

From [2]

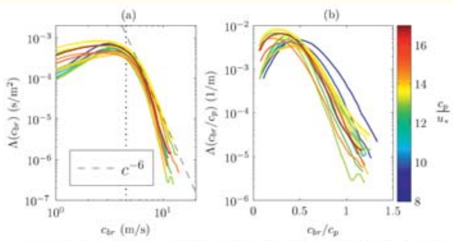

FIG. 9. (a) The $\Lambda(c_{br})$ distributions (Kleiss and Melville 2010) color coded according to the wave age c_p/u_*; the black dashed line is a reference power law of c^{-6} (Phillips 1985) and the vertical dotted line shows $c_p = 4.5$ m s^{-1}, corresponding to the lower limit of the $\Lambda(c_{br})$ data used in this study. (b) The breaking speed c_{br} is normalized by c_p and is scaled by c_p such that $\Lambda(c_{br}/c_p)d(c_{br}/c_p) = \Lambda(c_{br})dc_{br}$. From [1]

Acknowledgement

This work has been funded by th Norwegian Center for Offshor Wind Energy (NORCOWE) unde grant of the Research Council c Norway.

Summary

In this research cruise, different aspects of air-sea interactions were measured using different fixed and moving atmospheric and oceanographic sensors. All platforms were recovered except bottom frame platform. We are analysing both camera data based on image processing and MATS subsurface platform to measure amount of energy and momentum induced to the water column as a result of wave breaking, wave-current, and wave-turbulence interactions. In image proccessing of surface wave images, we calculated physical dimensions of some choosed images using intrinsic properties of camera. Furthermore, we provided required image proccessing algorithms for transformation of images from camera coordinate frame to the world global coordinate system. This can been done with different open source softwares. To approaching goal of this study, we also are runing the state of the art of identifications of whitcap foams and wave breaking using camera images. Important parameter which gives information about breaking crest characteristics is Philips breaking crest length per unit area. The implementations of calculating this parameter together with estimation of dissipation of waves into the water column have been done. However, there are some technical issue in using developed algorithm in our moving camera images mainly to strong platform motion contaminations.

References

[1] L. Romero, W.K. Melville, and J.M. Kleiss, Spectral energy dissipation due to surface wave breaking, J. Phys. Ocean. 2012

[2] A. H. Callaghan, G. Deane, M. Dale Stokes, and B. Ward, Observed variation in the decay time of oceanic whitecape foam, J. Geophy. Res., 2013.

Stochastic Particle Trajectories in the Wake of Large Wind Farm

Geofysisk institutt
Universitetet i Bergen

M Bakhoday Paskyabi, A. Valinejad
Geophysical Institute, University of Bergen, Bergen, Norway

norcowe
Norwegian Centre for Offshore Wind Energy

Introduction

The main goal of this study is to investigate pollutant diffusions with carrier flow and their temporal-spatial evolution in the wake regions of a large wind farm. The important feature of current study can be explained by its ability to focus on non-linear interactions between farm, passive tracers, and surface gravity waves by the means of the stochastic diffusion. Here, we specify a wind farm with a characteristic length, L, and assuming an analytical 2D U-shaped wake profile based on educated knowledge of wind deficit behind farm. For the numerical simulation, we modify 2D shallow water wave equations by including wave breaking and wave-current interaction effects. With progressive wave energy evolution and stochastic wave orbital motions, we solve Lagrangian equations of motions for pollutants. Then, we compare the particle trajectories in the wind-generated symmetrical range-dependent dipoles to highlight the temporal-spatial tendency of passive tracers with and without wave forcing with those calculated by vanishing farm contribution. Results also confirm the role of stochastic modeling of pollutants to capture more realistically the underlying physics by reducing the related uncertainties, especially during the strong oceanic upwelling and downwelling that influence marine life strongly, by bringing colder, nutrient rich water to the surface zone that there is enough light to provide appropriate conditions for growing and reproduction of phytoplankton.

Large Wind turbine and Wind Stress

➢**By vertical integrating momentum and continuity equations in the presence of wave effect, the following differential equations are obtained**

$$\frac{\partial(uh)}{\partial t}-f(v+vs)+\mathbf{F}_{ds}^{x}=-\frac{\partial\left(u^2h+0.5gh^2\right)}{\partial x}-\frac{\partial(uvh)}{\partial y}+\frac{1}{\rho_w}\left(\tau_x-\tau_x^w-\tau_B^x\right)$$

$$\frac{\partial(vh)}{\partial t}+f(u+us)+\mathbf{F}_{ds}^{y}=-\frac{\partial(uvh)}{\partial x}-\frac{\partial\left(v^2h+0.5gh^2\right)}{\partial y}+\frac{1}{\rho_w}\left(\tau_y-\tau_y^w-\tau_B^y\right)$$

$$\frac{\partial h}{\partial t}+\left(\frac{\partial(uh)}{\partial x}+\frac{\partial(vh)}{\partial y}\right)=0$$

➢**where u and v are the mass transports in the x and y directions, By assuming a thin layer of fluid with density ρ_0 and thickness *h* overlying a deep, motionless abyssal layer, assuming constant wind and wave characteristics, and by ignoring bottom friction and wave-induced momentum redistribution term $\mathbf{F}_{ds}$, we can obtain another simplified expression.**

➢Finite Volume Technique

The conservation form of Eq. (1) can be written as

$$\frac{\partial\theta}{\partial t}+\frac{\partial F(\theta)}{\partial x}+\frac{\partial G(\theta)}{\partial y}=S(t)$$

where source term is given as

$$\mathbf{S}(t)=\frac{1}{\rho_w}\begin{bmatrix}0\\ \tau_x-\tau_{in}^x-\tau_B^x\\ \tau_y-\tau_{in}^y-\tau_B^y\end{bmatrix}+\begin{bmatrix}0\\ f_{cor}(v+v_s)-\mathbf{F}_{ds}^x\\ -f_{cor}(u+u_s)-\mathbf{F}_{ds}^y\end{bmatrix}$$

We use Lax-Friedrichs technique as a member of finite volume (FV) to discretize homogenous version of Eq. (3) as

$$\boldsymbol{\theta}_{i,j}^{n+1}=\boldsymbol{\theta}_{i,j}^{n}-\frac{\Delta t}{\Delta x}\left(\mathbf{F}_{i+\frac{1}{2},j}^{n+\frac{1}{2}}-\mathbf{F}_{i-\frac{1}{2},j}^{n+\frac{1}{2}}\right)-\frac{\Delta t}{\Delta y}\left(\mathbf{G}_{i,j+\frac{1}{2}}^{n+\frac{1}{2}}-\mathbf{G}_{i,j-\frac{1}{2}}^{n+\frac{1}{2}}\right)$$

in which

$$\mathbf{F}_{i+\frac{1}{2},j}^{n+\frac{1}{2}}=\frac{\mathbf{F}(\boldsymbol{\theta}_{i,j}^{n})+\mathbf{F}(\boldsymbol{\theta}_{i+1,j}^{n})}{2}-\frac{1}{2}\left|\lambda\left(\frac{\boldsymbol{\theta}_{i,j}^{n}+\boldsymbol{\theta}_{i+1,j}^{n}}{2}\right)\right|\left(\boldsymbol{\theta}_{i+1,j}^{n}-\boldsymbol{\theta}_{i,j}^{n}\right)$$

λ **is non-linear advection speed. The external force is imposed to technique by following ordinary differential equation**

$$\frac{\partial\boldsymbol{\theta}}{\partial t}=\mathbf{S}(t)$$

➢Stochastic Lagrangian Particle Trajectories

The particle trajectory can be estimated using stochastic differential equation as

$$dX_t=f(X_t,t)\,dt+dW_t=\varepsilon f(X_t,t)\,dt+dW_t$$

where f is the orbital , W_t is the Brownian motion with $dW_t\sim N(0,\sigma^2 dt)$
$\varepsilon=kA/\omega$, and $dW_t\sim N(0,\sigma^2dt)$

If $(x(t),y(t))$ is the particle trajectory

$$\frac{dx}{dt}=u,\qquad \frac{dy}{dt}=v,$$

a perturbation series of X_t for the small parameter ε:

$$X_t=X_t^{(0)}+\varepsilon X_t^{(1)}+\varepsilon^2X_t^{(2)}+O\left(\varepsilon^3\right).$$

➢Numerical Results

➢**In this study for constant wind and wave the following analytical expression is proposed [1,3]:**

$$\Lambda=\Lambda_{init}-\Delta\Lambda_*\,\mathbf{P}(X,Y)$$

in which *X* and *Y* show the horizontal axes, Λ is wind-wave forcing vector, $\Delta\Lambda_*$ is wind-wave forcing fluctuation, and $\mathbf{P}$ gives the distribution of forcing behind wind farm. Wind and wave forcing are determined based on introduced shape function (Fig. 1) [3].

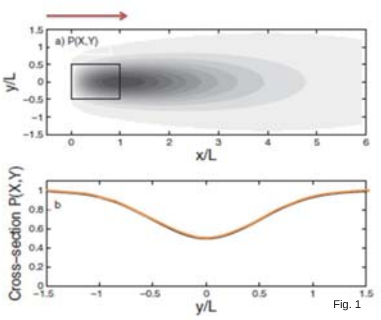

Fig. 1

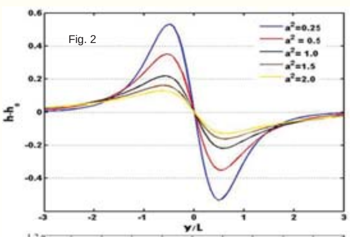

Fig. 2

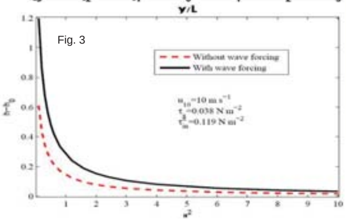

Fig. 3

➢**In fact, this parameter states how large the internal deformation radius is compared to the size of wind turbine farm (Fig. 2). The maximum value of pycnocline and the strength of upwelling as a function of *a* is shown in figure 3. It can be seen that the amplitude of response decreases rapidly with *a* that highlights the role of physical size of wind wake in upper ocean response [3].**

➢**Figure 4 shows the rising of pycnocline in the southern side of wind farm and corresponding falling due to geostrophic adjustment on the northern side. Further, including wave effect modifies ocean response by larger amplitude of pycnocline height.**

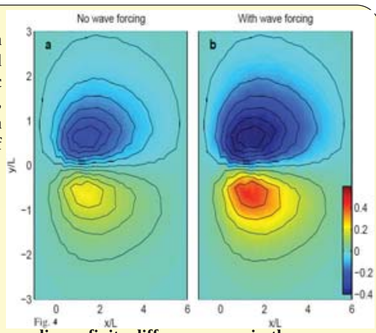

Fig. 4

➢**Here, we consider 5000 stochastic Particles.**

Figures 5 and 6 shows the linear FV runs, non-linear finite difference runs in the presence of bottom friction and advection term, and ROMS model results [3].

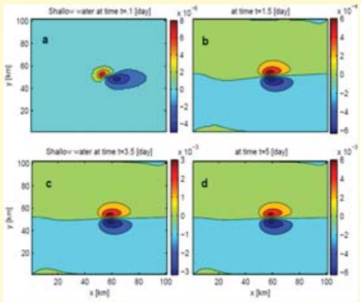
Fig. 5

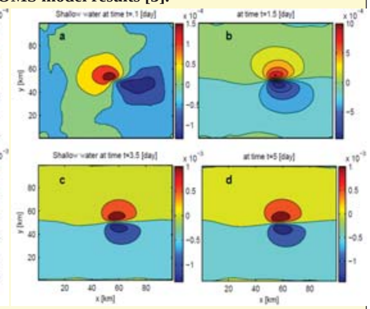
Fig. 6

➢**Temporal and spatial evolutions of Particles are shown in Fig. 7 for the scenario presented in Figs 8 and 9. To highlight the particles' trajectories in more details, we marked a moving particle for t=0, 1.5, 3.5, and 5 days, Respectively.**

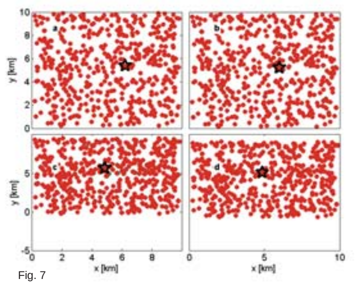

Fig. 7

➢**In Figs. 8 and 9, we show the trajectorie 4 stochastic particles in the presence of**

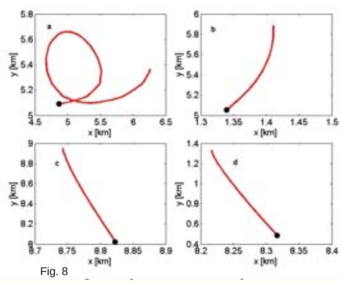

Fig. 8

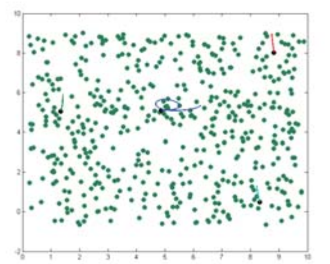
Fig. 9

trajectories have been shown in Fig. 8. These Figures show that wind farm modify the tracers trajectories, especially at the center of diploes.

Acknowledgement

This work has been funded by the Norwegian Center for Offshore Wind Energy (NORCOWE) under grant of the Research Council of Norway.

Summary

Growing the offshore wind industry necessitates investigations of different aspects of interaction between large wind farms and atmosphere, as well as ocean. Regarding to the later, upper ocean reveals direct but slow response to the wake strength and vertical extent of wind profile behind farm. All kind of variations in the atmospheric forcing conditions influence the wake pattern and structure downstream of wind farm and increase complexity of studying interaction between upper ocean and large farm. Among different issues of interest about this interaction, environmental effects of wind farm getting more important as a result of continual technological advances in design, installation, maintenance, and transport of energy from wind farm to power markets.
We showed that the max amplitude of pycnocline height with the wave effect is greater than that in no-wave case and this height approach to zero when *a* goes to infinity in both cases. Including non-linear term, horizontal diffusion, and the bottom friction led to decreasing of the strength of eddies. But, the amplitude of disturbances in the lee regions of the farm becomes weaker after almost three days. Furthermore, the wind turbine effects on the passive tracers have been studied in terms of stochastic lagrangian technique. We showed introductory results of these interactions suggesting small contribution of wind farm in distribution of surface particles. The results are preliminary and we plan to further study this interaction.

References

[1] Brostrom G. (2008): On the influence of large wind farms on the upper ocean circulation, *Journal of Marine Systems*, 74, 585-591.
[2] M. Bakhoday-Paskyabi, I. Fer, A. D. Jenkins, Surface gravity wave effects on the upper ocean boundary layer: modification of a one-dimensional vertical mixing model, Cont. Shelf Res. 2012.
Bakhoday Paskyabi, et. al, 2012, Upper Ocean Response to Large Wind Farm Effect in the Presence of Surface Gravity Waves, Energy Procedia.

LIMECS - LiDAR Measurement Campaign Sola

Valerie-Marie Kumer[1], Joachim Reuder[1], Birgitte R. Furevik[2]

[1]Geophysical Institute, University of Bergen, Norway, [2]Norwegian Meteorological Institute

LiDAR

An increase in nacelle height and rotor diameter of wind turbines in recent years have made measurements of wind profiles via meteorological masts difficult. In response LIDAR remote sensing has become increasingly important. With this technique, wind information at different heights is easily accessible and enables an analysis of boundary layer processes.

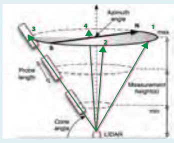

Figure 1: Measurement principal of the Doppler LIDAR WINDCUBE™ V1

WindCube v1

The WindCube v1 (figure 2) is a pulsed LiDAR system using the Doppler Beam Swing (DBS) technique to retrieve prevailing wind profiles. With 10 user defined altitudes the device can measure simultaneously up to a height of 200 m with a data accumulation time of 4 seconds.

Figure 2: WindCube v1 manufactured by Leosphere

WindCube 100S

The WindCube 100S (figure 3) is a scanning pulsed LiDAR system using Plan Position Indicator (PPI), Range Height Indicator (RHI) and DBS scanning techniques to picture 2D ambient flow fields, as well as wind profiles. With a range gate resolution of 50 m the device can measure to a distance of 3 km from the instrument.

Figure 3: WindCube 100S manufactured by Leosphere

Campaign & Methods

Figure 4: a) Map of the measurement site 1 and 2. Blue marks refer to reference measurements (tower and radio soundings), red and yellow indicate locations of the WindCubes. b) Picture of site 1 looking to the East.

Campaign

LIMECS was launched from beginning of March until mid of August 2013 at two different sites near the airport of Stavanger. The scanning WindCube 100S (WLS100S-8) and a WindCube v1 (WLS7-67) measured wind fields and profiles above the rooftop of the fire brigade building at Stavanger airport (site 1) respectively. At site 2, 2.3 km southeast of site 1, the other WindCube v1 (WLS7-65) measured wind profiles next to autosonde from the Norwegian Meteorological Institute (figure 4).

During the period of the campaign we temporarily increased the radiosonde launches from 2 to 4 releases per day. The two WindCubes v1 measured every 20 m from 40 to 200 m the three dimensional wind vector with a 4 second independent sampling rate, while the WindCube 100S measured at higher ranges between 150 and 3000 m, with a range gate of 75 m. In addition to wind profiles, the WindCube 100S also measured vertical and horizontal cross-sections of radial wind fields (figure 5), for a certain repetitive scanning pattern.

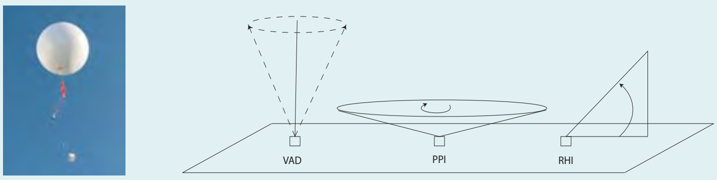

Figure 5: Picture of ascending radiosonde in a) and a sketch of possible scanning techniques with the WindCube 100S from left to right in b): Velocity Azimuth Display (VAD), PPI, RHI, leading to wind profiles, horizontal and vertical flow cross sections respectively.

Methods

The collected LiDAR measurements are going to be compared among each other, as well as to wind data collected by radiosonde ascents of the Norwegian Meteorological Institute (figure 7). In order to compare LiDAR to radiosonde measurements, the closest LiDAR profile to the time of the radiosonde launch is picked and compared to an over the range gate averaged wind speed of the radiosonde.

Results

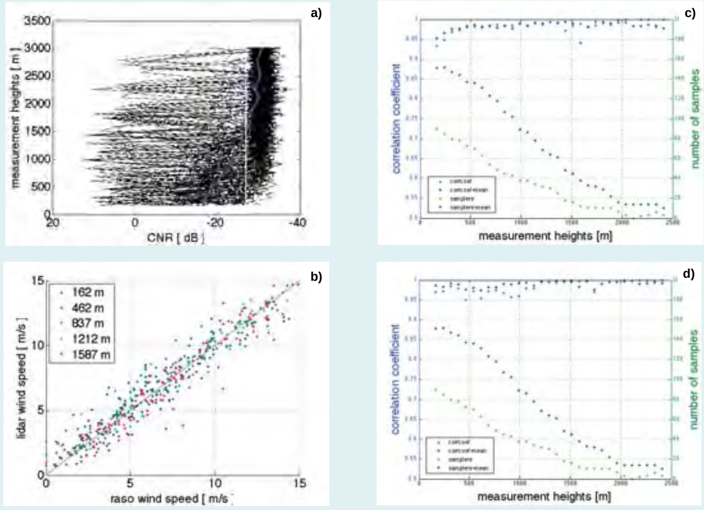

Figure 6: a) CNR profiles of the WindCube 100S for the period of comparison. The blue line indicates the average CNR profile and the white line shows the CNR threshold for data availability. b) Correlations of wind speeds of the same profiles to radiosonde wind measurements for different measurement heights. c) Correlation coefficients between WindCube 100S and radiosonde wind speeds as a function of height. In green the number of available measurements. d) Correlation coefficients between WindCube 100S and radiosonde wind directions as a function of height. In green the number of available measurements.

LiDAR-radiosonde comparison

First comparisons between 156 wind profiles measured by both, the LiDAR (WLS100S) and radiosonde show a correlation coefficient of 0.95 and 0.99 for wind speeds at measurement height of 162 m and above 500 m, respectively (figure 7). For wind direction the two measurement principles agree even a bit better, especially for 10 min averaged LiDAR wind directions.

During the analyzed period from mid March to mid July the average measurement range of the WindCube 100S was limited to around 1.5 km, as the data availability is dependent on weather conditions and aerosol concentrations.

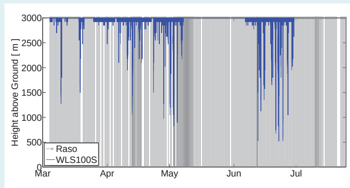

Figure 7: Data availability of WLS100S and radiosonde measurements over the whole measurement period. The blue lines indicate the maximal available measurement height.

Case study – Land breeze

Measurements show a case study of a land breeze circulation captured with the WindCube 100S on March 12th 2013. The surface near reversed flow layer is heading towards the sea with wind speeds of about 2 m/s and a depth of around 300 m (figure 6a).

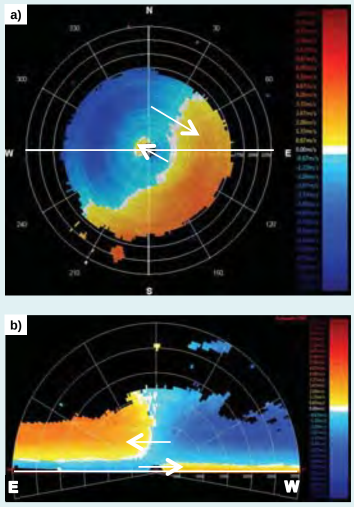

Figure 8: a) PPI scan of WLS100S on March 12th 2013 at 08:30 UTC. b) RHI scan of WLS100S on March 12th 2013 at 08:45 UTC. Red color indicate motion away from the LiDAR and blue towards the LiDAR.

Conclusions

- The compared WindCube 100S data is available on average until 1.5 km above ground level.
- Correlation coefficients between LiDAR and radiosonde wind measurements are height dependent and increase from 0.6 at 50 m to 0.99 at altitudes above 500 m.
- The WindCube 100S is able to capture costal boundary layer structures as shown in the case of a land breeze. Therefore it is a nice tool for boundary layer studies.

EERA DeepWind 2014

22. – 24.01.2014, Trondheim, Norway

Contacts: *Valerie Kumer* valerie.kumer@gfi.uib.no,

***Joachim Reuder* joachim.reuder@gfi.uib.no**

Fatigue Reliability-Based Inspection and Maintenance Planning of Gearbox Components in Wind Turbine Drivetrains

NTNU – Trondheim
Norwegian University of Science and Technology

NOWITECH Norwegian Research Centre for Offshore Wind Technology

Amir R. Nejad[1], Yi Guo[2], Zhen Gao[1], Torgeir Moan[1]

[1]Norwegian Research Centre for Offshore Wind Technology (Nowitech) and Center for Ships and Ocean Structures (CeSOS)

[2]National Wind Technology Centre (NWTC), National Renewable Energy Laboratory (NREL), USA

Abstract

This paper introduces a reliability-based maintenance plan for wind turbine gearbox components. The gears and bearings are graded based on their fatigue damage and a maintenance map is developed to focus on those components with higher probability of fatigue damage and lower level of reliability. The main aim of this paper is to propose a method for developing the "vulnerability map" which can be used for maintenance team to identify the components with lower reliability. The fatigue damage for gears and bearings are calculated at rated wind speed by SN curve approach. The load duration distribution (LDD) method is used to obtain the stress cycles for gears and load cycles for bearings from the load and load effect time series. During routine inspection and maintenance, the vulnerability map can be used to find the faulty component by inspecting those with highest probability of failure rather than examining all gears and bearings. Such maps can be used for fault detection during routine maintenance and can reduce the down time and efforts of maintenance team to identify the source of problem. The proposed procedure is exemplified by 750 kW NREL gearbox and a vulnerability map is developed for this case study gearbox.

Methodology

In this paper, the 750 kW NREL GRC gearbox is used. The loads on gears and bearings are obtained from the decoupled analysis. The global loads on the drivetrain are measured using a NREL dynamometer test bench. Next, these loads are used as inputs to a multi-body (MBS) drivetrain model in SIMPACK. See Fig. 1 for an illustration of drivetrain. The main shaft loads, or the forces and moments, are applied at the end of the main shaft where the rotor hub is connected.

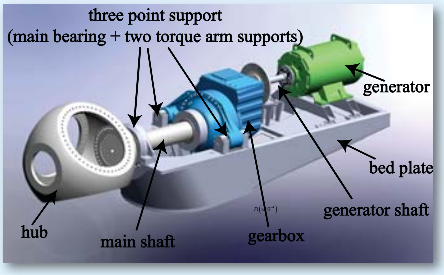

Figure 1: NREL 750 kW wind turbine.

In Fig. 2 the decoupled approach is presented.

Step I:

NREL dynamometer test bench.

Torque time series

Step II:

Torque time series are applied on Gearbox MBS model.

Step III:

Loads on gears and bearings are measured.

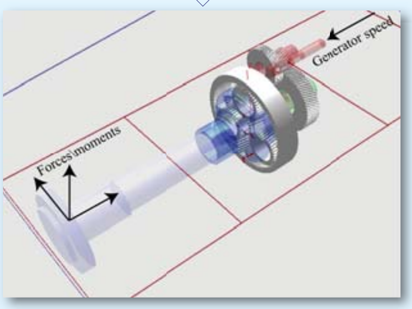

Figure 2: Decoupled analysis method.

Results

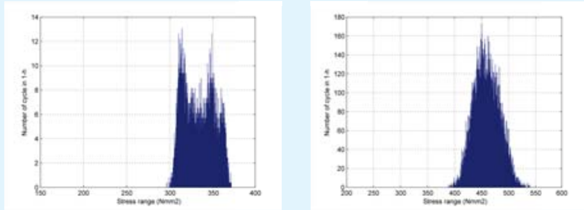

Figure 3: Stress range and number of stress cycles, planet gear (left); 3rd stage gear (right).

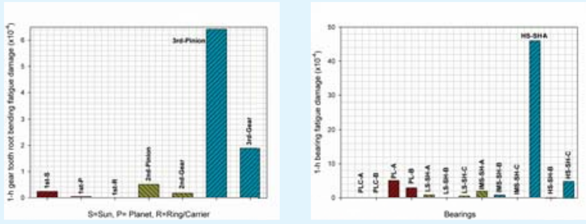

Figure 4:1-h fatigue damage of gears (left); bearings (right).

The fatigue damages of gears and bearings in the 750 kW case study gearbox are calculated and shown in Table 1 and Fig. 5.

Table 1: Gears and bearings sorted based on 1-h fatigue damage at rated wind speed.

Rank	Gear or Bearing	Name	*Damage* x 10^{-4}
1	Bearing	HS-SH-A	46.00
2	Gear	3rd Pinion	6.423
3	Bearing	PL-A	5.064
4	Bearing	HS-SH-C	4.846
5	Bearing	PL-B	2.921
6	Bearing	IMS-SH-A	1.954
7	Gear	3rd Gear	1.893
8	Bearing	LS-SH-A	0.812
9	Bearing	IMS-SH-B	0.777
10	Gear	2nd Pinion	0.509
11	Bearing	LS-SH-C	0.507
12	Gear	1st Sun Gear	0.241
13	Gear	2nd Gear	0.171
14	Bearing	HS-SH-B	0.096
15	Gear	1st Planet Gear	0.039
16	Bearing	IMS-SH-C	0.021
17	Bearing	LS-SH-B	0.020
18	Gear	1st Ring Gear	0.004
19	Bearing	PLC-A	0.000
20	Bearing	PLC-B	0.000

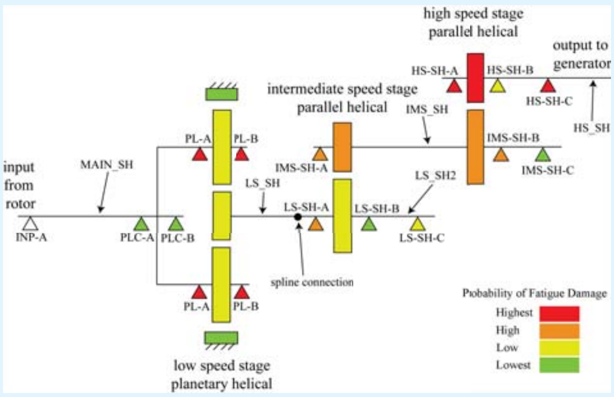

Figure 5: "Vulnerability map" of 750 kW case study gearbox based on component fatigue damage ranking.

Conclusions

In this paper an inspection and maintenance planning map based on the fatigue damage of gears and bearings is presented. The procedure for calculating the short-term fatigue damage for gears and bearings is described and exemplified for the NREL GRC 750 kW gearbox. The gearbox components are then sorted based on their fatigue damage. A "vulnerability map" is constructed indicating the components with highest to lowest fatigue damage. This maintenance map can be used for maintenance planning and inspection of components during routine preventive maintenance inspections. This approach can give the advantage of detecting the source of fault in shorter time. By using this plan, the maintenance inspector looks for defects from those with higher probability of failure, instead of examining all gears and bearings.

Assessment of environmental influence on fatigue crack growth in an Electron Beam (EB) welded flange connection

P. Noury[a], M. Pavlovic[a], M. Möller[a], M. Veljkovic[a]

[a]Luleå University of Technology, Division of Structural and Construction Engineering, Luleå 97187, Sweden

Abstract. Fatigue assessment of the ring-bolted flange connection under variety of load levels and corresponding number of cycles has shown to be more critical than that of fracture using Engineering Critical Assessment (ECA). The main objective of this paper is to determine the maximum acceptable flaw size of wind tower flanges which have a weld made by electron beam welding. The lowest temperature of a construction site used in the case study is -40 °C. Comparison is made between on-shore and off-shore conditions according to the recommended Paris law parameters acc. to BS 7910 and ASME, Sect. XI. Fatigue crack growth for a range of flaw length/depth (aspect ratio) from 1 to 10 is considered for centric and eccentric embedded flaw in a plate t=24mm (the shell segment closest to the ring flange), and internal and external circumferential surface flaw in the shell.

METHODOLOGY

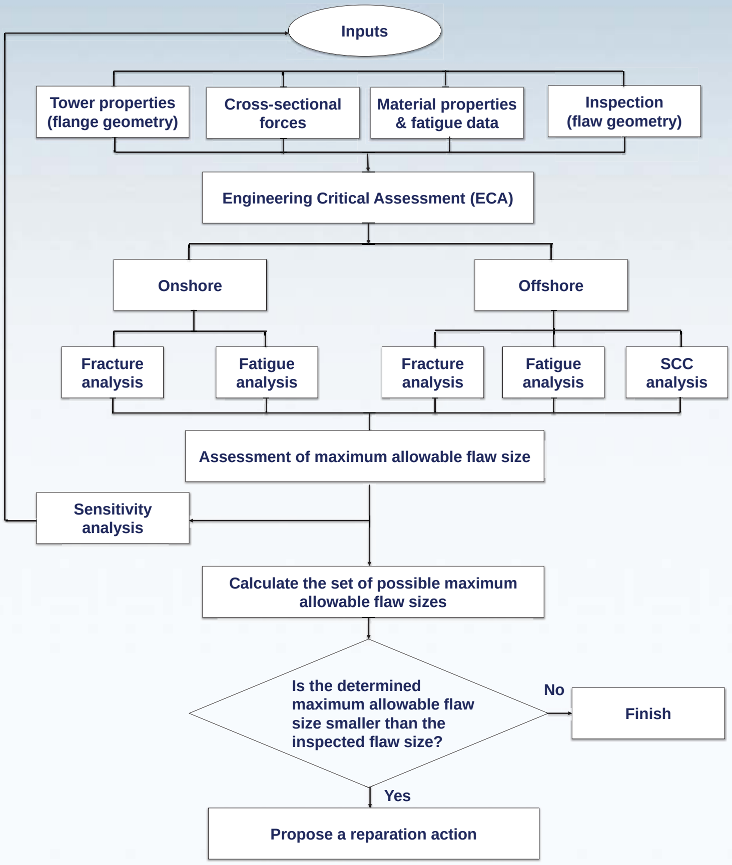

CASE STUDY

- FEA using the commercial ABAQUS finite element software have been used to define the stress levels of 3374 mm diameter EB welded ring flange connection used in towers for wind turbines.

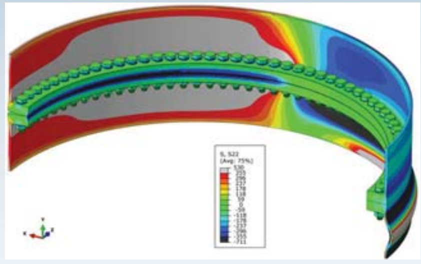

- The fracture toughness of the flange made of S355 at -50°C (the most sever operational conditions) has been determined using the Charpy values in terms of T_{27J} , and master curve approach.
- Fatigue assessment using Paris law is performed according to BS 7910 and ASME.

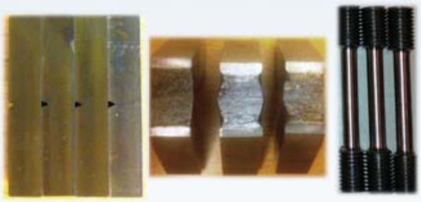

- The maximum allowable size of flaws, assuming the same loading conditions both for on-shore and off-shore conditions during wind tower's lifespan (25 years), have been determined for the sake of comparison.
- Effect of flaw geometries on the fatigue crack growth, internal and external surface flaws in cylinder oriented circumferentially and centric and eccentric embedded flaws in plate have been considered.

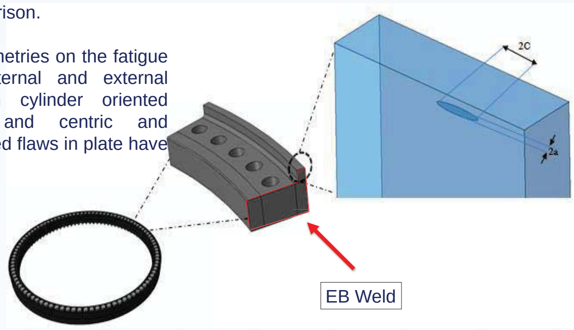

MAIN RESULTS

The acceptance criteria calculated for an eccentric embedded flaw (e = 10 mm) in a plate for fatigue of steel in the air and marine environment (acc. to the recommended Paris law parameters in BS 7910 and ASME, Sect XI).

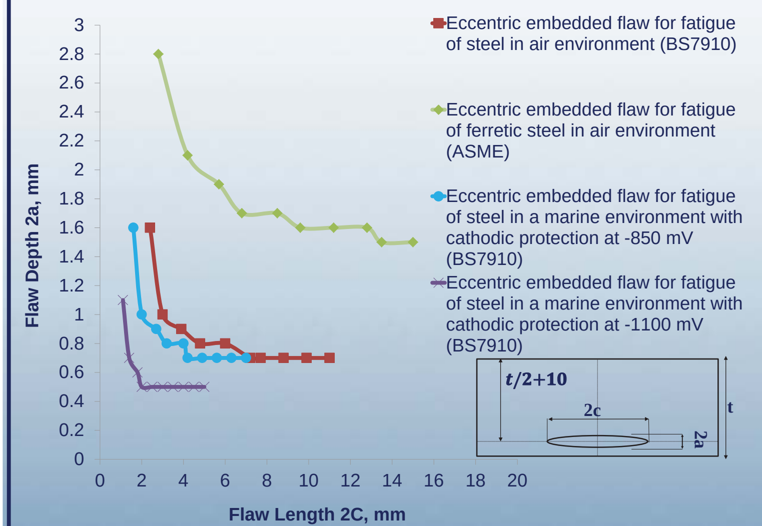

The set of acceptance flaws calculated for internal and external surface flaw position in the shell (circumferential orientation) and centric and eccentric embedded flaw in the shell for ferritic steels in the air environment (acc. to the recommended Paris law parameters in ASME, Sect XI).

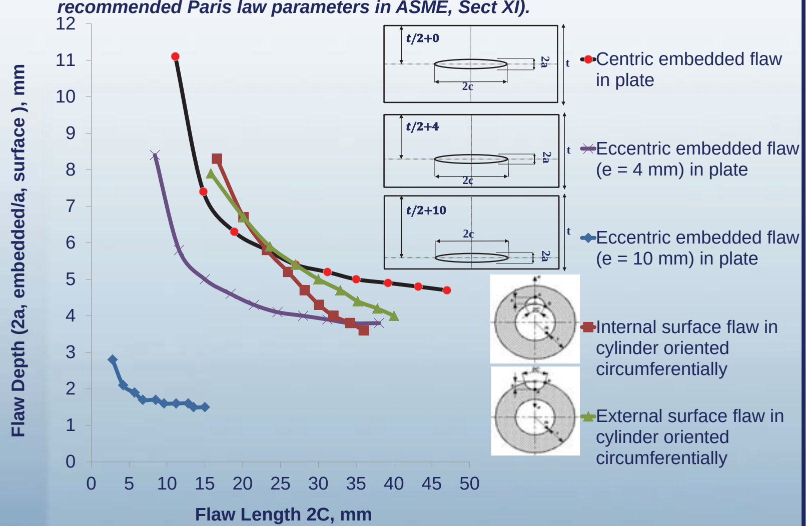

CONCLUSIONS

- Eccentric embedded flaw (e = 10 mm) represents most critical acceptance criteria of those considered.
- ASME is predicted less conservative acceptance criteria in comparison to BS 7910 for fatigue of steel in air or other non-aggressive environments.
- Eccentric embedded flaw (e = 10 mm) for fatigue of steel in a marine environment with cathodic protection at -1100 mV (according to the recommended fatigue flaw growth parameters in BS 7910) represents most critical acceptance criteria.
- The validation study demonstrates that the ECA procedure can be used for failure assessment of wind turbine tower structures containing flaws.

Acknowledgment. The research leading to these results has received funding from the European Union's Seventh Framework Programme managed by REA-Research Executive Agency http://ec.europa.eu/research/rea (FP7/2007-2013) under grant agreement n° FP7-SME-2011-286603

Refrences:

- BS 7910:2005. *Guide to methods for assessing the acceptibility of flaws in metallic structures.* The British Standard, July 2005.
- P. Dillstrom et al. *A combined deterministic and probabilistic procedure for safty assessment of components with cracks handbook*. Swedish Radiation Safety Authority, 2004.

A HYBRID NUMERICAL AND STATISTICAL MODEL FOR WIND POWER FORECASTING

Adil Rasheed[1], Jakob Kristoffer Süld[2], Ingrid Vik[3], Magne Røen[3],Trond Kvamsdal[1]
[1]Applied Mathematics SINTEF ICT, [2]MET Norway , [3]TrønderEnergi AS

Abstract: A large scale introduction of wind energy in power sector causes a number of challenges for electricity market and wind farm operators who will have to deal with the variability and uncertainty in the wind power generation in their scheduling and trading decisions. Numerical wind power forecasting has been identified as an important tool to address the increasing variability and uncertainty and to more efficiently operate power systems with large wind power penetration. The work clearly demonstrates the power of a hybrid numerical and statistical model developed in the FSI-WT project.

Why do a few turbines under-perform consistently in wind farms ? Can a RANS based model capture the flow behaviour in a complex terrain ?

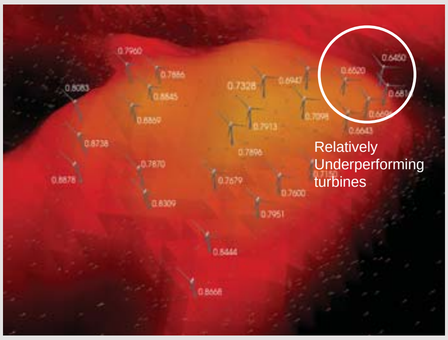

Offline simulations conducted with the most frequently encountered wind and stratification conditions:

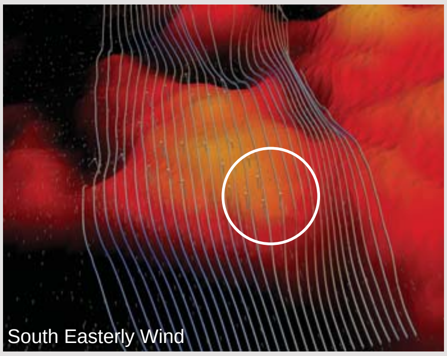

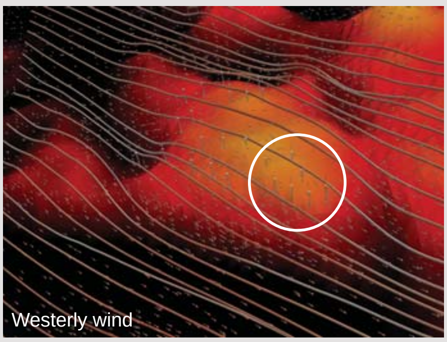

Stream limes for two most dominant wind directions. The figure clearly shows that the wind has a tendency to go around the hill which is perhaps related to the strong stratification in the region thus avoiding a few turbines which consistently underperform.

Three steps to improve Power production

STEP 1: A Multiscale Wind Forecast System

HARMONIE-SIMRA coupling

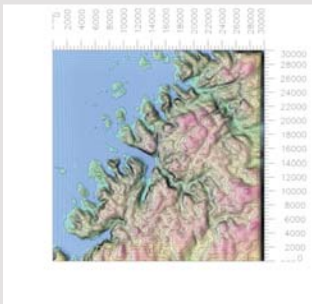

Wind, Temperature and Turbulent Kinetic Energy Field

Kalman filter using the historical wind observation data from the wind mast located In the wind farm

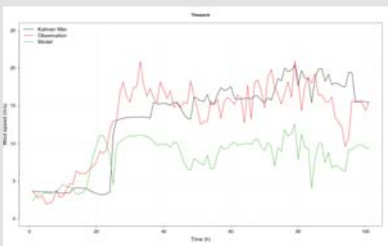

STEP 2: Uncertainty quantification by running 10 different ensemble runs

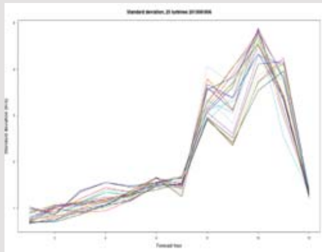

STEP 3: Better dynamic wind to power conversion curve using historical power production data

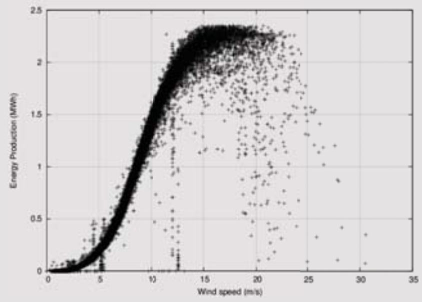

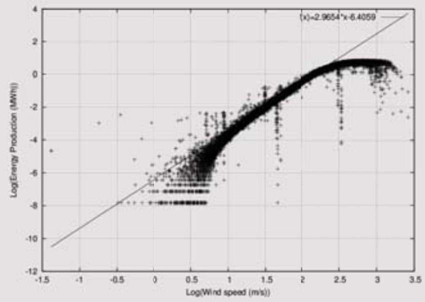

Improved power production in real time with quantified uncertainty

The authors acknowledge the financial support from the Norwegian Research Council and the industrial partners of the FSI-WT-project (216465/E20) | Contact: adil.rasheed@sintef.no

SINTEF | NTNU Norwegian University of Science and Technology | FFI Forsvarets forskningsinstitutt | Meteorologisk institutt | TrønderEnergi | windsim | Statoil | Kjeller Vindteknikk | Forskningsrådet

NOWITECH

The NOWITECH Reference Wind farm

A base case model to be used in offshore wind farm research

Further work for the NRW

To define among others: HVDC-system, turbine controller, park controller and turbine spacing including wake modelling

Current situation in wind farms

66 kV collector grid technology is available and enables higher power flow and lower losses.

Both the converter station platform and the offshore substation transforms the voltage.

The substation and converter platforms make up ~7 % of the total investment cost for a wind farm.

Contact: henrik.kirkeby@sintef.no, karl.merz@sintef.no,

Henrik Kirkeby and Karl Merz
SINTEF Energy Research

CENTRE FOR ENVIRONMENT-FRIENDLY ENERGY RESEARCH

Established by the Research Council of Norway

SINTEF

The NOWITECH Reference Wind Farm

Cost reductions due to electrical design in wind farms

The NOWITECH reference wind farm (NRW) is created to have a base case research model that enables focus on specific research topics. The initial focus of the NRW has been to design an electrical system that minimizes the lifetime cost of the internal grid.

Project focus

- Can untraditional design of the internal grid in an offshore wind farm lower lifetime costs?
- Is 66 kV collector grid a better option for large wind farms such as UK Round 3 projects?
- Can offshore transformer substations be eliminated in HVDC connected wind farms?
- Between these two possibilities and the more traditional solution with 33 kV collector grid and substations: Which is the most cost effective over the lifetime of the wind farm?

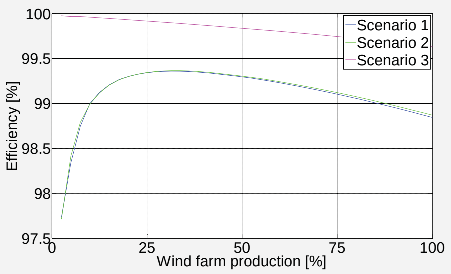

Simulation results for power losses in the internal grid

Results and findings

Upgrading the collector grid voltage level to 66 kV and eliminating the offshore transformer substation **save 137 M€** when compared to the standard configuration.

That is approximately **50 % of the investment** on the internal grid from the circuit breakers in the WTG to the circuit breakers on the converter platform.

Upgrading the voltage saves a small amount due to lower losses, but mostly due to the lower diameter required in the subsea cables. It is therefore a better solution in large farms.

Power losses go down when eliminating the substation transformer because the distance to the converter platform is small, so the substation is not necessary in the internal grid.

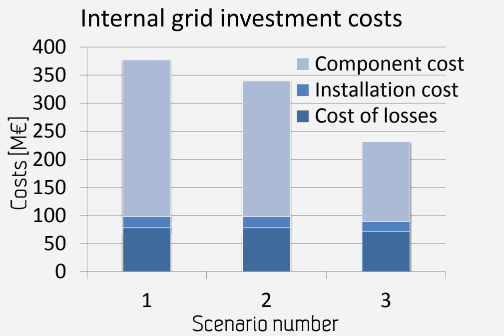

Methods

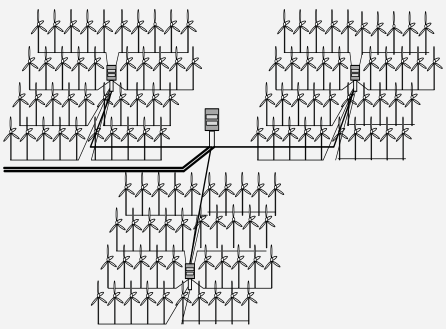

The NOWITECH Reference Wind Farm, scenario 2

The NRW quick facts:

- A MATLAB Simulink model
- 120 10 MW NOWITECH reference turbines
- 200 km long VSC-HVDC cable at ±420 kV
- Similar to the Dogger Bank Creyke Beck A wind farm

Three scenarios for the electrical system has been evaluated:

- Scenario 1 is the base case using the traditional solution with 33 kV collector grid and substations.
- Scenario 2 with substations and a 66 kV collector grid.
- Scenario 3 is without substations and with a 66 KV collector grid.

Methods cont.

To find the most cost effective solution, approximate numbers for installation and component costs were required from earlier projects and cost overview reports.

To find the cost for energy losses, minimum energy losses for different production levels are found through simulations. Empirical production data gave the duration for each production level, and the total energy loss was found. Energy price per year is given by the CfD incentive scheme in the UK and expected power prices.

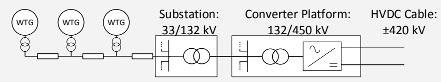

Scenario 1: 33 kV collector grid voltage and three substations

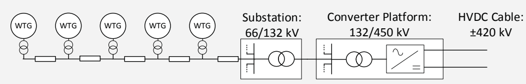

Scenario 2: 66 kV collector grid voltage and three substations

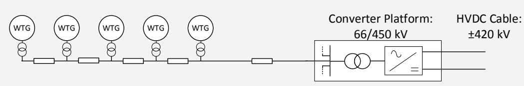

Scenario 3: 66 kV collector grid voltage and eliminated substations

Actuator disk wake model in RaNS

Vitor M. M. G. da Costa Gomes & José M. L. M. Palma
vitor.costa.gomes@fe.up.pt   jpalma@fe.up.pt

Faculdade de Engenharia da Universidade do Porto
Centre for Wind Energy and Atmospheric Flows

Abstract

A Wind Turbine (WT) wake model was integrated into a CFD code, in an attempt to bring the complex flow solving capabilities of state-of-the-art CFD solvers to the engineering level of wind farm development tools. For that purpose the tool does not require input other than standard manufacturer data on WTs (dimensions and power/thrust curves) and adds little computational cost to that already required by the CFD solver by itself. The present results are encouraging, as the model is able to predict satisfyingly the operating point (in the power/thrust curves) of the WT, thus estimating its performance, both in undisturbed flow and in the wake of another WT.

Introduction

In off-shore applications, the present engineering solutions to estimate wake losses may prove unreliable due to the interaction between the numerous Wind Turbine (WT) wakes or less-than-ideal wind conditions, like heterogeneous or unsteady inflow. By modelling the WT presence into the iterating equations of a RaNS solver, the risk of increased error due to biased calibration is reduced. This solution should be of interest both at the layout planning and energy yield prediction phases.

Objectives

An engineering minded RaNS-solved WT wake model should:

- Avoid need for precursor solutions to evaluate WT performance;
- Require minimum user input and calibration;
- Accurately estimate isolated WT wake behaviour;
- Predict wake interaction and WT behaviour in wake-disturbed inflow;

Proposed model

An actuator disk model based on Froude's Actuator Disk and momentum theory model was integrated into a RaNS code, allowing WT performance to be estimated in real time as the CFD code's solution converges. This was possible by introducing sink terms into the momentum equations, equivalent to the effect the WT has on the flow passing through its rotor.

By using Betz's conclusions regarding one dimensional momentum theory applied to the actuator disk (2), the model can estimate the force-per-unit-area (using Equation 1) applied by the rotor on the flow and re-distribute it over the actuator disk surface, which represents the span of the WT rotor.

$$d\mathrm{F} = \frac{1}{2}\rho \mathrm{C_T} \mathrm{U_\infty}^2 \, d\mathrm{A} \tag{1}$$

An estimate of free-stream velocity $\mathrm{U_\infty}$ at the WT location undisturbed by the WT itself, is necessary to close the model and interpolate into the manufacturer's thrust coefficient $\mathrm{C_T}$ curve (see Figure 2). An absolutely undisturbed velocity is obtained only through a precursor simulation, so that should be the standard against $\mathrm{U_\infty}$ estimates should be compared. The simplest way to estimate $\mathrm{U_\infty}$ is to consider the velocity some distance upstream of the WT (two diameters here) as an appropriate approximation. The proposed alternative is to use the velocity at the hub position (inside the actuator disk) as input to iterate Equation 3 with the $\mathrm{C_T}$ curve.

$$\mathrm{C_T} = 4\mathrm{a}\,(1-\mathrm{a})\ , \qquad \mathrm{a} = 1 - \frac{\mathrm{U_{hub}}}{\mathrm{U_\infty}} \tag{2}$$

Knowing the applied force, actuator disk's mechanical power can be determined by integrating the force-velocity product over the disk's surface. Considering a given electrical-mechanical conversion efficiency η_e of 97%, Equation 3 allows the model to estimate the WT's electical power.

$$d\mathrm{P} = \eta_e \, d\mathrm{F}\, \mathrm{U} \tag{3}$$

Results

As stated previously, the estimation of the free-stream velocity is key to predict the performance of a WT. Figure 1 shows that either estimation method proves to have high accuracy in the case of a WT in undisturbed flow. There are small deviations at low velocities from the $\mathrm{U_\infty}$ obtained from a precursor simulation, but the relative error falls with velocity.

When attempting to simulate the manufacturer's power curve, either prescribing the value for $\mathrm{U_\infty}$ used by the model, probing upstream or using the proposed momentum theory based iterative model seem to provide the same results (see Figure 2): reasonable agreement up to about 18 m/s, from whereon power estimation diverges significantly from the manufacturer's curve. This is believed to be due to a significant drop in aerodynamic efficiency of the rotor, result of some change in WT control strategy to limit electric power.

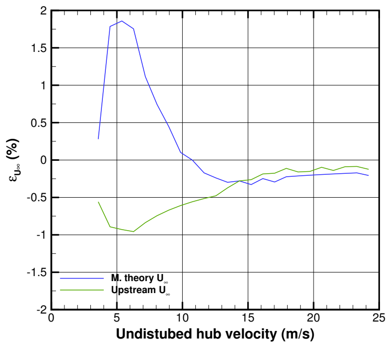

Figure 1: Deviation between free-stream velocity estimations and actual undisturbed velocity at WT hub over full wind speed range.

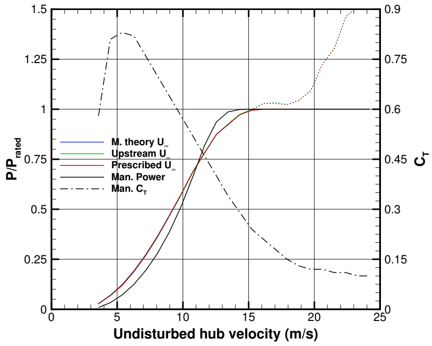

Figure 2: Power estimation over the WT's operating range, for different $\mathrm{U_\infty}$ estimation methods. Dotted lines show total modelled power if assuming absolute aerodynamic efficiency.

Upstream velocity probing proves limited when estimating free-stream velocity in the wake of another WT: comparison with the velocity undisturbed by the WT itself shows both an over-estimation of the velocity deficit and under-estimation of the wake width. The proposed method on the other hand shows good agreement on both terms.

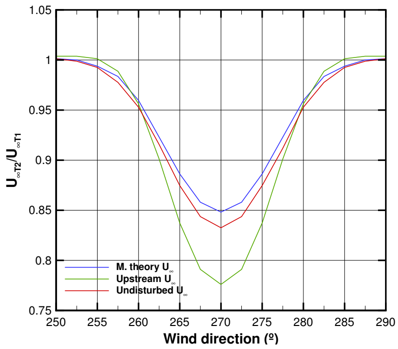

Figure 3: Free-stream velocity ratio for WT 5 diameters downstream of operating WT, for different $\mathrm{U_\infty}$ estimation methods.

Conclusions

- For an isolated WT, $\mathrm{U_\infty}$ estimation is in good agreement with the undisturbed velocity at the hub position over the operating range;
- WT rotor's aerodynamic efficiency unaccounted for in manufacturer data, visible by detachment between modelled WT power and manufacturer's curve at the top end of the operating range; elsewhere reasonable agreement is achieved
- $\mathrm{U_\infty}$ estimation by the proposed method in good agreement with velocity at the WT position in disturbed flow;

Acknowledgements

This research is funded by and conducted under the EERA-DTOC (1) project FP7-ENERGY-2011-1/ n°282797.

References

[1] *EERA Design tool for offshore clusters*, www.eera-dtoc.eu.

[2] G.A.M. Van Kuik. *On the Limitations of Froude's Actuator Disc Concept*. PhD thesis, Technical University of Eindhoven, 1991.

Interactive design of wind farm layout using CFD and model reduction

Chad Jarvis[1] , Yngve Heggelund, Marwan Khalil, Lene Sælen
Christian Michelsen Research, Bergen, Norway

[1] email: chad@cmr.no, phone: +47 950 26 778

Abstract

A theoretical framework for model reduction of the steady state Reynolds Averaged Navier-Stokes (RANS) equations for solving wind farm flow problems is presented. The method is developed for an interactive wind farm layout design tool considering offshore or flat terrain conditions.

Test cases are verified with corresponding flow field solutions from CMR-Wind, a Computational Fluid Dynamics (CFD) simulator. The developed method computes flow fields within seconds rather than several hours for full CFD simulations and provides accurate approximations to CFD solutions for application for interactive design of wind farms.

Objectives

The overall objective is to reduce the Cost of Energy of offshore wind farms by more optimal placement of turbines with respect to power losses due to wakes and maintenance costs due to wake induced fatigue loads.

Our first step is to develop an interactive tool for layout design, which can later interact with other software tools for layout assessment and optimization.

By basing our method on Computational Fluid Dynamics (CFD) and the full RANS equations, we believe that we can offer a method that is more accurate than the current state of the art for fast flow field assessment.

Methods

- ***Tile*** – *a subdomain of the wind farm*
- ***Snapshot*** – *the CFD solution within a tile for a given simulation.*
- ***Modes*** – *the set of orthogonal vectors/functions representing the reduced space*

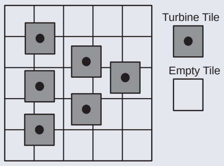

1. Run multiple RANS CFD simulations for varying setups (turbine positions, wind speeds). Extract snapshots for each simulation.

Example with two CFD simulations. Three tiles per Simulation.

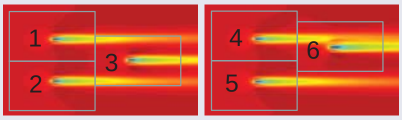

Extract six snapshots

2. Apply Singular Value Decomposition (SVD) to produce a reduced space solution basis of orthogonal modes.

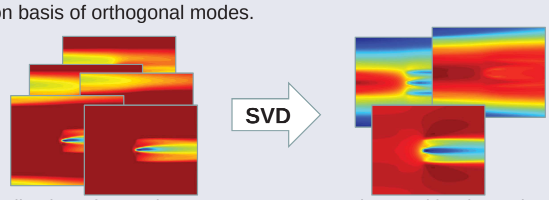

Collection of snapshots | Orthogonal basis modes

3. Interactively move tiles into arbitrary configurations. Solve the RANS equations and boundary matching in the reduced space spanned by the solution basis.

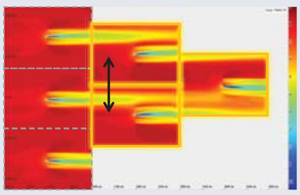

4. Compare solutions to RANS CFD solutions. If necessary improve the solution basis by running more CFD simulations and repeating steps 1-4.

Results

The simulations consisted of ten turbines with a uniform distance aligned with a neutrally stratified ambient flow over a surface with roughness length of 3 cm. The turbines were of type BONUS 2MW with a hub height of 76 m. The CFD simulations were performed with CMR-Wind [1].

1. Solution bases were created from a CFD simulation with turbine distance of 5 rotor diameters using only snapshots from the first N turbines. *These bases were used to test how well they could predict the power production of each of the ten turbines.*

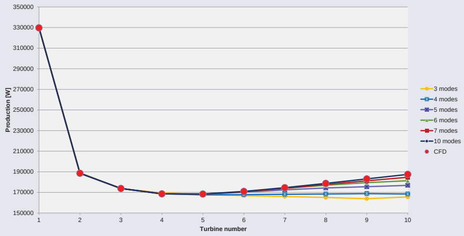

The power production of each turbine. The basis constructed from the first 3 turbines of the CFD simulation is labeled 3 modes etc. The deviation of the total production is less than **3.5%** compared to CFD when using 3 or more modes.

2. Solution bases were created from two different CFD simulations with turbine distances of 5 and 9 rotor diameters respectively. The bases were constructed from the first N turbines of each CFD simulation. *These bases were used to test how well they could predict the power production of each of the ten turbines for turbine distances of 6, 7 and 8 rotor diameters.*

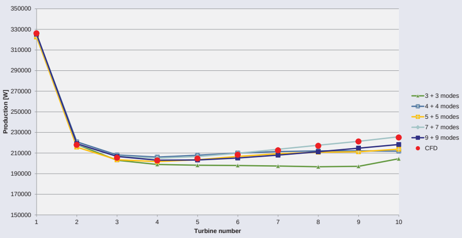

The power production of each turbine with a distance of 7 rotor diameters. The basis constructed from the first 3 turbines of each CFD simulation is labeled 3 + 3 modes etc. The deviation of the total production is less than **3.3%** compared to CFD when using 4 + 4 or more modes.

Model reduction result for a turbine distance of 7 rotor diameters, using a basis constructed from 4 snapshots each from the 5 and 9 rotor diameter CFD simulations.

Conclusions

A model reduction technique based on CFD has been presented [2]. For the test cases, the model reduction technique provides accurate approximations of the CFD results in **seconds rather than hours**.

We have previously presented the ability to simulate cases where the user can interactively move turbines in the crosswind direction [3].

Here we have shown that the model reduction technique is able to simulate the multiple wake effect for a long row of turbines from a relatively small set of basis modes.

Full three dimensional fields are computed, including the turbulent kinetic energy.

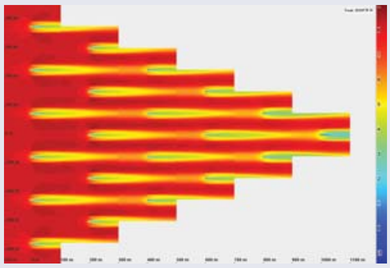

21 turbines, simulated in the reduced space within a second.

Future plans and perspectives:

- Verify the model reduction technique for more general setups and for more wind speeds and wind directions.
- Assess the wake induced fatigue loading on turbines by coupling the flow field and turbulent kinetic energy field to an external tool.

References

1. Khalil M. and Sælen, L. 2013 . Near and far wake validation study for two turbines in line using two sub-grid turbine models. EWEA conference, Vienna, Austria, 4-7 February 2013.
2. Heggelund, .Y, Khalil, M., Jarvis, C. and Sælen, L., Interactive design of wind farm layout using CFD and model reduction, EWEA Offshore 2013, Frankfurt, Germany, 19-21 November 2013.
3. Heggelund, Y., Skaar, I.M., and Jarvis, C., 2012, Interactive design of wind farm layout using CFD and model reduction of the steady state RANS equation, 11th World Wind Energy Conference, Bonn, Germany. 3-5 July 2012.

Energy yield prediction of offshore wind farm clusters at the EERA-DTOC European project

E. Cantero[1], J. Sanz[1], S. Lozano[1], C. B. Hasager[2], G. Sieros[3], P. Stuart[4], T. Young[4], A. Palomares[5], J. Navarro[5], M. Waechter[6], A. Morales[6]
1 CENER, Pamplona, Spain, 2 DTU Wind Energy, Risø Campus, Roskilde, Denmark, 3 CRES, Athens, Greece,
4 RES, London, United Kingdom, 5 CIEMAT, Madrid, Spain, 6 Forwind, Oldenburg, Germany

Abstract

A new integrated design tool for optimization of offshore wind farm clusters is under development in the European Energy Research Alliance – Design Tools for Offshore wind farm Cluster project (EERA DTOC). The project builds on already established design tools from the project partners and possibly third-party models. Wake models have been benchmarked on the Horns Rev-1 and, currently, on the Lillgrund wind farm test cases. Dedicated experiments from 'BARD Offshore 1' wind farm will using scanning lidars will produce new data for the validation of wake models. Furthermore, the project includes power plant interconnection and energy yield models all interrelated with a simplified cost model for the evaluation of layout scenarios. The overall aim is to produce an efficient, easy to use and flexible tool - to facilitate the optimized design of individual and clusters of offshore wind farms. A demonstration phase at the end of the project will assess the value of the integrated design tool with the help of potential end-users from industry.

In order to provide an accurate value of the expected net energy yield, the offshore wind resource assessment process has been reviewed as well as the sources of uncertainty associated to each step.

Methodologies for the assessment of offshore gross annual energy production are analyzed based on the Fino 1 test case. Measured data and virtual data from Numerical Weather Prediction models have been used to calculate long term mean wind speed, vertical wind profile and gross energy yield.

Objectives

The main objective of this work is to check methodologies and techniques used in the assessment of the Net Annual Energy Production of offshore wind farms and the associated uncertainties. Given the lack of available data from operational wind farms it is challenging to validate the proposed methodologies, especially regarding uncertainty quantification which is very case-specific.

Methods

In order to provide an accurate value of the expected net energy yield, the offshore wind resource assessment process has been reviewed as well as the sources of uncertainty associated to each step.

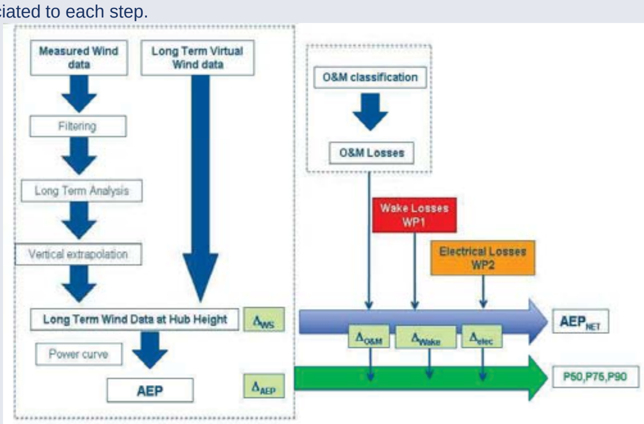

Based on FINO 1 input data several institutes and companies have estimated the Gross Annual Energy production using own methodologies. To analyze the different techniques in a homogeneous way, the next information has been requested to each participant:

1. For each measured level the mean wind speed before filtering
2. Mean measured wind conditions after filtering for the 100 meters level.
3. Long term wind speed distribution as a function of wind direction sector at 100 m level. Long term reference data is not provided as an input such that each participant can use own reference information (meteorological station or virtual data from databases like MERRA, GFS, World Wind Atlas Data…); this will allow assessing the impact from different reference data sources and Measure-Correlate-Predict (MCP) methods of temporal extrapolation.
4. Mean wind speed at hub height (120 meters).
5. Long-term prediction of gross energy yield in GWh/year, before wake effects and any other losses.
6. The estimated uncertainty of the long term 10-year equivalent predicted gross AEP, including a breakdown of the individual uncertainty components that have been estimated or assumed.
7. Details of how the particular methodology of each participant, in particular on how the wind speed prediction has been carried out (e.g. MCP technique), if measured or modeled wind shear was used, etc.

To analyze the NWP outputs as offshore virtual masts the gross annual energy production has been calculated based on data from nearest grid point of Skiron mesoscale model simulations.

Results

FINO 1 research platform, which is situated in the North Sea has been used as test case for estimating Gross Energy in a hypothetical wind farm.

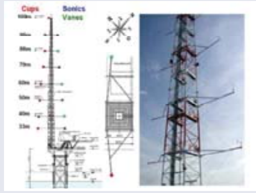

Ten minutes time series of controlled measured mean, standard deviation and maximum wind speed, mean and standard deviation of wind direction, temperature and pressure from 13/01/2005 to 01/07/2012 and a generic power and thrust curves have been provided as input.

According to the steps analyzed in the FINO 1 Gross energy estimation some critical points have been detected:

1.Filtering: the large deviations in the data recovery after filtering, mainly due to the mast shadowing effect show the need to have clear rules to filtered erroneous data specially in the case of mast shadowing influence. The data quality checking should be for all the measure period available and after this with all the relevant information select the full year analysis period.

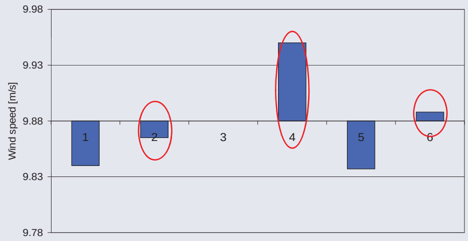

Mean wind speed after filtering at 100 m obtained as mean of ten minutes value. Mean value ± 1.0%. Red circles indicates that mast shadow effect has been filtered

2.Long term: a great variety of reference data and long term correlation methods are used, in each case and depending on the quality of the available data a exhaustive long term analysis should be done including validation and uncertainty assessment.

Participant	Long term period	Long term method
1	From Jan 2005 to Dec 2011	No long term correction
2	From Jan 1983 to Dec 2012	Long-term correction based on monthly NCAR data.
3	From Jan 1996 to Jun 2012	Long-term correction based hourly MERRA data as the reference source. A matrix correlation method was used.
4	From Jan 1979 to Dec 2011	Long-term correction based on monthly reanalysis data. The MCP method was applied for 12 different directional sectors.
5	From Jun 2005 to May 2012	No reference.
6	From Jan 1981 to Dec 2012	Long-term correction based hourly MERRA data as the reference source. A lineal correlation method was used.

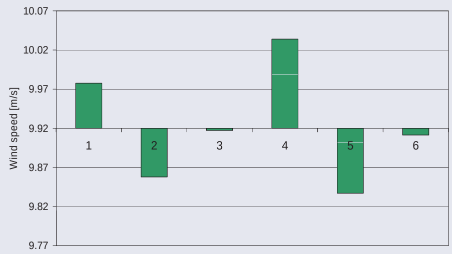

Long term mean wind speed at 100 m obtained from frequency distribution of hours in the year as a function of wind speed and direction. Mean value ± 1.5%

3.Vertical extrapolation: everybody has used the Hellmann exponential law that has good results for annual mean values but no when profiles are classified in terms of the observed atmospheric stability and, where the wind shear is overestimated during unstable conditions and underestimated in stable conditions. Stability and how it could be applied for wind resource assessment estimation should be analyzed.

4. Gross Energy: the deviations in the methodologies applied in before steps increasing in the gross energy estimation. According to the results new methodologies, should be explored and traditional methodologies should be checked to avoid big discrepancies like in the case of team 1 who with a similar wind speed distribution and the same power curve has obtained higher gross energy than the others participants.

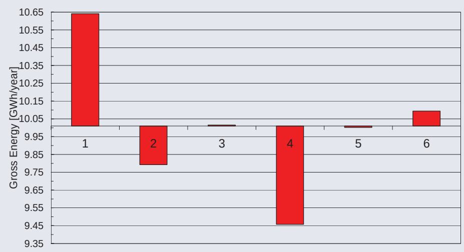

Gross Energy (P50) at hub height. Mean value ± 6.5%

5.Uncertainty: the sources of the uncertainty are clear but they are not enough to estimate it

6.Virtual masts: the results obtained for Skiron outputs for the FINO 1 site are very good, but more sites to validate are need to conclude that virtual masts are a alternative for initial offshore wind resource assessment.

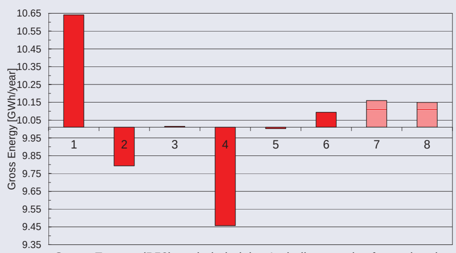

Gross Energy (P50) at hub height. Including results from virtual data, cases 7 and 8. Mean value ± 6.5%

Conclusions

The FINO 1 test case demonstrate the need of clear and common methodologies and standards to do the wind energy yield assessment in offshore wind farms.

New methodologies should be explored and incorporate to the wind energy yield assessment, like the analysis of atmospheric stability to define the wind profile or the NWP outputs as source of information to estimate the offshore wind resource.

To develop and validate methodologies and procedures wind farm data are need.

Acknowledgement to EERA DTOC project FP7-ENERGY-2011-1/ n°282797

A Model to Size Offshore Wind Energy Storage for Oil Platforms

Franz LaZerte, NTNU, Franzpl@stud.ntnu.no
Erling Næss, NTNU, Lars Sætran, NTNU

Why Energy Storage?

Grid-independent consumers can lower GHG emissions and combat rising fuel prices and emission taxes by switching to offshore wind power. However, wind alone must rely on supplementary generators due to its intermittency. Localized energy storage (ES) can reduce and eliminate dependency on fossil fuels. This model sizes an ES system to minimise energy required from Back-Up (BU) generators.

Future Development

Known Issues:

- Optimisation based solely on reducing back-up energy requirement, resulting in oversized ES
- No visual on how often certain charging power is reached
- Dumped energy is calculated but not factored into the optimisation

Next Steps:

- Track high ES charging and BU power occurrences
- Cost-based optimisation
- Optimise wind park size
- Investigate grid code implementation
- Grid-Dependent consumers

Acknowledgements:

Special thanks to Jillis Raadschelders, Petra de Boer, and many other DNV GL employees their advice, expertise and knowledge, including the normalized wind power data that was used to generate the wind power curves. Additional thanks to SINTEF Energy for sharing related academic papers and providing advice. Lastly, thanks to my supervisors, Erling and Lars, for their support and keeping me on track.
Funding for this project and MATLAB License is provided by NTNU

Methodology and Model

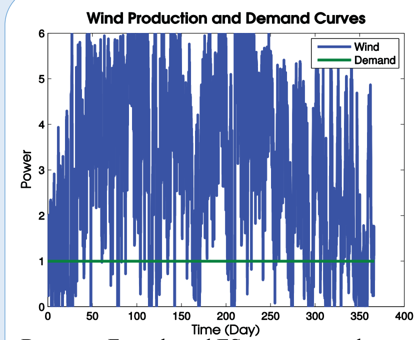

Purpose: For selected ES parameters, the difference between normalised wind power data and an off-grid consumer demand curve over a year is extracted and the following is simulated

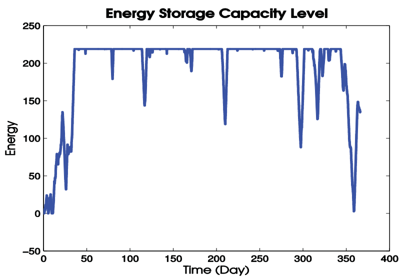

1. ES Performance

The model is coded using **MATLAB** and is split into three main stages:

1. ES Performance
2. Optimisation of ES
3. Wind Park Comparison

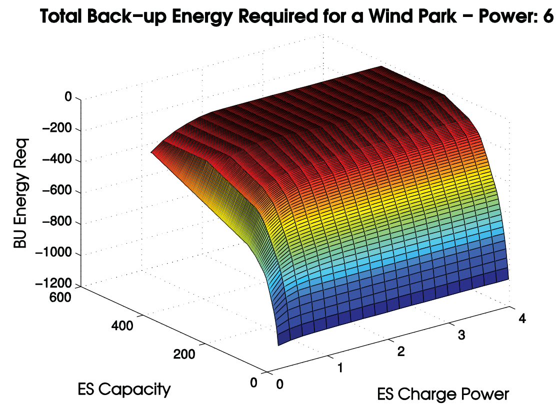

Purpose: to find the lowest ES Capacity and Charging Power combination that will require the lowest yearly Back-Up energy through iteration

2. Optimisation of ES

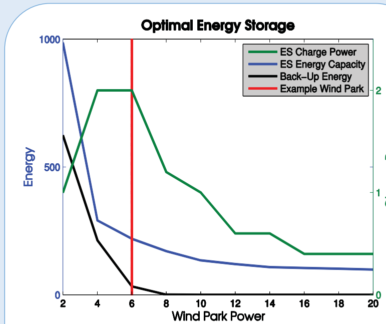

Purpose: Run optimisation with several different wind-park sizes

3. Wind Park Comparison

ES Parameters:

- Charge/Discharge Power
- Efficiency
- Min/Max Storage Capacity (Energy)
- Initial Capacity

Outputs (Over Time):

- Resultant ES Power/Energy
- Capacity Level Change
- Dump Load/Energy
- Back-Up Power/Energy

Assumptions:

- Constant Demand of 1
- Discharge Power set to match Demand
- Charge/Discharge Efficiency of 0.8
- Initial ES Capacity of 0

Literature:

D. Rastler, "Electicity Energy Storage Technology Options," *Electric Power Research Institute,* December 2010.
L. Warland, M. Korpås, W. He and J. O. G. Tande, "A Case-Study on Offshore Wind Power Supply to Oil and Gas Rigs," *Energy Procedia,* no. 24, pp. 18-26, 2012.
E. D. Castronuovo and J. A. P. Lopes, "Optimal operation and hydro storage sizing of a wind-hydro power plant," *Electrical Power and Energy Systems,* no. 26, pp. 771-778, 2004.
C. Abbey and G. Joós , "A Stochastic Optimization Approach to Rating of Energy Storage Systems in Wind-Diesel Isolated Grids," *IEEE Transactions on Power Systems,* vol. 24, no. 1, 2009.

Unsteady aerodynamics of attached flow for a floating wind turbine

Lene Eliassen and Jasna B. Jakobsen, University of Stavanger
Finn Gunnar Nielsen, Statoil/ University of Bergen

The dynamic response of a wind turbine is influenced by the aerodynamic loads, which are normally evaluated using the beam element momentum (BEM) method. This is an approach based on steady state conditions, and the unsteady aerodynamics are normally included by a semi-empirical model, e.g. Beddoes-Leishman method. The term unsteady aerodynamics is often used to describe dynamic stall, but the term also includes the unsteady conditions during attached flow. This study will focus on the unsteady aerodynamics during attached flow that occurs during normal operation of an offshore floating wind turbine.

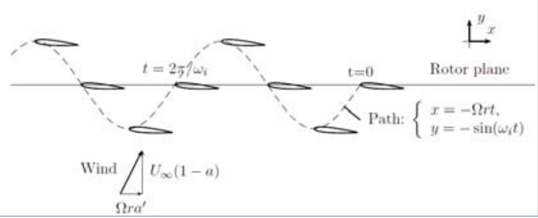

Figure 1: The oscillating path of a rotor blade.

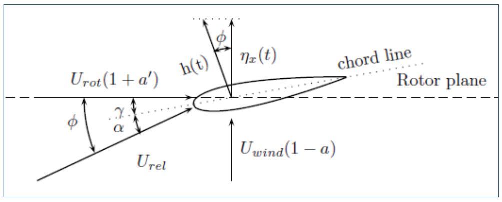

Figure 2: Angles and velocities relative to the airfoil and rotor plane

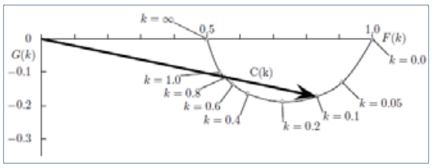

Figure 3: The imaginary and real part of the Theodorsen function.

Table 1: The oscillating path of a rotor blade.

Property	Angular frequency	Mass / inertial	Critical damping
Platform Pitch	0.21 rad/s	$5.8 * 10^{10}\ kg\ m^2$	$2.44 * 10^{10}$
1st elastic tower bending mode	2.95 rad/s	$3.9 * 10^5\ kg$	$2.31 * 10^6$

Table 2: Properties of OC-3 Hywind.

Property	Unit	Value
Rotor diameter	[m]	126
Nacelle mass	[Te]	240
Rotor mass	[Te]	110
Hub height	[m]	90

Introduction

A floating wind turbine may have very long eigen-periods for the surge and pitch motions. These motions in the axial direction of the rotor are dominated by quasi-steady aerodynamics. However, the eigen-frequency of the first bending tower mode is significantly higher and similar to that of a fixed onshore wind turbine. Thus the unsteady aerodynamic effects may be important. Theodorsen derived the unsteady aerodynamic forces in frequency domain for a flat plate in 1925. The corresponding time-domain formulations have been adopted for wind turbine applications and are implemented in today's aero-elastic wind turbine codes. In the present work, the effect of the unsteady aerodynamics during attached flow conditions is evaluated in the context of the aerodynamic damping for an offshore floating wind turbine.

Method

The aerodynamic damping for a floating offshore wind turbine rotor oscillating in the axial direction is estimated using Theodorsen's solution and a vortex panel code. Theodorsen solution for the thin airfoil is formulated analytically in the frequency domain, and is computaionally efficient. On the other hand, the vortex panel method van be used to simulate flow around an arbitary shaped airfoil. They are both based on potential flow theory, and are limited to attached flow condition. The wind turbine studied is the OC3-Hywind wind turbine and the main properties are shown in Table 2. Details regarding distributed aerodynamic properties of the blade can be found in ref [1].

The unsteadiness is measured using the reduced frequency, k. This is defined as $k = \omega c/2U_{rel}$, where ω is the rotational frequency, c is the chord length and U_{rel} is the relative wind speed, see Figure 2. In Figure 4, k along the blade for three different wind velocities is shown. According to [3] the flow can be assumed steady when k<0.01. For increasing values of k, the unsteadiness of the aerodynamics is increasing.

In Figure 1, the circular path of a rotor blade segment is unfolded into a straight line and the rotor oscillations in the axial direction are represented as departures from the mean rotor plane. The damping coefficient is extracted from the resulting thrust load in phase with the axial velocity of the nacelle. In this study, the rotor is assumed rigid, and the velocity of the nacelle is therefore equal to the velocity of the airfoil in axial direction.

The panel vortex code is a time-domain method. Constant strength panel elements are used to model the flow. At the surface of the airfoil both sources and doublets are used, and in the wake, only doublets are applied. The track of doublets in the wake is a part of the solution. The airfoil is forced to move along the path shown in Figure 1.

Theodorsen function describes the lift as a function of the plunging motion in the frequency domain. The lift force is related to the thrust force of the wind turbine with the flow angle ϕ. The real part of the function is related to the mass or inertia, and the imaginary part is related to the damping:

$$T_{2d} = -\left[M_{a,2d}(i\omega)^2 + C_{a,2d}(i\omega) + K_{a,2d}\right]$$

In this presentation, only the damping is presented. The damping according to the Theodorsen function is:

$$C_{a,2d} = \rho c U_{rel} \pi F(k) cos^2\phi$$

Where U_{rel} is the relative wind (see Figure 2), ϕ is the flow angle (see Figure 2) and F(k) is the real part of the Theodorsen function illustrated in Figure 4. For steady state, k=1, F(k) is 1. The value decreases with increases reduced frequency.

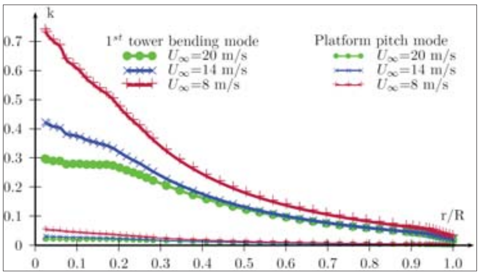

Figure 4: The reduced frequency relative to the radial position along the wind turbine blade.

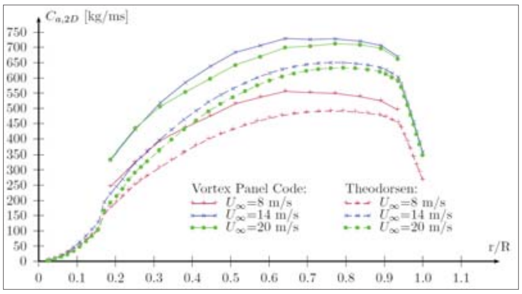

Figure 5: The local aerodynamic damping coefficient along the span of the blade for the platform pitch mode.

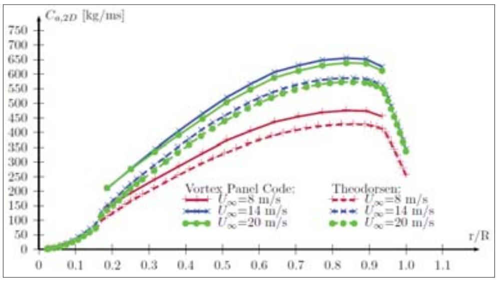

Figure 6: The local aerodynamic damping coefficient along the span of the blade for the 1st elastic tower bending mode.

Results

The local damping coefficients at the different blade sections for three different wind speeds are shown in Figure 5 and Figure 6. By summing up the damping coefficient along the blade and including the modal properties, the damping coefficient is estimated. For the platform pitch the top mass is multiplied by the squared distance to the water line, and the first is multiplied with the modal displacement. The ratio between the aerodynamic damping and the critical damping is the damping ratio, ξ. The results are listed in Table 3.

Discussion

The level of unsteadiness is measured using the reduced frequency, k, shown in Figure 4. The 1st tower mode is the most unsteady and the platform pitch has almost steady aerodynamic behaviour. The difference between the vortex panel method and the Theodorsen method, should only be related to the effect that the vortex panel code includes the thickness of the airfoil. This will have an influence on the slope of the lift curve, which is an important factor for steady aerodynamic damping.
In these simulations the panel vortex method shows higher damping relative to the Theodorsen method. The highest wind speed has the most steady aerodynamics, but also the largest difference in damping between the methods.

The most unsteady aerodynamics is for the 1st tower bending mode with the lowest wind speed. The local damping has the same trend, and the difference is so small that it is not visible in the damping ratio.

Conclusion

The aim of this study is to investigate the unsteady effects of attached flow. The main effect of increasing unsteadiness is reduced aerodynamic damping. The Theodorsen method and the vortex panel code give relative similar results.

Table 3: The aerodynamic damping results

	Wind speed [m/s]	Panel vortex method		Theodorsen method	
		C_a	ξ	C_a	ξ
Platform Pitch	8	$2.20 * 10^9 kg\ ^{m^2}/_{s}$	9%	$2.09 * 10^9 kg\ ^{m^2}/_{s}$	8.5%
	14	$2.92 * 10^9 kg\ ^{m^2}/_{s}$	12.0%	$2.74 * 10^9 kg\ ^{m^2}/_{s}$	11.2%
	20	$2.82 * 10^9 kg\ ^{m^2}/_{s}$	11.6%	$2.60 * 10^9 kg\ ^{m^2}/_{s}$	10.7%
1st elastic tower bending mode	8	$5.17 * 10^4 kg\ /s$	2.2%	$5.16 * 10^4 kg\ s$	2.2%
	14	$7.21 * 10^4 kg\ /s$	3.1%	$7.09 * 10^4 kg\ s$	3.1%
	20	$7.01 * 10^4 kg\ /s$	3.0%	$6.82 * 10^4 kg\ s$	3.0%

Acknowledgement
This study is part of the research performed by the Norwegian Center for Offshore Wind Energy (NORCOWE).

Corresponding author:
Lene Eliassen, e-mail: lene.eliassen@uis.no

References:
[1] J. Jonkman, S. Butterfield, W. Muscial, G. Scott, *Definition of a 5 MW Reference Wind Turbine for Offshore System Development.* National Renewable Laboratory. NREL/TP-500-38060. February 2009
[2] J. Jonkman, *Definition of the Floating System for Phase IV,* National Renewable Laboratory. NREL/TP-500-47535. May 2010.
[3] J. G. Leishman, *Challenges in modelling the unsteady aerodynamics of wind turbines*, Wind Energy 2002, 5 (2-3); 85-132

FloVAWT: Development of a Coupled Dynamics Design Tool for Floating Vertical Axis Wind Turbines

Cranfield UNIVERSITY

Michael Borg, Maurizio Collu, Andrew Shires

Energy & Power Division, Cranfield University

Introduction & Motivation

The ever-increasing need to curb climate change has led to an increased demand in alternatives to conventional energy sources. Offshore wind energy is one promising alternative energy source as large wind resources may be found offshore. To exploit such resources, wind turbines must be placed in the harsh marine environment, and in many cases, also sited in waters deeper than 50 metres where fixed foundations do not remain economically viable [1].

Whilst floating horizontal axis wind turbines (HAWTs) have been studied for a number of years, floating vertical axis wind turbines (VAWTs) are now gaining interest due a number of advantages over HAWTs for floating applications [2]. To investigate the technical feasibility of such floating systems, it is important to use appropriate engineering models to gain a first insight into their behaviour in the offshore environment.

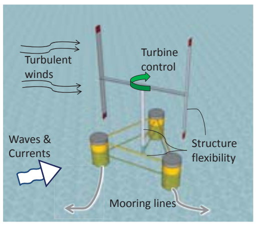

Fig. 1 – Dynamics of a floating VAWT

This involves integrating aerodynamics, hydrodynamics, control dynamics, structural dynamics and mooring line dynamics, that are all present for a floating wind turbine, as illustrated in Figure 1. This work deals with presenting the first attempt to develop a coupled model of dynamics for floating VAWTs, called FloVAWT, with the objectives to perform preliminary assessments of the motion response, system loading and power predictions. The developed model is briefly described, and a case study involving a combined wind-wave energy converter illustrates the capabilities of FloVAWT.

The motivation supporting the development of FloVAWT is the EU FP7-funded H2Ocean project. H2Ocean is aimed at the feasibility study of a multiuse offshore platform, incorporating wind and wave energy, hydrogen fuel production, aquaculture production and biomass [3]. This work illustrates the combined floating VAWT-wave energy converter concept currently being developed in this project.

Coupled Model Development

The first generation of FloVAWT has mainly focussed on interfacing a VAWT aerodynamic model with a hydrodynamic model and including a mooring line model, with the objective to investigate global platform motion, power predictions and characteristics of loads acting on/produced by floating VAWTs in the offshore environment.

The development of such a design tool for the preliminary assessment of floating VAWTs requires the integration of a number of engineering models, usually sourced from other research areas/industries. To overcome typical interfacing problems faced when attempting to couple software packages from different industries, FloVAWT has been developed entirely in the MATLAB/Simulink environment to allow for more robust and efficient interfacing between modules, accelerated model development and easier collaboration between researchers. The visual nature of Simulink also allows for the model to be readily used as a educational tool.

FloVAWT has been developed with the following methodologies in mind:

- Use the same programming language/environment where possible to enable standard interfacing.
- Take a modular approach; reduce models to a number of simpler blocks that can be easily chagnged/verified/validated.
- Where possible, pre-process data to avoid additional computations during simulations to maximise computational efficiency.
- Employ a loose-coupling scheme (allowing for the modular approach), enabling sub-cycling of individual modules to optimise computational efficiency of design tool.

The various engineering models implemented in FloVAWT are briefly illustrated in the following sections below and the process flowchart of FloVAWT is depicted in Figure 2.

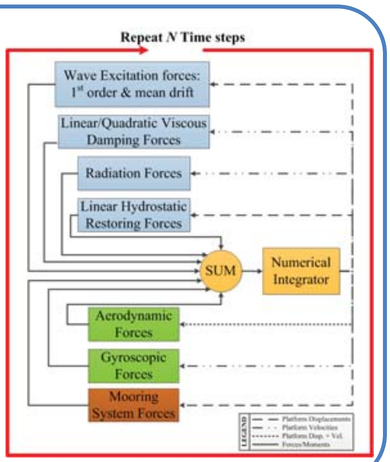

Fig. 2 – Process flowchart of FloVAWT coupled time-domain simulations

Aerodynamics Module

The aerodynamics module is based on the Double Multiple Streamtube momentum model, with several modifications to include dynamic stall (Gormont-Berg) model, tower shadow, tip and junction losses, 3D effects and turbulent incident wind. An alternative vector velocity formulation was implemented to better account for unsteady platform motion. Figure 3 illustrates the module process flow during simulations. Figure 4 provides the validated power curve for the VAWT 260 H-type turbine. Collu et al. [4,5] provides more details on model implementation and validation.

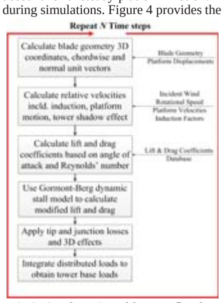

Fig. 3 –Aerodynamic model process flowchart

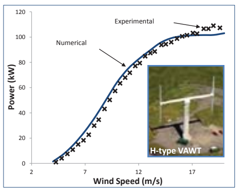

Fig. 4 –Aerodynamic model validation for the H-type VAWT 260 turbine

Hydrodynamics/Inertial Module

The hydrodynamics module is based on the time-domain Cummins equation, with a radiation-force state-space model approximation. The module was constructed using the Marine Systems Simulator Toolbox by Fossen and Perez [6], with a number of modifications and additions relevant to floating VAWTs. Numerical integration of the platform 6 DOF motion is performed in this module. Hydrodynamic aspects considered include:

- 1st order and mean drift wave excitation
- Linear hydrostatic restoring
- Radiation
- Linear/Quadratic global viscous damping

Inertial aspects considered:

- Gyroscopic moments in roll/pitch due to rotating rotor coupled with platform motion
- Time-dependent inertia matrix due to rotating rotor

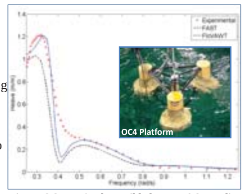

Fig. 5 –OC4 semi-submersible heave RAO predicted by FloVAWT and FAST and experimental data [7] (inset image obtained from [7])

This module has been validated for a number of cases, e.g. GVA4000 semi-submersible and DeepCwind OC4 semi-submersible (see Collu et al. [4,5]). Figure 5 shows validation in heave for the OC4 semi-submersible, also comparing to FAST predictions obtained from Coulling et al. [7].

Mooring Lines Module

The mooring line module is based on the quasi-static approach for catenary moorings and a linearised stiffness matrix for tensioned moorings. In the case of catenary moorings, the model is implemented through a nonlinear force-displacement relation database, which is obtained before running coupled time-domain simulations. The principle of minimum energy is used to solve the quasi-static catenary equations, producing a more robust and computationally efficient formulation, particularly with unconventional mooring designs. Through the use of coordinate system transformations, the platform 6 DOF motion is considered in the 2 DOF quasi-static catenary model. Figure 6 gives an example relation for horizontal (marked x) and vertical (marked y) fairlead forces of a catenary line as a function of heave and surge platform motion, as calculated by the above-described model.

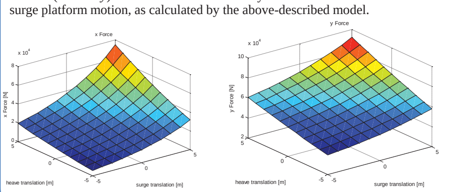

Fig. 6 –Nonlinear horizontal (left) and vertical (right) fairlead forces of a catenary mooring line as a function of heave and surge

Coupled Time-Domain Simulations: Case Study of the H2Ocean Concept

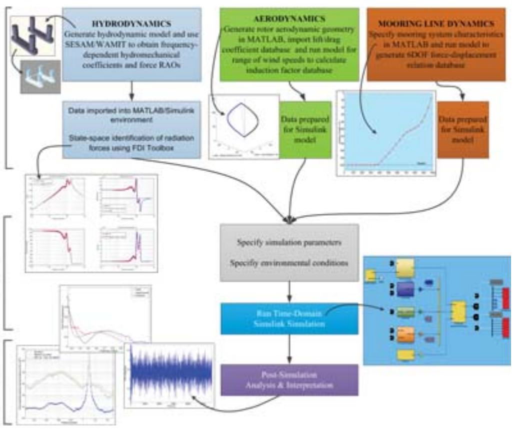

Fig. 7 – FloVAWT model preparation, simulation and analysis process

Fig. 8 – Simplified wind-wave energy converter concept

OUTLINE

Figure 7 presents the overall process of preparing and running a FloVAWT numerical model. To demonstrate the capabilities of FloVAWT, a case study was carried out on the combined floating wind-wave energy converter concept being developed in the H2Ocean project. The P80 wave energy converter (WEC) has been developed by Floating Power Plant [8], and is the result of a number of design iterations that have been experimentally tested at different model and prototype scales. The conceptual three-bladed H-type vertical axis wind turbine has been designed by Cranfield University as part of the H2Ocean project. The turbine has a 5MW rated capacity at a wind speed of 12 m/s and 7.5RPM. A simplified illustration of the device is shown in Figure 8.

A number of simulations were run to obtain a preliminary assessment of the performance of this combined wind-wave device, considering met-ocean conditions to investigate the combined dynamics of the device.

COMPUTATIONAL PERFORMANCE

Using a typical desktop PC with an Intel i5-2400 3.1GHz 64-bit processor and 8GB RAM, *simulation ratios of 23:1* were achieved when running the model on a single CPU and with a time step of 0.1 seconds. This efficiency results in many iterative simulations being run over a very short period of time, allowing for engineers and researchers to quickly assess and compare preliminary floating VAWT designs.

RESULTS & DISCUSSION

Figures 9 and 10 present the Amplitude Spectral Densities (ASDs) of the aerodynamic and wave excitation forces/moments in heave and pitch, respectively, for three met-ocean conditions: below-rated (U_{wind}=8m/s), rated (U_{wind}= 12m/s) and above-rated (U_{wind}=25m/s). As can be seen in Figure 10, aerodynamic heave forces are several orders of magnitude (o.o.m) lower than wave excitation forces, as was expected. In pitch, aerodynamic forces are 1 o.o.m lower than wave excitation forces, and in some cases of similar of similar magnitude, particularly around the platform natural frequency, where platform-induced motion augment the VAWT aerodynamic forces. It would be beneficial to further develop the platform and mooring system to shift the platform natural frequencies further away from this frequency range.

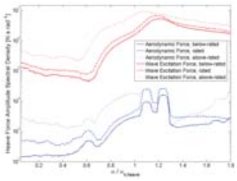

Fig. 9 –H2Ocean concept heave excitation forces

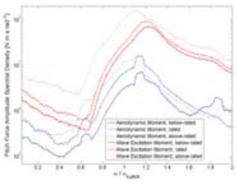

Fig. 10 –H2Ocean concept pitch excitation forces

Conclusions

Need to understand coupled dynamics of floating VAWTs,
Development of efficient coupled aero-hydro-servo-elastic model of dynamics dedicated to floating VAWTs

Approach to coupled model development described,
Description and validation of individual modules presented

Numerical model preparation, simulation and analysis process outlined
H2Ocean concept case study presented

Future Work

The next developments envisaged for FloVAWT are:

- Inclusion of an structural model to investigate internal loading and aeroelasticity
- Inclusion of second-order hydrodynamic forces
- Inclusion of hydroelastic models
- Inclusion of multi-member quadratic hydrodynamic viscous drag model
- Assessment of other aerodynamic models to better capture VAWT dynamics
- Inclusion of a dynamic mooring line model to include hydrodynamic phenomena

References

[1] Jonkman, J. M. and Matha, D. (2011), "Dynamics of offshore floating wind turbines-analysis of three concepts", Wind Energy, vol. 14, no. 4, pp. 557-569.
[2] Borg, M., Collu, M. and Brennan, F. P. (2012), "Offshore floating vertical axis wind turbines: advantages, disadvantages, and dynamics modelling state of the art", *The International Conference on Marine & Offshore Renewable Energy (M.O.R.E. 2012)*, 26-27 September, 2012, London, RINA.
[3] http://www.h2ocean-project.eu
[4] Collu, M., Borg, M., Shires, A. and Brennan, F. P. (2013), "Progress on the development of a coupled model of dynamics for floating offshore vertical axis wind turbines", *Proceedings of the ASME 2013 32nd International Conference on Ocean, Offshore and Arctic Engineering*, 9-14 June, 2013, Nantes, France, ASME.
[5] Collu, M., Borg, M., Shires, A., Rizzo, N. F. and Lupi, E. (2014), "FloVAWT: Further progresses on the development of a coupled model of dynamics for floating offshore VAWTs", *ASME 33rd International Conference on Ocean, Offshore and Arctic Engineering*, 8-13 June 2014, San Francisco, USA.
[6] Fossen, T. I. and Perez, T. , MSS. Marine Systems Simulator (2010).
[7] Coulling, A. J., Goupee, A. J., Robertson, A. N., Jonkman, J. M. and Dagher, H. J. (2013), "Validation of a FAST semi-submersible floating wind turbine numerical model with DeepCwind test data", *Journal of Renewable and Sustainable Energy*, vol. 5, no. 2.
[8] http://www.floatingpowerplant.com/

Acknowledgements

The research leading to these results has been performed in the frame of the H2OCEAN project (www.h2ocean-project.eu) and has received funding from the European Union Seventh Framework Programme (FP7/2007-2013) under grant agreement nº 288145.

It reflects only the views of the author(s) and the European Union is not liable for any use that may be made of the information contained herein.

Contact: Michael Borg, m.borg@cranfield.ac.uk

COOPERATION

H2Ocean

Use of an Industrial Strength Aeroelastic Software Tool for Educating Wind Turbine Engineers

P. Thomassen (Simis as), O. Dahlhaug (NTNU), T. Meisler (HiST)

AESW in Education

The use of aeroelastic analysis software (AESW) for wind turbines is today a well-established practice in the industry. In addition to wind turbine manufacturers, suppliers, consultancy companies as well as research institution are among the users of aeroeastic software.

Still, aeroeastic software apparently has seen little use in university level wind turbine technology classes. This is particularly so at an introductory level – at an advanced level AESW has seen some use, but mostly in a project context and typically not as a teaching or learning tool.

Use of AESW in an educational context at university level potentially has many benefits:

•Students get to know an important kind of tool for the industry

•Students get an improved knowledge of the work flow in the industry

• AESW has the potential of being an effective teaching tool for lecturers as well as an effective learning tool for students

The goal of introducing AESW in education has recently received focused attention from at least two groups. In addition to Ashes developed bySimis Fraunhofer IWES is developing *OneWind for Students*

Ashes @ NTNU

Ashes has been used in the class *TEP 4175 Energy from Environmental Flows* taught by Prof. Ole G. Dahlhaug during fall semester 2013. The class had app. 150 students.

The main portion of the class was a group project where the students were asked to design and test the rotor and the generator of a model scale wind turbine.

Ashes was successfully used in the design of the rotor and subsequently to export the designed blade to the CAD program AutoDesk Inventor. The wooden rotor was finally manufactured in a milling machine.

The project was largely considered a success and will be continued in 2014. The following improvements are among those planned for the use of Ashes in the project:

•A relatively elastic plastic material will be used instead of wood. Ashes will be extended to allow for accurate analysis of the large deflections of a solid blade in a soft material.

•As Mac computers have become very popular among students Ashes will also be delivered as a Mac version..

Ashes @ HiST

In 2012 the University College in Sør-Trøndelag (HiST) established a BSc degree in renewable energy focusing on hydro power and wind power. HiST and Simis have established a cooperation to leverage the use of Ashes in teaching wind turbine technology. In particular, Ashes will be used in the class *TFNE2003 Wind power and hydro power* taught by Håvard Karoliussen. Ashes has already been introduced in the elective class *AIM306V Wind power – An introduction* taught by Terje Meisler.

As a part of the cooperation with HiST a set of exercises is being developed where learning wind turbine technology is integrated with learning to use an aeroelastic tool in general and Ashes in particular.

Ashes will be offered for use in project and thesis work for the students of renewable energy at a later stage. Of particular interest is using Ashes in a context with the small scale wind turbines available at the HiST campus.

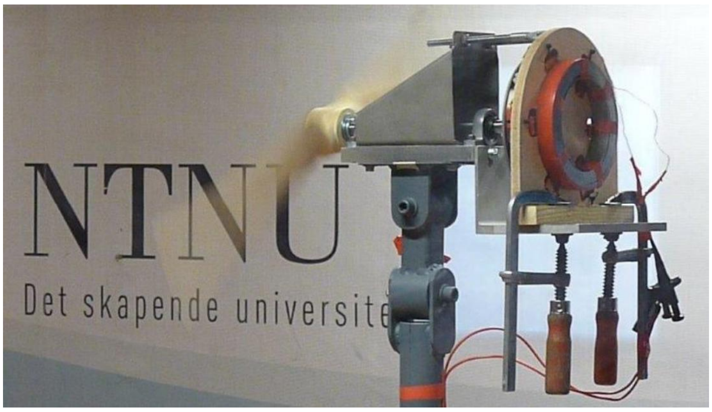

Model scale wind turbine tested in the NTNU wind tunnel. Photo: B. Brandåstrø

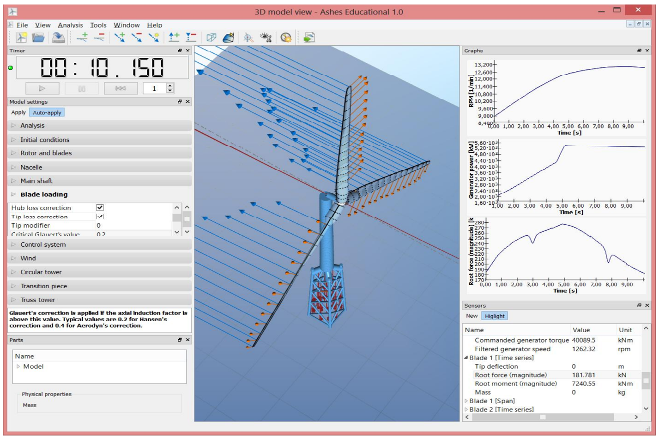

Graphical user interface for Ashes Educational 1.0

Conclusions

The aeroelastic software Ashes has been successfully introduced as a tool for teaching wind turbine technology for 150 students at NTNU. Ashes is particularly well suited for use by students because of the emphasis on a rich graphical user interface, visualization, as well as real-time analysis.

The development of Ashes will continue in cooperation with academic partners to optimize the benefit for both students and teachers. Software tools introduced for students will typically be compared to modern software used in other contexts rather than traditional engineering software. To be seen as a learning tool rather than a chore by the students this is likely to require an excellent user experience.

HiST TRONDHEIM

NTNU Norwegian University of Science and Technology

DeepWind'2014, Trondheim, 22-24 Jan. 2014

Offshore ramp forecasting using offsite data

Pål Preede Revheim, Hans Georg Beyer, Department of Engineering, University of Agder, Grimstad, Norway

UNIVERSITY OF AGDER

Objectives

The increasing use of wind power as an energy source poses new challenges for the management of electrical grids. One of the major challenges is dealing with sudden large changes in wind power production, normally referred to as wind power ramp events. The sooner and more accurate ramp events can be predicted, the smoother and more efficiently they can be dealt with. As a result of the large size of future offshore wind farms, and thus also large capacity, ramp forecasts will be of particular importance. At the same time the offshore location will pose additional challenges since the possibilities of using wind speed measurements from surrounding sites as early warnings will either be limited or costly.

Here on-site NWP wind forecasts and already available historical offsite wind measurements are used as input to forecast whether the next hour falls into one of the three categories "no ramp", "up ramp" or "down ramp". For doing this, the techniques random forests (RanFor) [1] and multinomial logistic regression (MLR) [2] are evaluated .

Case and data

The data used are wind speeds from three sources – the nacelle of Hywind, met-stations at 6 oil-platforms in the North sea (see map in Fig. 1) and Hirlam 4*4 km forecasts run by the Norwegian Meteorological Institute. Hywind serves as the site of interest, While the oil-platforms are used as off-sites. From Hywind the wind speeds are given as 500 second averages, From the oil-platforms at 10 minute averages measured once every 6 hours and from Hirlam as hourly forecasts rerun every 24 hours. All wind speeds are transformed to an uniform height by the use of a logarithmic profile, and computed into wind power using a generic wind turbine model. The data covers the time-period 01.01.2009 – 17.12.2011, in total 982 observations.

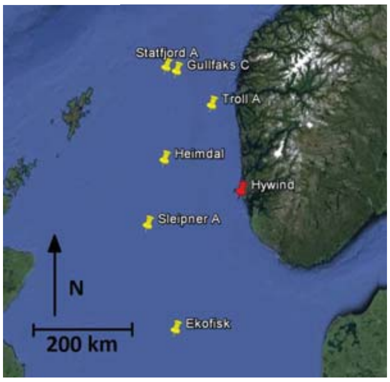

Fig. 1 – Map of locations (Google Earth)

The ramp forecasts are performed in three stages. First the ramp events are identified, then the datasets used for the random forest and MLR scheme s is constructed, and finally the forecast models are fitted.

For Hywind it is assumed that the forecast for the next hour and the measurements from a number of previous hours contain information about the probability of a ramp. For the off-sites it is assumed that there is a high probability of the ramp event one wants to predict occurred at a upwind site at an earlier time, hence that the ramps are subject to spatial propagation from upwind sites to downwind sites. Similarly to for Hywind this is included through information about the forecast for the next hour together with measurements from a previous hour. Because of the 6 hour interval between the off-site measurements only one hour at a time is included for these. This gives a dataset of 11 columns and 982 rows.

Wind power ramps

A main challenge of ramp forecasting is how to define a ramp event. In the literature there is no consensus about a standard formal definition of a ramp [3]. A part of the reason for this is that a ramp is described primarily by the function it has, and that this will vary depending on the location and size of the wind farm, the flexibility of the grid, other energy sources connected to the grid etc. There are good practical reasons for this, so the lack of consensus about a definition cannot be considered a problem in itself.

Here, the ramps are identified using the following definition:

$$P(t+\Delta_t)-P(t)>P_{val}, \qquad (1)$$

where Δ_t is a pre-defined time increment set to 3 hours and P_{val} is a threshold value set to 0.3, i.e. is a change in wind power production of more than 30% within 3 hours considered a ramp. The result of the ramp identification process is that 852 of the observations are identified as no-ramp, 62 as up-ramps and 63 as down-ramps.

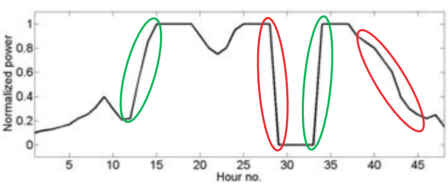

Fig. 2 – Example of normalized wind power production over 48 hours. Up-ramps (according to the definition in (1)) indicated with green cirkles and down-ramps indicated with red cirkles.

Methods

RanFor (Fig. 3) is an ensemble learning method for classifications that operate by constructing a large collection of de-correlated decision trees, and then predicts a class through a majority vote. Decision trees are able to capture complex structures in the data while at the same time having a relatively low bias, but they are notoriously noisy and hence tend to have a high variance. Averaging over *B* de-correlated and identically distributed trees, as is done when building a RF, reduces the variance by *1/B*. A thorough description of RanFor is found in [1].

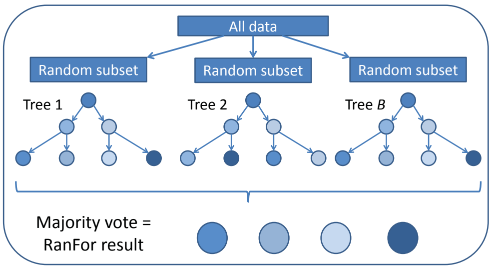

Fig. 3 – Visualization of random forest procedure

MLR is a generalization of logistic regression that allows more than two discrete outcomes, and is widely used for a variety of applications . Instead of directly providing a category as the output the MLR gives the probabilities that each observation belongs to each of the categories. The predicted category can then be found by selecting the outcome with the highest probability. A thorough description of MLR is found in [2].

Results

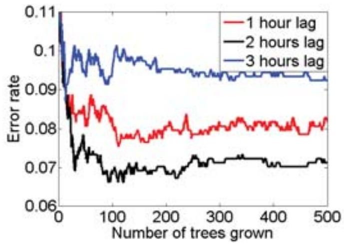

Fig. 4 – Error rates (fraction of wrong classification) for time-lags 1-3 hours for random forests of up to 500 trees.

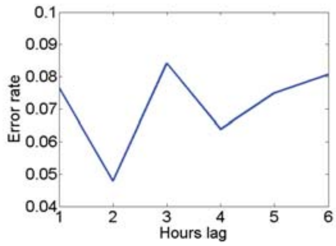

Fig. 5 – Error rate for time lags 1-6 hours for multinomial logistic regression

Figure 4 shows that the error rates of the RanFor stabilize from approx. 300 trees and that including additional trees after this does not give improved results. Figures 4 and 5 show the error rates for RanFor and MLR for different time-lags from the measurements at the off-sites. Both models give the lowest error rates for ramp forecasts based on measurements made two hours earlier. The decline in error rate from hour 3 to hour 4 that is found for MLR is not present for RanFor (graph not shown). It should be noted that as a result of the very low update rate of the measurements (6 hours) these results are the subject of large uncertainties.

Tab. 1 – Confusion matrix for random forest, multinomial logistic regression and unprocessed numerical weather prediction. Correct forecasts on the diagonal. Forecast errors off the diagonal.

Random forest/ Multinomial logistic regression/ Numerical weather prediction		Forecasted		
		No ramp	Up ramp	Down ramp
Observed	No ramp	845/ 843/ 778	6/ 8/ 42	6/ 6/ 37
	Up ramp	30/ 20/ 48	32/ 42/ 13	0/ 0/ 1
	Down ramp	28/ 13/ 48	0/ 0/ 1	35/ 50/ 19

Table 1 shows the confusion matrix (classification/misclassification) for RanFor and MLR as well as for a ramp forecast made from the NWP forecast without any post-processing (for comparison). From the table it is obvious that both RanFor and MLR has a much higher number of correct classifications (and thus also forecasts) than the raw NWP. Ranfor is slightly more conservative than MLR, predicting 25 more observations as no-ramps. This gives MLR slightly better results than RanFor, but the differences are small.

Conclusions

- Measurements from upwind off-sites can give positive contributions to the precision of wind power ramp forecasts.
- Off site measurements made only once every six hours gives very large uncertainties and is not well suited for the purpose of ramp forecasting.
- Both random forests and multinomial logistic regression gives large improvements in the number of correctly predicted ramps compared to an unprocessed NWP forecast.

References

[1] Breiman, Leo (2001). Random Forests. Machine learning, 45, 5-32.
[2] Agresti, Alan (2013). Categorical Data Analysis, 3rd Edition. Wiley.
[3] Ferreira, C. et al. (2010). A Survey on Wind Power Ramp Forecasting. ANL/DIS-10-13, Argonne Nat. Lab.

Significance of unsteady aerodynamics in floating wind turbine design

Roberts Proskovics[a], Julian Feuchtwang[a] and Shan Huang[b,c]

[a]Wind Energy Systems Centre for Doctoral Teaching, University of Strathclyde, Glasgow, UK
[b]Naval Architecture and Marine Engineering Department, University of Strathclyde, Glasgow, UK
[c]Upstream Engineering Centre, BP Exploration, Chertsey Road, Sunbury on Thames, TW16 7LN, UK

University of Strathclyde Engineering

Introduction

In the future, as floating offshore wind turbines evolve, engineers will probably need to redesign turbines completely to be better integrated with their floating support. For such a design process, it is not enough to be able to analyse an existing design; they will need to know what can be simplified and/or ignored in the initial design. In particular, as a step towards determining which types of motion are the most damaging, it becomes necessary to find out how important unsteady aerodynamics are.

Methodology

Theodorsen's model [1] and an analytical model of Van der Wall and Leishman [2], discretised in the time domain and coded in MATLAB, were used to analyse the fully-attached unsteady aerodynamics. Quasi-steady and fully-attached unsteady models were matched by comparing loads on the NREL 5MW base turbine blade [3].

A parallel study was performed in FAST [4] using the OC3-Hywind model [5]. This study included the whole spectrum of unsteady aerodynamics (dynamic inflow, attached flow, separated flow and dynamic stall).

Conclusions

Two different theories were used to compare quasi-steady and fully-attached unsteady loads on a turbine. Both theories showed a very good agreement of results with fully-attached unsteady loads having a slightly larger mean thrust load, smaller thrust amplitude and a phase lag compared to the quasi-steady results.

Fully-unsteady results, obtained using FAST, showed some similarities to the fully-attached codes. Mainly, in the higher mean loads compared to the quasi-steady results. However, the amplitude of the loading was always larger in the fully-unsteady aerodynamics when compared to quasi-steady loads.

A much higher aerodynamic damping was obtained using fully-unsteady aerodynamics assumption (3.7 % vs. 2.3 % in quasi-steady).

High non-linearity of dynamic inflow leads to more pronounced wave harmonics, which, when coinciding with other natural frequencies of the system, can be very damaging to system.

References

[1] Theodorsen T. "General Theory of Aerodynamic Instability and the Mechanism of Flutter." *NACA Report* 496, 1935.
[2] Van der Wall, B. G., and J. G. Leishman. "On the influence of time-varying flow velocity on unsteady aerodynamics." Journal of the American Helicopter Society 39.4 (1994): 25-36.
[3] Butterfield, Sandy, Walter Musial, and G. Scott. Definition of a 5-MW reference wind turbine for offshore system development. Colorado: National Renewable Energy Laboratory, 2009.
[4] NWTC Computer-Aided Engineering Tools (FAST by Jason Jonkman, Ph.D.). http://wind.nrel.gov/designcodes/simulators/fast/. Last modified 4-October-2013; accessed 16-October-2013.
[5] Jonkman, Jason Mark. Definition of the Floating System for Phase IV of OC3. National Renewable Energy Laboratory, 2010.

Results

A simple calculation using reduced frequency, a non-dimensional parameter that helps to identify the unsteadiness of the flow, shows that for an excitation frequency of 0.2 Hz different blade sections of an NREL 5 MW turbine's blade would see varying flow states over its span, including unsteady and highly-unsteady (Fig. 1).

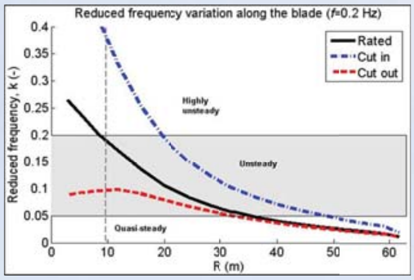

Fig. 1 – Reduced frequency variation along the blade span

Theodorsen showed that fully-attached lift on a rigid blade in harmonic plunging (heaving) and pitching motion can be expressed using Theodorsen's function.

Fig. 2 shows thrust force on the NREL 5 MW turbine's blade in plunging (a) and pitching (b) motion calculated using Theodorsen's function.

Reduction in the thrust force amplitude and phase shift are clearly seen in both motions.

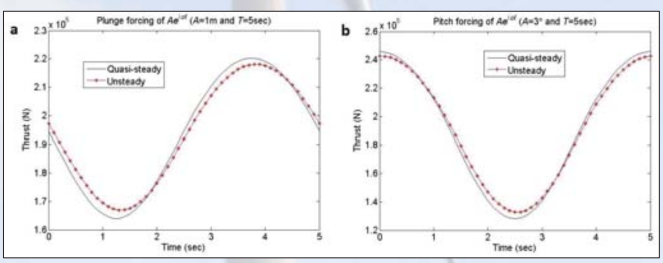

Fig. 2 (a) Thrust force on an NREL 5 MW blade in harmonic plunging; (b) pitching

Theodorsen theory applies only to constant free-stream velocity, which is rarely the case for wind turbines.

Van der Wall and Leishman improved the work of Theodorsen to account for the varying free-stream velocity by inserting it in the Duhamel's integral form.

Also, comapred to Theodorsen's theory, Van der Wall's and Leishman's theory is not constrained to any specific motion.

Fig. 3 (a) shows thrust force on an NREL 5 MW turbine blade calculated using Van der Wall and Leishman model for thin aerofoil theory (thin) and C_L look-up tables (look-up) using quasi-steady and fully-attached unsteady aerodynamics assumption.

Both sets of results show a phase shift and reduction in loading amplitude in the fully-attached unsteady case compared to quasi-steady. This is consistent with findings from Theodorsen theory (Fig. 2 (a) and (b)).

Fig. 3 (b) shows the difference in the amplitude of thrust force as the percentage of quasi-steady. These results show no dependence on amplitude of motion as thin aerofoil theory is purely linear. As the period of motion increases, the fully-attached results tend to quasi-steady.

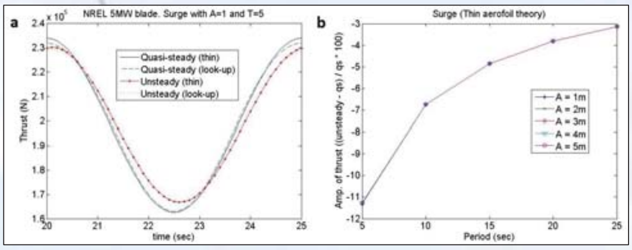

Fig. 3 (a) Thrust force on an NREL 5 MW blade; (b) Percentage difference in thrust amplitude

OC3-Hywind was analysed using FAST. Each degree-of-freedom was simulated separately, and loads on the turbine compared between the quasi-steady and unsteady aerodynamic models.

In Fig. 4 amplitudes of displacement (a) are almost identical, while the amplitude of thrust force on the rotor (b) is significantly larger in the unsteady aerodynamics simulations, which, partially, is the result of the aerodynamic damping, which for 1.57 m displacement in surge, was shown to be 2.3 and 3.7 % for the quasi-steady and unsteady simulations.

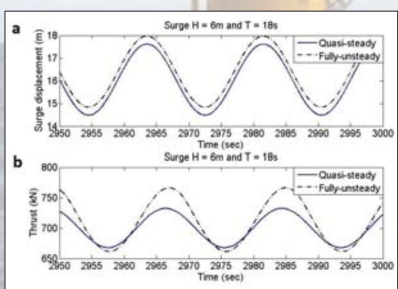

Fig. 4 (a) Surge displacement; (b) Thrust force on the rotor

Tower base side-side moment and the corresponding amplitude spectrum are shown in Fig. 5. Fully-unsteady results show a much large loading on the tower base with many more frequency components present in the amplitude spectrum.
A combination of the 7[th] wave harmonic and tower side-side mode results in a significant increase of the amplitude of that frequency component.

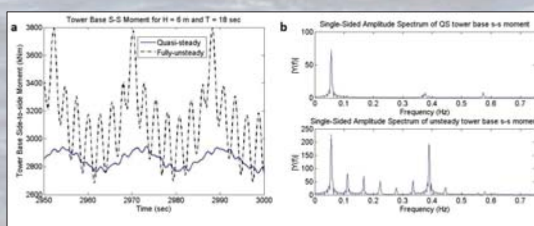

Fig. 5 (a) Tower base side-side moment; (b) Amplitude spectrum of the side-side moment

Acknowledgment: This work has been funded by the EPSRC, project reference number EP/G037728/1.

EPSRC

(Background photo: Trude Refsahl / Statoil)

WIND TUNNEL TESTING OF A FLOATING WIND TURBINE MOVING IN SURGE AND PITCH

NTNU
Det skapende universitet

J. Bartl, L. Sætran

Department of Energy and Process Engineering
Norwegian University of Science and Technology, N-7491 Trondheim, Norway

1. MOTIVATION

Large water depths (> *50 m*) in many costal regions around the world, e.g. Norway, Spain, Portugal, Japan or United States

Floating offshore wind turbine concepts could be an economic option

+ various concepts for floating structures proposed
+ higher flexibility of installation and easier decommissioning

Floating turbine concepts pose new challenges

- controlling of wind and wave induced turbine motion
- complex modelling in the design process: coupling of wind-wave climate, wind turbine, its support structure and mooring lines

Floating wind turbines are exposed to larger motions due to wave-induced hydrodynamic forces

⇨ Turbine rotor might move into and out of its own wake under certain wind and wave conditions
⇨ Need for computational codes that are capable to simulate aerodynamics correctly

2. OBJECTIVE

Investigation of rotor and wake aerodynamics affected by harmonic surge and pitch motions

- Rotor thrust C_T and turbine performance C_P
- Rotor induced velocities
- Wake bunching effect

} at different oscillation frequencies and amplitudes

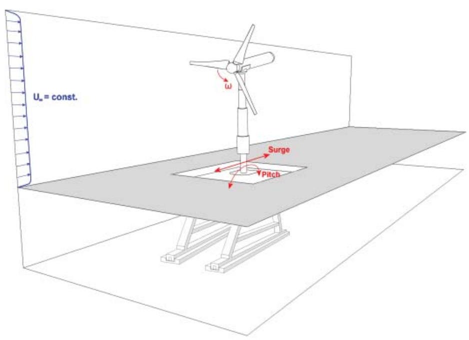

Fig.1: Sketch of the model wind turbine installed on a surge-pitch test rig in the wind tunnel

3. EXPERIMENTAL METHODS

TEST FACILITIES

- Closed-loop wind tunnel with a test section of *1.9 m* (height) x *2.7 m* (width) x *11.0 m* (length) at NTNU EPT
- 2D surge-pitch test rig capable to induce motions of approximately *1.0 Hz* (frequency) and *1.0 m* (amplitude) at NTNU IMT

MODEL WIND TURBINE AND INSTRUMENTATION

- Model wind turbine with a rotor diameter D_{Rotor} = *0.90 m*
- Turbine equipped with torque sensor and RPM sensor for power measurements
- Turbine placed on force plate for thrust force measurements
- Hot-wire probe for mean and turbulent velocities in wake

4. ILLUSTRATION OF WAKE FLOW

Effect of wake bunching at different oscillation modes

⇨ *Computational study by J. B. de Vaal, M.O.L. Hansen, T. Moan (NTNU/DTU)*
⇨ *Vortex Ring CFD model aimed at capturing unsteady rotor inflow*

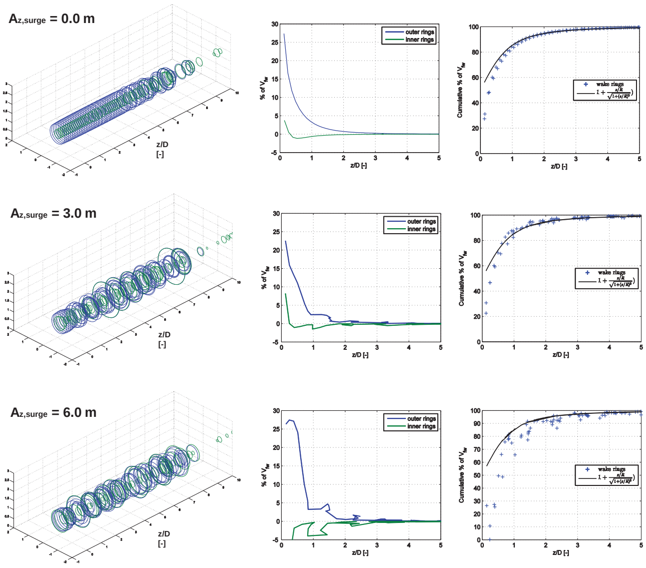

Fig.2: Wake shape (left), Incremental induced velocity (middle) and cumulative induced velocity (right) computed for a simplified NREL 5MW wind turbine operated at U_{wind} = 11.4 m/s and TSR = 7.0, oscillating in surge at a frequency f_{surge} = 0.08 Hz

[Source Fig. 2: with kind permission of Jacobus B. de Vaal, Institute of Marine Technology, NTNU]

5. EXPERIMENTAL CHALLENGES

Unsteady effects on aerodynamic forces and wake are expected for **fast motions** and **large motion amplitudes**

⇨ oscillation motion should reach convective wake velocity
⇨ not possible to impose fast motions and large amplitudes with test rig

High frequencies and motion amplitudes imply very high inertial forces

⇨ for accurate measurements the aerodynamic forces on the rotor should be in the same order as the inertial forces due to the turbine movement

EXPERIMENTAL PROGRESS PLAN

1. Solid **drag disc** in **surge** motion: Drag force and wake measurements
2. **Turbine** in **surge** motion: Rotor thrust & power and wake measurements
3. **Turbine** in **pitch** motion: Rotor thrust & power and wake measurements

REFERENCES

[1] A.R. Henderson, D. Witcher, "*Floating Offshore Wind Energy – A Review of the Current Status and an Assessment of the prospects*", Wind Engineering 34, pp. 1-16, 2010

[2] H. Bredmose, S.E. Larsen, D. Matha, A. Rettenmeier, E. Marino, L. Sætran, "*MARINET D2.4: Collation of offshore wind-wave dynamics*", 2012

[3] J.M. Jonkman, "*Dynamics Modeling and Loads Analysis of an Offshore Floating Wind Turbine*", Technical Report NREL/TP-500-41958, 2007

[4] J.B. de Vaal, M.O.L. Hansen, T. Moan, "*Effect of wind turbine surge motion on rotor thrust and induced velocity*", Wind Energy, DOI: 10/1002/we.1562, 2012

NOWITECH

Value-added of Offshore Energy Storage for Deep-sea Wind Farms

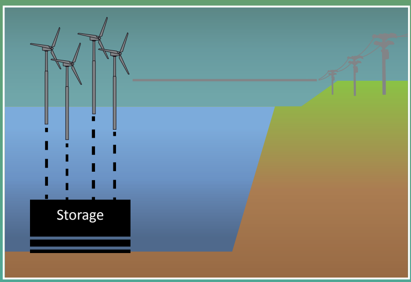

Use Case:

Wind Farm

- 400 MW offshore wind farm
- Located 30 km away from shore
- Connected to the UK grid
- NOWITECH 10 MW reference turbine

Energy Storage

- 300 MW storing and generation capacity
- 2000 MWh energy storage capacity
- 85 % round-trip efficiency

Objective:

Estimate the gross value of an offshore energy storage

Why Offshore?

- Reduced required cable capacity
  => lower initial investment
- Reduced influence of NIMBY
- Limited ecological impact compared to onshore alternative

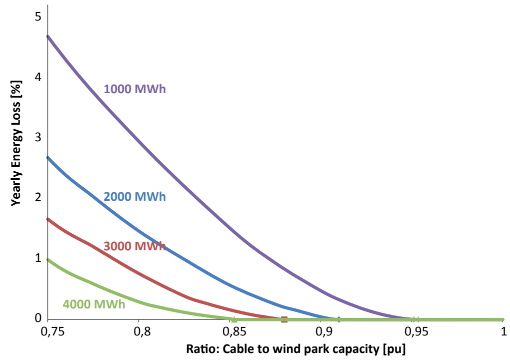

Right: Required cable capacity decreases with increasing storage capacity

Results:

The value is quantified assuming the following benefits:

1 Classical pumped-storage operation
2 Countering wind forecast error to avoid balance cost
3 Reduced cable capacity rating
4 Avoiding the need for onshore infrastructure reinforcements
5 Offering ancillary services

The study is giving indicative values only, relying on literature survey and simplistic calculations.

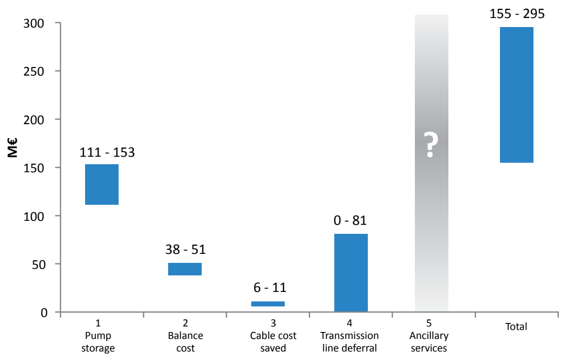

Total value of the energy storage unit broken into individual parts (20yr period, 7% annuity factor).

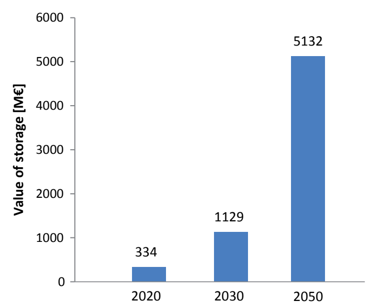

The total value of the energy storage will increase for future scenarios. Source: Carbon Trust

Subhydro Storage Concept

- Large scale pumped storage
- Sub-sea installation at depths up to 1000m
- Energy production by letting water in
- Energy storage by pumping water out

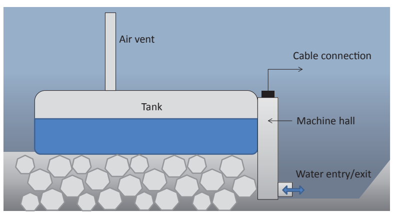

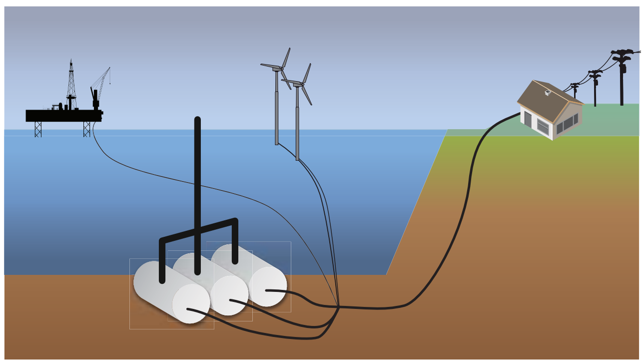

Acknowledgements:
The project has been funded and supported by NOWITECH in collaboration with Subhydro and SINTEF Energy Research. The wind data has been provided by the FINO project, which is sponsored by the BMU (Bundesministerium fuer Umwelt, Federal Ministry for the Environment, Nature Conservation and Nuclear Safety) and the PTJ (Projekttraeger Juelich, project executing organisation).

Contacts:
Ole Christian Spro SINTEF Energi AS olechristian.spro@sintef.no
John Olav Tande, SINTEF Energi AS john.o.tande@sintef.no
Rainer Schramm, Subhydro AS rainer.schramm@subhydro.com

CENTRE FOR ENVIRONMENT-FRIENDLY ENERGY RESEARCH

SINTEF

How can more advanced failure modelling contribute to improving life-cycle cost analyses of offshore wind farms?

Kari-Marie H. Holmstrøm: University of East London – Centre for Alternative Technology (kammarie.h.h@gmail.com)

Abstract

Accurate failure modelling is fundamental in reliability analyses and for optimisation of maintenance strategies to minimize life cycle costs (LCC) of offshore wind (OW) farms. Due to lack of (or reluctance among operators to share) sufficient wind turbine failure data, many operation and maintenance (O&M) models - simulating the operational phase of an OW farm with all maintenance activities and costs - rely on simple failure-time distributions for modelling failure events. The exponential distribution with its constant failure rate is widely used. It is often associated with the homogenous Poisson process (HPP) which assumes that a system is as good as new after repair.

Wind turbines' reliability is not necessarily improved by repairing components, and they are usually not as good as new unless completely overhauled. It was therefore investigated if a more advanced failure model, capable of taking such facts into account, was available for use in (models like) the Norwegian Offshore Wind cost and benefit (NOWIcob) model developed by NOWITECH.

Objectives

- ✓ Establish and implement a new, more flexible failure model to test, on a representative base case, how it affects the results and if it can contribute to more accurately simulate a realistic O&M phase and associated LCC of an OW farm.
- ✓ Provide, through the resulting evaluation, an overview of the failure model's behaviour compared to the existing one and compared to governing background theory for verification.

Method

Knowing that wind turbines are repairable, electro-mechanical systems that degrade with time, it was assumed that their overall failure behaviour follows the bathtub curve (BTC) through three distinct life-phases:

1: Burn-in period (decreasing failure rate, “infant mortality”)
2: Useful life (constant, low failure rate, random failures)
3: Burn-out period (increasing failure rate due to aging, wear and tear)

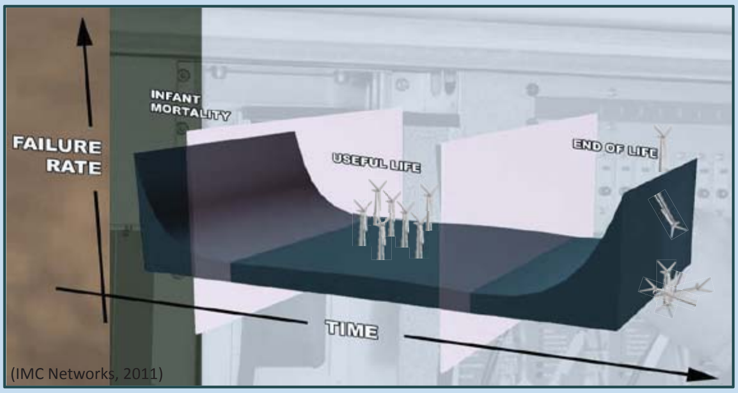

(IMC Networks, 2011)

Potential stochastic failure models were investigated and evaluated in terms of their complexity and capability of representing the three phases. A more advanced model, and a natural extension (being a generalisation) of the HPP used in NOWIcob, is the Non-Homogenous Poisson Process (NHPP) which with a proper failure intensity function λ(t), can handle trends, aging or reliability growth (Kim, 2009).

An example is the NHPP with Power Law (PL) intensity (NHPP_PL):

Rate of Occurrence of Failures (ROCOF) = $\lambda(t) = \frac{1}{\alpha}\beta t^{\beta-1}$

By changing the β-value, the NHPP_PL can be used to model systems in which ROCOF increases with time (β >1), decreases with time (β <1), or remains constant with time (β=1 → NHPP=HPP). NHPP assumes that a system is as bad as old after repair, and that repair time is negligible.

Based on the NHPP_PL a new model for the time to the next failure was established using the inverse transform method (Crow, 2004) and the condition that the previous failure-time is known. The model was coded in MATLAB and implemented in NOWIcob.

$$t_{next} = \left[\frac{\ln(1-U)}{\lambda} + t_{previous}^{\beta}\right]^{1/\beta}$$

To verify correct implementation, the model it was run under various combinations of the input parameters and empirical results were compared to theoretical ones. Further verification was done by confirming the time-dependency of the intensity function.

Results

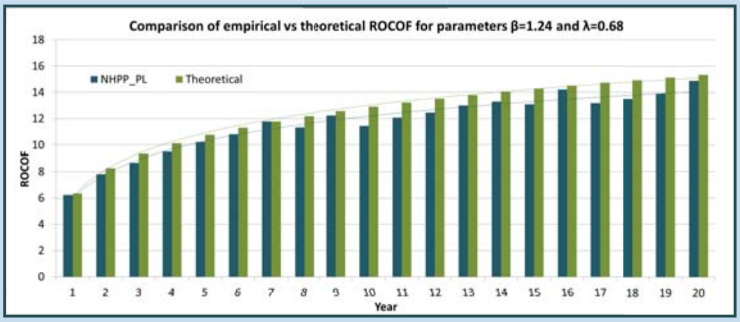

The new failure model, NHPP_PL, behaves according to theory, and can be used to model both increasing, decreasing and constant ROCOF development. In the example above, ROCOF is increasing with time for β >1. Empirical values are slightly lower, and the difference increases with time, because repair time associated with the failure scenario modelled is not negligible like theory assumes.

The higher ROCOF the lower availability. The capability of modelling time-dependent failure intensity is an important feature of the NHPP_PL model. The chart below shows how the availability decreases more and more with increasing β for longer simulation horizons.

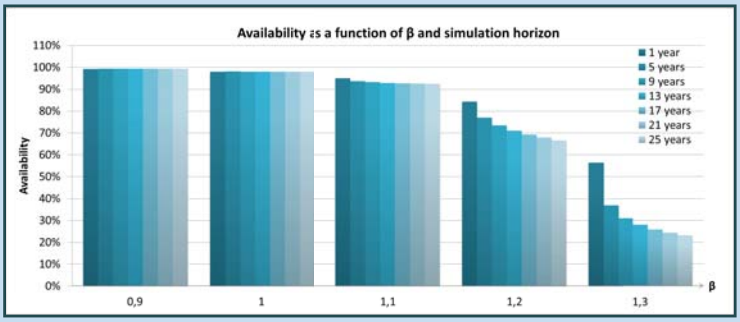

Conclusions

Models simulating the operation and maintenance phase of offshore wind farms often rely on failure models based on the simple exponential distribution. The non-homogenous Poisson process with power law intensity has great potential for improving wind farm life-cycle cost analyses in such models. More advanced failure models are available, but data requirements as well as their complexity might consequently make them harder to implement.

Until sufficient failure history from a representative number of offshore wind farms become available, it is reasonable to assume that on a system level, wind turbines' failure behaviour follows the bathtub curve. The flexibility of the power law makes it possible to model a time-dependent rate of occurrence of failures, which opposed to the constant rate modelled by the exponential distribution, is more realistic for wind turbines as they are known to degrade with time.

References

Crow, L.H. (2004) 'Practical Methods for Analysing the Reliability of Repairable Systems', *Reliability Edge*, 5(1), pp.3,5-7,9 [Online]. Available at: http://www.reliasoft.com/pubs/reliabilityedge_v5i1.pdf (Accessed: 13 Nov. 2013).

IMC Networks (2011) *MTBF, MTTR, MTTF & FIT: Explanation of Terms.* Available at: http://www.imcnetworks.com/Assets/DocSupport/WP-MTBF-0311.pdf (Accessed: 18 Dec .2013).

Kim H.K. (2009) *Reliability modelling and evaluation in aging power systems.* MSc thesis. Texas A&M University [Online]. Available at: http://repository.tamu.edu/bitstream/handle/1969.1/ETD-TAMU-2009-08-7011/KIM-THESIS.pdf (Accessed: 11 Oct .2013).

Will 10 MW wind turbines bring down the operation and maintenance cost of offshore wind farms?

Matthias Hofmann (matthias.hofmann@sintef.no), Iver Bakken Sperstad (iver.bakken.sperstad@sintef.no),
SINTEF Energy Research

Abstract

In the deployment of offshore wind power, a clear trend towards larger wind turbines can be observed. Prototypes of 7 MW offshore wind turbines are currently being installed, and plans and designs for 10 MW turbines are being developed, such as the reference turbine of the NOWITECH research programme. Larger wind turbines are believed to be advantageous from an investment and installation perspective. However, it is more uncertain, whether and to which extent larger wind turbines can contribute to a reduction in operation and maintenance (O&M) cost. This analysis will investigate this question.

Objectives

Main objective: Analyse how O&M costs are likely to be affected due to the transition from 5 MW wind turbines to 10 MW wind turbines.

High uncertainty of future O&M costs is mainly due to the uncertain development of failure rates, maintenance durations and spare part costs when scaling up the rated power of wind turbines. The analysis will therefore take into consideration the effect of the uncertainty in these parameters.

Method

A simulation study was performed using the NOWIcob model, which is a discrete-event simulation model for the operational phase of an offshore wind farm, focusing on maintenance tasks and related logistics. The study compares two hypothetical wind farms, each having a total rated production of 400 MW: One wind farm consisting of 80 x 5 MW turbines and the other wind farm consisting of 40 x 10 MW turbines. As a base case, it is assumed that one is able to achieve the same failure rates, the same durations of corrective and scheduled maintenance tasks, and the same spare part costs for 10 MW turbines as for 5 MW turbines. This has to be understood as the starting point for the analysis and not as a realistic assumption. Starting from this base case, the three parameters are sequentially increased to find the limit where the total O&M cost of the 10 MW turbine wind farm exceeds the O&M cost of the 5 MW turbine wind farm. Total O&M cost includes lost income due to downtime.

The approach assumes the same logistic setup for all cases: 3 crew transfer vessels, 1 field support vessel, 1 heavy-lift vessel and 25 technicians. This can be unrealistic for some of the cases. Therefore a careful examination of this assumption is undertaken by means of a sensitivity analysis.

Results

The simulation results show, not unsurprisingly, a decrease of ca. 24 % in the total O&M cost when replacing two 5 MW turbines by one 10 MW turbine, all other parameters being equal. However, as presented in the figure below, the O&M cost are highly dependent on how important maintenance parameters will develop.

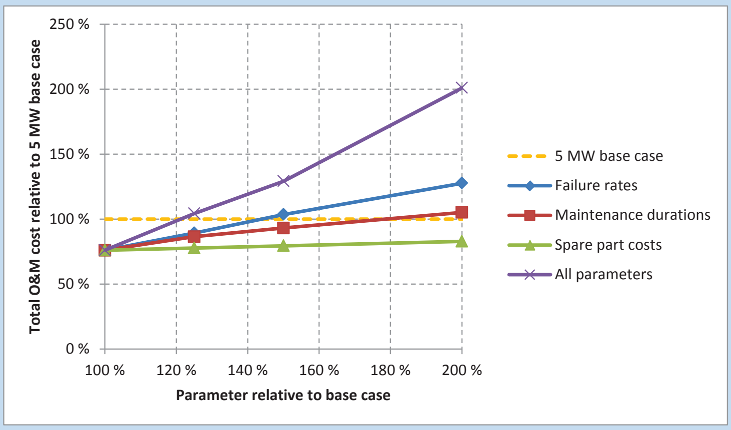

The results show that the O&M cost is highly sensitive to an increase in failure rates or an combined increase of the maintenance parameters. The following figures give an insight into how much the maintenance parameters can increase before larger wind turbines are turning less beneficial compared to 5 MW turbines.

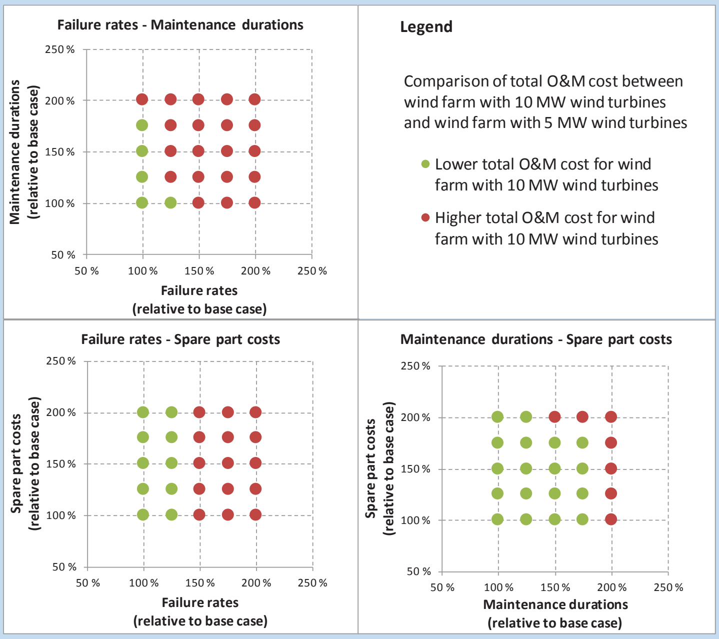

A parallel increase of the maintenance durations and failure rates by only 25 % already leads to an increase of the total O&M cost of a wind farm consisting of 10 MW wind turbines above the level of a similar wind farm consisting of 5 MW wind turbines. Spare part costs have only a minor effect on the total O&M cost.

The additional sensitivity analysis of the logistic setup showed that the setup is sufficient for all cases, even though it may not be the optimum. Total O&M cost for logistic strategies closer to the optimum are only up to a few percentages better. The assumption of equal logistic setup should therefore not bias the results.

Conclusions

The total O&M cost of wind farm with 10 MW wind turbines will not necessarily be lower compared with existing wind farms. Whether larger wind turbines are beneficial from an O&M perspective are first and foremost dependent on how the failure rates for such wind turbines will develop compared to 5 MW wind turbines. Also the maintenance durations have a major effect on the O&M cost. It is therefore difficult to say whether moving to 10 MW wind turbines by itself can help to reduce the O&M cost.

Based on the results of this analysis, it can be concluded that higher failure rates quite fast will counterbalance the benefits of larger wind turbines. One therefore has to focus on the reliability of the wind turbines, and further work should look more into the uncertainty around estimates for reliability of future 10 MW wind turbines.

References

1. NOWITECH 10 MW reference turbine. http://www.ntnu.edu/research/offshore-energy/wind-turbine
2. Hofmann, Matthias; Sperstad, Iver Bakken (2013): NOWIcob – A Tool for Reducing the Maintenance Costs of Offshore Wind Farms. DeepWind 2013. In Energy Procedia 35, pp. 177–186.
3. Hofmann, Matthias; Sperstad Iver Bakken (2013): Analysis of sensitivities in maintenance strategies for offshore wind farms using a simulation model. EWEA offshore 2013, Frankfurt, Germany.

Modelling of Lillgrund Wind Farm: *Effect of Wind Direction*

Mihaela Popescu, Balram Panjwani, Jon Samseth, Ernst Meese

SINTEF

Flow Technology Department
SINTEF Materials and Chemistry
Norway

Motivation

The recent years have shown dramatic development of offshore wind energy due to the better wind speeds availability compared to on land. The wakes of upstream turbines affect the flow field of the ones behind them, decreasing power production and increasing mechanical loading. The power production from a wind farm depends mainly on wind magnitude and direction, therefore quantitative and qualitative assessment of wind farm performance under different direction is necessary. In the present study, OffWindSolver[1] tool and OffWindEng tool are used to characterize the wind direction effect on the power production from the Lillgrund offshore wind farm.

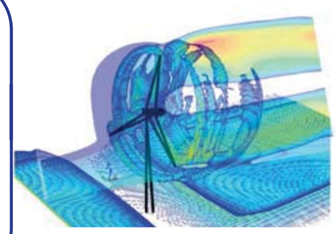

flow through wind turbine

OffWindSolver model

Actuator Line Turbine Model

- Blade is model as a set of discret points along each blade: Aerodynamics blade forces are governed by velocities obtained locally & tabulated 2D aerofoil data

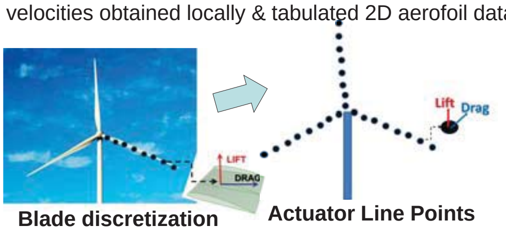

Blade discretization Actuator Line Points

Actuator Disc Model

- The actuator disk model resolve the rotor as a porous disk. AD

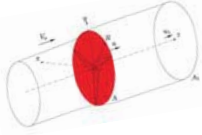

OffWindEng model

- Model of the wake effect includes:
  - Effects of wind direction
  - Wind speed time delay
  - Cumulative impact of multiple shadowing,

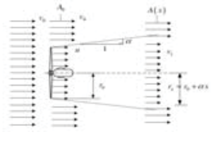

$$u_{i,power}{}^3 = \frac{\int_{S_{rotor}} u_i^3 ds}{S_{rotor}}$$

Influence of the wind direction on the wind farm production:

- **Minimum power production is obtained for around 220⁰ wind direction (WD)**
  - Almost total shading of the wind turbines situated in the lee of other turbine
  - the power production is only 50% from designed wind farm power (without any wake loss)
- **Maximum power production is obtained for around 280⁰ wind direction (WD)**
  - The shading for the wind turbine is low
  - the power production is around 80% from designed wind farm power (without any wake loss)

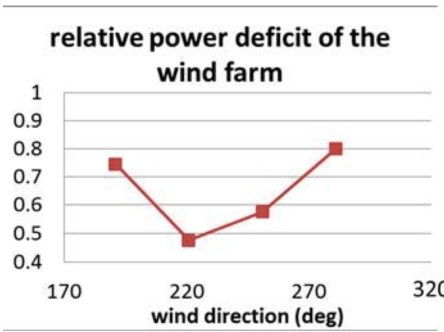

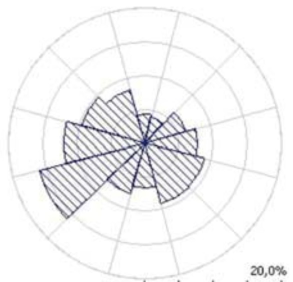

Wind rose - Lillgrund wind farm

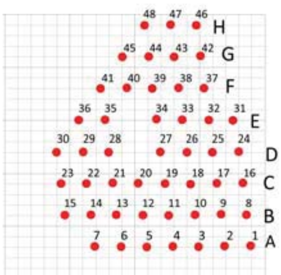

Lillgrund wind farm

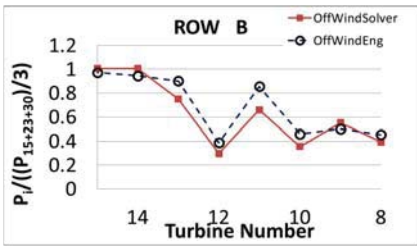

Wind power- wind direction = 281⁰

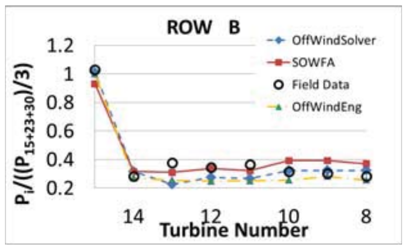

Wind power- wind direction = 221⁰

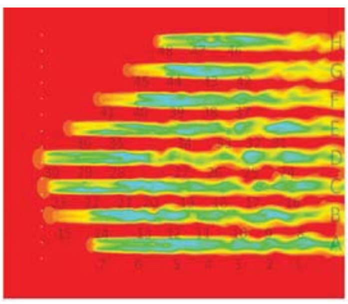

Velocity Distribution - WD = 221⁰

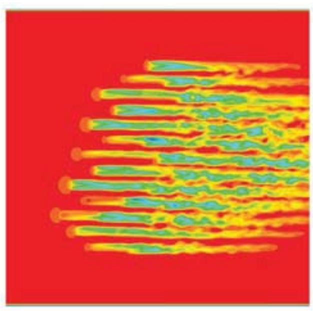

Velocity Distribution - WD = 251⁰

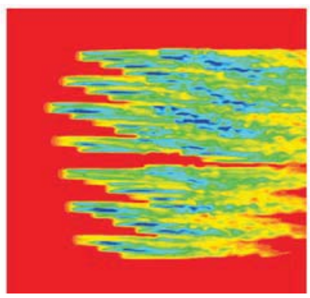

Velocity Distribution - WD = 281⁰

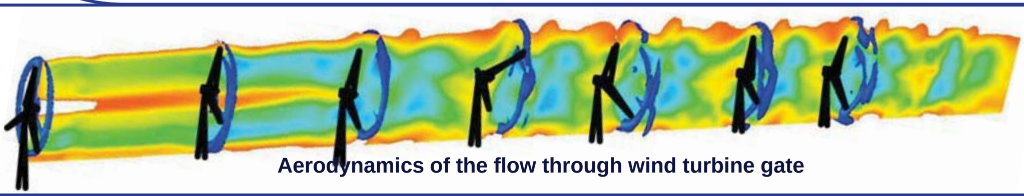

Aerodynamics of the flow through wind turbine gate

Acknowledgments

The OffWind project is supported by the **Nordic Energy Research**

norden
Nordic Energy Research

Balram Panjwani, Mihaela Popescu, Jon Samseth, Ernst Meese and Jafar Mahmoudi, "**OffWindSolver: Wind Farm Design Tool Based on Actuator Line/Actuator Disk Concept in OpenFoam architecture** ", First Symposium on OpenFOAM in Wind Energy, Oldenburg, 2013

NOWITECH

Lab-scale implementation of a multi-terminal HVDC grid connecting offshore wind farms

Objective:

- This work presents a lab-scale implementation of a multi-terminal HVDC system connecting an offshore wind farm

System:

- The system is composed by four voltage-source converters (VSC) replicating a future North Sea HVDC grid, where Norway, Germany and UK are interconnected together with an offshore wind farm.
- DC voltage droop is implemented on all terminals, except the wind node.
- The VSCs are built using FPGA-control. Opal RT and Labview is used for supervisory control and monitoring.

R&D topics:

- Operation and control, converter interoperability, system stability, fault handling and system services.

Smart grid laboratory SINTEF/NTNU

Main equipment:

- 55 kW wind turbine emulator with induction generator
- 50 kW low speed wind turbine emulator with PMSG
- 17 kW synchronous generator
- 60 kVA VSC units with in-house developed FPGA control
- Real time "hardware in the loop" simulator (Opal RT)
- Short circuit emulator
- Transformer substation model with protection relays
- Line models (RLC) and controllable loads
- Overall monitoring and control (Labview)

The laboratory is suitable for experiments within a wide range of fields:

- Smartgrid systems
- Wind power integration
- Multi-terminal HVDC systems
- Distributed energy production systems
- Weak grids and island mode grid operation
- Fault and transient handling

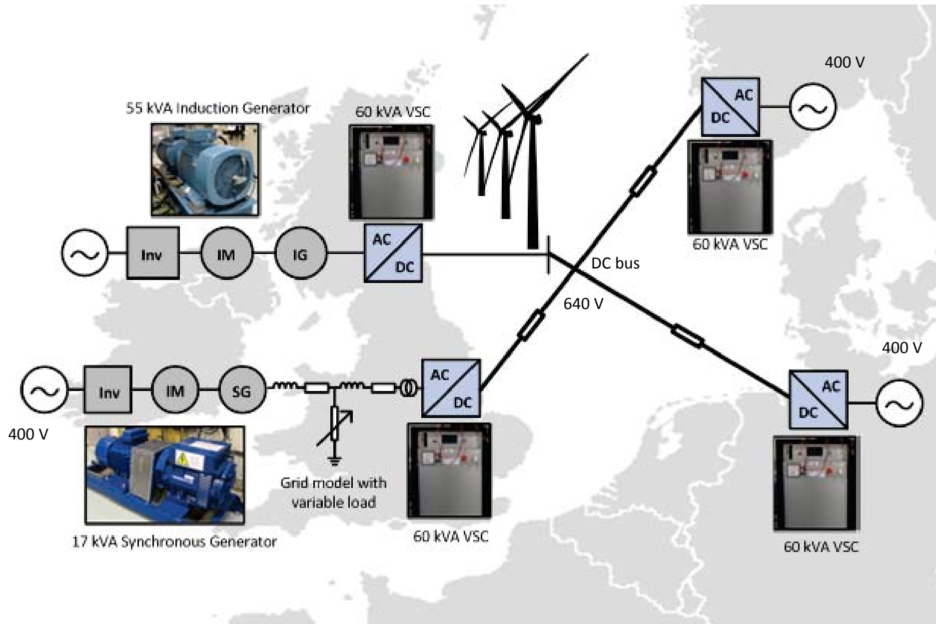

From left to right: Raymundo E. Torres, Hanne Støylen, Atle Rygg Årdal and Atsede G. Endegnanew

Contacts

Kjell Ljøkelsøy	kjell.ljokelsoy@sintef.no
Atle Rygg Årdal	atle.ardal@sintef.no
Raymundo E. Torres-Olguin	raymundo.torres-olguin@sintef.no
Atsede G. Endeganew	atsede.g.endegnanew@sintef.no
John Olav Tande	john.o.tande@sintef.no

SINTEF

Results

A) **Variation in wind production with different droop constants.** Experimental results show that the wind power is distributed proportionally to the droop constants.

B) **Loss of two terminals during full wind production.** When one terminal is disconnected the power is shared between the remaining terminals.

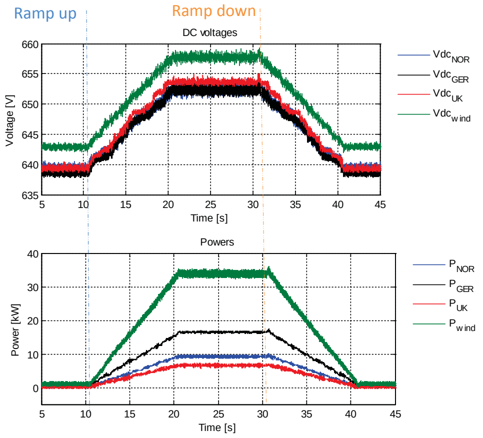

A)

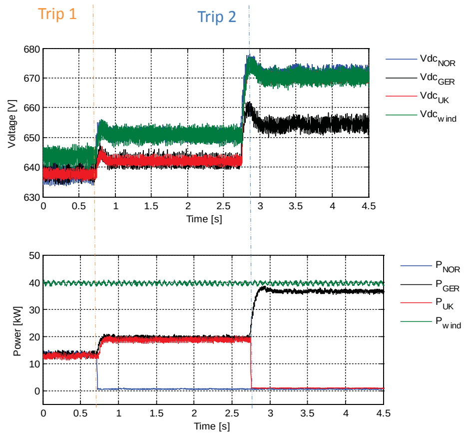

B)

Closing session – Strategic Outlook

Floating wind technology – future development; Johan Slätte, DNV

Results from the Offshore Wind Accelerator Programme; Jan Matthiesen, Carbon Trust

Offshore wind developments, Prof Leonard Bohmann, Michigan Tech

DNV·GL

ENERGY

Floating wind technology

Future development

Johan Slätte
24 January 2014

 SAFER, SMARTER, GREENER

DNV GL Group

DNV GL Group
Headquarter: Oslo, Norway
Group President & CEO: Henrik O. Madsen

Maritime	Oil & Gas	Energy	Business Assurance
Headquartered in Hamburg, Germany	Headquartered in Høvik, Norway	Headquartered in Arnhem, Netherlands	Headquartered in Milan, Italy
Appr. 6000 employees	Appr. 4500 employees	Appr. 3000 employees	Appr. 2000 employees

DNV GL Renewables Advisory
DNV GL Renewables Certification

---

1. Floating wind energy – DNV GL's work
2. Industry status, pathway to commercialization and costs
3. Visions for a future floating wind industry
   - Demonstration projects and small scale arrays – New applications
   - Cost compression and technology developments
   - What the future may look like
4. Concluding remarks

---

1. **Floating wind energy – DNV GL's work**
2. Industry status, pathway to commercialization and costs
3. Visions for a future floating wind industry
   - Demonstration projects and small scale arrays – New applications
   - Cost compression and technology developments
   - What the future may look like
4. Concluding remarks

Vast resources – supreme energy yield sites

Hotspots for floating wind developments:

- In Europe:
  - Towards the Atlantic: UK, Ireland, Spain and Portugal
  - The Northern North Sea, off the coasts of Norway and the UK
- The US
- Japan

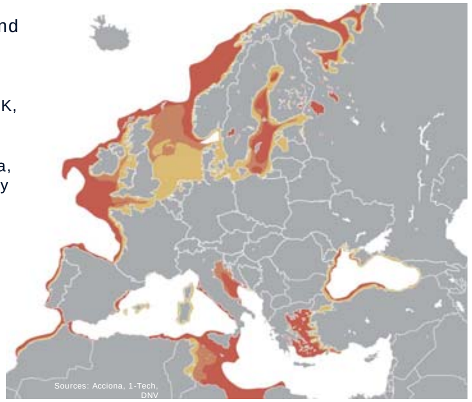

An emerging industry - An ocean of different concepts

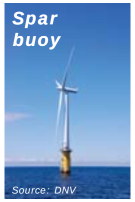

Hywind

WindFloat

PelaStar


Kabashima

Tri-Floater

GICON

Time for innovation….and consolidation

DNV GL have closely followed the development of the floating wind industry from its early days;

Core activities by DNV GL:

- Benchmarking studies
- Market analysis
- Technology evaluations
- Guideline and Standard development
- Conceptual design verification
- Prototype certification / Project certification

Standard development; DNV-OS-J103

- DNV-OS-J103 Design of Floating Wind Turbine Structures was published in June 2013
- Can be downloaded for free on **www.dnv.com**
- Developed through a Joint Industry Project (JIP) during 2011 – 2013
- Industry hearing April 2013
- Participants:
  - Statoil
  - Nippon Steel & Sumitomo Metal Corporation
  - Sasebo Heavy Industries
  - STX
  - Navantia
  - Gamesa
  - Iberdrola
  - Alstom
  - Glosten Associates
  - Principle Power

Contents of DNV-OS-J103 – Technical issues covered

- Safety philosophy and design principles
- Site conditions, loads and response
- Materials and corrosion protection
- Structural design
- Design of anchor foundations
- Floating stability
- Station keeping
- Control system
- Mechanical system
- Transport and installation
- In-service inspection, maintenance and monitoring
- Cable design (structural)
- Guidance for coupled analysis (appendix)

Mitsui

Why is a standard for floaters important?

- Expert / industry consensus on design principles
- Capturing industry experience
- Economically optimized designs through rules considering the unique aspects of floating wind turbines

DNV-OS-J103 Design of Floating Wind Turbine Structures, published in June 2013

Application of the standard - Pelastar TLP demonstration project

- Floating wind turbine demonstration project in UK
- Funded by Energy Technology Institute (ETI)
- Glosten Associates' Pelastar TLP design has been selected
- The TLP will support Alstom's 6 MW Haliade turbine
- DNV performs certification of the design against the new standard, DNV-OS-J103
- The project is currently in Front End Engineering Design (FEED) phase
- Planned installation2015/2016

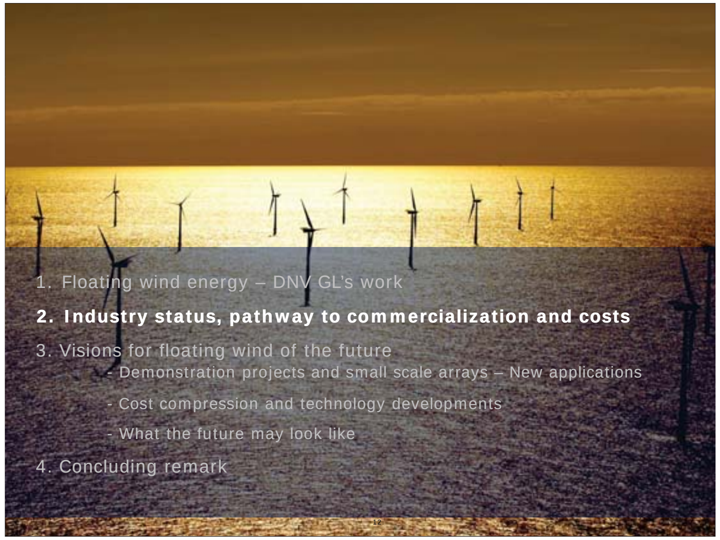

1. Floating wind energy – DNV GL's work
2. **Industry status, pathway to commercialization and costs**
3. Visions for floating wind of the future
   - Demonstration projects and small scale arrays – New applications
   - Cost compression and technology developments
   - What the future may look like
4. Concluding remark

Floating wind technology – A rapid development

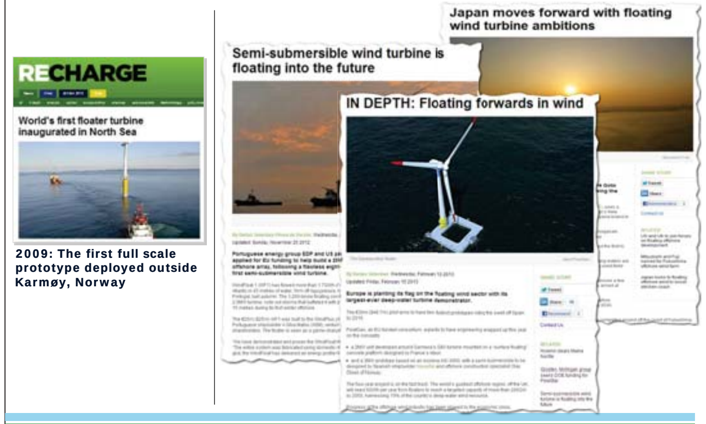

2009: The first full scale prototype deployed outside Karmøy, Norway

Typical development phases for new technologies

There are several natural steps in the development of a new technology:

1. **Proof of concept in the lab**
2. **Concept development and scale testing**
3. **Prototype demonstration**
4. **Commercial demonstration and system development**

TRL (Technology readiness level) scale can be used to describe the development process.

Today
Full scale demonstration for a number of concepts.

3 – 5 years
Small arrays likely for the most developed concepts.

7 – 10 years
Potential large arrays for the most developed concepts, commercially viable technology.

CAPEX estimations – floating vs. bottom fixed turbines

Floating wind turbine CAPEX is estimated to be ***approximately 20 % higher for than bottom-fixed wind energy.***

DNV (2012) The Crown Estate – UK Market Potential and Technology Assessment for floating offshore wind power

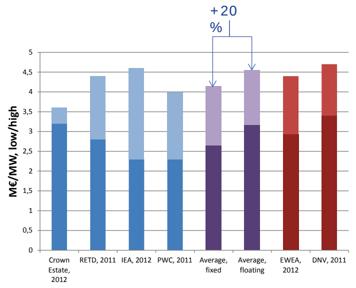

Considering potential for a higher energy yield as well as an OPEX at least equal with bottom fixed wind turbines, the cost of energy gap could be considered even smaller

Higher energy yield and an efficient supply chain

- Mass production
- No specialized vessels
- Minimum offshore operations


Image: Renewable Energy Magazine

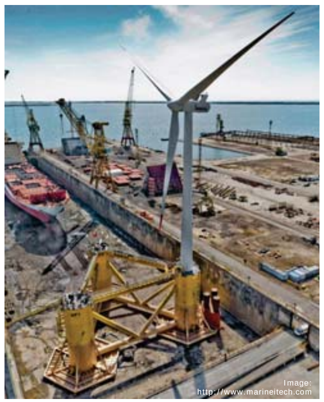
Image: http://www.marineitech.com

1. Floating wind energy – DNV GL's work
2. Industry status, pathway to commercialization and costs
3. **Visions for floating wind**
   - **Demonstration projects and small scale arrays – New applications**
   - **Cost compression and technology developments**
   - **What may the future look like**
4. Concluding remark

Era of demonstration projects and small scale arrays

Demonstration projects/small arrays

- **Hywind**
- **WindFloat**
- **Fukushima project**
  Phase 1, 2013:
  - Floating substation
  - 2 MW semi-submersible substructure

  Phase 2, 2015:
  - Two 7 MW turbines on semi-sub and spar solution respectively
- **Kabashima project**: 2 MW spar buoy installed fall 2013
- PelaStar (2016), IDEOL, GICON, Tri-Floater, VertiWind……more to come

- **Hywind Scotland (30 MW)**
- **WindFloat (27 MW)**
- **Japan initiatives, UK initiatives, US initiatives**

Are there situations where power from floating wind turbines could be a cost effective solution already today?

A potential future demonstration project?
Integration of offshore wind and Oil & Gas activities on the NCS

- High-level assessment of using floating wind turbines to power subsea water injection pumps, replacing gas turbines on the host platform.
- Cost drivers: Long step-out distances between host platform & injection well, platform conversion costs, fuel costs for running gas turbines, emission costs on the NCS
- Recent successes with raw-seawater injection (Tyrihans) and new subsea water treatment systems under development
- *High-level indicators of economic and technical performance show an interesting window of opportunity for applications that can tolerate unprocessed seawater for injection in oil fields and also other configurations are possible*

The onshore experience

- Total cost compressions of close to 75% are indicated during a 28 year period.
- Onshore wind is a mature industry compared to offshore wind, however, IEA have estimated that the cost of generating energy will continue to decrease with another 26% up until 2050 and their corresponding assessment for offshore wind implies a reduction in the cost of generating energy of 52 %. Both analyses accounting for increasing capacity factors.

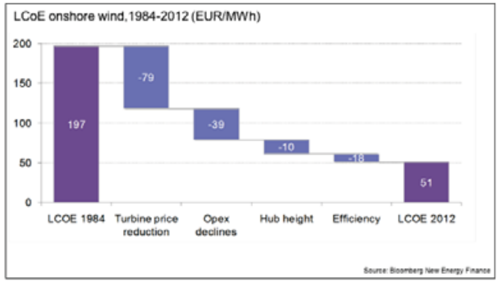

Historical developments in LCoE for onshore wind. Source: Bloomberg New Energy Finance

Concluding remarks

Demonstration projects:
- Design optimization and R&D efforts are obvious focus areas
- Technologies are being proven, the first small arrays on the way and commercialisation can be within the next few years

- Need not only to show the technical feasibility but also the ability to reduce costs – large potential for cost reductions
- New applications are possible – Integration with other offshore interests
- Stable, long-term policies are needed to create investor confidence
- DNV GL have strong belief in the floating wind industry focuses on its further development, assisting the industry through verification, certification, technology assessment and market studies!

Thank you

Johan Slätte
Johan.Slaette@dnvgl.com
+47-917 38 338

www.dnvgl.com

SAFER, SMARTER, GREENER


Carbon Trust
Offshore Wind Accelerator
Driving down the cost of offshore wind
24 Jan 2014
EERA DeepWind 2014
CARBON TRUST
DONG energy
e·on
MAINSTREAM RENEWABLE POWER
RWE The energy to lead
SCOTTISHPOWER RENEWABLES
SSE Renewables
Statkraft
Statoil
VATTENFALL


Offshore wind
Situation analysis
CARBON TRUST
Offshore wind is a young industry, near the start of the learning curve
– 22 years old vs 75 for gas, 115 for coal
– ~6GW installed vs 2,500GW gas, 2,400GW coal
Plenty of scope for cost reduction
– Mainly from innovation…
– …and also from supply chain and finance
For a healthy, sustainable industry, costs need to come down from ~£150/MWh to ~£100/MWh by 2020
If we can get innovations to market quickly, the industry can deliver significant cost reduction
2

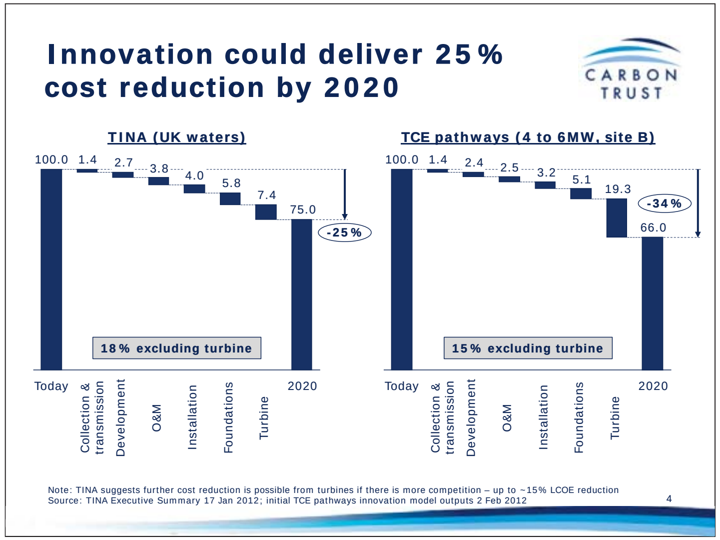
Innovation could deliver 25% cost reduction by 2020
CARBON TRUST
TINA (UK waters)
100.0 1.4 2.7 3.8 4.0 5.8 7.4 75.0
-25%
18% excluding turbine
Today
Collection & transmission
Development
O&M
Installation
Foundations
Turbine
2020
TCE pathways (4 to 6MW, site B)
100.0 1.4 2.4 2.5 3.2 5.1 19.3 66.0
-34%
15% excluding turbine
Today
Collection & transmission
Development
O&M
Installation
Foundations
Turbine
2020
Note: TINA suggests further cost reduction is possible from turbines if there is more competition – up to ~15% LCOE reduction
Source: TINA Executive Summary 17 Jan 2012; initial TCE pathways innovation model outputs 2 Feb 2012
4


Significant opportunity for innovation to drive down costs
CARBON TRUST
Development
Electrical
Foundations
Installation
Turbine
O&M
HIGH VOLTAGE
5

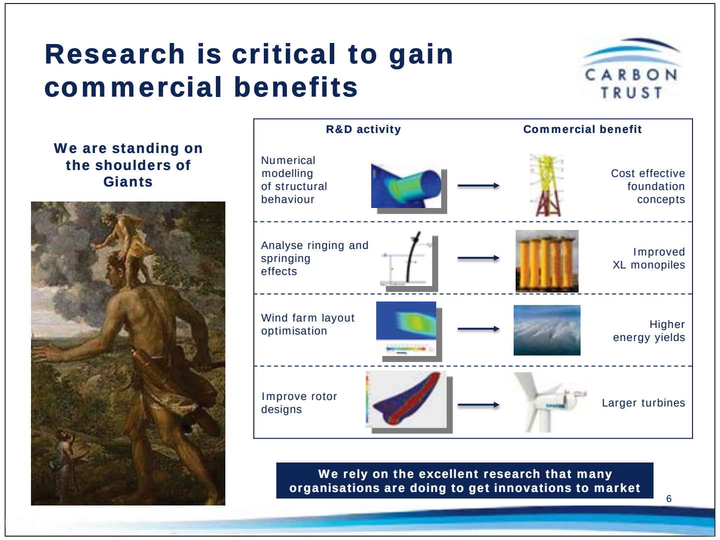
Research is critical to gain commercial benefits
CARBON TRUST
We are standing on the shoulders of Giants
R&D activity
Commercial benefit
Numerical modelling of structural behaviour
Cost effective foundation concepts
Analyse ringing and springing effects
Improved XL monopiles
Wind farm layout optimisation
Higher energy yields
Improve rotor designs
Larger turbines
We rely on the excellent research that many organisations are doing to get innovations to market
6

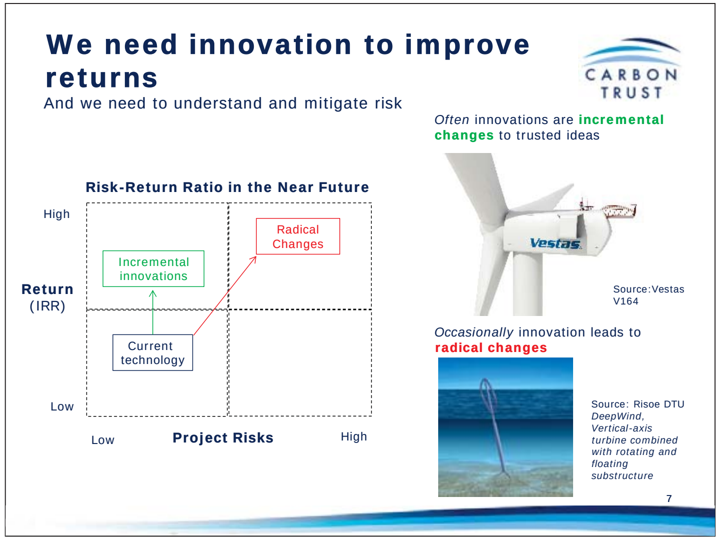
We need innovation to improve returns
And we need to understand and mitigate risk
CARBON TRUST
Risk-Return Ratio in the Near Future
High
Return (IRR)
Low
Low
Project Risks
High
Incremental innovations
Radical Changes
Current technology
Often innovations are incremental changes to trusted ideas
Vestas
Source:Vestas V164
Occasionally innovation leads to radical changes
Source: Risoe DTU DeepWind, Vertical-axis turbine combined with rotating and floating substructure
7

Evaluating Technology on its way to the market?

CARBON TRUST

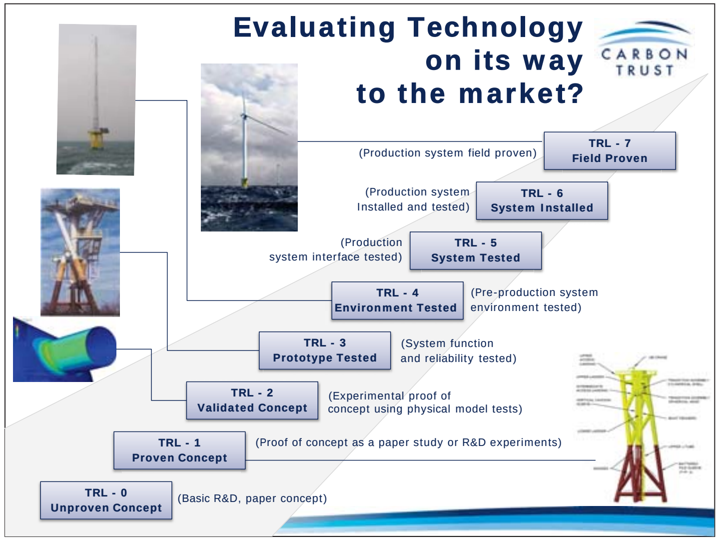

A challenging road from basic research to commercial product

CARBON TRUST

How do innovations reach the market?

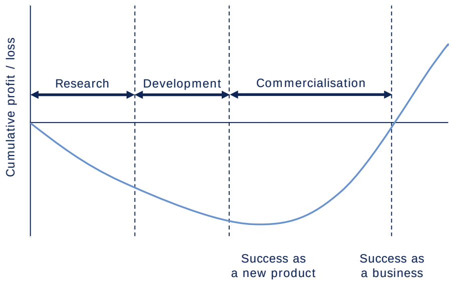

- From basic research to a commercial product is challenging process.
- Often a 'funding gap' exists between basic research and commercialization of a new product.
- This 'valley of death' is especially challenging in offshore wind for components that are high capex and which have a very large consequence if something goes wrong (ie, foundations or turbines).

Getting innovation into commercial projects is tough

Commercial project developers have a lot to worry about

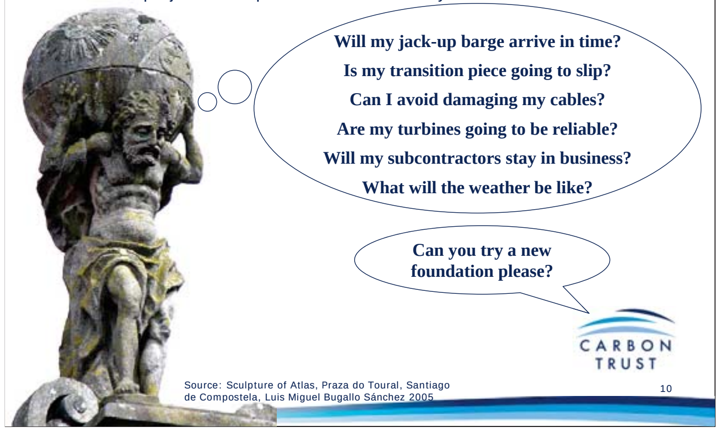

CARBON TRUST

Source: Sculpture of Atlas, Praza do Toural, Santiago de Compostela, Luis Miguel Bugallo Sánchez 2005

How do we make innovations attractive to the market?

CARBON TRUST

- **Developers must be confident new technologies are sufficiently proven and de-risked before deploying them in commercial projects**
- **Scaled testing, onshore or offshore demonstration is often required**
- **Technology needs to demonstrate clear advantages such as cost reduction**
- **Any outstanding risks must be well understood**
- **Industry collaboration can help to accelerate the derisking, demonstration and acceptance of new technologies**
  - Sharing costs, risks
  - Learning from each other
  - Pooling sites and resources

Offshore Wind Accelerator

CARBON TRUST

Objective: Reduce cost of energy by 10% in time for Round 3

CARBON TRUST · DONG energy · e.on · MAINSTREAM RENEWABLE POWER · RWE The energy to lead · SCOTTISHPOWER RENEWABLES · SSE Renewables · Statkraft · Statoil · VATTENFALL

77% (36GW) of licensed capacity in UK waters

- **Joint industry project involving 9 developers + Carbon Trust**
- **Only developers are members**
  - Aligned interests, commercially-focused
  - International outlook for best ideas
- **£45-60m programme**
  - 2/3 industry, 1/3 public (DECC)
- **Two types of project**
  - Common R&D – concept development and knowledge building
  - Discretionary Projects – demonstrations
- **Value to members**
  - New lower-cost technologies, ready to use
  - Insights into best technologies for Round 3
  - Funding for demo projects
- **Set up 2009, runs to 2016**

OWA is an example of market-pull innovation

CARBON TRUST

Two approaches to innovation

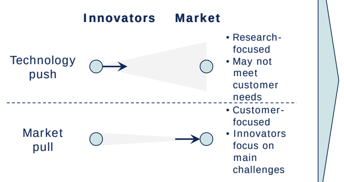

UK offshore wind R&D customer-driven

Offshore Wind Accelerator

Source: Carbon Trust 2011


We need international collaboration
OWA works with organisations around the North Sea
CARBON TRUST
UK
ATKINS
J P KENNY
tnei
SSE
South Boats
Norway
Statkraft
Nexans
Statoil
Denmark
DONG energy
DTU
A2 SEA
Universal Foundation
Netherland
Ballast Nedam
GeoSea
SPT Offshore
Grontmij
Germany
Schneider Electric
e.on
RWE
BILFINGER BERGER

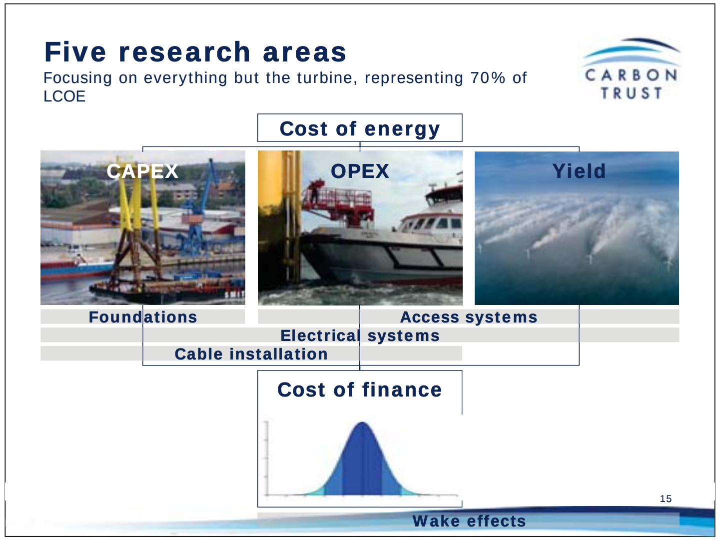
Five research areas
Focusing on everything but the turbine, representing 70% of LCOE
CARBON TRUST
Cost of energy
CAPEX
OPEX
Yield
Foundations
Access systems
Electrical systems
Cable installation
Cost of finance
Wake effects
15

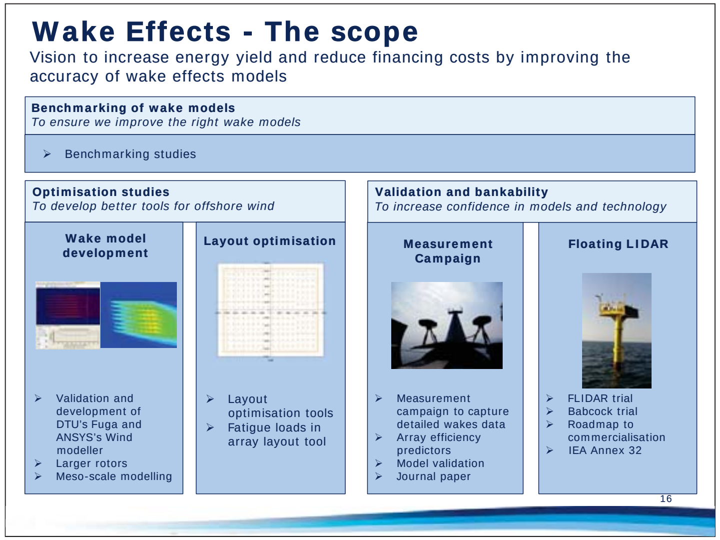
Wake Effects - The scope
Vision to increase energy yield and reduce financing costs by improving the accuracy of wake effects models
Benchmarking of wake models
To ensure we improve the right wake models
➢ Benchmarking studies
Optimisation studies
To develop better tools for offshore wind
Validation and bankability
To increase confidence in models and technology
Wake model development
➢ Validation and development of DTU's Fuga and ANSYS's Wind modeller
➢ Larger rotors
➢ Meso-scale modelling
Layout optimisation
➢ Layout optimisation tools
➢ Fatigue loads in array layout tool
Measurement Campaign
➢ Measurement campaign to capture detailed wakes data
➢ Array efficiency predictors
➢ Model validation
➢ Journal paper
Floating LIDAR
➢ FLIDAR trial
➢ Babcock trial
➢ Roadmap to commercialisation
➢ IEA Annex 32
16

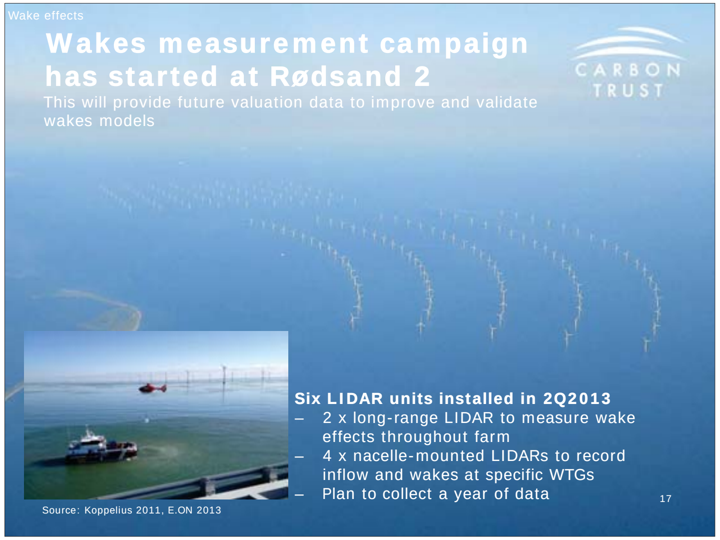
Wake effects
Wakes measurement campaign has started at Rødsand 2
This will provide future valuation data to improve and validate wakes models
CARBON TRUST
Six LIDAR units installed in 2Q2013
– 2 x long-range LIDAR to measure wake effects throughout farm
– 4 x nacelle-mounted LIDARs to record inflow and wakes at specific WTGs
– Plan to collect a year of data
Source: Koppelius 2011, E.ON 2013
17

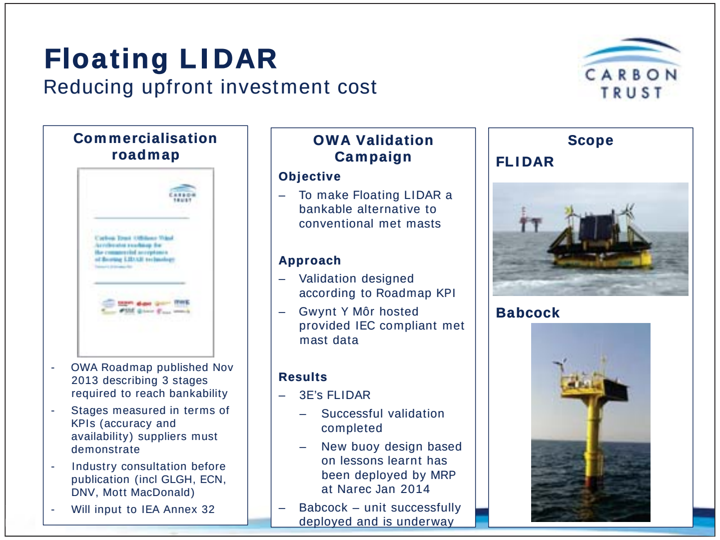
Floating LIDAR
Reducing upfront investment cost
CARBON TRUST
Commercialisation roadmap
- OWA Roadmap published Nov 2013 describing 3 stages required to reach bankability
- Stages measured in terms of KPIs (accuracy and availability) suppliers must demonstrate
- Industry consultation before publication (incl GLGH, ECN, DNV, Mott MacDonald)
- Will input to IEA Annex 32
OWA Validation Campaign
Objective
– To make Floating LIDAR a bankable alternative to conventional met masts
Approach
– Validation designed according to Roadmap KPI
– Gwynt Y Môr hosted provided IEC compliant met mast data
Results
– 3E's FLIDAR
– Successful validation completed
– New buoy design based on lessons learnt has been deployed by MRP at Narec Jan 2014
– Babcock – unit successfully deployed and is underway
Scope
FLIDAR
Babcock

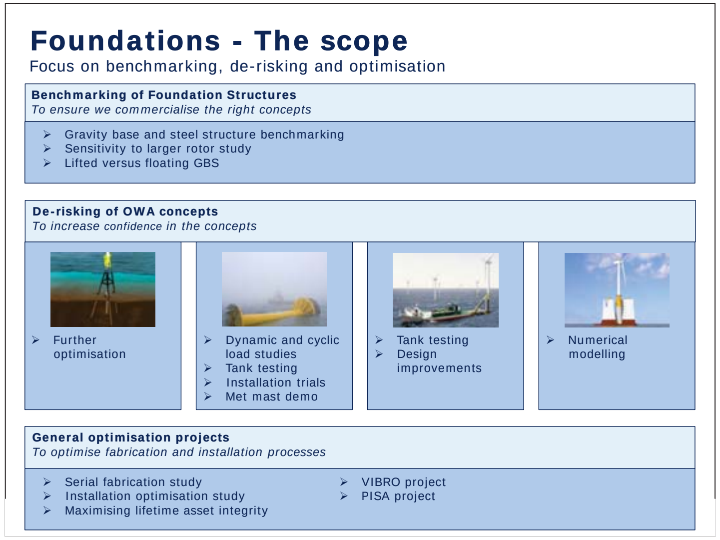
Foundations - The scope
Focus on benchmarking, de-risking and optimisation
Benchmarking of Foundation Structures
To ensure we commercialise the right concepts
➢ Gravity base and steel structure benchmarking
➢ Sensitivity to larger rotor study
➢ Lifted versus floating GBS
De-risking of OWA concepts
To increase confidence in the concepts
➢ Further optimisation
➢ Dynamic and cyclic load studies
➢ Tank testing
➢ Installation trials
➢ Met mast demo
➢ Tank testing
➢ Design improvements
➢ Numerical modelling
General optimisation projects
To optimise fabrication and installation processes
➢ Serial fabrication study
➢ Installation optimisation study
➢ Maximising lifetime asset integrity
➢ VIBRO project
➢ PISA project


Foundations
Two Universal Foundations installed at Dogger Bank
February and September 2013, 150km offshore, 25m depth
CARBON TRUST
Benefits
– Simple fabrication
– Few marine operations
– Fred. Olsen end-to-end EPC offer
– Significant cost reduction potential
Image: Forewind, 2013
20

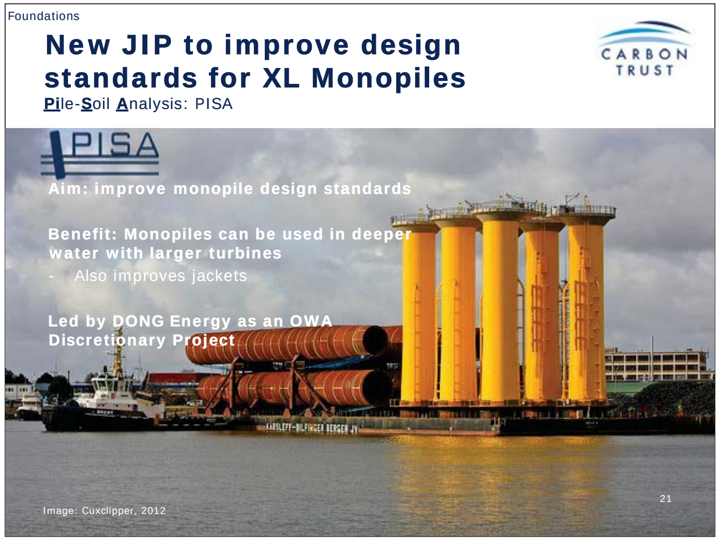
Foundations
New JIP to improve design standards for XL Monopiles
Pile-Soil Analysis: PISA
CARBON TRUST
PISA
Aim: improve monopile design standards
Benefit: Monopiles can be used in deeper water with larger turbines
- Also improves jackets
Led by DONG Energy as an OWA Discretionary Project
Image: Cuxclipper, 2012
21

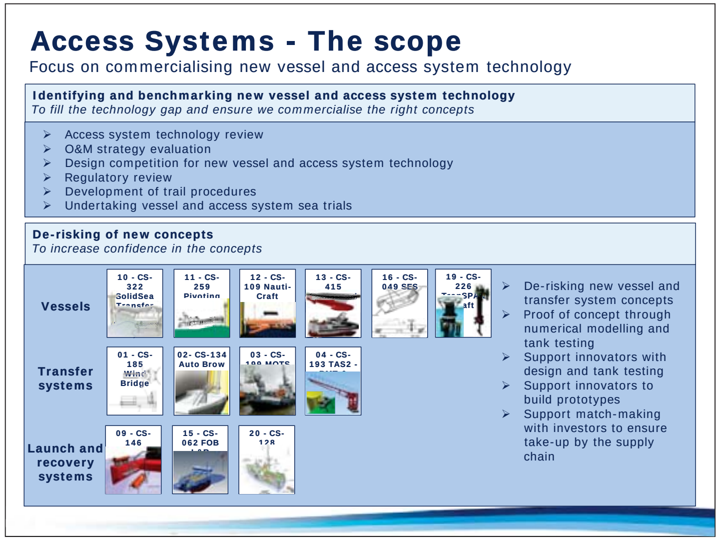
Access Systems - The scope
Focus on commercialising new vessel and access system technology
Identifying and benchmarking new vessel and access system technology
To fill the technology gap and ensure we commercialise the right concepts
➢ Access system technology review
➢ O&M strategy evaluation
➢ Design competition for new vessel and access system technology
➢ Regulatory review
➢ Development of trail procedures
➢ Undertaking vessel and access system sea trials
De-risking of new concepts
To increase confidence in the concepts
Vessels
Transfer systems
Launch and recovery systems
10 - CS-322 SolidSea
11 - CS-259
12 - CS-109 Nauti-Craft
13 - CS-415
16 - CS-049 SES
19 - CS-226
01 - CS-185
02- CS-134 Auto Brow
04 - CS-193 TAS2 -
09 - CS-146
15 - CS-062 FOB
➢ De-risking new vessel and transfer system concepts
➢ Proof of concept through numerical modelling and tank testing
➢ Support innovators with design and tank testing
➢ Support innovators to build prototypes
➢ Support match-making with investors to ensure take-up by the supply chain


First of six Fjellstrand WindServers is now in the water
CARBON TRUST
Advantage
- Fast and efficient
- Stability in station-keeping
Source: Fjellstrand 2013
23


NautiCraft has just built an 8m prototype
CARBON TRUST
DNV·GL
Advantage
- Fast, comfortable
- Hydraulic connections system compensates heave
Warp mode
Pitch mode
Roll mode
Source: NautiCraft, 2013
24


Umoe Mandal's Wave Craft
Successfully tank tested
CARBON TRUST
Advantage
- Speed
- Air cushion compensates motions
WAVECRAFT
Source: Umoe Mandal 2013
25

Electrical Systems - The scope

Significant focus on higher voltage arrays

Technology review
To ensure we focus on the opportunities that promise most cost reduction

- Technology evaluation

Feasibility and optimisation studies
To increase confidence in the concepts

66KV

- Higher voltage engineering design study
- 66kV component acceleration
- 66kV cable qualification

HVDC

- HVDC technology review
- Supplier engagement
- HVDC optimisation study

AC and DC

- DC array feasibility study
- AC optimisation study

Why 66kV?

CARBON TRUST

33kV

5MW Turbines
200 Turbines
1000MW capacity

3 Substation
Radial configuration

66kV

5MW Turbines
200 Turbines
1000MW capacity

2 Substation
Ring configuration

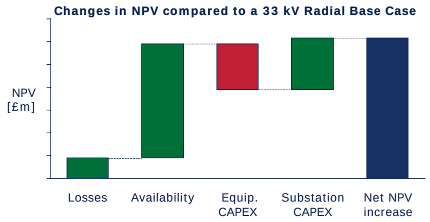

- Improvement in NPV is driven by reduced lost revenue due to increased availability (i.e. the ring design).
- The reduction in the number of substation and associated equipment is benefiting
- Some cost penalty in terms of wind turbine equipment – i.e. transformers and switchgear

Note: 0.015 failures/km/year was assumes

27

Cable Installation - The scope

Focus on improving cable installation techniques

Technology review
To ensure we focus on the opportunities that promise most cost reduction.

- Technology evaluation

Feasibility and optimisation studies
To increase confidence in the technology

Cable entry systems

- Technology review

Free hanging cables

- Feasibility study for free hanging cables

Cable burial

- Cable burial methodology and risk mitigation study

Cable installation

CARBON TRUST

Vision: Reduce cable failure rates and installation costs

J-tubeless, free-hanging cables: cables would be hung from transition piece, rather than pulled through the foundation

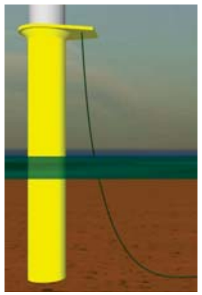

Benefits to dynamic cables

- No J-tubes
- No divers
- No cable pull, leading to faster installation

Lower costs
Fewer risks

Image: Orcaflex 2013

29

Conclusions

CARBON TRUST

- **Offshore wind costs need to come down from ~£150/MWh to ~£100/MWh by 2020**
- **Innovation has the potential to deliver three-quarters of this**
- **Research is critical to achieve cost reduction but commercialisation is challenging**
- **The industry is international, and we need to work together to get the best ideas – we won't find the answers alone**
- **OWA, EERA and TPWind are good examples of collaborative R&D in offshore wind**
- **We need industry to pull the innovations to market.**

30

Whitacre Presentation – Texas Tech
October 26, 2010

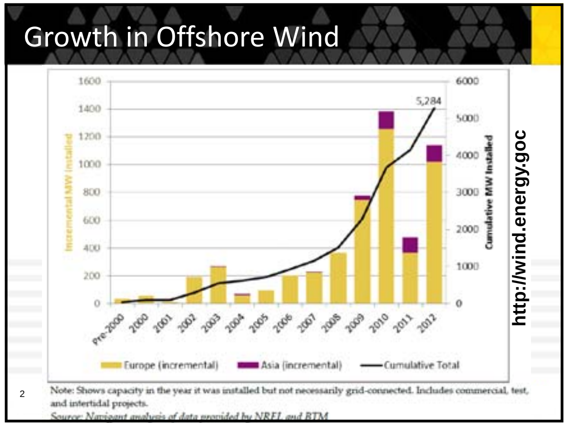

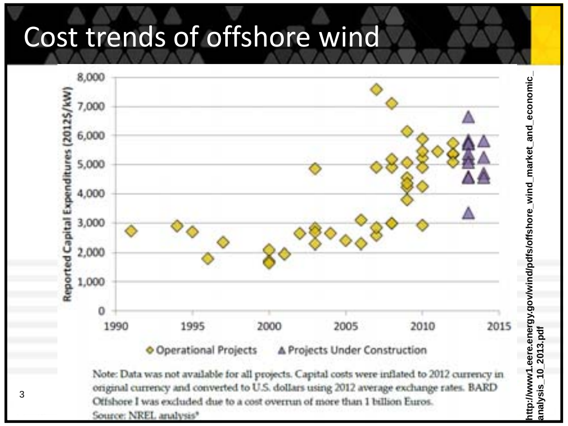

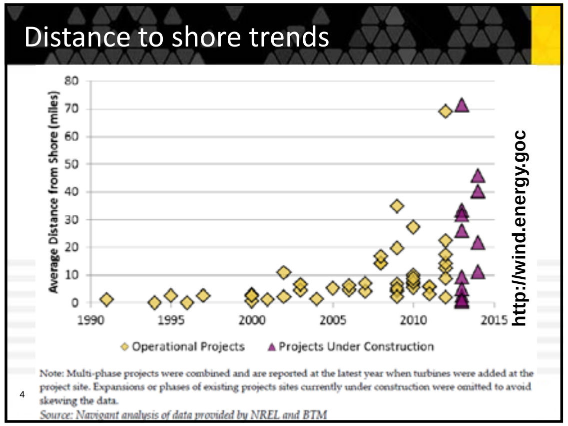

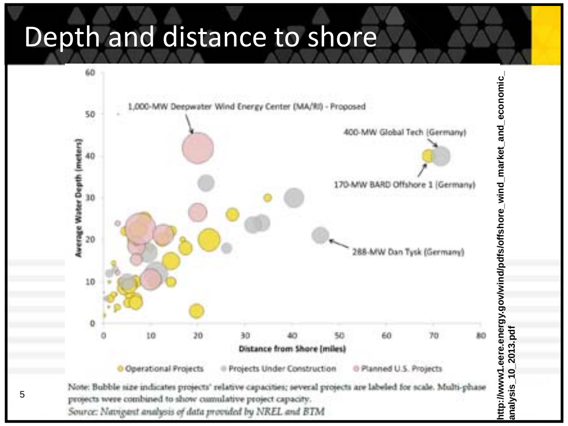

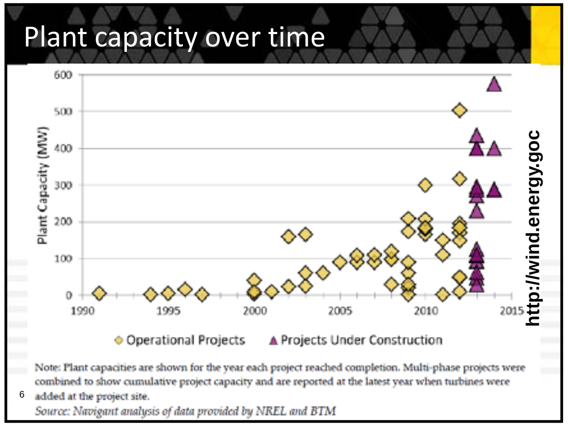

Whitacre Presentation – Texas Tech
October 26, 2010

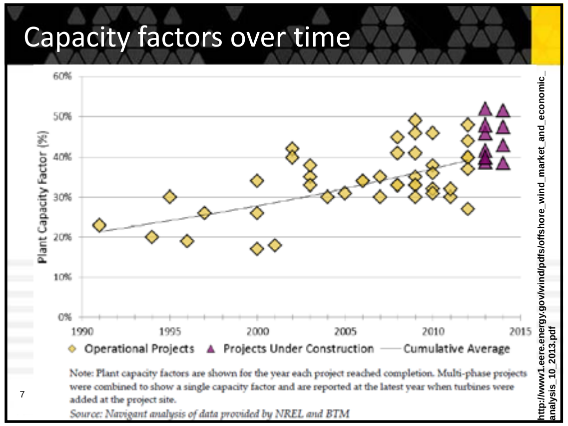

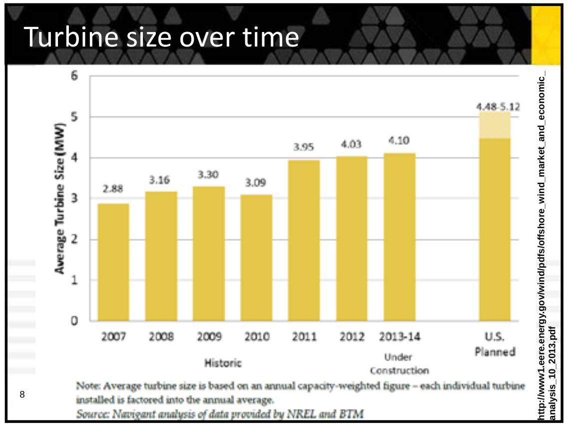

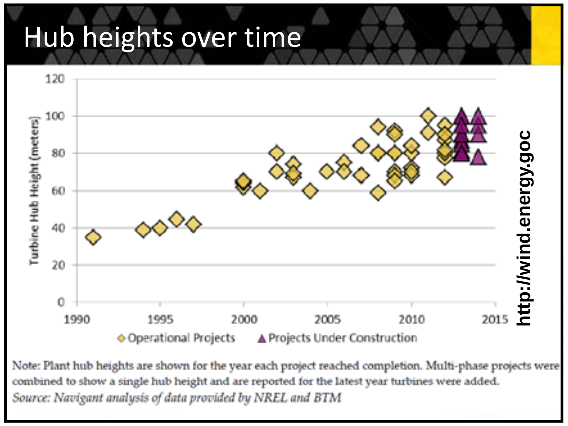

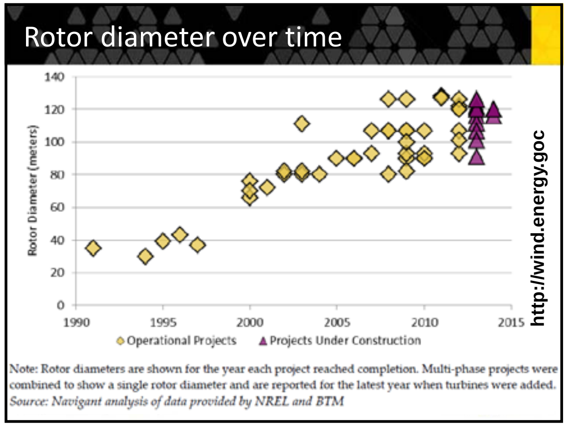

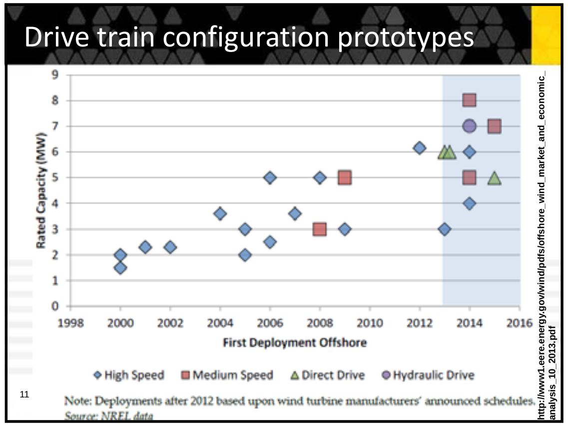

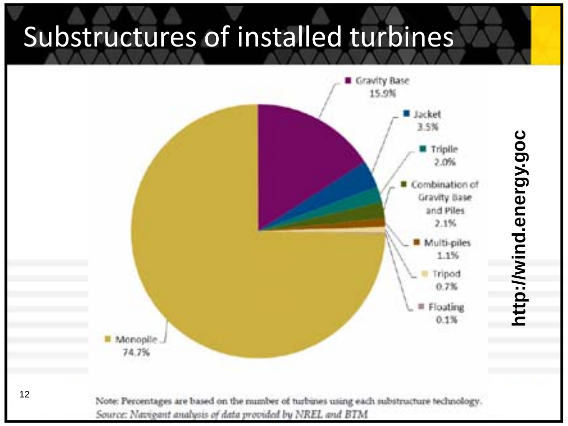

Whitacre Presentation – Texas Tech
October 26, 2010

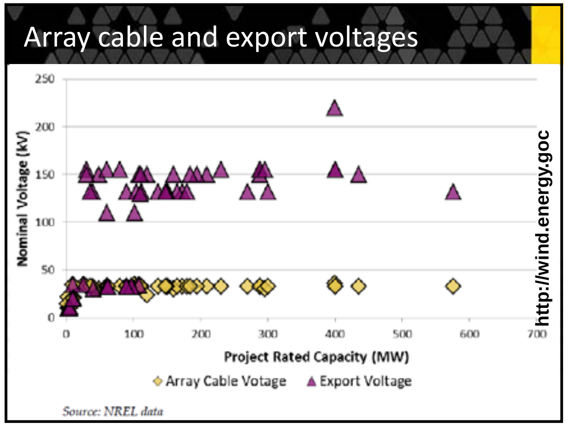

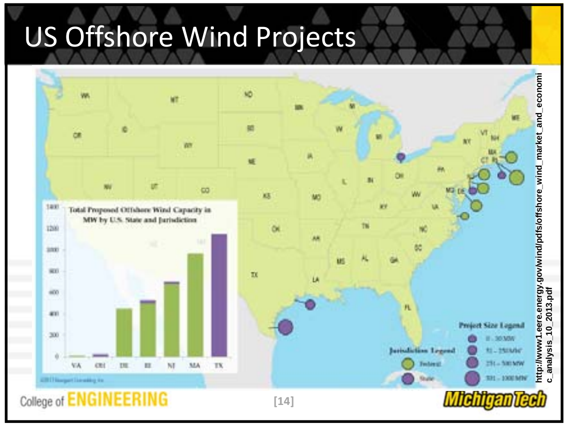

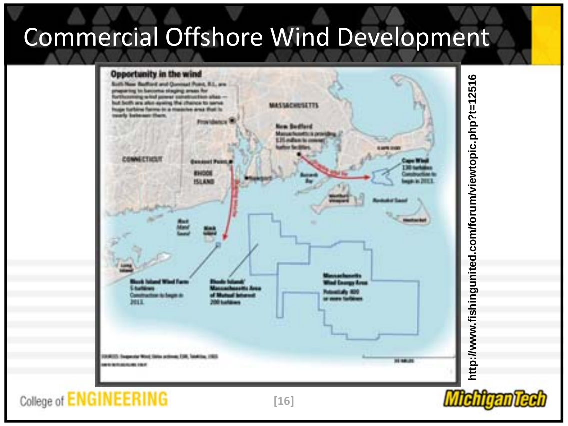

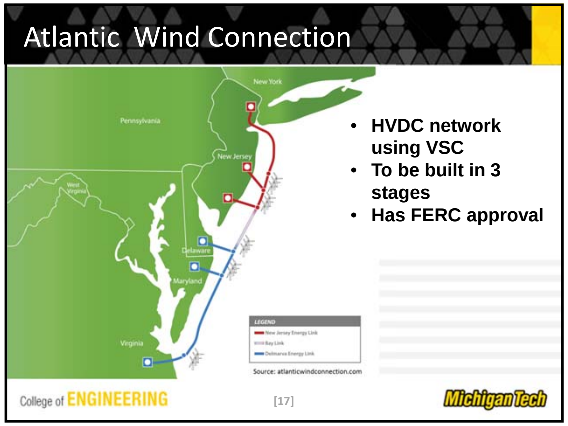

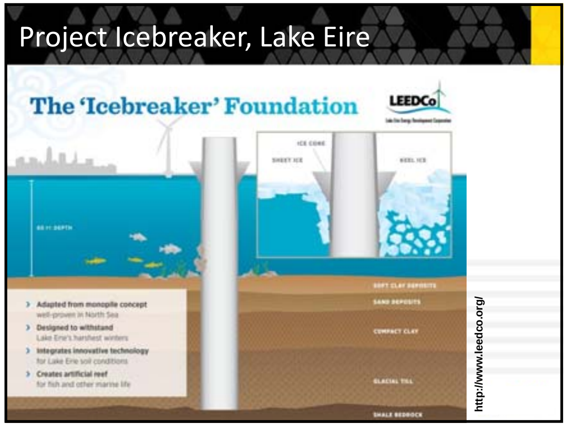

Whitacre Presentation – Texas Tech
October 26, 2010

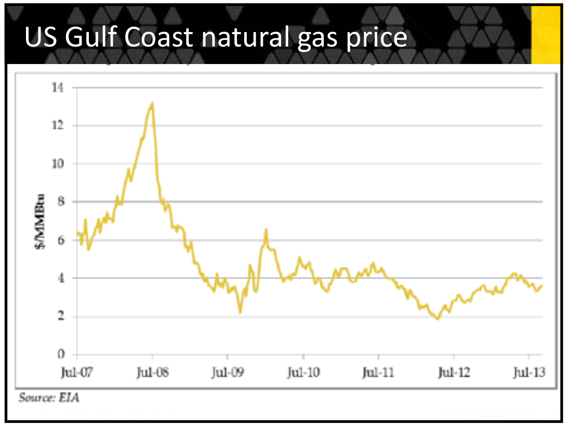

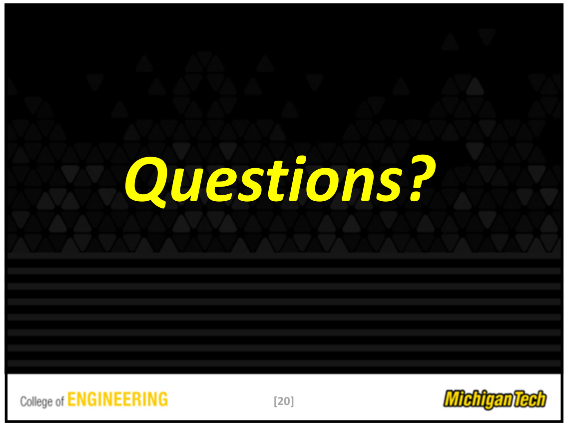

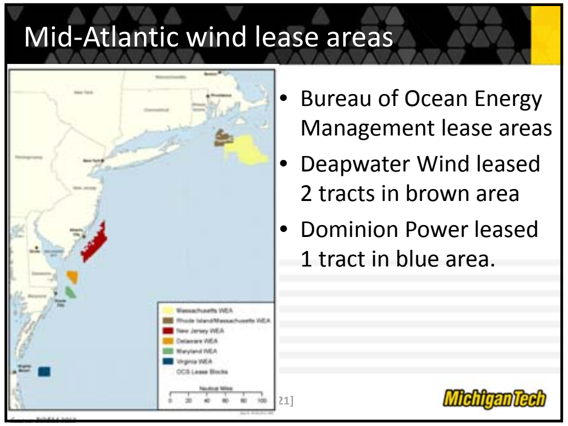

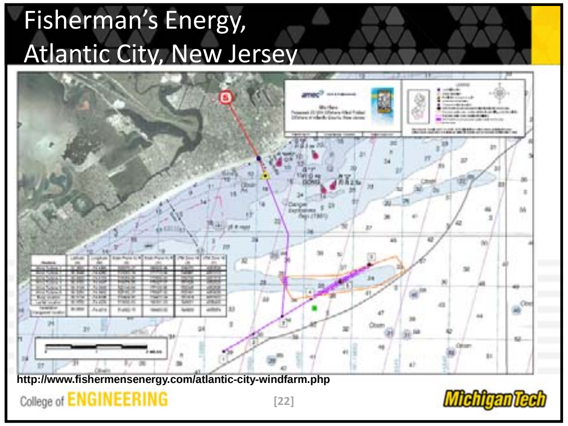

Whitacre Presentation – Texas Tech
October 26, 2010

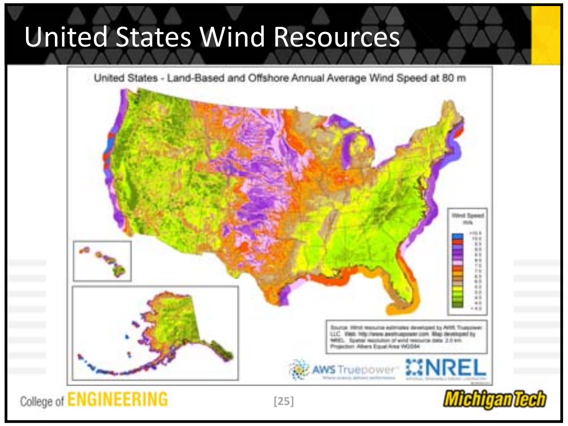

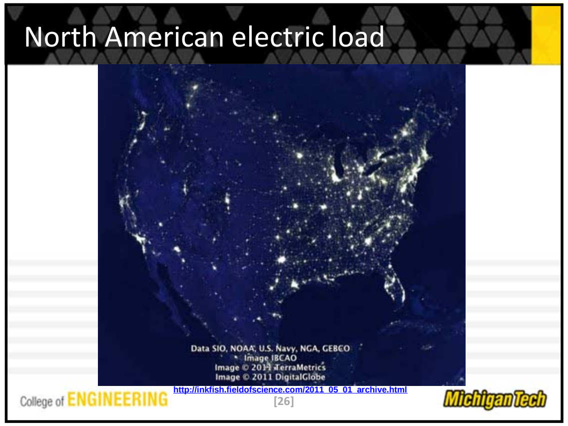

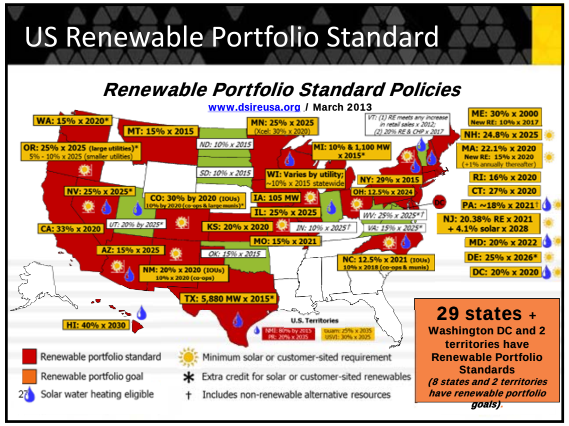

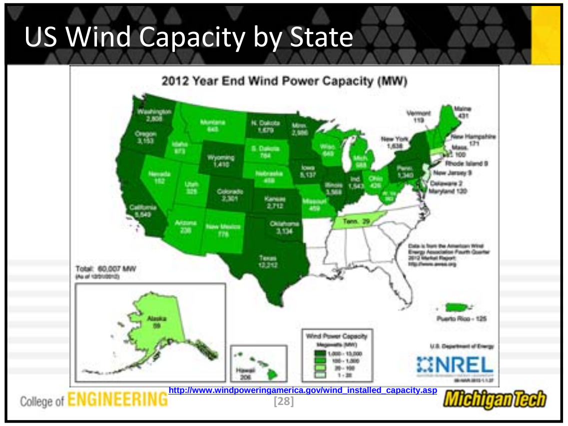

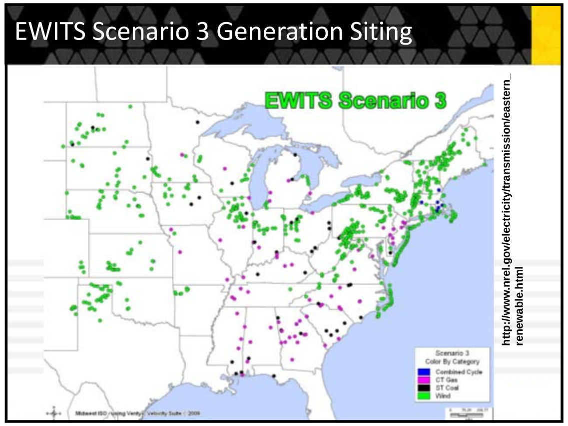

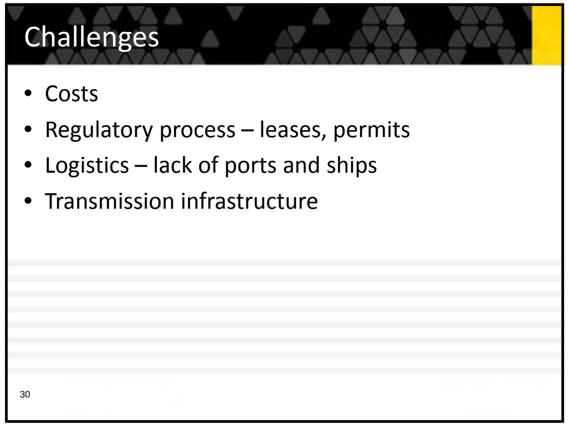

US Department of Energy

Off Shore Demonstration Projects

http://www1.eere.energy.gov/wind/index.html

College of ENGINEERING [31] MichiganTech

Statoil, Boothbay Harbor, Maine

http://www.renewbl.com/2011/06/28/statoil-selling-onshore-wind-assets-in-norway-moves-focus-on-offshore-wind.html

College of ENGINEERING [32] MichiganTech

GOWind, Gulf of Mexico, Texas

http://www.baryonyxcorp.com/

College of ENGINEERING [33] MichiganTech

Lake Eire Project

College of ENGINEERING [34] MichiganTech

Wind Float, Coos Bay, Oregon

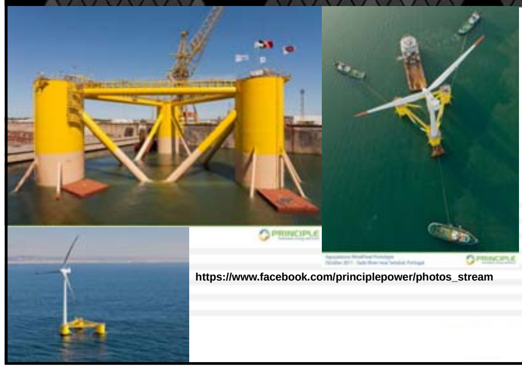

https://www.facebook.com/principlepower/photos_stream

Coos Bay Project

College of ENGINEERING [36] MichiganTech

Other Offshore Projects

College of ENGINEERING [37] Michigan Tech

Galveston Offshore Wind (Costal Energy)

College of ENGINEERING [38] Michigan Tech

Boothbay Harbor, Maine project

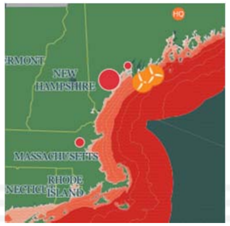

College of ENGINEERING [39] Michigan Tech